

ÉCOLE DOCTORALE SCIENCES DE LA VIE ET DE LA SANTÉ

Institut de recherche sur les maladies virales et hépatiques, UMR_S1110

THÈSE présentée par

Natascha Larissa RÖHLEN

Soutenue le 21 septembre 2021

Pour obtenir le grade de **Docteur de l'Université de Strasbourg**

Discipline/Spécialité : Sciences Médicales/Hépatogastroentérologie

**The functional role of Claudin-1 as a mediator and
therapeutic target in liver fibrogenesis and
hepatocarcinogenesis**

Thèse dirigée par :

Thomas Baumert

PU-PH, Université de Strasbourg

Catherine Schuster

DR Inserm, Université de Strasbourg

Rapporteurs :

Tobias Böttler

PD. Dr., Université de Fribourg, Allemagne

Magdalena Filipowicz Sinnreich

PD. Dr., Université de Bâle, Suisse

Examineurs :

Gabriel Malouf

PU-PH, Université de Strasbourg

Richard Moreau

DR Inserm, Université de Paris

Acknowledgements

I would like to acknowledge several persons for their support during realization of my PhD:

I would first like to thank my thesis director, Thomas Baumert, who initiated the projects of this thesis and whose expertise and close supervision guided all research questions and methodology. Your insightful feedback pushed me to learn new techniques, overcome technical difficulties and to develop new research ideas.

I'd like to acknowledge Catherine Schuster and Joachim Lupberger, who have guided me throughout my doctoral studies by critical scientific discussions, manuscript editing, and helped me focusing during times of endless deadlines and seemingly insurmountable amount of work.

I would also like to thank my colleagues, especially Hussein and Emilie, who integrated me into the project and helped acquiring experimental or bioinformatical skills that were crucial for the progress of this thesis.

Finally, I'd like to thank my family and friends for their wise counsel and invaluable distractions to rest my mind outside of research.

This doctoral thesis was supported by a grant from the German research foundation (DFG, RO 5983/1-1).

Table of contents

Acknowledgements	3
List of Tables	6
List of Figures	6
List of Annexes	6
Abbreviations	7
1. Introduction	10
1.1 The global burden of chronic liver disease	10
1.1.1 Chronic hepatitis B infection	11
1.1.2 Chronic hepatitis C infection	12
1.1.3 Non-alcoholic fatty liver disease	13
1.1.4 Alcoholic liver disease	15
1.2 Progression of chronic liver disease to liver fibrosis	15
1.2.1 Clinical monitoring and diagnosis of liver fibrosis	16
1.2.2 Pathophysiology of liver fibrosis	17
1.2.3 Fibrosis regression and therapeutic perspectives for patients with liver fibrosis	19
1.3 Progression of chronic liver disease to HCC	20
1.3.1 Clinical diagnosis of HCC	21
1.3.2 Pathophysiology of HCC	21
1.3.3 Role of the liver microenvironment in liver carcinogenesis	24
1.3.4 Role of epithelial-mesenchymal transition in HCC progression	26
1.3.5 Molecular subclassification of HCC	28
1.3.6 Management of HCC and therapeutic perspectives	29
1.4 Tight junction proteins in chronic liver disease and HCC	31
1.4.1 CLDN1 – Expression pattern and functional role	31
1.4.2 Role of CLDN1 in chronic liver disease and HCC – state of the art	36
1.4.3 Development of monoclonal antibodies targeting non-junctional CLDN1	38
1.5 Liver disease target discovery in the era of single cell RNA sequencing and transcriptomic pathway analyses	39
1.5.1 Single cell RNA sequencing	39
1.5.2 Gene set enrichment analysis (GSEA)	41
2 Thesis goals	43
3 Results	44
3.1 Non-junctional CLDN1 as a therapeutic target for treatment of liver fibrosis	44
3.1.1 Results summary and own contribution	44

3.1.2	Publication of the results.....	47
3.1.3	Results article I.....	48
3.2	Non-junctional CLDN1 as a therapeutic target for treatment of HCC.....	154
3.2.1	Results summary and own contribution	154
3.2.2	Publication of the results.....	156
3.2.3	Results article II.....	157
4	Discussion and perspectives	209
4.1	Considerations on the expression of CLDN1 on multiple cell types in liver fibrosis and HCC.....	210
4.2	Considerations on anti-fibrotic and chemopreventive effects of non-junctional CLDN1 targeting mAbs	212
4.3	Considerations on tumor-therapeutic effects of non-junctional CLDN1 targeting mAbs	213
4.4	Considerations on the molecular mechanism of CLDN1 mAb mediated antifibrotic, chemopreventive and tumortherapeutic effects	214
4.5	Considerations on the role of non-junctional CLDN1 in other fibrotic and malignant diseases	218
4.6	Final concluding remarks.....	219
5	Résumé français de la thèse de doctorat	220
6	References.....	228
7	Annexes	246
8	Curriculum vitae.....	321

List of Tables

Table 1. Compounds in clinical development for treatment of NASH.....	14
Table 2. Reported perturbations of CLDN1 expression in human diseases.....	34
Table 3. Reported implications of CLDN1 in intracellular cellular signaling cascades in human disease.....	35

List of Figures

Figure 1. The prevalence of chronic liver disease is increasing worldwide.....	10
Figure 2. Liver fibrosis is the main determinant of mortality in patients with chronic liver disease.....	16
Figure 3. General mechanisms involved in liver fibrogenesis..	18
Figure 4: Liver cell plasticity during fibrotic liver disease progression.....	19
Figure 5. Incidence and etiology of HCC worldwide.	20
Figure 6. Sequential evolution of HCC in cirrhotic liver..	22
Figure 7. Model of different cancer cell origins in HCC..	23
Figure 8. Complex interaction of cancer cells with its immunogenic microenvironment.	25
Figure 9. Cancer-associated fibroblasts of the tumor microenvironment promote hepatocarcinogenesis, tumor progression and treatment resistance.....	26
Figure 10. The role of EMT transition in cancer.....	27
Figure 12. Therapeutic management of HCC according to BCLC stage.	30
Figure 13. Model of CLDN1 structure.....	32
Figure 14. CLDN1 expression on epithelial cells and current concept of interactions.....	33
Figure 15: Functional role of basolateral CLDN1 as an HCV cell entry factor.....	37
Figure 16: Development of non-junctional CLDN1 targeting monoclonal antibodies.	39
Figure 17. Gene set enrichment analysis (GSEA).....	42
Figure 18: ScRNAseq analysis for high-resolution studies on liver pathophysiology.	40
Figure 19. Schematic illustration of the main findings of the work presented in this thesis..	209

List of Annexes

Introductory article I – Liver fibrosis: Mechanistic concepts and therapeutic perspectives.....	246
Introductory article II – The role of the liver microenvironment in liver carcinogenesis.....	287
Introductory article III – Tight Junction Proteins and the Biology of Hepatobiliary Disease.....	298

Abbreviations

ACC	Acetyl CoA Carboxylase
ANGPT ½	Angiopoietin ½
Apo	Apolipoprotein
APOC	Apolipoprotein C
AFP	Alpha-fetoprotein
ALD	Alcoholic liver disease
ALT	Alanine aminotransferase
AIH	Autoimmune hepatitis
BC	Bile canaliculi
BCLC	Barcelona Clinic Liver Cancer
BCR	B cell receptor
CAFs	Cancer associated fibroblasts
CCL2	Chemokine (C-C motif) ligand 2
CD81	Cluster of Differentiation 81
CLDN	Claudin
CSCs	Cancer Stem Cells
DAA	Direct acting antivirals
DAMPs	Damage-associated molecular patterns
DDLT	Deceased Donor Liver Transplant
ECM	Extracellular matrix
ECOG	Eastern Cooperative Oncology Group
ECL1	Extracellular loop 1
ECL2	Extracellular loop 2
EMT	Epithelial-mesenchymal transition
EPCAM	Epithelial cell adhesion molecule
EGFR	Epithelial growth factor receptor
ERK	Extracellular-signal regulated kinase
ES	Enrichment Score
FAK	Focal adhesion kinase
FDA	Food and Drug Administration
FGF19	Fibroblast Growth Factor 19

FGF20	Fibroblast Growth Factor 20
FXRs	Farnesoid X-Activated Receptors
GLP1	Glucagon-like Peptide 1
GSEA	Gene set enrichment analysis
HBV	Hepatitis B virus
HBsAg	Hepatitis B surface Antigen
HCC	Hepatocellular carcinoma
HCV	Hepatitis C virus
HDV	Hepatitis D virus
HGDNs	High-grade dysplastic nodules
HLMF	Human liver myofibroblasts
HRas	HRas Proto-Oncogene
HS	Heparan sulfate
HSCs	Hepatic stellate cells
iCCA	Intrahepatic cholangiocarcinoma
IL-10	Interleukin 10
ITGB1	Integrin beta 1
mAbs	Monoclonal Antibodies
MAPK	Mitogen-activated protein kinase
MDSC	Myeloid-derived suppressor cell
MMP	Matrix metalloproteinase
NAFLD	Non-alcoholic fatty liver disease
NASH	Non-alcoholic steatohepatitis
NISCH	Neonatal ichthyosis and sclerosing cholangitis
NPC1L1	Niemann-Pick C1-Like 1
OCA	Obetichol acid
OCLN	Occludin
OS	Overall survival
PBC	Primary biliary cirrhosis
PDGF	Platelet Derived Growth Factor
PHH	Primary human hepatocytes
PLS	Prognostic Liver Signature

PNPLA3	Phospholipase domain-containing protein 3
PPARs	Peroxisome proliferator-activated receptor
PSC	Primary sclerosing cholangitis
Pro-MMP	Pro-Matrix metalloproteinase
LDLT	Live Donor Liver Transplant
LDLR	Low density lipoprotein receptor
LGDNs	Low-grade dysplastic nodules
RNAseq	RNA sequencing
RTCs	Randomized Controlled Trials
RTKs	Receptor tyrosine kinases
SCD-1	Stearoyl coenzyme A desaturase 1
scRNAseq	Single cell RNA sequencing
SGLT2	Sodium glucose cotransporter 2
SR-B1	Scavenger receptor class B type 1
TACE	Transarterial chemoembolization
TE	Transient elastography
TERT	Telomerase reverse transcriptase
TfR1	Transferrin receptor 1
TGF- β	Transforming Growth Factor Beta
THR β	Thyroid Hormone Receptor beta
TNF	Tumor necrosis factor
T _{reg} cell	Regulatory T cell
TJ	Tight junction
t-SNE	T-distributed stochastic neighbour embedding
US	United States
VEGF	Vascular endothelial growth factor
ZO	Zonula Occludens

1. Introduction

1.1 The global burden of chronic liver disease

Chronic liver diseases constitute a global health problem, affecting more than 1.5 billion people worldwide. The major causes of chronic liver disease include chronic hepatitis B and C, alcoholic liver disease (ALD) and non-alcoholic fatty liver disease (NAFLD). Moreover, genetic diseases and autoimmune disorders such as autoimmune hepatitis (AIH) and primary biliary cirrhosis (PBC) are rare causes of chronic hepatic injury. Despite breakthroughs in therapeutic management of viral hepatitis, the prevalence of chronic liver disease is increasing worldwide (**Figure 1**). This is especially due to the rising incidence of obesity and NAFLD within the last years (Younossi, 2019). Apart from increased health care utilization and impaired quality of life, chronic liver diseases are associated with a high mortality, due to complications such as liver fibrosis and hepatocellular carcinoma (HCC). In fact, recent mortality evaluations indicate chronic liver diseases to account for more than two million deaths per year worldwide (Moon *et al.*, 2020).

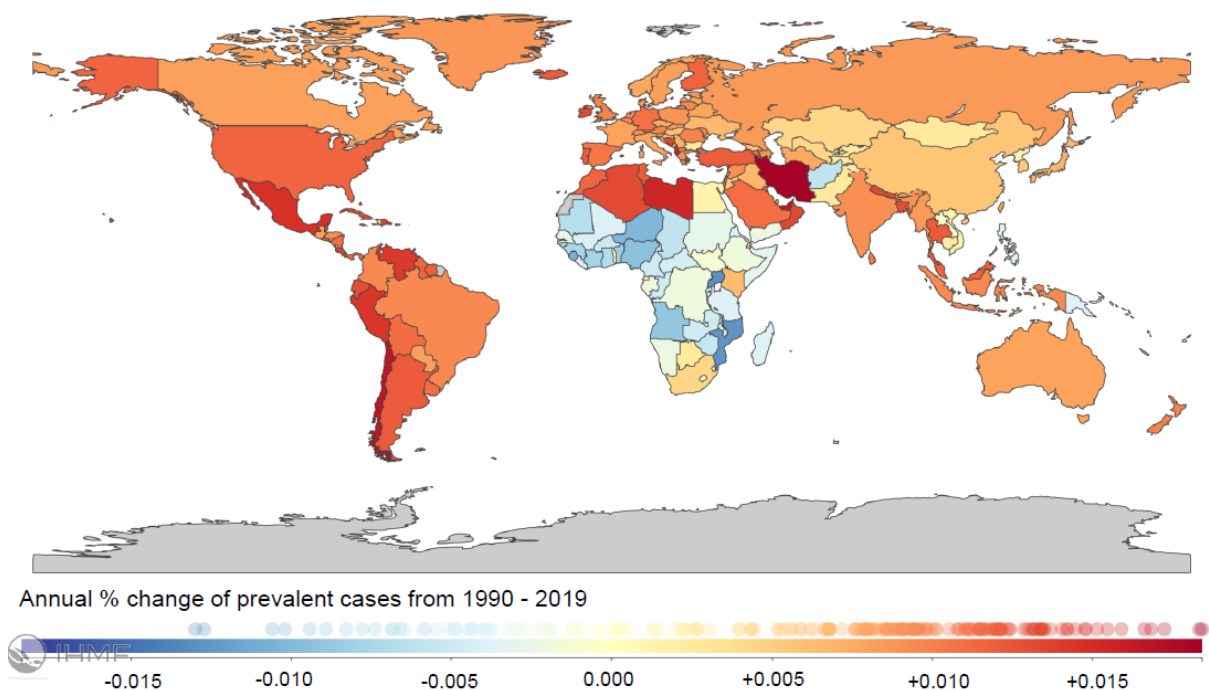


Figure 1. The prevalence of chronic liver disease is increasing worldwide. The annual % change of prevalent cases per 100.000 inhabitants (both genders, all ages, year 1990-2019) is shown. Adapted from the Global Burden of Disease study (Sung *et al.*, 2021) (<https://vizhub.healthdata.org/gbd-compare/>).

1.1.1 Chronic hepatitis B infection

The hepatitis B virus (HBV) belongs to the *Hepadnaviridae* family of DNA viruses and has first been described in 1970 (Cossart and Field, 1970). Characterized by a complex viral life cycle with unique similarities to retroviruses, HBV only infects human and orangutan hepatocytes (Guidotti and Chisari, 2006). While HBV itself does not directly induce hepatocyte death, the host's immune system determines the course of the disease. Acute HBV infection hereby ranges from self-limiting asymptomatic hepatitis to fulminant hepatic failure. Chronic hepatitis B is diagnosed if Hepatitis B surface antigen and HBV DNA persist and is determined by virus-induced immune escape. In adults, approximately 95% of HBV infections result in a self-limiting, transient hepatitis with viral clearance and development of protective antibodies (for a review see: Li *et al.*, 2019). However, about 90 % of vertical transmissions and 20-30% of infections during childhood result in chronic hepatitis, which has been attributed to the immaturity of the adaptive immune system in infants and children (Fattovich *et al.*, 2008). Patients with untreated chronic HBV infection develop liver cirrhosis in 15-40% of all cases and are at high risk for HCC development (Tang *et al.*, 2018).

Importantly, HBV encoded envelope proteins enable hepatic cell entry and dissemination of another hepatotropic virus, hepatitis D virus (HDV). Thus, HDV infection can only occur in association with HBV (Hughes *et al.*, 2011). Whereas simultaneous infection with HBV and HDV results in clearance of both viruses in the majority of individuals, super-infection of an HBV-infected individual with HDV typically results in chronic HBV/HDV co-infection, the most severe and rapidly progressive form of chronic viral hepatitis. In fact, chronic HBV/HDV co-infection is associated with an unfavorable outcome due to the development of liver cirrhosis, liver failure, and eventually HCC within 5-10 years (for a review see: Sureau and Negro, 2016). The development of effective prophylactic vaccines against HBV has led to a strong decrease in prevalence of chronic HBV infection in western countries. However, due to insufficient implementation of universal vaccination programs especially in low-income countries, HBV infection remains a global health problem. Worldwide more than 350 million are chronically

infected with HBV, of which approximately 5% show chronic HBV/HDV infection (Yuen *et al.*, 2018). Recent estimations attribute 1 million deaths/year to chronic HBV and HBV/HDV co-infections due to its complications of liver fibrosis and HCC (Li *et al.*, 2019). Approved medications for treatment of chronic hepatitis B include interferon formulations, nucleoside or nucleotide analogues, such as lamivudine. These treatments have shown to significantly suppress HBV replication and to reduce hepatic inflammation, though do not allow viral clearance (Lok *et al.*, 2016). Current treatment options for chronic HBV/HDV co-infection consist of pegylated interferon- α (pegIFN α). However, this treatment is effective only in a minority of patients and may cause severe side effects (Koh *et al.*, 2019). New and promising therapeutic approaches, e.g. the entry-inhibitor bulevirtide, are currently in clinical trials (Asselah *et al.*, 2020).

1.1.2 Chronic hepatitis C infection

Following the first description of a non-A non-B posttransfusion hepatitis in 1975 (Feinstone *et al.*, 1975), hepatitis C virus (HCV) was discovered in 1989 as the causative virus (Choo *et al.*, 1989). HCV is an enveloped RNA virus belonging to the *Flaviviridae* family. In developed countries, the main risk factor for HCV infection is chronic intravenous drug abuse, while in developing countries most infections are healthcare-associated due to poor standards of infection control and injection safety. Vertical (mother-to-infant) transmission is the most common cause of HCV infection in children (for a review see: Lanini *et al.*, 2016).

Only approximately 25% of patients with acute HCV infection show clinical symptoms of disease, but 70-80% develop chronic HCV infection (Bukh, 2016). Of note, about 15-35% of patients with chronic HCV infection develop progressive fibrosis and cirrhosis. Once HCV-associated liver cirrhosis is established, HCC occurs at an annual rate of 2-3% (For a review see: Thrift *et al.*, 2017).

Scientific milestones of HCV research including the development of experimental recombinant cell culture systems and the elucidation of HCV's viral life cycle have paved the way from

relatively ineffective interferon monotherapy to highly efficient HCV enzyme inhibitors, namely direct-acting antivirals (DAA). In fact, current DAA therapies can cure over 90% of HCV infections and significantly reduce the risk of cirrhosis and HCC development (Kanwal *et al.*, 2017). Still, approximately 71 million people worldwide have chronic HCV infection with an estimated number of 1.8 million new infections per year (Moon *et al.*, 2020). This is mainly due to a high rate of undiagnosed HCV infections, ranging from 68% in North America to 94% in Africa (Cooke *et al.*, 2019). Moreover, curative HCV treatment with DAA is still often not accessible to a high proportion of infected individuals, due to associated costs and limited reachability of populations-at-risk (Wiessing *et al.*, 2014; Marshall *et al.*, 2018). The development of protective vaccines against HCV infection has yet been hampered by the genetic diversity of HCV, the lack of suitable *in vivo* models and virus immune escape (for a review see: Luxenburger *et al.*, 2018). A recent phase 1/2 clinical trial failed in preventing chronic HCV infection by a vaccine regime based on recombinant adenoviral vectors (Page *et al.*, 2021).

1.1.3 Non-alcoholic fatty liver disease

Non-alcoholic liver disease (NAFLD) describes a liver disease associated with the metabolic syndrome and is characterized by excess accumulation of fat in hepatocytes. Main risk factors for NAFLD include adipositas (body mass index ≥ 30), insulin resistance, type 2 diabetes and hyperlipidemia (Younossi, 2019). Although most patients with NAFLD are obese, NAFLD can also occur in underweight or normal weight patients (lean NAFLD). The occurrence of lean NAFLD is strongly associated with genetic factors (PNPLA3 polymorphisms), congenital metabolic defects (e.g. lysosomal acid lipase deficiency), as well as specific medication (e.g. amiodaron, total parenteral nutrition) (for a review see: Kumar and Mohan, 2017).

The clinical spectrum of NAFLD ranges from simple steatosis to non-alcoholic steatohepatitis (NASH) with significant hepatocyte cell death and histological signs of inflammation. NASH can lead to liver fibrosis, cirrhosis and HCC. Given the increasing rates of obesity especially in

western countries, the prevalence of NAFLD has strongly increased, essentially contributing to the rising numbers in liver disease associated mortality in the last years (Kim *et al.*, 2018). Thus, NAFLD currently affects 25% of the general population (ranging from 13% in Africa to 30.45% in south America) (Younossi *et al.*, 2019) and is expected to become the leading cause of liver-related death in the future (for a review see: Diehl and Day, 2017).

Weight loss exhibits beneficial effects on biochemical and histological markers of NASH activity, however, the realization of recommended lifestyle changes is often unsuccessful (Vilar-Gomez *et al.*, 2015; Romero-Gomez *et al.*, 2017). Bariatric surgery has been shown to be highly effective in resolution of NASH but is invasive, irreversible and potentially associated with severe complications (Lassailly *et al.*, 2020). Within the last decade, multiple compounds for pharmacological treatment of NAFLD and NASH have been developed and are currently investigated in clinical trials (For a review see: Shen and Lu, 2021 and Guirguis *et al.*, 2021) (**Table 1**). The most promising compounds in clinical development include obeticholic acid (OCA), Fibroblast Growth Factor 19/21 (FGF19/21) analogues and anti-diabetics, such as Glucagon-like Peptide 1 (GLP1) agonists (Attia *et al.*, 2021). However, yet, no therapy has been approved for treatment of NAFLD and NASH.

Table 1. Compounds in clinical development for treatment of NASH.

Target	Compound	Phase of clinical development	Reference or Clinicaltrials.gov identifier
FXRs	OCA	Phase 3	(Younossi <i>et al.</i> , 2019)
	MET409	Phase 2a	(Harrison <i>et al.</i> , 2021)
	EDP305	Phase 2b	NCT04378010
	EYP001	Phase 2a	NCT03812029
PPARs	Elafibranor	Phase 3 terminated	NCT02704403
	Lanifibranor	Phase 2b	(Sven <i>et al.</i> , 2020)
	Saroglitazar	Phase 2	(Gawrieh <i>et al.</i> , 2021)
FGF19/21	Aldafermin	Phase 2b	(Harrison <i>et al.</i> , 2021)
	Pegbelfermin	Phase 2b	(Sanyal <i>et al.</i> , 2019)
	Efruxifermin	Phase 2b	(Harrison <i>et al.</i> , 2021)
THRβ	Resmetirom	Phase 3	(Harrison <i>et al.</i> , 2019)
	VK2809	Phase 2	NCT4173065
ACC	PF-05221304	Phase 2	NCT03248882
	Firsocostat	Phase 2b	(Loomba <i>et al.</i> , 2018)
SCD-1	Aramchol	Phase 3	NCT04104321
GLP1	Semaglutide	Phase 2	(Newsome <i>et al.</i> , 2021)
SGLT2	Empagliflozin	Phase 4	NCT04639414

Abbreviations: ACC= Acetyl CoA carboxylase (ACC); FGF19/21= Fibroblast Growth Factor 19/21; FXRs= Farnesoid X-Activated Receptors; GLP1= Glucagon-like peptide 1; OCA= Obeticholic acid; PPARs= Peroxisome proliferator-activated receptor; SCD-1= Stearoyl coenzyme A desaturase 1; SGLT2= Sodium glucose cotransporter 2; THRβ= Thyroid Hormone Receptor beta.

1.1.4 Alcoholic liver disease

Excessive alcohol consumption currently affects approximately 2.3 billion people in the world (WHO, 2018). Liver disease can be attributed to alcohol consumption in men who consume more than 30 g and women who consume more than 20 g alcohol per day. The first clinical sign of ALD is steatosis that develops in more than 90% of individuals with alcohol abuse over decades (for a review see: Lieber, 2004). Alcoholic hepatitis is a severe acute clinical presentation of ALD and occurs in 30-40% of patients with chronic alcohol abuse (Lefkowitz, 2005). The prevalence of ALD is rising with the highest prevalence in European countries. In 2016, approximately 27% of chronic liver disease related deaths worldwide were attributable to alcohol consumption (Seitz *et al.*, 2018). No specific treatment exists for ALD. Current management includes potential short-term treatment with corticosteroids in severe alcoholic hepatitis and lifestyle recommendations (for a review see: Stickel *et al.*, 2017).

1.2 Progression of chronic liver disease to liver fibrosis

Despite etiology-specific characteristics in terms of early pathophysiology, all major etiologies of chronic liver disease are characterized by the risk of progressing fibrosis and cirrhosis (Kim *et al.*, 2018). Approximately 25-30% of patients with chronic liver disease develop significant fibrosis or cirrhosis over the course of 15-20 years. Given millions of people being affected by chronic liver disease worldwide, this causes an enormous socioeconomic and public health burden (for a review see: Moon *et al.*, 2020). Risk factors for disease progression to cirrhosis include etiology-specific and un-specific factors, such as genetic susceptibility, age, gender and extent of liver-toxic conditions (e.g. alcohol intake and obesity). Moreover, simultaneous presence of multiple liver-damaging conditions (e.g. HBV/HCV co-infections, ALD and NASH) strongly increases the risk for fibrotic disease progression (Bataller and Brenner, 2005). The degree of fibrosis is the main determinant of mortality in patients with chronic liver disease (Kim *et al.*, 2018). In fact, impaired liver function and portal hypertension account for high risk of

complications in patients with liver cirrhosis. Acute decompensation typically manifests with ascites, bleeding events or hepatic encephalopathy and is associated with a high short-term mortality. Moreover, acute-on-chronic liver failure can occur at any stage from compensated to decompensated cirrhosis and has a 28-day mortality of 30% (Moreau *et al.*, 2013; for a review see: Arroyo *et al.*, 2016) (**Figure 2**)

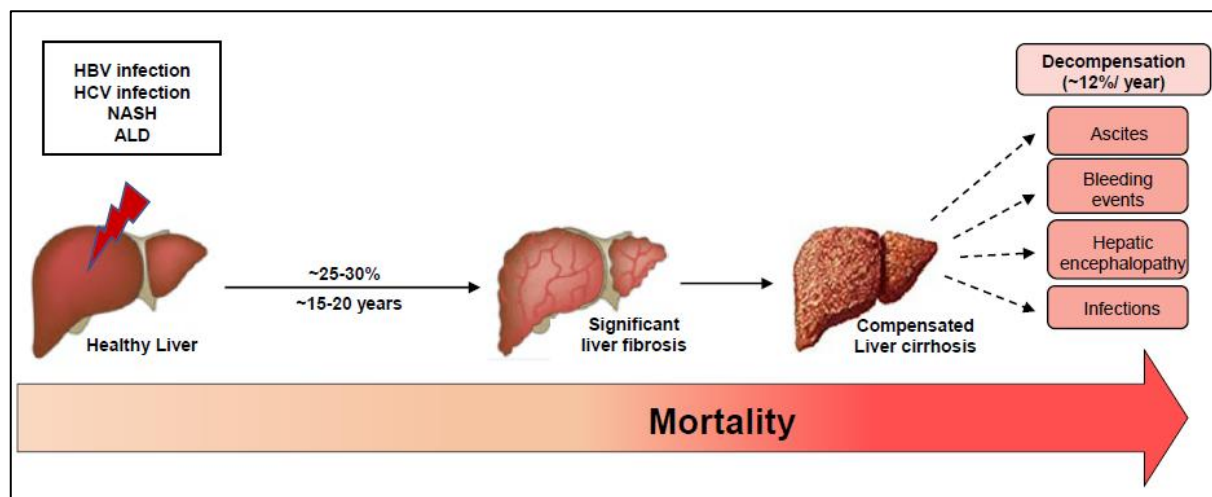


Figure 2. Liver fibrosis is the main determinant of mortality in patients with chronic liver disease. In approximately 25-30% of patients, chronic liver disease progresses to significant liver fibrosis or cirrhosis. Patients with liver cirrhosis have a high risk for complications such as bleeding events, infections and hepatic encephalopathy (Pinzani *et al.*, 2005; Fleming *et al.*, 2010; Nusrat *et al.*, 2014).

1.2.1 Clinical monitoring and diagnosis of liver fibrosis

Due to the high risk of progressing liver fibrosis, regular monitoring including physical examination, ultrasound as well as blood tests is recommended in patients with chronic liver disease. Transient elastography (TE, Fibroscan®) represents the most widely used imaging technique for clinical liver fibrosis assessment in Europe with a good sensitivity and specificity for liver cirrhosis detection (~90%). However, the diagnostic value in the pre-cirrhotic stage of liver fibrosis is significantly lower (sensitivity 70-80%) and TE is limited by frequent uninterpretable results (up to 22% due to e.g. ascites, obesity and narrow intercostal spaces) and confounding factors, such as liver inflammation (Papastergiou *et al.*, 2012). Non-invasive serological biomarkers to assess liver fibrosis include direct (class 1) biomarkers of extracellular matrix (ECM) turnover (e.g. pro-collagen), and indirect (class 2) biomarkers that

are related to liver function and inflammation (e.g. serum alanine aminotransferase (ALT)). Combination of several biomarkers into algorithms, such as the PGAA index, Forns index or ELF test have been validated in independent studies and are already in use in clinical practice (for a review see: Fallatah, 2014). However, serological assessments mostly depict dynamic processes and are therefore recommended for monitoring of disease progression and treatment response but insufficient to predict a specific fibrosis stage at fixed timepoints (Fallatah, 2014). Thus, despite potential mortality and morbidity as well as high inter-observer variability, liver biopsy still remains the gold standard for fibrosis diagnosis and staging. Moreover, histological examination of liver biopsies enables assessment of the severity of necroinflammation and fibrosis according to scoring systems, such as METAVIR and Scheuer Score (for a review see: Pinzani *et al.*, 2005).

1.2.2 Pathophysiology of liver fibrosis

Liver fibrosis is a paradigm of chronic inflammation-associated tissue scarring that can occur in virtually any organ of the human body as the result of a wound healing response to chronic inflammatory injury. Despite diverse primary injuries, fibrogenesis is driven by common mechanisms, including parenchymal cell death, inflammatory responses and activation of collagen-producing mesenchymal cells (Henderson *et al.*, 2020). While fibroblast activation and collagen production can be balanced by scar-resolving mechanisms upon short-term injury, fibrosis is characterized by excessive accumulation of ECM leading to disruption of normal tissue architecture and organ dysfunction (for a review see: Weiskirchen *et al.*, 2019). In liver fibrosis, metabolic stress or chronic viral infection lead to hepatocyte damage and release of damage-associated molecular patterns (DAMPs) that activate hepatic stellate cells (HSC's) and promote recruitment and activation of lymphocytes and macrophages. On the molecular basis, liver fibrogenesis is orchestrated by a complex network of different signaling pathways with particular importance of $\text{TNF}\alpha$ - $\text{NF}\kappa\text{B}$ -, $\text{TGF}\beta$ -, and PDGF-signaling (for a review see: Roehlen *et al.*, 2020) (**Figure 3**).

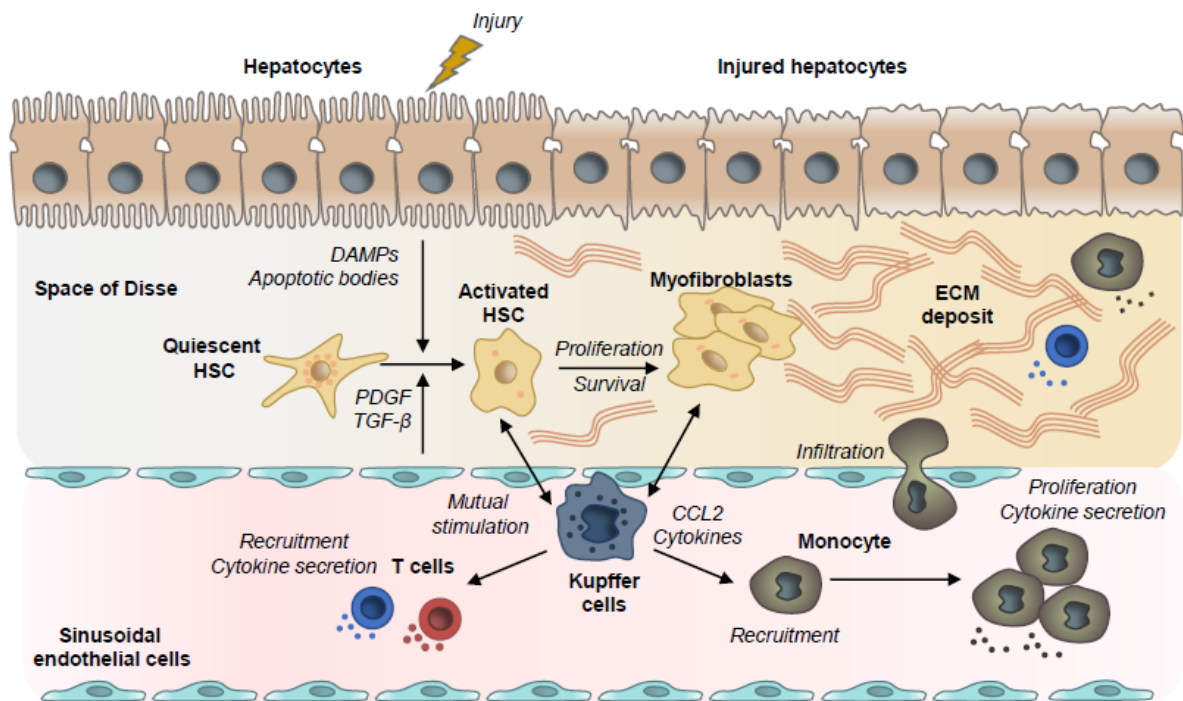


Figure 3. General mechanisms involved in liver fibrogenesis. Figure modified from (Roehlen et al., 2020). Chronic hepatocyte injury causes release of DAMPs and apoptotic bodies that activate HSCs and recruit immune cells. Complex multidirectional interactions of activated HSCs with Kupffer cells as well as innate immune cells promote trans-differentiation into proliferative and ECM producing myofibroblasts. Abbreviations: PDGF = Platelet Derived Growth Factor; TGF- β = Transforming Growth Factor Beta; CCL2 = chemokine (C-C motif) ligand 2.

Trans-differentiation of HSCs into liver myofibroblasts is a well characterized feature of liver fibrosis and the main driver of excessive ECM production and tissue disruption (Schuppan *et al.*, 2018). Interestingly, recent studies indicate specific differentiation states also of other non-parenchymal cells to contribute to fibrosis progression. Thus, Ramachandran *et al.* identified terminally differentiated TREM2⁺CD9⁺ scar-associated macrophages to expand in cirrhotic liver and to promote collagen production in HSC's. Moreover, scar-associated PLVAP⁺ endothelial cells were found to drive liver fibrosis progression by enhancing leukocyte transmigration (Ramachandran *et al.*, 2019). Collectively, these data reveal liver cell plasticity as a new concept in liver fibrogenesis (**Figure 4**).

A detailed overview of pathophysiological mechanisms involved in liver fibrogenesis is provided in the **Supplementary article I** (Roehlen N. *et al.*, Liver fibrosis: Mechanistic Concept and Therapeutic Perspectives, *Cells*, 2020, Apr 3;9(4):875; **Annex**).

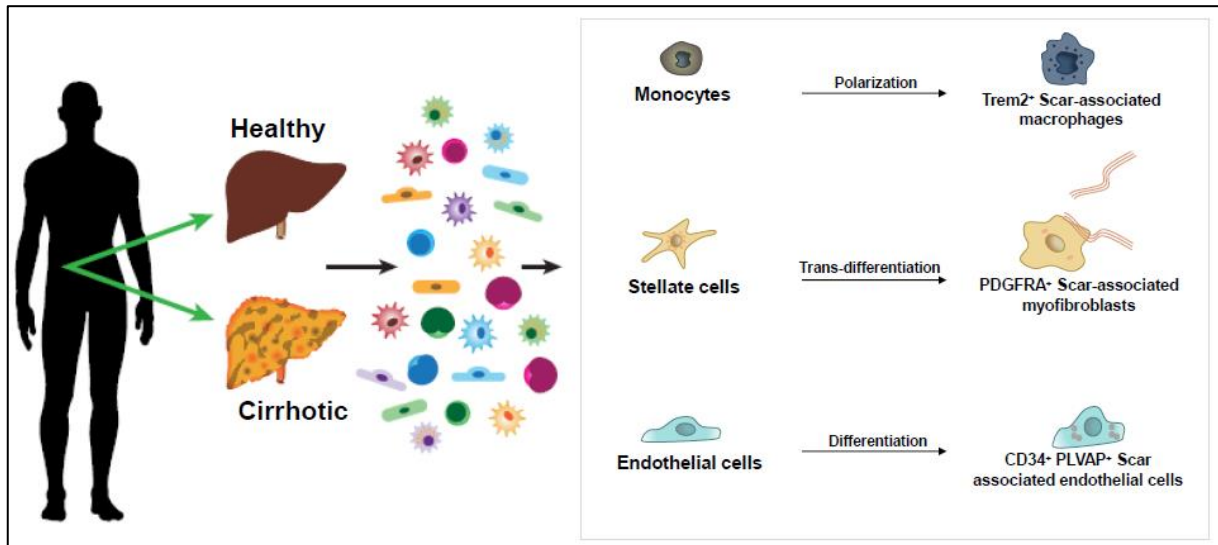


Figure 4: Liver cell plasticity during fibrotic liver disease progression. Figure modified and extended from (Ramachandran et al., 2019). Single cell RNA sequencing on healthy and cirrhotic liver indicated expansion of specific scar-associated phenotypes of non-parenchymal cells in liver fibrosis with distinct pro-fibrogenic functions (Ramachandran et al., 2019).

1.2.3 Fibrosis regression and therapeutic perspectives for patients with liver fibrosis

Fibrosis regression upon viral cure or bariatric surgery indicates that liver fibrosis is (at least partially) reversible (D'Ambrosio *et al.*, 2012; Marcellin *et al.*, 2013; Lassailly *et al.*, 2020). Pathophysiologically, fibrosis regression has been associated with myofibroblast apoptosis and macrophage-executed scar resolution (Fallowfield *et al.*, 2007; Troeger *et al.*, 2012; Campana and Iredale, 2017). However, spontaneous resolution after removal or treatment of the causative injury occurs slowly and infrequently, indicating the urgent need of specific therapies.

Unfortunately, until today, no antifibrotic therapies to treat liver fibrosis have been approved. Consequently, the only curative treatment option for patients with advanced liver fibrosis and cirrhosis is liver transplantation (Parola and Pinzani, 2019). Compounds in pre-clinical and clinical studies can be classified into direct antifibrotics targeting HSC activation or scar-resolving mechanisms as well as indirect antifibrotics that aim to suppress inflammation. While many of these compounds have shown strong antifibrotic effects in preclinical investigations, the effects in clinical trials are less robust (Schuppan *et al.*, 2018).

A detailed overview of therapeutic concepts and current compounds in clinical development is provided in the **Supplementary article I** (Roehlen N. *et al.*, Liver fibrosis: Mechanistic Concept and Therapeutic Perspectives, *Cells*, 2020, Apr 3;9(4):875; **Annex**).

1.3 Progression of chronic liver disease to HCC

With an annual incidence of 1-6%, HCC represents the leading cause of death among patients with liver cirrhosis (Trinchet *et al.*, 2015). Importantly, HCC nearly always arises in the context of chronic liver disease with liver cirrhosis representing the strongest risk factor. Moreover, several socioeconomic factors increase the risk of HCC, including age, male gender, hispanic ethnicity, smoking as well as genetics (for a review see: Llovet *et al.*, 2021). Among different etiologies, chronic HBV infection is still the strongest risk factor for HCC, accounting for 50% of all HCC cases (Akinyemiju *et al.*, 2017). NASH represents the fastest growing etiology of HCC, particularly in western countries (Estes *et al.*, 2018). Of note, overall HCC incidence is strongly increasing and currently the fourth leading cause of cancer-related death in the world (Sung *et al.*, 2021). It is estimated that by 2025 more than 1 million people per year will be affected by liver cancer globally (Sung *et al.*, 2021) (**Figure 5**).

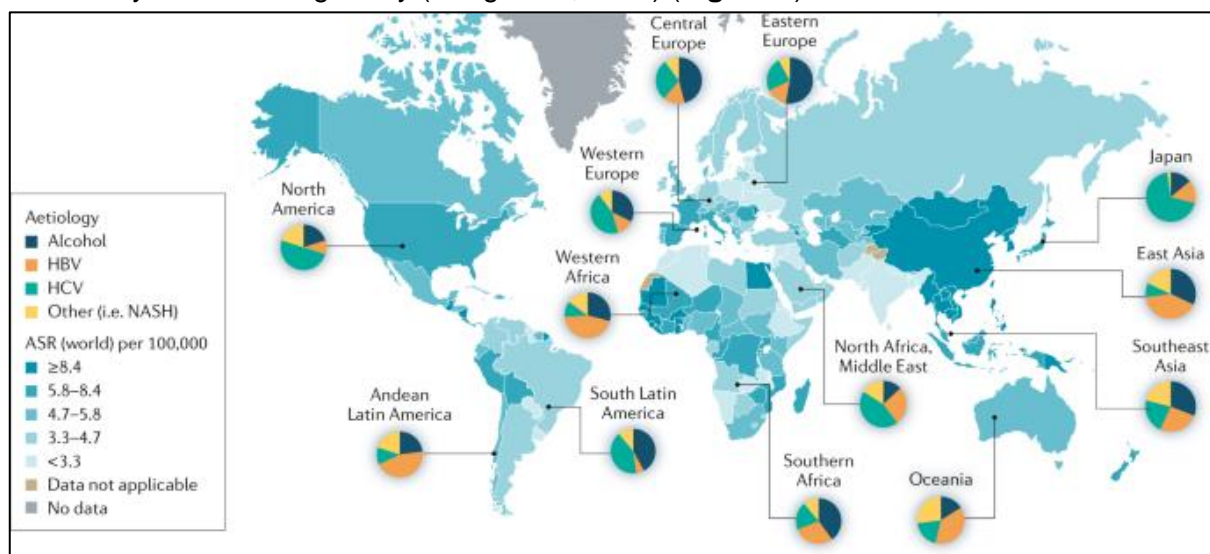


Figure 5. Incidence and etiology of HCC worldwide. Figure modified from (Llovet *et al.*, 2021). Highest incidence of HCC in East Asia with HBV infection as the leading etiology. Alcoholic liver disease and chronic HCV infection represent the most common causes of HCC in Europe. Abbreviations= NASH= Non-alcoholic steatohepatitis.

1.3.1 Clinical diagnosis of HCC

Considering the high risk of HCC development, regular screening by ultrasound imaging as well as serum α -fetoprotein (AFP) measurement is recommended in patients with chronic liver disease (Llovet *et al.*, 2021). However, given poor implementation of serological and ultrasound-based screening especially in developing countries, still 50% of HCC diagnoses are incidental and often associated with advanced stage (Llovet *et al.*, 2021). In patients under regular surveillance, elevated serum AFP levels (>20 ng/ml) and/or lesions > 1 cm in liver ultrasound are indications for subsequent diagnostic evaluation by quadruple-phase CT or dynamic contrast-enhanced MRI (Marrero *et al.*, 2018). The radiological characteristics of arterial enhancement and delayed washout have a sensitivity and specificity of up to 90%, justifying diagnosis without histological confirmation (Marrero *et al.*, 2018; van der Pol *et al.*, 2019). In case of atypical appearance by imaging but persisting clinical suspicion, liver biopsy or alternative contrast-enhanced imaging techniques are recommended (Marrero *et al.*, 2018).

1.3.2 Pathophysiology of HCC

Hepatocarcinogenesis describes a complex multi-stage process influenced by multiple cellular drivers and diverse oncogenic pathways. In chronically diseased livers, inflammation, oxidative stress and parenchymal cell damage promote chronic error-prone repair processes that lead to hepatocyte proliferation, somatic mutations and finally the development of dysplastic nodules. Low-grade dysplastic nodules (LGDNs) can transform to high-grade dysplastic nodules (HGDNs) and early HCCs within a mean time course of five to seven years (Marquardt *et al.*, 2015). The molecular events determining malignant transformation are only partially understood. Large-scale transcriptomic characterizations of dysplastic nodules and early HCCs revealed mutations affecting telomerase maintenance (telomerase reverse transcriptase = TERT), chromatin modifiers and inflammatory pathways to represent common early genetic events in the sequential evolution of HCC (Marquardt *et al.*, 2015). Thus, TERT-activations are

believed to account for delimited hepatocyte proliferation and are found in ~6% of LGDNs, ~20% of HGDNs and up to 61% of early HCCs (Nault *et al.*, 2014). Cumulative genetic alterations in the course of HCC development finally cause dysregulation of key oncogenic pathways, such as PI3K/AKT, Wnt- β -catenin and IL6/JAK/STAT3 signaling, whose specific contributions characterize the genomic heterogeneity of HCC (Marquardt *et al.*, 2015). Transcriptomic profiling of 243 liver tumors revealed eleven recurrently altered pathways (Figure 6) (Schulze *et al.*, 2015). Some altered driver genes were found to be characteristic for specific etiologies, such as CTNNB1 (alcohol liver disease) and TP53 (chronic HBV infection). In contrast HCC's related to chronic HCV infection and NASH show strong transcriptomic heterogeneity (Schulze *et al.*, 2015).

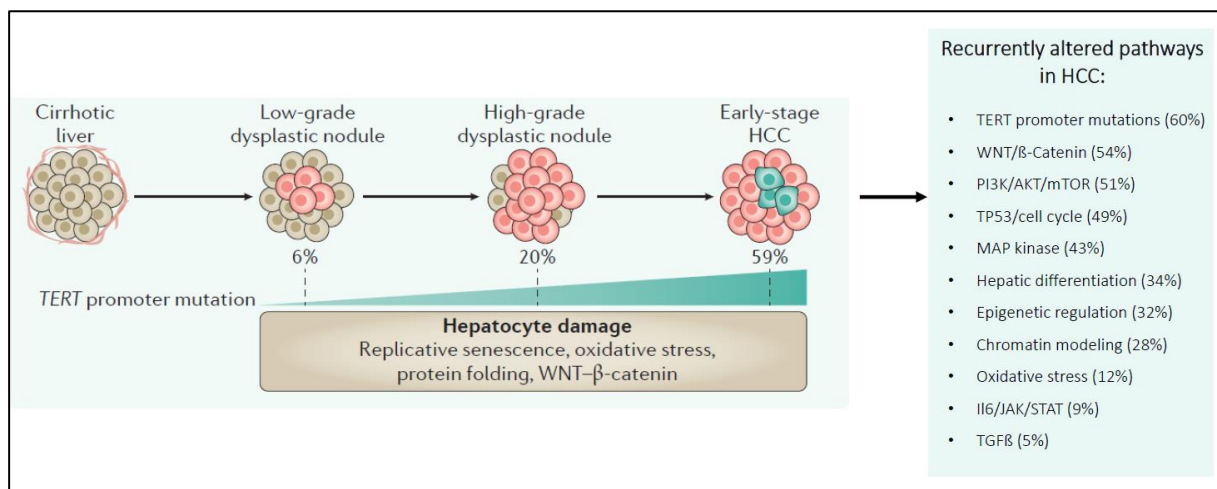


Figure 6. Sequential evolution of HCC in cirrhotic liver. Figure modified and extended from (Llovet *et al.*, 2016). Hepatocyte damage during chronic liver injury induces development of dysplastic nodules that progress to early HCC's within 5 to 7 years. This step wise malignant transformation is associated with increasing frequency of TERT promoter mutations. Accumulating genetic alterations during malignant transformation leads to aberrant activation of oncogenic pathways most frequently related to Wnt/ β -catenin and PI3K/AKT signaling (Schulze *et al.*, 2015). Abbreviations: HCC= Hepatocellular carcinoma.

HCC is characterized by a broad histological pattern, ranging from well-differentiated HCC to poorly differentiated HCC and tumors showing intermediate phenotypes between hepatocytes and cholangiocytes (so called mixed HCC-iCCA) (Marquardt *et al.*, 2015). The phenotypic heterogeneity of liver cancer is believed to be influenced by the cellular origin of the malignant transformation. Two main cell types of the liver parenchyma have been suggested as potential cellular origins of HCC: hepatocytes and adult liver progenitor cells (Yamashita and Wang,

2013;Sia *et al.*, 2017). Thus, HCCs with mature hepatocyte gene signatures have been described to develop via malignant transformation of mature hepatocytes. HCCs with a stem-cell like or intermediate (so called mixed HCC-CCAs) phenotype on the other hand have been attributed to de-differentiation of hepatocytes into precursor cells or direct transformation of adult liver progenitor cells (for a review see: Sia *et al.*, 2017) (**Figure 7**). Of note, lineage tracing methods in mice could yet only validate hepatocytes as cellular origins of HCC (Shin *et al.*, 2016). However, reports of hepatocyte de-differentiation during chronic liver injury (Nishikawa *et al.*, 2015) and phenotypic resemblance of HCC cells with liver progenitor cells (Aizarani *et al.*, 2019) support the recognition of hepatocyte progenitor cells as cancer cell origins in the field.

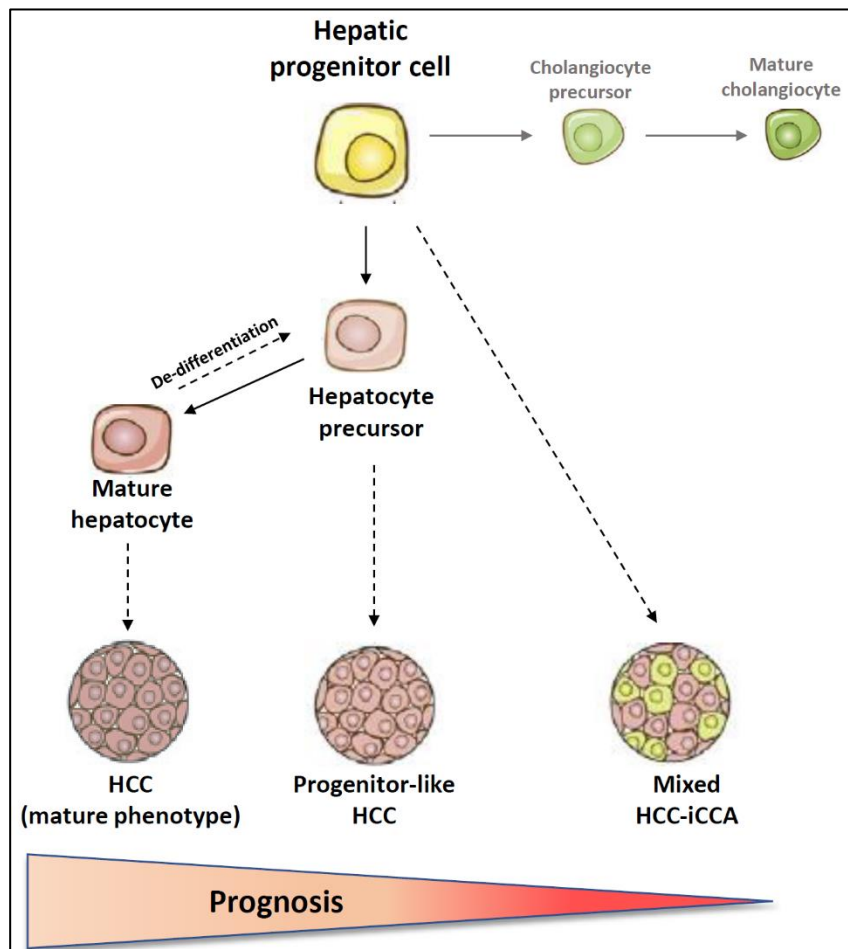


Figure 7. Model of different cancer cell origins in HCC. HCC's with a mature hepatocyte phenotype are usually associated with a better prognosis than progenitor-like HCC's. Mixed-iCCAs are highly aggressive tumors with poor prognosis. Image modified from (Sia *et al.*, 2017). Abbreviations: HCC= Hepatocellular carcinoma; iCCA= intrahepatic cholangiocarcinoma.

1.3.3 Role of the liver microenvironment in liver carcinogenesis

More than 90% of HCCs develop under conditions of chronic inflammation and fibrosis (Llovet *et al.*, 2021). Accordingly, the stromal and immunogenic microenvironment has been characterized to play a tremendous role in initiation and progression of hepatocarcinogenesis. In fact, crosstalk between parenchymal and non-parenchymal cells, alterations of the ECM and immune cell dysfunction contribute to tumorigenesis (Tahmasebi Birgani and Carloni, 2017). The interaction between cancer and immune cells have been summarized under the term “immunoediting”, that is composed of three phases: elimination, equilibrium and escape. In the initial phase, tumor cells, which express immunogenic neoantigens, are recognized and eliminated by the immune system. During the equilibrium phase, tumor cells acquire features that allow immune evasion. Finally, prolonged immune activation and cancer cell-derived growth factors contribute to the development of an immune-tolerant, pro-tumorigenic microenvironment (Craig *et al.*, 2020). Immune cells can hereby accelerate hepatocarcinogenesis and tumor aggressiveness by secreting TNF α , IL-6 and lymphotoxin- α (Llovet *et al.*, 2021) (**Figure 8**).

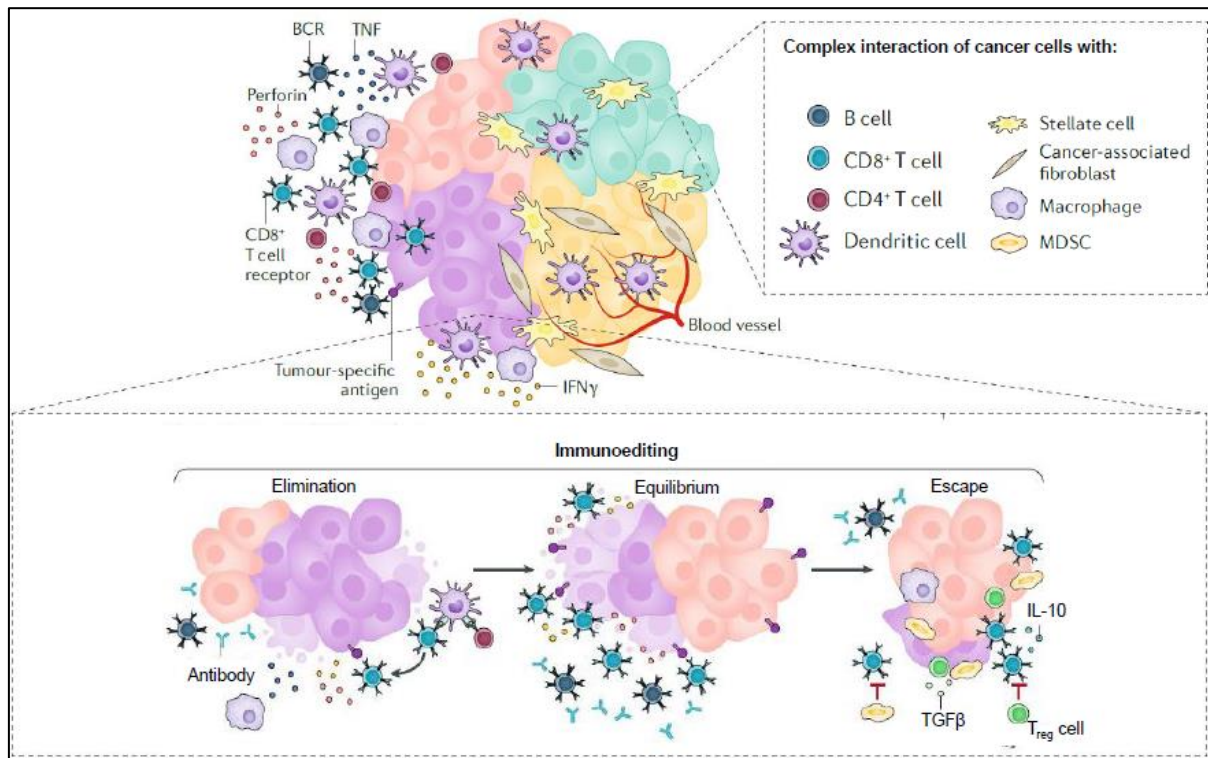


Figure 8. Complex interaction of cancer cells with its immunogenic microenvironment. Figure modified from (Craig *et al.*, 2020). The term “immunoediting” describes the interaction between cancer cells and immune cells that lead to establishment of an immuno-tolerant, pro-tumorigenic microenvironment. **Abbreviations:** BCR= B cell receptor; IL-10= Interleukin 10; MDSC= myeloid-derived suppressor cell; TGFβ= Transforming Growth factor beta; TNF= Tumor necrosis factor; T_{reg} cell= Regulatory T cell.

Besides immune cells, the tumor microenvironment is characterized by enriched populations of stromal cells and increased ECM deposition. Cancer-associated fibroblasts (CAFs) support cancer cell survival, angiogenesis and invasion by releasing cytokines and growth factors, such as TGFβ, vascular endothelial growth factor (VEGF) and IL6. In addition, CAF's contribute to an immunosuppressive microenvironment by promoting M2 polarization of cancer-associated macrophages (Baglieri *et al.*, 2019) that facilitate cancer cell migration and invasion by inducing ECM remodeling (Deng *et al.*, 2021). Finally, abnormal ECM deposition and scarring can promote cancer cell invasion via mechano-signaling pathways and contribute to development of a hypoxic pro-angiogenic milieu (for a review see: Petrova *et al.*, 2018) (**Figure 9**).

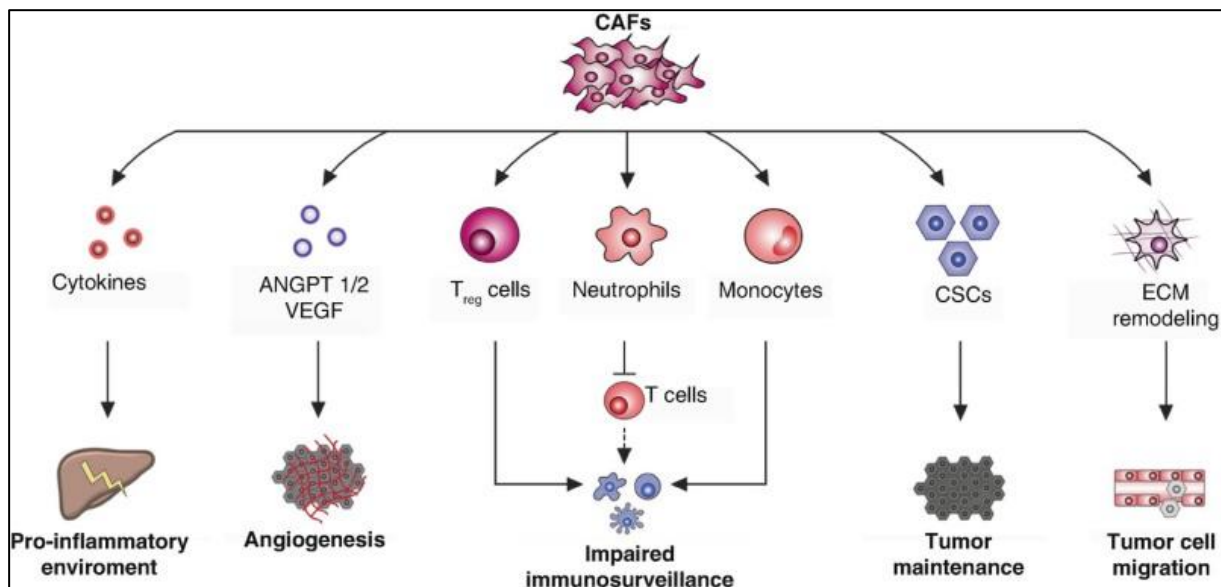


Figure 9. Cancer-associated fibroblasts of the tumor microenvironment promote hepatocarcinogenesis, tumor progression and treatment resistance. Figure derived from (Saviano *et al.*, 2019). CAFs interact with immune cells and reduce immune surveillance. By paracrine interactions as well as secretion of angiogenic factors and prooncogenic cytokines CAFs promote cancer cell proliferation and drive tumor angiogenesis. CAFs are also reported to recruit cancer stem cells, hereby affecting tumor maintenance, heterogeneity and treatment resistance. By ECM remodeling, CAFs promote HCC cancer cell invasion and migration. **Abbreviations:** ANGPT 1/2= Angiopoietin 1/2; CAFs= Cancer-associated fibroblasts; CSCs= Cancer Stem Cells; ECM= Extracellular Matrix; Treg cells= regulatory T cells; VEGF= Vascular Growth Factor.

The current concepts on the role of the tumor microenvironment in hepatocarcinogenesis are discussed in detail in the **Supplementary article II** (Saviano A., Roehlen N. *et al.*: Stromal and Immune drivers of Hepatocellular Carcinoma. 2019 Aug 6. In: Hoshida Y, editor. Hepatocellular Carcinoma: Translational Precision Medicine Approaches. Cham (CH): Humana Press; 2019. Chapter 15; **Annex**).

1.3.4 Role of epithelial-mesenchymal transition in HCC progression

Epithelial-to-mesenchymal transition (EMT) describes a reversible process, by which epithelial cell types gradually develop mesenchymal characteristics leading to higher motility and invasive properties (for a review see: Nieto *et al.*, 2016). EMT occurs physiologically during embryonic development and wound healing but also represents a pathological mechanism of cancer cells, that promotes tumor aggressivity. In HCC, hepatocytes and cancer cells can undergo epithelial reprogramming due to genetic and epigenetic changes that activate

transcription factors of the SNAIL, Twist and ZEB family. TGF β -signaling represents the strongest activator of EMT (Giannelli *et al.*, 2016). Considering that TGF β is stored or activated in the fibrotic niche (Roehlen *et al.*, 2020), the stromal microenvironment plays a tremendous functional role in EMT.

Typical indicators of EMT in the liver are the downregulation of E-cadherin and simultaneous upregulation of mesenchymal markers such as fibronectin and vimentin on hepatocytes (Giannelli *et al.*, 2016). EMT markers have been reported to be expressed in 56% of HCC patients (Yang *et al.*, 2009). In line with the associated molecular phenotype of more migratory and invasive cancer cells, several of these markers correlate with tumor dissemination and shorter patients' survival (Kim *et al.*, 2010; Mima *et al.*, 2013; Yamada *et al.*, 2014; Zhai *et al.*, 2014). The association of EMT with cancer stemness and chemoresistance further substantiated numerous studies investigating EMT as a target for HCC therapy (**Figure 10**).

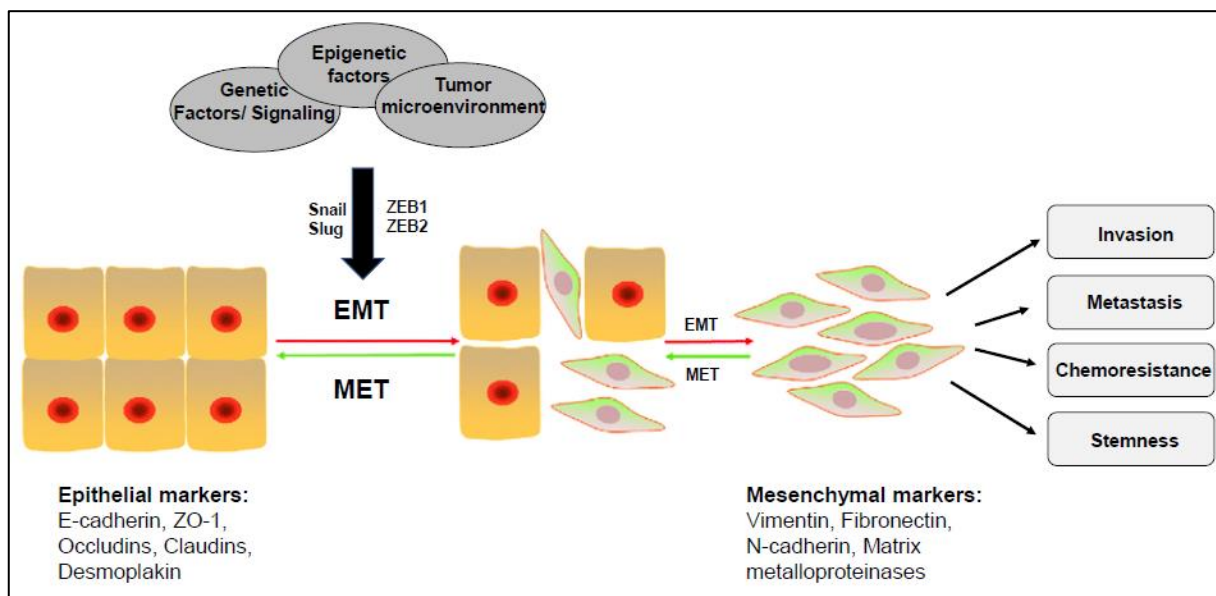


Figure 10. The role of EMT transition in cancer. Figure adapted and extended from (Song *et al.*, 2019). Epigenetic and genetic changes as well as crosstalk of cancer cells with their microenvironment lead to enhanced activation of signaling pathways such as TGF β - or Wnt- signaling that promotes EMT via upregulation of the transcription factors Snail, Slug, Zeb1 or Zeb2. Cells undergoing EMT show decreased expression of epithelial markers and upregulated expression of mesenchymal markers such as Vimentin or Fibronectin. The process of EMT is hereby associated with the development of a migratory and invasive cell phenotype that correlates with metastasis, tumor invasion, cancer stemness and chemoresistance in patients. Abbreviations: EMT= Epithelial-mesenchymal Transition; MET= Mesenchymal-epithelial transition; ZO-1= Zonula occludens.

1.3.5 Molecular subclassification of HCC

The complex and multi-factorial pathogenesis of HCC led to the establishment of a molecular and immune tumor subclassification (for a review see: Llovet *et al.*, 2021). Tumors can hereby be divided into two major molecular groups that are either characterized by poor differentiation and aggressive behavior or moderate to well differentiation and better prognosis. The poor-prognosis “*Proliferation class*” is typically associated with chronic HBV infection and often shows histological features of a progenitor or mixed phenotype (e.g. epithelial cell adhesion molecule (EPCAM) or AFP expression) and activated Wnt-TGF β signaling. The “*Non-proliferation class*” is characterized by a higher chromosomal stability, frequent TERT promoter mutations and CTNNB1 mutations. Each of these two main subclasses can be further subclassified according to immunological features (Llovet *et al.*, 2021)(**Figure 11**).

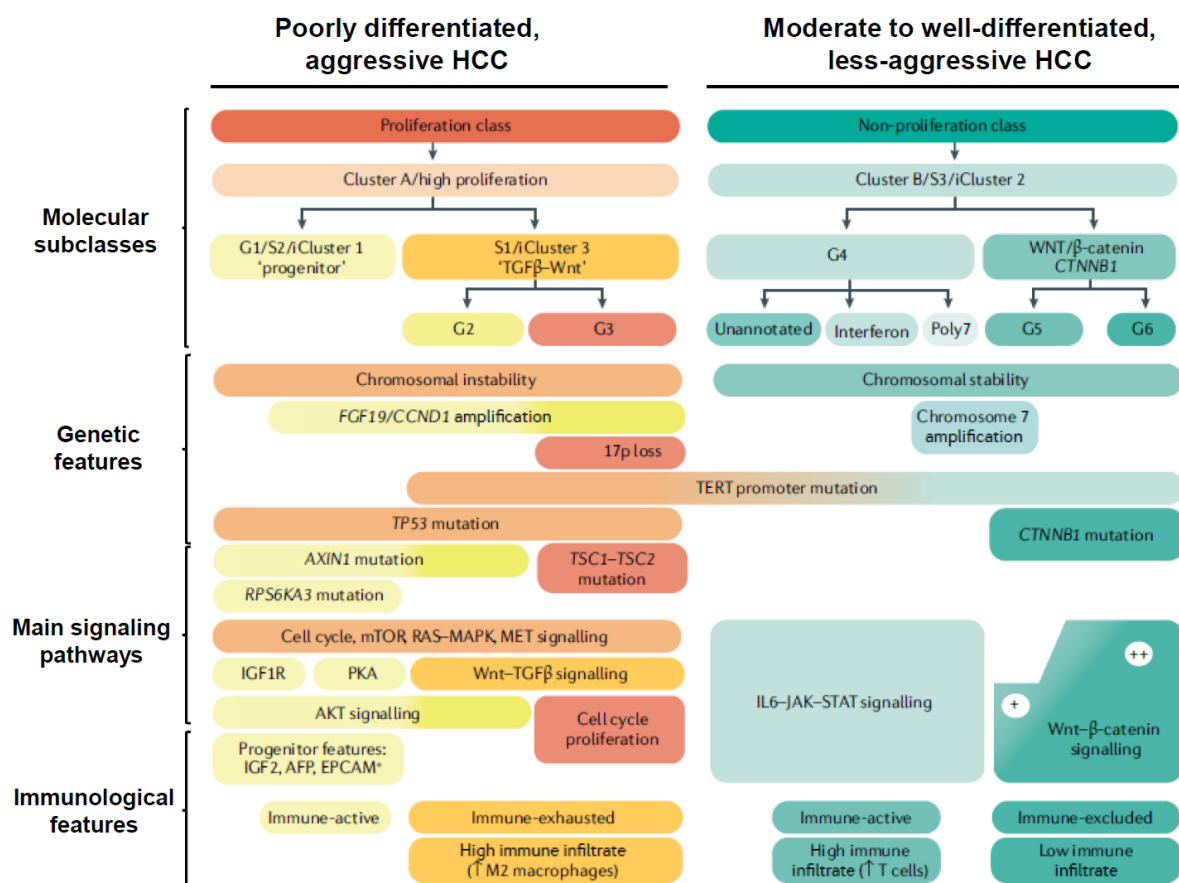


Figure 11. Molecular and immune classification of HCC. Molecular subclasses Cluster A/B; Proliferating/ non-proliferating; G1-6 and S1-3 are described elsewhere (Lee *et al.*, 2006; Boyault *et al.*, 2007; Chiang *et al.*, 2008; Hoshida *et al.*, 2009; Cancer Genome Atlas Research Network, 2017). Figure modified from (Llovet *et al.*, 2021).

Approximately 20% of HCC's are immune-active and show enriched proportions of T helper (CD4⁺)- and cytotoxic T (CD8⁺) cells. Immune-exhausted tumors show CD8⁺ T cell exhaustion, while immune-excluded tumors are characterized by an increase of Treg cells and paucity of T-cell infiltrates (Llovet *et al.*, 2021). Interestingly, immune-excluded HCC tumors have been recently associated with therapeutic response to immune checkpoint inhibitors (Ruiz de Galarreta *et al.*, 2019). The molecular subclassification of HCC has further stimulated research on molecular therapies specifically targeting features of subclasses (Goossens *et al.*, 2015). Thus, although yet not applied in clinical therapeutic management, the molecular and immune subclassification of HCC may guide therapeutic decision-making in the future.

1.3.6 Management of HCC and therapeutic perspectives

Therapeutic options for HCC strongly depend on the patient's overall health status, the grade of fibrosis and the tumor's size and have therefore led to the implementation of the Barcelona clinic liver cancer (BCLC) stage system in therapeutic management strategies. Briefly, patients with small tumors and preserved liver function (BCLC0 and A) are recommended to receive local ablation, resection or liver transplantation, while patients with intermediate-stage HCC (BCLC B) are candidates for chemoembolization (TACE). Following a decade of sorafenib therapy representing the only available systemic treatment for patient with advanced disease (BCLC C) (Llovet *et al.*, 2008), recently new compounds with comparable or better efficacy and safety have been developed (Kudo *et al.*, 2018; Finn *et al.*, 2020). Currently available HCC therapeutics can be classified into two main subclasses: the multi kinase inhibitors (MKIs) with primarily anti-angiogenic effects (e.g. sorafenib or Lenvatinib) and the checkpoint inhibitors (e.g. atezolizumab and nivolumab). Promising results of combining molecularly targeted therapies with immunotherapy to augment tumor-responsiveness in several human solid cancer types (Zappasodi *et al.*, 2018) have further substantiated several ongoing phase III clinical trials of immune checkpoint blockade-based combination therapies for advanced HCC. These include the COSMIC-312 study (Lenvatinib+Pembrolizumab, NCT03755791) (Kelley

et al., 2020) and the LEAP program (Cabozantinib+Atezolizumab, NCT03713593) (Taylor *et al.*, 2021) that are expected to be completed in December 2021 and May 2022, respectively (Figure 12).

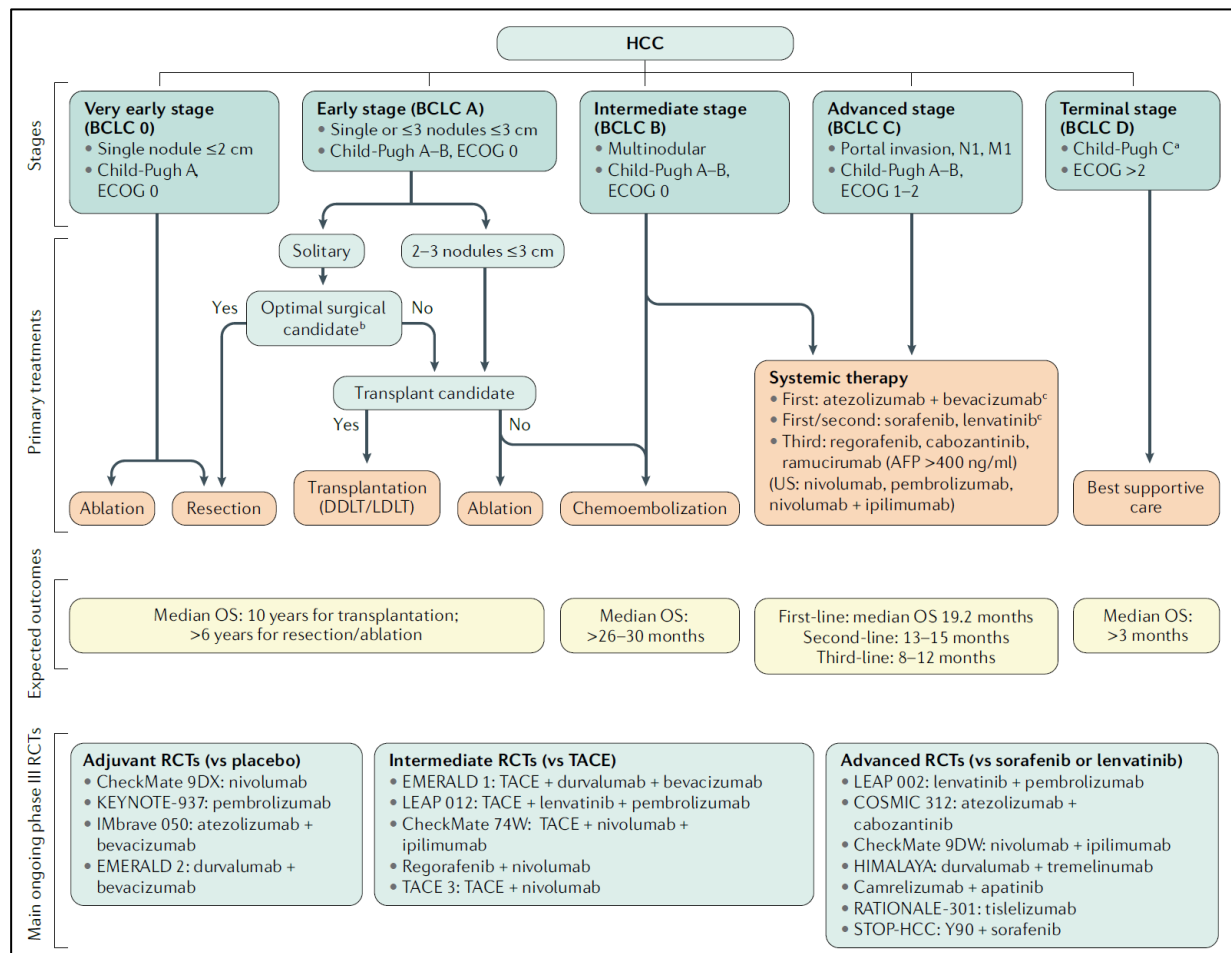


Figure 12. Therapeutic management of HCC according to BCLC stage. Figure derived from (Llovet *et al.*, 2021). Abbreviations: AFP= alpha fetoprotein; BCLC= Barcelona Clinic Liver Cancer; DDLT= Deceased Donor Liver Transplant; ECOG= Eastern Cooperative Oncology Group; HCC= Hepatocellular carcinoma; LDLT= Live Donor Liver Transplant; OS= Overall survival; RTCs= Randomized Controlled Trials; TACE= Transarterial chemoembolization; US= United States.

Despite major improvements in therapeutic management of HCC within the last years, HCC survival under treatment still remains poor. In fact, recurrence of HCC following surgical intervention is a frequent event, occurring in up to 70% of the patients after liver resection and in 10-15% after liver transplantation within 5 years (Imamura, 2003; Roayaie *et al.*, 2013; Llovet *et al.*, 2021). Early HCC recurrence within the first 2 years after surgical resection typically results from micrometastases, while tumor recurrence at later timepoints usually results from de-novo HCC development in a pre-carcinogenic microenvironment (Imamura, 2003). In

patients with advanced HCC, the current preferred first-line therapy, a combination of atezolizumab and bevacizumab, improves the 12-month survival only to 67.2 % compared to 54.6 % under sorafenib treatment (Finn *et al.*, 2020). Moreover, only 5.5 % of the patients show complete remission under atezolizumab and bevacizumab treatment (Finn *et al.*, 2020). Thus, new therapeutic strategies and novel targets for treatment of HCC are urgently needed.

1.4 Tight junction proteins in chronic liver disease and HCC

Tight junctions are intercellular adhesion complexes that regulate paracellular diffusion and maintain apicobasal polarization. Beyond the initial model as simple rigid diffusion barriers, multiple studies in the recent years revealed tight junctions to be highly dynamic and to associate with complex cellular functions including cell-cell or cell-matrix interactions as well as intracellular signaling (Zihni *et al.*, 2016). Moreover, classical components of tight junctions, such as Claudin (CLDN) and Zonula occludens (ZO) proteins have been shown to be also expressed outside of tight junctions and to be involved in the pathogenesis of chronic inflammatory, infectious and malignant diseases (for a review see: Zeisel *et al.*, 2019). The association of tight junction proteins with benign and malignant liver diseases was reviewed in detail in the **Supplementary article III** (Roehlen N. *et al.*: Tight Junction Proteins and the Biology of Hepatobiliary Disease, Int J Mol Sci. 2020 Jan 28;21(3):825; **Annex**).

1.4.1 CLDN1 – Expression pattern and functional role

Among all tight junction proteins, most functional data regarding the involvement in disease biology and cancer exist for CLDN1 (Zeisel *et al.*, 2019;Bhat *et al.*, 2020), the first identified member of the claudin family of tight junction proteins (Furuse *et al.*, 2002). With a molecular

weight of 23 kDa CLDN1 consists of four transmembrane domains, two extracellular loops and intracellularly oriented N and C termini (Tsukita and Furuse, 2000) (**Figure 13**).

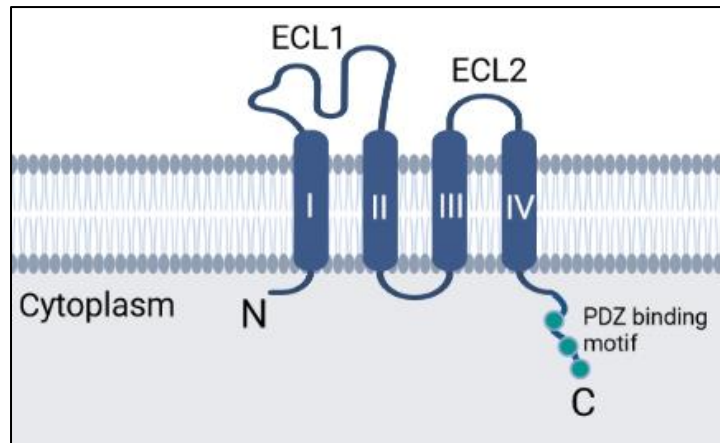


Figure 13. Model of CLDN1 structure. CLDN1 is a tetraspanin with 2 extracellular loops and intracellularly oriented N- and C termini. Image created with BioRender.com. Abbreviations: ECL1 =Extracellular loop 1; ECL2 Extracellular loop 2.

CLDN1 is highly expressed in epithelial cells of most organs, especially the skin, the liver and the lung. The major fraction of CLDN1 is expressed at the apical membrane of epithelial cells in tight junctions. At this localization, CLDN1 has been well characterized to control paracellular permeability, hereby contributing to cell polarity and maintenance of the epithelial barrier (Tsukita and Furuse, 2000; Furuse *et al.*, 2002). However, a minor pool of CLDN1 can also be detected non-junctionally at the basolateral membrane of epithelial cells in the liver, the lung or the kidney (Reynolds *et al.*, 2008; Mee *et al.*, 2009; Hagen, 2017). This is consistent with reports of CLDN1 expression in non-epithelial cells, such as macrophages and HLMFs, that do not form tight junctions (Van den Bossche *et al.*, 2012; Aoudjehane *et al.*, 2015). The physiological function of non-junctionally expressed CLDNs is only poorly understood. However, several studies indicate a role of non-junctional CLDNs in cell-cell and cell-matrix interactions. Interestingly, non-junctional CLDN1 was found to interact with integrins at focal adhesion complexes and to activate MAPK signaling in intestinal cells (Hagen, 2017). In line, in colon cancer cells basolateral expressed CLDN1 was found to form a complex with epithelial cell adhesion molecule (EPCAM) (Wu *et al.*, 2013), a transmembrane glycoprotein characterized to orchestrate cellular signaling by interaction with growth receptors and integrins (Chen *et al.*, 2020; Yang *et al.*, 2020). Further indicating a functional role in ECM

remodeling, non-junctional CLDN1 has been described to promote activation of matrix metalloproteinase 2 (MMP-2) in melanoma cells (Leotlela *et al.*, 2007) (**Figure 14**). Taking together, these data suggest non-junctional CLDN1 to integrate and translate bi-directional signals from cell-cell and cell-matrix interactions.

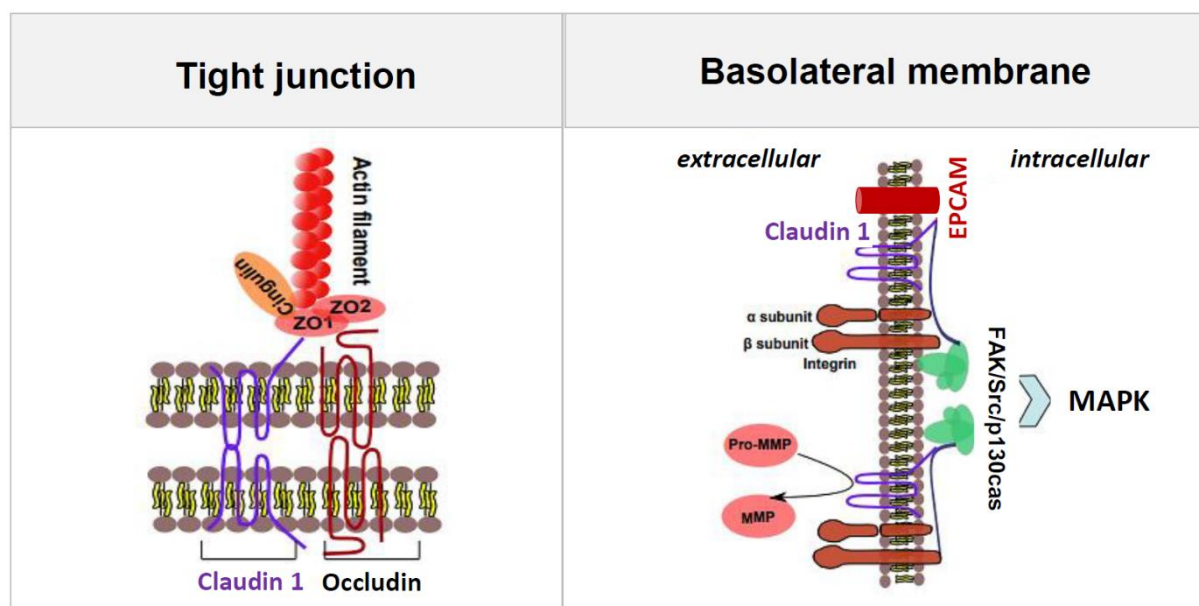


Figure 14. CLDN1 expression on epithelial cells and current concept of interactions. Figure modified from (Roehlen *et al.*, 2020). CLDN1 is mainly expressed at the apical membrane of epithelial cells, where it forms tight junctions between neighboring cells and controls paracellular permeability and epithelial polarity. Non-junctionally expressed CLDN1 at the basolateral membrane of epithelial cells has been described to form complexes with membrane receptors such as integrins or epithelial-cell adhesion molecule (EPCAM) and to impact on intracellular signaling such as MAPK signaling. Moreover, CLDN1 has been described to recruit and activate pro-MMPs. Abbreviations: EPCAM= epithelial cell adhesion molecule; FAK= Focal adhesion kinase; MAPK= Mitogen-activated protein kinase; pro-MMP= pro-Matrix metalloproteinase; ZO1/2= Zonula occludens 1/2.

Numerous studies indicate a functional role of CLDN1 in human disease. Implications in benign, inflammatory diseases are mostly related to the functional role of CLDN1 for epithelial polarity at junctional localization. For instance, CLDN1 has been shown to be downregulated in atopic dermatitis, potentially contributing to an impaired skin barrier function (De Benedetto *et al.*, 2011). Similarly, CLDN1 is downregulated and delocalized in eosinophilic oesophagitis (Masterson *et al.*, 2019). CLDN1 expression have further been reported to be perturbed in numerous human cancer entities (Bhat *et al.*, 2020). While most studies report an overexpression of CLDN1 in cancer entities, such as colon and lung cancer, conversely decreased CLDN1 expression has been associated with cancer progression and metastasis in prostate cancer (Seo *et al.*, 2010) and estrogen receptor positive (ER⁺) breast cancer

(Blanchard *et al.*, 2009). Beyond up- and downregulation, nuclear and cytoplasmic delocalization of CLDN1 has been reported in ER⁻ basal-like breast cancer (Blanchard *et al.*, 2009), colorectal cancer (Dhawan *et al.*, 2005) as well as melanoma (French *et al.*, 2009) (Table 2).

Table 2. Reported perturbations of CLDN1 expression in human diseases.

Disease	CLDN1 expression	Clinical associations	Reference
Atopic dermatitis	Downregulated	-	(De Benedetto <i>et al.</i> , 2011)
Eosinophilic oesophagitis	Downregulated	-	(Masterson <i>et al.</i> , 2019)
Melanoma	Upregulated, cytoplasmic delocalization	-	(Leotlela <i>et al.</i> , 2007; French <i>et al.</i> 2009)
Oral Squamous Cell Carcinoma	Upregulated	-	(Oku <i>et al.</i> , 2006)
Prostate Cancer	Downregulated	Correlation of decreased expression with cancer progression and poor survival	(Vare <i>et al.</i> , 2008; Seo <i>et al.</i> , 2010)
Lung Cancer	Downregulated in lung adenocarcinoma Upregulated in lung squamous cell carcinoma	Correlation of decreased expression with poor survival in lung adenocarcinoma	(Paschoud <i>et al.</i> , 2007; Eftang <i>et al.</i> , 2013)
ER+ Breast Cancer	Downregulated in ER+ breast cancer, upregulated and delocalized in ER- breast cancer	Association of high CLDN1 expression with the basal-like subtype of breast cancer, that shows poor outcome	(Blanchard <i>et al.</i> , 2009)
Thyroid Cancer	Upregulated	-	(Nemeth <i>et al.</i> , 2010; Zwanziger <i>et al.</i> , 2015)
Ovarian Cancer	Upregulated	Association of CLDN1 overexpression with poor patients' survival	(Kleinberg <i>et al.</i> , 2008)
Colon Cancer	Upregulated, cytoplasmic delocalization	Low CLDN1 expression is associated poorer overall- and disease-free survival	(Dhawan <i>et al.</i> , 2005; Kinugasa <i>et al.</i> , 2010; Zuo <i>et al.</i> , 2020)
Gastric Cancer	Upregulated	Association of CLDN1 overexpression with poor patients' survival	(Eftang <i>et al.</i> , 2013)
Pancreatic Cancer	Upregulated	Association of CLDN1 expression with ductal differentiation of pancreatic tumors	(Tsukahara <i>et al.</i> , 2005; Borka, 2009)
HCC	Upregulated	Loss of CLDN1 expression in poorly differentiated HCC	(Reynolds <i>et al.</i> , 2008; Holczbauer <i>et al.</i> , 2014; Zhou <i>et al.</i> , 2015)

The description of CLDN1 as both a tumor suppressor and promoter in different cancer types suggests a complex functional role in human carcinogenesis (Bhat *et al.*, 2020). Mechanistic studies hereby indicate CLDN1 to be especially implicated in cell survival and cell differentiation by interacting with various different signaling cascades (Table 3). In colon cancer cells CLDN1 overexpression was found to promote Src-, PI3K/AKT- and NOTCH signaling

(Singh *et al.*, 2011; Singh *et al.*, 2012; Pope *et al.*, 2014). Moreover, CLDN1 has been reported to interact with TNF α and Wnt/ β -catenin signaling in a bidirectional way. While TNF α and Wnt/ β -catenin pathway activation increases CLDN1 expression in different epithelial cancer cells, CLDN1 overexpression in turn mediates downstream effects on inflammation, cell proliferation and apoptosis. Of note, functionality of CLDN1 for cellular signaling have yet only been reported for epithelial cells. Due to the technical challenge to investigate signaling networks specific to CLDN1 subcellular localization, the respective contributions of the different cellular expression sites remain elusive.

Table 3. Reported implications of CLDN1 in intracellular cellular signaling cascades in human disease.

Signaling pathway	Disease context	Proposed interaction	Affect cell function	Reference
c-Abl-PKC	Liver cancer	CLDN1 overexpression increases c-Abl kinase activity	EMT, invasion	(Yoon <i>et al.</i> , 2010; Suh <i>et al.</i> , 2013)
PKC	Follicular thyroid cancer	CLDN1 downregulation is associated with decreased PKC activation	Cell proliferation, migration, invasion	(Zwanziger <i>et al.</i> , 2015)
Src-AKT	Colon cancer	CLDN1 interacts with Src and activates AKT signaling	Apoptosis	(Singh <i>et al.</i> , 2011; Singh <i>et al.</i> , 2012)
	Gastric cancer	CLDN1 overexpression activates Src and Akt signaling	Anoikis	(Huang <i>et al.</i> , 2015)
PI3K/AKT	Colon cancer	CLDN1 overexpression upregulates Akt phosphorylation	EMT	(Singh <i>et al.</i> , 2011)
Notch	Inflammatory bowel disease/Colon cancer	CLDN1 overexpression upregulates Notch signaling	Inflammation, Cell differentiation, proliferation	(Pope <i>et al.</i> , 2014)
	Lung cancer	CLDN1 knockdown suppresses Notch signaling	EMT, migration	(Lv <i>et al.</i> , 2017)
TNFα	Colon cancer, breast cancer, lung cancer and pancreatic cancer	CLDN1 expression \leftrightarrow TNF α pathway activation	EMT, invasion/migration, cell proliferation	(Kondo <i>et al.</i> , 2008; Liu <i>et al.</i> , 2012; Shiozaki <i>et al.</i> , 2012; Bhat <i>et al.</i> , 2016)
Wnt/β-catenin	Colon cancer	CLDN1 expression \leftrightarrow Wnt/ β -catenin pathway activation	EMT	(Miwa <i>et al.</i> , 2001; Singh <i>et al.</i> , 2011)
	Gastric cancer	CLDN1 knockdown decreases membranous β -catenin expression	Cell-cell adhesion, Anoikis	(Huang <i>et al.</i> , 2015)

1.4.2 Role of CLDN1 in chronic liver disease and HCC – state of the art

Several studies have reported an involvement of CLDN1 in liver disease and HCC. Loss of CLDN1 function in the liver and the skin due to congenital *CLDN1* mutations causes the genetic disease *neonatal ichthyosis and sclerosing cholangitis* (NISCH) syndrome. With to date only 18 reported patients, the hepatic manifestation of this ichthyosis syndrome typically presents with neonatal sclerosing cholangitis, hepatomegaly and elevated serum bile acids that have been attributed to the loss of CLDN1 expression in hepatocyte tight junctions and an impaired blood-biliary barrier. However, despite complete CLDN1 knockout phenotype in all individuals, the hepatic manifestation is highly variable ranging from mild cholestasis to progressive liver disease and liver failure. This indicates that CLDN1 loss-of-function at tight junctions might be compensable in humans (Izurieta Pacheco *et al.*, 2020).

The best studied example for the involvement of basolateral expressed CLDN1 in liver disease is its function for HCV cell entry. HCV entry glycoproteins E1E2 can bind to the first extracellular loop (EL1) of basolateral CLDN1 that promotes viral internalization via interaction with CD81 (for a review see: Zeisel *et al.*, 2019). This interaction has been shown to augment virus-induced MAPK signaling (Mailly *et al.*, 2015). Moreover, besides cell-entry, CLDN1 has also been reported to be involved in HCV cell-cell transmission (Timpe *et al.*, 2008). Established HCV infection in the liver has been shown to upregulate CLDN1 expression (Reynolds *et al.*, 2008; Nakamuta *et al.*, 2011; Zadori *et al.*, 2011) (**Figure 15**).

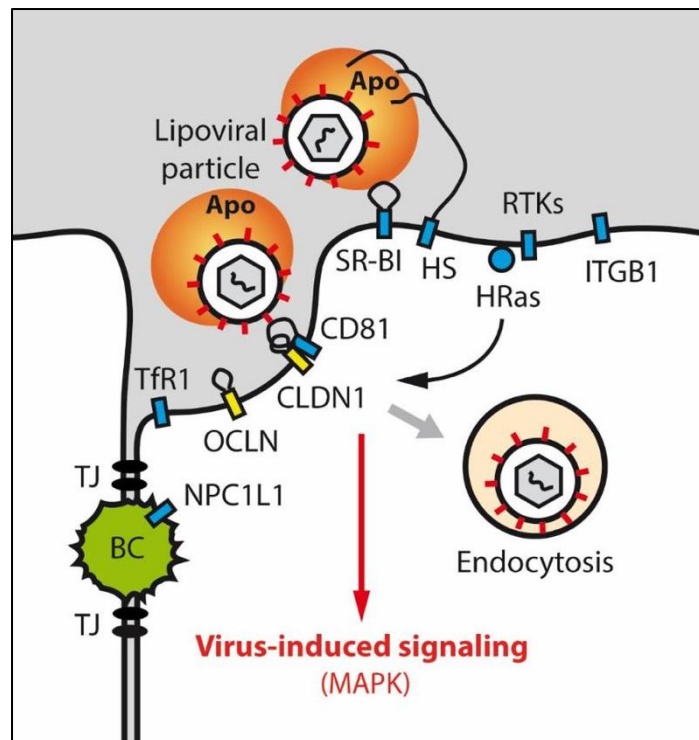


Figure 15: Functional role of basolateral CLDN1 as an HCV cell entry factor. Figure derived from (Roehlen *et al.*, 2020). CLDN1 belongs to the four main HCV entry factors and mediates HCV entry and virus induced signaling by interaction with CD81. Abbreviations: Apo= Apolipoprotein; BC=Bile canaliculi; CD81=Cluster of Differentiation 81; CLDN1= Claudin 1; HRas= HRas Proto-Oncogene, GTPase; HS=Heparan sulfate; ITGB1= Integrin beta 1; MAPK=Mitogen-activated protein kinase; NPC1L1= Niemann-Pick C1-Like 1; OCLN= Occludin; RTKs= Receptor tyrosine kinases; SR-B1= Scavenger receptor class B type 1; TfR1= Transferrin receptor 1; TJ= Tight junction.

Accumulating data further indicate a functional role of CLDN1 in chronic liver disease independent of HCV infection. In a small cohort of 30 patients, Reynolds *et al.* reported CLDN1 protein expression not only to be increased in livers of patients with chronic HCV infection, but also in patients with ALD, AIH and PBC (Reynolds *et al.*, 2008). Moreover, recent studies revealed expression of CLDN1 in human liver myofibroblasts, the most important non-parenchymal cell type in liver fibrosis, driving ECM production and scarring (Aoudjehane *et al.*, 2015).

Several studies further suggest a role of CLDN1 in liver carcinogenesis. In fact, CLDN1 was not only found to be overexpressed in HCC (Reynolds *et al.*, 2008; Holczbauer *et al.*, 2014; Zhou *et al.*, 2015) but was also reported to promote migration and invasion of human hepatoma cells by inducing epithelial-mesenchymal transition (EMT) (Yoon *et al.*, 2010; Kim *et al.*, 2011; Suh *et al.*, 2013; Lee *et al.*, 2015). In particular, CLDN1 overexpression upregulated the

transcriptional EMT regulators ZEB1 and SLUG via c-Abl-Ras-Raf-1-ERK pathway activation (Yoon *et al.*, 2010; Suh *et al.*, 2013). Similar associations with migratory and invasive cell capacities have been reported in other cancer cell types (Oku *et al.*, 2006; Leotlela *et al.*, 2007; Dos Reis *et al.*, 2008; Zhang *et al.*, 2013; Babkair *et al.*, 2016) corroborating a pro-oncogenic function of CLDN1. Nevertheless, the wide range of reported associations of CLDN1 with signaling pathways and cell functions (**Table 3**) but incomplete allocation of these interactions to different cellular fractions underlines our yet incomplete understanding of the complex role of CLDN1 in liver disease biology.

1.4.3 Development of monoclonal antibodies targeting non-junctional CLDN1

The identification of CLDN1 as an HCV cell entry factor (Evans *et al.*, 2007) has led to the development of monoclonal antibodies (mAbs) targeting CLDN1 as potential antiviral agents. By genetic immunization of Wistar rats, the laboratory of Prof. Baumert developed several mAbs targeting the first extracellular loop (EL1) of native human CLDN1. Detailed *in vitro* investigations demonstrated high efficacy of anti-CLDN1 mAbs in inhibiting HCV infection of all major genotypes without detectable toxicity in primary human hepatocytes (PHH) (Fofana *et al.*, 2010). Detailed studies in liver-chimeric mice did not only confirm the anti-viral efficacy and absent toxicity of the leading candidate rat anti-human CLDN1 mAb OM-7D3-B3, but also revealed selective binding to non-junctional CLDN1 (Mailly *et al.*, 2015) (**Figure 16**). Corroborating the current hypothesis of non-junctional CLDN1 as signaling hubs, CLDN1 mAb treatment was associated with suppression of HCV induced MAPK signaling (Mailly *et al.*, 2015). In preparation of clinical development, the rat anti-human CLDN1 mAb OM-7D3-B3 was humanized using CDR grafting (Colpitts *et al.*, 2018). This further allowed confirmation of the anti-viral efficacy of a fully humanized anti-CLDN1 mAb in primary human hepatocytes (Colpitts *et al.*, 2018).

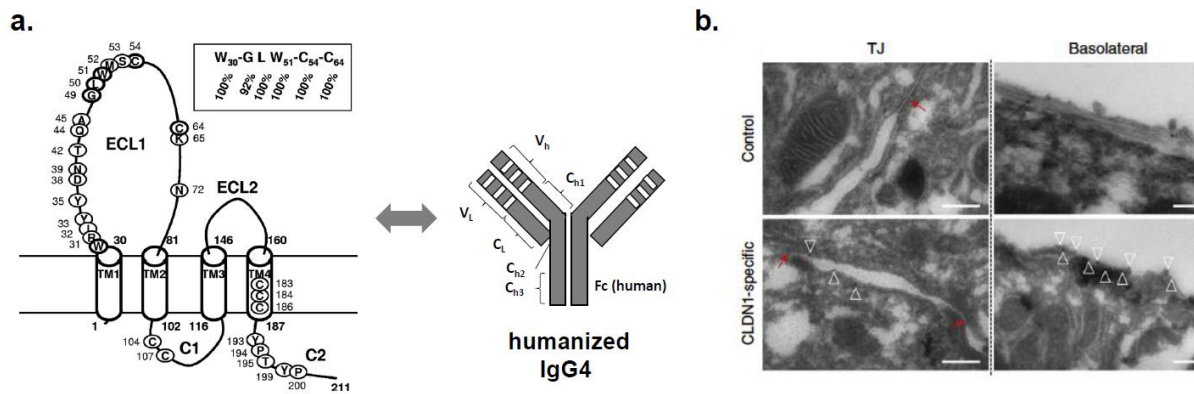


Figure 16: Development of non-junctional CLDN1 targeting monoclonal antibodies. Figure modified from (Mailly *et al.*, 2015). **a.** Humanized CLDN1 specific mAbs target a conformational epitope of Claudin-1 ECL1 **b.** Binding of CLDN1 mAbs to hepatocytes of human liver chimeric mouse livers was assessed by transmission electron microscopy and immunogold labeling. Red arrows indicate tight junctions, empty triangles indicate immunogold staining. Abbreviations: CLDN1= Claudin1; TJ= Tight junction.

1.5 Liver disease target discovery in the era of single cell RNA sequencing and transcriptomic pathway analyses

High-throughput sequencing technologies have markedly developed in the past years and have driven the discovery of biomarkers and therapeutic targets in human diseases (Boyault *et al.*, 2007; Hoshida *et al.*, 2009). Emerging techniques, such as single cell RNA sequencing (scRNAseq) enable the study of cell heterogeneity, and rare or previously unknown cell types, that is crucial for pathophysiological decoding of complex diseases such as liver fibrosis and HCC (for a review see: Saviano *et al.*, 2020). Computational tools for assessment of large transcriptomic data such as gene set enrichment analysis (GSEA) not only allow molecular characterization of different disease states or cell types (Armingol *et al.*, 2021), but also mechanistic evaluation of targeted therapies (Crouchet *et al.*, 2021).

1.5.1 Single cell RNA sequencing

RNAsequencing is a highly sensitive method for measuring gene expression across the transcriptome. While bulk RNAseq techniques are valuable instruments to assess molecular

mechanisms in homogenous samples such as cell lines, its significance in reproducing cellular states in complex cellular compositions, such as liver tissue is limited. Thus, bulk RNAseq of human tissue gives an average readout of gene expression information from a heterogeneous cell mix and is therefore highly influenced by a cell type's prevalence. However, rare cell types and specific cell subtypes can be crucial in the pathogenesis of human diseases (Aizarani *et al.*, 2019). ScRNAseq is a high-resolution technique for genome-wide RNA profiling in individual cells and has emerged as a valuable method to study heterogeneous tissues and complex diseases (Saviano *et al.*, 2020). It requires dissociation of patient samples into a single cell suspension, followed by a subsequent general workflow of sorting, capturing and sequencing, for which different alternative techniques are available (Picelli *et al.*, 2013; Macosko *et al.*, 2015; Hashimshony *et al.*, 2016; Ziegenhain *et al.*, 2017). The generated expression profile of thousands of gene transcripts per cell are usually represented as t-distributed stochastic neighbor embedding (t-SNE) maps that cluster cells according to their transcriptomic similarity (Li *et al.*, 2017) (**Figure 17**).

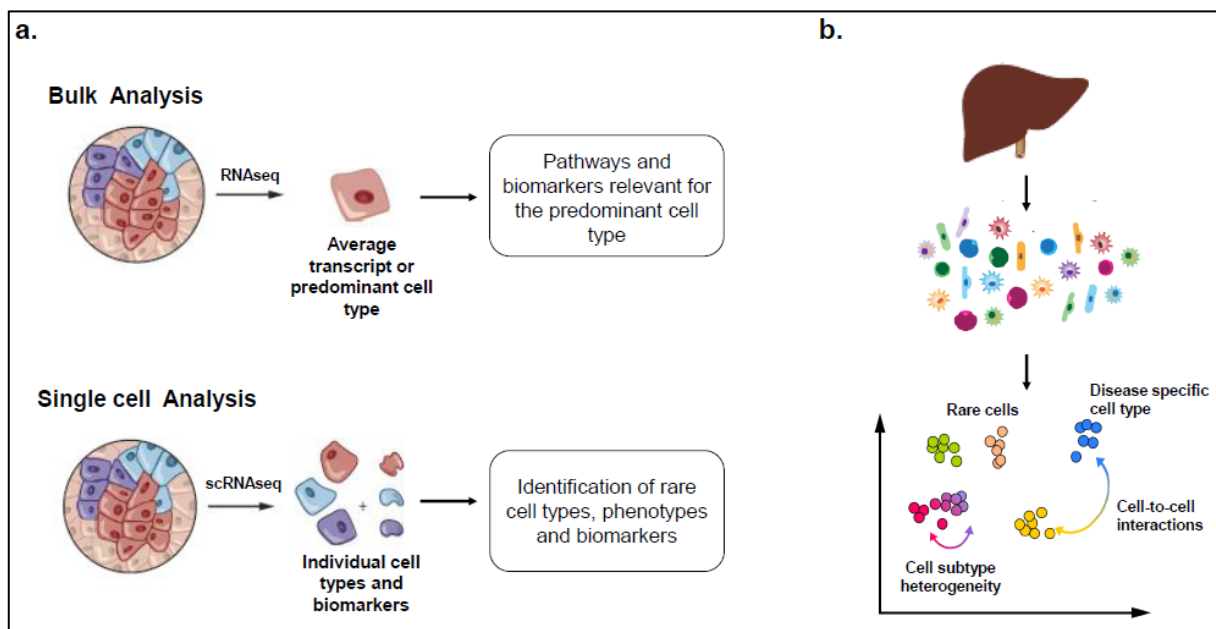


Figure 17: ScRNAseq analysis for high-resolution studies on liver pathophysiology. **a.** Bulk RNAseq can only recapitulate pathways and biomarkers relevant for the predominant cell type or average transcript. ScRNAseq allows identification of rare cell types, phenotypes and biomarkers. Figure modified from (Shalek and Benson, 2017) **b.** Simplified illustration of scRNAseq in the liver allowing study of rare cell types, cell phenotypes and cell-cell interactions. Liver tissue is dissociated into single cells that are sequenced using different approaches. Thousands of transcripts per cell are typically presented in a t-SNE plot where each dot represents a cell and the distance between the dots depicts transcriptomic similarity. Figure modified and extended from (Saviano *et al.*, 2020) and (Ramachandran *et al.*, 2019). Abbreviations: ScRNAseq= Single cell RNA sequencing; RNAseq= RNA sequencing.

Besides the identification and characterization of rare or unknown cell types (Aizarani *et al.*, 2019), computational tools, such as pseudo-time diffusion mapping (Haghverdi *et al.*, 2016) or RNA velocity (La Manno *et al.*, 2018) enable lineage tracing and cell differentiation analyses in scRNAseq data sets. However, despite its value in high-resolution profiling, high-throughput application of scRNAseq is still hampered by costs and technical challenges. In particular, optimized tissue dissociation is critical for unbiased cell yield and minimal manipulation-associated transcriptomic changes (van den Brink *et al.*, 2017). This is challenging in case of liver tissue, with hepatocytes exhibiting high susceptibility to mechanical manipulations and cholangiocytes being difficult to extract. Moreover, bioinformatical analysis of single cell data is challenging and often complicated by so-called “drop-outs” and undesired doublet cell captures (DePasquale *et al.*, 2019; Lahnemann *et al.*, 2020).

1.5.2 Gene set enrichment analysis (GSEA)

Gene set enrichment analysis represents one of the most widely used approaches for computational analysis of RNAseq data. Complementing traditional differential expression assessments that capture only strongest differences in single genes regardless of its biological relevance, GSEA evaluates RNAseq data in the context of previously defined gene sets. These can be genes related to a specific signaling pathway or genes associated with a specific cell differentiation state. The comparison of this gene set in samples from two or more biological conditions by GSEA results in a gene ranking based on the correlation of the respective gene's expression with a biological condition (signal-to-noise metric). This allows the assessment whether the genes within this gene set are randomly distributed or significantly enriched, hence primarily ranked to one of the assessed conditions. The enrichment score (ES) reflects the degree of overrepresented genes of the entire ranked gene list in one condition and is calculated by a weighted Kolmogorov–Smirnov-like statistic (Subramanian *et al.*, 2005) (**Figure 18**).

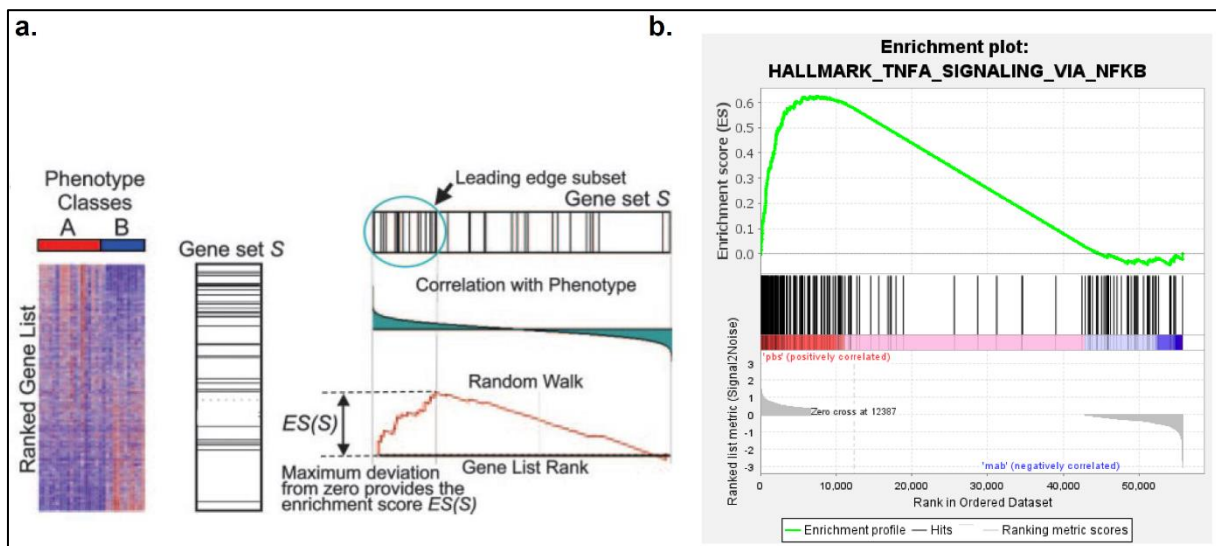


Figure 18. Gene set enrichment analysis (GSEA). **a.** Method illustration. Predefined gene sets are compared between two or more groups of conditions with available RNAseq or microarray data. The genes are ranked according to correlation with a phenotype. The enrichment score recapitulates to which extent the genes are over-represented at either the top or the bottom of the list. **b.** Example for a typical output of GSEA on the example of the Hallmark gene set TNFA_SIGNALING_VIA_NFKB that is enriched in the condition “pbs”. Abbreviations: ES= Enrichment Score.

By normalizing the ES (normalized enrichment score = NES) GSEA compensates differences in gene set size and correlations between the expression dataset and the gene set. The false discovery rate (FDR) accounts for multiple hypothesis testing and estimates the probability of a false positive finding. Unless small numbers of samples are compared, an FDR < 25 % is usually regarded as statistically significant (Subramanian *et al.*, 2005). As a powerful tool for high-throughput differential transcriptomic analysis, GSEA can be applied for molecular characterization of patient-derived samples, such as low or high-grade patient tumor samples (Wang, 2011; Wu *et al.*, 2019). In the context of target discovery and drug development, GSEA allows assessment of signaling pathway-, cell differentiation- or disease specific gene sets in samples from perturbation studies (Crouchet *et al.*, 2021).

2 Thesis goals

Despite major advances in the understanding of liver fibrosis and HCC pathogenesis, efficient antifibrotic therapies to treat liver fibrosis are absent and treatment options for advanced HCC only improve patient's prognosis to low extent and in a minor population (Finn *et al.*, 2020, for a review see: Llovet *et al.*, 2021)). Especially the strong causal link between liver fibrosis and HCC development has only been insufficiently addressed. Thus, compounds in clinical development for treatment of liver fibrosis not only have limited efficacy in suppressing fibrosis progression but also do not show any chemopreventive effects. Similarly, current HCC therapeutics show no effects on liver fibrosis, a major determinant of mortality in these patients. Thus, new compounds for treatment of liver fibrosis, HCC chemoprevention and HCC therapy are urgently needed.

The perturbation of CLDN1 expression in both liver fibrosis and HCC suggests a functional role of CLDN1 in liver disease progression, which constitutes the main hypothesis of this thesis. Given the association of especially non-junctional CLDN1 with oncogenic and pro-inflammatory cell signaling and absent toxic effects of specific non-junctional CLDN1 targeting mAbs (Mailly *et al.*, 2015; Colpitts *et al.*, 2018) this project aimed to evaluate non-junctional CLDN1 as a therapeutic target for I) treatment of advanced liver fibrosis and II) HCC therapy. Addressing the widely accepted hypothesis of common fibrosis driving cellular and molecular mechanisms, antifibrotic effects of non-junctional CLDN1 targeting therapies were further evaluated in the context of two other organs systems, the kidney and the lung. A main focus of this study was the application of authentic patient-derived 3D model systems as well as in-depth assessments of the targeted cell populations and mediated molecular effects using scRNAseq and GSEA.

3 Results

The results related to the two main aims of this thesis are an integral part of two manuscripts that are included in the following sections. In addition to project management and manuscript writing as first-author, my individual experimental contributions are highlighted in the respective summary sections prior to the article. Detailed descriptions of the respective material and methods are included at the end of each article.

3.1 Non-junctional CLDN1 as a therapeutic target for treatment of liver fibrosis

3.1.1 Results summary and own contribution

I) CLDN1 is overexpressed in liver tissue of patients with chronic liver disease and correlates with fibrosis progression (major contribution, Article figures 1A-D).

In order to evaluate the functional role of CLDN1 in chronic liver disease, the host laboratory investigated *CLDN1* gene expression in liver tissue of patients with NASH. In fact, *CLDN1* overexpression was observed in livers of NASH patients and showed significant correlation with advanced fibrosis stages. Following up on this observation, I assessed *CLDN1* gene expression in liver microarray data of several publicly available patient cohorts and found *CLDN1* not only to be upregulated in patients with NASH but also in liver tissue of patients with chronic HBV and HCV infection. Interestingly, *CLDN1* expression in patients with chronic HCV infection was significantly associated with the risk of fibrotic disease progression. By assessing *CLDN1* expression in publicly available liver scRNAseq datasets derived from healthy and cirrhotic livers, I further identified hepatocytes, cholangiocytes and liver progenitor cells as the main cellular sources of *CLDN1* expression in healthy liver. Moreover, I could demonstrate that hepatocytes in cirrhotic livers exhibit enhanced *CLDN1* expression and simultaneously show transcriptomic resemblance to liver progenitor cells. All together my analyses suggest *CLDN1*

expression to be perturbed in chronic liver disease of all main etiologies and indicate an association of CLDN1 with hepatocyte de-differentiation during liver disease progression.

II) CLDN1 is expressed on multiple liver resident cell types and upregulated by TNF α -NF κ B signaling (major contribution: Article Figures 1A-D; 1G-M)

My analysis of liver scRNAseq datasets indicates that *CLDN1* is predominantly expressed in liver hepatocytes and progenitor cells but also in non-parenchymal cells albeit at lower levels. In order to specifically characterize membranous and therefore targetable CLDN1 in liver resident cell types, I acquired an isolation technique allowing high-throughput isolation and purification of primary human hepatocytes (PHH), liver myofibroblasts (HLMFs), Kupffer cells and liver sinusoidal endothelial cells (LECs) from resected human liver tissue (Kegel *et al.*, 2016). Using this method, I could show that CLDN1 is not only expressed on epithelial cells of the liver but also on Kupffer cells and HLMFs. Linking CLDN1 overexpression with inflammation, I identified TNF α -NF κ B signaling, one of the main signaling pathways involved in fibrotic liver disease progression (Roehlen *et al.*, 2020), as a strong inducer of *CLDN1* expression in these cell types.

II) Targeting non-junctional CLDN1 by CLDN1 mAbs inhibits liver fibrosis and tumor development (co-authors and collaborators)

To evaluate non-junctional CLDN1 as a therapeutic target, the group of Prof. Baumert and collaborators assessed CLDN1 mAb treatment in several patient-derived *in vivo*, *ex vivo* and 3D *in vitro* models of liver fibrosis. In fact, CLDN1 mAb treatment markedly and significantly suppressed fibrosis markers in patient-derived liver spheroids and bioprinted liver tissue. Moreover, transcriptomic profiling of CLDN1 mAb- or control mAb-treated patient-derived precision cut liver slices indicated CLDN1 perturbation to strongly suppress cell circuits related to liver disease progression and HCC risk. In addition, CLDN1 mAb treatment showed strong anti-fibrotic and tumorpreventive effects in two independent state-of the-art mouse models of

liver fibrosis, validating a functional role of non-junctional CLDN1 in liver fibrosis and HCC development.

III) CLDN1 mAb suppresses fibrosis and carcinogenesis associated signaling and interferes with liver cell plasticity (major contribution: Article Figures 5A-B, 5D, 6A-O)

In order to evaluate the molecular mechanism of CLDN1 mAb-mediated anti-fibrotic and tumor-preventive effects, we performed RNAseq and GSEA on non-tumorous liver tissue derived from the two NASH fibrosis mouse models. By comparing the liver transcriptome in CLDN1 mAb- or control treated-mice with that of NASH patients with mild or advanced fibrosis, I observed CLDN1 mAb-treatment to suppress multiple pro-fibrogenic and oncogenic signaling pathways associated with liver disease progression *in situ*. Moreover, the assessment of scRNAseq-derived cell differentiation specific gene sets revealed that CLDN1 mAb treatment affects fibrosis-associated liver cell plasticity. In fact, I could validate strong inhibitory effects of CLDN1 mAb-treatment on hepatocyte dedifferentiation, scar-associated myofibroblast differentiation and macrophage polarization in cell culture systems using Huh7.5.1 cells, primary patient-derived HLMFs and Kupffer cells.

IV) Non-junctional CLDN1 is a potential target for treatment of lung and kidney fibrosis (contribution: in vitro experiments and bioinformatical analyses, Article Figures 7I-L)

Considering that CLDN1 is not only expressed in the liver but also in other organs such as the kidney and the lung we aimed to assess its functional role in other fibrotic diseases. In fact, investigation of publicly available cohorts of patients with chronic kidney disease and lung fibrosis indicated an association of CLDN1 with fibrosis also in other organs than the liver. Interestingly, a collaboration of the Baumert laboratory with SMC Laboratories (Tokyo, Japan) revealed strong anti-fibrotic effects of CLDN1 mAb-treatment in a bleomycin lung fibrosis and a unilateral ureteral obstruction (UUO) mouse model of renal interstitial fibrosis. To question similar molecular effects of CLDN1 mAb-treatment in these organs, I characterized CLDN1 expression on patient-derived kidney and lung fibroblasts and performed perturbation studies

in cell culture. Interestingly, I found both kidney and lung fibroblasts to express CLDN1 in a TNF α -NF κ B dependent manner, similar to the liver. Moreover, corroborating an organ-independent functional role of CLDN1 in fibroblast differentiation and activation, CLDN1 mAb-treatment of lung fibroblasts strongly suppressed gene sets specific for scar-associated fibroblast differentiation states.

V) Clinical translatability (collaborators)

In order to evaluate the clinical applicability of CLDN1 mAbs the Baumert laboratory performed pilot toxicology and pharmacokinetic studies in non-human primates in collaboration with *Alentis Therapeutics*. Application of high doses of CLDN1 mAb up to 150mg/kg in macaques did not show any detectable toxicity. Moreover, pharmacokinetic assessments predicted therapeutic mAb concentrations to be achievable in humans, supporting the evaluation of CLDN1 mAb-treatment in clinical studies.

3.1.2 Publication of the results

These results were integrated into the manuscript “A monoclonal antibody targeting non-junctional Claudin-1 inhibits liver fibrosis in patient-derived models by modulating cell plasticity and signaling”, which is currently under revision in *Science Translational Medicine*.

3.1.3 Results article I

A monoclonal antibody targeting non-junctional Claudin-1 inhibits fibrosis in patient-derived models by modulating cell plasticity.

Natascha Roehlen^{1,2†}, Antonio Saviano^{1,2,3†}, Houssein El Saghire^{1,2†}, Emilie Crouchet^{1,2}, François H.T. Duong^{1,2}, Frank Juehling^{1,2}, Sara Cherradi^{1,2}, Marine A. Oudot^{1,2}, Victor Gonzalez Motos^{1,2}, Sarah C. Durand^{1,2}, Patrick Pessaux^{1,2,3}, Emanuele Felli^{1,2,3}, Andrea Cavalli⁴, Jacopo Sgrignani⁴, Christine Thumann^{1,2}, Olga Koutsopoulos^{1,2}, Bryan C. Fuchs⁵, Yujin Hoshida⁶, Greg Elson⁷, Markus Meyer⁷, Roberto Iacone⁷, Tamas Schweighoffer⁷, Mathias Heikenwälder⁸, Laurent Mailly^{1,2}, Mirjam B. Zeisel^{1,2}, Catherine Schuster^{1,2}, Joachim Lupberger^{1,2}, Thomas F. Baumert^{1,2,3,9*}

Affiliations:

¹Université de Strasbourg, Strasbourg, France.

²Inserm, U1110, Institut de Recherche sur les Maladies Virales et Hépatiques; Strasbourg, France. ³Institut Hospitalo-Universitaire, Pôle Hépatodigestif, Nouvel Hôpital Civil; Strasbourg, France.

⁴Institute for Research in Biomedicine, Università della Svizzera Italiana; Bellinzona, Switzerland.

⁵Massachusetts General Hospital Cancer Center, Harvard Medical School; Charlestown, MA, USA.

⁶Liver Tumor Translational Research Program, Harold C. Simmons Comprehensive Cancer Center, Division of Digestive and Liver Diseases, University of Texas Southwestern Medical Center; Dallas, TX, USA.

⁷Alentis Therapeutics; Basel, Switzerland.

⁸Division of Chronic Inflammation and Cancer, German Cancer Research Center; Heidelberg, Germany.

⁹Institut Universitaire de France; Paris, France.

† These authors contributed equally to this work

*Correspondance should be addressed to: Prof. Thomas F. Baumert, MD, Inserm U1110, Institut de Recherche sur les Maladies Virales et Hépatiques, Université de Strasbourg, 3 rue Koeberlé, 67000 Strasbourg, France. E-mail: thomas.baumert@unistra.fr.

One Sentence Summary: Non-junctional Claudin-1 is a mediator and therapeutic target for organ fibrosis.

Abstract: Tissue fibrosis is a key driver of end-stage organ failure and cancer, overall accounting for up to 45% of deaths in developed countries. There is a large unmet medical need for anti-fibrotic therapies. Claudin-1 (CLDN1) is a member of the tight junction (TJ) protein family. While the role of CLDN1 incorporated in TJ is well established, the function of non-junctional CLDN1 is largely unknown. Using highly specific monoclonal antibodies targeting a conformation-dependent epitope of non-junctional CLDN1, we show in patient-derived liver 3D fibrosis and human liver chimeric mouse models that non-junctional CLDN1 is a previously unknown mediator and target for liver fibrosis. Targeting non-junctional CLDN1 reverted inflammation-induced hepatocyte pro-fibrogenic signaling and cell fate and suppressed the pro-fibrogenic differentiation of Kupffer cells and myofibroblasts. Safety studies of a fully humanized antibody in non-human primates did not reveal any significant adverse events even at high steady-state concentrations. Our results provide preclinical proof-of-concept for CLDN1-specific mAbs for treatment of advanced liver fibrosis and cancer prevention. Antifibrotic effects in lung and kidney fibrosis models further indicate a role of CLDN1 as a therapeutic target for tissue fibrosis across organs. In conclusion, our data pave the way for further therapeutic exploration of CLDN1-targeting therapies for fibrotic diseases in patients.

INTRODUCTION

Organ fibrosis is the result of excessive accumulation of extracellular matrix (ECM) that results from a wound healing response to repeated and chronic tissue injury. Leading to distortion of tissue architecture and loss of organ function, organ fibrosis accounts for up to 45% of death in developed countries(1). Moreover, fibrosis is a major risk factor for tumor development across organs(2). Yet, approved therapies that aim to prevent or resolve fibrosis are either absent as for the liver or show limited efficacy and safety(3-5). One explanation for the lack of efficient anti-fibrotic therapies is the fact that the cell circuits driving the disease biology are still only partially understood(3). Importantly, several key features and cellular drivers appear to be similar across different organs(1). Primary tissue injury initiates inflammation and leads to the release of proinflammatory, vasoactive and profibrotic cytokines. These then promote pro-fibrogenic differentiation of resident or recruited fibroblast progenitor cells that drive production of a fibrotic scar. Perturbated ECM-resolving mechanisms due to repeated or chronic tissue inflammation ultimately result in ECM accumulation and disruption of normal tissue architecture(1, 3).

In the liver, the major causes of liver fibrosis are chronic hepatitis B and C, alcoholic liver disease (ALD) and non-alcoholic steatohepatitis (NASH). The end-stage of liver fibrosis are cirrhosis and hepatocellular carcinoma (HCC)(6). Common pathways mediate the progression of liver fibrosis and its transition to HCC irrespective of the etiology(7). Of note, HCC nearly always arises in the context of advanced liver fibrosis(7, 8). While removal of the cause of injury in the early stage of disease can restore liver function and outcome, patients with advanced fibrosis remain at risk for HCC(9). This has been elegantly illustrated by the observation that HCV cure in advanced fibrosis only partially reduces but not eliminates the risk of HCC(9). Thus, direct anti-fibrotic agents are urgently needed to improve patient survival and outcome in advanced fibrosis by preventing liver disease progression, cancer risk and mortality(10).

Claudin-1 (CLDN1) is a member of the tight junction (TJ) protein family. While its function within the TJs for cell-cell-adhesion is well established, the role of non-junctionally expressed CLDN1 is largely unknown. In the liver CLDN1 serves as a cell entry factor of hepatitis C virus (HCV), a major cause of liver fibrosis(11). We have previously developed a humanized monoclonal antibody (mAb) targeting the extracellular loop 1 (EL1) of CLDN1 expressed on the hepatocyte basolateral membrane(12, 13). By inhibiting CLDN1 co-receptor interactions this mAb potentially inhibits viral entry and infection of hepatocytes(13, 14).

Using a panel of mAbs targeting the EL1 of CLDN1 combined with patient-derived models and perturbation studies, we aimed to investigate the role of non-junctional CLDN1 as a mediator and therapeutic target for liver fibrosis and cancer prevention. Finally, in preparation for clinical translation, we characterized the pharmacological and safety properties of a humanized anti-CLDN1 antibody in non-human primates.

RESULTS

CLDN1 expression is associated with liver fibrosis and disease progression

To investigate the role of CLDN1 as a therapeutic target in liver fibrosis, we first analyzed its expression in patients with chronic liver disease of viral and non-viral etiologies. Analysis of total *CLDN1* gene expression levels in patient liver tissues retrieved from Gene Expression Omnibus (GEO) database(15-17) and a cohort from the University of Strasbourg (**Suppl. Table 1**) showed marked and significant upregulation of *CLDN1* in liver disease of all major etiologies including chronic hepatitis C, B and NASH ($p<0.0001$, $p=0.003$, $p<0.001$, Student's t-test (t-test), respectively, **Fig. 1A**). Of note, the level of *CLDN1* expression was significantly associated with fibrotic disease progression in patients with NASH(17) and HCV-infected individuals post transplantation(15) ($p<0.001$, t-test and $p=0.04$, Mann Whitney U-test (U-test), **Fig. 1B**).

We next investigated *CLDN1* mRNA expression on single cell level in the healthy and diseased liver. Analysis of recently published single cell RNAseq data(18) revealed *CLDN1* to

be most highly expressed on EPCAM⁺ epithelial liver progenitor cells and hepatocytes in patients without chronic liver disease (**Fig. 1C**). In cirrhotic liver, *CLDN1* expression on hepatocytes was markedly increased (**Fig. 1D**)(19) and correlated with upregulation of liver progenitor markers(18), including epithelial cell adhesion molecule (*EPCAM*) and Tumor Associated Calcium Signal Transducer 2 (*TACSTD2* (data retrievable at: <https://shiny.igmm.ed.ac.uk/livercellatlas/>). Within the fibrotic mesenchyme, *CLDN1* mRNA was strongly expressed on mesothelial cells, a yet poorly investigated cell type associated with liver fibrosis (**Fig. 1D**)(19). Lineage tracing methods in mice have recently indicated mesothelial cells to serve as HSC and myofibroblast progenitor cells in liver fibrogenesis(20).

Taken together, the significant up-regulation of *CLDN1* expression in hepatocytes of fibrotic liver and its association with disease progression among different etiologies suggests a functional role in the pathogenesis of liver fibrosis. High expression in mesothelial cells, solely detectable in fibrotic liver(19), further suggest a functional role of *CLDN1* in this yet poorly characterized putative mesenchymal progenitor cell population. *CLDN1* expression in other liver mesenchymal cells and macrophages at lower levels (**Fig. 1D**) warrant further *ex vivo* characterization.

CLDN1 is expressed both in tight junctions as well as outside the tight junctions(11). We have previously established a panel of humanized *CLDN1*-specific antibodies targeting a conformation-dependent epitope of EL1 in non-junctional *CLDN1*(12-14). A subsequent genome-wide protein array demonstrated that these antibodies selectively bind human *CLDN1* without any cross-reactivity to other *CLDN* family members and 5000 other membrane and secreted proteins tested (**Suppl. Fig. 1**). Furthermore, structural modeling revealed that the epitope recognized by the mAb in EL1 is only accessible outside TJs (**Fig. 1E**) and not in TJ due its conformation (**Fig. 1F**).

To specifically characterize non-junctional *CLDN1* expression in the liver, primary liver cells were isolated from human liver (**Suppl. Table 2**) and investigated by flow cytometry or immunofluorescence using the humanized mAb H3L3(12-14). In addition to the expected strong binding to primary human hepatocytes (PHH, **Fig. 1G**), the mAb specifically bound to

non-junctional CLDN1 expressed on patient-derived primary human liver myofibroblasts (HLMFs, **Fig. 1H**), the main fibrosis effector cells in chronic liver disease(3). Liver macrophages are the largest non-parenchymal cell (NPC) fraction characterized by high plasticity and phenotypic variations that depend on the disease environment(3). Flow cytometric analyses on native cells revealed CLDN1 expression at the membrane of primary Kupffer cells (**Fig. 1I**). In contrast, liver endothelial cells (LECs) lacked expression of CLDN1 (**Fig. 1J**).

We next aimed to elucidate molecular drivers of CLDN1 upregulation in chronic liver disease. TNF α -NF κ B signaling is a key signaling pathway upregulated in chronic inflammatory liver tissue and is functionally involved in liver fibrogenesis and carcinogenesis(3). Interestingly, treatment of HLMFs with TNF α markedly and significantly enhanced non-junctional CLDN1 expression accessible to CLDN1 mAb ($p<0.0001$, t-test, **Fig. 1K**). A similar upregulation was observed in TNF α treated PHH, albeit to a lower magnitude than in HLMFs ($p<0.0001$, t-test, **Fig. 1L**). TNF α -mediated upregulation was reduced following pharmacological inhibition of NF κ B signaling in both HLMF and PHH ($p<0.0001$ and $p=0.008$, t-test, respectively, **Fig. 1K-L**).

Studying CLDN1 expression in a subpopulation of patient-derived Kupffer cells (**Fig. 1I**), we used the peripheral blood monocyte-derived cell line THP1 to evaluate *CLDN1* expression in different macrophage differentiation states(21). We revealed that *CLDN1* is expressed in M1 macrophages but not or poorly in monocytes and M0 macrophages ($p<0.0001$, $p=0.004$, U test, respectively, **Fig. 1M**, left panel). M1 macrophages are key drivers of chronic inflammation and liver fibrogenesis and the main source of TNF α *in situ*(3) (**Fig. 1M**, right panel). Interestingly, in a pilot study, incubation of HLMF with M1 macrophage-conditioned medium significantly upregulated *CLDN1* expression ($p=0.04$, t-test, **Fig. 1N**). Collectively, these results suggest TNF α -NF κ B signaling as a driver of CLDN1 upregulation in chronic inflammatory liver disease and identify PHHs, HLMFs and M1 Kupffer cells as target and effector cells for non-junctional CLDN1 binding mAbs.

Targeting non-junctional CLDN1 by a highly specific monoclonal antibody reduces fibrosis and tumor burden in a human liver chimeric mouse model for liver fibrosis

To investigate the functional role of non-junctional CLDN1 as a mediator and target for liver fibrosis, we next assessed the therapeutic effect of the humanized CLDN1 mAb H3L3(13) in a chimeric, patient-derived animal model that is closely recapitulating key features of clinical liver fibrosis and expressing human CLDN1. As a model we used *Fah^{-/-}/Rag2^{-/-}/Il2rg^{-/-} (FRG)-NOD* mice robustly repopulated with PHH(22). While these mice do not harbor any T or B cells, they carry liver macrophages, myofibroblasts and LECs(22). Among all liver fibrosis animal models, high-fat diet models are considered to be closest to the human disease(23, 24). Thus, we applied a well-established long-term choline-deficient, L-amino acid-defined, high fat diet (CDA-HFD)(24) to induce advanced liver fibrosis.

Following establishment of advanced liver fibrosis over 16 weeks of diet, mice were randomized in 2 groups and received a weekly i.p. injection of either the humanized CLDN1 mAb or an equivalent vehicle control for 8 weeks (**Fig. 2A**) while the diet was continued. A total of two independent studies were performed (**Fig. 2**). We first studied effects of CLDN1 mAb on liver fibrosis and identified humanized areas in the mouse liver by fumarylacetoacetate hydrolase (FAH) staining, which is absent in mouse cells(22). Sirius red staining and automated analysis of the collagen proportionate area (CPA) revealed markedly and significantly reduced total liver fibrosis and fibrosis in humanized areas in CLDN1 mAb treated mice in both independently performed studies (**Fig. 2B-D, Suppl. Table 3**). In the first experiment, the median total fibrosis level was 6.59% in the control group (Q1-Q3 6.43-8.54%) and 2.34% in CLDN1 mAb-treated humanized mice (Q1-Q3 1.31-4.51%, $p=0.03$, U test) (**Fig. 2C**, left panel). The median fibrosis level in humanized areas was 4.66% in the control group (Q1-Q3 4.00-5.48%) and 1.09% in CLDN1 mAb group (Q1-Q3 0.59-1.65%, $p=0.03$, U test, **Fig. 2c**, right panel). Similar antifibrotic effects were observed in the second, independent experiment ($p=0.01$, U test, respectively, **Fig. 2D, Suppl. Table 3**).

Corroborating the histological findings, humanized mice treated with CLDN1 mAb showed significantly downregulated hepatic gene expression of fibrosis markers, including collagen type II alpha 1 chain (*COL2A1*), *TIMP1* and platelet-derived growth factor subunit A (*PDGFA*)(3) ($p=0.03$, $p=0.02$ and $p=0.009$, t-test, respectively, **Fig. 2E**). Finally, CLDN1 mAb treated mice exhibited strongly reduced plasma levels of C-reactive protein (*CRP*), a secreted inflammatory biomarker ($p<0.01$, U-test, **Fig. 2F**).

Due to the chronic liver disease induced by FAH-deficiency and CDA-HFD, the humanized mice also developed liver tumors. Macroscopic and histological examination of humanized livers revealed significantly reduced tumor burden in CLDN1 mAb-treated mice in both experiments confirming the potential of CLDN1 mAb in preventing HCC ($p<0.05$ and $p<0.01$, U-test, respectively, **Fig. 2G-I**). Taken together these data indicate that the humanized CLDN1 mAb H3L3(13) significantly reduces diet-induced liver fibrosis and diminishes liver tumor formation in a patient-derived mouse liver fibrosis model.

A murinized CLDN1-specific mAb reduces fibrosis, liver disease progression and hepatocarcinogenesis in a mouse model of diet-induced fibrosis and HCC

To further validate anti-fibrotic and cancer-preventive effects of targeting non-junctional CLDN1 in a fully immunocompetent mouse model, we engineered a murinized version of our previously established rat anti-human CLDN1 mAb(12). Thus, as described for its humanized version(13) the complementarity-determining regions (CDRs) of rat anti-human CLDN1 mAb were fused to a murine Fc part (designated TAR-Rm). Of note, the epitope recognized by rat, humanized and murinized anti-human CLDN1 mAbs is similar. Reflecting species-specific variations in CLDN1 structure, the binding affinity of the murinized anti-human CLDN1 mAb to mouse CLDN1 was lower than the affinity of the previously developed humanized CLDN1 mAb(13) to human CLDN1 expressed on PHH. Still, the murinized CLDN1 mAb showed satisfactory target-engagement as demonstrated by a robust inhibition of CLDN1-mediated HCV entry into 293T cells expressing mouse CLDN1 (**Suppl. Fig. S2A-F**). Pharmacokinetic studies with the

murinized mAb in mice revealed an approximate half-life of 7.7 days. An injection of 25 mg/kg resulted in plasma doses saturating receptor binding with robust target engagement (**Suppl. Fig. S2C, G**) suggesting that the murinized mAb is suitable for *in vivo* studies in mouse models.

Similarly as in the humanized mouse model we chose a CDA-HFD(24) to induce NASH and fibrosis. To study also the effect of the mAb on advanced liver disease progressing to cancer, we injected one dose of diethylnitrosamine (DEN) to accelerate hepatocarcinogenesis. This DEN-CDA-HFD model recapitulates NASH histological and metabolic features, including fibrosis, and results in induction of liver tumors after 24 weeks(24). Following the establishment of NASH-like features within 9 weeks, the mice were randomized in 2 groups and received a weekly i.p. injection of either the murinized CLDN1 mAb or an equivalent vehicle control for 16 weeks (**Fig. 3A**). Two mice in the control group died during the experiment for unknown causes; no deaths occurred in the CLDN1 mAb-treated mice.

For functional characterization of CLDN1 mAb effects on chronic liver disease progression *in vivo*, we first analyzed key hallmarks of NASH, including liver inflammation, steatosis and fibrosis. A histological assessment of liver steatosis and inflammation revealed marked and significant improvement of liver steatosis levels and the NALFD activity score(25) in CLDN1 mAb-treated animals (**Fig. 3B** upper panel and **Fig. 3C**, left panels, $p < 0.05$ and $p < 0.01$, U-test, respectively). Similarly, 16 weeks administration of the CLDN1 mAb was accompanied by a significant reduction of ALT levels (10.2%, $p = 0.03$, U-test), whereas total bilirubin and alkaline phosphatase levels remained unchanged (**Suppl. Table 4**). Sirius red staining and automated analysis of the collagen proportionate area (CPA) revealed markedly and significantly reduced fibrosis in the CLDN1 mAb group compared to the control group with a relative median fibrosis improvement of 28.4% ($p = 0.003$, U-test, **Fig. 3B-C**, middle panels, **Suppl. Table 5**). Furthermore, treatment of animals with the CLDN1 mAb reduced alpha smooth muscle actin (α -SMA) expression, a specific marker of myofibroblasts(3) ($p < 0.05$, U-test, **Fig. 3B**, lower panel and **Fig. 3C**, right panel). The antifibrotic effect of the CLDN1 mAb were confirmed by transcriptomics showing impaired expression of collagen type I alpha 1

chain (*COL1A1*), alpha smooth muscle actin (*ACTA2*) and Platelet Derived Growth Factor Subunit B (*PDGFB*) (**Fig. 3D**).

As observed in the humanized mice model (**Fig. 2**), macroscopic and microscopic examination of mouse livers showed a marked difference in short-term liver tumor development and growth. While 17/18 mice of the control group had liver tumors (94.4%; 10 mice with >6 nodules), the CLDN1 mAb-treated group tumors were only found in 6/20 (30%; 1 mouse >6 nodules) mice ($p<0.0001$ and $p<0.01$, U-test, respectively, **Fig. 3E**, upper panel and **Fig. 3F**, left panel). These findings were also confirmed by histological analysis where 83.3% of mice in the control group had tumors >1mm compared to 40% in the CLDN1 mAb group ($p=0.007$, U-test, **Fig. 3F**, right panel). Moreover, the tumor burden in terms of number and size was significantly higher in the control group ($p=0.001$, U-test, respectively, **Fig. 3G**, left panels, **Suppl. Table 5**). Liver tumors were further stained for the heat-shock protein 70 (Hsp70) (**Fig. 3E**, lower panel), a marker used for the clinico-pathological diagnosis of HCC. In the CLDN1 mAb group the prevalence of mice with at least one Hsp70-positive tumor was only 5.0% (1/20 mice), which was significantly lower than the prevalence in the control group (8/18, 44.4% mice with at least one Hsp70-positive tumor ($p<0.01$, U-test, **Fig. 3G**, right panel).

Extensive safety studies including histopathology of major organs, complete serum chemistry and renal and liver function tests did not show any detectable adverse effects (**Suppl. Fig. S3** and **Suppl. Table 4**). Collectively, these data show that a CLDN1-specific mAb reverses NASH-associated liver fibrosis, steatosis, and inflammation and prevents hepatocarcinogenesis in a state-of-the-art diet model for NASH-induced fibrosis and HCC.

Validation of the profibrogenic role of non-junctional CLDN1 in patient-derived 3D liver fibrosis and NASH models

We next validated the antifibrotic effects of CLDN1 mAb in patient-derived *ex vivo* models. The 3D ExVive Human Liver Tissue model (Organovo) mimics distinct features of NASH and fibrosis and allows the assessment of liver disease therapeutics(26). In this model PHH, LECs,

Kupffer cells (KCs) and hepatic stellate cells (HSCs) are exposed to steatogenic and inflammatory stress. They are co-cultured on a bioprinted scaffold using transwell technology, which recapitulates the human liver multicellular structure with a compartmentalized architecture resembling native liver (**Fig. 4A**, left panel)(26). In this human NASH model, CLDN1 mAb markedly reduced hepatocyte ballooning and macro- and micro-steatosis in three out of four tissue preparations (**Fig. 4B**). Overall incidence of bridging fibrosis as well as the thickness of collagen fibrils around steatotic and ballooned hepatocytes was reduced in the tissues treated with CLDN1 mAb. Image-based quantification of the collagen proportionate area (8 slices per tissue preparation) revealed that the median fibrosis level in CLDN1 mAb-treated ExVive tissues was strongly reduced compared to control mAb-treated tissues (2.69% vs. 6.14%, $p < 0.0001$, t-test, **Fig. 4C**).

Next, we studied effects of CLDN1 mAb on fibrosis in patient-derived human liver spheroids. Spheroids are cultured as 3D micro-tissues and thereby recapitulate the liver microenvironment, relevant for a therapeutic response(27). Thus, patient-derived multicellular spheroids are considered as one of the most relevant and translatable model systems to assess the effect of liver-therapeutic agents(28). Liver tissues from patients with and without chronic liver disease and fibrosis (**Suppl. Table 6**) were dissociated and cultured in ultra-low attachment plates (**Fig. 4D**). This protocol allows the formation of patient-derived spheroids harboring original liver cell populations, including ASGPR1⁺ hepatocytes, CD31⁺ endothelial cells, CD68⁺ Kupffer cells and α SMA⁺ myofibroblasts (**Fig. 4E**). Validating the functionality of the liver microenvironment in this 3D spheroid model, treatment with transforming growth factor beta (TGF- β) induced the expression of *COL1A1*, *COL1A4*, and the secretion of CCL3, a well described immune cell derived pro-fibrogenic cytokine(29) (**Fig. 4F**). Treatment of patient spheroids with CLDN1 mAb suppressed the induction of these pro-fibrogenic markers ($p < 0.05$, Fisher's exact test, respectively, **Fig. 4F**). Moreover, CLDN1 mAb treatment suppressed collagen deposition with superior effects compared to compounds in clinical development, such as elafibranor(30) (**Fig. 4G**). Finally, CLDN1 mAb treatment of spheroids derived from fibrotic livers reduced expression of fibrosis markers, including *ACTA2* and *PDGFB* (**Fig. 4H**).

Given the significant and robust inhibition of fibrosis progression and tumor development *in vivo* (**Figs. 2-3**), we aimed to validate the effect of CLDN1 mAb on cell circuits associated with disease progression and carcinogenesis in liver tissues from patients with advanced fibrosis(31). Gene expression signatures have been established to predict progression of fibrotic liver disease to HCC independent of the etiology. These include an FDA-approved prognostic liver 186-gene signature (PLS) in stromal liver cirrhosis tissue of HCC in all major etiologies(32-36). The clinical PLS can be used as a treatment-responsive tool to evaluate the effect of antifibrotic compounds on prognosis relevant cell circuits in *ex vivo* models, such as precision cut slices(31, 37). Liver slices of NASH patients with different stages of fibrosis (**Suppl. Table 7**) were incubated with CLDN1 mAb or control and analyzed for expression of the clinical PLS (**Fig. 4I**). As shown in **Fig. 4J**, CLDN1 mAb markedly and significantly reverted the PLS from poor to good-prognosis status for all patients (FDR<0.25, Kolmogorov-Smirnov test). Collectively, these results validate the functional impact of CLDN1 as a mediator and target for treatment of liver fibrosis in state-of-the-art multi-cellular patient-derived 3D model systems for liver fibrosis.

Targeting non-junctional CLDN1 restores perturbation of liver cell circuits and signaling mediating chronic inflammation and fibrosis

Next, we aimed to elucidate the molecular mechanism of CLDN1 mAb mediated anti-fibrotic and tumor preventive effects *in vivo* using RNAseq and gene set enrichment analysis (GSEA)(38). To evaluate the most relevant cell circuits involved in liver disease progression *in situ*, we analyzed transcriptional signatures of fibrosis- and carcinogenesis-related signaling side-by-side in mouse models and a human NASH cohort with mild and advanced fibrosis (GSEA49541(17)) (**Fig. 5A**). As demonstrated in **Fig. 5B**, fibrotic livers in both NASH fibrosis mouse models exhibited upregulated fibrosis-associated pathways, including TNF α -NF κ B or TGF β signaling similar to NASH patients with advanced compared to mild fibrosis. Treatment with CLDN1 mAb robustly and significantly reversed the induction of these fibrogenic circuits with most pronounced effects on TNF α -NF κ B signaling (FDR<0.001, Kolmogorov Smirnov

test, respectively, **Fig. 5B**). Similarly, carcinogenesis-associated pathways, including K-Ras signaling and epithelial-mesenchymal transition (EMT) are upregulated in NASH patients with advanced fibrosis but significantly suppressed by CLDN1 mAb treatment in both animal models (FDR<0.25, Kolmogorov Smirnov test, **Fig. 5B**). Using a large clinical data base of >500 cirrhotic patients, a recent study defined 31 human cirrhosis gene modules relevant for liver disease progression, fibrosis and hepatocarcinogenesis(31). These modules enable clinical translation of transcriptomic signatures beyond single signaling pathways(31). Consistently, the expression of gene modules related to inflammatory signaling (module 7 and 24), as well as myofibroblast activation and ECM production (module 1 and 24), were markedly induced in the clinical cohort of NASH patients with advanced fibrosis compared to mild fibrosis, as well as in the NASH fibrosis mouse models. At the same time, the expression of gene modules associated with physiological hepatocyte metabolism (modules 9, 22 and 23) were suppressed in NASH patients with advanced fibrosis and livers of fibrotic mice (**Fig. 5B**). Corroborating the clinical relevance of observed suppressive effects on fibrosis-associated signaling, CLDN1 mAb strongly suppressed gene expression of modules related to ECM proteins, immune signaling and myofibroblast differentiation, while gene expression patterns associated with physiological hepatocyte metabolism were restored (**Fig. 5B**). Finally, assessment of the clinical PLS(31-33, 36), revealed robust and highly significant reversion of the PLS poor prognosis to good prognosis status suggesting a treatment-induced improvement of liver disease progression and decreased HCC risk (FDR<0.001, Kolmogorov-Smirnov test, respectively, **Fig. 5C**).

We next validated CLDN1 mAb effects on fibrogenic and carcinogenic signaling in cell-based models. Since PHH undergo rapid de-differentiation during cell culture accompanied by a loss of key physiological functions, we used DMSO-differentiated Huh7.5.1 cells (Huh7.5.1^{dif}) exhibiting a hepatocyte-like phenotype(39-41) as a surrogate model for functional studies. Our recent study has shown that this model recapitulates key cell circuits of liver disease progression of patients(42). As shown in **Fig. 5D**, RNAseq and GSEA confirmed the observed CLDN1 mAb-mediated suppression on hepatocyte pro-fibrogenic and carcinogenic signaling

in cell culture models for both viral and metabolic liver disease. Furthermore, proteomic assessment of signaling using phospho-specific antibody capture arrays revealed a CLDN1 mAb-induced suppression of Src family kinase activation (**Fig. 5E**). Src signaling cascades are key drivers of liver fibrogenesis(43) and converge on several other pathways identified, including NFκB, MAPK and STAT signaling(44). Consistently, CLDN1 mAb treatment suppressed phosphorylation of downstream effectors of these pathways, including p38a, CREB5 (MAPK(45)) and TOR (PI3K-AKT signaling(46)) (**Fig. 5E**).

Using stable CLDN1 knockout (KO) and pharmacological intervention we demonstrate that CLDN1 is a driver of the poor prognosis status of the PLS predicting liver disease progression and HCC risk for all major liver disease etiologies (FDR<0.25, Kolmogorov-Smirnov test, respectively, **Suppl. Fig. S4**). Reversal of the poor prognosis status of the PLS was hereby dose-dependent, with most robust effects at 10 µg/mL, the saturating concentration for mAb binding to CLDN1 on hepatocytes (**Suppl. Fig. S2**). Collectively, these findings demonstrate that targeting non-junctional CLDN1 by a highly specific mAb suppresses hepatocyte pro-fibrogenic and carcinogenic signaling pathways.

Targeting non-junctional CLDN1 reverses inflammation-induced perturbation of hepatocyte cell fate and plasticity

Single cell RNA sequencing (scRNAseq) has transformed our understanding of the cellular states in health and disease. In the liver, scRNASeq has revealed distinct differentiation states of parenchymal and non-parenchymal cells(18, 19). Well characterized examples are EPCAM⁺ bipotent liver progenitor cells as well as scar-associated myofibroblasts(18, 19). Interestingly, liver cirrhosis-derived hepatocytes show marked upregulation of liver progenitor cell marker genes, such as Prominin 1(PROM1) and SRY-Box Transcription Factor 9 (SOX9) and simultaneous downregulation of mature hepatocyte markers (e.g., apolipoprotein F, APOF) on single cell level(19) (data retrievable at: <https://shiny.igmm.ed.ac.uk/livercellatlas/>) suggesting a transformation of chronically injured mature hepatocytes towards an immature liver

progenitor cell-phenotype. To evaluate whether this fibrosis-associated perturbation of cell fate and plasticity can be detected on bulk RNAseq level, we assessed scRNAseq derived cell lineage marker genes (MSigDB and (18, 19)) in livers of NASH patients (GSE49541(17)) and human liver chimeric mice (**Fig. 6A**). Interestingly, gene sets encompassing marker genes of the EPCAM⁺ progenitor compartment(18), including PROM1 and SOX9 were markedly enriched in NASH patients with advanced compared to mild fibrosis(17) (FDR<0.001, Kolmogorov Smirnov test, **Fig. 6B**, and p=0.005, p=0.0004, t-test, **Fig. 6C**). Moreover, genes characterizing healthy mature hepatocytes(18), such as APOF, were strongly suppressed during liver disease progression in NASH fibrosis patients(17) (FDR<0.02, Kolmogorov Smirnov test, **Fig. 6B** and p=0.002, t-test, **Fig. 6D**, left panel). Similar results were obtained in fibrotic livers derived from two NASH fibrosis mouse models (**Suppl. Fig. S5A-B**). Importantly, treatment with CLDN1 mAb considerably suppressed the disease-induced upregulation of hepatocyte progenitor markers in both mouse models (**Fig. 6E-F**, **Suppl. Fig. S5C-D**). Mature hepatocyte marker gene expression on the other hand was restored (**Fig. 6D**, right panel, **Fig. 6E** and **Suppl. Fig. S5D**, right panel). Similar results were obtained in liver cell-based models (**Fig. 6G**), strongly corroborating the relevance of our findings for hepatocyte fate. Collectively, these data suggest that CLDN1-specific mAb treatment reverts the disease-induced immature hepatocyte phenotype back to a mature phenotype of non-diseased hepatocytes.

Targeting non-junctional CLDN1 reverses pro-fibrogenic differentiation and activation of human liver myofibroblasts and Kupffer cells

Scar-associated mesenchymal cells express several key markers that differentiate these cells from its quiescent progenitor cells beyond the classical myofibroblast activation markers(19). Expression of marker genes of PDGFRA⁺ scar-associated myofibroblasts(19) (**Suppl. Table S8**) was significantly induced both in livers of NASH patients with advanced compared to mild fibrosis (FDR<0.001, Kolmogorov Smirnov test, **Fig. 6H**, left panel), as well as fibrotic mouse livers compared to healthy controls (FDR=0.001, Kolmogorov Smirnov test, **Suppl. Fig. S5E**). CLDN1 mAb-treatment significantly suppressed myofibroblast activation gene

signatures (FDR<0.001 Kolmogorov Smirnov test, **Fig. 6I**, left panel) as well as expression of HLMF marker genes (i.e., *PDGFRA*) (**Fig. 6H, I**, right panels). Corroborating our findings *in vivo*, RNAseq and GSEA(38) of CLDN1 mAb treated primary patient-derived HLMFs validated suppression of liver fibrosis associated myofibroblast differentiation states (**Fig. 6J**). Thus, marker genes of scar-associated myofibroblasts type A (**Suppl Table 9**), the major phenotype of myofibroblasts reported to expand in fibrotic liver(19) were significantly suppressed in CLDN1 mAb treated HLMFs compared to cells treated with a control antibody (FDR=0.06, Kolmogorov Smirnov test, **Fig. 6J**). Genes related to scar-associated myofibroblasts type B (portal fibroblasts, **Suppl. Table 10**) on the other hand remained unchanged by CLDN1 mAb (**Fig. 6J**)(19). Similar as observed in hepatocytes, CLDN1 mAb strongly suppressed TNF α -NF κ B signaling in HLMFs (FDR= 0.03, Kolmogorov, Smirnov-test, **Fig. 6K**). Finally, we confirmed the direct downstream effects on myofibroblast effector functions, such as fibroblast contractility and ECM production. CLDN1 mAb treatment of HLMFs from different donors (**Suppl. Table 2**) markedly suppressed key activation markers, including *ACTA2*, *COL1A1* and fibronectin (*FN1*) (p=0.003, p=0.01 and p=0.02, Wilcoxon matched pairs test, **Fig. 6L**). Collectively, these data suggest that CLDN1 mAb reverses the differentiation of profibrogenic myofibroblasts by interfering with TNF α -NF κ B signaling.

Focusing next on immune cell signatures in liver tissues of patients and animal models, we observed a strong and significant suppressive effect of CLDN1 mAb treatment on fibrosis-associated macrophage activation (GO: POSITIVE_REGULATION_OF_MACROPHAGE_ACTIVATION, MSigDB) (FDR<0.01, Kolmogorov Smirnov-test, **Fig. 6M**). Expression of ITGAX, also known as CD11c(47) as well as TREM2, recently defined as the key marker of scar-associated pro-fibrogenic macrophages(19) was markedly downregulated in the livers of CLDN1 mAb treated NASH fibrosis mice (**Fig. 6N**). Consistently, in pro-inflammatory (M1) primary Kupffer cells (**Suppl. Table 2**), CLDN1 mAb treatment suppressed *TNF α* and *IL6* gene expression, two cytokines implicated in liver fibrogenesis and hepatocarcinogenesis (p=0.03 and p=0.01, Wilcoxon matched pairs test, respectively, **Fig. 6O**, left panels). Moreover, CLDN1 mAb treatment

significantly reduced *TIMP1* expression, a potent inhibitor of matrix degradation and macrophage-mediated resolution of fibrosis ($p=0.03$, Wilcoxon matched pairs test, **Fig. 6O**, right panel). These data suggest that CLDN1 mAb inhibits the differentiation and activation of Kupffer cells into a pro-inflammatory and pro-fibrogenic phenotype.

Collectively, our integrative analyses in patient liver tissues, patient-derived mouse models, cell lines and primary cells, demonstrate that treatment with CLDN1 mAb reverses fibrosis-associated cell fate and plasticity in the three major cell types mediating fibrosis.

CLDN1 is a candidate target for treatment of lung and kidney fibrosis

As the discovered mechanistic role of CLDN1 during fibrosis is not necessarily limited to the liver, a CLDN1-targeted therapy holds the potential to be effective for other fibrotic diseases. Indeed, several studies have suggested a role of CLDN1 in the pathogenesis of chronic kidney disease(48, 49). However, its role as therapeutic target remains unknown. Upregulation of *CLDN1* expression in patients with glomerulonephritis as well as murine fibrotic kidneys(50) ($p=0.009$ and $p<0.0001$, t-test, respectively, **Fig. 7A**) validates the involvement of *CLDN1* in the pathogenesis of renal fibrotic disease. Furthermore, *CLDN1* was significantly overexpressed in patients with idiopathic pulmonary fibrosis (IPF)(51) as well as lung fibrosis(52), independent of the etiology ($p=0.0001$ and $p<0.0001$, t-test, respectively, **Fig. 7B**). Strikingly, *CLDN1* expression was also significantly upregulated in lungs of patients with COVID19 disease ($p<0.0001$, t-test, **Fig. 7B**, right panel) associated with high morbidity and mortality due to pulmonary complications including fibrosis(53). These findings indicate an implication of CLDN1 in fibrogenesis across organs.

To investigate the role of CLDN1 as a therapeutic target we used two state-of-the-art mouse models for kidney and lung fibrosis (**Fig. 7C**). Treatment with the murinized CLDN1-specific mAb (**Suppl. Fig. S2**) resulted in robust anti-fibrotic effects in the unilateral ureteral obstruction (UUO) mouse model of kidney fibrosis(54) as shown by a marked and significant decrease in collagen proportionate area in kidney sections of mAb-treated compared to the

control group (median collagen proportionate area: 2.89% vs. 7.49%, $p=0.0003$, U-test, **Fig. 7D-E, Suppl. Table 11**). Moreover, histological assessment of mouse kidneys revealed a suppression of macrophage infiltration by CLDN1 mAb (**Fig. 7F**).

In lung fibrosis, the effects of CLDN1 mAb were studied in a bleomycin-induced pulmonary fibrosis mouse model compared to dexamethasone, a frequently off-label used drug with protective effects in lung fibrosis patients(4) (**Fig. 7C**). Treatment with CLDN1 mAb suppressed lung fibrosis in these animals as shown by a significant decrease in Ashcroft score(55) ($p=0.04$, U-test, **Fig. 7G, Suppl. Table 12**) as well as Masson's Trichrome staining (**Fig. 7H**). Similar to the liver, CLDN1 was expressed and regulated via $\text{TNF}\alpha$ - $\text{NF}\kappa\text{B}$ signaling in both lung (**Fig. 7I-J**, left panel) and kidney fibroblasts (**Fig. 7J**, right panel) ($p<0.0001$ and $p<0.001$, t-test, respectively). In line with the role of CLDN1 in liver cell fate and differentiation (**Figs. 5-6**), treatment of IPF patient-derived myofibroblasts with CLDN1 mAb resulted in reversal of previously described pro-fibrogenic lung fibroblast differentiation states (56) (**Fig. 7K**). CLDN1 mAb strongly suppressed expression of marker genes of ACTA2^+ myofibroblasts, PLIN2^+ lipomyofibroblasts, and HAS1^{hi} fibroblasts (**Suppl. Table 13-15**), that were reported to expand in fibrotic IPF lungs (FDR=0.04, FDR=0.05 and FDR=0.03, Kolmogorov-Smirnov-test, respectively)(56). As observed in HLMFs, CLDN1 mAb-treatment suppressed $\text{TNF}\alpha$ - $\text{NF}\kappa\text{B}$ signaling in primary lung fibroblasts (FDR=0.01, Kolmogorov-Smirnov test, **Fig. 7L**). Collectively, these findings uncover CLDN1 as a previously unknown candidate target for kidney and lung fibrosis which warrants further investigation.

ALE.F02, an anti-CLDN1 therapeutic candidate antibody for treating human fibrotic diseases, is safe in cynomolgus monkeys

Given the role of CLDN1 in the barrier function of epithelial cells, a thorough and in-depth safety analysis of non-junctional CLDN1 targeted therapies is key for any clinical translation. Our safety studies in mice including epithelial function tests, histopathology of major organs, complete serum chemistry and renal and hepato-biliary function tests did not identify any

detectable adverse effects of CLDN1-targeting mAbs (**Suppl. Fig. S3, Suppl. Table 4**). To ensure the safety of CLDN1-mAbs in a species with full human target homology and equivalent antibody affinity, toxicity studies were expanded to non-human primates (**Suppl. Table 16**). As a candidate for future human therapeutic applications, we chose a fully humanized variant derived from the same original OM-7D3-B3 rat anti-human CLDN1 antibody clone(12, 13) as H3L3 which we designated ALE.F02. Differently from H3L3, the Fc region of the ALE.F02 molecule contains three mutations (L234F, L235E and P331S) which have been introduced to reduce binding to Fc gamma receptors whilst maintaining binding to the neonatal Fc receptor. To conduct a combined non-GLP dose-range finding and toxicology study, we chose cynomolgus monkeys (*M. fascicularis*), where the sequence of CLDN1 and its binding epitope is 100% conserved. A rapid escalation protocol achieved safe, multiple weekly dosing up to the highest tested dose of 150 mg/kg. No major clinical / behavioral changes were observed and temperature, feeding, bodyweight remained normal throughout the observational period. Most importantly, there was no indication of NISCH syndrome in the animals, a condition caused by genetic CLDN1-deficiency in humans associated with defects in the epithelial barrier function. These confirmed that CLDN1-targeted therapies are safe *in vivo* and that ALE.F02 did not affect the integrity or barrier function of tight junctions. ALE.F02 serum levels were analyzed by ELISA and PK modeling were performed, indicating a dose-dependent, sustainable and effective antibody level in macaques (**Fig. 8A**). Using the monkey data, CLDN1 receptor occupancy in humans were predicted for single doses of 0.3, 1, 3, 10 and 30 mg/kg ALE-F02. Simulations with an inter-individual variability predicted that PK profiles in humans with a single dose of ~10 mg/kg ALE-F02 fully saturate CLDN1 for about 2 weeks (**Fig. 8B**).

DISCUSSION

In this study we uncovered non-junctional CLDN1 as a mediator and therapeutic target for tissue fibrosis – a major global health challenge with limited therapeutic options. Using the liver

as a model of chronic inflammation-associated fibrogenesis and carcinogenesis we show that targeting non-junctional CLDN1 by highly specific mAbs effectively inhibit tissue fibrosis progression and tumor development across a large series of complementary patient-derived *in vivo* and *ex vivo* model systems. Our data show that targeting non-junctional CLDN1 by specific mAbs (i) robustly reduce liver inflammation, fibrosis, tumor development and tumor burden in NASH fibrosis mouse models (**Fig. 2-3**); (ii) strongly reduces liver fibrosis in state-of-the-art *ex vivo* patient-derived models (**Fig. 4**) and (iii) reverses transcriptomic liver disease signatures predictive for liver fibrosis progression and HCC risk *in vivo* and *ex vivo* (**Fig. 4-5**).

A key strength of our study is its focus on authentic patient-derived model systems, the consistency of results across complementary model systems, different organs and patient cohorts supporting its validity and translatability into the clinic. While knockout studies in cell-based models confirmed the functional role of CLDN1 as a driver of cell circuits in liver fibrosis (**Suppl. Fig. S4**), a potential limitation could be the absence of genetic *in vivo* knockout studies. Since a genetic KO will result in loss of CLDN1 tight junction barrier function, it would therefore be not suitable to study the specific role of non-junctional CLDN1. Indeed, due to its key role in development and barrier function(57), congenital CLDN1 knockout is lethal in mice(58).

Our comprehensive analysis and results suggest the following model (**Suppl. Fig. S6**): Persistent inflammation due to chronic liver disease results in the upregulation of non-junctional CLDN1 on the cell membrane in Kupffer cells, myofibroblasts and hepatocytes via TNF α -NF κ B signaling (**Fig. 1**). Within the cell membrane non-junctional CLDN1 is part of a membranous complex that cross-talks with receptor tyrosine kinases (RTKs) and growth factor signaling. Interference of CLDN1-RTK interaction by CLDN1 mAb inhibits pro-fibrogenic and pro-carcinogenic signaling, i.e., NF κ B, MAPK, Src(3, 43) (**Fig. 5-6**). Our detailed gene expression analyses revealed that non-junctional CLDN1 plays a key role in cell fate and plasticity of hepatocytes and non-parenchymal cells which is line with its functional role in EMT and organ development(59). The reprogramming of hepatocytes and its microenvironment ultimately results in the attenuation of tissue fibrosis and HCC risk (**Fig. 5-6**).

CLDN1-targeting strategies for treatment of liver fibrosis are a novel, effective and differentiated concept. The large majority of liver disease therapeutics target metabolism, inflammation or cell death, which are relevant in the early stage of disease. Only few compounds with potential anti-fibrotic properties have entered clinical development with largely disappointing results in terms of efficacy, while displaying considerable safety issues(60-62). Moreover, as shown recently for GLP1 analogues(63), robust improvement of steatosis and inflammation does not necessarily induce improvement of fibrosis. A key differentiator of CLDN1-specific mAb is the combination of robust anti-fibrotic and HCC preventive effect as demonstrated across preclinical models (**Fig. 1-4**), which addresses the key unmet medical need in advanced liver fibrosis.

Our data obtained here and in previous studies(12-14) demonstrates that the administration of the antibody is safe without detectable adverse and off-target effects. This is due to a specific binding of the developed mAb to a conformation-dependent epitope on CLDN1 which is concealed in CLDN1 functionally associated in TJs(12) (**Fig. 1**). Safety studies in non-human primates (**Fig. 8** and **Suppl. Table 16**) demonstrate that even repeated high dose administration does not induce any major adverse effects and support a further clinical development in humans. Given the preclinical data, the target population for CLDN1 mAb therapies will be patients with F3/F4 fibrosis at risk for HCC.

Beyond the liver, our *in vivo* data suggest that CLDN1 is also a previously unrecognized candidate target for kidney and lung fibrosis – two entities of high morbidity and mortality with unsatisfactory treatment options(4, 5). Given the observed upregulation of *CLDN1* expression in lung tissues of patients with COVID19 (**Fig. 7**), CLDN1-targeting approaches may also offer an approach for prevention and treatment of COVID19-associated lung fibrosis(53). Our functional studies suggest common mechanisms across organs as demonstrated by similar inhibition profiles of lung fibroblast differentiation by CLDN1 mAb via interference with TNF α -NF κ B signaling (**Fig. 7**). However, given the expression of CLDN1 in organ-specific cell types of distinct function such as parietal epithelial cells in the kidney(64) or aberrant basaloid(65) in the lung, it is likely that also additional organ-specific mechanisms are at play.

Collectively, the development of CLDN1-specific mAb provides an opportunity for the clinical development of a first-in-class compound for treatment of organ fibrosis, a major and rapidly growing unmet medical need world-wide. Good tolerability, absence of adverse toxicological finding, and adequate pharmacokinetic profile of a lead candidate antibody suggest that such a therapeutic approach may become reality in the near future.

MATERIAL AND METHODS

Study design. The primary objective of this study was to evaluate non-junctional CLDN1 as a driver of organ fibrosis. This was accomplished by combining target expression analysis in healthy and diseased patients with complementary intervention studies in patient-derived *in vivo* and *ex vivo* model systems and mechanistic studies. Thus, computational transcriptomic analyses were conducted in publicly available and own patient cohorts of chronic liver disease. Target expression was characterized on major primary liver cell populations derived from at least 3 different donors. Genetic knockout-studies were performed to validate CLDN1 as a driver of liver disease progression and HCC risk. Non-junctional CLDN1 accessible by highly specific humanized mAb was further evaluated as a target to treat fibrosis in a large set of complementary *in vivo* (humanized and NASH fibrosis mouse model, UUO kidney fibrosis and bleomycin lung fibrosis model) and *ex vivo* models (bioprinted tissues, patient-derived spheroids and precision cut liver slices). Finally, transcriptomic analyses of liver tissues derived from *in vivo* mouse studies were used to determine the molecular mechanism of CLDN1 mAb mediated treatment effects. Key elements of CLDN1 mAb mediated molecular effects were validated in patient-derived fibroblasts and Kupffer cells, as well as cell line models of chronic liver disease. Finally, in preparation for clinical translation, we characterized target specificity and validated the pharmacological and safety properties of a humanized anti-CLDN1 antibody in non-human primates. Experiments were not blinded and performed in triplicates in at least three independent experiments, unless otherwise stated. Patient tissues for *ex vivo* and *in vitro* studies were randomly assigned.

Human subjects and patient cohorts. Human liver tissue samples were obtained from patients who had undergone liver resections between 2014 and 2020 at the Center for Digestive and Liver Disease (Pôle Hépatodigestif) at the Strasbourg University Hospitals, University of Strasbourg, France. All patients provided a written informed consent, the protocol followed the ethical principles of the declaration of Helsinki and was approved by the ethics committee of the University Hospital of Strasbourg and the local independent ethics committee

(comités de protection des personnes). Demographic data and clinical characteristics of patients enrolled are summarized in **Suppl. Table 1-2 and 5-6**, respectively. Datasets of clinical cohorts with chronic liver disease (GSE34798, GSE83148, GSE49541), chronic kidney disease (GSE11585), kidney fibrosis (GSE60685(50)), IPF (GSE2052(51)), lung fibrosis (GSE24988(52)) and COVID 19 disease (GSE150316) were selected following comprehensive database analysis, where we identified CLDN1 as part of the microarray data. Liver scRNAseq data (GSE124395 and GSE136103) were investigated using publicly available webtools (<http://human-liver-cell-atlas.ie-freiburg.mpg.de/> and <https://shiny.igmm.ed.ac.uk/livercellatlas/>).

Bioinformatic and statistical analyses. Human RNAseq data was mapped using HISAT2(66) to the human genome hg19. Mouse RNAseq data was mapped to the mouse genome mm10 and annotated using the Gencode vM15 gene annotation. Data from humanized mice were mapped similarly, but to an artificial genome consisting of all human (hg19) and mouse (mm10) chromosomes, and only reads mapping to human chromosomes were kept for further analysis as described(67). Reads were counted with htseq-count, and a differentially expression analysis was performed with DESeq2 applying GENCODE 19(68). Gene Set Enrichment Analysis (GSEA)(38) was used for unbiased pathway analysis using Molecular Signature Database (MSigDB)(69). Unbiased assessment of HALLMARK(70), Gene ontology and curated gene sets(69) were used for primary screening of clinical relevant signaling pathways and cell circuits, that were then subsequently analyzed in RNAseq data of our mouse models. Results from GSEA were adjusted for the false discovery rate (FDR). $FDR < 0.25$ was considered as statistically significant. All gene sets used for final analysis (**Fig. 5**) are listed in **Suppl. Table 17**. All other data was compared using t-test, when normally distributed or non-parametric tests (U-test and Fisher test) when non-normally distributed (Shapiro-Wilk test). Functional results in patient-derived liver cells were compared using Mann-Whitney matched paired test. Results with a p-value < 0.05 were considered statistically significant.

REFERENCES

1. D. C. Rockey, P. D. Bell, J. A. Hill, Fibrosis--a common pathway to organ injury and failure. *The New England journal of medicine* **372**, 1138-1149 (2015).
2. C. Chandler, T. Liu, R. Buckanovich, L. G. Coffman, The double edge sword of fibrosis in cancer. *Transl Res* **209**, 55-67 (2019).
3. N. Roehlen, E. Crouchet, T. F. Baumert, Liver Fibrosis: Mechanistic Concepts and Therapeutic Perspectives. *Cells* **9**, (2020).
4. L. Richeldi, F. Varone, M. Bergna, J. de Andrade, J. Falk, R. Hallowell, S. Jouneau, Y. Kondoh, L. Morrow, W. Randerath, M. Streck, G. Tabaj, Pharmacological management of progressive-fibrosing interstitial lung diseases: a review of the current evidence. *Eur Respir Rev* **27**, (2018).
5. M. Ruiz-Ortega, S. Rayego-Mateos, S. Lamas, A. Ortiz, R. R. Rodrigues-Diez, Targeting the progression of chronic kidney disease. *Nat Rev Nephrol* **16**, 269-288 (2020).
6. D. Kim, A. A. Li, B. J. Perumpail, C. Gadiparthi, W. Kim, G. Cholankeril, J. S. Glenn, S. A. Harrison, Z. M. Younossi, A. Ahmed, Changing trends in etiology-based and ethnicity-based annual mortality rates of cirrhosis and hepatocellular carcinoma in the United States. *Hepatology* **69**, 1064-1074 (2019).
7. L. Kulik, H. B. El-Serag, Epidemiology and Management of Hepatocellular Carcinoma. *Gastroenterology* **156**, 477-491 e471 (2019).
8. H. Hagstrom, P. Nasr, M. Ekstedt, U. Hammar, P. Stal, R. Hultcrantz, S. Kechagias, Fibrosis stage but not NASH predicts mortality and time to development of severe liver disease in biopsy-proven NAFLD. *Journal of hepatology* **67**, 1265-1273 (2017).

9. F. Kanwal, J. Kramer, S. M. Asch, M. Chayanupatkul, Y. Cao, H. B. El-Serag, Risk of Hepatocellular Cancer in HCV Patients Treated With Direct-Acting Antiviral Agents. *Gastroenterology* **153**, 996-1005 e1001 (2017).
10. P. Manka, A. Zeller, W. K. Syn, Fibrosis in Chronic Liver Disease: An Update on Diagnostic and Treatment Modalities. *Drugs* **79**, 903-927 (2019).
11. M. B. Zeisel, P. Dhawan, T. F. Baumert, Tight junction proteins in gastrointestinal and liver disease. *Gut*, (2018).
12. I. Fofana, S. E. Krieger, F. Grunert, S. Glauben, F. Xiao, S. Fafi-Kremer, E. Soulier, C. Royer, C. Thumann, C. J. Mee, J. A. McKeating, T. Dragic, P. Pessaux, F. Stoll-Keller, C. Schuster, J. Thompson, T. F. Baumert, Monoclonal anti-claudin 1 antibodies prevent hepatitis C virus infection of primary human hepatocytes. *Gastroenterology* **139**, 953-964, 964 e951-954 (2010).
13. C. C. Colpitts, R. G. Tawar, L. Mailly, C. Thumann, L. Heydmann, S. C. Durand, F. Xiao, E. Robinet, P. Pessaux, M. B. Zeisel, T. F. Baumert, Humanisation of a claudin-1-specific monoclonal antibody for clinical prevention and cure of HCV infection without escape. *Gut* **67**, 736-745 (2018).
14. L. Mailly, F. Xiao, J. Lupberger, G. K. Wilson, P. Aubert, F. H. T. Duong, D. Calabrese, C. Leboeuf, I. Fofana, C. Thumann, S. Bandiera, M. Lutgehetmann, T. Volz, C. Davis, H. J. Harris, C. J. Mee, E. Girardi, B. Chane-Woon-Ming, M. Ericsson, N. Fletcher, R. Bartenschlager, P. Pessaux, K. Vercauteren, P. Meuleman, P. Villa, L. Kaderali, S. Pfeffer, M. H. Heim, M. Neunlist, M. B. Zeisel, M. Dandri, J. A. McKeating, E. Robinet, T. F. Baumert, Clearance of persistent hepatitis C virus infection in humanized mice using a claudin-1-targeting monoclonal antibody. *Nature biotechnology* **33**, 549-554 (2015).
15. A. L. Rasmussen, N. Tchitchek, N. J. Susnow, A. L. Krasnoselsky, D. L. Diamond, M. M. Yeh, S. C. Proll, M. J. Korth, K. A. Walters, S. Lederer, A. M. Larson, R. L. Carithers,

- A. Benecke, M. G. Katze, Early transcriptional programming links progression to hepatitis C virus-induced severe liver disease in transplant patients. *Hepatology* **56**, 17-27 (2012).
16. W. Zhou, Y. Ma, J. Zhang, J. Hu, M. Zhang, Y. Wang, Y. Li, L. Wu, Y. Pan, Y. Zhang, X. Zhang, X. Zhang, Z. Zhang, J. Zhang, H. Li, L. Lu, L. Jin, J. Wang, Z. Yuan, J. Liu, Predictive model for inflammation grades of chronic hepatitis B: Large-scale analysis of clinical parameters and gene expressions. *Liver international : official journal of the International Association for the Study of the Liver* **37**, 1632-1641 (2017).
 17. C. A. Moylan, H. Pang, A. Dellinger, A. Suzuki, M. E. Garrett, C. D. Guy, S. K. Murphy, A. E. Ashley-Koch, S. S. Choi, G. A. Michelotti, D. D. Hampton, Y. Chen, H. L. Tillmann, M. A. Hauser, M. F. Abdelmalek, A. M. Diehl, Hepatic gene expression profiles differentiate presymptomatic patients with mild versus severe nonalcoholic fatty liver disease. *Hepatology* **59**, 471-482 (2014).
 18. N. Aizarani, A. Saviano, Sagar, L. Mailly, S. Durand, J. S. Herman, P. Pessaux, T. F. Baumert, D. Grun, A human liver cell atlas reveals heterogeneity and epithelial progenitors. *Nature* **572**, 199-204 (2019).
 19. P. Ramachandran, R. Dobie, J. R. Wilson-Kanamori, E. F. Dora, B. E. P. Henderson, N. T. Luu, J. R. Portman, K. P. Matchett, M. Brice, J. A. Marwick, R. S. Taylor, M. Efremova, R. Vento-Tormo, N. O. Carragher, T. J. Kendall, J. A. Fallowfield, E. M. Harrison, D. J. Mole, S. J. Wigmore, P. N. Newsome, C. J. Weston, J. P. Iredale, F. Tacke, J. W. Pollard, C. P. Ponting, J. C. Marioni, S. A. Teichmann, N. C. Henderson, Resolving the fibrotic niche of human liver cirrhosis at single-cell level. *Nature* **575**, 512-518 (2019).
 20. Y. Li, J. Wang, K. Asahina, Mesothelial cells give rise to hepatic stellate cells and myofibroblasts via mesothelial-mesenchymal transition in liver injury. *Proceedings of*

- the National Academy of Sciences of the United States of America* **110**, 2324-2329 (2013).
21. Z. Zong, J. Zou, R. Mao, C. Ma, N. Li, J. Wang, X. Wang, H. Zhou, L. Zhang, Y. Shi, M1 Macrophages Induce PD-L1 Expression in Hepatocellular Carcinoma Cells Through IL-1beta Signaling. *Front Immunol* **10**, 1643 (2019).
 22. H. Azuma, N. Paulk, A. Ranade, C. Dorrell, M. Al-Dhalimy, E. Ellis, S. Strom, M. A. Kay, M. Finegold, M. Grompe, Robust expansion of human hepatocytes in Fah^{-/-}/Rag2^{-/-}/Il2rg^{-/-} mice. *Nature biotechnology* **25**, 903-910 (2007).
 23. A. Teufel, T. Itzel, W. Erhart, M. Brosch, X. Y. Wang, Y. O. Kim, W. von Schonfels, A. Herrmann, S. Bruckner, F. Stickel, J. F. Dufour, T. Chavakis, C. Hellerbrand, R. Spang, T. Maass, T. Becker, S. Schreiber, C. Schafmayer, D. Schuppan, J. Hampe, Comparison of Gene Expression Patterns Between Mouse Models of Nonalcoholic Fatty Liver Disease and Liver Tissues From Patients. *Gastroenterology* **151**, 513-525 e510 (2016).
 24. N. Kishida, S. Matsuda, O. Itano, M. Shinoda, M. Kitago, H. Yagi, Y. Abe, T. Hibi, Y. Masugi, K. Aiura, M. Sakamoto, Y. Kitagawa, Development of a novel mouse model of hepatocellular carcinoma with nonalcoholic steatohepatitis using a high-fat, choline-deficient diet and intraperitoneal injection of diethylnitrosamine. *BMC gastroenterology* **16**, 61 (2016).
 25. D. E. Kleiner, E. M. Brunt, M. Van Natta, C. Behling, M. J. Contos, O. W. Cummings, L. D. Ferrell, Y. C. Liu, M. S. Torbenson, A. Unalp-Arida, M. Yeh, A. J. McCullough, A. J. Sanyal, Design and validation of a histological scoring system for nonalcoholic fatty liver disease. *Hepatology* **41**, 1313-1321 (2005).
 26. D. Carter, S. Presnell, B. David, A. Chen, Modeling NAFLD using 3D bioprinted human liver tissue. *Journal of hepatology* **68**, (2018).

27. D. Antoni, H. Burckel, E. Josset, G. Noel, Three-dimensional cell culture: a breakthrough in vivo. *International journal of molecular sciences* **16**, 5517-5527 (2015).
28. Y. Song, J. S. Kim, S. H. Kim, Y. K. Park, E. Yu, K. H. Kim, E. J. Seo, H. B. Oh, H. C. Lee, K. M. Kim, H. R. Seo, Patient-derived multicellular tumor spheroids towards optimized treatment for patients with hepatocellular carcinoma. *Journal of experimental & clinical cancer research : CR* **37**, 109 (2018).
29. D. Heinrichs, M. L. Berres, A. Nellen, P. Fischer, D. Scholten, C. Trautwein, H. E. Wasmuth, H. Sahin, The chemokine CCL3 promotes experimental liver fibrosis in mice. *PLoS One* **8**, e66106 (2013).
30. J. J. Connolly, K. Ooka, J. K. Lim, Future Pharmacotherapy for Non-alcoholic Steatohepatitis (NASH): Review of Phase 2 and 3 Trials. *J Clin Transl Hepatol* **6**, 264-275 (2018).
31. S. Nakagawa, L. Wei, W. M. Song, T. Higashi, S. Ghoshal, R. S. Kim, C. B. Bian, S. Yamada, X. Sun, A. Venkatesh, N. Goossens, G. Bain, G. Y. Lauwers, A. P. Koh, M. El-Abtah, N. B. Ahmad, H. Hoshida, D. J. Erstad, G. Gunasekaran, Y. Lee, M. L. Yu, W. L. Chuang, C. Y. Dai, M. Kobayashi, H. Kumada, T. Beppu, H. Baba, M. Mahajan, V. D. Nair, M. Lanuti, A. Villanueva, A. Sangiovanni, M. Iavarone, M. Colombo, J. M. Llovet, A. Subramanian, A. M. Tager, S. L. Friedman, T. F. Baumert, M. E. Schwarz, R. T. Chung, K. K. Tanabe, B. Zhang, B. C. Fuchs, Y. Hoshida, Molecular Liver Cancer Prevention in Cirrhosis by Organ Transcriptome Analysis and Lysophosphatidic Acid Pathway Inhibition. *Cancer cell* **30**, 879-890 (2016).
32. Y. Hoshida, A. Villanueva, M. Kobayashi, J. Peix, D. Y. Chiang, A. Camargo, S. Gupta, J. Moore, M. J. Wrobel, J. Lerner, M. Reich, J. A. Chan, J. N. Glickman, K. Ikeda, M. Hashimoto, G. Watanabe, M. G. Daidone, S. Roayaie, M. Schwartz, S. Thung, H. B. Salvesen, S. Gabriel, V. Mazzaferro, J. Bruix, S. L. Friedman, H. Kumada, J. M. Llovet,

- T. R. Golub, Gene expression in fixed tissues and outcome in hepatocellular carcinoma. *The New England journal of medicine* **359**, 1995-2004 (2008).
33. Y. Hoshida, A. Villanueva, A. Sangiovanni, M. Sole, C. Hur, K. L. Andersson, R. T. Chung, J. Gould, K. Kojima, S. Gupta, B. Taylor, A. Crenshaw, S. Gabriel, B. Minguez, M. Iavarone, S. L. Friedman, M. Colombo, J. M. Llovet, T. R. Golub, Prognostic gene expression signature for patients with hepatitis C-related early-stage cirrhosis. *Gastroenterology* **144**, 1024-1030 (2013).
 34. L. Y. King, C. Canasto-Chibuque, K. B. Johnson, S. Yip, X. Chen, K. Kojima, M. Deshmukh, A. Venkatesh, P. S. Tan, X. Sun, A. Villanueva, A. Sangiovanni, V. Nair, M. Mahajan, M. Kobayashi, H. Kumada, M. Iavarone, M. Colombo, M. I. Fiel, S. L. Friedman, J. M. Llovet, R. T. Chung, Y. Hoshida, A genomic and clinical prognostic index for hepatitis C-related early-stage cirrhosis that predicts clinical deterioration. *Gut*, (2014).
 35. N. Goossens, Y. Hoshida, W. M. Song, M. Jung, P. Morel, S. Nakagawa, B. Zhang, J. L. Frossard, L. Spahr, S. L. Friedman, F. Negro, L. Rubbia-Brandt, E. Giostra, Nonalcoholic Steatohepatitis Is Associated With Increased Mortality in Obese Patients Undergoing Bariatric Surgery. *Clinical gastroenterology and hepatology : the official clinical practice journal of the American Gastroenterological Association* **14**, 1619-1628 (2016).
 36. A. Villanueva, Y. Hoshida, C. Battiston, V. Tovar, D. Sia, C. Alsinet, H. Cornella, A. Liberzon, M. Kobayashi, H. Kumada, S. N. Thung, J. Bruix, P. Newell, C. April, J. B. Fan, S. Roayaie, V. Mazzaferro, M. E. Schwartz, J. M. Llovet, Combining clinical, pathology, and gene expression data to predict recurrence of hepatocellular carcinoma. *Gastroenterology* **140**, 1501-1512 e1502 (2011).
 37. T. Luangmonkong, S. Suriguga, E. Bigaeva, M. Boersema, D. Oosterhuis, K. P. de Jong, D. Schuppan, H. A. M. Mutsaers, P. Olinga, Evaluating the antifibrotic potency of

- galunisertib in a human ex vivo model of liver fibrosis. *Br J Pharmacol* **174**, 3107-3117 (2017).
38. A. Subramanian, P. Tamayo, V. K. Mootha, S. Mukherjee, B. L. Ebert, M. A. Gillette, A. Paulovich, S. L. Pomeroy, T. R. Golub, E. S. Lander, J. P. Mesirov, Gene set enrichment analysis: a knowledge-based approach for interpreting genome-wide expression profiles. *Proceedings of the National Academy of Sciences of the United States of America* **102**, 15545-15550 (2005).
 39. S. Bandiera, S. Pernot, H. El Saghire, S. C. Durand, C. Thumann, E. Crouchet, T. Ye, I. Fofana, M. A. Oudot, J. Barths, C. Schuster, P. Pessaux, M. H. Heim, T. F. Baumert, M. B. Zeisel, Hepatitis C Virus-Induced Upregulation of MicroRNA miR-146a-5p in Hepatocytes Promotes Viral Infection and Deregulates Metabolic Pathways Associated with Liver Disease Pathogenesis. *Journal of virology* **90**, 6387-6400 (2016).
 40. O. Bauhofer, A. Ruggieri, B. Schmid, P. Schirmacher, R. Bartenschlager, Persistence of HCV in quiescent hepatic cells under conditions of an interferon-induced antiviral response. *Gastroenterology* **143**, 429-438 e428 (2012).
 41. J. Lupberger, T. Croonenborghs, A. A. Roca Suarez, N. Van Renne, F. Juhling, M. A. Oudot, A. Virzi, S. Bandiera, C. Jamey, G. Meszaros, D. Brumaru, A. Mukherji, S. C. Durand, L. Heydmann, E. R. Verrier, H. El Saghire, N. Hamdane, R. Bartenschlager, S. Fereshetian, E. Ramberger, R. Sinha, M. Nabian, C. Everaert, M. Jovanovic, P. Mertins, S. A. Carr, K. Chayama, N. Dali-Youcef, R. Ricci, N. M. Bardeesy, N. Fujiwara, O. Gevaert, M. B. Zeisel, Y. Hoshida, N. Pochet, T. F. Baumert, Combined Analysis of Metabolomes, Proteomes, and Transcriptomes of Hepatitis C Virus-Infected Cells and Liver to Identify Pathways Associated With Disease Development. *Gastroenterology* **157**, 537-551 e539 (2019).
 42. F. Juhling, N. Hamdane, E. Crouchet, S. Li, H. El Saghire, A. Mukherji, N. Fujiwara, M. A. Oudot, C. Thumann, A. Saviano, A. A. Roca Suarez, K. Goto, R. Masia, M. Sojoodi,

- G. Arora, H. Aikata, A. Ono, P. Tabrizian, M. Schwartz, S. J. Polyak, I. Davidson, C. Schmidl, C. Bock, C. Schuster, K. Chayama, P. Pessaux, K. K. Tanabe, Y. Hoshida, M. B. Zeisel, F. H. Duong, B. C. Fuchs, T. F. Baumert, Targeting clinical epigenetic reprogramming for chemoprevention of metabolic and viral hepatocellular carcinoma. *Gut* **70**, 157-169 (2021).
43. H. Y. Seo, S. H. Lee, J. H. Lee, Y. N. Kang, J. S. Hwang, K. G. Park, M. K. Kim, B. K. Jang, Src Inhibition Attenuates Liver Fibrosis by Preventing Hepatic Stellate Cell Activation and Decreasing Connetive Tissue Growth Factor. *Cells* **9**, (2020).
 44. H. Li, C. Zhao, Y. Tian, J. Lu, G. Zhang, S. Liang, D. Chen, X. Liu, W. Kuang, M. Zhu, Src family kinases and pulmonary fibrosis: A review. *Biomed Pharmacother* **127**, 110183 (2020).
 45. T. Zarubin, J. Han, Activation and signaling of the p38 MAP kinase pathway. *Cell research* **15**, 11-18 (2005).
 46. S. Wullschleger, R. Loewith, M. N. Hall, TOR signaling in growth and metabolism. *Cell* **124**, 471-484 (2006).
 47. M. Itoh, T. Suganami, H. Kato, S. Kanai, I. Shirakawa, T. Sakai, T. Goto, M. Asakawa, I. Hidaka, H. Sakugawa, K. Ohnishi, Y. Komohara, K. Asano, I. Sakaida, M. Tanaka, Y. Ogawa, CD11c+ resident macrophages drive hepatocyte death-triggered liver fibrosis in a murine model of nonalcoholic steatohepatitis. *JCI insight* **2**, (2017).
 48. K. Hasegawa, S. Wakino, P. Simic, Y. Sakamaki, H. Minakuchi, K. Fujimura, K. Hosoya, M. Komatsu, Y. Kaneko, T. Kanda, E. Kubota, H. Tokuyama, K. Hayashi, L. Guarente, H. Itoh, Renal tubular Sirt1 attenuates diabetic albuminuria by epigenetically suppressing Claudin-1 overexpression in podocytes. *Nat Med* **19**, 1496-1504 (2013).

49. F. R. Fritzsche, B. Oelrich, M. Johannsen, I. Kristiansen, H. Moch, K. Jung, G. Kristiansen, Claudin-1 protein expression is a prognostic marker of patient survival in renal cell carcinomas. *Clin Cancer Res* **14**, 7035-7042 (2008).
50. S. Lovisa, V. S. LeBleu, B. Tampe, H. Sugimoto, K. Vадnagara, J. L. Carstens, C. C. Wu, Y. Hagos, B. C. Burckhardt, T. Pentcheva-Hoang, H. Nischal, J. P. Allison, M. Zeisberg, R. Kalluri, Epithelial-to-mesenchymal transition induces cell cycle arrest and parenchymal damage in renal fibrosis. *Nat Med* **21**, 998-1009 (2015).
51. A. Pardo, K. Gibson, J. Cisneros, T. J. Richards, Y. Yang, C. Becerril, S. Yousem, I. Herrera, V. Ruiz, M. Selman, N. Kaminski, Up-regulation and profibrotic role of osteopontin in human idiopathic pulmonary fibrosis. *PLoS Med* **2**, e251 (2005).
52. M. Mura, M. Anraku, Z. Yun, K. McRae, M. Liu, T. K. Waddell, L. G. Singer, J. T. Granton, S. Keshavjee, M. de Perrot, Gene expression profiling in the lungs of patients with pulmonary hypertension associated with pulmonary fibrosis. *Chest* **141**, 661-673 (2012).
53. P. M. George, A. U. Wells, R. G. Jenkins, Pulmonary fibrosis and COVID-19: the potential role for antifibrotic therapy. *Lancet Respir Med* **8**, 807-815 (2020).
54. R. L. Chevalier, M. S. Forbes, B. A. Thornhill, Ureteral obstruction as a model of renal interstitial fibrosis and obstructive nephropathy. *Kidney Int* **75**, 1145-1152 (2009).
55. R. H. Hubner, W. Gitter, N. E. El Mokhtari, M. Mathiak, M. Both, H. Bolte, S. Freitag-Wolf, B. Bewig, Standardized quantification of pulmonary fibrosis in histological samples. *Biotechniques* **44**, 507-511, 514-507 (2008).
56. A. C. Habermann, A. J. Gutierrez, L. T. Bui, S. L. Yahn, N. I. Winters, C. L. Calvi, L. Peter, M. I. Chung, C. J. Taylor, C. Jetter, L. Raju, J. Roberson, G. Ding, L. Wood, J. M. S. Sucre, B. W. Richmond, A. P. Serezani, W. J. McDonnell, S. B. Mallal, M. J. Bacchetta, J. E. Loyd, C. M. Shaver, L. B. Ware, R. Bremner, R. Walia, T. S. Blackwell,

- N. E. Banovich, J. A. Kropski, Single-cell RNA sequencing reveals profibrotic roles of distinct epithelial and mesenchymal lineages in pulmonary fibrosis. *Sci Adv* **6**, eaba1972 (2020).
57. N. Roehlen, A. A. Roca Suarez, H. El Saghire, A. Saviano, C. Schuster, J. Lupberger, T. F. Baumert, Tight Junction Proteins and the Biology of Hepatobiliary Disease. *International journal of molecular sciences* **21**, (2020).
 58. M. Furuse, M. Hata, K. Furuse, Y. Yoshida, A. Haratake, Y. Sugitani, T. Noda, A. Kubo, S. Tsukita, Claudin-based tight junctions are crucial for the mammalian epidermal barrier: a lesson from claudin-1-deficient mice. *The Journal of cell biology* **156**, 1099-1111 (2002).
 59. D. H. Kim, T. Xing, Z. Yang, R. Dudek, Q. Lu, Y. H. Chen, Epithelial Mesenchymal Transition in Embryonic Development, Tissue Repair and Cancer: A Comprehensive Overview. *Journal of clinical medicine* **7**, (2017).
 60. S. A. Harrison, M. F. Abdelmalek, S. Caldwell, M. L. Shiffman, A. M. Diehl, R. Ghalib, E. J. Lawitz, D. C. Rockey, R. A. Schall, C. Jia, B. J. McColgan, J. G. McHutchison, G. M. Subramanian, R. P. Myers, Z. Younossi, V. Ratziu, A. J. Muir, N. H. Afdhal, Z. Goodman, J. Bosch, A. J. Sanyal, U. S. Gs, G.-U.-. Investigators, Simtuzumab Is Ineffective for Patients With Bridging Fibrosis or Compensated Cirrhosis Caused by Nonalcoholic Steatohepatitis. *Gastroenterology* **155**, 1140-1153 (2018).
 61. A. Mullard, FDA rejects NASH drug. *Nature reviews. Drug discovery* **19**, 501 (2020).
 62. A. J. Sanyal, N. Chalasani, K. V. Kowdley, A. McCullough, A. M. Diehl, N. M. Bass, B. A. Neuschwander-Tetri, J. E. Lavine, J. Tonascia, A. Unalp, M. Van Natta, J. Clark, E. M. Brunt, D. E. Kleiner, J. H. Hoofnagle, P. R. Robuck, C. R. N. Nash, Pioglitazone, vitamin E, or placebo for nonalcoholic steatohepatitis. *The New England journal of medicine* **362**, 1675-1685 (2010).

63. P. N. Newsome, K. Buchholtz, K. Cusi, M. Linder, T. Okanoue, V. Ratziu, A. J. Sanyal, A. S. Sejling, S. A. Harrison, N. N. Investigators, A Placebo-Controlled Trial of Subcutaneous Semaglutide in Nonalcoholic Steatohepatitis. *The New England journal of medicine* **384**, 1113-1124 (2021).
64. R. Koda, A. Yoshino, Y. Imanishi, S. Kawamoto, Y. Ueda, E. Yaoita, J. J. Kazama, I. Narita, T. Takeda, Expression of tight junction protein claudin-1 in human crescentic glomerulonephritis. *Int J Nephrol* **2014**, 598670 (2014).
65. J. Lv, B. Sun, Z. Mai, M. Jiang, J. Du, CLDN-1 promoted the epithelial to migration and mesenchymal transition (EMT) in human bronchial epithelial cells via Notch pathway. *Mol Cell Biochem* **432**, 91-98 (2017).
66. D. Kim, B. Langmead, S. L. Salzberg, HISAT: a fast spliced aligner with low memory requirements. *Nat. Methods* **12**, 357-360 (2015).
67. N. Hamdane, F. Juhling, E. Crouchet, H. El Saghire, C. Thumann, M. A. Oudot, S. Bandiera, A. Saviano, C. Ponsolles, A. A. Roca Suarez, S. Li, N. Fujiwara, A. Ono, I. Davidson, N. Bardeesy, C. Schmidl, C. Bock, C. Schuster, J. Lupberger, F. Habersetzer, M. Doffoel, T. Piardi, D. Sommacale, M. Imamura, T. Uchida, H. Ohdan, H. Aikata, K. Chayama, T. Boldanova, P. Pessaux, B. C. Fuchs, Y. Hoshida, M. B. Zeisel, F. H. T. Duong, T. F. Baumert, HCV-Induced Epigenetic Changes Associated With Liver Cancer Risk Persist After Sustained Virologic Response. *Gastroenterology* **156**, 2313-2329 e2317 (2019).
68. J. Harrow, F. Denoeud, A. Frankish, A. Reymond, C. K. Chen, J. Chrast, J. Lagarde, J. G. Gilbert, R. Storey, D. Swarbreck, C. Rossier, C. Ucla, T. Hubbard, S. E. Antonarakis, R. Guigo, GENCODE: producing a reference annotation for ENCODE. *Genome Biol.* **7** Suppl 1, S4 1-9 (2006).

69. A. Liberzon, A. Subramanian, R. Pinchback, H. Thorvaldsdottir, P. Tamayo, J. P. Mesirov, Molecular signatures database (MSigDB) 3.0. *Bioinformatics* **27**, 1739-1740 (2011).
70. A. Liberzon, C. Birger, H. Thorvaldsdottir, M. Ghandi, J. P. Mesirov, P. Tamayo, The Molecular Signatures Database (MSigDB) hallmark gene set collection. *Cell Syst* **1**, 417-425 (2015).
71. H. Suzuki, K. Tani, A. Tamura, S. Tsukita, Y. Fujiyoshi, Model for the architecture of claudin-based paracellular ion channels through tight junctions. *J Mol Biol* **427**, 291-297 (2015).
72. H. M. Berman, J. Westbrook, Z. Feng, G. Gilliland, T. N. Bhat, H. Weissig, I. N. Shindyalov, P. E. Bourne, The Protein Data Bank. *Nucleic Acids Res* **28**, 235-242 (2000).
73. M. P. Jacobson, D. L. Pincus, C. S. Rapp, T. J. Day, B. Honig, D. E. Shaw, R. A. Friesner, A hierarchical approach to all-atom protein loop prediction. *Proteins* **55**, 351-367 (2004).
74. M. P. Jacobson, R. A. Friesner, Z. Xiang, B. Honig, On the role of the crystal environment in determining protein side-chain conformations. *J Mol Biol* **320**, 597-608 (2002).
75. K. Zhu, T. Day, D. Warshaviak, C. Murrett, R. Friesner, D. Pearlman, Antibody structure determination using a combination of homology modeling, energy-based refinement, and loop prediction. *Proteins* **82**, 1646-1655 (2014).
76. N. K. Salam, M. Adzhigirey, W. Sherman, D. A. Pearlman, Structure-based approach to the prediction of disulfide bonds in proteins. *Protein Eng Des Sel* **27**, 365-374 (2014).

77. H. Beard, A. Cholleti, D. Pearlman, W. Sherman, K. A. Loving, Applying physics-based scoring to calculate free energies of binding for single amino acid mutations in protein-protein complexes. *PLoS One* **8**, e82849 (2013).
78. M. A. Lomize, I. D. Pogozheva, H. Joo, H. I. Mosberg, A. L. Lomize, OPM database and PPM web server: resources for positioning of proteins in membranes. *Nucleic Acids Res* **40**, D370-376 (2012).
79. W. L. Jorgensen, J. Chandrasekhar, J. D. Madura, R. W. Impey, L. M. Klein, Comparison of simple potential functions for simulating liquid water. *J Chem Phys* **79**, 926-935 (1983).
80. K. Roos, C. Wu, W. Damm, M. Reboul, J. M. Stevenson, C. Lu, M. K. Dahlgren, S. Mondal, W. Chen, L. Wang, R. Abel, R. A. Friesner, E. D. Harder, OPLS3e: Extending Force Field Coverage for Drug-Like Small Molecules. *Journal of Chemical Theory and Computation* **15**, 1863-1874 (2019).
81. G. Martyna, D. Tobias, M. Klein, Constant pressure molecular dynamics algorithms. *The Journal of Chemical Physics* **101**, 4177-4189 (1994).
82. G. J. Martyna, M. L. Klein, M. Tuckerman, Nosé–Hoover chains: The canonical ensemble via continuous dynamics. *The Journal of Chemical Physics* **97**, 2635-2643 (1992).
83. K. J. Bowers, E. Chow, H. Xu, R. O. Dror, M. P. Eastwood, B. A. Gregersen, J. L. Klepeis, I. Kolossvary, M. A. Moraes, F. D. Sacerdoti, J. K. Salmon, Y. Shan, D. E. Shaw, paper presented at the Proceedings of the 2006 ACM/IEEE conference on Supercomputing, Tampa, Florida, 2006.
84. T. Tubiana, J.-C. Carvaille, Y. Boulard, S. Bressanelli, TTClust: A Versatile Molecular Simulation Trajectory Clustering Program with Graphical Summaries. *Journal of Chemical Information and Modeling* **58**, 2178-2182 (2018).

85. R. Tibshirani, G. Walther, T. Hastie, Estimating the number of clusters in a data set via the gap statistic. *Journal of the Royal Statistical Society. Series B: Statistical Methodology* **63**, 411-423 (2001).
86. G. C. P. van Zundert, J. Rodrigues, M. Trellet, C. Schmitz, P. L. Kastiris, E. Karaca, A. S. J. Melquiond, M. van Dijk, S. J. de Vries, A. Bonvin, The HADDOCK2.2 Web Server: User-Friendly Integrative Modeling of Biomolecular Complexes. *J Mol Biol* **428**, 720-725 (2016).
87. C. Dominguez, R. Boelens, A. M. J. J. Bonvin, HADDOCK: A Protein–Protein Docking Approach Based on Biochemical or Biophysical Information. *Journal of the American Chemical Society* **125**, 1731-1737 (2003).
88. J. Z. a. B. A. M. J. J. Francesco Ambrosetti F., A protocol for information-driven antibody-antigen modelling with the HADDOCK2.4 webserve. *arXiv*, (2020).
89. A. Vangone, A. M. Bonvin, Contacts-based prediction of binding affinity in protein-protein complexes. *Elife* **4**, e07454 (2015).
90. J. Freeth, J. Soden, New Advances in Cell Microarray Technology to Expand Applications in Target Deconvolution and Off-Target Screening. *SLAS Discov* **25**, 223-230 (2020).
91. M. Charni-Natan, I. Goldstein, Protocol for Primary Mouse Hepatocyte Isolation. *STAR Protoc* **1**, 100086 (2020).
92. V. Kegel, D. Deharde, E. Pfeiffer, K. Zeilinger, D. Seehofer, G. Damm, Protocol for Isolation of Primary Human Hepatocytes and Corresponding Major Populations of Non-parenchymal Liver Cells. *J Vis Exp*, e53069 (2016).
93. L. Aoudjehane, G. Bisch, O. Scatton, C. Granier, J. Gaston, C. Housset, P. Roingeard, F. L. Cosset, F. Perdigao, P. Balladur, T. Wakita, Y. Calmus, F. Conti, Infection of

- Human Liver Myofibroblasts by Hepatitis C Virus: A Direct Mechanism of Liver Fibrosis in Hepatitis C. *PloS one* **10**, e0134141 (2015).
94. M. Boeckh, M. M. Berrey, R. A. Bowden, S. W. Crawford, J. Balsley, L. Corey, Phase 1 evaluation of the respiratory syncytial virus-specific monoclonal antibody palivizumab in recipients of hematopoietic stem cell transplants. *J. Infect. Dis.* **184**, 350-354 (2001).
 95. C. A. Schneider, W. S. Rasband, K. W. Eliceiri, NIH Image to ImageJ: 25 years of image analysis. *Nat. Methods* **9**, 671-675 (2012).
 96. S. Fafi-Kremer, I. Fofana, E. Soulier, P. Carolla, P. Meuleman, G. Leroux-Roels, A. H. Patel, F. L. Cosset, P. Pessaux, M. Doffoel, P. Wolf, F. Stoll-Keller, T. F. Baumert, Viral entry and escape from antibody-mediated neutralization influence hepatitis C virus reinfection in liver transplantation. *The Journal of experimental medicine* **207**, 2019-2031 (2010).
 97. K. J. Livak, T. D. Schmittgen, Analysis of relative gene expression data using real-time quantitative PCR and the 2^{(-Delta Delta C(T))} Method. *Methods* **25**, 402-408 (2001).
 98. E. R. Verrier, C. C. Colpitts, C. Bach, L. Heydmann, A. Weiss, M. Renaud, S. C. Durand, F. Habersetzer, D. Durantel, G. Abou-Jaoude, M. M. Lopez Ledesma, D. J. Felmlee, M. Soumillon, T. Croonenborghs, N. Pochet, M. Nassal, C. Schuster, L. Brino, C. Sureau, M. B. Zeisel, T. F. Baumert, A targeted functional RNA interference screen uncovers glypican 5 as an entry factor for hepatitis B and D viruses. *Hepatology* **63**, 35-48 (2016).
 99. V. J. Barbero-Becerra, P. J. Giraudi, N. C. Chavez-Tapia, M. Uribe, C. Tiribelli, N. Rosso, The interplay between hepatic stellate cells and hepatocytes in an in vitro model of NASH. *Toxicology in vitro : an international journal published in association with BIBRA* **29**, 1753-1758 (2015).

ACKNOWLEDGMENTS

The authors thank the CRB (Centre de Ressources Biologiques-Biological Resource Centre) of the Strasbourg University Hospitals for the management of patient-derived liver tissue. The authors thank Dr. R. Bartenschlager (University of Heidelberg, Germany), Dr. C. Rice (Rockefeller University, NY) for providing plasmids for production of HCVcc Jc1 strains, Dr. M. Evans (Mount Sinai Hospital, NY) for providing mouse and human CLDN1 expression plasmids, Dr. F. Chisari (The Scripps Research Institute, La Jolla, CA) for the gift of Huh7.5.1 cells, Dr. S. Friedman (Mount Sinai Hospital, New York) for the gift of the LX2 stellate cell line, Dr. F. Habersetzer (Strasbourg University Hospitals) for patient serum samples for isolation of infectious HBV and Dr. D. Root (Broad Institute of MIT and Harvard, Cambridge, MA) for providing expression plasmids for lentiviruses and sgRNAs for CLDN1 KO. We thank C. Ponsolles for contribution to *in vitro* experiments, Prof. A. Schmitt-Graeff (Dept. of Pathology, University Hospital Freiburg) and Dr. H. Jacobs (ICS Mouse Clinic, IGBMC, Illkirch) for histopathological analyses of animal tissues and Dr. Lynda Audjehane (Human HepCell, Faculté de Médecine Pierre et Marie Curie, Site Saint-Antoine, Paris, France) for providing human myofibroblasts for part of the staining experiments.

FUNDING

European Research Council Grant ERC-AdG-2014 *HEPCIR* (T.F.B.); European Research Council Grant ERC-AdG-2020 *FIBCAN* (T.F.B.); European Research Council Grant ERC-PoC-2016 *PRELICAN* (T.F.B.); European Research Council Grant ERC-PoC-2018 *HEPCAN* (T.F.B.); European Research Council Consolidator grant *HepatoMetabopath* (M.H.); European Union EU H2020 *HEPCAR* (T.F.B. and M.H.); ARC Grant *TheraHCC2.0* IHUARC IHU201301187 (T.F.B.); ANRS Grant ECTZ103701 *CLAUDIN-1* (T.F.B.); SATT Conectus, University of Strasbourg (CANCLAU) (T.F.B.); French National Research Agency LABEX ANR-10-LABX-0028_ *HEPSYS* (T.F.B.); German Research Foundation (DFG) RO 5983/1-1 (N.R.)

AUTHOR CONTRIBUTIONS

T.F.B. initiated and coordinated the study. H.E.S., N.R., E.C., L.M., C.T, V.G.M., M.A.O., S.C., F.H.T.D., S.C.D, M.H., C.S., J.L., M.B.Z. and T.F.B. designed or performed experiments and analyzed data. A.S., S.C.D. analyzed histopathology of mouse liver tissue. Y.H. analyzed gene expression of the prognostic liver signature in part of the cell lines. F.J., H.E.S. and N.R. performed computational analyses, E.F. and P.P. prepared liver resections for *ex vivo* models. B.C.F. co-designed animal experiments and edited the manuscript. A.C. and J.S. performed structural modeling of CLDN1 mAb binding to CLDN1. G.E., M.M., R.I., T.S. designed and conducted the experiments in non-human primates. M.B.Z, C.S., J.L. and O.K. edited the manuscript. N.R., H.E.S., A.S. and T.F.B. designed the figures and wrote the manuscript.

COMPETING INTERESTS

Inserm, the University of Strasbourg, the Strasbourg University Hospitals and the Institut Hospitalo-Universitaire have filed patent applications for the use of anti-claudin-1 monoclonal antibodies for the treatment of liver disease, NASH and HCC (PCT/EP2016/055942, PCT/EP2017/056703), which have been licensed to Alentis Therapeutics, Basel.

DATA AND MATERIAL AVAILABILITY

Transcriptomic data reported in this paper have been deposited with the Gene Expression Omnibus database (GEO). All other data associated with this study are available in the main text or the supplementary materials.

Figure 1

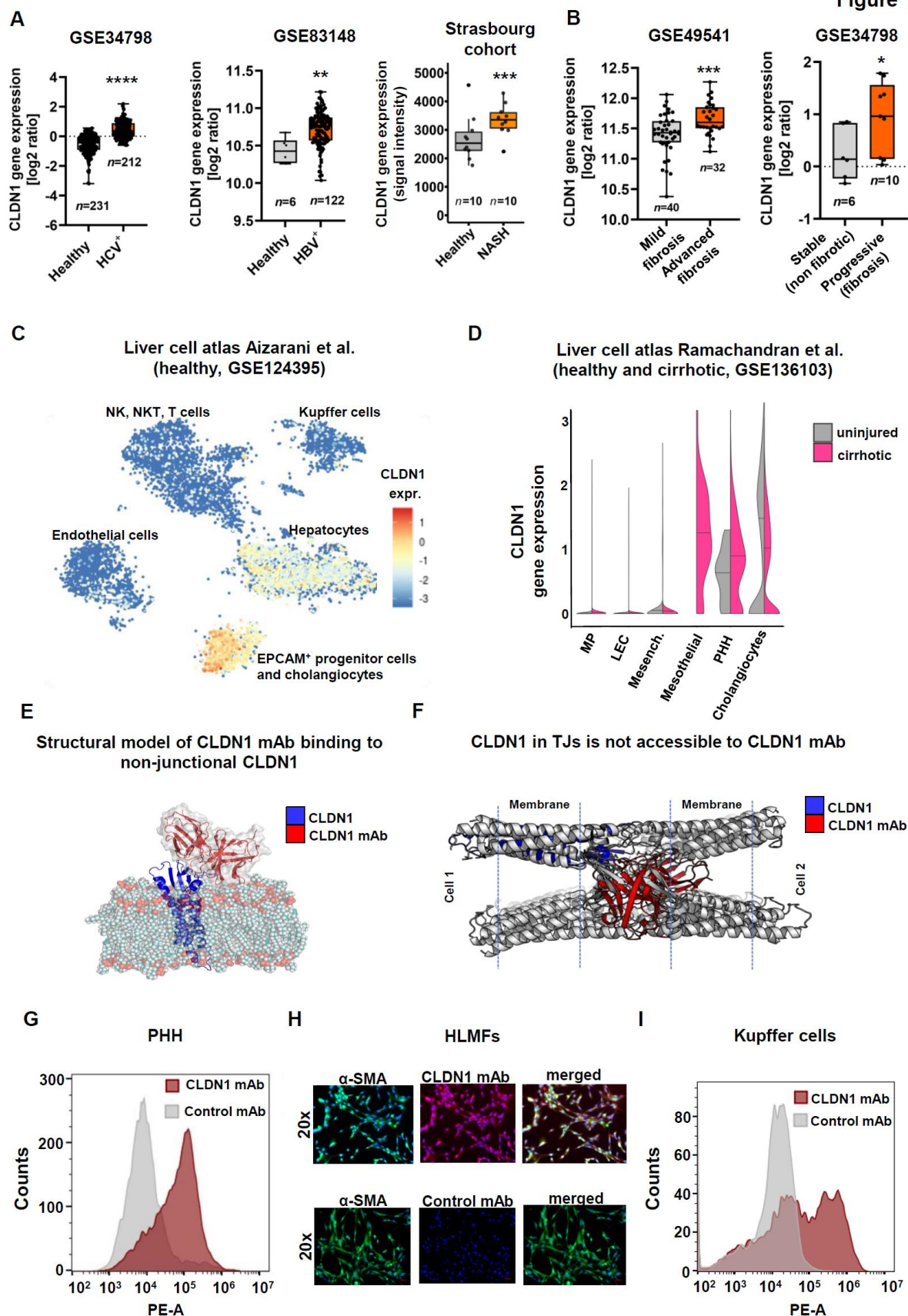


Figure 1 continued

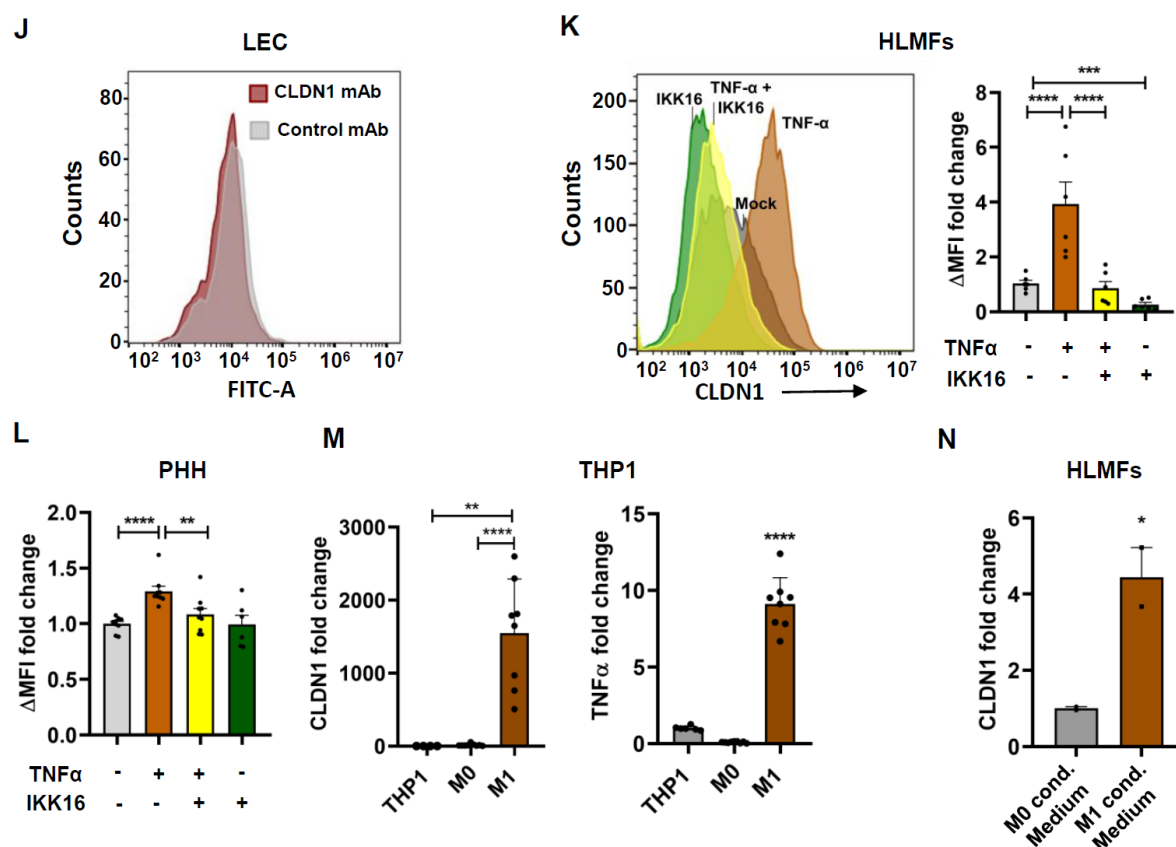


Fig. 1. CLDN1 is overexpressed in chronic liver disease. **A.** CLDN1 overexpression in liver tissues of patients with chronic HCV (GSE34798, left panel), HBV infection (GSE83148, middle panel) and NASH (U Strasbourg cohort, right panel). **B.** CLDN1 expression in livers of NASH patients with mild (F1-2) or advanced fibrosis (F3-4) (GSE49541, left panel) and liver tissues of HCV-infected patients after liver transplantation with stable or progressive fibrotic disease (GSE34798, right panel). **C.** CLDN1 expression on single cell level in different liver resident cell types derived from healthy liver tissue(18) is shown as gene tSNE. **D.** CLDN1 expression on single cell level in cirrhotic tissue-derived liver cells compared to healthy liver(19) is shown as gene violins. **E.** Computationally predicted structural model of the non-junctional CLDN1/CLDN1 mAb H3L3 complex. **F.** Structural model of the CLDN1/CLDN1 mAb H3L3 complex aligned on the model of the claudin tight junctions proposed by Suzuki *et al.*(71). Claudin-1 and the antibody are represented as blue and red cartoons, respectively. **G.** Representative flowcytometric assessment of CLDN1 mAb H3L3 binding to PHH. **H.** Representative images of CLDN1 mAb H3L3 binding to patient derived HLMFs, as assessed

by immunofluorescence. **I-J.** Representative flowcytometric assessment of CLDN1 mAb H3L3 binding to primary patient-derived Kupffer cells (**I**) and LECs (**J**). **K-L.** HLMFs (**K**) and PHH (**L**) were treated with TNF α , IKK-16 or TNF α + IKK16 and subjected to flowcytometric analysis of CLDN1 mAb H3L3 binding. Δ MFI of CLDN1 mAb to control mAb is shown for each treatment group as fold change compared to untreated cells. **M.** *CLDN1* and *TNF α* gene expression in THP1, THP-1-derived differentiated macrophages (M0) and THP1-derived pro-inflammatory M1 macrophages (M1) is shown as fold change compared to untreated THP1 cells. **N.** HLMFs were incubated with conditioned medium derived from M0 or M1 differentiated THP1 cells. *CLDN1* gene expression is shown as fold change. Bars show mean \pm SEM and single data points (\bullet). **** p <0.0001, *** p <0.001, ** p <0.01, * p <0.05, t-test (**A, B, K-L, N**) and U-test (**M**) respectively. Abbreviations: CLDN1=Claudin-1; HBV=Hepatitis B virus; HCV= Hepatitis C virus; LEC= Liver endothelial cells; MFI= Mean fluorescence intensity; MP=mononuclear phagocyte; NASH= Non-alcoholic steatohepatitis; PHH= Primary human hepatocytes.

Figure 2

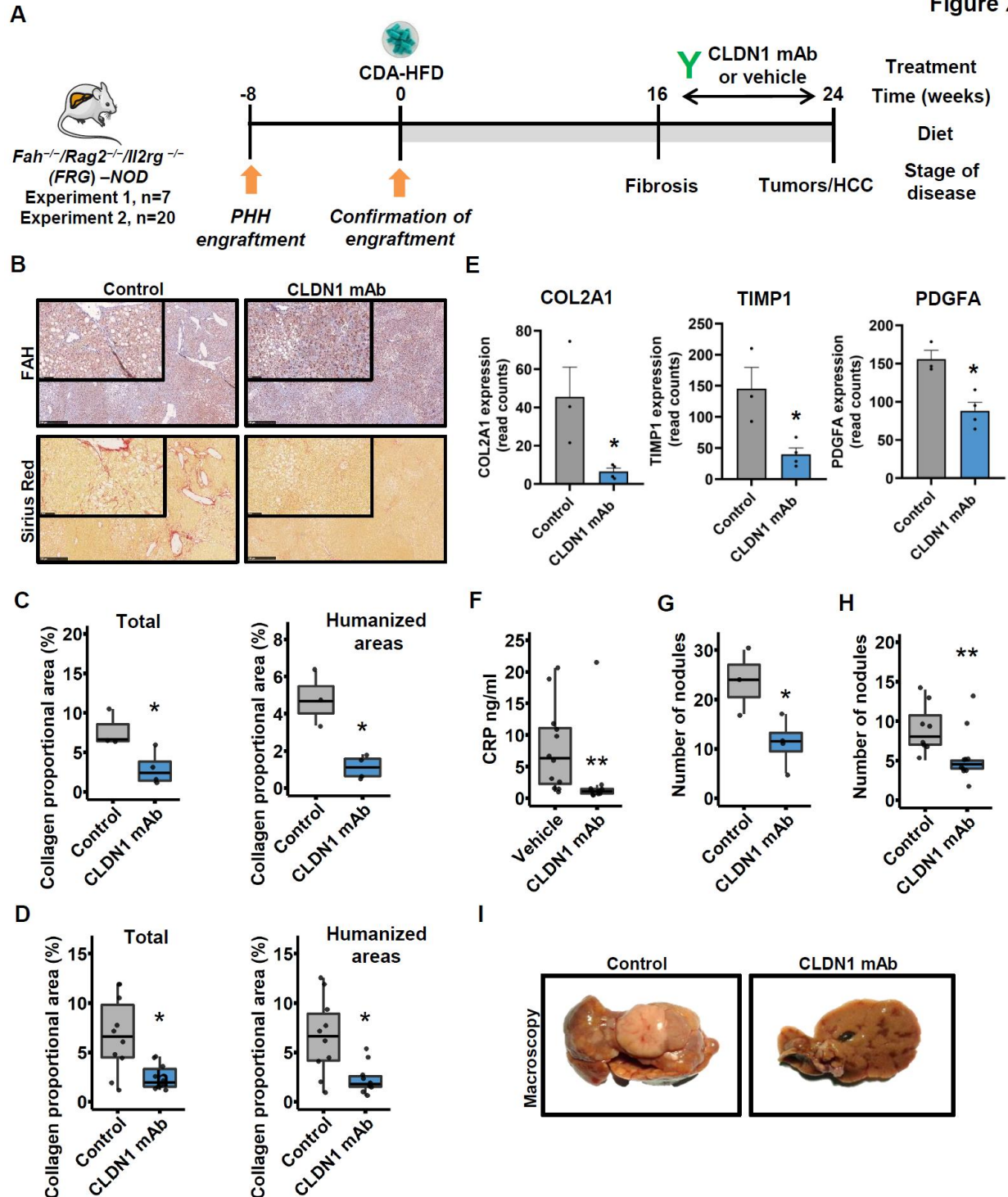


Fig. 2. Treatment with CLDN1 mAb reduces liver fibrosis and tumor burden in a patient-derived human liver chimeric mouse model for liver fibrosis. A. Study protocol of humanized mouse NASH model. **B.** Representative histological images of FAH (humanized areas, upper panel) and Sirius red (lower panels) staining in both treatment groups. **C-D.** Collagen proportional area in the total liver tissue and humanized areas of experiment 1 (**C**),

and experiment 2 (**D**). **E**. Gene expression of fibrosis markers *COL2A1*, *TIMP1* and *PDGFA* in humanized mice livers. **F**. CRP levels detected by ELISA in mouse plasma. **G-H**. Tumor burden in CLDN1 mAb vs. control-treated humanized mice (**G**: experiment 1, **H**: experiment 2). **I**. Representative macroscopic images of tumor burden in humanized mouse livers. Scale bars in (**B**) correspond to 50 μm and 150 μm , respectively. Boxplots represent median (**—**), 1st and 3rd quartile (bottom and top of the box) and single data points (**•**). Bars show mean \pm SEM. * $p < 0.05$, ** $p < 0.01$, U-test (**C-D**, **G-H**), t-test (**E-F**), respectively. Abbreviations: CDA-HFD=choline-deficient, L-amino acid-defined, high fat diet; COL2A1=collagen type 2 alpha 1 chain; FAH=fumarylacetoacetate hydrolase; FDR=False discovery rate; HCC=Hepatocellular carcinoma; PDGFA=Platelet Derived Growth Factor Subunit A; PHH=primary human hepatocytes; TIMP1=TIMP Metalloproteinase Inhibitor 1.

Figure 3

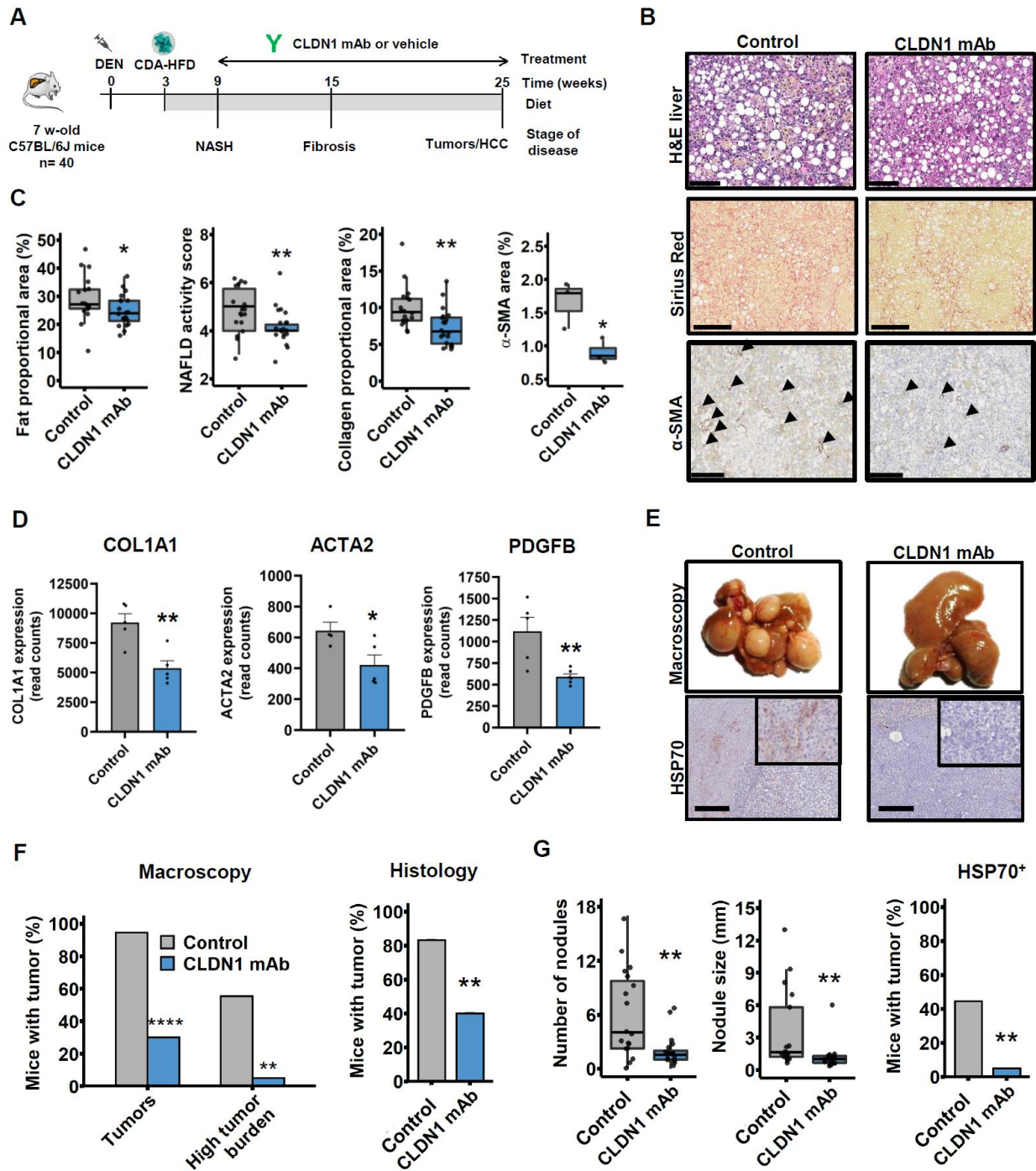


Fig. 3. Targeting non-junctional CLDN1 by CLDN1 mAb reduces fibrosis and tumor development in a NASH fibrosis mouse model. A. Study protocol of DEN-CDA-HFD NASH fibrosis mouse model. **B.** Representative histological images of steatosis (upper panel), fibrosis (middle panel) and myofibroblast activation (bottom panel) in mouse livers. **C.** Quantitative assessment of liver fat proportional area and NAFLD activity score (left panels), as well as

collagen and α -SMA proportional areas (right panels) in treatment groups. **D.** Gene expression of fibrosis markers *COL1A1*, *ACTA2* and *PDGFB* in livers of NASH fibrosis mice. **E.** Representative images of macroscopic tumor burden and HSP70⁺ areas in mouse livers. **F.** Macroscopic (left panel) and histological (right panel) assessment of tumor burden. **G.** Number (left panel), size (middle panel) of tumor nodules and proportion of HSP⁺ tumors (right panel) in mice livers. Scale bars in **(B)** and **(E)** correspond to 100 μ m and 500 μ m, respectively. Boxplots represent median (**—**), 1st and 3rd quartile (bottom and top of the box) and single data points (**•**). Bars show mean \pm SEM. * $p < 0.05$, ** $p < 0.01$, *** $p < 0.001$, **** $p < 0.0001$, U-test (**C**, **F**, **G**) and t-test (**D**), respectively. Abbreviations: ACTA2(gene)/ α -SMA(protein)=alpha smooth muscle actin; COL1A1=collagen type 1 alpha 1 chain; CDA-HFD=choline-deficient, L-amino acid-defined, high fat diet; DEN=Diethylnitrosamine; HCC=Hepatocellular carcinoma; H&E=Haematoxylin and Eosin; HSP70=Heat-shock protein 70; NASH=Non-alcoholic steatohepatitis; PDGFA=Platelet Derived Growth Factor Subunit B; SEM=standard error of the mean.

Figure 4

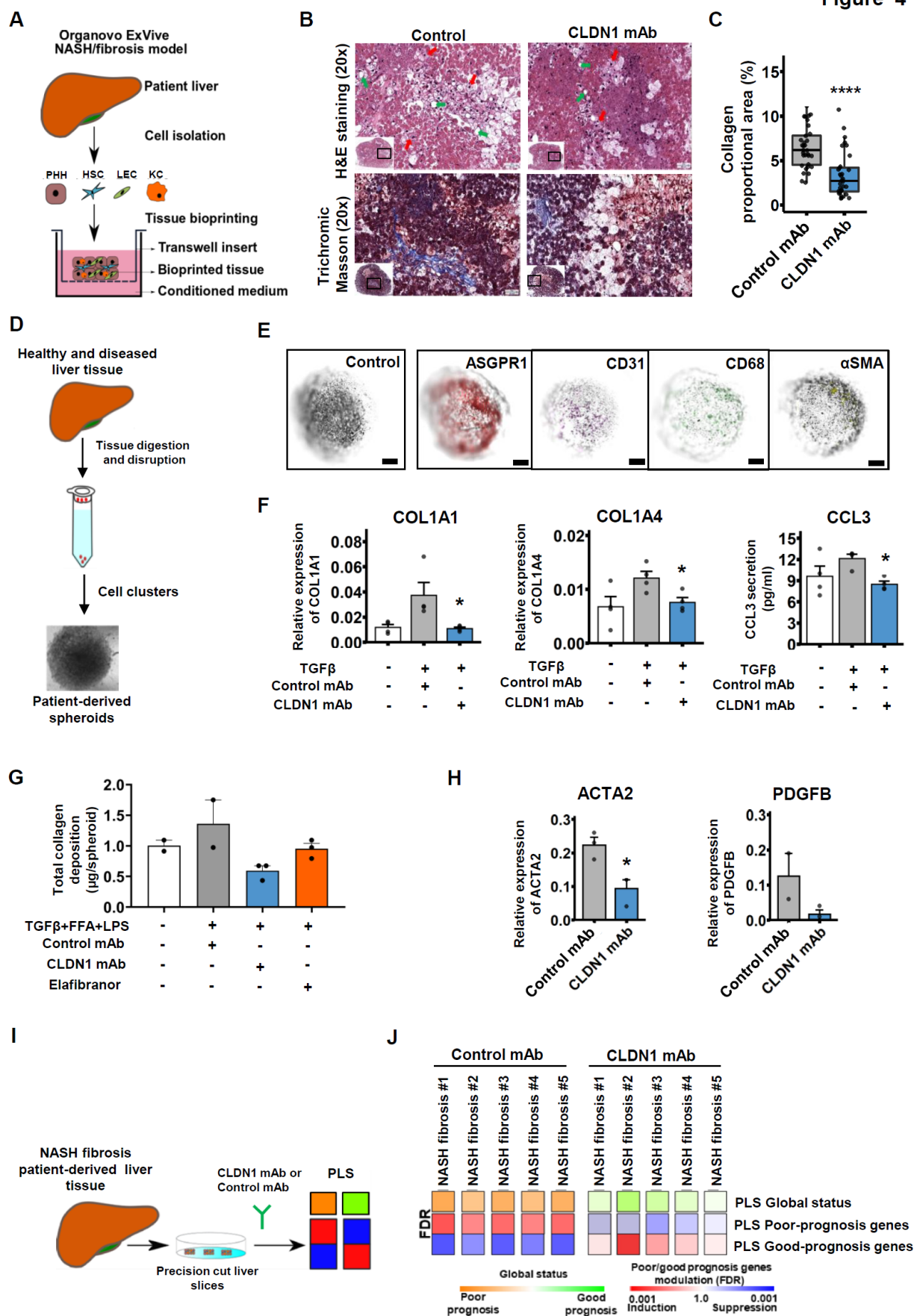


Fig. 4. Modeling of fibrosis in patient-derived *ex vivo* models of chronic liver disease and therapeutic effect of CLDN1-specific mAb. **A.** Illustration of Organovo ExVive fibrosis model. **B.** Images of Trichromic Masson and H&E staining in Organovo ExVive Human Liver Tissues sections treated with CLDN1 mAb or control mAb. Macrovascular steatosis is indicated by green and microvascular steatosis by red arrows. Scale bars correspond to 40 μ m. **C.** Quantitative assessment of collagen proportional area in Organovo ExVive Human Liver Tissues. **D.** Illustration of liver spheroid establishment from patient liver tissues. **E.** Immunostaining of ASPGR1, CD31, CD68 and α -SMA in patient-derived liver spheroids. Staining with anti-mouse AF647 conjugated secondary antibodies were used as a control. Spheroids were visualized by Celigo imaging cytometer. Scale bar corresponds to 500 μ m. **F.** Gene expression of *COL1A1*, *COL1A4* and *CCL3* concentration in spheroid supernatant in TGF β exposed liver spheroids treated with either CLDN1 mAb or control mAb. **G.** Total collagen deposition in patient-derived liver spheroids stimulated with FFA+LPS+TGF β and treated with CLDN1 mAb, control mAb or Elafibranor. **H.** Gene expression of *ACTA2* and *PDGFB* in CLDN1 mAb or control mAb-treated liver spheroids derived from fibrotic liver tissue. **I.** Illustration of precision cut liver slices study protocol. **J.** Modulation of PLS to good (green) or poor (orange) prognosis status in precision cut liver slices. The significance (FDR, Kolmogorov smirnov test) of induction (red) or suppression (blue) of PLS poor- or good-prognosis genes is illustrated below. Boxplots represent median (—), 1st and 3rd quartile (bottom and top of the box) and single data points (\bullet). Bars show mean \pm SEM. * $p < 0.05$, **** $p < 0.0001$, t-test (**C**), Fishers exact test (**F**, **H**). Abbreviations: COL1A1=collagen type 1 alpha 1 chain; COL1A4=collagen type 1 alpha 4 chain; ECs=Endothelial cells; FDR=False discovery rate; H&E=Haemotoxylin and Eosin; HCs=Hepatocytes; HSCs=Hepatic stellate cells; KCs=Kupffer cells; NASH=Non-alcoholic steatohepatitis; PLS=Prognostic liver signature; SEM=standard error of the mean.

Figure 5

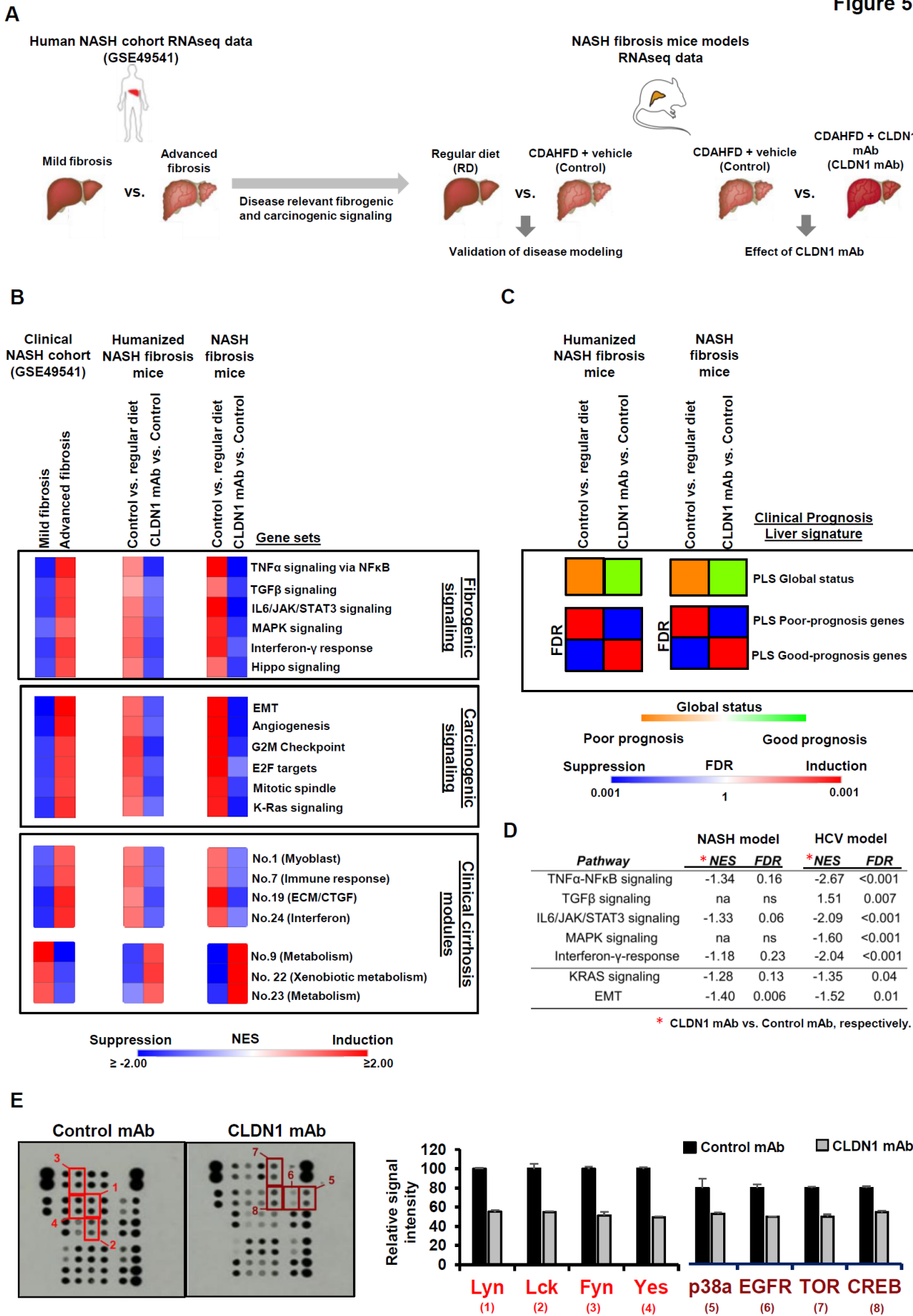


Fig. 5. Treatment with CLDN1-specific mAb suppresses liver cell circuits mediating inflammation, fibrosis and carcinogenesis. **A.** Graphical illustration of methodological approach. **B.** Modulation of fibrogenic and carcinogenic signaling pathways and human cirrhosis gene modules(31) in NASH patients with mild or advanced fibrosis (GSE49541(17), left panels), humanized NASH fibrosis mice treated with CLDN1 mAb or control (middle panels) and regular NASH fibrosis mice treated with CLDN1 mAb or control (right panels). Heatmaps illustrate NES of altered gene sets (all FDR<0.25 except for induction of fibrogenic, Kras signaling and cirrhosis modules #1, #7, #19, #24 and #23 in humanized mice control tissues and reversal of E2F targets, TGF β signaling and cirrhosis modules #1, #7 and #24 in CLDN1 mAb treated NASH fibrosis mice, FDR>0.25). **C.** Modulation of PLS and NAFLD/NASH signature to good (green) or poor (orange) prognosis status in liver tissues of NASH fibrosis mice and humanized NASH fibrosis mice treated with CLDN1 mAb or control. The significance (FDR, Kolmogorov smirnov test) of induction (red) or suppression (blue) of PLS poor- or good-prognosis genes is illustrated below. **D.** Modulation of fibrosis- and carcinogenesis-associated signaling pathways by CLDN1 mAb in the HCV and NASH *in vitro* model. **E.** Effect of CLDN1 mAb on phosphokinase signaling in the NASH *in vitro* model. Abbreviations: ECM= Extracellular Matrix; EMT= epithelial-mesenchymal transition; FDR=False discovery rate; MSigDB= Molecular Signature Database; na= not applicable; ns= non-significant; NASH=Non-alcoholic steatohepatitis.; NES= Normalized enrichment score; RD=Regular diet.

Figure 6

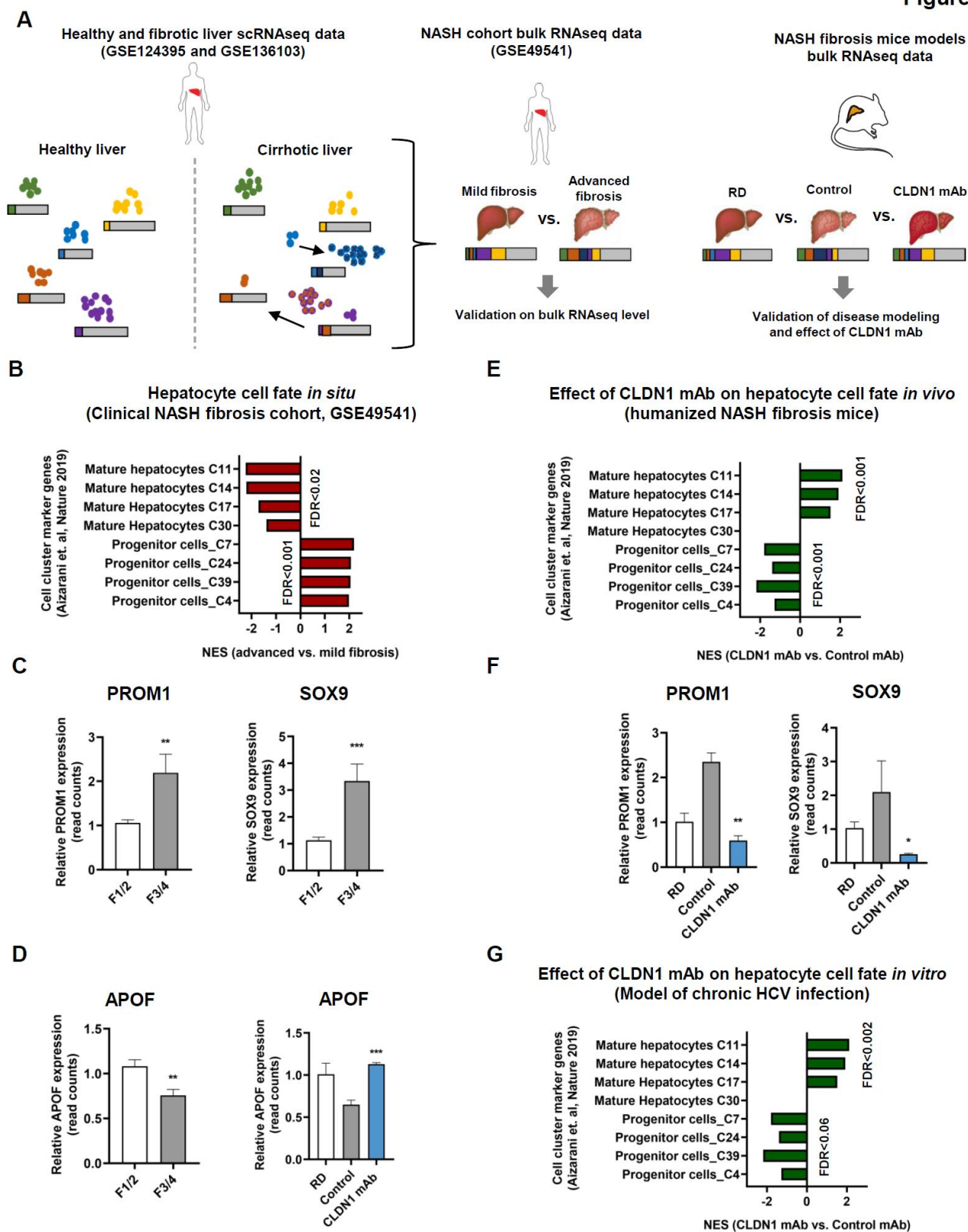


Figure 6 continued

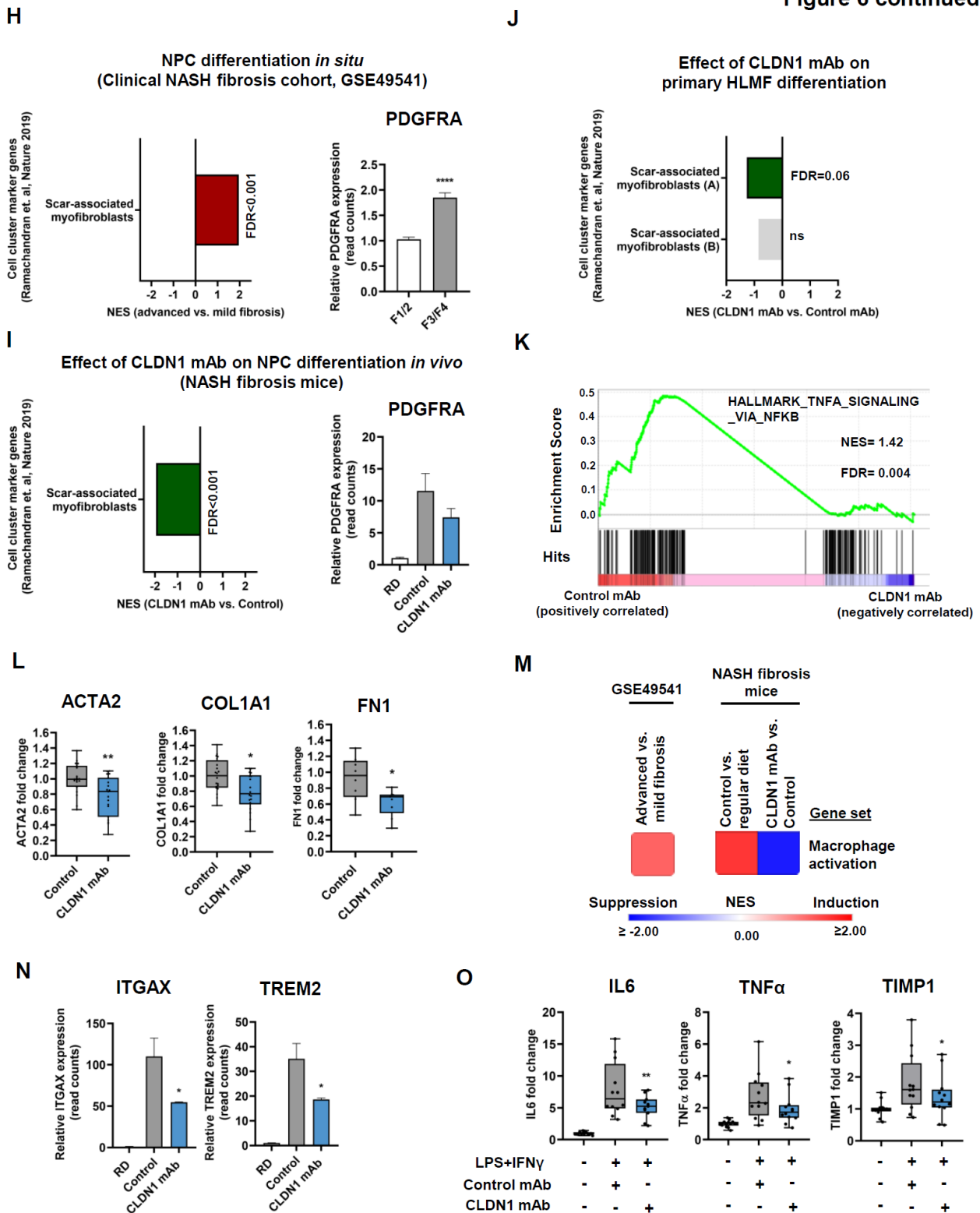


Fig. 6. Targeting non-junctional CLDN1 inhibits fibrosis-associated phenotypes of PHH, HLMF and Kupffer cells by interfering with TNF α -NF κ B, MAPK and Src signaling. A.

Graphical illustration of methodological approach. **B.** Modulation of gene sets characterizing mature hepatocytes ((18) and MSigDB: AIZARANI_LIVER_C11/C14/C17C30_HEPATOCYTES) and immature progenitor cells ((18) and MSigDB: AIZARANI_LIVER_C4/C7/C24/C39_EPCAM_POS_BILE_DUCT_CELLS) in NASH patients with mild or advanced fibrosis (GSE49541 (17)). **C.** Gene expression of *PROM1* and *SOX9* in NASH patients with mild or advanced fibrosis (GSE49541 (17)). **D.** Gene expression of *APOF* in NASH patients with mild or advanced fibrosis (GSE49541 (17)) and humanized NASH fibrosis mice is shown. **E.** Effect of CLDN1 mAb on liver progenitor and mature hepatocyte marker gene sets in humanized NASH fibrosis mice. **F.** Gene expression of *PROM1* and *SOX9* in humanized NASH fibrosis mice. **G.** Modulation of liver progenitor and mature hepatocyte related gene sets in Huh7.5.1^{diff} infected with HCV and treated with CLDN1 mAb or control mAb. **H.** Differential expression of a gene set characterizing scar-associated myofibroblasts (**Suppl Table 8** and (19)) (left panel) and gene expression of *PDGFRA* (right panel) in NASH patient with mild compared to advanced fibrosis. **I.** Effect of CLDN1 mAb on expression of scar-associated myofibroblast marker genes in the regular NASH fibrosis mouse model. **J.** Effect of CLDN1 mAb on scar-associated myofibroblast type A and B marker genes (**Suppl. Table 9-10**) in patient derived HLMF. **K.** Enrichment plot for TNF α -NF κ B signaling (HALLMARK_TNFA_SIGNALING_VIA_NFKB) in HLMFs treated by CLDN1 mAb compared to control mAb. **L.** Expression of *ACTA2*, *COL1A1*, and *FN1* in HLMFs (n=7 donors) treated with CLDN1 mAb or control is shown as fold change compared to untreated cells. **M.** Modulated expression of gene sets related to macrophage activation (GO: POSITIVE_REGULATION_OF_MACROPHAGE_ACTIVATION, MSigDB) is shown as heatmaps, indicating NES of significant (FDR<0.25) alterations. **N.** Gene expression of *ITGAX* and *TREM2* in treatment groups of the NASH fibrosis mice models. **O.** Expression of *IL6*, *TNF α* , and *TIMP1*, in Kupffer cells (n= 5 donors) treated with IFN γ +LPS in presence of CLDN1 mAb or control mAb is shown as fold change compared to untreated cells. Vertical bars show mean \pm SEM and single data points (●). Horizontal bars indicate NES of significantly (FDR<0.25) altered gene sets. *p<0.05, ** p<0.01, **** p<0.0001, t-test (**C, D, F, H-I, N**),

Wilcoxon matched pairs test (**L**, **O**), respectively. Abbreviations: APOF=Apolipoprotein F; FDR=False discovery rate; HLMFs=Human liver myofibroblasts; ITGAX=Integrin Subunit Alpha X; NASH=Non-alcoholic steatohepatitis. NES=Normalized enrichment score; PDGFRA=Platelet Derived Growth Factor Receptor Alpha; PROM1=Prominin 1; SOX9=SRY-Box Transcription Factor 9; TREM2=Triggering Receptor Expressed On Myeloid Cells 2.

Figure 7

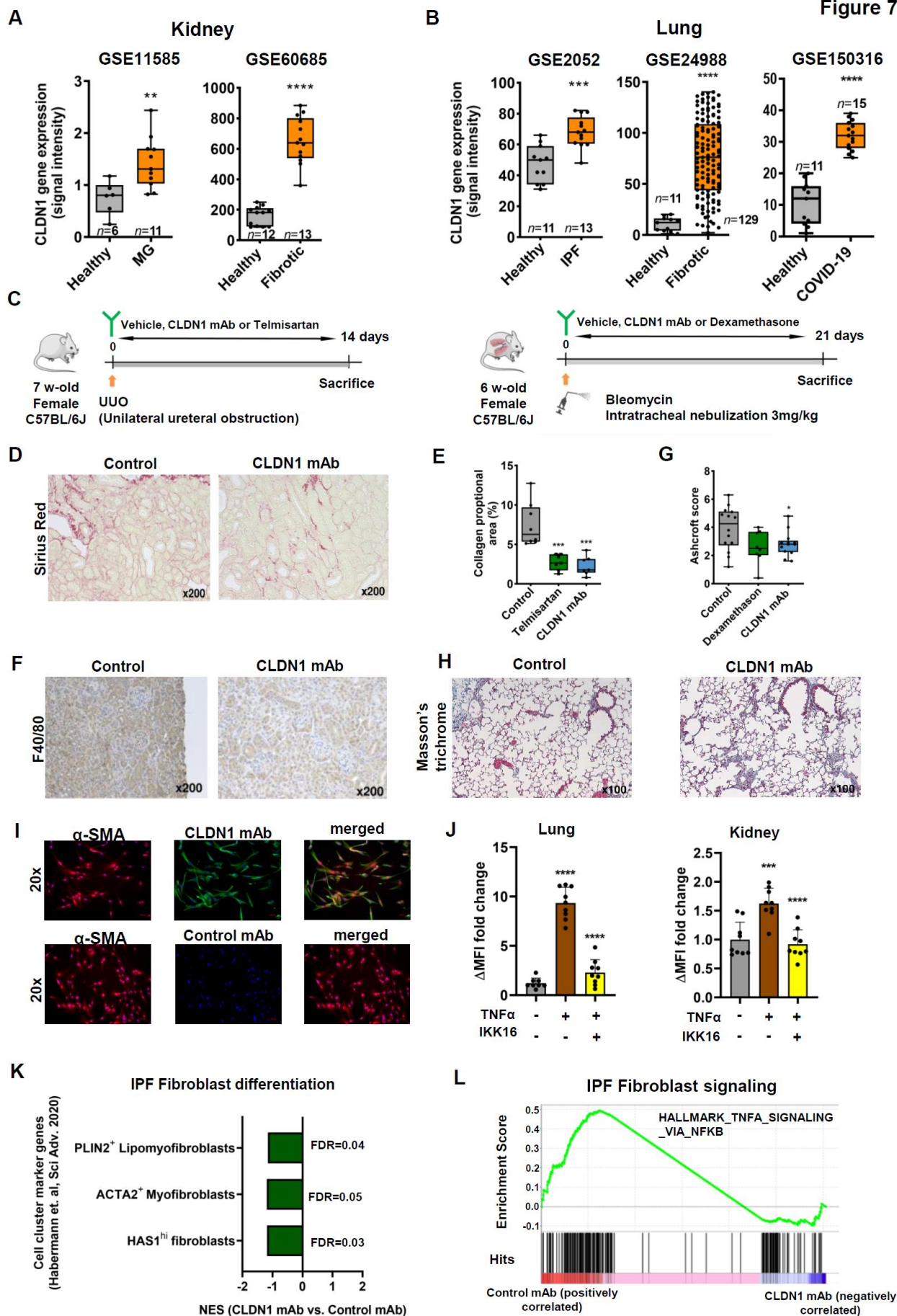


Fig. 7. CLDN1 is overexpressed in fibrotic kidney and lung diseases including COVID19 and targeting CLDN1 reduces fibrosis in lung and kidney fibrosis mouse models. **A.** *CLDN1* gene expression in renal tissues of MG (left panel, GSE11585) and fibrotic kidney tissue (right panel, GSE60685(50)) compared to respective healthy kidneys is shown as signal intensity values. **B.** *CLDN1* gene expression in pulmonary tissues of patients with IPF (left panel: GSE2052(51)), pulmonary fibrosis (middle panel: GSE24988(52)) and postmortal lung tissues of patients with COVID19 disease (right panel: GSE150316) compared to healthy lung tissue (GSE2052(51)) is shown as signal intensity values. **C.** Illustration of the UUO and bleomycin mouse models of kidney and lung fibrosis. **D.** Representative images of Sirius-red staining in kidneys from vehicle control and CLDN1 mAb-treated animals. **E.** Quantitative assessment of liver collagen proportional area in UUO mice treated with vehicle control, Telmisartan or murinized CLDN1 mAb (n=8, respectively). **F.** Representative images of F40/80 immunostaining in kidney tissues of CLDN1 mAb or control-treated animals. **G.** Representative images of Trichochrom masson staining of lung tissue from vehicle control and CLDN1 mAb-treated animals. **H.** Histological evaluation of pulmonary fibrosis by Ashcroft score(55) in vehicle control (n=14), CLDN1 mAb (n=13) and dexamethasone (n=8) treated animals. **I.** Representative images of CLDN1 mAb binding to CLDN1 on lung fibroblasts. Scale bar correspond to 100 μ m. **J.** Kidney fibroblasts (left panel) and lung fibroblasts (right panel) were treated with TNF α (10 ng/mL), IKK-16 (1 μ M), TNF α + IKK16 or vehicle control and subjected to fluorocytometric analysis of CLDN1 mAb H3L3 binding, respectively. Δ MFI of CLDN1 mAb to control mAb is shown as fold change compared to untreated cells. **K.** Modulation of gene sets characterizing lung fibrosis-associated fibroblast differentiation states(56) in CLDN1 mAb or control mAb treated IPF patient derived fibroblasts. **L.** Enrichment plot for TNF α -NF κ B signaling (HALLMARK_TNFA_SIGNALING_VIA_NFKB) in IPF fibroblasts treated by CLDN1 mAb compared to control mAb. Boxplot represents median (—), 1st and 3rd quartile (bottom and top of the box) and single data points (\bullet). Vertical bars show mean \pm SEM and and single data points (\bullet). Horizontal bars indicate NES of significantly (FDR<0.25) altered gene sets. *p<0.05, ***p<0.001, **** p<0.0001, t-test (**A-B, E, G, J**). Abbreviations: α -SMA=alpha smooth

muscle actin; IPF=idiopathic pulmonary fibrosis; MFI=Mean fluorescence intensity;
MG=membranous glomerulonephritis; UUO=unilateral ureteral obstruction.

Figure 8

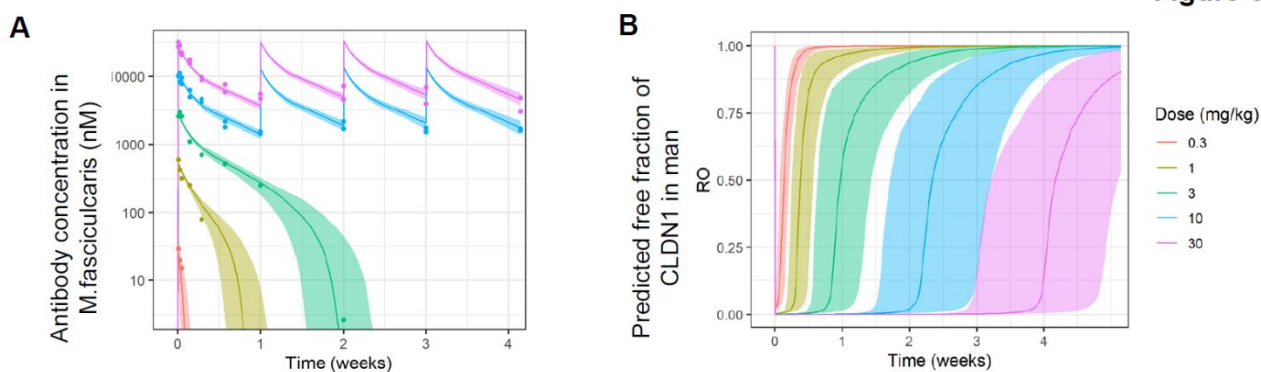


Fig. 8. CLDN1 mAb pharmacokinetic in non-human primates. A. Predicted exposure of the anti-CLDN1 antibody ALE.F02 in macaca (median, 5th and 95th percentiles from 200 simulated profiles). Dots are the observed serum concentrations. All data in nmol/L, color correspond to the dose levels. **B.** Predicted receptor occupancy in human, indicating the total systemic free accessible CLDN1 not occupied by the administered antibody as a function of time. Shown are median, 5th and 95th percentiles from 100 simulated PK/PD profiles.

Supplementary Information

SUPPLEMENTARY MATERIAL AND METHODS

Modeling of the claudin-1/antibody complex. Generation of a CLDN1 structural model: To date the structure of CLDN1 has not been solved and no structure is available in the protein data bank (PDB)(72). We therefore generated an atomistic model by homology modeling. Sequence analysis revealed that claudin-19 (CLDN19) has a sequence similarity of 57% with CLDN1 and was therefore selected as a template. A structural model of CLDN1 was generated and optimized using PRIME, a dedicated pipeline implemented in the Schrodinger suite for molecular modeling(73, 74). Generation of the antibody model: The structure of the antibody was generated using the antibody modelling pipeline implemented in the Schrodinger suite for molecular modeling(75-77). MD simulations: To explore conformational variability and dynamics of CLDN1, we performed extensive molecular dynamics (MD) simulations. An atomistic model of CLDN1 in a membrane was build using the OPM webserver(78). In particular CLDN1 was immersed in a POPC lipid bilayer with a concentration of 0.15M NaCl. Furthermore, the TIP3P model(79) was used to describe the water molecules while all the other parts of the system were described by the OPLS3e force field(80). The full system was then equilibrated using the following protocol: 1. Brownian Dynamics was run for 100 ps in an NVT ensemble ($T=10$ K) applying harmonic restraints on solute heavy atoms (force constant 50 kcal/mol/Å²); 2. NVT ($T=10$ K) MD simulation of 12 ps in NVT ensemble conserving the same restraints applied in 1.; 3. NPT ($T=300$ K and $P=1$ atm) MD simulation (12 ps) conserving the same restraints applied in 1.; 4. NPT ($T=300$ K and $P=1$ atm) MD simulation (24 ps) without restraints. Pressure and the temperature were fixed at 300 K and 1 atm by the Martyna-Tobias-Klein barostat(81) and the Nose-Hoover chain thermostat (82), respectively. Finally, three independent production runs of 1 μ s were performed. The DESMOND software in its GPU implementation was used as simulations engine(83). Finally, a cluster analysis was run to

extract the most relevant conformations from the MD trajectories. This analysis was carried out with the *ttclust* program(84). The CLDN1 backbone atoms were considered for both alignment and clustering, the optimal number of clusters was automatically determined using the “elbow” method with *kmeans* (85). *Modeling of Claudin-1/Antibody complex:* Cluster analysis identified six different clusters. However, only two included more than 20% of the conformations sampled during MD. The centers of these two clusters were, therefore, used for the modelling of the structure of the claudin-1/antibody complex. CLDN1/antibody docking were performed using the Haddock v2.4 webserver(86, 87) following the procedure described by Bonvin and coworkers(88) and the definition of the epitope given in Fofana et al.(12) Finally, two complex structures, one for each representative CLDN1 structure, were selected for further investigations. Next, to optimize the CLDN1/antibody interface and account for induced-fit effects on the proteins, two complexes were simulated by MD for 500ns using the same set-up described before, and the trajectories analyzed by cluster analysis. Finally, the interaction free energy (ΔG) for the most representative structure from the two largest clusters were computed using the PRODIGY software(89) and the model with the best (more negative) ΔG was selected as the final model of the Claudin-1/Antibody complex.

Retrogenix study: Retrogenix’s cell microarray technology was performed, as described(90). Briefly, 5484 expression vectors, encoding both ZsGreen1 and a full-length human plasma membrane protein or a cell-surface tethered human secreted protein, were arrayed in duplicate across 16 microarray slides (‘slide-sets’) for primary screen. An expression vector (pIRES-hEGFR-IRES-ZsGreen1) was spotted in quadruplicate on every slide and was used to ensure that a minimal threshold of transfection efficiency had been achieved or exceeded on every slide. Human HEK293 cells were used for reverse transfection/expression. The test antibody was added to each slide after cell fixation giving a final concentration of 2 $\mu\text{g/ml}$. Detection of binding was performed by using AlexaFluor 647 labelled anti-human IgG Fc detection antibody. Fluorescent images were analysed and quantitated (for transfection) using ImageQuant software. A protein ‘hit’ was defined as a duplicate spot showing a raised signal compared to

background levels. Hits were classified as 'strong, medium, weak or very weak', depending on the intensity of the duplicate spots. To confirm the hits and assess specificity, vectors encoding all hits identified in the primary screens, plus vectors encoding CD20 and EGFR, were arrayed and expressed in HEK293 cells on new slides. Confirmation/Specificity screens and analyses were carried out as for primary screening except that identical slides were treated, after cell fixation, with the test antibody individually at the same concentration as before (2 µg/ml), 1 µg/ml Rituximab biosimilar, or no test antibody/secondary only (n=2 slides per treatment).

Isolation of primary liver cells. Mouse: Primary Mouse Hepatocytes (PMH) were isolated from fresh non-diseased mouse liver tissue, as described(91). Human: Isolation of PHH and non-parenchymal cells from patients' liver tissue (**Suppl. Table 2**) was performed as previously described(92). Briefly, human liver tissue samples from surgical interventions were digested using a two-step EGTA/collagenase perfusion technique. PHH were depleted by initial centrifugation at 50xg and NPC's were further purified by serial centrifugation at different speed and density gradient centrifugation. Fast attachment of Kupffer cells to culture plates as well as magnetic separation of endothelial cells using CD31 microbeads (CD31 MicroBead Kit, human, Miltenyi, France) further allowed separation and cultivation of Kupffer cells, HSC's and LEC's(92).

Binding studies of murinized and humanized CLDN1 specific mAbs by flow cytometry.

Binding of murinized and humanized CLDN1 mAb to cells was analyzed by flow cytometry with ~1x10⁵ cells in triplicate per condition. PHH and PMH (primary antibody staining): Isolated PHH and PMH were incubated with increasing concentrations of humanized CLDN1 mAb H3L3 or murinized mAb CLDN1 mTAR (0.01-100 µg/mL), respectively. 293-T cells (primary antibody staining): 293-T cells were transfected with plasmids encoding for human or mouse CLDN1 fused with cerulean fluorescent protein or empty plasmid fused with cerulean fluorescent protein (kindly provided by M. Evans, Mount Sinai Hospital, New York). Transfected cells were incubated with increasing concentrations of humanized CLDN1 mAb H3L3, murinized CLDN1 mAb mTAR or the respective isotype control antibodies. HLMF (primary antibody staining):

Isolated HSC's were differentiated into HLMFs within 10 days of culture on plastic(93). Phenotypic identity was subsequently confirmed by α -SMA positive staining using immunofluorescence (see below). For flowcytometric analysis of CLDN1 mAb binding under conditions of inflammation, transdifferentiated HLMFs were treated with TNF- α (10 ng/mL), IKK-16 (1 μ M) or TNF- α (10 ng/mL) + IKK-16 (1 μ M) for 24 h, prior to incubation with humanized CLDN1 mAb H3L3 or isotype control mAb at 10 μ g/mL. Kupffer cells (primary antibody staining): Phenotypic identity of patient derived Kupffer cells was confirmed by CD68 positive staining using immunofluorescence (see below). Kupffer cells were then incubated with humanized CLDN1 mAb H3L3 or isotype control mAb at 50 μ g/mL. LEC's (primary antibody staining): Isolated LEC's were co-stained with anti-CD31 FITC conjugated antibody (Beckman Coulter, France, 1:20) and humanized CLDN1 mAb H3L3 or isotype control mAb at 50 μ g/mL, followed by assessment of CLDN1 mAb binding to CD31⁺ LECs by flow cytometry. Secondary antibody staining (all cell types): Following incubation with the respective mAbs concentrations for 1h, all cells were washed and incubated with phycoerythrin (PE)-conjugated species-specific (human or mouse) secondary antibodies at 4 °C for 45 min to allow detection of binding. Cells were subsequently washed and fixed with 2% paraformaldehyde (PFA). Data were acquired using Cytoflex B2R2V0 (Beckman Coulter) and analyzed using CytExpert 2.1 and FlowJo v10 (Beckman Coulter). All experiments were repeated in at least 3 independent experiments (and/or donors) in triplicate. CLDN1 expression was calculated as the difference of the mean fluorescence intensities of cells stained with CLDN1 mAb and cells stained with the isotype control mAbs. The kinetics of the interaction between humanized or murinized mAb against human or mouse CLDN1, respectively, were determined by gating in cerulean positive cells using FlowJo and the Michaelis-Menten mathematical model using R 3.5.1 (<http://www.R-project.org/>).

Reagents and antibodies. The following reagents were used for *in vitro* experiments in this study: DMSO, oleic acid and palmitic acid (Sigma-Aldrich, St. Louis, Missouri), IL6 (Sigma-Aldrich, St. Louis, Missouri), TGF β (R&D Systems, Minneapolis, USA), IFN γ (Thermo Fisher

Scientific, Freiburg, Germany), PMA (Sigma-Aldrich, St. Louis, Missouri). Humanized CLDN1 specific mAb H3L3 has been described(13) and were produced by Evitria, Schlieren. Murinized CLDN1 specific mAb (TAR-Rm) was generated by co-transfecting chinese hamster ovary (CHO) cells with plasmids containing appropriate heavy and light chain variants as described(13) by Evitria, Schlieren. The isotype control antibodies used are palivizumab IgG4(94) (Evitria, Schlieren) and motavizumab (Eviteria, Switzerland).

Liver fibrosis mouse models. All experiments were performed at the animal facility of Inserm U1110 according to local laws and ethics committee approval (institutional protocol approval number APAFiS #3559 and #7216). ***Pharmacokinetics studies.*** Three C3H male mice (6-8 weeks old) were i.p. injected with 500 µg of murinized CLDN1 specific mAb TAR-R-mIgG. At day 1, 3, 8 and 15 after injection, 100 µL blood was harvested under general anesthesia (isoflurane 3%) by retro-orbital puncture with dry capillaries. Serum levels of the murinized CLDN1 specific mAb were quantified by flow cytometry as described(14). Briefly, 3×10^4 CLDN1-overexpressing Huh7.5.1 cells were incubated for 30 min at 4 °C with 20 µL of 1/50-diluted serum or serial concentrations (0, 0.1, 0.3, 1, 3, 10 and 30 µg/mL) of CLDN1 specific mAb TAR-R-mIgG in 1:50-diluted serum from an untreated C3H mouse. After extensive washing, cells were labelled with PE-conjugated goat-anti-mouse Abs (Jackson ImmunoResearch Laboratories, Pennsylvania, USA) and fixed with 2% paraformaldehyde. Cells were analyzed on a BD LSRII FACS. To determine the mAb concentration at each time point, the PE mean fluorescence intensity (MFI) of all viable cells in experimental samples were compared with that of the titration curve. The mAb serum levels were then plotted against time and the half-life was calculated for each mouse using its regression curve. ***DEN-CDA-HFD model:*** Forty 7-week old male C57BL/6J mice (Charles River Laboratories, MA, United States) received a single i.p. injection of DEN (100 mg/kg) (Sigma-Aldrich, France) and were subsequently fed with the CDA-HFD (A06071302, Research Diet, NJ, USA) after 3 weeks. After 6 weeks of diet, the mice were randomized in 2 groups, receiving weekly i.p. injections of 500 µg of either CLDN1 specific mAb or vehicle control for 16 weeks. After 16 weeks of

treatment, all mice were sacrificed, the blood was sampled and the liver as well as other major organs (i.e., brain, heart, lung, kidney, stomach, intestine, spleen, bladder and skin) were harvested and underwent macroscopic and microscopic examination (**Suppl. Fig. S2**).

Humanized liver NASH mouse model: *Fah^{-/-}/Rag2^{-/-}/Il2rg^{-/-} (FRG) –NOD* breeding mice were kept at the Inserm Unit 1110 SPF animal facility and maintained with 16 mg/L of 2-(2-nitro-4-trifluoro-methyl-benzoyl)-1,3 cyclohexanedione (NTBC; Swedish Orphan Biovitrum) in drinking water. Six-week old mice were intravenously injected with 1.5×10^9 plaque forming units (pfu) of an adenoviral vector encoding the secreted form of the human urokinase-like plasminogen activator (Ad-uPA)(22). Forty-eight hours later, 10^6 PHH were injected intrasplenically via a 27-gauge needle. For the procedure, the mice were kept under gaseous isoflurane anesthesia and received a subcutaneous injection of buprenorphine at the dose of 0.1 mg/kg. After the transplantation the NTBC was gradually decreased and completely withdrawn in 7 d. The transplant success was evaluated 2 months after the procedure by dosing human albumin in mouse serum as previously described(14). The mice successfully transplanted were fed with CDA-HFD for 16 weeks and then treated with humanized CLDN1 specific mAb 500 µg or vehicle for additional 8 weeks. CRP was measured in collected plasma of the humanized mice using Human C-Reactive Protein/CRP Quantikine ELISA Kit (R&D Systems, France) according to the manufacturer's instructions. Histological and image analysis. All organs were immediately fixed in a 10% formalin solution after harvesting and subsequently included in paraffin. Liver slices stained with hematoxylin & eosin (H&E) and Sirius Red were obtained for all mice. An immunohistochemistry staining for HSP70, FAH and α -SMA were performed respectively in the DEN-CDA-HFD and humanized NASH experiments. For each mouse, 5 to 10 consecutive images at 10x or 20x magnification per staining were captured and analyzed or the entire histological slide scanned and analyzed using ImageJ software v1.51j8 (Rasband W, National Institutes of Health, USA). For the collagen proportional area quantification in humanized areas, two consecutive liver cuts were stained with FAH and Sirius Red. The corresponding FAH positive area in the Sirius Red histological slide was selected as region of interest and then the collagen proportional area quantified using ImageJ software(95).

Kidney fibrosis (unilateral ureteral obstruction model, UUO) mouse model: Seven-week-old female C57BL/6J mice were obtained from Japan SLC, Inc. (Japan) and housed and cared for in accordance with the Japanese Pharmacological Society Guidelines for Animal Use at SMC laboratories, Japan. Animals were housed and fed with a normal diet (CE-2; CLEA Japan, Japan) under controlled conditions. On day 0, UUO surgery was performed under mixed anesthetic agents (medetomidine, midazolam, butorphanol). CLDN1 mAb (500 µg in 100 µL/mouse, $n=8$) or vehicle (100 µl, $n=8$) was administered intraperitoneally of twice weekly for 14 days. Telmisartan (30 mg/kg, $n=8$) was administered orally once daily for 14 days. The animals were sacrificed by exsanguination through direct cardiac puncture under isoflurane anesthesia (Pfizer Inc.) at day 14. For plasma biochemistry, non-fasting blood was collected in polypropylene tubes with anticoagulant (Novo-Heparin, Mochida Pharmaceutical Co. Ltd., Japan) and centrifuged at 1,000 \times g for 15 min. at 4 °C. The supernatant was collected and stored at -80 °C until use. Plasma urea nitrogen was measured by FUJI DRI-CHEM 7000 (Fujifilm, Japan). *Histological and image analysis.* To visualize collagen deposition, kidney sections were stained using picro-Sirius red solution (Waldeck, Germany). For quantification of interstitial fibrosis area, bright field images in the corticomedullary region were captured using a digital camera (DFC295) at 200-fold magnification, and the positive areas in 5 fields/section were measured using ImageJ software. For immunohistochemistry, sections were cut from paraffin blocks and deparaffinized and rehydrated. Endogenous peroxidase activity was blocked using 0.3% H₂O₂ for 5 min., followed by incubation with Block Ace (Dainippon Sumitomo Pharma Co. Ltd., Japan) for 10 min. The sections were incubated with a 100-fold dilution of anti-F4/80 antibody (BMA Biomedicals, Switzerland) at room temperature for 1 hour. After incubation with secondary antibody (HRP-Goat anti-rat antibody, Invitrogen, USA), enzyme-substrate reactions were performed using 3, 3'-diaminobenzidine/H₂O₂ solution (Nichirei Bioscience Inc., Japan). For quantitative analysis of inflammation areas, bright field images of F4/80-immunostained sections were captured using a digital camera (DFC295) at 200- and 400-fold magnifications.

Lung fibrosis (Bleomycin-induced) mouse model: Six-week-old female C57BL/6J mice were obtained from Japan SLC, Inc. (Japan) and housed and cared in accordance with the Japanese Pharmacological Society Guidelines for Animal Use at SMC laboratories, Japan. Animals were housed and fed with normal diet (CE-2; CLEA Japan, Japan) under controlled conditions. On day 0, mice were anesthetized with a mixture of medetomidine (Nippon Zenyaku Kogyo, Japan), midazolam (Sandoz K.K., Japan) and butorphanol (Meiji Seika Pharma, Japan) anesthesia and intratracheally administered BLM (Nippon Kayaku, Japan) in saline at a dose of 3 mg/kg, in a volume of 50 μ L per animal using a Microsprayer (Penn-Century, USA). CLDN1 mAb (500 μ g/mouse and 5 mL/kg, $n=9$) or vehicle (5 mL/kg, $n=9$) was administered intraperitoneally twice weekly from day 0 to 20. Dexamethasone (0.25 mg/kg, $n=9$) was administered orally once daily from day 0 to 20. The animals were sacrificed at day 21 by exsanguination through the abdominal aorta under a mixture of medetomidine, midazolam and butorphanol anesthesia. Histological and image analysis. Right lung tissues prefixed in 10% neutral buffered formalin were embedded in paraffin and sectioned at 4 μ m. For Masson's Trichrome staining, the sections were stained with Masson's Trichrome staining Kit (Sigma, USA) according to the manufacturer's instructions. The degree of pulmonary fibrosis was evaluated using the Ashcroft score(55).

Non-human primate study. This study was performed and controlled by Charles River Laboratories, under study number CRL 20229915. Pharmacokinetic modeling was performed by LYO-X (Allschwil, Switzerland); in brief, for parameter estimation and diagnostic plots, Monolix Suite 2019R2, and for the human PK-binding simulations, Simulx (Monolix Suite 2019R2), mlxR 4.1.0 (Lavielle 2019) and R 3.6.0 (R Development Core Team 2008) were used.

Functional assessment of the murinized CLDN1 specific mAb. Mouse CLDN1-transfected 293-T cells were pre-incubated with control mAb or murinized CLDN1 mAb (100 μ g/mL) for 1 h at 37 °C and subsequently exposed to HCV pseudoparticles (HCVpp) for 4 h at 37 °C, as described(96). HCVpp entry was analyzed by measuring intracellular luciferase activity after

72 h (relative light units, RLU). Inhibition was expressed as a percentage relative to cells treated with Control mAb as described(14).

RNA extraction from human and murine liver tissue. Liver cells were lysed in TRI-reagent (Molecular Research Center), and RNA was purified using Direct-zol RNA MiniPrep (Zymo Research) according to the manufacturer's instructions. RNA quantity and quality were assessed using NanoDrop (ThermoScientific). Gene expression profiling was performed using 250-500 ng total RNA.

Prognostic liver signature expression analyses. Profiling of the prognostic liver signature (PLS) was performed using Nanostring nCounter assay as described(34). Induction or suppression of the PLS in gene expression data was determined as previously reported using the Gene Set Enrichment Analysis (GSEA)(38), implemented in GenePattern genomic analysis toolkits. False discovery rate (FDR) <0.25 was regarded as statistically significant(38). Global status corresponds to the difference between low-risk and high-risk gene enrichments.

Organovo ExVive Human Liver Tissue NASH fibrosis model. The study was conducted by Organovo (San Diego, CA, USA). PHH and nonparenchymal cell populations (LEC, HSC and Kupffer cells) cultured in conditioned medium (sugars, free fatty acids and inflammatory inducers) were bioprinted in 3D using the NovoGen Bioprinter platform as described(26). Four NASH induced ExVive Human Liver Tissues with Kupffer cells were exposed to CLDN1 mAb H3L3 or isotype control mAb at 10 µg/mL daily for 21 days. After 21 days, tissues were stained with hematoxylin and eosin and Trichromic Masson. Eight sections of each tissue replicate underwent histological quantification. One image per each of the eight sections for the four tissue replicates stained with Trichromic Masson underwent fibrosis quantification (total 32 images). Image analysis was performed using ImageJ software.

Patient-derived liver spheroids and tumorspheres. Liver tissues from patients with or without chronic liver disease (**Suppl. Table 6**) were gently digested using a two-step digestion with EGTA for 15 min on ice and 0.02% collagenase P for 30 min at 37 °C. The sample was

then washed with PBS 1x and loaded on a 70 µm cell strainer. Digested tissue was gently smashed, and the cell strainer washed with up to 10 mL PBS 1x. Collected cell clusters were further filtered through a 0.45 µm filter and centrifuged for 5 min at 800xg. The cell pellet containing all liver cell types was then re-suspended in Mammocult basal medium (StemCell), supplemented with human proliferation supplement (3.4%), hydrocortisone (0.056%) and heparin (0.011%) and cultured in 96 well ultra-low attachment plates (Corning, Sigma Aldrich, France). Cell characterization in spheroids by immunofluorescence: Spheroids were fixed with formaldehyde (4% for 2 hours), permeabilized with Triton 0.5%, blocked with 5% FBS, and incubated with ASGPR1- PE (REA608, Miltenyi, 1:50), αSMA (ab5694, 1:50), CD68 (Biolegend Y1/82A, 1:50) or CD31-FITC (CST 89C2, 1:50) overnight. Respective species-specific secondary antibodies (CK18, αSMA and CD68) were added for 1h, followed by washing steps. Spheroids were visualized by Celigo™ imaging cytometer. Spheroid fibrosis model: Following spheroid formation overnight, spheroids derived from fibrotic liver tissue were incubated with CLDN1 mAb or control mAb (10 µg/mL, respectively) for 6 days. For chemical induction of fibrogenesis in spheroids derived from non-fibrotic healthy liver tissue, culture medium was supplemented with TGF-β (10 ng/mL in presence of CLDN1 mAb or control mAb (10 µg/mL, respectively). After 7 days of culture, spheroids were lysed, and RNA was extracted using Arcturus PicoPure RNA Isolation Kit (Applied Biosystems, France). Subsequently, total RNA was reverse transcribed (H Minus First Strand cDNA synthesis Mix, ThermoScientific, France) on a Thermocycler (Bio-Rad T100, Bio-Rad, Hercules, CA, USA). Quantitative PCR was performed on the CFX96 Touch Real-Time PCR Detection system with 10 µL reaction volumes containing 5 µL SYBR Green 2x mix (Bio-Rad), 2 µL of RNase-free water and 250 nM gene specific sense and antisense primers. For qPCR analyses Prime PCR SYBR Green Assays for *ACTA2*, *COL1A1*, *COL1A4*, and *PDGF-β* (Biorad, France) were applied according to the manufacturer's instructions. Gene expression were normalized to the housekeeping gene GAPDH (Biorad, France) using the $\Delta\Delta C_t$ method(97). Spheroid culture supernatant was processed for CCL3 quantification by ELISA (ab214569, Abcam, France) according to the manufacturers' instructions. Assessment of collagen deposition in spheroids: Healthy liver

tissue (**Suppl. Table 6**) was processed into multicellular spheroids, stimulated with FFA (100ng/ml), LPS (100ng/ml) and TGF β (10ng/ml), and then treated with Elafibranor (10 μ M), isotype control antibody (10 μ g/ml), or CLDN1 mAb (10 μ g/ml) for 4 days. Total collagen deposition was quantified using Total Collagen Assay Kit perchlorate-free (Abcam), according to the manufacturer's instructions.

Precision cut ex vivo liver slice culture. Liver tissue slices (200-500 μ m-thick) were prepared from surgically resected non-tumorous liver tissues from NASH patients who underwent liver resection for HCC (**Suppl. Table 7**). The slices derived from adjacent non-tumorous tissue were cultured with CLDN1 specific mAb or isotype control mAb (10 μ g/mL) for 24 h and harvested for gene expression analysis, as described above. Gene expression data from non-diseased liver tissues (University Strasbourg NASH cohort, **Suppl. Table 1**) were used as reference controls to verify the induction of the PLS in the studied NASH patients.

Genome wide RNA-seq analyses. RNA-Seq libraries were generated from 300 ng of total RNA using TruSeq Stranded mRNA Sample Preparation Kit (Illumina, Part Number RS-122-2101). Briefly, following purification with poly-T oligo attached magnetic beads, the mRNA was fragmented using divalent cations at 94 °C for 2 min. The cleaved RNA fragments were copied into first strand cDNA using reverse transcriptase and random primers. Strand specificity was achieved by replacing dTTP with dUTP during second strand cDNA synthesis using DNA Polymerase I and RNase H. Following addition of a single 'A' base and subsequent ligation of the adapter on double stranded cDNA fragments, the products were purified and enriched with PCR (30 sec at 98 °C; [10 sec at 98 °C, 30 sec at 60 °C, 30 sec at 72°C] x 12 cycles; 5 min at 72°C) to create the cDNA library. Surplus PCR primers were further removed by purification using AMPure XP beads (Beckman Coulter) and the final cDNA libraries were checked for quality and quantified using 2100 Bioanalyzer (Agilent). Libraries were sequenced on the Illumina HiSeq 4000 as Single-Read 50 base reads following Illumina's instructions. Image analysis and base calling were performed using RTA v2.7.3 and bcl2fastq v2.17.1.14.

In vitro perturbation studies on THP1 cell line and primary Kupffer cells. THP1: Human monocytic cell line THP1 (ATCC cell bank) was cultured in DMEM supplemented with 10% heat-inactivated fetal bovine serum at 37°C and 5% CO₂. Differentiation into M0 macrophages was induced by treatment of THP1 cells (1.5 x10⁵ cells per well in 12 well plates) with phorbol 12-myristate 13-acetate (PMA) for 320nM hours. Differentiation into M1 macrophages was induced by subsequent treatment with LPS (100ng/mL) + IFN (20ng/mL) of THP1-derived M0 macrophages for 24 h(21). All experiments were performed in at least three independent experiments in triplicate. Kupffer cells: Primary Kupffer cells were isolated from non-tumorous patients liver tissue as described(92) and maintained in RPMI supplemented with 10% heat-inactivated fetal bovine serum at 37°C and 5% CO₂. Identity and purification of Kupffer cells was validated by expression of CD68 (CUSABIO, USA) as assessed by immunofluorescence (see below). For CLDN1 gene expression analysis, primary Kupffer cells (1.5 x10⁵ cells per well in 12 well plates) were differentiated into M1 phenotype by incubation with LPS (100ng/mL) + IFN (20ng/mL) for 24 h or treated with TNFα (10ng/mL) for 24 h. For perturbation studies of CLDN1 mAb effects on M1 Kupffer cell differentiation, primary patient-derived Kupffer cells were treated with vehicle Control (Mock) or LPS (100ng/mL) + IFN (20ng/mL) in presence of CLDN1 mAb or control mAb (50µg/mL, respectively) for 3 days(21). Kupffer cells were derived from n= 5 different donors (**Suppl. Table 2**) and experiments were performed in triplicate per condition and donor.

In vitro perturbation studies on human liver myofibroblasts (HLMF). Isolated human hepatic stellate cells (HSCs)(92) were seeded at a density of 5 x 10⁴ cells/cm² in DMEM with 10% FBS on collagen-coated 12 well plates. Following 10 days of cultivation on plastic, all cells showed a HLMF-like phenotype(93). At this stage (10d of culture) identity and purity of HLMF's were validated by expression of α-SMA (ab5694, Abcam, France), as assessed by immunofluorescence (see below). For analysis of CLDN1 mAb effects on HLMFs activation markers, primary HLMFs were seeded at 5 x 10⁴ cells/cm² in 12 well plates and treated with

CLDN1 mAb (50 ug/mL) or vehicle control for 3 days. HLMFs were derived from n= 7 different donors (**Suppl. Table 2**) and experiments were performed in triplicate per condition and donor.

Immunofluorescence. Cells were seeded onto 8-chamber cover glasses (Lab-Tek II #1.5, Sigma-Aldrich). The next day, cells were washed twice with PBS and fixed with 4% PFA for 15 min at room temperature, followed by permeabilization with 0.1% Triton-X for 10 min. After two washing steps, cells were blocked for 30 min with 10% FBS. Primary antibody staining with anti- α -SMA Ab (1:100, Abcam, France) or anti-CD68 (1:100, CUSABIO, USA) and CLDN1 mAb H3L3 or control mAb (10 μ g/mL, respectively) was performed overnight at 4 °C. Cells were washed with PBS and incubated with goat anti-human Alexa Fluor 488 and/or goat anti-rabbit Alexa Fluor 647 secondary antibodies (Jackson, United Kingdom) at a dilution of 1:200. Nuclear staining was done using DAPI (1 μ g/mL) and cells were visualized using epifluorescence microscopy. Results were confirmed in at least 3 independent experiments.

Gene expression analyses in 2D cell culture experiments. Total RNA extraction from 2D cell cultures was performed using RNAeasy Mini Kit (Quiagen, France) according to the manufacturer's instructions. Subsequently, 100-500 ng RNA was reverse transcribed (H Minus First Strand cDNA synthesis Mix, ThermoScientific, France) on a Thermocycler (Bio-Rad T100, Bio-Rad, Hercules, CA, USA). Quantitative PCR was performed on the CFX96 Touch Real-Time PCR Detection system with 20 μ L reaction volumes containing 10 μ L SYBR Green 2x mix (Bio-Rad), 4 μ L of RNase-free water and 250 nM gene specific sense and antisense primers. The primer sequences were as follows: *ACTA2* Fw: 5'-TGA AGA GCA TCC CAC CCT, Rv: 5'-ACG AAG GAA TAG CCA CGC; *COL1A1*: Fw: 5'-CCT CAA GGG CTC CAA CGA G, Rv: 5'-TCA ATC ACT GTC TTG CCC CA; *TNFA*: Fw: 5'-GAG GCC AAG CCC TGG TAT G, Rv: 5'-CGG GCC GAT TGA TCT CAG C; *IL6*: Fw: 5'-ACT CAC CTC TTC AGA ACG AAT TG, Rv: 5'-CCA TCT TTG GAA GGT TCA GGT TG; *TIMP1*: Fw: 5'-GCC CAG AGA GAC ACC AGA GAA C, Rv: 5'-CTA TCA GCC ACA GCA ACA AC AGG. All gene expression levels were normalized to housekeeping genes *HPRT1* (Fw: 5'-CTG GAA AGA ATG TCT TGA TTG TGG, Rv: 5'-TTT GGA TTA TAC TGC CTG ACC AAG in HLMFs) and *GAPDH* (Fw: 5'-GTC

TCC TCT GAC TTC AAC AGC G, Rv: 5'-ACC ACC CTG TTG CTG TAG CCA A) using the $\Delta\Delta\text{Ct}$ method(97).

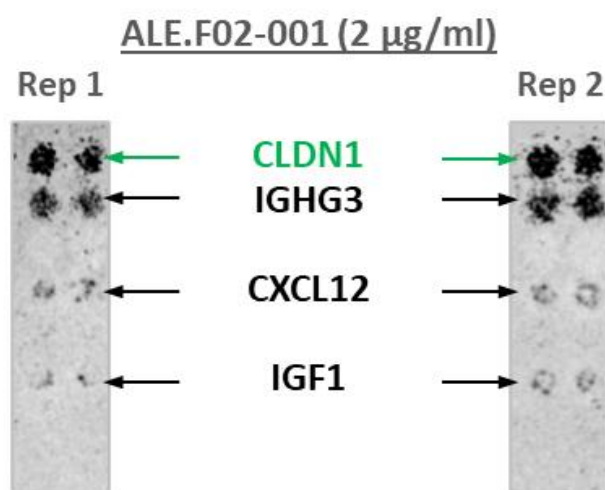
In vitro models of hepatocyte chronic injury. Huh7.5.1 and LX2 stellate cells were cultured in Dulbecco's Modified Eagle Medium (DMEM) containing 10% fetal bovine serum (FBS) and 1% DMSO for differentiation (Huh7.5.1^{dif} cells) as described(39-41). NTCP-overexpressing HepG2 (HepG2-NTCP) cells were selected using puromycin and cultured in DMEM with 10% FBS as previously described(98). HCV: DMSO-differentiated Huh7.5.1^{dif} cells were plated in 6-well plates and infected with HCVcc Jc1 (genotype 2a/2a) as described(39). HCV infection was assessed at day 10 by qRT-PCR of intracellular RNA as described(39). CLDN1 mAb or control mAb (10 $\mu\text{g/mL}$, respectively) were added for 3 days following HCV infection. HBV: HepG2-NTCP cells were plated in 12-well plates and infected with HBV purified from patient serum(98) in presence of CLDN1 mAb or control mAb (10 $\mu\text{g/mL}$, respectively). HBV infection was assessed at day 7 post-infection by qRT-PCR quantification of HBV pre-genomic RNA (pgRNA)(98). FFA-NASH model: DMSO-differentiated Huh7.5.1^{dif} cells co-cultured with LX2 cells (20%) were plated in 12-well plates and exposed to FFA (800 μM oleic acid and 400 μM palmitic acid) for 48 hours as described(99). CLDN1 mAb or control mAb (10 $\mu\text{g/mL}$, respectively) were added for 3 days following FFA treatment. Ethanol-ALD model: DMSO-differentiated Huh7.5.1^{dif} cells were plated in 6-well plates and exposed to ethanol (40 mM) in presence of CLDN1 mAb or control mAb (10 $\mu\text{g/mL}$, respectively) for 10 days. Fresh medium containing ethanol and mAbs was replenished daily. Each cell culture model was assessed in at least three independent experiments, performed in triplicate.

Analysis of phosphokinase phosphorylation. Phosphokinase phosphorylation was assessed in cell lysates derived from the NASH *in vitro* model using the Proteome Profiler Human Phosphokinase Array Kit (R&D Systems Inc.), according to the manufacturer's instructions. Levels of phosphokinases were assessed using biotinylated detection antibodies followed by chemiluminescence detection.

CLDN1 knockout using CRISPR-Cas9 technology. Huh7.5.1 stably expressing Cas-9 endonuclease (Huh7.5.1-Cas9) were DMSO-differentiated for 7 days (Huh7.5.1-Cas9^{diff}), and then either co-cultured with LX-2 stellate cells (20%) and treated with free fatty acids (FFA; 800 μ M oleic acid and 400 μ M palmitic acid) or infected using HCV Jc1. After 3 (FFA treatment) or 7 days (HCV Jc1 infection), cells were transduced with lentiviruses expressing control single guide RNA (sgRNA) or sgRNA targeting *CLDN1* gene expression (sgCLDN1). Expression plasmids were provided by Dr. David Root (Broad Institute of Harvard and MIT, Cambridge, USA). Transduced cells were selected under hygromycin treatment (500 μ g/mL) for 3 days and lysed using iScript™ RT-qPCR sample preparation reagent. The HCV- or FFA-induced PLS was analyzed using nCounter Nanostring technology in cell lysates. In parallel, cells were used to analyze CLDN1 expression by flow cytometry using a CLDN1 specific mAb (10 μ g/mL).

SUPPLEMENTARY FIGURES

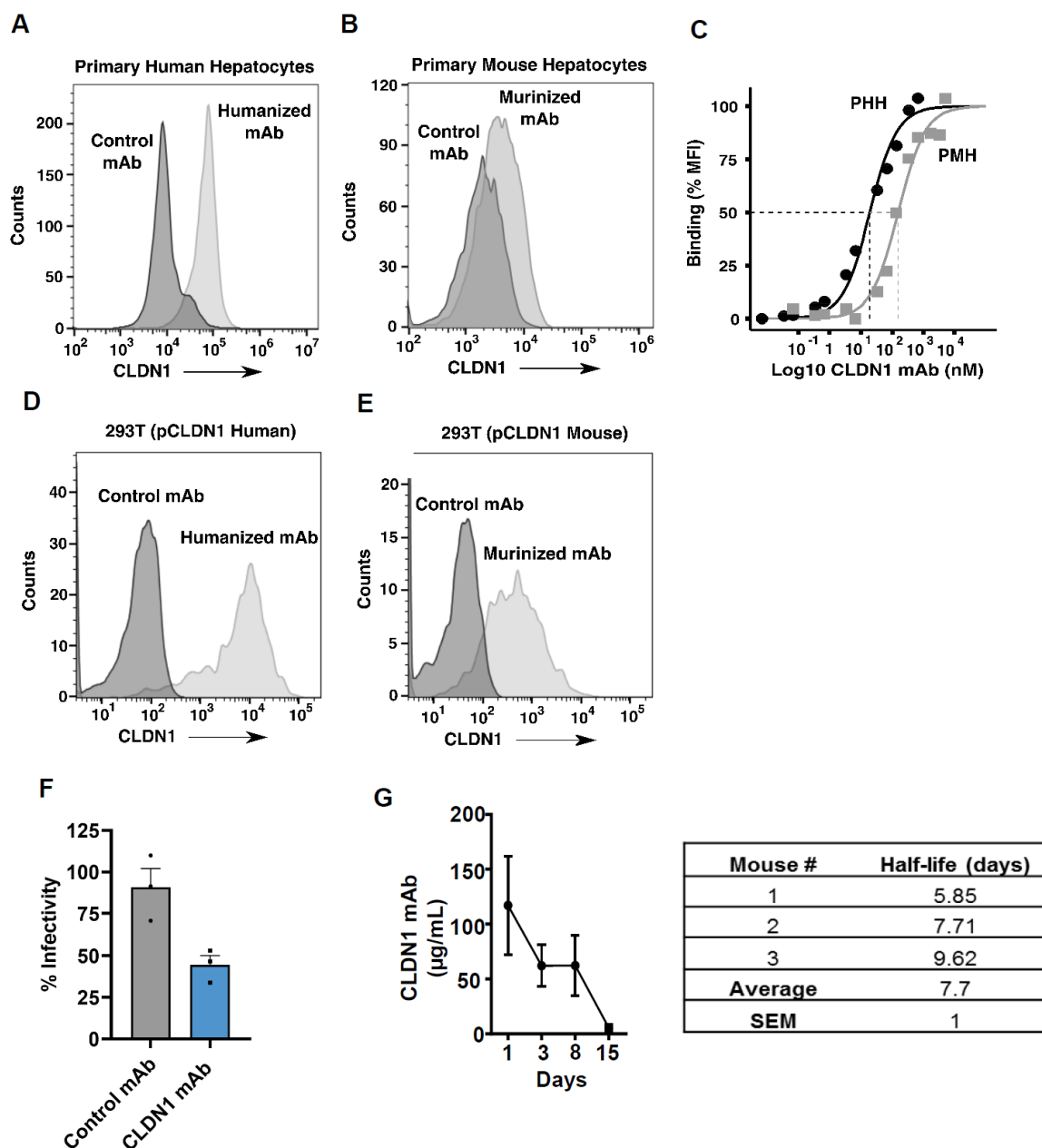
Supplementary Figure S1, related to Fig. 1. CLDN1 mAbs are highly specific for human CLDN1.



Gene Id	ALE.F02-001 interaction detected?
CLDN1	Yes
CLDN2	No
CLDN3	No
CLDN4	No
CLDN5	No
CLDN6	No
CLDN7	No
CLDN8	No
CLDN9	No
CLDN10	No
CLDN11	No
CLDN12	No
CLDN14	No
CLDN15	No
CLDN16	No
CLDN17	No
CLDN18	No
CLDN19	No
CLDN20	No
CLDN22	No
CLDN23	No
CLDN24	No
CLDN25	No
CLDN34	No

Interaction of CLDN1 mAbs (representatively shown for ALE.F02) with human plasma membrane and secreted proteins, as assessed by Retrogenix assay is shown. A strong positive signal was only detected for hCLDN1 and the IgG heavy chain. No cross-reactivity was found for >5000 other proteins tested. Minor non-specific interactions were found for CXCL12 and IGF1. Abbreviations: CLDN=Claudin; CXCL12=C-X-C Motif Chemokine Ligand 12; IGHG3=Immunoglobulin Heavy Constant Gamma 3; IGF=Insulin like growth factor 1; Rep=Replicate.

Supplementary Figure S2, related to Fig. 3. Functional assessment and pharmacokinetics of the murinized and humanized anti-human CLDN1-specific mAb.

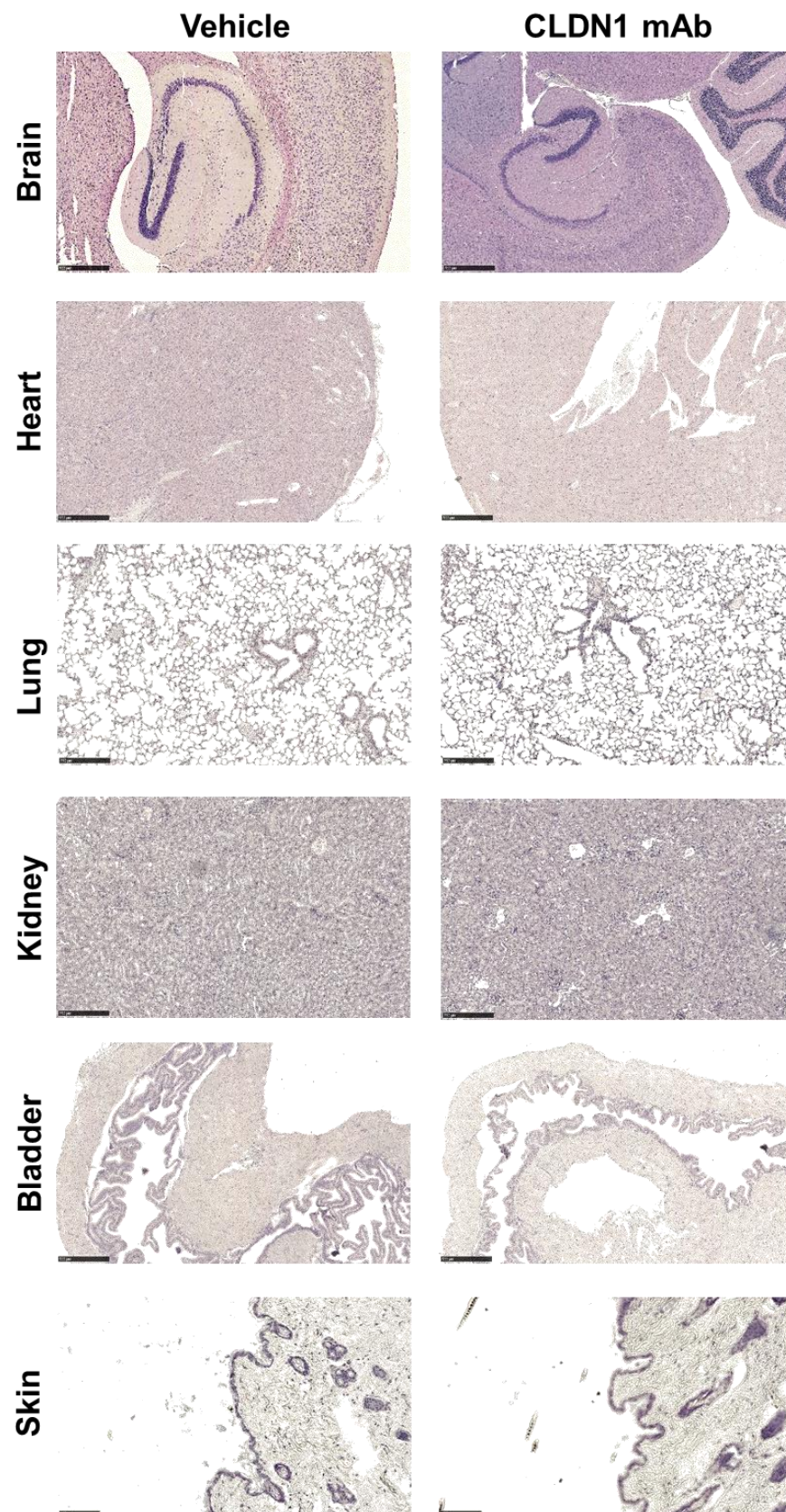


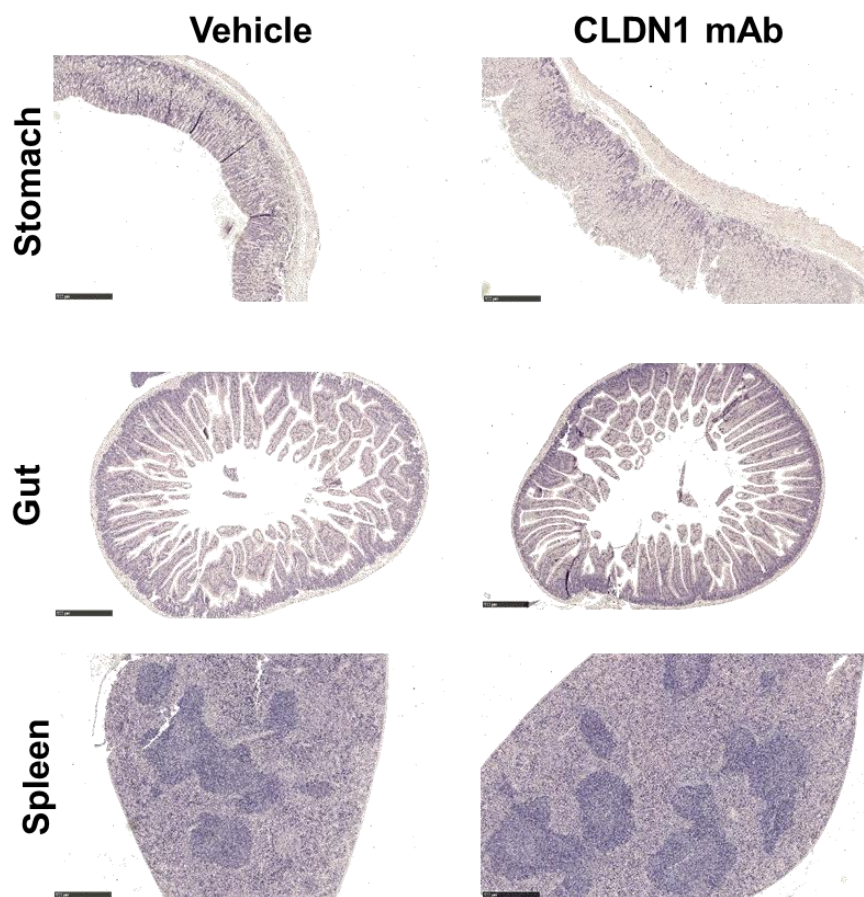
A-B. Binding of humanized anti-CLDN1 mAb H3L3 or murinized CLDN1 mAb to CLDN1 expressed on primary human (PHH) (**A**) or mouse hepatocytes (PMH) (**B**) as assessed by flow cytometry is shown **C**. The binding kinetics of the interaction between humanized or murinized mAb against human or mouse CLDN1 expressed on PHH and PMH were determined by applying the Michaelis-Menten mathematical model (PHH: black, apparent K_d of ≈ 19 nM;

PMH: grey, apparent K_d of ≈ 154 nM), respectively. **D-E.** The humanized and murinized CLDN1 mAb show robust binding to 293T cells, engineered to express human or murine CLDN1 (mCLDN1), respectively. **F.** mCLDN1 expressing 293T cells were incubated with a murinized CLDN1 mAb (100 μ g/mL) for 1 h at 37 °C prior to incubation with HCV pseudoparticles bearing glycoproteins JHF1 genotype 2a of HCV. HCVpp entry into 293T cells was assessed by measuring luciferase activity after 72 h and is shown as percentage relative to entry into untreated cells. * $p < 0.05$, Student's t-test. **G.** Left panel: Serum concentrations of the murinized CLDN1 mAb were determined at the indicated time points after a single i.p. injection of 500 μ g (25 mg/kg) of murinized mAb into three C3H mice. Right panel: The half-life of the murinized CLDN1-specific is shown, as determined using regression curve analyses.

Abbreviations: SEM=standard error of the mean; PHH=primary human hepatocytes; PMH=primary mouse hepatocytes.

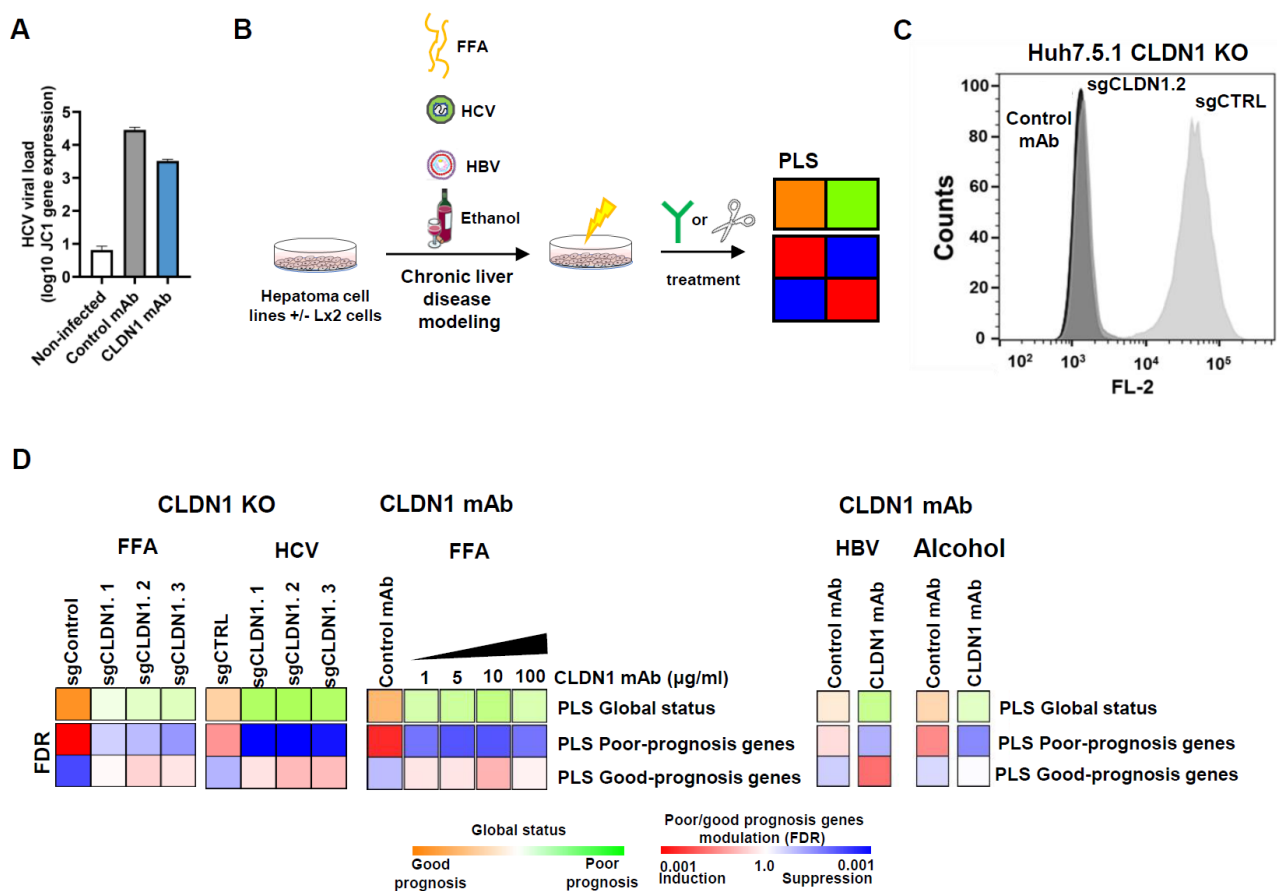
Supplementary Figure S3, related to Fig 3. Histopathology of organs in DEN-CDA-HFD mouse model treated with CLDN1-specific mAb or vehicle Control for 16 weeks.





All the organs were fixed in formalin, embedded in paraffin, stained by hematoxylin and eosin and analyzed by an expert veterinary pathologist from Phemonin-ICS, Illkirch, France. One-hundred-twenty-eight histological slides were analyzed. Eosin was weak on some sections (as shown in the brain image of the vehicle control group) without affecting the quality of the analysis.

Supplementary Figure S4, related to Fig. 5. CLDN1 mAb reverses the poor prognosis status of the clinical PLS in models of all major etiologies of chronic liver disease.

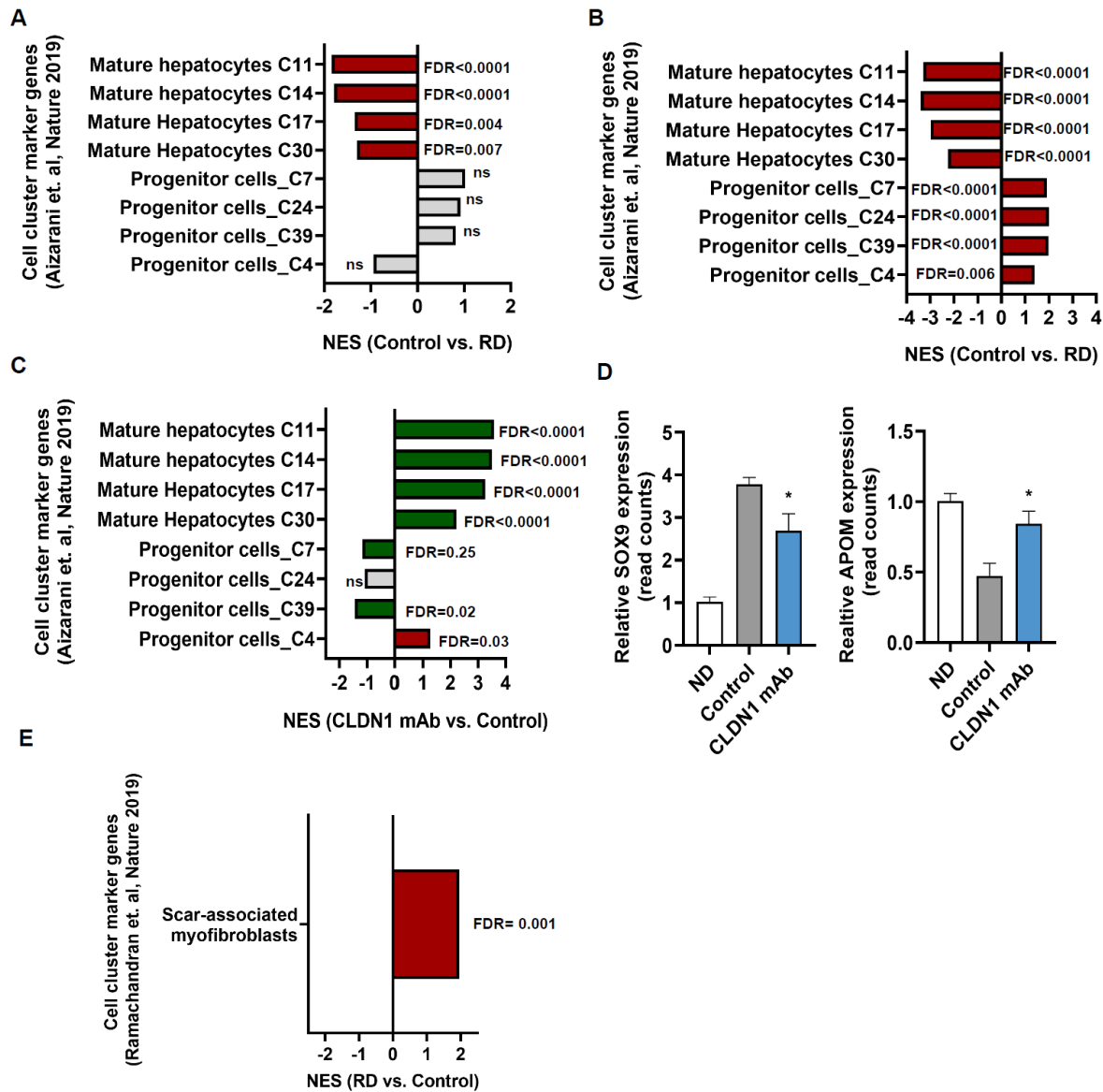


A. Quantification of viral load by JC1 gene expression analysis in Huh 7.5.1^{diff} cells after infection with HCVccc for 10 days and subsequent treatment with CLDN1 mAb or Control mAb.

B. Graphical illustration of PLS assessment in *in vitro* models of all major etiologies of chronic liver disease. **C.** Absent binding of humanized CLDN1 mAb to *Huh7.5.1-Cas9* cells expressing single guide RNAs (sgRNAs), assessed by flowcytometry is shown. **D.** Modulation of PLS to good (green) or poor (orange) prognosis status in sgCLDN1 or sgCTRL transfected- as well as CLDN1 mAb or control mAb-treated *in vitro* models of NASH, alcoholic liver disease, HBV and HCV infection compared to Mock cells. The significance (FDR, Kolmogorov smirnov test) of induction (red) or suppression (blue) of PLS poor- or good-prognosis genes is illustrated below. Abbreviations: HBV= Hepatitis B Virus; HCV= Hepatitis C virus; FDR= False discovery

rate; FFA= Free fatty acids; KO= Knockout; PLS= Prognostic Liver Signature; SEM= Standard error of the mean; sg= single guides.

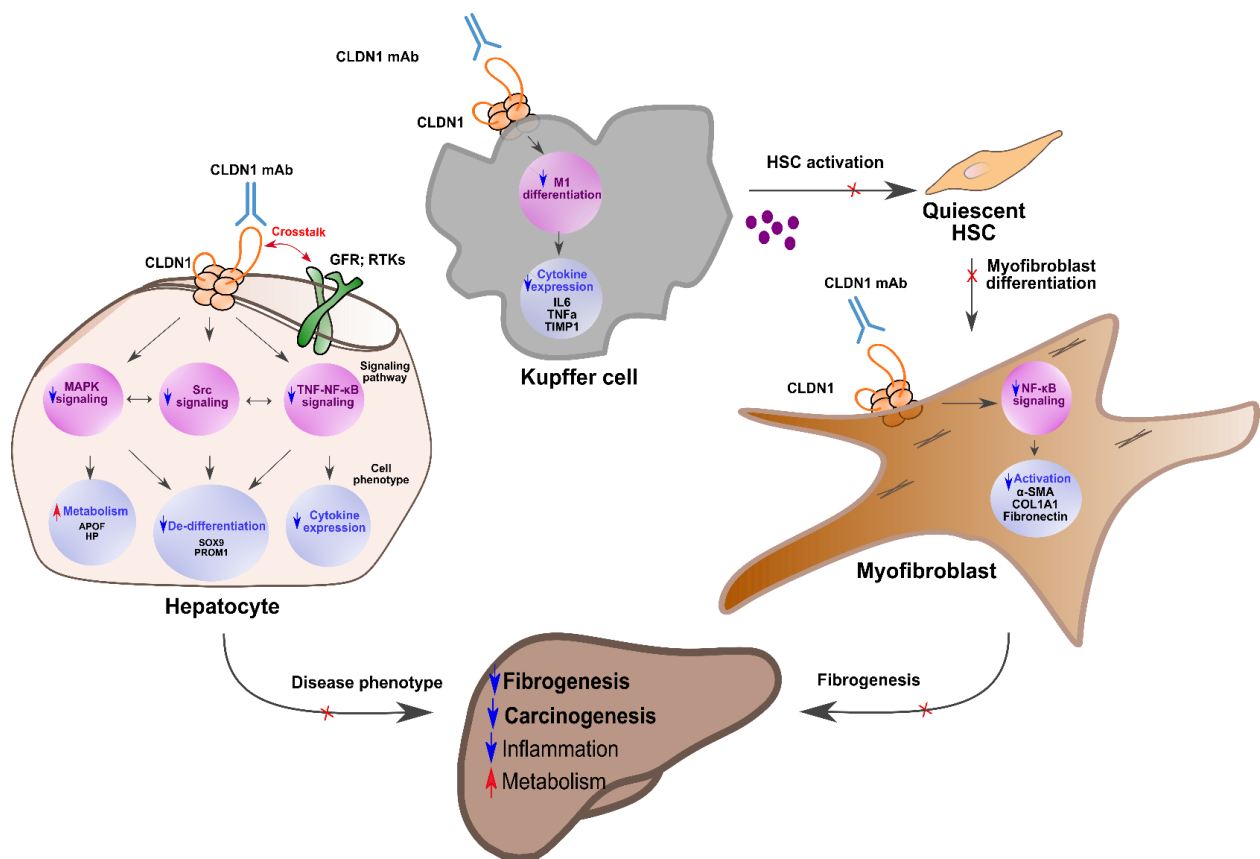
Supplementary Figure S5, related to Fig. 6. Reversal of injury-induced hepatocyte differentiation by CLDN1 mAb in humanized and NASH fibrosis model.



A-B. Differential expression of gene sets characterizing mature hepatocytes ((18) and MSigDB: AIZARANI_LIVER_C11/C14/C17C30_HEPATOCYTES) and immature progenitor cells ((18)and MSigDB: AIZARANI_LIVER_C4/C7/C24/C39_EPCAM_POS_BILE_DUCT_CELLS) in healthy (RD) versus fibrotic livers in the humanized (A) and classical NASH fibrosis mouse model (B) is

shown. **C.** Effect of CLDN1 mAb on hepatocyte de-differentiation in NASH fibrosis mice. **D.** Gene expression of SOX9 and APOM in NASH fibrosis mice treated with CLDN1 mAb or Control are shown. **E.** Modulation of gene sets characterizing scar-associated myofibroblasts in healthy (RD) versus fibrotic livers in the classical NASH fibrosis mouse model. Colored horizontal bars indicate NES of significantly (FDR<0.25, Kolmogorov Smirnov test, respectively) altered gene sets. Vertical bars show mean \pm SEM. *p<0.05, t-test, respectively. Abbreviations: Apolipoprotein M=APOM; False discovery rate=FDR; NASH= Non-alcoholic steatohepatitis; Normal diet= ND; Normalized enrichment score=NES; SRY-Box Transcription Factor 9=SOX9.

Supplementary Figure S6: Model for CLDN1 mAb mechanism of action



Model of mechanism of action. Within the cell membrane CLDN1 forms a complex that cross-talks with growth factor receptors (GFR) and receptor tyrosine kinases (RTKs). The CLDN1 specific mAb interferes with the CLDN1 complex formation modulating intracellular signaling, such as MAPK-, Src and TNF-NFκB signaling in hepatocytes, hereby suppressing hepatocyte de-differentiation and pro-fibrogenic cytokine expression and restoring mature hepatocyte metabolism. CLDN1-specific mAb further binds to M1 Kupffer cells, reducing the expression of secreted myofibroblast activators and pro-fibrogenic factors. Interference of CLDN1 mAb with NFκB signaling in myofibroblasts suppresses activation and thus production of extracellular matrix and scarring. Collectively, modulation of hepatocyte, Kupffer cell and myofibroblast signaling by CLDN1 specific mAb inhibits fibrosis associated cell plasticity, inflammation, fibrogenesis and carcinogenesis and at the same time improves metabolic functions of the hepatocyte. Abbreviations: αSMA=alpha smooth muscle actin; APOF=Apolipoprotein F; CLDN1=Claudin-1; Col1A1=collagen 1A1; FN1=Fibronectin; GFR=Growth factor receptors;

HP=Haptoglobin; HSC=Hepatic stellate cell; IL6=Interleukin 6; MAPK=Mitogen-activated protein kinases; PROM1=Prominin 1; RTK=Receptor tyrosine kinase; SOX9= SRY-Box Transcription Factor 9; TIMP1=TIMP Metalloproteinase Inhibitor 1; TNF α =Tumor necrosis factor alpha.

SUPPLEMENTARY TABLES

Supplementary Table 1, relating to Fig. 1a. Demographic and clinical characteristics of the University of Strasbourg NASH cohort.

	Control (n=10)	NASH (n=10)
Age (years)	43 (23-73)	39 (25-54)
Female (%)	18 (90)	4 (40)
Waist circumference (cm)	98.5 (75-149)	136 (100-170)
BMI (kg/m²)	31.9 (22.4-50.0)	46.9 (40.5-60.5)
Blood fasting glucose (mg/dL)	84 (66-130)	114 (83-162)
Insulin (μUI/mL)	6.1 (1.7-29.5)	9.2 (4.8-83.5)
HOMA-IR index	1.14 (0.33-5.90)	3.31 (0.99-33.40)
Total cholesterol (mg/dL)	166 (113-288)	151 (93-181)
Triglycerides (mg/dL)	122 (60-209)	194 (93-273)
FFA (mg/dL)	26 (8-36)	24 (13-35)
LDL cholesterol (mg/dL)	106 (59-217)	81 (46-101)
HDL cholesterol (mg/dL)	41 (31-67)	31 (18-42)
AST (UI/L)	21.5 (12-85)	48.5 (20-176)
ALT (UI/L)	18 (5-122)	56.5 (27-229)
ALP (UI/L)	60 (36-122)	54.5 (35-97)
GGT (UI/L)	20.5 (5-221)	35.5 (19-114)
Total bilirubin (mg/dL)	0.6 (0.3-1.01)	0.6 (0.3-0.9)
Iron (μg/dL)	76 (30-197)	66 (30-146)
Ferritin (ng/mL)	70.5 (14-399)	155 (10-2380)
Transferrin saturation %	27.5 (9-81)	23.5 (10-49)
CRP (mg/L)	2.84 (0.18-9.59)	6.27 (1.39-19.40)

Continuous variables are indicated as median and range. Abbreviations: ALP=alkaline phosphate, ALT=alanine aminotransferase, AST=aspartate aminotransferase, BMI=Body Mass Index, CRP=C-reactive protein, FFA=free fatty acid, GGT=gamma-glutamyl transferase, HDL=high density lipoprotein, HOMA-IR=homeostatic model assessment of insulin resistance,

LDL=low density lipoprotein, NAFL=non-alcoholic fatty liver, NASH=non-alcoholic steatohepatitis.

Supplementary Table 2, relating to Fig.1 and 6. Demographic and clinical characteristics of patients recruited for isolation of Kupffer cells, LECs and HSCs.

ID	Age(y)	Sex	Chronic liver disease	Indication for liver resection	Isolated cell type
304	52	F	No	CCM	LEC, Kupffer cells
352	48	M	No	CCM	HSCs
372	51	M	No	CCM	HSCs
374	59	F	No	CCM	HSCs
383	71	F	No	CCM	HSCs, Kupffer cells
389	82	F	HCV cured +NAFLD (F2)*	CCA	HSCs, Kupffer cells
397	23	F	No	PHL	HSCs, LECs, Kupffer cells
401	36	F	No	CCM	HSCs, LECs, Kupffer cells
429	62	M	No	CCM	Kupffer cells

*Fibrosis stage(25)

Abbreviations: CCA= Cholangiocellular Carcinoma, CCM= Colon cancer liver metastasis; HSC=Hepatic stellate cells; LECs= Liver endothelial cells, NAFLD= Non-alcoholic fatty liver disease, PHL= Primary hepatic leiomyosarcoma, y= years.

Supplementary Table 3, relating to Fig 2. Individual data of the main efficacy endpoints of the humanized NASH mice treated with vehicle control or humanized CLDN1 mAb.

Experiment #1

Group	Mouse ID	Total fibrosis %	Fibrosis in humanized area %	Tumor Number
Vehicle	4409	10.495	6.30	24
	4411	6.589	4.66	30
	4412	6.261	3.35	17
Median		6.59	4.66	24.00
Mean		7.78	4.77	23.67
s.e.m.		1.36	0.86	3.76
CLDN1 mAb	4405	1.101	0.51	17
	4407	5.843	1.80	5
	4408	3.168	1.51	12
	4424	1.516	0.68	11
Median		2.34	1.09	11.50
Mean		2.91	1.12	11.25
s.e.m.		1.08	0.31	2.46
Test		MW	MW	MW
p-value		0.0339	0.0339	0.0498

Abbreviations: MW= Mann Whitney U test, s.e.m.= standard error of the mean.

Experiment #2

Group	Mouse ID	Total fibrosis %	Fibrosis in humanized area %	Tumor Number
Vehicle	1005	7.708	7.708	9
	1006	11.862	12.531	10
	4472	11.8925	11.8925	NA
	4477	6.048	4.438	22
	4478	1.167	0.886	13
	4479	10.4915	9.34	14
	4490	4.751	4.046	7
	4491	1.881	2.017	7
	4492	7.13	7.13	7
	4493	4.401	6.152	5
Median		6.59	6.64	9.00
Mean		6.73	6.61	10.44
s.e.m.		1.21	0.84	1.75
CLDN1 mAb	1001	2.11	2.667	5
	1002	4.55	5.352	5
	1008	1.48	1.48	4
	1009	4.446	4.5225	4
	1010	1.716	1.716	4
	4470	1.618	1.864	2
	4471	1.1705	1.5995	4
	4483	2.556	2.308	5
	4484	3.552	0.96	13
	4485	1.322	0.583	10
Median		1.91	1.79	4.50
Mean		2.45	2.31	5.60
s.e.m.		0.41	0.48	1.05
Test		MW	MW	MW
p-value		0.013	0.013	0.0093

Abbreviations: MW= Mann Whitney U test, s.e.m.= standard error of the mean

Supplementary Table 4, relating to Fig. 3. Metabolic parameters and CLDN1 mAb concentrations in DEN-CDA-HFD mice treated with vehicle control or murinized CLDN1 mAb.

	Vehicle (mean \pm s.e.m.)	CLDN1 mAb (mean \pm s.e.m.)	p-value (MW test)
ALT (UI/L)	244 \pm 12	217 \pm 14	0.033
AST (UI/L)	276 \pm 16	271 \pm 20	0.664
ALP (UI/L)	129 \pm 30.2	103.1 \pm 3.3	0.584
Total bilirubin (μmol/L)	3.89 \pm 0.40	4.57 \pm 0.62	0.511
Total proteins (g/L)	46.2 \pm 0.8	49.1 \pm 0.4	0.013
Albumin (g/L)	22.4 \pm 0.7	23.8 \pm 0.5	0.275
Creatinine (μmol/L)	8.79 \pm 0.50	7.98 \pm 0.39	0.316
Urea (mmol/L)	9.01 \pm 0.18	8.75 \pm 0.39	0.371
Sodium (mmol/L)	145.0 \pm 1.7	147.7 \pm 0.7	0.059
Potassium (mmol/L)	5.33 \pm 0.14	5.04 \pm 0.13	0.152
Calcium (mmol/L)	2.05 \pm 0.04	2.09 \pm 0.02	0.602
Glucose (mmol/L)*	8.25 \pm 0.51	9.12 \pm 0.31	0.179
Total cholesterol (mmol/L)*	1.08 \pm 0.06	1.12 \pm 0.05	0.784
CLDN1 mAb (μg/mL)	--	125.8 \pm 8.5	--

*Mice not fasted.

Abbreviations: ALT= alanine aminotransferase, AST= aspartate aminotransferase, ALP= alkaline phosphatases, MW= Mann Whitney U test, s.e.m.= standard error of the mean.

Supplementary Table 5, relating to Fig. 3. Individual data of the main efficacy endpoints of DEN-CDA-HFD mice treated with vehicle control or CLDN1 mAb.

Group	Mouse ID	Fibrosis %	Tumor macroscopy (Y=1/N=0)	Tumor N at histology	Max tumor size (mm)	Tumor HSP70+ (Y=1/N=0)
Vehicle	621	11.25	1	9	5.8	1
	622	8.59	1	7	2.2	1
	623	14.19	1	8	7.0	1
	624	9.95	1	3	1.5	0
	625	11.07	1	1	1.2	0
	631	9.53	0	0	NA	0
	632	18.69	1	3	1.5	0
	633	6.83	1	2	0.9	0
	634	7.69	1	1	2.1	0
	635	11.46	1	2	1.6	0
	641	8.28	1	11	1.2	1
	642	11.89	1	4	0.6	0
	643	8.24	1	3	1.0	0
	644	8.01	1	13	1.6	0
	645	8.79	1	10	8.1	1
	652	9.52	1	11	9.3	1
	653	6.67	1	17	13.0	1
	654	9.26	1	4	1.6	1
Median		9.39	NA	4.00	1.62	NA
Mean		10.00	0.94	6.06	3.55	0.44
s.e.m.		0.68	0.06	1.15	0.89	0.12
CLDN1 mAb	626	9.92	0	1	1.4	0
	627	11.76	1	7	6.0	1
	628	8.29	0	0	NA	0
	629	8.93	0	0	NA	0
	630	8.81	0	1	0.9	0
	636	5.16	0	2	0.5	0
	637	4.64	0	3	0.8	0
	638	6.57	1	2	1.3	0
	639	4.76	1	2	1.3	0
	640	6.87	0	1	1.1	0
	646	6.05	0	0	NA	0
	647	6.29	0	1	0.7	0
	648	13.55	1	2	1.1	0
	649	4.33	0	1	0.6	0
	650	6.06	0	1	0.6	0
	656	4.39	1	6	1.5	0
	657	7.91	0	0	NA	0
	658	8.60	0	2	0.4	0
	659	4.94	0	2	0.8	0
	660	7.97	1	3	1.1	0
Median		6.72	N/A	1.50	1.00	N/A
Mean		7.29	0.30	1.85	1.25	0.05
s.e.m.		0.56	0.11	0.41	0.33	0.05
Test		MW	FT	MW	MW	FT
Per mouse						
p-value		0.003				
Per image						
		<0.001		0.001	0.001	0.007
<0.001						

Abbreviations: FT= Fisher test, HSP70= heat shock protein 70, MW= Mann Whitney U test,

N/A= not applicable., s.e.m.= Standard error of the mean.

Supplementary Table 6, relating to Fig. 4. Demographic and clinical characteristics of patients shown in **Fig. 4c-g**.

ID	Age(y)	Sex	Chronic liver disease	Indication for liver resection	Fibrosis stage	Applied type of tissue
353	83	M	NAFLD	HCC	F2	diseased, non-tumorous
351	78	M	NAFLD	CCM	F0	diseased, non-tumorous
410	70	M	-	CCM	F0	healthy, non-tumorous
471	70	M	-	GBC	F0	healthy, non-tumorous
525	50	F	-	BCM	F0	healthy, non-tumorous

Abbreviations: BCM= breast cancer metastasis, CCM= colon cancer liver metastasis, F= female, GBC= Gallbladder adenocarcinoma, HCC= Hepatocellular carcinoma, M= male, NAFLD= Non-alcoholic fatty liver disease, NASH=Non-alcoholic steatohepatitis, y= years.

Supplementary Table 7, relating to Fig. 4. Demographic and clinical characteristics of patients shown in **Fig. 4h**.

	NASH #1	NASH #2	NASH #3	NASH #4	NASH #5
Age (years)	74	60	74	81	75
Sex (Male/Female)	Male	Male	Male	Male	Male
Fibrosis stage(25)	4	3	3	4	2
Obesity (Yes/No)	Yes	No	No	No	No
Diabetes (Yes/No)	Yes	Yes	No	No	Yes
Hypertension (Yes/No)	Yes	Yes	No	No	No

Abbreviations: NASH= Non-alcoholic steatohepatitis.

Supplementary Table 8, relating to Fig.6. Scar-associated myofibroblast marker genes*.

DCN	TMSB10	FBLN1	RPL36	CYR61	MARCKSL1
C1R	EFEMP1	CD81	PRSS23	CCL2	THBS2
LUM	BGN	MMP2	IL32	RPS12	CTSC
COL3A1	MMP23B	PDGFRA	ANXA1	ADAMTSL2	TCEAL4
C1S	IFITM3	FBLN5	NR2F1	IGFBP7	EMP3
C7	PPIB	COLEC11	TSPAN4	CTSD	WBP5
COL1A2	NNMT	CD74	COL5A1	ITGBL1	RPLP1
COL1A1	NPC2	SPON2	ENG	IGFBP3	RPS17
CFH	COL6A1	COL6A3	RPL37	FSTL1	RPS23
TIMP1	MARCKS	COL14A1	ISLR	PPIC	RPS15
PCOLCE	AEBP1	G0S2	RPS15A	FCGRT	HLA-DPA1
CST3	THY1	LTBP4	PTGDS	PLTP	COL4A2
OLFML3	HLA-DRB1	RCN3	RRBP1	SSR2	TFPI
CXCL12	SRPX	IGFBP4	EFEMP2	RPS18	HLA-DRA
CLEC11A	COL6A2	LY6E	INMT	CLEC2B	IGF2
GGT5	S100A10	MGP	SPARC	IGFBP6	LAMB1
CD63	MEG3	RPL13	ECM1	TIMP2	CCL21
FTL	EMILIN1	LGALS3BP	CCDC80	VCAN	CEBPD
RARRES2	RPL12	TMEM176A	SERPING1	ALDH1A1	RARRES1
ASPN	S100A11	PRELP	FN1	TPT1	DAAM1
S100A13	LRP1	TYROBP	LXN	QSOX1	
RBP1	ADH1B	TMEM176B	MFAP4	RPS24	
SERPINF1	CYBA	IFITM1	RPL39	RAMP1	
DPT	RPL28	RPS28	VKORC1	F2R	

*derived from(19).

Supplementary Table 9, relating to Fig.6. Scar-associated myofibroblast type A marker genes*.

COLEC11	HLA-A	EDNRB	CALM2	MASP1	PTGIR
IGFBP7	HLA-DRB1	HGF	CITED2	ALDH1A1	HLA-DRB5
PPP1R14A	HLA-B	HLA-C	TMEM204	TMSB4X	ITM2C
GGT5	C11orf96	TPM1	COX7A1	CTSD	SGCA
CALD1	LTBP4	ENG	BST2	HLA-DPA1	ARHGAP15
TYROBP	4-Sep	COL4A2	CCL21	MARCKS	RGS16
B2M	MYL9	RAMP1	RBPMS	ASPN	COL4A1
ADAMTSL2	C8orf4	IGFBP3	RBP1	GPX3	

*derived from(19).

Supplementary Table 10, relating to Fig.5. Scar-associated myofibroblast type B marker genes*.

COL1A2	IGF1	NNMT	RPLP0	YBX3	LXN
S100A6	RARRES1	TSHZ2	VIM	MMP2	CCND2
C3	SERPINF1	ADIRF	ANXA1	RPSA	SFRP2
FBLN1	MDK	STEAP1	RPS3	PTGIS	IGFBP4
CCDC80	CLU	CTHRC1	S100A16	IGFBP2	DNAJB1
COL1A1	FSTL1	COL6A3	DHRS3	NR4A2	PLP2
OGN	SLIT3	LGALS1	VCAN	SVIL	CAV1
SPARCL1	ANXA2	OSR1	COL6A1	BOC	MGP
S100A4	IGFBP6	OAF	MMP23B	GPRC5A	CAPZB
NBL1	COL3A1	S100A10	CRABP2	PCOLCE	

*derived from(19).

Supplementary Table 11, relating to Fig.7. Individual Sirius-red positive areas in renal fibrosis UO mice treated with vehicle control or CLDN1 mAb.

Control						CLDN1-specific mAb					
Mouse ID	Photo No.	Total area (pixel)	Positive area (pixel)	Positive area (%)	Positive area (%)	Mouse ID	Photo No.	Total area (pixel)	Positive area (pixel)	Positive area (%)	Positive area (%)
101	1	3145728	344415	10.95	8.88	201	1	2942661	91823	3.12	3.14
	2	3145728	277600	8.82			2	3145728	9667	0.31	
	3	3145728	616310	19.59			3	3145728	178982	5.69	
	4	3145728	106844	3.40			4	3145728	105012	3.34	
	5	2525427	41941	1.66			5	3145728	102614	3.26	
102	1	3145728	54042	1.72	6.88	202	1	2955677	149707	5.07	4.26
	2	1852892	282606	15.25			2	3145728	157964	5.02	
	3	2901737	105846	3.65			3	3145728	158958	5.05	
	4	2680358	270561	10.09			4	3145728	137962	4.39	
	5	1677944	61894	3.69			5	3145728	55942	1.78	
103	1	2613185	45756	1.75	12.74	203	1	3145728	106839	3.40	3.01
	2	3145728	79596	2.53			2	3145728	96460	3.07	
	3	3145728	105531	3.35			3	3145728	104407	3.32	
	4	2128925	256408	12.04			4	3145728	108886	3.46	
	5	1805725	795103	44.03			5	3145728	56876	1.81	
104	1	1907636	96743	5.07	5.62	204	1	2053687	221370	10.78	7.07
	2	3145728	116189	3.69			2	2922969	175727	6.01	
	3	2498956	300009	12.01			3	3145728	280234	8.91	
	4	3145728	197408	6.28			4	3145728	95235	3.03	
	5	3145728	32587	1.04			5	3145728	208497	6.63	
105	1	3145728	107920	3.43	5.12	205	1	3145728	26479	0.84	1.70
	2	3145728	228570	7.27			2	3145728	113376	3.60	
	3	3145728	57914	1.84			3	3145728	31501	1.00	
	4	3145728	163861	5.21			4	3145728	24949	0.79	
	5	3145728	247323	7.86			5	3145728	71784	2.28	
106	1	2391160	25941	1.08	5.31	206	1	3145728	56743	1.80	1.77
	2	2481193	192484	7.76			2	3145728	84916	2.70	
	3	2409692	128920	5.35			3	3145728	52829	1.68	
	4	3145728	46287	1.47			4	3145728	61369	1.95	
	5	3145728	343353	10.91			5	3145728	22164	0.70	
107	1	2952140	36770	1.25	9.96	207	1	3145728	44821	1.42	0.79
	2	1283270	262341	20.44			2	3145728	33427	1.06	
	3	1882451	145227	7.71			3	3145728	33393	1.06	
	4	3145728	140876	4.48			4	3145728	5123	0.16	
	5	2652902	421933	15.90			5	3145728	7575	0.24	
108	1	3145728	225836	7.18	5.42	208	1	3054515	39178	1.28	1.41
	2	3145728	302298	9.61			2	3016949	51887	1.72	
	3	3145728	207383	6.59			3	2771583	44394	1.60	
	4	3145728	88954	2.83			4	2615483	39127	1.50	
	5	3145728	28495	0.91			5	2568128	23833	0.93	

Supplementary Table 12, relating to Fig.7. Individual Ashcroft scores in bleomycin pulmonary fibrosis mice treated with vehicle control or CLDN1 mAb.

Group	Mouse ID	Photo No.																				Mean
		1	2	3	4	5	6	7	8	9	10	11	12	13	14	15	16	17	18	19	20	
Control	101																					
	102	5	3	3	3	3	3	1	2	2	2	1	2	1	2	1	2	2	2	2	1	2.2
	103	4	6	7	7	3	6	7	7	6	6	7	5	4	3	5	3	2	1	3	1	4.7
	104	5	3	3	3	3	3	2	3	3	4	3	3	3	3	3	3	2	3	1	1	2.9
	105	5	6	6	6	6	3	4	8	7	3	3	4	6	5	6	7	5	3	2	1	4.8
	106	4	5	3	4	5	5	3	3	5	6	6	3	3	2	2	4	3	4	3	3	3.8
	107	3	3	3	3	5	2	3	5	6	8	8	7	6	7	6	3	4	3	8	8	5.1
	108																					
	109	3	6	8	8	5	2	5	3	4	3	7	8	8	8	5	4	5	8	6	6	5.6
	110	2	1	2	1	1	1	1	1	2	1	1	1	1	1	1	1	1	1	2	1	1.2
	111	2	2	2	2	1	2	2	2	1	3	3	2	1	1	1	2	2	2	2	2	1.9
	112																					
	113																					
	114	4	5	4	4	2	2	2	3	3	4	3	2	1	2	2	2	3	3	3	3	2.9
	115	4	4	6	3	5	3	3	3	3	3	3	3	3	4	4	3	2	3	2	3	3.4
	116	7	7	7	7	7	7	7	7	7	7	7	8	7	7	6	6	5	4	3	3	6.3
	117	5	5	3	5	7	7	3	8	5	7	7	7	7	5	4	5	3	3	3	5	5.2
	118	5	7	6	5	7	6	6	3	4	5	6	3	3	8	5	5	4	3	4	3	4.9
CLDN1-specific mAb	201	2	3	3	2	2	3	1	3	1	1	1	3	1	3	4	1	3	2	3	2	2.2
	202																					
	203	1	1	1	3	0	2	3	3	1	2	0	0	1	1	0	2	2	2	4	3	1.6
	204	1	1	2	3	2	1	0	0	1	1	0	0	2	1	2	5	4	3	2	3	1.7
	205	4	3	3	3	3	3	3	4	3	3	2	4	3	2	3	3	3	3	3	5	3.2
	206	3	4	2	3	4	4	2	3	3	3	3	2	1	2	3	3	3	3	3	2	2.8
	207	3	4	3	3	3	3	3	3	2	2	2	2	3	3	3	4	3	3	2	3	2.9
	208	2	1	3	1	2	2	2	2	3	3	1	1	1	4	3	4	2	3	3	2	2.3
	209	3	1	3	3	3	3	1	3	3	3	3	1	2	4	2	3	3	3	3	2	2.6
	210																					
	211																					
	212	1	1	3	4	3	3	3	4	3	4	2	3	3	2	3	5	2	4	3	2	2.9
	213	2	3	3	3	3	3	3	3	3	4	5	7	8	8	8	8	7	3	7	5	4.8
	214	3	3	3	3	3	2	3	2	3	3	2	3	4	3	4	2	3	3	3	2	2.9
	215	3	5	3	6	4	5	3	3	4	2	3	3	4	6	6	8	2	4	3	3	4.0
	216	2	3	3	2	3	3	3	3	3	2	3	3	3	3	2	3	3	3	3	3	2.8
	217																					
	218																					

Supplementary Table 13, relating to Fig.7. HAS^{high} fibroblast marker genes*.

AC090498.1	ETF1	GNPTAB	CSTB	MESDC1	ANKRD37	ATPIF1	HLA-C
MT-CYB	KIAA1324L	LITAF	RCAN1	RAB3A	TLE1	ZFAND3	METAP2
A2M	PGM3	MYL9	MID1	SLC25A33	RCN3	CD70	PPP4R2
CDKN2A	PTGES3	ISG20L2	PKM	CEBPZ	OSER1	PFKFB3	NR2F2
GALNT13	FAT1	CDKN1A	MAP1LC3B	CACNA2D1	IGF2	VCAN	ADD3
HSP90AA1	CXorf40B	SLC16A1	MTRNR2L12	SMARCA1	CD276	EDNRA	WTAP
HSPE1	PTP4A1	GPRC5A	COL6A2	SEMA3C	YPEL2	EMP1	EFEMP1
LINC01605	CD9	PRRC2C	GXYLT2	SKIL	GOLM1	CDC42EP2	MT1M
HSPD1	CERCAM	MGP	ATXN7	UCK2	HINT1	SPCS1	ARPC5L
FHL2	ARF4	PNPLA8	CTSL	HBEGF	CREM	QSOX1	PDLIM4
KIAA1217	COL1A1	HAS1	RALGPS2	S1PR3	PPIC	ARMCX3	WT1
PDLIM3	EIF5A	PLK2	THBS3	FGF2	OAF	JARID2	FRZB
NAF1	FAM180A	FKBP4	MT-ND5	TOB1	BAG2	TFG	KDEL2
TNFSF9	MORF4L2	BTA1F1	ARC	SFTPC	CCDC71L	SOCS3	IFITM3
LINC00152	ISLR	RPL17	GAS7	FLNA	THBS2	CXCL14	XBP1
MT-ATP8	INSIG1	ARHGAP5	CYB5A	RHOC	PCDH7	MAP2K3	CYP1B1
SELK	MEDAG	VEGFA	PITPNB	ATP5G2	ERVK3-1	ARSI	ADGRD1
SLC12A8	ZBTB21	IFITM2	CMTM3	PPRC1	NAV1	MYH9	LIMCH1
MT-CO2	MAP4K5	SLC4A7	TAF13	MT-ND4	CPNE8	WWTR1	H3F3A
TLL1	BLOC1S6	C16orf45	TCF21	SCGB1A1	ARHGDIB	MINOS1	SFPQ
AC113404.1	STIP1	KLHL21	IPMK	PTRH2	MAP3K4	SCG2	PSAP
MT-CO3	TPM2	FERMT2	BAZ1A	ECM1	ALDH2	HLA-DPB1	CHSY1
HSP90AB1	RP11-210L7.3	ROR1	HSPB8	ADAMTS16	YWHAQ	GLA	KDM5B
CDKN2B	AHSA1	PAMR1	VAT1	TEX10	COX4I2	PGAP1	PTGES
HSPA4L	GEM	TXN	JOSD1	CLDN11	EBF1	MAGED1	LAMC1
FEM1C	ITGB1	UBE2B	CTC-444N24.11	MICAL2	CALM1	LY96	USP2
ABL2	OSMR-AS1	ZNF460	VIM	TFB2M	IGF1	SRGN	ATP5L
HSPA8	MEG3	BAIAP2	NDEL1	CTSD	EIF3J	GOPC	PCBP2
MXRA5	KDM6B	ASB1	MCC	TUBB2A	EIF2S1	CHIC2	PDGFRL
MT-CO1	PTHLH	IQCJ-SCHIP1	UBAP1	NGF	SEPW1	RSL1D1	ZFC3H1
GPX3	SULF1	MYC	MIR22HG	JAG1	SAMD9	CTSK	BNC2
RP11-474O21.5	ACLY	COL3A1	TUBB3	HTRA3	COX4I1	PNO1	HNRNPAB
RABGEF1	MIR4435-2HG	HSD3B7	HMG2N	MAPRE1	GART	ANGPT1	SPG20
LINC01060	CCT2	HSPA1A	RUNX2	HMG2N3	RCN1	CSNK1A1	MAPK1IP1L
UGDH	PDK4	GNG12	LRRC59	MLF1	STAG1	ANXA5	KRT18
GCLM	TES	ARL5B	BMP1	GTPBP4	LSM12	NNMT	SRP14
USP12	FAM3C	CEBPD	SDC2	DOT1L	DENND4A	LOX	LRRC17
TAGLN	CHMP1B	PLIN3	OSMR	CCNK	PXDN	TGIF1	PHGDH
NRIP1	NR4A3	PRKCI	MSC	3-Mar	CD248	EPHX1	CLIP1
DNAJA1	EIF1	ANKRD28	TSR1	TMEM263	SMS	ANK2	HNRNPF

DCBLD2	NR4A2	PRRX1	HBP1	RRM1	ANGPTL4	C1QTNF3	IGFBP7
CRABP2	ELOVL5	FBN1	NOTCH2	ADAMTSL1	SESN3	CDC42SE1	AMD1
ZBTB38	STX4	RARG	KIAA1462	CRIP2	RGS2	FKBP14	TMEM59
RLF	FNIP2	VAPB	TGM2	NDFIP2	SSR4	SH3D19	LOXL1
BAG3	SCGB3A1	CDK17	KPNA4	AC058791.1	TPBG	FLNB	TOR1AIP2
CHORDC1	SERTAD1	SLC19A2	SERTAD2	KTN1	UBQLN1	ARPC3	ANKLE2
SPARC	SGK1	RND3	ADAMTS2	NOP58	MYL6	FKBP5	CTTN
DYRK3	SLC30A1	BZW2	EGR3	KLF4	BDNF	NUP58	PER3
ZSWIM6	HERC4	TXNRD1	FOSB	ZMAT3	GALNT2	UQCR10	GLUD1
PLA2G4A	HAS2	HIVEP2	TUBA1C	FSCN1	RBP1	CXCL6	CCDC80
CPXM1	ZDBF2	RAB7A	NFE2L2	CCNT1	ZC3HAV1	CMSS1	SMDT1
SERPINH1	DPYSL3	PANX1	SMIM3	SLFN11	PSME1	ITPRIP	KPNA2
DOK5	PRRG3	SELM	RNF149	UBE2D3	RNASEK	HSPB1	PEG10
MT-ND4L	HDLBP	ALDH1A3	AKAP12	FNDC1	AGO2	OTUD4	COX6A1
HSPA4	COQ10B	CPZ	EGFL6	SEPP1	CLMP	TUBB2B	CHCHD10
ANXA1	ASCC3	CADPS2	CTNNAL1	TIMP2	H3F3B	RC3H1	GPC1
ARL4C	DNAJB6	ATP13A3	HMOX1	TCEB1	S100A4	NUPR1	MYL12A
COL1A2	MT-ND2	FBXO34	C10orf10	RPS6KA3	TAF1D	RARRES1	ARHGAP21
SQSTM1	TIPARP	IPO7	ITGAV	CIRBP	AFG3L2	SERINC5	EPB41L2
TCP1	MTRNR2L8	HRH1	MAPK6	DDX21	SH3PXD2B	EDIL3	LY6E
PHLDA1	TSC22D2	INPP1	RGMB	IDI1	NIFK	ADH1C	ADAMTS15
NT5E	P4HA1	TNFRSF10B	MMP2	CCDC109B	CD44	PTPN1	CXCL12
ARID5B	MT-ND3	TNFAIP6	METRNL	MYOF	FAM110B	TRAF4	ETNK1
ROR1-AS1	JAM3	UAP1	SPON2	BZW1	DDX3X	ABHD2	PLA2G5
SNAI2	TWIST1	PLAUR	TIMP3	NTM	SEMA4A	DSTN	GRPEL1
GJA1	PPP1R14A	UCHL3	MAP4K4	GPSM2	UHRF1BP1L	DSEL	CILP2
LIMA1	PTGIS	JUN	CNTN4	EMILIN2	TRIO	NFATC1	FBLN2
LRRC8C	LMCD1	CD74	UTP4	AFF4	KCNE4	FKBP10	SUMO2
ZFAND2A	TPM4	FGFR1	CLEC11A	NOP16	USP15	SPSB1	HMGB1
SPAG9	IL1R1	ERRFI1	AFAP1	TSPO	MIR222HG	UBE3A	NOV
HSPH1	ANGPTL2	PLOD2	NOLC1	CADM3	GABPB1	TMEM2	ALDH1A1
RPS26	RPL41	GABARAPL1	TNFRSF12A	CTNNB1	AOC3	SOX4	CA12
CHD1	REL	GNAI3	LRIF1	TTC3	RGS5	SRGAP1	HIGD1B
EIF4E	KCTD9	YWHAZ	ZFP36L1	AKIRIN1	GNL2	IL33	PERP
YWHAG	ELL2	SACS	CLIC4	FRS2	MDM2	FABP5	KLF2
CBLB	DDX3Y	FRMD6	IFI16	GSTP1	EMP2	SEC23A	PABPC1
DNAJB4	FAM198B	PPTC7	NXT1	GNL3	UFM1	COX8A	NFAT5
MSX2	C1QTNF6	COL4A1	MRPL18	HIST3H2A	SLC40A1	CCT3	C14orf2
RAB23	PPDPF	COL4A2	DNTTIP2	ITGA11	IL6R	PEBP1	BCAP31
PEA15	TICAM1	MAFF	DNAJB9	SLC20A1	SEMA3B	NUFIP2	HOTAIRM1
DRAM1	TOP1	NBPF14	ALG13	PRMT9	ELN	RGCC	SEMA6A
EIF4A3	COL6A1	WDR43	FKBP9	NDUFA4	HLA-DPA1	DES	NDUFA3
LHFPL2	ETV3	MLLT11	MED13	CREB3L1	COL5A1	PIM1	ACSL3
DNAJB1	WBP5	HNRNPA2B1	LATS2	CCT4	PFDN2	DDX5	OLFML3
IL6ST	SOD3	DNMBP	NUP153	ESYT2	HIVEP1	AHNAK	EIF5

ACTA2	SLPI	SDCBP	SERBP1	TPT1	HIPK3	FLRT2	PHLDB2
YES1	ABI3BP	CD55	C3orf58	CRY1	APP	IGFBP6	CD68
ADH1B	CREB5	NAA50	FOSL1	TRIM69	EIF1AX	PAICS	MAP3K8
GLIS3	MMP14	MAT2A	KLF3	HEG1	FLNC	SSC5D	PCDHGC3
MT-ND1	DPT	CAMSAP2	FAM114A1	CYP51A1	ANKH	KDELR3	ANXA2
HSPA9	PTGFRN	RCOR1	PCBP1	HNRNPH3	ARL4D	IER3	KRTCAP2
C1orf21	SYAP1	HSPA1B	USP36	MRC2	UBL3	CKAP4	COL5A2
SNX9	APOD	GPC6	ACSL4	TSC22D1	PHLDB1	RAB1A	INHBA
RYBP	GFPT2	HNRNPA0	TSPAN5	NDUFA4L2	EDF1	ASAH1	NPM1
TXNIP	PRSS23	CYCS	SAMD8	PXDC1	CD200	SNRPB	CD81
CACYBP	RUNX1	HECTD2	COX5B	FAP	DCLK1	NIP7	FILIP1
FSTL1	BIN1	WDR45B	SAR1A	AHNAK2	PPP1R15B	ATP1B3	HLA-A
GNPNAT1	MT-ND6	THBS1	HLA-DRB1	CSRNP1	EIF4G2	HSPA5	EEA1
RANBP2	FAM46A	STK17A	MEST	MEIS2	PPP2R2A	POLR1C	RP11-14N7.2
KLF6	PTGS2	SPRY2	SLC38A2	TSPAN3	KRAS	NR4A1	SLC39A14
ZFAND5	CALM2	IPO5	NRBF2	THAP2	NUP98	LHFP	FOSL2
U2AF1L5	DDX27	CMBL	TUBB6	SLC39A6	IFI27	HMGA1	LAMA4
ITIH5	NSUN2	DUSP5	SPHK1	CLIC2	ANTXR2	SEC31A	OPTN
JMJD1C	HNRNPU	H2AFJ	HLA-DRA	TOB2	COPS2	NR1D2	PAFAH1B1
HOMER1	COL14A1	APBB3	MMP23B	KLF9	MRPS6	PDGFD	NOTCH3
EPHB2	RASAL2	BACH1	S100A16	TMED5	B4GALT1	MYLK	DAZAP2
DCUN1D3	ZNF703	RAP1B	TSHZ2	PFKP	C2	ATF4	ATF3
PLXDC1	KLHL4	CLCF1	APOE	MCL1	MYO1E	PLAU	RASL11A
AES	GPM6B	KCTD20	LDHB	ZBTB16	SCGB3A2	LMOD1	PDPN
RBBP6	UGCG	HMCN1	C8orf4	ATP5D	PNP	SNHG12	TPI1
RELB	FTH1	MFAP5	ABCA1	ABCA9	TINAGL1	TRIB1	ARL6IP4
TNXB	PTP4A3	KITLG	F10	DBN1	GOLGA4	CAST	MIR155HG
HLA-DRB5	TALDO1	DCXR	PFDN5	LRRN4CL	CALU	OLFML2B	CFD
SLC3A2	PTRF	NDUFS5	SPATS2L	NUDT4	SAMHD1	LYZ	RORA
PLAGL1	PPP1R10	NEU1	CFI	WDR83OS	SGCE	EIF4G1	DUSP4
FAM126A	PTN	GUK1	ANTXR1	ACKR3	DBNDD2	CNN1	HIF1A
SFRP1	PTGDS	COL15A1	UGP2	CD82	FGF7	MGST3	PRR13
RPS19	NDUFB10	G3BP1	CAPN2	ARFGAP3	CD4	FNDC3B	UQCR11
RPL22L1	ATP6V0E1	BRD2	FKBP1A	EIF3A	NFIL3	LGALS3BP	CIB1
NDUFV2	CLEC2B	CHN1	NDUFA13	VPS28	S100A6	ZEB2	CD34
MBNL2	GPC3	RRBP1	USMG5	DNAJA4	ANAPC16	LDHA	S100A11
SCPEP1	GGT5	COX5A	EIF3K	NGFRAP1	TCEB2	LINC00657	GDF15
KRT8	MARCKS	SELENBP1	GPCPD1	EDNRB	LXN	ABLIM1	NCL
UQCRB	MFAP2	IL1RL1	CHPF	RDH10	ADIRF	SPTAN1	ADAM12
EGFR	TNS1	TACC1	GPNMB	RGN	GRINA	SYNCRIP	MACF1
SLC7A5	C2orf40	LPL	CLEC3B	NDUFB7	TGFB111	COX6B1	VASN
PCOLCE	STAT3	CTSS	LEPR	DKK3	SFRP4	ITGA1	CXCL8
ATP5J	ADGRF5	COMP	MT1A	ROBO2	NME3	MEF2C	LSP1
CCL26	SCN7A	DKK1	RNASE1	SGCA	S100A10	OSR1	AURKAIP1

MXRA8	RSRP1	NPNT	ARL6IP5	PIEZO2	CHRD1	SLC16A7	SLC2A3
SYPL1	MT1X	HILPDA	TGFBR3	PSME2	CD302	MARCKSL1	TUBA1A
COMT	KCNMA1	CXCL2	TBX2	PODN	BCL3	NBL1	
HGF	DDIT4	HOPX	NDFIP1	4-Sep	THY1	CES1	
CYBA	SFTP8	ABHD5	TNFRSF1A	CSRP1	C7	ITGA8	
RBM39	TYROBP	AKR1C1	SCARA5	IGFBP4	ATP6V1F	SH3BGRL	

* Derived from(56)

Supplementary Table 14, relating to Fig.7. ACTA2⁺ myofibroblast marker genes*.

FN1	TFPI2	FAP	CD34	MGST1	SMPDL3A	TNFRSF1A	LPP
LTBP2	FGFR4	CD302	LGALS3	SOD3	CFH	ATP13A3	ID3
LIMCH1	SLC40A1	CD248	EFEMP1	PMP22	CPXM1	PLN	FHL1
CDH11	ASPN	ARC	CTGF	ANTXR1	SELENBP1	MAFF	SERPINA3
ADIRF	DNAJB1	CD55	SLC25A4	NOLC1	HNRNPF	EIF4A1	CILP
PLA2G2A	COL5A2	CHD1	NCL	TCF12	FAM162B	ARL4D	FIBIN
A2M	PALLD	MDK	MYH11	ADGRD1	IGFBP7	MYOC	FABP4
MACF1	EIF4A3	GJA4	NR4A2	WDR43	EZR	EGR3	C1R
ITGBL1	TCF21	CALM1	COL1A1	NAMPT	CLCF1	RARRES1	MAP1B
CES1	PLIN2	EFHD1	ESAM	KCTD12	MYL6	PDK4	C2orf40
HAS1	MT1M	HMGNI	NDNF	PCBP1	PDLIM5	SFPQ	KIAA1217
MYC	G0S2	PTP4A1	MMP19	PRSS23	SLC4A7	PIK3R1	HTRA1
TM4SF1	NPNT	ITM2A	RPL41	ABLIM1	MIR22HG	SPTBN1	SRGN
MOXD1	HSP90AB1	FOSL1	HNRNPAB	FKBP4	WISP2	SEMA3C	THBS1
COL6A3	TMEM119	DNAJA1	NT5E	CXCL12	CHMP1B	AEBP1	TGM2
MAMDC2	NR4A3	BCAM	WT1	INPP4B	CFB	SRSF3	SLC2A3
ROBO2	ANGPT1	ENC1	LMO4	CLEC3B	ACTG2	UBC	CEBPB
ERRFI1	SPINT2	TPM2	TNC	PI16	ADAMTS9	UGP2	SERPINA3.1
COL8A1	SLC38A5	LSP1	MTRNR2L12	KRT8	ZNF331	PHLDA2	MGP
UGDH	CTHRC1	HMOX1	ATF3	MXRA8	LGALS1	LMOD1	IFI6
MFAP2	SELK	ISYNA1	KLF9	PFDN2	CREB5	CRISPLD2	SERPINE1
CCDC80	PTGIS	OSR1	NOTCH3	FLNC	GABARAPL1	LGALS3BP	TXNIP
MEDAG	ADAMTS1	NDRG1	PLAU	11-Sep	MEF2C	PIM3	CXCL1
CDKN1A	RGS5	3-Mar	PCOLCE2	ZYX	FAM46A	IL32	FHL2
EMILIN1	SFRP1	NRP2	SRSF2	RABGEF1	RANBP2	ITGA5	HIF1A
GPRC5A	SMOC2	ITGA2	MTHFD2	PPP1R12A	ENO1	NUDT4	BGN
UAP1	DES	EPS8	ELL2	FIGF	YBX3	MT-CYB	FBN1
PLXDC2	LDHA	FKBP1A	FBLN5	OSTC	RP11-14N7.2	NRIP1	PDPN
MT1A	DIO2	SEPP1	MMP2	JUNB	GNL3	ARID5B	THBD
PLEKHH2	NOP16	NDUFA4L2	COL10A1	ITM2C	CCL11	S100A13	RGS16
QSOX1	CRIP1	HSD11B1	EGFL6	ENAH	HNRNPU	MMP14	BTG2
IGF2	TDO2	ETV1	GNG11	WDR1	UACA	HEYL	INHBA
C3	HIGD1B	PTP4A3	CTSB	YWHAG	INSIG1	EDNRA	RASD1
RHOB	LUM	RSPO3	LSAMP	ATP1A1	TUBB3	AKR1C1	CHRD1

RARRES2	HSPH1	ELN	COL1A2	ACTA2	PLK2	TCF4	KLF2
GPC3	COL16A1	C1QTNF1	SPARC	TPT1	STMN1	TIMP3	C10orf10
SCN7A	DDX21	CNN2	LBH	TUBB2A	RSL1D1	CBLB	TSC22D3
DKK3	TUBB4B	SCARB2	LHFP	PA2G4	HSPB6	MINOS1	FGF7
ITGA8	SGK1	MFGE8	ZNF106	BTG3	ANGPTL4	FMO2	HSPB8
HSPD1	CDC42EP2	TAGLN2	ADGRF5	NPC2	XBP1	HSPA1A	TNFRSF12A
MT2A	CPE	PPIB	NAP1L1	LINC01133	PTMA	DDX3X	MEG3
POSTN	KRT18	HSPA8	SCARA5	CADM3	SNRPB	TXN	EGR1
CD82	TSPAN13	COL5A1	VEGFA	DSTN	F2R	SOCS3	COL12A1
COMP	GDF10	F3	TSPAN8	DNTTIP2	ARL6IP5	FAT1	AC090498.1
IGFBP6	HSP90AA1	C16orf45	ZFAND5	ABL2	MLLT11	SPSB1	PTGDS
EIF1	NKD2	EIF5A	HES4	RPS27	TUBA1B	MT1G	LINC00152
NBL1	IFITM1	ID4	NXT1	FOSL2	HSPB1	VASN	FOSB
MAT2A	DST	C1QTNF7	TIPARP	BAZ1A	HSPA1B	CST3	ZFP36
FST	SLPI	PLPP1	LRRN4CL	SLC16A1	EMP2	IGF1	CFD
COX4I2	ACKR3	FAT4	FHL5	C1QTNF3	RAB31	CYSTM1	CXCL2
HSPE1	ALDH1A3	TUBA1C	GNPNAT1	NR2F1	SH3BP5	PIM1	IGFBP3
ENPP2	SNHG15	PTK7	ALDH2	MMP23B	PDLIM4	EPAS1	SOD2
BAG3	ROBO1	COL15A1	MFAP4	FMO3	HSPA9	HMGA1	PTGS2
LTBP1	BDKRB1	CYP7B1	DBNDD2	ADAMTS4	KLF3	CYR61	SFRP4
ATP1B3	AKAP12	STEAP4	PDGFRL	CEBPZ	EIF4E	MYO1B	CXCL3
CYCS	TNFRSF19	SRSF7	ALDH1A1	KLF4	CSRNP1	IFI16	DPT
BMP5	MCAM	SORBS2	SH3PXD2A	EDNRB	ACTN4	MT1X	DCN
CTSL	CREM	NR4A1	TOB1	NPM1	LAMB1	RRBP1	CRABP2
GFPT2	COL3A1	EIF1B	ETF1	KDM6B	ISG15	MARCKS	GPX3
HMCN1	SNCG	SLC20A1	PHLDA1	SNU13	CSRP2	SRPX	SFRP2
MYL9	PNRC1	AMD1	RGS3	SLIT2	PDGFRB	TPM1	ADH1B
MFAP5	LAMA2	LITAF	APOLD1	TCP1	NREP	TAGLN	ADM
TINAGL1	GSN	TCEB1	UBA2	CRYAB	ZFP36L1	COL6A1	ICAM1
RGCC	EBF1	RAN	DKK1	NOP58	PLAUR	GPNMB	CH25H
SPON1	COL13A1	H3F3B	SH3D19	ACTB	TXNRD1	PPP1R15A	PPP1R14A
ACSL4	PIEZO2	MAOB	CNN1	CYP1B1	TMSB10	HILPDA	
VCAN	PROCR	PMEPA1	NRP1	WNT2	SERTAD1	COL18A1	
IFI27	MYH10	STOM	SFTA1P	MT1E	IGFBP2	CXCL8	

* Derived from(56)

Supplementary Table 15, relating to Fig.7. PLIN2⁺ lipomyofibroblast marker genes*.

CTSL	AOC3	ANGPT1	LARP4	METAP2	SARAF	ARF5	PLN
MT-CYB	EIF4A3	RABGEF1	KCTD20	NABP1	EMP3	MIR222HG	MINOS1
BGN	MGST1	PA2G4	ITGA8	NFIL3	ANAPC16	FAM180A	HIST1H4C
MYL9	DNAJC2	STK40	COX5B	C1S	PRRC2C	EIF3M	INPP4B
TAGLN	LIMA1	ZNF800	SLC43A3	OLFML3	ANXA6	MT1A	GJA4
ACTA2	MEG3	LINC00473	NRIP1	PHLDB1	RGN	NME3	ADAMTS9
UAP1	FBN1	IL1R1	THBS1	SRM	ARPC5	FGFR4	CNN3
ACSL4	NR4A3	CCND2	CD151	PRKCDBP	H3F3A	CSNK1A1	S100A4
PLIN2	RNF149	DDX27	ESYT2	NNMT	PLSCR1	LGALS3BP	ADIRF
TMSB4X	TSC22D1	RSPO3	COLEC12	PTP4A3	ILF2	NEAT1	LGALS1
GFPT2	NDUFA4L2	FBL	BAG3	SRSF1	DAZAP2	ARL6IP4	CNN2
CRIP2	MT2A	SRGAP1	LMOD1	TCEB1	4-Sep	CDKN1A	ALDH2
IGF2	CAV2	TMED5	SNED1	IVNS1ABP	CHCHD10	APOLD1	RUNX1
PPP1R14A	ARL4D	KDM6B	FAM162B	AKIRIN1	EDNRB	NFIA	LITAF
DDK3	SLC4A7	CLDN11	FGF2	CRIP1	ELL2	CHURC1	OGN
TPM2	F3	SH3BGRL	PIM1	BICC1	H3F3B	RTN4	UGCG
NOP16	MYH9	GPNUMB	PRDM2	SEMA3B	TGIF1	TCF21	HMOX1
EIF1B	CSRP1	SAT1	COX6A1	MAMDC2	ASAH1	SOD3	LTBP1
GPRC5A	C1R	FN1	FRZB	ADM	CTHRC1	SH3PXD2B	MFGE8
CXCL12	PNO1	LRRC59	TIPARP	INTS6	CES1	NUPR1	SLPI
MT-ATP8	SRSF2	EIF5A	B2M	CREM	CTSF	FIS1	ETS2
FST	THBS2	PTP4A1	PXDC1	CFD	PALLD	COX7C	CLEC3B
DDX21	BDKRB2	ASPN	DBNDD2	LURAP1L	RNASEK	JMJD1C	SRGN
3-Mar	GNPNAT1	MCL1	MT1X	MYL12A	GCLM	TMEM47	PIK3R1
MT-CO2	FLNA	PLTP	EIF1AX	CYCS	PTMS	CHMP1B	HSPA5
ITM2A	ATP1B3	C1orf21	WTAP	TWISTNB	SLC16A7	FCGRT	JUND
SPSB1	PIM3	VASH2	TWIST2	GABARAPL1	RPS29	LPP	TFPI2
NCL	BRIX1	HLA-C	TSPAN8	EIF4E	SPAG9	SRSF3	HSPB8
DSTN	HSPD1	FAM126A	TXNIP	MEF2C	TFRC	GJA1	GPC3
HNRNPAB	SERPINF1	ALDH1A3	EIF3A	TCP1	RAN	HSPB6	S100A13
MYLK	UBC	NR2F2	TUBB2B	ABLIM1	TIMP3	HSPA2	IFITM1
ERRFI1	SFPQ	EDIL3	C2orf40	G3BP1	TGM2	TRIB1	CSRP2
IGFBP7	HNRNPF	DKC1	BZW2	CHN1	EPAS1	PEA15	TM4SF1
MEDAG	NDUFA4	SOD2	ABCA9	PPP1R12A	PDLIM7	PLAT	ARID5B
MT-CO1	ZFP36L2	FGFR1	EFEMP1	TUBA4A	EHD2	RPS26	CH25H
HSP90AB1	COX4I2	DAB2	BCCIP	TGFB3	SPHK1	MACF1	HAS2
CYP1B1	PAMR1	SLC25A33	PCOLCE	H2AFJ	SNHG12	NREP	DUSP1
FGF7	ARHGDI	NIP7	SRSF5	PEBP1	NEDD9	MFAP5	HOPX
PDLIM4	SRPX	CTGF	ENO1	HEYL	CTSB	MT1M	PTGDS
FKBP1A	FOSL1	PNRC1	EGR1	MT-ND6	LAMB1	COX7A2	KLF2
MYC	MGST3	C7	TRMT10C	REXO2	RP11-14N7.2	MSRB3	CXCL1
EIF1	TUBB2A	BIN1	SVEP1	ADD3	GSN	PTX3	PDGFRA

MT-ND4L	COL4A1	PAICS	HNRNPDL	MOXD1	EDF1	LRP1	BTG1
AC090498.1	MESDC1	PTGIS	PPP3CA	CLCF1	GLT8D2	NDUFB7	COL6A2
NOP58	DCAF13	EGFR	BCAM	ARPC3	COMP	S100A16	REL
VEGFA	IGF1	NAMPT	FUS	TNFAIP6	ADGRF5	PTN	ELN
SRSF7	NT5E	TUBB6	C10orf10	SDCBP	CCNL1	TCEAL4	NR4A2
WT1	PTRH2	CYBRD1	EXOSC4	TGFB11	HMG2N	RRAD	IGFBP2
CALD1	PLBD1	TXNRD1	TXN	BAIAP2	RASL12	IGSF10	S100A10
BTG3	CD82	B4GALT1	TUBB3	PLEKHH2	SORBS2	TUBA1B	FBLN2
MYL6	SH3BP5	CPXM2	SERTAD1	VAMP8	STRAP	MT-ND3	CRABP2
C16orf45	C16orf89	NOTCH3	TPBG	ISYNA1	TIMP2	C1QTNF3	HSPA1B
PDGFRL	HNRNPU	EMILIN2	CCDC109B	NEGR1	TGFB1	UQCR10	PLK2
LSP1	CYP26B1	GPX3	ABHD5	PCBP1	TNS1	DDX24	ARC
EGFL6	NFE2L2	TNXB	INPP1	STAT3	TMEM204	C9orf16	SFRP2
ATP13A3	XBP1	KRT18	RANBP2	INSIG1	F2R	PDGFRB	HSPA1A
PLAU	KLF3	TINAGL1	PLPP3	IPO7	CTSD	SLC39A14	QSOX1
CCDC80	MYH11	DES	RPF2	CREB5	BRD2	ACTG1	COL14A1
ZFP36L1	FSTL1	POSTN	RBM25	TBX2	EIF3K	JUNB	GADD45B
HSPA8	SNU13	ITGBL1	SGCA	CCDC47	ZC3H15	STEAP1	HIGD1B
MAT2A	OSR1	SYNCRIP	OSMR	CTSH	SLC3A2	HLA-DRB1	ID2
CHD1	BZW1	TOP1	PROS1	MIDN	KRT8	PSME1	CXCL3
CEBPZ	CPXM1	PLS3	ST3GAL1	SERTAD2	COX6B1	SCN7A	RGS2
PPDPF	STK17A	POLR1C	HNRNPA0	SNRPB	DDR2	C12orf57	NBL1
NPM1	TNFRSF1A	SLC40A1	TPT1	UGP2	C8orf4	ANK2	CXCL2
ATP5G2	GRPEL1	ABL1	CILP	FAM46A	CFL1	ENAH	RGCC
C3	SEPW1	CD34	GABARAP	FABP5	PRRX1	RARRES1	RHOB
EZR	METRNL	TOMM5	TFAM	ACTN1	UBE2N	ANKRD28	EMP1
AMD1	RFK	SCARA5	DDX3Y	CDH11	RPL22L1	HIF1A	FABP4
LBH	KLF4	TNC	ABCA8	TMEM176B	HLA-DPB1	TSKU	ATF3
NXT1	EDNRA	UCK2	RBM39	COX4I1	PDE5A	TLN1	THBD
CHRD1	ABL2	IGFBP4	SLC16A1	RCAN2	MYL12B	SMOC2	CTSK
LTBP2	EBF2	EIF2S1	H2AFX	ADAMTS16	TSC22D3	GPM6B	G0S2
BDKRB1	NOP56	FBLN1	IGFBP6	SLC19A2	PARK7	COL15A1	PRG4
LRRN4CL	COL8A1	SLC20A1	SOAT1	HLA-DRA	HNRNPH1	FERMT2	SGK1
ETF1	MPZL1	TSPAN3	CYB5R3	MARCKSL1	ATPIF1	PLXDC2	FHL2
CAV1	COTL1	LIMCH1	SEMA6A	HIPK3	ABI3BP	SNAI2	APOE
WDR43	RGS5	SNRPD1	HMG2N	MYH10	TGFB2	RAB13	BMP5
CBLB	HSP90AA1	CALM1	HSPA9	HAS1	SPCS1	HCFC1R1	NR4A1
IFI16	NIFK	GTPBP4	SYNGR2	CD4	GUCY1A3	MCAM	NFKBIA
ACKR3	CIRBP	DNTTIP2	TAF1D	PLA2G2A	RBBP6	ESAM	JUN
LDHA	ARPC5L	GLIS3	SPARC	FLNB	COX7A1	TACC1	CTSC
EGR3	BAZ1A	DDX5	EIF5	PITPNB	IL33	MRC2	GEM
KLF9	SERBP1	CFI	CCT2	FOSB	WDR83OS	MSN	PTGS2
ITGA1	A2M	PERP	HMGA1	RDH10	ATP5D	NDUFB10	CFB
PLAUR	TSHZ2	EIF3J	CRIM1	ACTN4	PODN	TMEM70	C11orf96
RPL41	TUBB4B	GSPT1	NME1	APP	PAG1	WFDC1	CNN1

ATP1A1	TUBA1C	STEAP2	PNPLA8	COX8A	SPINT2	ILK	TNFAIP3
CALM2	CD248	NAA50	EIF5B	VAT1	VIMP	NEXN	VCAN
DCN	DNAJB1	IL6ST	USP36	EIF4A1	ACTG2	HMGNI	ADAMTS4
SFRP1	COL4A2	FAM198B	SPTSSA	UQCRB	SQSTM1	LXN	LMCD1
GNL3	TMEM176A	RIOK1	VASN	MT-ND2	HTRA3	MIR22HG	SERPINA3
RSL1D1	MLLT11	TRIO	UQCR11	SF1	TRAPPC1	LMNA	WISP2
YWHAG	MT-ND1	NUFIP2	ELOVL5	KPNA2	SNX9	TNFAIP2	IFI27
PFDN2	CPZ	ANGPTL4	DUSP6	CDC42EP2	GNG11	GAS7	COL3A1
ZNF593	SEMA3C	HSPH1	TNFRSF12A	WWTR1	HLA-B	SOCS3	
UGDH	RBMS1	OAF	ANXA1	ROBO2	FOSL2	MAFF	
MT-CO3	CD55	TXLNG	DDX3X	AKAP12	GUCY1B3	CCDC71L	
ADAMTS15	MT-ND5	SELM	SELK	LPL	ZFAS1	PDK4	
NOLC1	HRH1	MRTO4	RERG	CTNNAL1	NPNT	MALAT1	
DNAJA1	ITGA5	TPM1	DCLK1	CD9	PDPN	HSPE1	
MTRNR2L12	MT1G	CXCL8	DKK1	RGS16	CCL2	AKR1C1	

* Derived from (56)

Supplementary Table 16, relating to Fig.8. Overview of Non-GLP Study CRL 20229915 performed in cynomolgus monkeys with ALE.F02

Study type and duration of dosing	Species, origin, number of animals	Animal ID	Doses (mg/kg/day)	Administration
Single dose , 42 days	Cynomolgus monkey (Vietnam) 1 male/group	2001	0.3mg/kg	IV bolus
		2002	3mg/kg	IV bolus
		2003	15mg/kg	IV bolus
Repeat dose , 28 days, 4 doses applied weekly	Cynomolgus monkey (Vietnam) 2 males/group	2004 2005	60mg/kg	IV infusion (30 min)
		2006 2007	150mg/kg	IV infusion (30 min)

Supplementary Table 17, relating to Supplementary Methods and Fig. 5-6. Gene sets derived from Molecular Signatures Database v7.4 used in this study.

MSigDB source collection	Gene set
Hallmark gene sets	HALLMARK_TNFA_SIGNALING_VIA_NFKB
Hallmark gene sets	HALLMARK_TGF_BETA_SIGNALING
Hallmark gene sets	HALLMARK_IL6_JAK_STAT3_SIGNALING
Curated Gene sets	KEGG_MAPK_SIGNALING_PATHWAY
Hallmark gene sets	HALLMARK_INTERFERON_GAMMA_RESPONSE
Ontology gene sets	GO_HIPPO_SIGNALING
Hallmark gene sets	HALLMARK_EPITHELIAL_MESENCHYMAL_TRANSITION
Hallmark gene sets	HALLMARK_ANGIOGENESIS
Hallmark gene sets	HALLMARK_G2M_CHECKPOINT
Hallmark gene sets	HALLMARK_E2F_TARGETS
Hallmark gene sets	HALLMARK_MITOTIC_SPINDLE
Hallmark gene sets	HALLMARK_KRAS_SIGNALING_UP
Ontology gene sets	GO_POSITIVE_REGULATION_OF_MACROPHAGE_ACTIVATION

3.2 Non-junctional CLDN1 as a therapeutic target for treatment of HCC

3.2.1 Results summary and own contribution

*I) CLDN1 is overexpressed in HCC and correlates with tumor stemness and poor prognosis.
(Major contribution, Article figures 1D-J)*

In order to evaluate CLDN1 as a target for treatment of HCC, I assessed *CLDN1* gene expression in tumorous and adjacent liver tissue of several publicly available cohorts of patients with HCC. Interestingly, *CLDN1* was significantly overexpressed in pre-malignant dysplastic nodules and established HCC compared to non-tumorous liver tissue. Additionally, I found *CLDN1* overexpression to be associated with transcriptomic signatures related to tumor stemness as well as metastatic behavior and short recurrence free survival following surgical intervention. These data indicate a functional relevance of CLDN1 for tumor aggressiveness.

II) CLDN1 perturbation suppresses tumor cell proliferation and invasion in state-of-the art 3D culture models of HCC (Major contribution, Article figures 2A-F, 2H and 2K-L).

We next evaluated the functional role of CLDN1 as a therapeutic target for treatment of HCC in several 2D and 3D cell culture models using Huh7 cell line. Using 5-ethynyl-2'-deoxyuridine (EdU) proliferation- and transwell invasion assays, I could show that both CLDN1 knockout as well as CLDN1 mAb-treatment strongly suppressed proliferation and invasion of Huh7 cells. Considering the association of *CLDN1* gene expression with stemness in HCC liver tissue, I further assessed the effect of CLDN1 mAb-treatment in a sphere formation assay, that has been shown to recapitulate stem cell functionality. Intriguingly, CLDN1 mAb-treatment was associated with formation of markedly smaller tumor spheres and significantly decreased tumor sphere viability.

III) CLDN1 mAb suppresses tumor growth and epithelial-mesenchymal transition in patient-derived 3D culture models of HCC. (Major contribution, Article figures 3A-B, 3E-F).

The therapeutic effect of CLDN1 mAb-treatment was further assessed in several patient-derived models of HCC. I contributed to studies in patient-derived HCC tumorspheres, that demonstrated significant suppressive effect of CLDN1 mAb-treatment on tumor cell viability in patient-derived HCC tumorspheres with superior effects compared to sorafenib. Considering the previously observed strong effects of CLDN1 perturbation on tumor cell invasion, I assessed the effect of CLDN1 mAb treatment on EMT. In fact, CLDN1 mAb-treatment strongly suppressed expression of fibronectin, vimentin and SNAI2 in complementary model systems consisting of co-culture of Huh7 cells with primary CAFs in patient-derived liver ECM.

IV) CLDN1 mAb suppresses tumor growth in cell line- and patient-derived xenograft mouse models of HCC (co-authors and collaborators).

To validate the anti-tumor effects of CLDN1 mAb-treatment *in vivo*, the Baumert laboratory, in collaboration with *Alentis Therapeutics*, employed cell line-derived xenograft (CDX) and patient-derived xenograft (PDX) mouse models of HCC. Two independent studies with Huh7 CDX mice as well as 6 independent PDX mouse models confirmed strong suppressive effects of CLDN1 mAb-treatment on tumor growth *in vivo*.

V) CLDN1 mAb-treatment interferes with tumor cell survival, differentiation and oncogenic signaling (coauthors and own contribution to RNAseq and GSEA, Article Figs. 6A-B)

In order to evaluate the molecular mechanism of CLDN1 mAb-mediated anti-tumor effects, me and our laboratory's bioinformatician performed RNAseq and GSEA on liver tissue derived from CLDN1 mAb or control treated PDX mice. Interestingly we observed CLDN1 mAb treatment to strongly suppress transcriptomic signatures related to cell proliferation, EMT and stem cell differentiation. On the other hand, gene sets associated with physiological metabolism were strongly upregulated in CLDN1 mAb treated PDX mice. Finally, our assessments indicated CLDN1 mAb to suppress oncogenic signaling with the strongest effects

on transcriptomic signatures related to TNF α -NF κ B signaling, Wnt- β -catenin- and KRAS-signaling. Proteomic studies in Huh7 spheroids performed by the Baumert laboratory further indicated that CLDN1 mAb interferes with Src activation, a non-receptor tyrosine kinase that converges on several oncogenic pathways. Collectively, these data suggest CLDN1 mAb to suppress tumor growth by interfering with tumor cell differentiation and oncogenic signaling.

VI) Pathway analysis might predict response to CLDN1 mAb treatment (major contribution, Article Figure 7)

The evaluation of CLDN1 mAb treatment in patient-derived HCC tumorspheres as well as in the PDX mouse model indicated 46%- 66% of tumors to respond to CLDN1 mAb treatment by reduced growth. Hypothesizing an association of this treatment response with the molecular characteristics of these tumors I performed RNAseq and GSEA to characterize HCC liver tissue with known response or non-response to CLDN1 mAb treatment in either HCC spheroids or in the PDX mouse model. Interestingly I observed transcriptomic signatures related to EMT and embryonic development pathways to predict response to CLDN1 mAb treatment, while signatures related to oxidative stress, Myc and MTORC1 signaling predicted resistance to CLDN1 mAb treatment. Taken together these prediction analyses suggest that pathway analyses might enable patient selection for precision medicine using CLDN1-targeting treatment approaches.

3.2.2 Publication of the results

These results were integrated into the manuscript “A humanized Claudin-1 specific monoclonal antibody for treatment of hepatocellular carcinoma”, currently prepared for submission to *Cancer discovery*.

3.2.3 Results article II

A humanized Claudin-1 specific monoclonal antibody for treatment of hepatocellular carcinoma

Natascha Roehlen^{1,2}, Marion Muller^{1,2,3}, Sara Cherradi^{1,2}, Frank Jühling^{1,2}, Francois H.T. Duong^{1,2}, Nuno Almeida^{1,2}, Fabio Del Zompo^{1,2}, Mirian Fernández-Vaquero⁴, Tobias Riedl⁴, Hussein El Saghire^{2,5}, Antonio Saviano⁶, Sarah Durand^{1,2}, Clara Ponsolles^{1,2}, Marine Oudot^{1,2}, Emanuele Felli⁶, Patrick Pessaux⁶, Irwin Davidson⁷, Emilie Crouchet^{1,2}, Simonetta Bandiera^{1,2}, Christine Thumann^{1,2}, Brandon Nicolay⁸, Nabeel Bardeesy⁸, Patrice Laquerriere³, Mathias Heikenwälder⁴, Roberto Iacone⁵, Markus Meyer⁵, Greg Elson⁵, Tamas Schweighoffer⁵, Catherine Schuster^{1,2}, Laurent Mailly^{1,2}, Joachim Lupberger^{1,2}, Thomas F. Baumert^{1,2,5,§}

¹Université de Strasbourg, Strasbourg, France; ²Inserm, U1110, Institut de Recherche sur les Maladies Virales et Hépatiques, Strasbourg, France; ³CNRS, Institut Pluridisciplinaire Hubert Curien UMR 7178, Strasbourg, France; ⁴Division of Chronic Inflammation and Cancer, German Cancer Research Center; Heidelberg, Germany; ⁵Alentis Therapeutics, Basel, Switzerland; ⁶Institut Hospitalo-Universitaire, Pôle Hépatodigestif, Nouvel Hôpital Civil, Strasbourg, France; ⁷Department of Functional Genomics and Cancer, Institut de Génétique et de Biologie Moléculaire et Cellulaire, CNRS/INSERM/UDS, Illkirch, France; ⁸Massachusetts General Hospital Cancer Center, Harvard Medical School, Charlestown, MA.

Running title: CLDN1 is a target for treatment of HCC

Keywords: Liver cancer, tight junction, CLDN1, HCC, stemness.

Additional information:Financial support:

European Research Council Grant ERC-AdG-2014 *HEPCIR* (T.F.B.); European Research Council Grant ERC-AdG-2020 *FIBCAN* (T.F.B.); European Research Council Grant ERC-PoC-2016 *PRELICAN* (T.F.B.); European Research Council Grant ERC-PoC-2018 *HEPCAN* (T.F.B.); European Research Council Consolidator grant *HepatoMetabopath* (M.H.); European Union EU H2020 *HEPCAR* (T.F.B. and M.H.); ARC Grant *TheraHCC2.0* IHUARC IHU201301187 (T.F.B.); ANRS Grant ECTZ103701 *CLAUDIN-1* (T.F.B.); SATT Conectus, University of Strasbourg (CANCLAU) (T.F.B.); French National Research Agency LABEX ANR-10-LABX-0028_ *HEPSYS* (T.F.B.); German Research Foundation (DFG) RO 5983/1-1 (N.R.)

§Correspondance should be addressed to : Prof. Thomas F. Baumert, MD, Inserm U1110, Institut de Recherche sur les Maladies Virales et Hépatiques, Université de Strasbourg, 3 rue Koeberlé, 67000 Strasbourg, France. E-mail: thomas.baumert@unistra.fr.

Conflict of interest: Inserm, the University of Strasbourg and the Institut Hospitalo-Universitaire have filed patent applications for the use of anti-claudin-1 monoclonal antibodies for the treatment of liver disease, NASH and HCC (PCT/EP2016/055942, PCT/EP2017/056703).

Word count: 7198

Number of figures: 7

ABSTRACT

Hepatocellular carcinoma (HCC) is the fastest rising and fourth leading cause of cancer-related death worldwide. Despite new treatment approvals, prognosis of patients with advanced HCC remains poor. Claudin-1 (CLDN1) is a cell membrane protein mediating cell-cell adhesion, cell fate and differentiation. While the function of CLDN1 within tight junctions is well characterized, the role of non-junctional CLDN1 in HCC remains unexplored. Here we show that targeting non-junctional CLDN1 by humanized monoclonal antibodies robustly suppress tumor growth in a large series of patient-derived model systems, including multicellular tumorspheres and patient-derived xenograft (PDX) mouse models. Mechanistic studies revealed that CLDN1 mAbs suppress tumor cell proliferation and invasion by interfering with stemness and oncogenic signaling. Our results provide robust pre-clinical proof-of-concept for humanized CLDN1-specific mAbs for treatment of HCC. The novel and unique mechanism of action has the potential to break the plateau of limited response and survival offered by currently approved therapies.

SIGNIFICANCE: HCC is a deathly cancer with unsatisfactory treatment options. Here we identified CLDN1 as a novel target for treatment of advanced HCC. Monoclonal antibodies targeting non-junctional CLDN1 inhibit tumor growth, invasion and stemness in patient-derived *ex vivo* and *in vivo* models with superior efficacy and response rate compared to sorafenib.

INTRODUCTION

Hepatocellular carcinoma (HCC) is a major public health burden and currently the fourth leading and fastest rising cause of cancer related death worldwide (1). It is estimated that by 2025 more than 1 million people/year will be affected by liver cancer worldwide (2). HCC typically develops on the background of chronic liver diseases, such as viral infection or non-alcoholic steatohepatitis (NASH) (3). Despite diverse primary causes, common pathways are involved in HCC initiation and progression, irrespective of the etiology. HCC nearly always arises in the context of chronic inflammation and hepatic fibrosis or cirrhosis, underscoring the critical role of the liver microenvironment as a trigger for hepatocarcinogenesis (1). In fact, cancer-associated fibroblasts (CAFs) and tumor-associated macrophages (TAMs) have been suggested to promote tumor initiation and progression by fostering biological events such as epithelial-to-mesenchymal transition (EMT), stemness and immune-escape (4-6). The mechanism of malignant hepatocyte transformation has been shown to involve hyperactivation of the Ras–Raf–MAPK, PI3K–Akt–mTOR pathways and Wnt– β -catenin (7, 8). Association of oncofetal transcriptome signatures with HCC subtypes of poor prognosis and therapeutic resistance further indicates a functional role of cancer stem cells in HCC development and progression (9).

Despite a dramatic rise in prevalence, current treatment options for HCC are still unsatisfactory. Less than 30-40% of HCC patients are eligible for curative approaches such as liver transplantation, resection and local ablation. For advanced HCC, only few systemic therapies with very limited efficacy and safety are available (10). Of note, the most efficient and current first line combination therapy for advanced HCC (Barcelona-Clinic Liver Cancer (BCLC), stage C) atezolizumab and bevacizumab showed objective response in only 27.3% and complete remission in only 5.5% of the patients (11). Moreover, tumor recurrence is a frequent and unpredictable event affecting patients with HCC even after curative treatments (70% of patients at 5 years) (12). Given the absence of efficient drugs combined with the rising incidence of the disease, there is an urgent unmet medical need for novel therapeutic approaches to prevent HCC development and to treat its progression (13).

Accumulating evidence indicates a role of tight junction (TJ) proteins in human carcinogenesis (14, 15). Claudin-1 (CLDN1) is a transmembrane protein expressed in TJs, but also in free, non-junctional form, e.g., at the basolateral membrane of the human hepatocyte. Non-junctional CLDN1 serves as a cell entry factor of hepatitis C virus (HCV)(16), a major cause of HCC world-wide. During viral cell entry HCV-CLDN1 interactions result in the induction of pro-carcinogenic signaling such as activation of the EGFR-MAPK pathway (17-19). We previously developed monoclonal antibodies (mAb) targeting the extracellular loop 1 (EL1) specifically on non-junctional CLDN1(20). By inhibiting CLDN1 co-receptor interactions and CLDN1 signaling these mAbs eliminate chronic HCV infection without detectable toxicity in several *in vivo* and cell-based models (17, 21). Here, we combined genetic knockout (KO) studies with perturbation studies using humanized non-junctional CLDN1 targeting mAbs in a large series of patient-derived model systems and demonstrate that non-junctional CLDN1 is a novel driver and therapeutic target for HCC.

RESULTS

CLDN1 is overexpressed in HCC and correlates with tumor stemness and poor patient prognosis

To investigate the role of CLDN1 as a driver and therapeutic target in liver cancer, we first analyzed its expression in liver tissues of patients with HCC. Comprehensive computational analysis of protein and gene expression data retrieved from the Genomic Data commons platform (<https://portal.gdc.cancer.gov>) and the human protein atlas (22) revealed CLDN1 to be highly expressed in primary liver cancer at both gene and protein levels (**Fig. 1a-b**). Thus, compared to frequent loss of detectable expression for other CLDN family members, immunohistochemical staining of liver tumors indicated medium to high expression in >75% of the patients (**Fig. 1c**). Further indicating a functional implication in hepatocarcinogenesis, CLDN1 was significantly upregulated in pre-malignant dysplastic nodules of cirrhotic liver (GSE102383 (23), $p=0.03$, Student's t-test, **Fig. 1d**), as well as malignant tumorous HCC tissue

compared to matched non-tumorous adjacent liver (GSE113996, $p=0.02$, paired Student's t-test, **Fig. 1e**). Taken together these data suggest a role of CLDN1 in hepatocarcinogenesis and as a potential novel drug target.

HCC is characterized by strong inter-tumoral heterogeneity and various molecular phenotypes (1). Thus, we next evaluated *CLDN1* expression in regard to molecular tumor subtypes. Interestingly, *CLDN1* was markedly and significantly overexpressed in HCC exhibiting a hepatocyte progenitor/stem cell phenotype (HpSC-HCC) compared to a lower expression in HCC's with a mature hepatocyte signature (MH-HCC) (GSE5975(24), $p<0.0001$, Student's t-test, **Fig. 1f**). Consistently, gene set enrichment analysis (GSEA) (25) of liver RNA sequencing (RNA-seq) data derived from an independent large HCC cohort (26) revealed enrichment of well described tumor stem cell signatures (27, 28) and embryonic genes (29, 30) in HCC tumors with high *CLDN1* expression (GSE11279 (26), $FDR<0.001$, Kolmogorov-Smirnov test, respectively, **Fig. 1g**). Moreover, HCC's with high *CLDN1* expression were characterized by upregulation of gene sets associated with cell proliferation as well as distinct oncogenic signaling cascades, such as MYC, MAPK and IL6-JAK-STAT3 signaling ($FDR<0.005$, Kolmogorov-Smirnov test, respectively, **Fig. 1h**). Considering HpSC-HCC as a molecular subtype of poor prognosis (27, 28), we next assessed a potential correlation of *CLDN1* expression with clinical patient prognosis. Large-scale profiling of HCC patient liver tissue previously suggested that especially transcriptomic alterations of the tumor adjacent liver strongly predict patient's outcome (31). Of note, high *CLDN1* expression in HCC adjacent liver tissue was markedly and significantly associated with a metastatic behavior of the corresponding tumor (GSE5093(32), $p<0.0001$, Student's t-test, **Fig. 1i**). Moreover, evaluation of an independent HCC cohort revealed strong correlation of *CLDN1* expression in adjacent liver tissue with post-resection recurrence free survival (GSE76427 (33), $p=0.008$, log rank test, **Fig. 1j**). Taken together, high and robust overexpression as well as association with tumor stemness and clinical aggressiveness suggest CLDN1 as a candidate target for treatment of HCC.

CLDN1 mediates tumor cell proliferation, invasion and stemness

In order to evaluate CLDN1 as a target for HCC therapy, we assessed the effect of CLDN1 genetic knockout (KO) on hallmarks of cancer progression, such as tumor cell proliferation, stemness and invasion in hepatoma cell culture (Huh-7). CLDN1 loss of function potently impaired tumor cell proliferation ($p=0.001$, Student's t-test, **Fig. 2a**) and tumor cell viability ($p<0.0001$, Student's t-test, **Fig. 2b**) in both 2D and 3D cell culture assays and showed a significantly decreased expression of cell proliferation markers, such as *E2F1*, *CCNB1* and *CCNB2* ($p=0.02$, Student's t-test, respectively, **Fig. 2c**). Beyond its impact on cell proliferation, CLDN1 KO markedly and significantly suppressed the invasive capacity of tumor cells, as demonstrated by trans-well invasion assays ($p=0.007$, Student's t-test, **Fig. 2d**). In line with the association of *CLDN1* expression with tumor stemness (**Fig. 1f-h**), CLDN1 KO cells exhibited markedly and significantly decreased surface expression of well characterized liver stem cell markers, such as EPCAM, CD133 (PROM1) and CD90 (34) ($p<0.0001$, $p<0.0001$, $p=0.002$, Student's t-test, respectively, **Fig. 2e**). Taken together, these data suggest CLDN1 loss-of-function to mediate anti-tumorigenic effects and to interfere with tumor stemness.

We previously established fully humanized monoclonal antibodies specifically targeting the first EL of non-junctional CLDN1. Flow cytometry revealed robustly enhanced binding of CLDN1 mAb to non-junctional CLDN1 in tumor cells compared to matched non-tumoral cells derived from adjacent liver ($p=0.006$, 2-way ANOVA, **Fig. 2f**), validating these mAbs for subsequent functional studies. Of note, treatment of Huh7 cells with CLDN1 mAb significantly decreased tumor cell viability ($p=0.003$, Student's t-test, **Fig. 2g**) and invasion ($p=0.006$ and $p<0.0001$, Student's t-test, respectively, **Fig. 2h-i**) in 3D culture assays. In line with computationally assessed decrease in invasion area (**Fig. 2i** right panel), CLDN1 mAb treatment of Huh7 cells strongly decreased expression of matrix metalloproteinases (MMPs), such as MMP14 with consistent results at gene and protein levels ($p=0.0009$, Student's t-test, **Fig. 2j**). CLDN1 mAb effects were further studied in a tumorsphere formation assay that has been shown to specifically enrich subclones of cancer stem cells via serum deprivation and exposure to growth factors (35). We found that, CLDN1 mAb treated Huh7 cells formed

markedly smaller tumorspheres (**Fig. 2k**) and showed significantly decreased viability after 7 days of culture ($p < 0.0001$, Student's t-test, **Fig. 2l**). Taken together these data reveal strong effects of CLDN1 perturbation on cancer hallmarks, such as proliferation, clonal expansion and invasion. In line with the association of CLDN1 expression with stem cell signatures *in situ* (**Fig. 1**), the distinct impact on tumorsphere formation, growth and marker gene expression indicate that CLDN1 plays a critical role in cancer stemness.

Monoclonal antibodies targeting non-junctional CLDN1 suppress tumor growth and EMT in patient-derived *ex vivo* models with efficacies superior to sorafenib

To validate clinically relevant anti-tumorigenic effects, we next assessed CLDN1 mAb treatment in patient-derived model systems closely recapitulating human disease. Patient-derived liver scaffold culture systems allow assessment of cancer therapeutics in a three-dimensional growth microenvironment that mimics the native structures. Briefly, liver cells were removed from patient-derived liver tissues and repopulated with Huh7 hepatoma cells and patient-derived cancer-associated fibroblasts (CAFs) to study the effect of CLDN1 mAb on EMT, a hallmark of cancer cells closely related to stemness and invasion (4, 36) (study protocol illustrated in **Fig. 3a**). Treatment of repopulated liver scaffolds with TGF β induced markers of EMT, validating functionality of the cells in this system (**Fig. 3b**). Of note, CLDN1 mAb markedly and significantly suppressed several markers of EMT, including Vimentin (*VIM*), Fibronectin (*FN1*) and Snail Family Transcriptional Repressor 2 (*SNAI2*) ($p = 0.006$, $p = 0.04$ and $p = 0.04$, paired t-test, respectively, **Fig. 3b**). Analogous results were obtained in a complementary 3D model system, consisting of Huh7 cells co-cultured with primary CAFs in patient liver-derived fibrotic extracellular matrix hydrogel (**Suppl. Fig. 1**).

We next aimed to assess the effect of CLDN1 mAb on tumor growth in a fully patient-derived culture system, modeling tumor heterogeneity. Cultured as multicellular micro-tissues, primary HCC tumorspheres maintain original cell-cell contacts and recapitulate non-parenchymal cells of the tumor microenvironment, which are relevant for tumor progression

and therapeutic resistance (37, 38). As shown in **Fig. 3c**, CLDN1 mAb treatment markedly disrupted sphere formation capacity and architecture of HCC spheroids. Moreover, CLDN1 mAb showed a pronounced effect on HCC spheroid cell viability ($p=0.003$ and $p=0.04$, Student's t-test, **Fig. 3d**). In contrast, sorafenib, one of the current first-line treatments for advanced HCC (1), showed either no or minor effects (**Fig. 3d**). A subsequent large screen in HCC spheroids derived from a total number of 15 different HCC patients (patient characteristics shown in **Suppl. Table 1**), validated strong suppressive effects of CLDN1 mAb on tumor cell viability with superior response rate compared to sorafenib (47% vs. 30%, defined as decrease in cell viability of $>20\%$, **Fig. 3e**). Resistance of HCC cells to sorafenib have been attributed to tumor cell plasticity and stemness (39). Indeed, *CLDN1* is highly overexpressed in HCC tissue predicted to be resistant to sorafenib treatment (GSE109211(40), $p<0.0001$, Student's t-test, **Fig. 3f**).

Taken together, these data indicate strong suppressive effects of CLDN1 mAb on cancer cell plasticity and tumor growth with superior effects compared to current first-line treatment with sorafenib. Marked overexpression of CLDN1 in sorafenib resistant HCC tissue highlight its potential as a target in patients with MKI drug resistance.

A humanized CLDN1-specific mAb suppresses tumor growth in cell line-derived xenograft (CDX) mouse models

To further confirm anti-tumorigenic effects *in vivo*, we assessed the effect of CLDN1 mAb on tumor growth in Huh7 cell line-derived xenograft (CDX) mouse models. Thus, 5×10^6 Huh7 cells were subcutaneously injected into the right flank of 6 to 8 weeks old non-obese diabetic Rag1^{-/-} IL2Rgc^{-/-} (NRG) mice. When the tumor volumes reached 50 mm³, mice were randomized into treatment groups. Tumor growth was monitored three times a week and mice were sacrificed when ethical endpoints were reached (tumor volume ≥ 2000 mm³ or when the largest measure reached 2 cm) (study protocol illustrated in **Fig. 4a**). In a first study, treatment effects of CLDN1 mAb monotherapy were compared to treatment with a vehicle Control. No measurable adverse effects were observed in mice treated with CLDN1 mAb. As shown in **Fig.**

4b, CLDN1 mAb treatment significantly suppressed tumor growth with increasing effects over time of treatment ($p < 0.01$, Mann Whitney U test, respectively, **Fig. 4b**). In line, histological assessment of Ki67, a marker of cell proliferation, revealed marked and significant decrease in tumor cell proliferation in CLDN1 mAb treated CDX mice (**Fig. 4c, left panel**). Moreover, CLDN1 mAb treated CDX mice showed strongly suppressed expression of EPCAM and FN1 (**Fig. 4c, middle and right panel**), corroborating the functional effect of CLDN1 mAb treatment on cancer cell stemness and EMT observed in cell-based models (**Fig. 2e, 2k-l, Fig. 3b**). In a second independent study Huh7 engrafted mice were additionally randomized into groups receiving sorafenib (study protocol illustrated in **Fig. 4a**). Interestingly, CLDN1 mAb treatment showed superior anti-tumor efficacy compared to sorafenib (**Fig. 4d**), strongly corroborating our findings in HCC spheroids (**Fig. 3e**).

Positron emission tomography (PET) with 3'-deoxy-3'-[^{18}F]-fluorothymidine ([^{18}F]-FLT) represents a highly sensitive imaging technique for non-invasive assessment of tumor response and treatment efficacy in patients and preclinical models of cancer (41). The uptake of ^{18}FLT is regulated by the cell cycle dependent activity of thymidine kinase 1 (TK1) and therefore correlates with cell proliferation (42). Corroborating our clinical and histological findings, ^{18}FLT PET Scan of 2 representative CDX mice per group (study protocol illustrated in **Fig. 4e**) showed reduced uptake of ^{18}FLT in CLDN1 mAb- compared to control- treated animals (Maximum Standardized Uptake Value (SUV_{max})= 3.68 and 5.16 vs. 10.32 and 5.46, **Fig. 4f and 4g, left panel**). Moreover, the avid tumor volume (ATV) and total lesion proliferation (TLP) were markedly smaller in CLDN1 mAb- compared to control treated mice (**Fig. 4g, middle and right panel**).

We further evaluated the effect of CLDN1 mAb on cancer metabolism by 2-deoxy-2-[^{18}F]- fluoro- D-glucose ([^{18}F]-FDG) PET Scan. Of note, reduction in ^{18}FDG PET activity following tumor therapy have been shown to correlate with favourable effects on clinical endpoints and survival in cancer patients (43). Interestingly, ^{18}FDG PET Scan of CDX mice treated with control, sorafenib or CLDN1 mAb (study protocol illustrated in **Fig. 4h**) revealed strong suppressive effects of CLDN1 perturbation on glucose uptake in cancer cells (Total

lesion glycolysis (TLG), CLDN1 mAb vs. Control = 98.21 vs. 342.48, $p < 0.05$, **Fig. 4i-j**). In contrast, Sorafenib showed no effect on tumor cell glycolysis (Total lesion glycolysis (TLG), Sorafenib vs. Control = 378.62 vs. 342.48, **Fig. 4i-j**). Taken together these data validate the functional impact of CLDN1 mAb on HCC tumor growth and metabolism and highlight its superior efficacy compared to one of the current first-line HCC therapeutics sorafenib.

A humanized CLDN1-specific mAb suppresses tumor growth in patient-derived xenograft (PDX) mouse models

Molecular drivers and response to therapeutics strongly vary between different HCC subclasses and patients (1). In this context, PDX mouse models recapitulate tumoral heterogeneity and are currently the most powerful *in vivo* system for studying cancer therapeutics and predicting clinical outcomes (44). To evaluate anti-tumoral efficacy and response rate, CLDN1 mAb treatment was assessed in 6 different PDX mouse models (available clinical and histo-pathology data are shown in **Suppl. Table 2**). Following established tumor growth (16 to 115 days), mice from each tumor model were randomized into groups receiving weekly i.p. injections of 500 μ g CLDN1 mAb ($n=3$ per model) or vehicle control ($n=2$ per model). Tumor growth was monitored for 28 days (study protocol illustrated in **Fig. 5a**). Body weight in CLDN1 mAb treated animals remained unaltered compared to the control group throughout the study (**Suppl. Table 3**). Of note CLDN1 mAb markedly and significantly suppressed tumor growth by 38.5% on average in 4 out of 6 PDX models, a value superior to current treatment in clinical practice (1) (**Fig. 5b**). Strongest effects were observed in an AFP+ HCC PDX mouse model with an average decrease in tumor volume of 54% (LI6716, $p=0.003$, paired Student's t-test, **Fig. 5c**). Taken together these data validate anti-tumor effects of non-junctional CLDN1 targeting mAbs in tumor models and provide robust preclinical proof-of-concept for CLDN1 mAbs for the treatment of HCC.

CLDN1 mAbs mediate anti-tumorigenic effects by interfering with cancer cell differentiation, metabolism and oncogenic signaling

Next, we aimed to elucidate the molecular mechanism of CLDN1 mAbs mediating anti-tumorigenic effects. We performed RNA-seq and GSEA (25) on CLDN1 mAb-(n=3) vs. control (n=2) treated tumor tissues harvested from the CLDN1 mAb-responding PDX mouse model #LI6716 (**Fig. 5**). In line with our *in vitro* data (**Fig. 2**) and the observed tumor suppressive effect, gene sets associated with cell survival, such as E2F targets, G2M checkpoint and mitotic spindle were markedly downregulated in CLDN1 mAb treated PDX mice (**Fig. 6a**). Moreover, consistent with our results obtained in cell based models (**Fig. 2e, 2k-l, Fig. 3a-b**) and CDX mice (**Fig. 4c**), genes sets related to liver cancer stemness (28, 29) and EMT (45) were markedly suppressed in CLDN1 mAb treated PDX mice (**Fig. 6a**). Interestingly, transcriptomic assessment of cancer cell metabolism in PDX mice derived tumorous liver tissue revealed strong suppression of hypoxia related genes in CLDN1 mAb treated animals. On the other hand, genes associated with physiological hepatocyte metabolism, such as bile acid metabolism, glycolysis and cholesterol homeostasis were restored (**Fig. 6a**). Taken together these data validate CLDN1 mAb to strongly impact on cancer cell proliferation, metabolism and stem-cell like differentiation.

Proliferation, differentiation and metabolism in cancer cells are orchestrated by a broad range of different signaling cascades. Interestingly, CLDN1 has been previously reported to crosstalk with Src signaling (19, 46), a key transmitter of growth factor or integrin receptor activation that converges on several oncogenic signaling pathways. Thus, we next evaluated the effect of CLDN1 mAb treatment on transcriptomic signatures of cancer cell signaling in tumorous tissue derived from the PDX mouse model LI6716. In fact, mice treated with CLDN1 mAb showed strong suppression of several key oncogenic signaling pathways, with the strongest effects on TNF α -NF κ B, TGF β , IL6-JAK-STAT3 and KRAS signaling (47) (**Fig. 5c**). Assessing Src signaling and key downstream pathways in our Huh7 spheroid model system revealed that CLDN1 mAb robustly suppressed Src (pY416) phosphorylation in a dose

dependent manner (**Fig. 5c**). Moreover, phosphorylation of STAT3 (pY705), one of the downstream targets of Src signaling was significantly reduced in CLDN1 mAb compared to control mAb-treated cells (**Fig. 5c**). Taken together, these data indicate that CLDN1 mAb broadly interferes with oncogenic signaling to impact on tumor cell proliferation, differentiation and metabolism.

Transcriptomic signatures predict response to CLDN1 mAb therapy providing a perspective for biomarker development and individualized therapy

Strong inter-individual differences in treatment response warrant evaluation of treatment predictive biomarkers to enable precision medicine. We aimed to identify molecular signatures predicting response to CLDN1 mAb therapy in patient-derived tumorspheres and PDX mouse models. RNA-seq data from basal non-treated HCC tissue was therefore assessed by GSEA in relation to its response to CLDN1 mAb treatment in spheroid and PDX mouse models (Responders: #S06, #S07, #S15, LI6280, LI6716, LI6723, LI6688; Non-Responders: #S13, #S16, #S17, #S18, LI1055 and LI1068). Although HCCs used in this study were from (I) diverse etiologies, (II) tumor grade and (III) presented different histological features, we found that the dysregulation of few distinct pathways enabled us to predict if the cancer cells would respond to CLDN1 mAb in *in vivo* or *ex vivo* models. Gene sets specific for Wnt/ β -Catenin and EMT were found to be strongly enriched in HCC tumor tissues showing response to CLDN1 mAb in HCC tumorspheres and PDX mouse models (**Fig. 7**) in line with the observation that these signaling pathways were suppressed in CLDN1 mAb treated mice (**Fig. 6b**). Resistance to CLDN1 mAb on the other hand was associated with MYC signaling as well as gene sets related to oxidative stress and MTORC1 signaling (**Fig. 7**), that consistently rather showed induction upon CLDN1 mAb treatment (**Fig. 6b**). Taken together these data identify molecular subtypes of HCC with distinct susceptibility to CLDN1 mAb treatment.

DISCUSSION

In this study, we identified non-junctional CLDN1 as a novel therapeutic target for treatment of HCC, a public health burden with unsatisfactory treatment options (1). Applying novel and innovative patient-derived *ex vivo* and *in vivo* models, we provide robust pre-clinical proof-of-concept for highly specific CLDN1 mAbs for treatment of advanced HCC. This conclusion is supported by the following findings: i) CLDN1 is overexpressed in HCC and correlates with tumor stemness and poor patient prognosis (**Fig. 1**); ii) targeting CLDN1 by specific mAbs markedly suppressed tumor cell viability, invasion and stem cell state in cell line and patient-derived 3D culture systems (**Fig. 2-3**) and iii) markedly decreased tumor growth in CDX and PDX mouse models (**Fig. 4-5**). Of note, evaluation of CLDN1 mAb treatment response in a large set of different patient-derived HCC spheroids and xenograft mouse models indicated significant tumor suppressive effects in 47-67% of patients, which is superior to compounds in clinical practice (1, 11).

One of the key strengths of this study is its focus on authentic patient-derived model systems as well as the high consistency of results obtained among different model systems. Importantly, the response rate of 30% for sorafenib in HCC spheroids is consistent with assessments in clinical studies (1, 48) and therefore strongly corroborates the validity of our system to predict tumor susceptibility to CLDN1 targeting therapies.

Current HCC therapeutics can be mainly subclassified into the multi-kinase inhibitors (MKIs) that mediate anti-angiogenic effects, as well as checkpoint inhibitors, that target the tumor immune microenvironment (1). The molecular mechanism-of-action of CLDN1 mAb treatment mediated anti-tumor effects hereby represents a novel concept. Thus, CLDN1 mAb treatment not only inhibits tumor cell proliferation but also suppresses cancer cell de-differentiation and stemness, a hallmark of HCC tumors with therapeutic resistance and poor prognosis (39, 49). Moreover, targeting non-junctional CLDN1 by specific mAbs suppresses multiple oncogenic signaling pathways such as Wnt- β -Catenin, KRAS, PI3K and STAT3 signaling that have been shown to account for resistance to therapy with checkpoint inhibitors and MKIs in HCC (50, 51). This inhibition suggests opportunities for highly effective

combination therapies to break the plateau of limited response in HCC patients with intrinsic or acquired therapeutic resistance.

HCC arises almost exclusively in the context of liver fibrosis and chronic inflammation (4, 52). The stage of liver fibrosis hereby represents a key factor for patient outcome (1, 53). In addition to the strong tumor suppressive effects of CLDN1 mAb demonstrated in this study, we previously showed that non-junctional CLDN1 targeting mAbs further markedly suppress liver fibrosis (54). While current treatment strategies in HCC are frequently limited by the degree of liver cirrhosis (1), the combined antifibrotic and tumor suppressive effects of CLDN1 mAbs represent a unique opportunity to target not only tumor growth but also fibrosis and de-novo HCC development in the non-tumorous fibrotic microenvironment (31). Moreover, we previously demonstrated that anti-fibrotic effects of CLDN1 mAb treatment mediate improvement of liver function in fibrosis mouse models (54) suggesting potential downgrading in BCLC stage and bridging to curative treatment options.

Considering the urgent need for individualized molecular therapies for the heterogenous group of HCC tumors with multiple molecular drivers (1), this study further provides key prediction markers for patient selection to CLDN1 mAb therapies. Upregulation of EMT as well as signaling pathways implicated in stemness such as Wnt- β -Catenin, Hippo and NOTCH signaling (55, 56) strongly predicted response of HCC tumors to CLDN1 mAb treatment in both *ex vivo* and *in vivo* model systems (**Fig. 7**). Predicted resistance to CLDN1 mAb therapy in tumors with upregulated MTORC1 signaling on the other hand suggest evaluation of combination therapies with MTORC1 inhibitors, that are currently in clinical development (57).

CLDN1 is highly expressed in the liver but also in other organs such as the skin, intestine and lungs. Our data obtained here and in previous studies demonstrate that the administration of the antibody is safe without detectable adverse and off-target effects (17, 54, 58). Thus, non-human primates and mouse models did not reveal any major toxicity even when high doses largely exceeding the therapeutic need were repeatedly applied (54). The absence of toxicity and off-target effects are due to the specific binding of the mAb to non-junctional

CLDN1 without being able to access CLDN1 present in TJ (17). Thus, the antibody does not have any functional effect on liver or intestinal TJ barrier function in human cell culture models and in mouse models *in vivo* (17, 58).

Collectively our data provide robust pre-clinical proof-of-concept for CLDN1 mAbs as a first in-class compound with a perspective to break the plateau of limited treatment response in advanced HCC, raising the outlook for patients with currently poor prognosis.

Material and Methods:

Human subjects and patient cohorts. Human liver tissue samples were obtained from patients who had undergone liver resections between 2014 and 2021 at the Center for Digestive and Liver Disease (Pôle Hépatodigestif) at the Strasbourg University Hospitals, University of Strasbourg, France. Tissue samples were stored in HypoThermosol FRS Preservation Solution (Sigma-Aldrich) and kept at +4°C prior processing. All patients provided a written informed consent, the protocol followed the ethical principles of the declaration of Helsinki and was approved by the ethics committee of the University Hospital of Strasbourg and the local independent ethics committee (*comités de protection des personnes*). Demographic data and clinical characteristics of patients enrolled are summarized in **Suppl. Table 1-2**, respectively. The gene expression of different CLDNs in primary liver cancer were derived from *Genomic Data commons* platform (<https://portal.gdc.cancer.gov>). The protein expression and immunohistochemistry of CLDNs in patient tissues were retrieved from the human protein atlas (22). Datasets of clinical cohorts with HCC (GSE113996, GSE102383 (23), GSE5975 (24), GSE11279 (26), GSE5093 (32), GSE76427 (33)) were selected following comprehensive database analysis, where we identified CLDN1 as part of the microarray data.

Reagents and antibodies. The following reagents were used for *in vitro* experiments in this study: human recombinant TGFβ (MERCK, France), Matrigel (Corning, USA), Recombinant human EGF (R&D Systems, USA), human FGF-basic (FGF-2/bFGF, Gibco, Fisher Scientific, France), HypoThermosol (StemCell, #07935). Humanized CLDN1 specific mAb H3L3 has been described (21) and were produced by Evitria, Switzerland. The isotype control antibodies used are palivizumab IgG4 (59) (Evitria, Switzerland) and motavizumab (Eviteria, Switzerland).

CLDN1 knockout using CRISPR-Cas9 technology. Huh7 cells stably expressing Cas-9 endonuclease (Huh7-Cas9) were transduced with lentiviruses expressing control single guide RNA (sgRNA) or sgRNA targeting *CLDN1* gene expression (sgCLDN1). Expression plasmids were provided by Dr. David Root (Broad Institute of Harvard and MIT, Cambridge, USA).

Transduced cells were selected under hygromycin treatment (500 µg/mL) for 3 days. CLDN1 KO was confirmed by flow cytometry using a CLDN1 specific mAb (10 µg/mL).

Generation and treatment of Huh7 spheroids. Parental Huh7 cell line was kindly provided by Prof. Gerhard Christofori and maintained in DMEM Glutamax (Gibco, #10566032), supplemented with 10% FBS, 1% MEM non-essential amino acid solution (Gibco, #11140050) and 0.5% Gentamicin (Gibco, #11500506). For maintenance of Huh7_CLDN1 KO and Huh7_sgCTRL cells, medium was additionally supplemented with hygromycin (500 µg/mL) and puromycin (10 µg/mL). For spheroid establishment, cells were trypsinized and seeded at a density of 500 cells per well in ultralow attachment plates (Corning spheroid microplates, #CLS4515). Following spheroid formation overnight, parental Huh7 cell line was treated with 10 µg/mL of CLDN1-specific mAb (H3L3) or isotype control mAb (Motavizumab) for 3 days. Tumor spheroids viability was assessed at day 3 using CellTiterGlo 3D (Promega) according to the manufacturer's instructions. Tumorspheres invasion assay was performed by adding Matrigel (Corning Matrigel Basement Membrane Matrix) to established spheroids treated with CLDN1 mAb or control mAb for 3 days (ratio 1:1). The quantification of cell sprouting was assessed 48h later by measuring the invasion area using the "tumorspheroid invasion" setting from the Celigo imaging cytometer as described (60).

Tumorsphere formation assay. Tumorsphere formation assay was performed as described (35). Briefly 1×10^4 Huh7 cells were seeded in 96 well ultralow attachment plates (Corning) in serum free DMEM Glutamax supplemented with 20 ng/mL epidermal growth factor (EGF) and 10 ng/mL basic fibroblast growth factor (bFGF) and CLDN1 mAb (H3L3, 10 µg/mL) or isotype control mAb (Motavizumab). Sphere formation was visualized at day 3 and 7 using the "tumorsphere" setting from the Celigo imaging cytometer. Tumor spheroids viability was assessed at day 7 using CellTiterGlo 3D (Promega) according to the manufacturer's instructions.

Transwell invasion assay. Transwell invasion assay was performed as described (61). Briefly, 100 000 Huh7 or Hep3B cells/well were seeded in 12 well plates (Corning) and treated

with CLDN1 mAb or control mAb for 24h. Subsequently pre-treated parental Huh7 cells or Huh7_CLDN1 KO or Huh7_sgCTRL cells were seeded in 100µl serum-free medium (75%) and Matrigel (25%, Corning) on 24 well transwell plates (Corning). Following solidification for 10 min in an incubator (37°C, 5% CO₂), 600 µL serum (10%) supplemented medium was added to the bottom wells. Invaded cells were visualized after 16 hours (Huh7) or 4h (Hep3B) by staining with crystal violet (0.2%) and quantified using ImageJ.

EDU proliferation assay. Huh7 CLDN1_KO or Huh7_sgCTRL cells were seeded in 12 well plates (Corning) at 100 000/well. The following day, cells were incubated with EDU (10 µM) for 5 h. Cells were subsequently washed, fixed with PFA 4% and permeabilized with Triton X 0.5%. EDU incorporated proliferating cells were stained and quantified using Click it EDU Cell Proliferation kit (Invitrogen) according to the manufacturer's instructions.

Flowcytometric assessment of CLDN1 mAb binding to primary cells derived from tumorous and adjacent liver tissue. Fresh or cryopreserved tumorous and adjacent tissue was dissociated into single cell suspension using Gentle MACS dissociator (Miltenyi Biotec) using Human Tumor Dissociation Kit (Miltenyi Biotec) according to the manufacturer's instructions. Following filtration (70µm), centrifugation (300g, 5 min) and washing steps, cells were blocked with 10% FBS for 1 h at room temperature. Subsequently, cells were washed and incubated with rat anti human CLDN1 mAb (10 µg) (21) or respective Isotype control mAb (10 µg/mL) for 1 h. Incubation with secondary anti-rat AF647 conjugated antibodies (1:100, Jackson ImmunoResearch, France) was performed for 45 minutes at room temperature. Data were acquired using Cytotflex B2R2V0 (Beckman Coulter) and analyzed using CytExpert 2.1 and FlowJo v10 (Beckman Coulter).

Huh7 CAF coculture of patient-derived liver scaffolds and ECM hydrogel. Cancer-associated fibroblasts were purchased from Bio/VT and maintained according to the supplier's instructions. Patient normal and fibrotic liver-derived liver scaffolds and ECM hydrogel were purchased from Xylyx Bio. Re-population of liver scaffolds was performed according to the supplier's instructions. Briefly, 8x10⁴ Huh7 and 2x10⁴ CAFs were seeded in 20 µL volumes on

liver scaffolds and incubated for 45 min in an incubator at 37°C, 5% CO₂ before 200 µL of complete Stellate Cell medium SteCM (ScienCell, #5301) was added. Following incubation overnight, 200 µL medium supplemented with 20 ng/mL TGFβ and 50 µg/mL CLDN1 specific or isotype control mAb was added. For co-culture of Huh7 cells with CAFs in patient-derived ECM hydrogel, ECM substrates were prepared as recommended by the supplier. 8x10⁴ Huh7 and 2 x10⁴ CAFs were embedded in hydrogel at 50 µL volumes and Stellate Cell medium SteCM containing TGFβ (10 ng/mL) and CLDN1 mAb or control mAb (10 µg/mL, respectively) were added following solidification over 45 min at 37°C. After 3 d, scaffolds and ECM hydrogels were dissociated and lysed using TriReagent (Molecular Research Center) on a GentleMACS Dissociator (Miltenyi Biotec). RNA extraction, reverse transcription and qPCR assessment of marker genes were performed as described below.

Perturbation studies on HCC patient-derived spheroids. Fragments of tumor tissue (5x5mm to 8x8mm size) were excised from tumor mass of HCC patients and then processed with enzymatic and mechanical dissociation to generate clusters of tumor cells. Aggregates of cells are assembled into spheroids in 96-well Black/Clear Bottom Low Flange Ultra-Low Attachment Microplate (Corning) and cultured in MammoCult complete medium (STEMCELL Technologies). Tumorspheres were treated for 6 d with 10 µg/mL isotype control mAb, 10 µg/mL CLDN1 mAb or Sorafenib (10 µM) (Selleckchem). Tumorsphere viability was assessed at day 6 using CellTiterGlo 3D (Promega) according to the manufacturer's instructions.

CDX mouse model. All experiments were performed at the animal facility of Inserm U1110 according to local laws and ethics committee approval (institutional protocol approval number APAFiS #3559 and #7216). Non-Obese Diabetic Rag1^{-/-} IL2Rgc^{-/-} (NRG) mice were subcutaneously injected with 5 × 10⁶ cells of Huh7 cell line. After 7 to 10 days, when the average of tumor volumes reached 50 mm³, mice were randomized into different groups and treated for 6 weeks. In a first study mice were randomized into 2 groups: one was treated with CLDN1 mAb (25 mg/kg i.p. once per week), the other with vehicle control (i.p. once per week).

In a second independent study mice were randomized into 3 groups and treated with: a) H3L3 (25 mg/kg i.p. BIW); b) sorafenib 10mg/kg dissolved in Cremophor/Ethanol/PBS (5:5:90) by daily oral gavage; c) vehicle control of sorafenib by daily oral gavage, and PBS by BIW i.p. injection. Tumor growth was weekly monitored with a digital caliper and tumor volume was calculated using $1/2(\text{length} \times \text{width}^2)$ formula. When ethical endpoints were reached (*tumor volume $\geq 2000 \text{ mm}^3$ or when the largest measure reached 2 cm*) mice were sacrificed, and the tumors were harvested for immunohistochemistry, RNA and protein isolation.

[^{18}F]-FLT and [^{18}F]-FDG PET Scan of CDX mice. *PET procedure:* Imaging was conducted using a dedicated preclinical PET (IRIS PET, Inviscan). [^{18}F]-FLT or [^{18}F]-FDG was administered via tail vein injection at an activity dose of 7 to 12 MBq per mouse. Static image acquisitions were performed 90 min after injection of [^{18}F]-FLT, or 45min after injection of [^{18}F]-FDG. During the entire exam, each mouse was maintained under isoflurane anesthesia (2%, Minerve). Two photons detected within a 5 ns coincidence timing window and with an energy ranging from 250 to 750 keV were defined as a coincidence. For each PET exam, the coincidences were acquired for 10 min. Data were reconstructed into a 201x201x120 volume using the iterative 3D ordered-subset expectation-maximization algorithm. The resulting voxel size was equal to 0.42 mm in the transverse plane while the slice thickness was equal to 0.855 mm. PET data were fully corrected for normalization, random coincidences, radioactive decay, and dead time during the reconstruction process. No attenuation and scatter corrections were applied. *PET image Analysis:* All PET imaging datasets were analyzed using the AMIDE software package (62). For semiquantitative analysis, an elliptical volume of interest (VOI) was drawn on the tumor with a threshold of 60% of the maximum tracer uptake. Standardized Uptake Value (SUV) was calculated as ratio of measured radioactivity concentration (MBq/mL), divided by the administered dose at the time of injection (in MBq) divided by body weight (kg). Glucose metabolic activity and proliferative activity were quantified using the maximum SUV (SUV_{max}), mean SUV (SUV_{mean}), MTV (metabolic tumor volume) and PTV (proliferative tumor volume). Total lesion glycolysis (TLG) by FDG-PET and total lesion proliferation (TLP) by FLT-

PET were calculated by multiplying MTV and PTV with the corresponding SUV_{mean} for each tumor volume.

PDX mouse model. All experiments were performed at Crown Bio. The protocol and any amendment(s) or procedures involving the care and use of animals in this study were reviewed and approved by the Institutional Animal Care and Use Committee (IACUC) of CrownBio prior to execution. During the study, the care and use of animals were conducted in accordance with the regulations of the Association for Assessment and Accreditation of Laboratory Animal Care (AAALAC). Fresh tumor tissues from mice bearing established primary human liver cancer PDX model LI6280, LI6716, LI6723, LI1055 and LI1068) were harvested and cut into small pieces (approximately 2-3 mm in diameter) and inoculated subcutaneously at the upper right dorsal flank into female BALB/c nude mice for tumor development. The randomization started when the mean tumor size reached 100 mm³. A total of 5 mice were enrolled in each model. Randomization into groups receiving CLDN1 mAb (10 mg/kg, 10 mL/kg, QW x 4 doses, n=3) or vehicle control (10 mL/kg, QW x 4 doses, n=2) was performed based on "Matched distribution" method (Study Director TM software, version 3.1.399.19). The date of grouping was denoted as day 1. Dosing was started on day 1 and continued through day 25. After tumor inoculation, the animals were checked daily for morbidity and mortality. During routine monitoring, the animals were checked for any effects of tumor growth and treatments on behavior such as mobility, food and water consumption, body weight gain/loss (body weights would be measured twice per week after randomization), eye/hair matting and any other abnormalities. Mortality and observed clinical signs were recorded for individual animals in detail. Tumor volumes were measured twice per week after randomization in two dimensions using a caliper. The body weights and tumor volumes were measured by using Study Director TM software (version 3.1.399.19).

RNA extraction from human and murine liver tissue. Liver cells were lysed in TRI-reagent (Molecular Research Center), and RNA was purified using Direct-zol RNA MiniPrep (Zymo Research) according to the manufacturer's instructions. RNA quantity and quality were

assessed using NanoDrop (ThermoScientific). Gene expression profiling was performed using 250-500 ng total RNA.

Histological and image analysis. All organs were immediately fixed in a 10% formalin solution after harvesting and subsequently included in paraffin. Immunohistochemistry staining for KI67, EPCAM and Fibronectin were performed in 5-6 mice per group. For each mouse, images at 10x or 20x magnification per staining were captured and analyzed by image J.

Protein immunodetection. Cells derived from Huh7 spheroids were collected at the desired timepoints, washed and centrifuged at 300xg during 5 min. For obtaining whole cell lysates, cells were lysed with IP lysis buffer (Triton 1%; NaCl 50 mM; Tris 50 mM pH 7.6; MgCl₂ 2 mM in ddH₂O) with proteinase inhibitors (Roche) and phosphatase inhibitors (Sigma Phosphatase Cocktail number 2 and 3) during 30 min at 4°C with agitation. Then the samples were centrifuged at 16000xg during 15 min and the supernatant was collected. Protein quantification was assessed with Thermo Scientific BCA Kit. Gels were prepared following the Biorad TGX gel protocol (BioRad). The gels were transferred using the Biorad trans blot turbo protocol (BioRad) into PVDF membranes. Blocking of the membranes was performed with 3% BSA in TBS-T for 1 h. The membranes were incubated with MT1-MMP (MMP14) D1E4 rabbit mAb (Cell Signaling Technology) and monoclonal anti- β -Actin antibody produced in mouse (Sigma) in 3% BSA in TBS-T with a dilution of 1:2000 overnight at 4°C. The membranes were incubated with secondary peroxidase AffiniPure goat anti-rabbit IgG (H+L) mAb (Jackson ImmunoResearch) or ECL mouse IgG, HRP-linked whole Ab (from sheep) (Amersham) in 3% BSA in TBS-T with a dilution of 1:10000 for 1 h at room temperature. Protein immunodetection of the membranes was performed with Clarity ECL Western Blot Substrate (Biorad) in a ChemiDoc MP Imaging System (Biorad). Immunoblot images were analyzed using Fiji and the graphics were performed with GraphPad Prism 8.

Genome wide RNA-seq analyses. RNA-seq libraries were generated from 300 ng of total RNA using TruSeq Stranded mRNA Sample Preparation Kit (Illumina, Part Number RS-122-2101). Briefly, following purification with poly-T oligo attached magnetic beads, the mRNA was

fragmented using divalent cations at 94°C for 2 min. The cleaved RNA fragments were copied into first strand cDNA using reverse transcriptase and random primers. Strand specificity was achieved by replacing dTTP with dUTP during second strand cDNA synthesis using DNA Polymerase I and RNase H. Following addition of a single 'A' base and subsequent ligation of the adapter on double stranded cDNA fragments, the products were purified and enriched with PCR (30 sec at 98°C; [10 sec at 98°C, 30 sec at 60°C, 30 sec at 72°C] x 12 cycles; 5 min at 72°C) to create the cDNA library. Surplus PCR primers were further removed by purification using AMPure XP beads (Beckman Coulter) and the final cDNA libraries were checked for quality and quantified using 2100 Bioanalyzer (Agilent). Libraries were sequenced on the Illumina HiSeq 4000 as Single-Read 50 base reads following Illumina's instructions. Image analysis and base calling were performed using RTA v2.7.3 and bcl2fastq v2.17.1.14.

Gene expression analyses in cell culture experiments. Total RNA extraction from 2D cell cultures was performed using RNeasy Mini Kit (Qiagen) according to the manufacturer's instructions. RNA extraction from spheroids was performed using Arcturus PicoPure RNA Isolation Kit (Applied Biosystems). Subsequently, total RNA was reverse transcribed (H Minus First Strand cDNA synthesis Mix, ThermoScientific) on a Thermocycler (Bio-Rad T100, Bio-Rad). Quantitative PCR was performed on the CFX96 Touch Real-Time PCR Detection system with 10 µL reaction volumes containing 5 µL SYBR Green 2x mix (Bio-Rad), 2 µL of RNase-free water and 250 nM gene specific sense and antisense primers. All gene expression levels were normalized to housekeeping genes *HPRT1*, *GAPDH* or *GUSB* using the $\Delta\Delta C_t$ method(63).

Bioinformatic and statistical analyses. Human RNA-seq data was mapped using HISAT2(64) to the human genome hg19. Mouse RNA-seq data was mapped to the mouse genome mm10 and annotated using the Gencode vM15 gene annotation. Data from PDX mice were only further processed if >50% reads were mapped to the human genome. Only reads mapping to human chromosomes were kept for further analysis. Reads were counted with htseq-count, and a differentially expression analysis was performed with DESeq2 applying

GENCODE 19(65). Gene Set Enrichment Analysis (GSEA)(25) was used for unbiased pathway analysis (HALLMARK gene sets) using Molecular Signature Database (MSigDB)(66). Results from GSEA were adjusted for the false discovery rate (FDR). FDR<0.25 was considered as statistically significant. For evaluation of CLDN1 mAb treatment effects on the liver transcriptome in PDX mouse models, samples derived from CLDN1 mAb treated animals were compared to respective control samples of the same model. Only normalized enrichment scores (NES) of significant alterations are shown. Unless otherwise stated, *in vitro* analyses were performed in at least three independent experiments performed in triplicate. Results of *in vitro* analyses are expressed as % to the respective controls \pm sem. All data was compared using Students' t-test, when normally distributed or non-parametric tests (U-test and Fisher test) when non-normally distributed (Shapiro-Wilk test) (GraphPad Prism v9.1). Results derived from liver scaffolds experiments were compared using paired Student's t-test (GraphPad Prism v9.1). Results with a p-value <0.05 were considered statistically significant. **** $p < 0.0001$, *** $p < 0.001$, ** $p < 0.01$, * $p < 0.05$.

Acknowledgements

The authors thank the CRB (Centre de Ressources Biologiques-Biological Resource Centre) of the Strasbourg University Hospitals for the management of patient-derived liver tissue. The authors thank Dr. M. Evans (Mount Sinai Hospital, NY) for providing mouse and human CLDN1 expression plasmids, Dr. D. Root (Broad Institute of MIT and Harvard, Cambridge, MA) for providing expression plasmids for lentiviruses and sgRNAs for CLDN1 KO and Prof. Gerhard Cristofori for the gift of Huh7 cells.

Author contributions

T.F.B. initiated and led the study. N.R., S.C, F.H.D, E.C., C.S., J.L. and T.F.B. designed experiments and analyzed data. N.R., S.C., F.H.D., F. D., S.D., M.F., T.R., M.O. and N.A. performed experiment and analyzed data. M.M. performed and analyzed animal experiments. R.I., T.S., G.E. and M.M. designed PDX mice model studies. H.E. performed gene expression analyses. F.J. performed computational analyses. M. H. and I.D. gave critical conceptual input. E.F. and P.P. recruited and prepared patient liver tissues for *ex vivo* experiments. N.R., S.C., M.M. and N.A. designed figures and tables. N. R., J.L. and T.F.B. wrote the manuscript. All authors read and approved the final manuscript to be submitted.

References

1. J. M. Llovet, R. K. Kelley, A. Villanueva, A. G. Singal, E. Pikarsky, S. Roayaie *et al.*, Hepatocellular carcinoma. *Nat Rev Dis Primers* **7**, 6 (2021).
2. I. A. f. R. o. Cancer. (IARC, 2020).
3. e. e. e. European Association for the Study of the Liver. Electronic address, L. European Association for the Study of the, EASL Clinical Practice Guidelines: Management of hepatocellular carcinoma. *J Hepatol* **69**, 182-236 (2018).
4. J. Baglieri, D. A. Brenner, T. Kisseleva, The Role of Fibrosis and Liver-Associated Fibroblasts in the Pathogenesis of Hepatocellular Carcinoma. *Int J Mol Sci* **20**, (2019).
5. Q. Zhang, Y. He, N. Luo, S. J. Patel, Y. Han, R. Gao *et al.*, Landscape and Dynamics of Single Immune Cells in Hepatocellular Carcinoma. *Cell* **179**, 829-845 e820 (2019).
6. C. E. Lewis, J. W. Pollard, Distinct role of macrophages in different tumor microenvironments. *Cancer Res* **66**, 605-612 (2006).
7. K. Schulze, S. Imbeaud, E. Letouze, L. B. Alexandrov, J. Calderaro, S. Rebouissou *et al.*, Exome sequencing of hepatocellular carcinomas identifies new mutational signatures and potential therapeutic targets. *Nat Genet* **47**, 505-511 (2015).

8. C. Guichard, G. Amaddeo, S. Imbeaud, Y. Ladeiro, L. Pelletier, I. B. Maad *et al.*, Integrated analysis of somatic mutations and focal copy-number changes identifies key genes and pathways in hepatocellular carcinoma. *Nat Genet* **44**, 694-698 (2012).
9. M. Liu, Q. Yan, Y. Sun, Y. Nam, L. Hu, J. H. Loong *et al.*, A hepatocyte differentiation model reveals two subtypes of liver cancer with different oncofetal properties and therapeutic targets. *Proc Natl Acad Sci U S A* **117**, 6103-6113 (2020).
10. J. K. Heimbach, L. M. Kulik, R. S. Finn, C. B. Sirlin, M. M. Abecassis, L. R. Roberts *et al.*, AASLD guidelines for the treatment of hepatocellular carcinoma. *Hepatology* **67**, 358-380 (2018).
11. R. S. Finn, S. Qin, M. Ikeda, P. R. Galle, M. Ducreux, T. Y. Kim *et al.*, Atezolizumab plus Bevacizumab in Unresectable Hepatocellular Carcinoma. *N Engl J Med* **382**, 1894-1905 (2020).
12. S. Roayaie, K. Obeidat, C. Sposito, L. Mariani, S. Bhoori, A. Pellegrinelli *et al.*, Resection of hepatocellular cancer ≤ 2 cm: results from two Western centers. *Hepatology* **57**, 1426-1435 (2013).
13. E. Crouchet, S. Bandiera, N. Fujiwara, S. Li, H. El Saghire, M. Fernández-Vaquero *et al.*, A human liver cell-based system modeling a clinical prognostic liver signature combined with single-cell RNA-Seq for discovery of liver disease therapeutics. *Nat Commun*, (Accepted 06/21).
14. M. B. Zeisel, P. Dhawan, T. F. Baumert, Tight junction proteins in gastrointestinal and liver disease. *Gut* **68**, 547-561 (2019).
15. N. Roehlen, A. A. Roca Suarez, H. El Saghire, A. Saviano, C. Schuster, J. Lupberger *et al.*, Tight Junction Proteins and the Biology of Hepatobiliary Disease. *Int J Mol Sci* **21**, (2020).
16. M. J. Evans, T. von Hahn, D. M. Tscherne, A. J. Syder, M. Panis, B. Wolk *et al.*, Claudin-1 is a hepatitis C virus co-receptor required for a late step in entry. *Nature* **446**, 801-805 (2007).

17. L. Mailly, F. Xiao, J. Lupberger, G. K. Wilson, P. Aubert, F. H. T. Duong *et al.*, Clearance of persistent hepatitis C virus infection in humanized mice using a claudin-1-targeting monoclonal antibody. *Nat Biotechnol* **33**, 549-554 (2015).
18. J. Stebbing, A. Filipovic, G. Giamas, Claudin-1 as a promoter of EMT in hepatocellular carcinoma. *Oncogene* **32**, 4871-4872 (2013).
19. Y. Suh, C. H. Yoon, R. K. Kim, E. J. Lim, Y. S. Oh, S. G. Hwang *et al.*, Claudin-1 induces epithelial-mesenchymal transition through activation of the c-Abl-ERK signaling pathway in human liver cells. *Oncogene* **32**, 4873-4882 (2013).
20. I. Fofana, S. E. Krieger, F. Grunert, S. Glauben, F. Xiao, S. Fafi-Kremer *et al.*, Monoclonal anti-claudin 1 antibodies prevent hepatitis C virus infection of primary human hepatocytes. *Gastroenterology* **139**, 953-964, 964 e951-954 (2010).
21. C. C. Colpitts, R. G. Tawar, L. Mailly, C. Thumann, L. Heydmann, S. C. Durand *et al.*, Humanisation of a claudin-1-specific monoclonal antibody for clinical prevention and cure of HCV infection without escape. *Gut* **67**, 736-745 (2018).
22. M. Uhlen, P. Oksvold, L. Fagerberg, E. Lundberg, K. Jonasson, M. Forsberg *et al.*, Towards a knowledge-based Human Protein Atlas. *Nature biotechnology* **28**, 1248-1250 (2010).
23. S. Torrecilla, D. Sia, A. N. Harrington, Z. Zhang, L. Cabellos, H. Cornella *et al.*, Trunk mutational events present minimal intra- and inter-tumoral heterogeneity in hepatocellular carcinoma. *J Hepatol* **67**, 1222-1231 (2017).
24. T. Yamashita, J. Ji, A. Budhu, M. Forgues, W. Yang, H. Y. Wang *et al.*, EpCAM-positive hepatocellular carcinoma cells are tumor-initiating cells with stem/progenitor cell features. *Gastroenterology* **136**, 1012-1024 (2009).
25. A. Subramanian, P. Tamayo, V. K. Mootha, S. Mukherjee, B. L. Ebert, M. A. Gillette *et al.*, Gene set enrichment analysis: a knowledge-based approach for interpreting genome-wide expression profiles. *Proc Natl Acad Sci U S A* **102**, 15545-15550 (2005).

26. S. Shimada, K. Mogushi, Y. Akiyama, T. Furuyama, S. Watanabe, T. Ogura *et al.*, Comprehensive molecular and immunological characterization of hepatocellular carcinoma. *EBioMedicine* **40**, 457-470 (2019).
27. Y. Hoshida, S. M. Nijman, M. Kobayashi, J. A. Chan, J. P. Brunet, D. Y. Chiang *et al.*, Integrative transcriptome analysis reveals common molecular subclasses of human hepatocellular carcinoma. *Cancer Res* **69**, 7385-7392 (2009).
28. A. Villanueva, Y. Hoshida, C. Battiston, V. Tovar, D. Sia, C. Alsinet *et al.*, Combining clinical, pathology, and gene expression data to predict recurrence of hepatocellular carcinoma. *Gastroenterology* **140**, 1501-1512 e1502 (2011).
29. M. Ramalho-Santos, S. Yoon, Y. Matsuzaki, R. C. Mulligan, D. A. Melton, "Stemness": transcriptional profiling of embryonic and adult stem cells. *Science* **298**, 597-600 (2002).
30. S. Assou, T. Le Carrou, S. Tondeur, S. Strom, A. Gabelle, S. Marty *et al.*, A meta-analysis of human embryonic stem cells transcriptome integrated into a web-based expression atlas. *Stem Cells* **25**, 961-973 (2007).
31. Y. Hoshida, A. Villanueva, M. Kobayashi, J. Peix, D. Y. Chiang, A. Camargo *et al.*, Gene expression in fixed tissues and outcome in hepatocellular carcinoma. *N Engl J Med* **359**, 1995-2004 (2008).
32. A. Budhu, M. Forgues, Q. H. Ye, H. L. Jia, P. He, K. A. Zanetti *et al.*, Prediction of venous metastases, recurrence, and prognosis in hepatocellular carcinoma based on a unique immune response signature of the liver microenvironment. *Cancer Cell* **10**, 99-111 (2006).
33. O. V. Grinchuk, S. P. Yenamandra, R. Iyer, M. Singh, H. K. Lee, K. H. Lim *et al.*, Tumor-adjacent tissue co-expression profile analysis reveals pro-oncogenic ribosomal gene signature for prognosis of resectable hepatocellular carcinoma. *Mol Oncol* **12**, 89-113 (2018).
34. T. Yamashita, X. W. Wang, Cancer stem cells in the development of liver cancer. *J Clin Invest* **123**, 1911-1918 (2013).

35. X. L. Ma, Y. F. Sun, B. L. Wang, M. N. Shen, Y. Zhou, J. W. Chen *et al.*, Sphere-forming culture enriches liver cancer stem cells and reveals Stearoyl-CoA desaturase 1 as a potential therapeutic target. *BMC Cancer* **19**, 760 (2019).
36. M. A. Nieto, R. Y. Huang, R. A. Jackson, J. P. Thiery, Emt: 2016. *Cell* **166**, 21-45 (2016).
37. Y. Song, S. H. Kim, K. M. Kim, E. K. Choi, J. Kim, H. R. Seo, Activated hepatic stellate cells play pivotal roles in hepatocellular carcinoma cell chemoresistance and migration in multicellular tumor spheroids. *Sci Rep* **6**, 36750 (2016).
38. Y. Song, J. S. Kim, S. H. Kim, Y. K. Park, E. Yu, K. H. Kim *et al.*, Patient-derived multicellular tumor spheroids towards optimized treatment for patients with hepatocellular carcinoma. *J Exp Clin Cancer Res* **37**, 109 (2018).
39. S. Xia, Y. Pan, Y. Liang, J. Xu, X. Cai, The microenvironmental and metabolic aspects of sorafenib resistance in hepatocellular carcinoma. *EBioMedicine* **51**, 102610 (2020).
40. R. Pinyol, R. Montal, L. Bassaganyas, D. Sia, T. Takayama, G. Y. Chau *et al.*, Molecular predictors of prevention of recurrence in HCC with sorafenib as adjuvant treatment and prognostic factors in the phase 3 STORM trial. *Gut* **68**, 1065-1075 (2019).
41. V. R. Bollineni, G. M. Kramer, E. P. Jansma, Y. Liu, W. J. Oyen, A systematic review on [(18)F]FLT-PET uptake as a measure of treatment response in cancer patients. *Eur J Cancer* **55**, 81-97 (2016).
42. M. P. Dunphy, J. S. Lewis, Radiopharmaceuticals in preclinical and clinical development for monitoring of therapy with PET. *J Nucl Med* **50 Suppl 1**, 106S-121S (2009).
43. S. Ben-Haim, P. Ell, 18F-FDG PET and PET/CT in the evaluation of cancer treatment response. *J Nucl Med* **50**, 88-99 (2009).
44. C. Xu, X. Li, P. Liu, M. Li, F. Luo, Patient-derived xenograft mouse models: A high fidelity tool for individualized medicine. *Oncol Lett* **17**, 3-10 (2019).
45. G. Giannelli, P. Koudelkova, F. Dituri, W. Mikulits, Role of epithelial to mesenchymal transition in hepatocellular carcinoma. *J Hepatol* **65**, 798-808 (2016).

46. C. H. Yoon, M. J. Kim, M. J. Park, I. C. Park, S. G. Hwang, S. An *et al.*, Claudin-1 acts through c-Abl-protein kinase Cdelta (PKCdelta) signaling and has a causal role in the acquisition of invasive capacity in human liver cells. *J Biol Chem* **285**, 226-233 (2010).
47. J. Zucman-Rossi, A. Villanueva, J. C. Nault, J. M. Llovet, Genetic Landscape and Biomarkers of Hepatocellular Carcinoma. *Gastroenterology* **149**, 1226-1239 e1224 (2015).
48. J. M. Llovet, S. Ricci, V. Mazzaferro, P. Hilgard, E. Gane, J. F. Blanc *et al.*, Sorafenib in advanced hepatocellular carcinoma. *N Engl J Med* **359**, 378-390 (2008).
49. Y. C. Liu, C. T. Yeh, K. H. Lin, Cancer Stem Cell Functions in Hepatocellular Carcinoma and Comprehensive Therapeutic Strategies. *Cells* **9**, (2020).
50. M. Ruiz de Galarreta, E. Bresnahan, P. Molina-Sanchez, K. E. Lindblad, B. Maier, D. Sia *et al.*, beta-Catenin Activation Promotes Immune Escape and Resistance to Anti-PD-1 Therapy in Hepatocellular Carcinoma. *Cancer Discov* **9**, 1124-1141 (2019).
51. Y. J. Zhu, B. Zheng, H. Y. Wang, L. Chen, New knowledge of the mechanisms of sorafenib resistance in liver cancer. *Acta Pharmacol Sin* **38**, 614-622 (2017).
52. J. M. Llovet, J. Zucman-Rossi, E. Pikarsky, B. Sangro, M. Schwartz, M. Sherman *et al.*, Hepatocellular carcinoma. *Nat Rev Dis Primers* **2**, 16018 (2016).
53. F. Kanwal, J. Kramer, S. M. Asch, M. Chayanupatkul, Y. Cao, H. B. El-Serag, Risk of Hepatocellular Cancer in HCV Patients Treated With Direct-Acting Antiviral Agents. *Gastroenterology* **153**, 996-1005 e1001 (2017).
54. N. Roehlen, A. Saviano, H. El Saghire, E. Crouchet, F. H. T. Duong, F. Juehling *et al.*, A monoclonal antibody targeting non-junctional Claudin-1 inhibits fibrosis in patient-derived models by modulating cell plasticity. *Sci Transl Med.*, (Submitted, preparation of R1 revision).
55. J. H. Park, J. E. Shin, H. W. Park, The Role of Hippo Pathway in Cancer Stem Cell Biology. *Mol Cells* **41**, 83-92 (2018).
56. J. Wang, B. A. Sullenger, J. N. Rich, Notch signaling in cancer stem cells. *Adv Exp Med Biol* **727**, 174-185 (2012).

57. M. S. Matter, T. Decaens, J. B. Andersen, S. S. Thorgeirsson, Targeting the mTOR pathway in hepatocellular carcinoma: current state and future trends. *J Hepatol* **60**, 855-865 (2014).
58. C. C. Colpitts, R. G. Tawar, L. Mailly, C. Thumann, L. Heydmann, S. C. Durand *et al.*, Humanisation of a claudin-1-specific monoclonal antibody for clinical prevention and cure of HCV infection without escape. *Gut*, (2017).
59. M. Boeckh, M. M. Berrey, R. A. Bowden, S. W. Crawford, J. Balsley, L. Corey, Phase 1 evaluation of the respiratory syncytial virus-specific monoclonal antibody palivizumab in recipients of hematopoietic stem cell transplants. *J. Infect. Dis.* **184**, 350-354 (2001).
60. S. Cribbes, S. Kessel, S. McMenemy, J. Qiu, L. L. Chan, A Novel Multiparametric Drug-Scoring Method for High-Throughput Screening of 3D Multicellular Tumor Spheroids Using the Celigo Image Cytometer. *SLAS Discov* **22**, 547-557 (2017).
61. C. R. Justus, N. Leffler, M. Ruiz-Echevarria, L. V. Yang, In vitro cell migration and invasion assays. *J Vis Exp*, (2014).
62. A. M. Loening, S. S. Gambhir, AMIDE: a free software tool for multimodality medical image analysis. *Mol Imaging* **2**, 131-137 (2003).
63. K. J. Livak, T. D. Schmittgen, Analysis of relative gene expression data using real-time quantitative PCR and the 2(-Delta Delta C(T)) Method. *Methods* **25**, 402-408 (2001).
64. D. Kim, B. Langmead, S. L. Salzberg, HISAT: a fast spliced aligner with low memory requirements. *Nat. Methods* **12**, 357-360 (2015).
65. J. Harrow, F. Denoeud, A. Frankish, A. Reymond, C. K. Chen, J. Chrast *et al.*, GENCODE: producing a reference annotation for ENCODE. *Genome Biol.* **7 Suppl 1**, S4 1-9 (2006).
66. A. Liberzon, A. Subramanian, R. Pinchback, H. Thorvaldsdottir, P. Tamayo, J. P. Mesirov, Molecular signatures database (MSigDB) 3.0. *Bioinformatics* **27**, 1739-1740 (2011).
67. Z. D. Goodman, Grading and staging systems for inflammation and fibrosis in chronic liver diseases. *J Hepatol* **47**, 598-607 (2007).

68. S. N. Martins-Filho, C. Paiva, R. S. Azevedo, V. A. F. Alves, Histological Grading of Hepatocellular Carcinoma-A Systematic Review of Literature. *Front Med (Lausanne)* **4**, 193 (2017).
69. J. A. Marrero, L. M. Kulik, C. B. Sirlin, A. X. Zhu, R. S. Finn, M. M. Abecassis *et al.*, Diagnosis, Staging, and Management of Hepatocellular Carcinoma: 2018 Practice Guidance by the American Association for the Study of Liver Diseases. *Hepatology* **68**, 723-750 (2018).

Figure 1

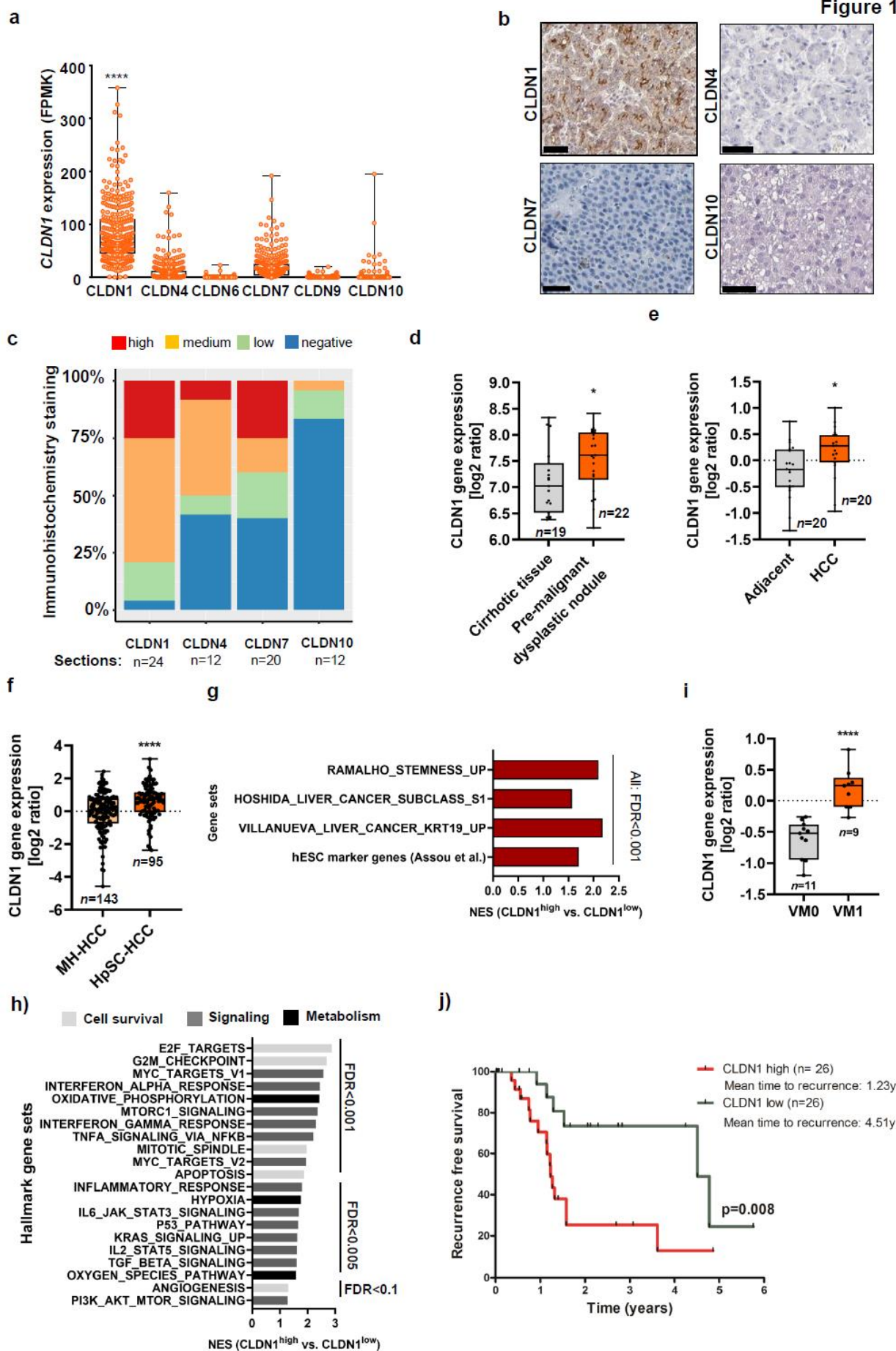


Figure 1. CLDN1 is overexpressed in HCC and correlates with stemness and poor clinical prognosis.

a. Gene expression of different claudin proteins in human liver cancer (n=365 patients, *Genomic Data commons* platform, <https://portal.gdc.cancer.gov>, $p < 0.0001$, One-way ANOVA). **b.** Immunostaining of different CLDNs in human HCC tissue derived from the human protein atlas (22) **c.** Quantification of CLDN1, 4, 7 and 10 protein expression in HCC patient tissue based on the human protein atlas (22). **d.** *CLDN1* expression in premalignant dysplastic nodules of cirrhotic liver compared to non-dysplastic cirrhotic tissue (GSE102383 (23), $p = 0.03$, Student's t-test) is shown. **e.** *CLDN1* expression in tumorous and matched adjacent liver tissue of patients with HCC (GSE113996, $p = 0.02$, paired Student's t-test). **f.** *CLDN1* expression in HCC tissue with a hepatocyte mature (MH-HCC) or a progenitor like stem cell signature (HpSC-HCC) (GSE5975 (24), $p < 0.0001$, Student's t-test) is shown. **g.** GSEA (25) analysis of embryonic genes (30) and gene sets related to stemness (MSigDB) in HCC liver tissue with high (50% above median) or low (50% below median) *CLDN1* expression (GSE11279 (26), $FDR < 0.001$, Kolmogorov-Smirnov test, respectively). **h.** Unbiased GSEA(25) of HALLMARK gene sets (MSigDB) in HCC liver tissue with high (50% above median) or low (50% below median) *CLDN1* expression (GSE11279 (26), $FDR < 0.1$, Kolmogorov-Smirnov test, respectively). **i.** *CLDN1* expression in non-cancerous tumor-microenvironment of HCC patients with venous metastasis (VM1) or without (VM0) (GSE5093(32), $p < 0.0001$ Students' t-test). **j.** Recurrence free survival in patient with high (50% above median) vs. low (50% below median) *CLDN1* expression in tumor adjacent liver tissue GSE76427 (33), $p = 0.008$, log rank test. Boxplot represents median (—), 1st and 3rd quartile (bottom and top of the box) and single data points (●). Vertical bars show NES of significantly ($FDR < 0.25$, Kolmogorov-Smirnov test, respectively) altered gene sets. * $p < 0.05$, ** $p < 0.01$, *** $p < 0.001$, **** $p < 0.0001$. Abbreviations: CLDN=Claudin; FPKM=Fragments Per Kilobase Million; HCC=Hepatocellular Carcinoma; MH-HCC=hepatocyte mature HCC; HpSC-HCC=progenitor like stem cell signature; VM0=HCC adjacent tissue without venous metastasis; VM1=HCC adjacent tissue with venous metastasis.

Figure 2

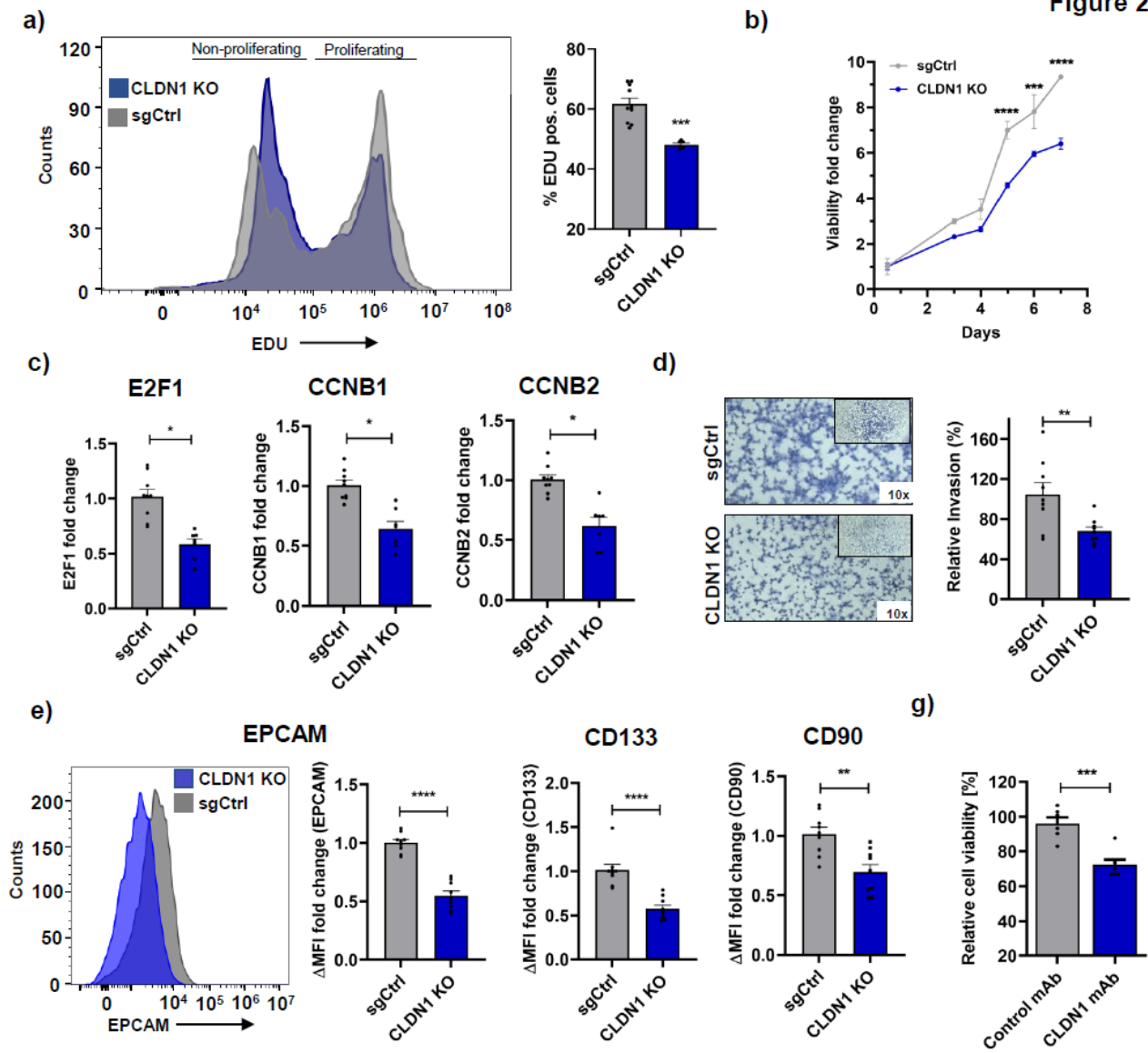


Figure 2 continued

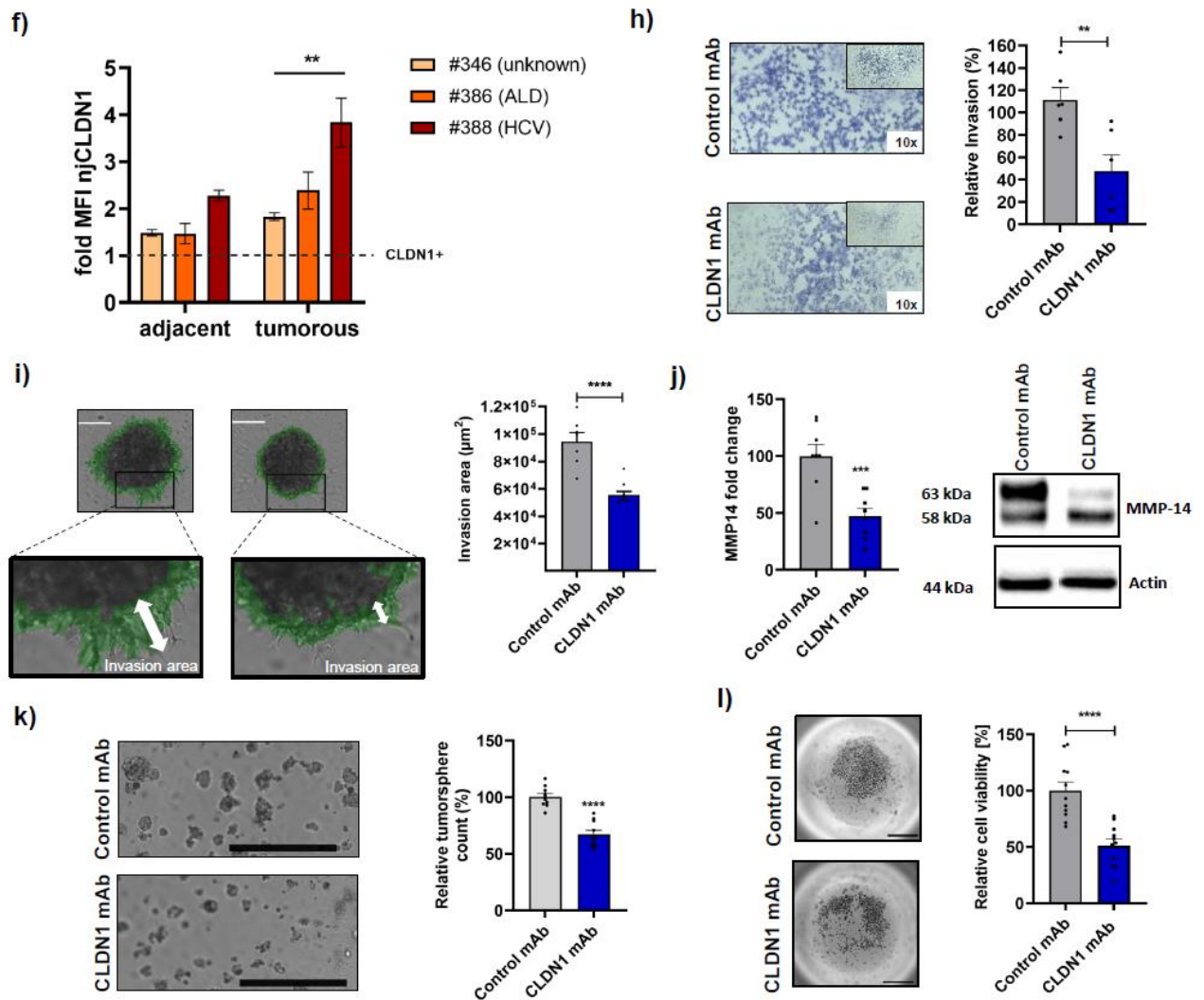


Figure 2. CLDN1 perturbation by genetic knockout or CLDN1 mAb mediated anti-tumorigenic effects.

a. Flowcytometric analysis of EDU-pos (proliferating) and EDU-neg (non-proliferating) cells in Huh7_CLDN1 KO and Huh7_sgCTRL cell line ($p < 0.001$, Student's t-test). **b.** Tumorsphere growth was assessed by ATP quantification over 7 days in Huh7_CLDN1 KO and Huh7_sgCTRL cells. Graph shows % tumor cell viability compared to post-seeding viability ($p < 0.001$, Student's t-test, respectively). **c.** Relative gene expression of proliferation markers *E2F1*, *CCNB1* and *CCNB2* in Huh7_CLDN1 KO compared to Huh7_sgCTRL cell is shown ($p = 0.02$, Student's t-test, respectively). **d.** Representative images showing crystal violet

visualized invading cells in transwell chamber assays. Bars show normalized ratio of invading cells ($p=0.007$, Student's t-test). **e.** Flowcytometric assessment of stemness markers EPCAM, CD133 (PROM1) and CD90 in Huh7_CLDN1 KO and Huh7_sgCTRL cells. Bars show Δ MFI of target-antibody stained vs. control antibody-stained cells normalized to Huh7_sgCTRL cells. **f.** Flowcytometric assessment of CLDN1 mAb binding to the total cell population derived from tumorous tissue compared to matched non-tumorous adjacent tissue. Bars show mean \pm SD of fold MFI (CLDN1 mAb compared to control mAb binding) ($p=0.006$, 2-way ANOVA). **g.** Tumorsphere growth was assessed by ATP quantification at day 3 post seeding in CLDN1 mAb or control mAb treated Huh7 cells. Graph shows %tumor cell viability normalized to cell viability in control mAb treated cells. ($p=0.003$, Student's t-test). **h.** Representative images showing crystal violet visualized invading cells in transwell chamber assays. Bars show normalized ratio of invading cells ($p=0.006$, Student's t-test). **i.** Left panel: Representative images showing assessment of tumor cell invasion in Matrigel embedded Huh7 spheroids treated with CLDN1 or isotype control mAb for 3 days using Celigo imaging cytometer. Green mask represents the delimitation used for the invasion area quantification. Right panel: Bars show computationally analysed invasion area. **j.** Left panel: Normalized gene expression of *MMP14* in Matrigel embedded Huh7 spheroids treated with CLDN1 or control mAb for 3 days. Right panel: Representative images of MMP14 immunoblots in Huh7 spheroids treated with CLDN1 or control mAb for 3 days. **k.** Left panel: Representative images showing Huh7 tumorsphere size on day 3 under EGF (20 ng/mL) + FGF (10ng/mL) and CLDN1 or control mAb treatment. Right panel: Quantitative assessment of tumorsphere number on day 7 under CLDN1 or control mAb treatment. **l.** Left panel: Representative images showing number and size of Huh7 tumorspheres on day 7 under EGF (20 ng/mL) + FGF (10 ng/mL) and CLDN1 or control mAb treatment. Right panel: Quantitative assessment of tumor cell viability by ATP quantification. Bars show mean \pm SEM and single data points (\bullet). * $p<0.05$, ** $p<0.01$, *** $p<0.001$, **** $p<0.0001$. Abbreviations: ALD=alcoholic liver disease; CLDN1=Claudin 1; EDU=5-ethynyl-2'-deoxyuridine; HCV=hepatitis C virus; KO=Knockout; sgCTRL=single guide control.

Figure 3

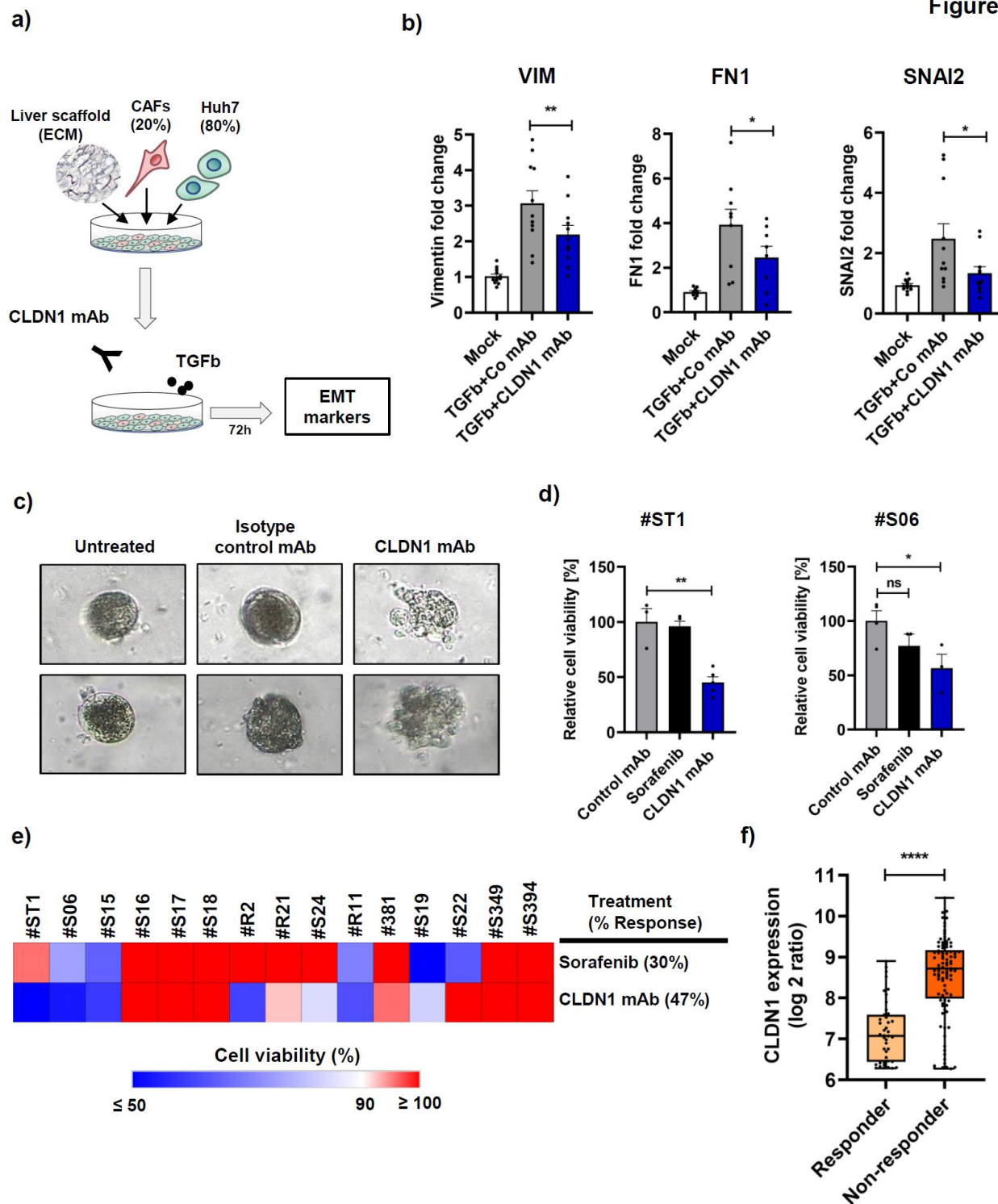


Figure 3. CLDN1 mAb suppresses epithelial-mesenchymal transition and tumor growth in patient-derived *ex vivo* models of HCC.

a. Illustration of study protocol for assessment of CLDN1 mAb treatment effects on Huh7 cells co-cultured with primary CAFs on patient-derived liver scaffolds. **b.** Normalized gene expression of EMT markers Vimentin (*VIM*), Fibronectin (*FN1*) and *SNAI2* in CLDN1 or control mAb treated Huh7+CAF liver scaffolds ($p=0.006$, $p=0.04$ and $p=0.04$, paired Student's t-test, respectively). **c.** Tumor spheroids were generated from HCC liver tissue and then treated with control mAb or with CLDN1 mAb. Representative microscopic pictures, taken on day 6 post-treatment are shown. **d.** Tumor spheroids were prepared from 15 HCC liver tissues and then treated with CLDN1 mAb or sorafenib. Heatmaps illustrate % cell viability compared to control mAb treated cells on day 6 using ATP quantification. **e.** *CLDN1* expression in HCC tissue predicted to confer response or resistance to sorafenib treatment (GSE109211(40), $p<0.0001$, Student's t-test). Boxplots represent median (—), 1st and 3rd quartile (bottom and top of the box) and single data points (●). Bars show mean \pm SEM. * $p<0.05$, ** $p<0.01$, *** $p<0.001$, **** $p<0.0001$. Abbreviations: CAFs= Cancer-associated fibroblasts; CLDN1=Claudin 1; ECM=Extracellular matrix.

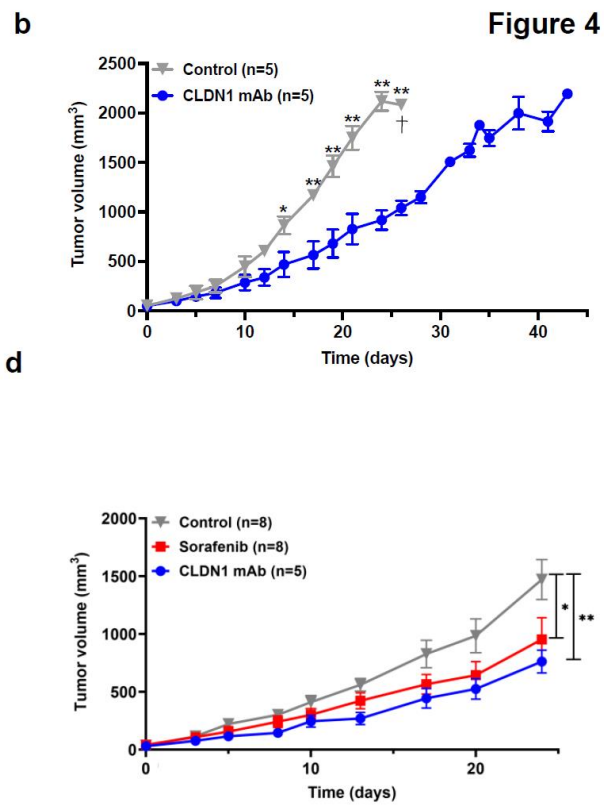
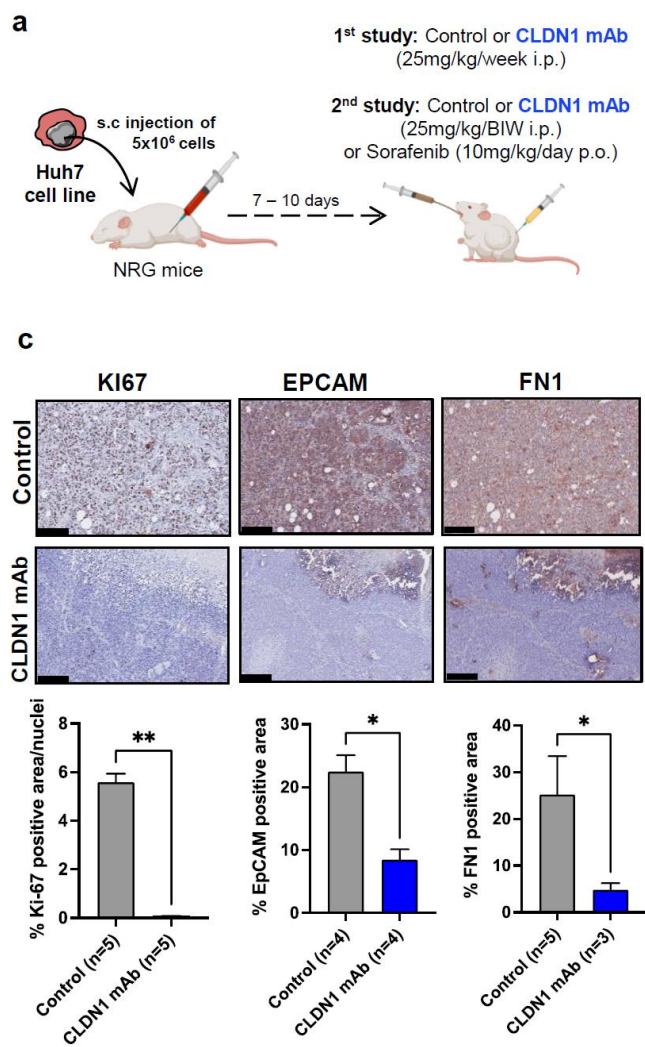
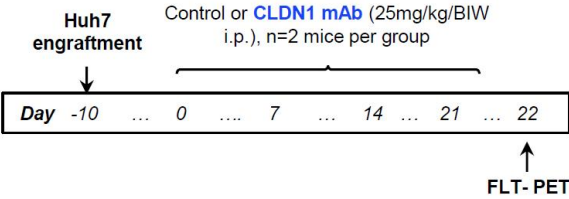
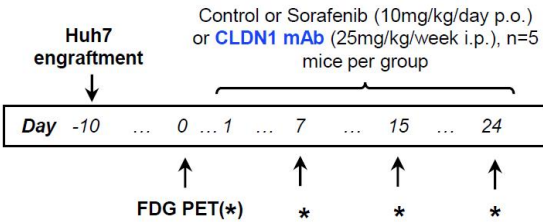


Figure 4 continued

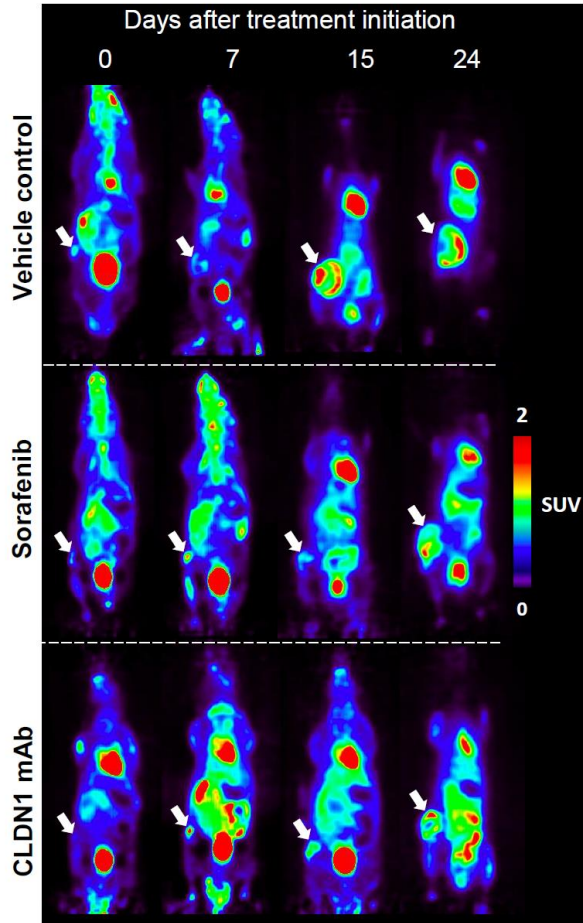
e



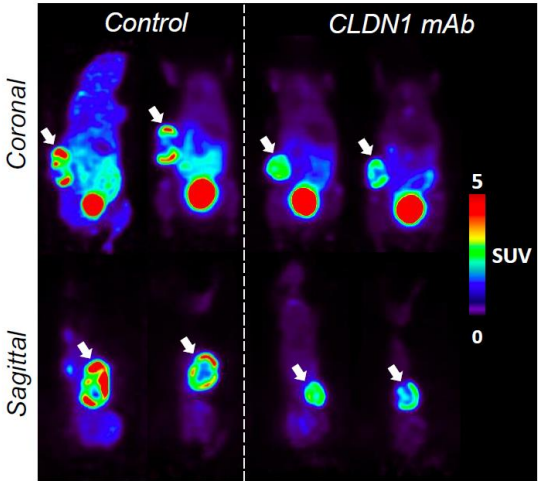
h



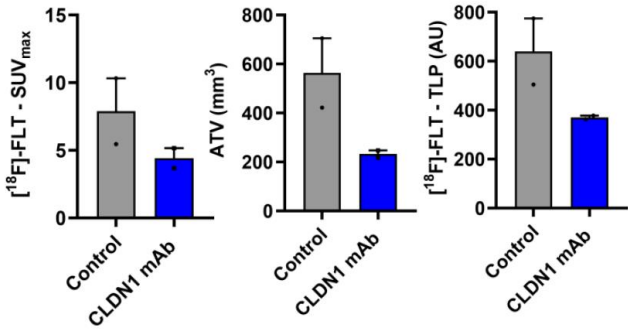
i



f



g



j

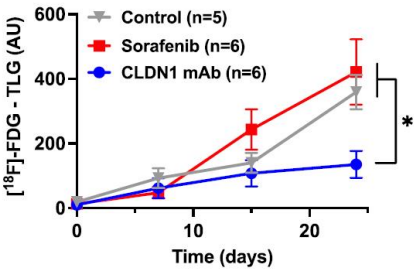


Figure 4. CLDN1 mAb suppresses tumor growth in Huh7 CDX mouse model.

a. Illustration of Huh7 CDX mice model study protocol (2 independent studies). **b.** Tumor growth in CLDN1 mAb or vehicle control treated Huh7 CDX mice (* $p < 0.05$, ** $p < 0.01$, Mann-Whitney U test, respectively). **c.** Immunohistochemical assessment of KI67, EPCAM and FN1 expression in tumor tissue derived from Control or CLDN1 mAb treated Huh7 CDX mice. Computational quantification of the respective marker expressions is shown below (* $p < 0.05$, ** $p < 0.01$, Mann-Whitney U test, respectively) **d.** Tumor growth in CLDN1 mAb, Control or Sorafenib treated Huh7 CDX mice (* $p < 0.05$, ** $p < 0.01$, Mann-Whitney U test, respectively). **e.** Illustration of [^{18}F]-FLT PET Scan study protocol in CLDN1 mAb or Control treated mice. **f.** Representative images showing [^{18}F]-FLT uptake in CLDN1 mAb or Control treated CDX mice. **g.** Quantitative assessment of SUX_{max} (left panel), ATV (middle panel) and TLP (right panel) in [^{18}F]-FLT PET Scans of CLDN1 mAb or Control treated Huh7 CDX mice. **h.** Illustration of [^{18}F]-FDG PET Scan study protocol in CLDN1 mAb, Sorafenib or Control treated mice. **i.** Representative images showing [^{18}F]-FDG uptake in CLDN1 mAb, Sorafenib or Control treated CDX mice. **j.** Quantitative assessment of TLG in [^{18}F]-FDG PET Scans of CLDN1 mAb, Sorafenib or Control treated Huh7 CDX mice (* $p < 0.05$, Mann Whitney U test). Abbreviations: [^{18}F]-FLT= 3'-deoxy-3'-[^{18}F]-fluorothymidine; [^{18}F]-FDG= 2-deoxy-2-[^{18}F]- fluoro- D-glucose; ATV= avid tumor volume; CDX=cell line-derived xenografts; CLDN1=Claudin 1; EPCAM= epithelial cell adhesion molecule; FN1= Fibronectin; HCC=Hepatocellular carcinoma; i.p.=intra peritoneal; SC=subcutaneous; SUV= standardized uptake value; TLG= total lesion glycolysis; TLP= total lesion proliferation.

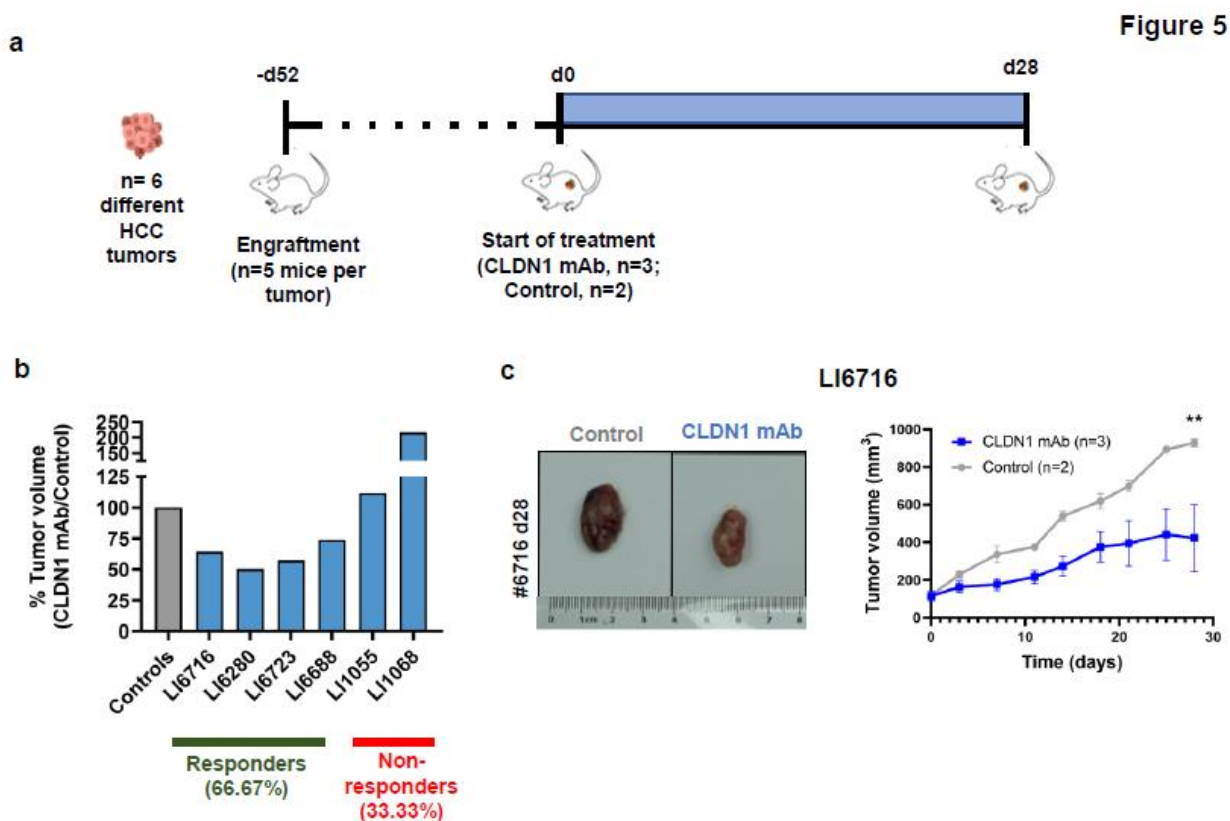
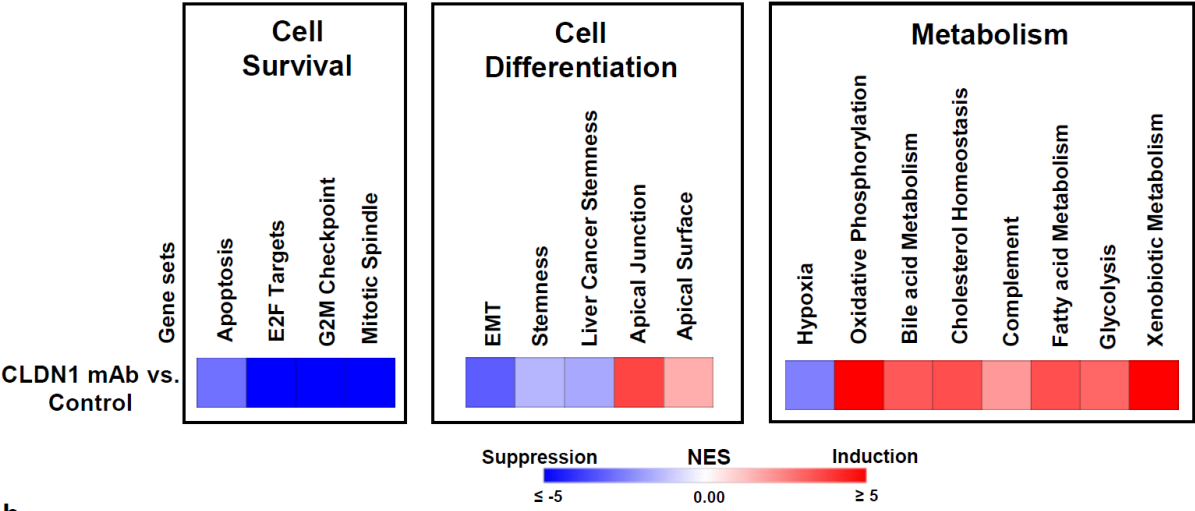


Figure 5. CLDN1 mAb suppresses tumor growth in PDX mouse models.

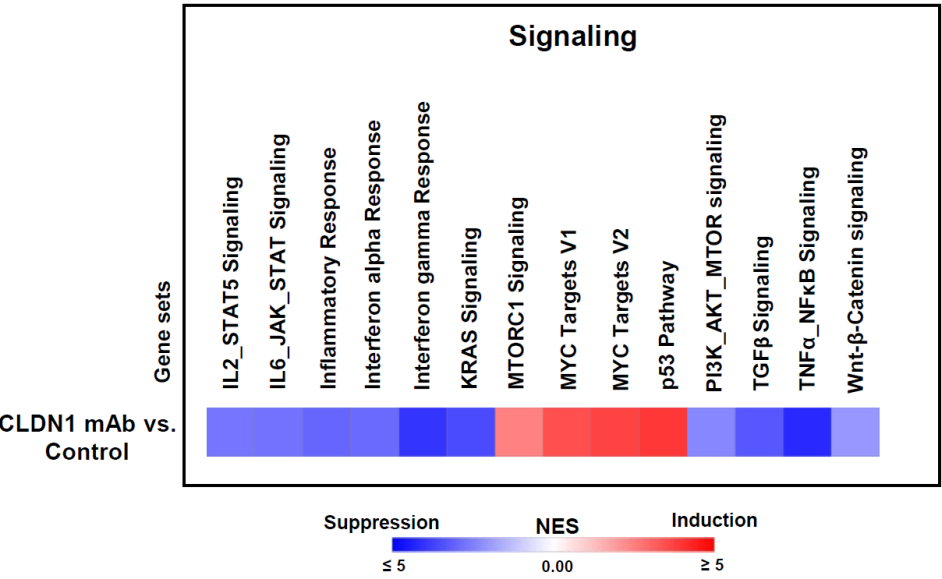
a. Illustration of PDX mice model study protocol (6 independent studies with n=6 different HCC tumors) **b.** Tumor growth in CLDN1 mAb treated PDX mice models is shown as % mean tumor volume compared to corresponding vehicle control treated mice. **c.** Representative macroscopic images of harvested tumors (day 28) derived from CLDN1 mAb or vehicle control treated mice of LI6716 PDX mice model. **d.** Tumor growth in CLDN1 mAb or vehicle control treated PDX mice (#LI6716, $p=0.003$, paired t-test). * $p<0.05$, ** $p<0.01$, *** $p<0.001$, **** $p<0.0001$. Abbreviations: CDX=cell line-derived xenografts; CLDN1=Claudin 1; HCC=Hepatocellular carcinoma; i.p.=intra peritoneal; PDX=patient-derived xenografts; SC=subcutaneous.

Figure 6

a



b



c

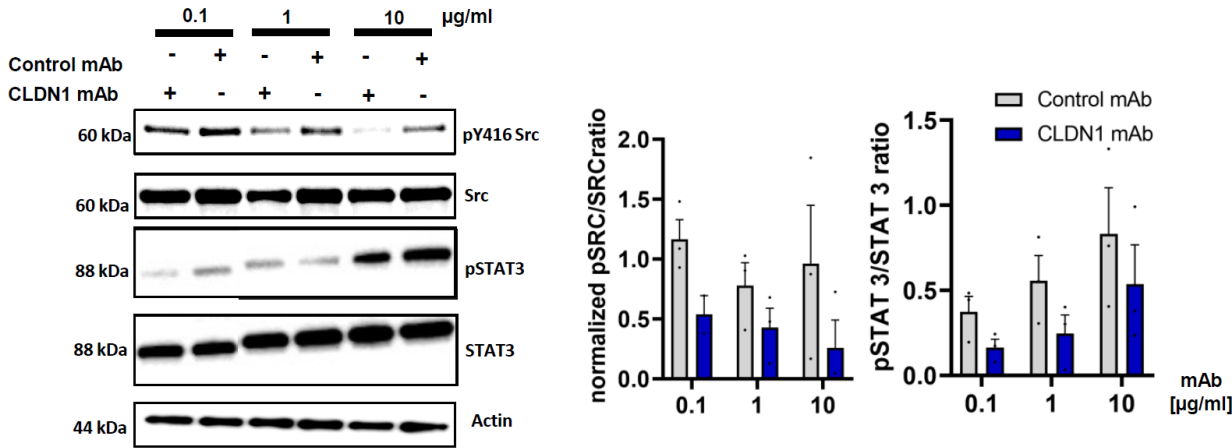


Figure 6. CLDN1 mAb suppresses tumor growth and stemness by interfering with Src mediated oncogenic signaling

a-b. Unbiased GSEA(25) analysis of the gene sets RAMALHO_STEMNESS_UP(29) (“stemness”) and VILLANUEVA_LIVER_CANCER_KRT19_UP(28) and HALLMARK gene sets related to cell survival, cell differentiation, metabolism (**a**) and signaling (**b**) in tumor tissue of CLDN1 mAb compared to vehicle control treated PDX mice (LI6716). Heatmaps show NES of significantly (FDR<0.25, Kolmogorov Smirnov test, respectively) altered gene sets. **c.** Left panel: Representative immunoblots of pY416 Src, Src, pY705 STAT3, STAT3 and Actin in Huh7 spheroids treated with different concentrations of CLDN1 mAb or control mAb. Right panel: Normalized Ratio of pSrc/Src and pSTAT3/STAT3 protein expression derived from n=3 independent experiments (p=0.01 and p=0.001, paired t-test, respectively). Bars show mean \pm SEM. *p<0.05, **p<0.01, ***p<0.001, ****p<0.0001. Abbreviations: CLDN1=Claudin-1; FDR=False discovery rate; NES=Normalized enrichment score.

Figure 7

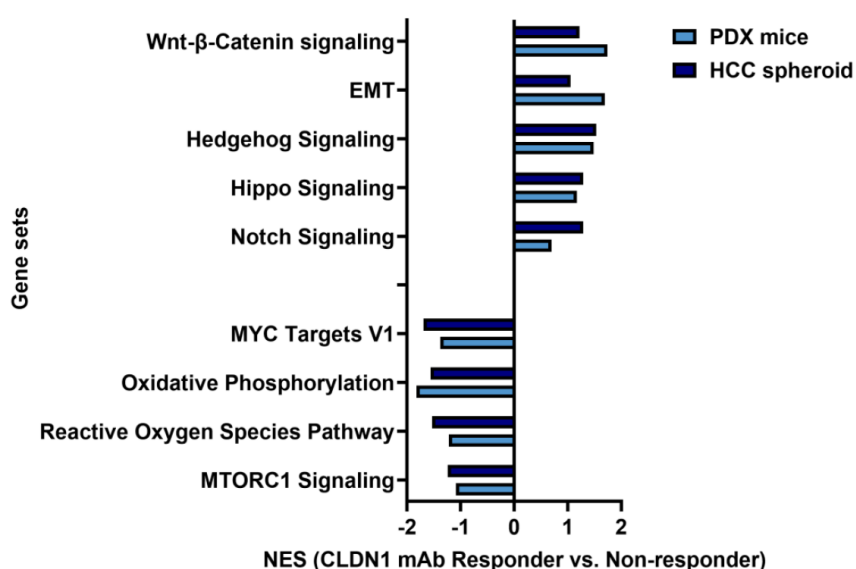


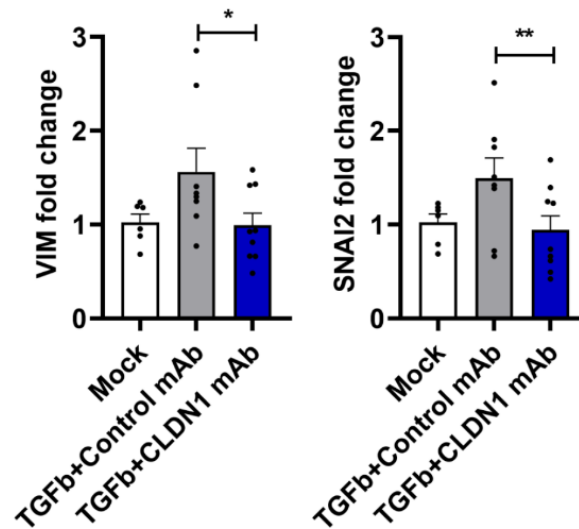
Figure 7. Response prediction to CLDN1 mAb in HCC spheroid and PDX mice models.

RNA-seq data from basal tissues of HCC tumors responding to CLDN1 mAb treatment in HCC spheroid models (#S06, #S07, #S15) or PDX mice models (LI6280, LI6716, LI6723, LI6688) were compared to non-responders (#S13, #S16, #S17, #S18, LI1055 and LI1068) by GSEA(25). Bars show NES of significantly (FDR<0.25 in either spheroid or PDX model tumors, Kolmogorov Smirnov test, respectively) enriched gene sets. Abbreviations: CLDN1=Claudin-1; HCC=Hepatocellular carcinoma; NES=Normalized enrichment Score; PDX=patient-derived xenograft.

A humanized Claudin-1 specific monoclonal antibody for treatment of hepatocellular carcinoma

Natascha Roehlen^{1,2}, Marion Muller^{1,2,3}, Sara Cherradi^{1,2}, Frank Jühling^{1,2}, Francois H.T. Duong^{1,2}, Nuno Almeida^{1,2}, Fabio Del Zompo^{1,2}, Mirian Fernández-Vaquero⁴, Tobias Riedl⁴, Hussein El Saghire^{2,5}, Antonio Saviano⁶, Sarah Durand^{1,2}, Clara Ponsolles^{1,2}, Marine Oudot^{1,2}, Emanuele Felli⁶, Patrick Pessaux⁶, Irwin Davidson⁷, Emilie Crouchet^{1,2}, Simonetta Bandiera^{1,2}, Christine Thumann^{1,2}, Brandon Nicolay⁸, Nabeel Bardeesy⁸, Patrice Laquerriere³, Mathias Heikenwälder⁴, Roberto Iacone⁵, Markus Meyer⁵, Greg Elson⁵, Tamas Schweighoffer⁵, Catherine Schuster^{1,2}, Laurent Mailly^{1,2}, Joachim Lupberger^{1,2}, Thomas F. Baumert^{1,2,5,§}

SUPPLEMENTARY INFORMATION



Suppl. Figure 1, relating to Fig. 3. CLDN1 mAb suppresses EMT in Huh7 cell co-cultured with CAFs in patient-derived extracellular matrix. Huh7 cells and CAFs were embedded in patient derived fibrotic and non-fibrotic ECM hydrogel and treated with TGF β (10ng/ml) and CLDN1 mAb or Control mAb (50 μ g/ml, representatively). Relative fold change of Vimentin (VIM) and SNAI2 gene expression is shown ($p=0.02$, $p=0.009$, paired t-test, respectively). Bars show mean \pm SEM. Abbreviations: CLDN1= Claudin 1, Snail Family Transcriptional Repressor 2, VIM= Vimentin.

Suppl. Table 1, relating to Fig. 3c-e. Clinical characteristics of HCC patients, recruited for HCC spheroid perturbation studies.

#	Gender	Age	Etiology of chronic liver disease	Fibrosis stage*	Histological characteristics#
ST1	M	77	hemochromatosis	F4	G1, no invasion, pT1b
S06	M	81	HCV1b, SVR	A2F2	-
S07	M	71	ASH	-	-
S15	M	65	HCV1a, SVR	A0F2	G2, vascular invasion pT2
S17	M	58	HCV1a, SVR	A0F4	G2, no vascular invasion pT2
S18	F	64	HCV	F2A2	G2-3, vascular invasion
S24	-	-	-	-	-
381	M	76	NASH	F1-2,A1-A2	G2, vascular invasion, pT2
S19	M	72	NASH	F3-4	G2, vascular invasion
S22	M	60	NASH	F3	G1-2, vascular invasion, pT2
S349	M	65	HCV	F1	G1, vascular invasion, pT1b
S394	M	61	No chronic liver disease	F0-1/A0	G4, poorly differentiated, vascular invasion
S13	M	65	NASH	-	-
S16	M	65	ASH	F4	G2-G3, vascular invasion, pT2
R2	M	80	ASH	F3	-
R21	M	72	ASH	F4	-
R11	M	65	HBV	F4	-

*fibrosis stage according to METAVIR score(67). #tumor grade according to Edmondson classification(68), tumor stage according to TNM classification(69).

Suppl. Table 2, relating to Fig. 5, Clinical and histopathological characteristics of HCC patients, recruited for perturbation studies in PDX mice models.

#	Gender	Age	Viral status	Histological characteristics*
LI1055	F	29	HBV-, HCV-, HIV-	Mixed HCC/CCA, lymphoid cells invade portal area with fibrous tissues hyperplasia, AFP(-), HEPA(-),CK19 (+)
LI1068	M	69	HBV+, HCV-	G2, tumor cells scattered within liver, tumor embolus in vessel, nodular cirrhosis, AFP(++), HEPA(+)
LI6280	M	59	HBV+, HCV-, HIV-	G3, HCC of spindle cell type, sarcomatoid type and mixed type cirrhosis, AFP (-)
LI6688	M	42	HBV+, HCV-, HIV-	G3
LI6716	F	45	-	HepPar-1 (3+), AFP (+)
LI6723	F	58	HBV-, HCV-, HIV-	G4, CK18 (3+), hep-1 (-), arg-1 (-)

Data provided by CrownBio * tumor grade according to Edmondson classification(68)

Suppl. Table 3, relating to Fig 5, Body weight change of CLDN1 or vehicle control treated PDX mice. Body weight change is shown in % at end of study compared to day 0.

#	Vehicle	CLDN1 mAb
LI1055	-2.62%	-5.72%
LI1068	1.57%	0.96%
LI6280	16.20%	11.43%
LI6688	-	-
LI6716	4.67%	6.76%
LI6723	-10.51%	-9.50%

Supplementary References:

1. Goodman, Z.D. Grading and staging systems for inflammation and fibrosis in chronic liver diseases. *J Hepatol* **47**, 598-607 (2007).
2. Martins-Filho, S.N., Paiva, C., Azevedo, R.S. & Alves, V.A.F. Histological Grading of Hepatocellular Carcinoma-A Systematic Review of Literature. *Front Med (Lausanne)* **4**, 193 (2017).
3. Marrero, J.A. et al. Diagnosis, Staging, and Management of Hepatocellular Carcinoma: 2018 Practice Guidance by the American Association for the Study of Liver Diseases. *Hepatology* **68**, 723-750 (2018).

4 Discussion and perspectives

In the framework of this thesis, non-junctional CLDN1 was identified as a target for treatment of advanced liver fibrosis and HCC. This conclusion is supported by the following findings: I) *CLDN1* is overexpressed in liver tissue of patients with liver fibrosis and HCC II) Targeting non-junctional CLDN1 by specific mAbs suppresses liver fibrosis progression, tumor development and tumor growth in state-of-the-art *ex-vivo* and *in-vivo* models and III) CLDN1 mAbs mediate broad suppression of pro-fibrogenic and carcinogenic signaling pathways and interfere with liver cell plasticity (**Figure 19**).

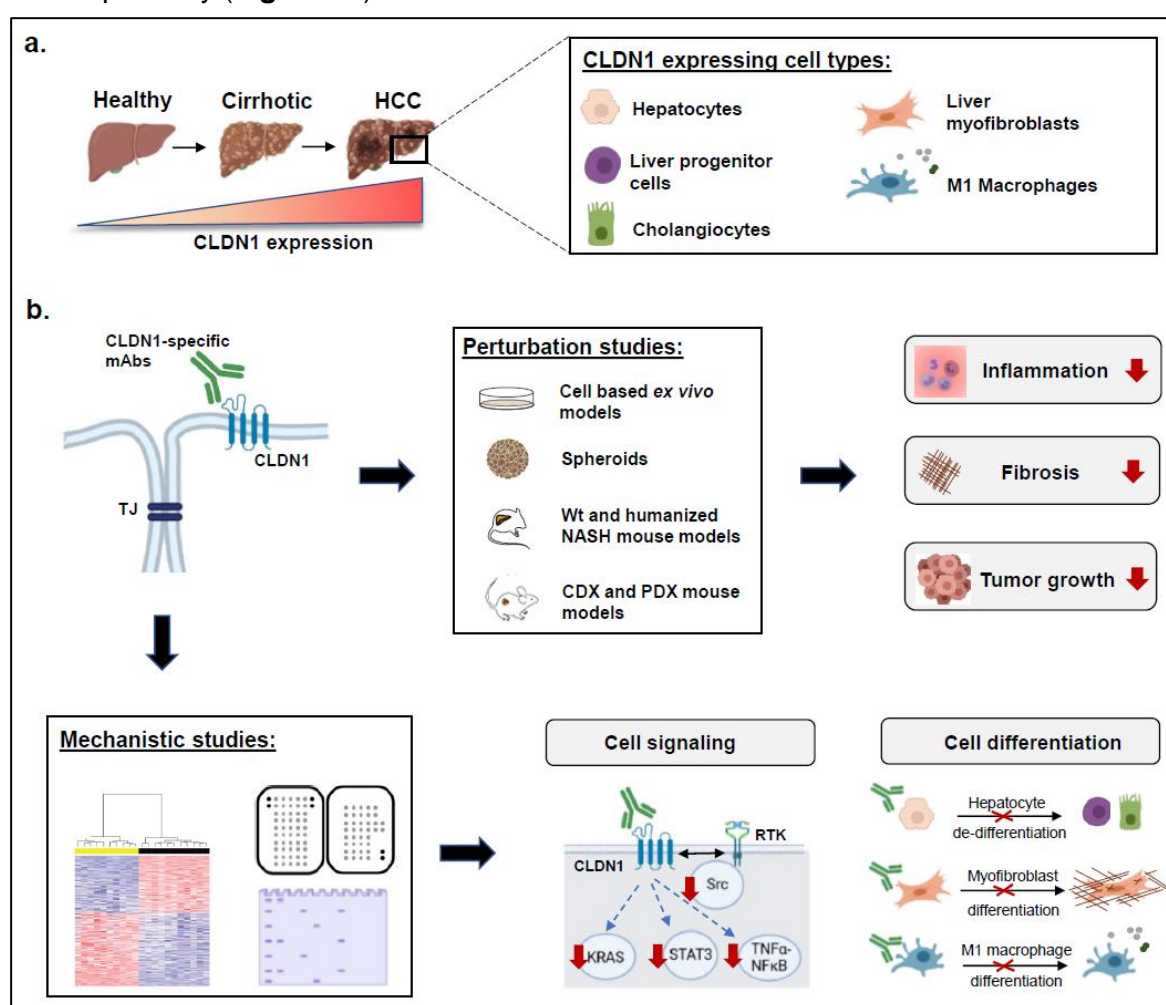


Figure 19. Schematic illustration of the main findings of the work presented in this thesis. a. *CLDN1* expression increases during liver disease progression towards liver fibrosis and HCC. Liver progenitor cells, cholangiocytes, hepatocytes, human liver myofibroblasts and M1 Macrophages are the main cell types expressing CLDN1 in the liver. **b.** Functional and mechanistic studies indicate CLDN1-specific mAbs to inhibit inflammation, liver fibrosis and tumor development by interfering with cell signaling and liver cell plasticity. Figure created with Biorender.com. **Abbreviations:** CLDN1= Claudin-1; HCC= Hepatocellular carcinoma; mAbs= Monoclonal antibodies; RTK= Receptor tyrosine kinases; TJ= Tight junction; wt= wild type.

The key findings of this study will be discussed in the context of the current literature in the following sections. To reduce redundancy a key focus of this separated discussion section are potential limitations as well as future perspectives of this study.

4.1 Considerations on the expression of CLDN1 on multiple cell types in liver fibrosis and HCC

In mammals 27 different isoforms of CLDNs have been described (for a review see: Roehlen *et al.*, 2020). CLDN1 hereby represents the most highly expressed CLDN family member in human liver (Uhlén M. *et al.*, 2015). Besides its physiological function for establishment of the blood biliary barrier, CLDN1 has been previously characterized to be involved in liver disease, such as HCV infection (for a review see: Zeisel *et al.*, 2019). Indicating a role of CLDN1 in liver disease beyond viral hepatitis, we could characterize hepatic *CLDN1* expression to be upregulated along the progression of primary injury to advanced liver fibrosis and HCC in all major etiologies, such as chronic HBV and HCV infection or NASH. This is consistent with previous reports of CLDN1 overexpression in liver tissue of small cohorts of patients with chronic HCV infection, liver cirrhosis and HCC (Zadori *et al.*, 2011; Holczbauer *et al.*, 2014). In line with the role of CLDN1 in embryonic development (Eckert and Fleming, 2008; Collins *et al.*, 2013) and cell differentiation (Suh *et al.*, 2013), we found *CLDN1* overexpression on diseased hepatocytes and cancer cells to be associated with an immature, progenitor-or stem cell like phenotype. Given pre-dominant expression of CLDN1 on liver progenitor cells in healthy liver, two hypotheses could explain this observation: I. CLDN1 overexpression is a *consequence* of liver progenitor cell differentiation and/or proliferation during chronic liver injury or II. otherwise induced CLDN1 overexpression in liver fibrosis and HCC (e.g. by TNF-NFκB pathway activation) *actively* impact on hepatocyte differentiation. While both models might apply, our data showing reversal of liver progenitor cell differentiation in CLDN1 mAb treated mice and hepatoma cells suggest CLDN1 to be functionally involved in liver cell plasticity (see

also 4.4). Interestingly, liver progenitor and stem cells have been shown to be functionally involved in both liver fibrogenesis and carcinogenesis. Thus, improper activation of hepatic progenitor cells is closely related to fibrotic responses leading to activation of liver myofibroblasts and ECM accumulation (Bria *et al.*, 2017). Moreover, de-differentiated hepatocytes and liver progenitor cells are putative cellular origins of cancer cells in HCC's of the progenitor-like type (Sia *et al.*, 2017). This HCC subclass is typically associated with a poor clinical prognosis (Llovet *et al.*, 2021). In line, patients with high hepatic *CLDN1* expression showed significantly shorter recurrence-free survival and frequent metastatic course compared to patients with low expression.

The association of *CLDN1* with liver fibrosis and HCC as well as patients' outcome suggests it as a potential attractive target for treatment of chronic liver disease progression. However, considering that junctional *CLDN1* is an important contributor to tight junction barrier function (Roehlen *et al.*, 2020), only non-junctional *CLDN1* appears to be a potential target for direct therapeutic approaches. Previous studies suggest that *CLDN1* delocalizes from tight junctions under pathological conditions such as inflammation and cancer (Suzuki, 2013; Bhat *et al.*, 2020). Accordingly, I could only detect non-junctional *CLDN1* expression in liver disease-associated phenotypes of non-parenchymal cells, such as liver myofibroblasts and M1 Kupffer cells but not in quiescent HSC's or non-activated monocytes and macrophages derived from healthy liver. While these data strongly suggest an association of non-junctional *CLDN1* with fibrosis-associated phenotypes of non-parenchymal cells, it remains unclear whether only non-junctional *CLDN1* is specifically overexpressed on diseased hepatocytes and HCC cancer cells. Thus, the specific distribution of *CLDN1* along the membrane of epithelial liver cells in healthy and diseased tissue still has to be analyzed in more detail. However, the determination of non-junctional *CLDN1* expression in human tissue sections is technically challenging due to the need of electron microscopy (Mailly *et al.*, 2015) or multi-color immunofluorescent staining with validated tight junction markers. High background signal from tight junctions yet limited our investigation of non-junctional *CLDN1* especially on non-epithelial cells. We are currently establishing optimized fixation and antigen retrieval protocols for the use of non-junctional

CLDN1-targeting mAbs for tissue staining. Characterization of HCC liver tissue and isolated cancer-associated cell types are further underway to clearly define the expression and distribution of CLDN1 on cancer cells and its stromal and immunogenic microenvironment. Taken together, the overexpression as well as association with clinical characteristics of poor outcome suggests CLDN1 as a target in chronic liver disease and HCC. The question whether perturbation of CLDN1 expression is specific for its non-junctional localization needs to be addressed by future investigations.

4.2 Considerations on anti-fibrotic and chemopreventive effects of non-junctional CLDN1 targeting mAbs

We studied the effect of non-junctional CLDN1 targeting mAbs in multiple patient-derived *ex vivo* and *in vivo* models of liver fibrosis. The consistent anti-fibrotic and chemopreventive effects of CLDN1 mAb treatment among different systems, such as bioprinted tissue and two different mouse models corroborate non-junctional CLDN1 to be a driver of fibrotic liver disease progression. A strength of our study is the focus on authentic patient-derived model systems, recapitulating all important cell types and allowing multi-directional cell interactions. Insufficient mimicry of the complex pathophysiology of liver fibrosis by regular 2D culture systems and singular mouse models have been previously attributed to account for high failure rates of antifibrotic agents in clinical studies (for a review see: Schuppan *et al.*, 2018).

Importantly, our data indicate CLDN1 mAb to markedly reverse liver fibrosis even in advanced disease stages. Thus, CLDN1 mAb treatment showed strong anti-fibrotic effects and restored signatures of mature hepatocytes in humanized mice that had already developed advanced fibrosis when treatment was started. Moreover, CLDN1 mAb strongly suppressed the poor-prognosis PLS in precision-cut liver slices derived from NASH patients with advanced fibrosis stage. This indicates a key differentiator to current compounds in clinical development that show mostly effects in early disease stages by targeting metabolism (Younossi *et al.*, 2019).

Future assessments in pre-clinical models and clinical trials should directly compare the antifibrotic efficacy of CLDN1 mAb treatment with other candidate compounds for treatment of liver fibrosis, such as OCA (Younossi *et al.*, 2019).

A potential limitation of our functional studies might be the absence of *in vivo* CLDN1 knockout and overexpression studies. Although CLDN1 mAb selectively targets non-junctional CLDN1, CLDN1 loss- and gain-of-function studies could corroborate CLDN1 as a driver of liver fibrosis. In contrast to humans (Izurieta Pacheco *et al.*, 2020), congenital knockout of CLDN1 is lethal in mice (Furuse *et al.*, 2002). Therefore, conditional knockouts using GalNAc mediated CLDN1 gene silencing (Foster *et al.*, 2018) in dietary mouse models of liver fibrosis are currently in preparation.

Our assessment of CLDN1 expression in clinical cohorts suggests a functional role of CLDN1 in liver fibrosis independent of the etiology of chronic liver disease. In addition to our current NASH mouse models, studies including carbon tetra chloride (CCL₄) or common bile duct ligation mouse models could therefore give additional insights into the role of non-junctional CLDN1 in toxin- and cholestatic injury-related liver fibrosis (Yanguas *et al.*, 2016).

4.3 Considerations on tumor-therapeutic effects of non-junctional CLDN1 targeting mAbs

The anti-tumorigenic efficacy of non-junctional CLDN1 targeting mAbs was studied in numerous cell line based as well as patient-derived models of HCC. Our hypothesis of CLDN1 as a driver of tumor progression is corroborated by the strong tumor suppressive effects of both CLDN1 KO and CLDN1 mAb treatment in different model systems. Especially the strong efficacy and high response rate in patient-derived model systems such as HCC spheroids and in the PDX mouse models support further pre-clinical and clinical evaluation of non-junctional CLDN1-targeting therapies for treatment of HCC. Thus, we are currently performing genetically

engineered mouse models of HCC with conditional CLDN1 gain- or loss-of function in the liver (Brown *et al.*, 2018).

A key differentiator of CLDN1 mAbs compared to current HCC therapeutics might be the combined antifibrotic and anti-tumorigenic effects. This is of high clinical importance since liver cirrhosis stage and liver function are key determinants for therapeutic options and outcome in patients with HCC (for a review see: Llovet *et al.*, 2021). While we studied the anti-fibrotic effect of CLDN1 mAb treatment in detail in mouse models of liver fibrosis, our cancer models yet lack independent validation of fibrosis suppression in the tumor microenvironment. Experimental set-ups with CLDN1 mAb treatment of NASH mice at time of established tumor growth could allow simultaneous evaluation of therapeutic effects on the tumor as well as the fibrotic adjacent tissue.

Our results further indicate potential opportunities for CLDN1 mAb as part of combination therapies in patients. Thus, we could show that HCC's with predicted resistance to sorafenib show significantly increased *CLDN1* expression. Moreover, CLDN1 mAb suppressed signaling pathways such as Wnt- β -catenin and KRAS signaling, that have been shown to be implicated in sorafenib resistance (Zhu *et al.*, 2017; Ruiz de Galarreta *et al.*, 2019). Given the emerging role of combination therapies for HCC, combinatory treatment with CLDN1 mAb and Sorafenib and PD1 or PD-L1 inhibitors such as Nivolumab (Yau *et al.*, 2020) are currently assessed in patient-derived HCC spheroids. Future perspectives further include the evaluation of combination therapies in immunocompetent mouse models (Li *et al.*, 2019).

4.4 Considerations on the molecular mechanism of CLDN1 mAb mediated antifibrotic, chemopreventive and tumortherapeutic effects

Our computational analyses of transcriptomic signatures in mouse models of liver fibrosis and HCC suggest CLDN1 mAb to interfere with multiple pro-inflammatory, pro-fibrogenic and pro-carcinogenic signaling pathways as well as with cell plasticity. This is in line with previous

associations of CLDN1 with EMT (Yoon *et al.*, 2010; Suh *et al.*, 2013) and the model of non-junctional CLDNs to function as signaling hubs that assemble and translate internal and external signals (Hagen, 2017).

One of the key pathways found to be suppressed by CLDN1 mAb-treatment in both our studies was Src signaling. Consistently, CLDN1 knockdown has been reported to suppress Src activation in hepatoma and colon cancer cells (Singh *et al.*, 2012; Suh *et al.*, 2013). Immunoprecipitation studies indicate CLDN1 to directly interact with Src at its C-terminal region (Singh *et al.*, 2012). As a key signal transducer of stroma-cell and cell-cell interactions, Src activation is closely related to PI3K-AKT-, TGF β -, KRAS- or JAK/STAT3 signaling (Hsu *et al.*, 2020; Du *et al.*, 2020) that have been shown to be affected by CLDN1 mAb-treatment but not yet been reported to directly interact with membranous CLDN1. The function of Src kinases as signaling transducers of the stromal microenvironment is especially important under conditions of enriched ECM, as observed in liver fibrosis and HCC. Thus, Src represents a candidate effector of CLDN1 mAb-mediated pleiotropic effects on signaling in fibrotic tissue (Parsons and Parsons, 2004). To further corroborate our hypothesis of Src as a mediator of CLDN1 mAb effects on signaling, further mechanistic studies especially on protein level are currently under way. These mechanistic studies include the assessment of key downstream pathways such as KRAS and TGF β signaling in CLDN1 mAb treated and Src silenced or overexpressing cells.

Given the interaction of CLDN1 with multiple other membrane proteins such as CD81, EGFR and integrins (for a review see: Zeisel *et al.*, 2019), binding of the CLDN1 mAb to EL1 of non-junctional CLDN1 might also perturbate other signaling relevant protein-protein interactions. In order to identify non-junctional CLDN1 interactants in an unbiased approach, we are currently performing CLDN1 co-immunoprecipitation coupled with mass spectrometry in CLDN1 mAb treated hepatoma cells. One example for a most likely Src-independently affected pathway is TNF α -NF κ B signaling since it has not yet been shown to directly interact with Src and appears to crosstalk with CLDN1 in a bi-directional way.

Another major molecular effect of CLDN1 mAb treatment is its impact on cell differentiation. CLDN1 mAb treated NASH mice showed strongly suppressed transcriptomic signatures of liver

progenitor cells, while CLDN1 mAb treatment strongly suppressed EMT and stemness in cancer models. These therapeutic effects of CLDN1 mAb are in line with the functional role of CLDNs in cell differentiation during embryonic development (Eckert and Fleming, 2008; Collins *et al.*, 2013) or in EMT (Suh *et al.*, 2013; Bhat *et al.*, 2016). Moreover, the expression pattern of CLDN1 in liver progenitor cells as well as its association with stemness signatures in HCC tissue supports its functional relevance for cell differentiation. Still, it remains elusive how CLDN1 perturbation induces these changes in cell differentiation and whether these effects might be related to CLDN1 mAbs's effect on signaling. Potential candidate pathways for CLDN1 mAb-mediated effects on cell differentiation are TNF α -NF κ B signaling as well as the TGF β pathway. TNF α has been reported to play a key role in liver progenitor cell differentiation and activation (Jing *et al.*, 2018), while TGF β represents a well characterized promoter of EMT and stemness (Xu *et al.*, 2009). To further elucidate the specific molecular effects of CLDN1 mAb on cell differentiation, additional cell culture experiments and mouse models have been initiated. The hepatic progenitor cell line HepaRG will be used to study the role of CLDN1 for hepatic progenitor cell proliferation and activation, as well as its differentiation into mature hepatocyte and cholangiocyte lineages (Dianat *et al.*, 2014; Lucifora *et al.*, 2020). Patient-derived model systems such as fibrotic liver- or HCC derived organoids (Broutier *et al.*, 2017; Prior *et al.*, 2019) could further allow evaluation of disease-specific functions of CLDN1 for liver progenitor cell functionality. Finally, additional *in vivo* experiments, employing mouse models for liver progenitor cell driven fibrosis and tumor development, such as 3,5-diethoxycarbonyl-1,4-dihydrocollidine (DDC)-fed mice (Forbes and Newsome, 2016) and CDX mice orthotopically engrafted with cancer stem cells (Yamashita *et al.*, 2009) are currently under way.

CLDN1 mAb treatment further affected the phenotype of liver myofibroblasts: genes specific for scar-associated myofibroblasts were strongly suppressed in both CLDN1 mAb treated NASH mice and primary HLMFs cell culture. CLDN1 mAb treated Kupffer cells on the other hand showed downregulation of genes related to the pro-inflammatory M1 phenotype. Signaling-wise we found the changes in myofibroblast differentiation to be correlated with

suppression of TNF α -NF κ B signaling. Interestingly, Ramachandran *et al.*, identified receptors of the TNF superfamily to be enriched in scar-associated fibroblasts within the fibrotic niche (Ramachandran *et al.*, 2019). This corroborates a role of TNF signaling in myofibroblast differentiation. Genetically engineered CLDN1 overexpression in HLMFs have been initiated for further conclusions on the role of CLDN1 in myofibroblast differentiation and its relationship to TNF α -NF κ B signaling.

Similar to liver fibrogenesis, perturbations of the stromal and immunogenic microenvironment of the liver are characteristic for the pathophysiology of HCC. Considering our observations of CLDN1 mAb treatment-mediated effects on Kupffer cells and myofibroblasts, current investigations focus on the role of CLDN1 in tumor-associated non-parenchymal cell types, such as TAMs and CAFs. Compared to my work on healthy liver tissue-derived non-parenchymal cells, these studies are technically challenging since the availability of HCC tumorous tissue as well as its quality in terms of tissue size and cell viability is limited.

Given the complex bi-directional crosstalk of CLDN1 mAb-targeted liver cells during liver fibrogenesis and carcinogenesis, a key experimental approach would be to evaluate the molecular effects of CLDN1 perturbation in authentic three-dimensional and multicellular model systems using scRNAseq. In fact, I have recently established a protocol allowing unbiased scRNAseq on patient-derived multicellular liver spheroids (data not presented in the thesis). The bioinformatical assessment of CLDN1 mAb-treatment-mediated effects on hepatocytes, macrophages and fibroblasts is currently ongoing. Ligand-receptor interactions analyses of CLDN1 mAb-targeted cells might reveal important insights into the role of CLDN1 in the complex interplay of parenchymal and non-parenchymal cells in liver fibrosis (Ramachandran *et al.*, 2019).

4.5 Considerations on the role of non-junctional CLDN1 in other fibrotic and malignant diseases

CLDN1 is not only expressed in the liver, but also in other organs, such as the skin, the intestine, the kidney and the lung (Uhlén M. *et al.*, 2015). Non-junctional expression of CLDN1 has been described in human epidermal, intestinal, kidney and lung epithelial cells (for a review see: Hagen, 2017). Additionally, we identified human kidney and lung myofibroblasts to express CLDN1.

Corroborating a role of CLDN1 in fibrogenesis among organs, we found CLDN1 not only to be overexpressed in liver fibrosis but also chronic kidney disease and idiopathic pulmonary fibrosis. Interestingly, CLDN1-gain-of-function has been previously reported to promote chronic kidney disease (Hasegawa *et al.*, 2013) and intestinal inflammation (Pope *et al.*, 2014). The robust antifibrotic effects of non-junctional CLDN1-targeting antibodies in the UUO and in the bleomycin mouse model suggest a potential therapeutic applicability of non-junctional CLDN1 targeting therapies for fibrotic diseases among organs. However, given distinct cell types (Adams *et al.*, 2020; Zheng *et al.*, 2020) and molecular mechanisms (Hill *et al.*, 2019; Yuan *et al.*, 2019) being involved in the pathophysiology of fibrosis in different organs, detailed future studies using patient-derived cell based and mouse models are needed for final conclusions regarding the role of CLDN1 mAbs for treatment of kidney and lung fibrosis.

Apart from HCC, CLDN1 has been reported to be overexpressed in other cancer types, such as triple-negative breast cancer, thyroid cancer, as well as gastric and colorectal adenocarcinoma (for a review see: Bhat *et al.*, 2020). Genetic or microRNA (miRNA)-mediated CLDN1 downregulation mediated protective effects in experimental models of multiple cancer entities (for a review see: Bhat *et al.*, 2020). Moreover, CLDN1 targeting antibodies have been shown to suppress tumor growth and metastasis in mouse models of colon cancer (Cherradi *et al.*, 2017). The description of a tumor suppressive function of CLDN1 in lung adenocarcinoma (Chao *et al.*, 2009) and esophageal squamous cell carcinoma (Kuo *et al.*, 2016) might indicate cell differentiation specific functions of CLDN1. This hypothesis becomes

especially evident in the example of breast cancer, where CLDN1 has been shown to increase cell migration and cell survival in estrogen receptor (ER)-negative subtypes, while promoting cancer cell apoptosis in ER-positive tumors (Zhou *et al.*, 2015).

Indicating an isotype-independent function of CLDNs in human tumorigenesis, oncogenic functions have further been reported for CLDN4 (Neesse *et al.*, 2012), 7 (Dahiya *et al.*, 2011) and 18.2 (Singh *et al.*, 2017) in human cancer. A monoclonal antibody targeting CLDN18.2 is currently in phase II clinical trial for treatment of gastric cancer (Sahin *et al.*, 2021).

Collectively, these data indicate an emerging role of CLDNs as therapeutic targets for fibrotic and malignant human diseases.

4.6 Final concluding remarks

Taking together, the research carried out within the framework of this thesis sheds light on non-junctional CLDN1 as a novel target for treatment of liver fibrosis and HCC. Interestingly, our data indicate the opportunity for holistic therapeutic approaches targeting both liver fibrosis progression as well as tumor development and growth. This introduces a new concept for treatment of patients with chronic liver disease. Complementing existing efficient therapies for treatment or prevention of the primary cause of liver injury, such as DAAs and HBV vaccination, clinical application of CLDN1 mAbs might revolutionize future management of patient with advanced liver disease. The description of CLDN1 perturbation in multiple other diseases and organs further unveils numerous future perspectives for the assessment of non-junctional CLDN1-targeting therapies. The potential mechanism of CLDN1 mAbs to mediate antifibrotic and tumor suppressive effects by affecting liver cell plasticity hereby recapitulates recent insights from scRNAseq studies showing liver cell differentiation to be implicated in numerous inflammatory, fibrotic and malignant diseases (Lindeboom *et al.*, 2021). This work therefore highlights the potential of scRNAseq for target discovery that might reshape future drug development.

Rôle fonctionnel de Claudin-1 comme médiateur et cible thérapeutique de la fibrogénèse et de la carcinogénèse hépatique

Contexte

Les maladies chroniques du foie constituent un problème de santé majeur à l'échelle mondiale, comme le démontrent leur association à une mortalité élevée causée par des complications telles que la cirrhose et le carcinome hépatocellulaire (CHC) (Kim *et al.*, 2019). La cirrhose décompensée est la quatrième cause de décès chez l'adulte en Europe et le CHC est la deuxième cause de décès par cancer dans le monde (Kim *et al.*, 2019). Les principales étiologies de la maladie hépatique avancée sont l'hépatite chronique B et C, la stéatohépatite alcoolique (ALD) et la stéatohépatite non alcoolique (NASH) (Kulik and El-Serag, 2019). Malgré la diversité des étiologies, la progression de la fibrose hépatique et son évolution vers le CHC, empruntent des voies communes. En effet, toutes les maladies chroniques du foie sont caractérisées par une inflammation chronique, une fibrose progressive et finalement le développement d'un CHC (Kulik and El-Serag, 2019). Il convient de noter que le CHC apparaît presque toujours dans le contexte d'une fibrose hépatique ou d'une cirrhose, ce qui démontre le rôle critique de la fibrose et du microenvironnement hépatique comme déclencheur de l'hépatocarcinogénèse (Kulik and El-Serag, 2019). Il a été démontré que le stade de la fibrose est l'indicateur pronostic le plus important pour estimer la chance de survie du patient et le risque de développer un CHC (Hagstrom *et al.*, 2017). Bien que l'élimination de la cause de la lésion puisse restaurer la fonction hépatique au stade précoce de la maladie, les patients atteints de fibrose avancée voient le risque de CHC persister malgré un changement de style ou d'hygiène de vie (Kanwal *et al.*, 2017). Il n'existe à ce jour aucune thérapie approuvée permettant de prévenir ou de guérir la fibrose hépatique et les médicaments en développement clinique sont limités en termes d'efficacité et de compatibilité (pour revue voir: Roehlen *et al.*, 2020). De même, les stratégies de traitement actuelles pour les patients atteints d'un CHC

avancé ne présentent qu'une efficacité qui se limite à quelques mois de gain d'espérance de vie (pour revue voir: Llovet *et al.*, 2021). Il existe donc un besoin médical urgent de développer de nouvelles stratégies thérapeutiques, afin de traiter la fibrose hépatique et de prévenir ou de traiter le CHC.

La protéine claudine-1 (CLDN1) est un membre de la famille des protéines des jonctions serrées ou *zona occludens*. Dans le foie, elle participe en association avec la protéine Occludin à l'étanchéité paracellulaire et à la polarité des cellules hépatiques. Une fraction de CLDN1 est toutefois présente sous forme libre, non jonctionnelle, par exemple à la membrane basale des cellules hépatiques. C'est sous cette forme qu'elle agit comme facteur d'entrée cellulaire pour le virus de l'hépatite C (VHC)(Evans *et al.*, 2007 ; Zeisel *et al.*, 2019).

Dans la littérature, CLDN1 est décrite comme étant impliquée dans l'adhésion cellulaire, la différenciation et la signalisation des cellules épithéliales (pour revue voir: Zeisel *et al.*, 2018 ; Roehlen *et al.*, 2020) et a été proposée comme cible thérapeutique potentielle dans divers cancers humains (Bhat *et al.*, 2020). Des données récentes indiquent, que CLDN1 est également exprimée dans les myofibroblastes du foie humain (HLMF) (Aoudjehane *et al.*, 2015). Les HLMF sont les cellules effectrices de la fibrogénèse du foie pour l'ensemble des étiologies des maladies chroniques du foie (pour revue voir: Roehlen *et al.*, 2020). Par la mise au point d'anticorps monoclonaux humanisés (AcM) ciblant la première boucle extracellulaire (EL1) de CLDN1 lorsque CLDN1 est exposée sous sa forme non-jonctionnelle, notre laboratoire a démontré, que ces AcM inhibaient l'entrée du VHC de manière génotype indépendante ainsi que la signalisation induite par le virus dans les hépatocytes (Mailly *et al.*, 2015 ; Colpitts *et al.*, 2018). Le rôle fonctionnel de CLDN1 non-jonctionnelle dans la fibrogénèse et la carcinogenèse du foie indépendamment de l'infection par le VHC restait encore inconnue lorsque j'ai débuté mes travaux de thèse.

Objectifs

L'objectif de ma thèse était :

- I) d'évaluer le rôle fonctionnel de CLDN1 dans la fibrogénèse et la carcinogenèse hépatiques indépendamment de l'étiologie de la maladie hépatique chronique
- II) de caractériser l'expression de CLDN1 dans divers types de cellules résidant dans le foie et impliquées dans la progression des maladies chroniques du foie,
- III) d'évaluer les effets thérapeutiques de nouvelles thérapies ciblant CLDN1 non-jonctionnelle sur la fibrogenèse et la carcinogenèse hépatiques
- IV) d'élucider le mécanisme moléculaire des effets thérapeutiques médiés par les AcM ciblant CLDN1 non-jonctionnelle.

Résultats

CLDN1 est dérégulée dans la fibrose hépatique et dans le CHC, indépendamment de l'étiologie de la maladie hépatique chronique.

Afin d'étudier le rôle de CLDN1 en tant que cible thérapeutique pour la fibrose hépatique et le CHC, j'ai dans un premier temps analysé et comparé son niveau d'expression chez des patients atteints de maladies hépatiques chroniques d'étiologie virale et non virale. L'évaluation des niveaux d'expression de l'ARNm de CLDN1 dans les tissus hépatiques de patients (données de cohortes publiques) a montré une augmentation marquée et significative de l'expression de l'ARNm de CLDN1 chez les patients atteints de NASH, ainsi que d'hépatite B et C chroniques (**Fig. 1a, article de résultats I**). De plus, le niveau d'expression de CLDN1 était significativement associé à la progression de la maladie fibrotique chez les patients infectés par le VHC ainsi que chez les patients atteints de NASH (**Fig. 1b, article de résultats I**). L'analyse de l'expression de l'ARNm de CLDN1 dans les tissus tumoraux de CHC comparés aux tissus adjacents non-tumoraux appariés, montre une surexpression significative de CLDN1 dans les tissus tumoraux suggérant un rôle fonctionnel de CLDN1 dans la carcinogenèse hépatique (**Fig. 1e, article de résultats II**). Enfin, j'ai observé que l'augmentation de l'expression de CLDN1 était corrélée de manière significative aux caractéristiques des cellules souches de la tumeur, à la récurrence tumorale et à l'évolution

métastatique (**Fig. 1f-j, article de résultats II**). Dans leur ensemble, ces données suggèrent un rôle fonctionnel de CLDN1 dans la fibrogénèse et la carcinogénèse du foie induites par différentes étiologies.

CLDN1 est exprimée dans plusieurs types de cellules résidant dans le foie et son expression est régulée par la voie de signalisation TNF α -NF κ B.

Par la suite, j'ai analysé le niveau d'expression de CLDN1 dans les principaux types de cellules résidant dans le foie. L'analyse computationnelle des données de séquençage d'ARN à l'échelle de la cellule unique (*single cell RNA sequencing, scRNASeq*) récemment publiées (Aizarani *et al.*, 2019) a révélé que CLDN1 était le plus fortement exprimée dans les cellules progénitrices épithéliales hépatiques et les hépatocytes dans le foie de patients sans maladie hépatique chronique (**Fig. 1c, article de résultats I**). Dans le foie fibrotique, l'expression de CLDN1 dans les hépatocytes était nettement accrue (**Fig. 1d, article de résultats I**) et corrélée à l'augmentation des marqueurs des progéniteurs hépatiques, notamment EPCAM et TACSTD2 (Aizarani *et al.*, 2019). Les cellules mésenchymateuses du foie et les macrophages exprimaient CLDN1 à un niveau plus faible (**Fig. 1d, article de résultats I**).

Afin de définir le niveau de CLDN1 non-jonctionnelle à la surface des types de cellules hépatiques et d'évaluer le potentiel thérapeutique de l'anticorps monoclonal (AcM) CLDN1 établi au laboratoire, j'ai isolé et séparé les principaux types de cellules hépatiques parenchymateuses et non parenchymateuses de patients sains. L'analyse cytométrique de la liaison de l'AcM CLDN1 à ces cellules a confirmé l'expression non-jonctionnelle de CLDN1 à la surface des hépatocytes, des myofibroblastes de foie humain et d'une sous-population de cellules de Küpffer (**Figure 1g-j, article de résultats I**). L'évaluation de l'effet de plusieurs cytokines associées à la fibrogénèse et à la carcinogénèse a révélé, que l'expression de CLDN1 était nettement et significativement augmentée suite à l'activation de la voie de signalisation TNF α -NF κ B (**Figure 1k-l, article de résultats I**). Globalement, ces données indiquent que les hépatocytes, les HLMF, ainsi qu'une sous population des macrophages hépatiques, sont des médiateurs potentiels de la fonctionnalité de CLDN1 dans le foie. La voie

de signalisation TNF α -NF κ B a ainsi été identifiée comme un médiateur potentiel de l'augmentation de l'expression de CLDN1 dans les maladies chroniques du foie.

Le ciblage de CLDN1 non-jonctionnelle par des AcM spécifiques supprime la fibrose hépatique dans les modèles 3D ex vivo et dans les modèles murins humanisés.

Afin d'étudier CLDN1 comme cible de traitement potentielle de la fibrose hépatique, l'efficacité des AcM ciblant CLDN1 a été évaluée dans deux modèles murins de fibrose hépatique associée à la NASH. Le traitement des souris avec l'AcM CLDN1 freine significativement la progression de la fibrose hépatique et le développement de tumeurs chez des souris de type sauvage et des souris chimériques humanisées soumises à un régime riche en graisses et pauvre en choline induisant le développement d'une maladie chronique avancée du foie (**Fig. 2 et 3, article de résultats I**). L'effet antifibrotique et chimiopréventif de l'AcM CLDN1 a été validé dans plusieurs modèles *ex vivo* de fibrose hépatique à partir de tissus dérivés de patients. Ainsi, le traitement par l'AcM CLDN1 a montré des effets antifibrotiques marqués et significatifs dans les sphéroïdes hépatiques dérivés de patients atteints de NASH et dans le tissu hépatique reconstitué par la méthode Bioprint (Antoni *et al.*, 2015; Kizawa *et al.*, 2017) (**Fig. 4a-h, article de résultats I**). En analysant les éléments de la signature hépatique pronostique permettant d'évaluer la progression de la maladie hépatique vers un bon ou un mauvais pronostic établi par nos collaborateurs (Hoshida *et al.*, 2008 ; Crouchet E., 2021) nous avons observé que l'AcM CLDN1 supprime les signatures génétiques associées à la progression de la maladie hépatique et au risque de CHC (**Fig. 4i-j, article de résultats I**). L'ensemble de ces données indique que des thérapies ciblant CLDN1 non-jonctionnelle peuvent stopper la progression de la fibrose hépatique et le développement des tumeurs.

Le ciblage de CLDN1 inhibe la croissance et l'invasion tumorale dans des modèles cellulaires et murins de CHC.

Afin d'évaluer les effets chimiopréventifs de thérapies ciblant CLDN1, j'ai ensuite analysé d'une part, l'effet de l'inactivation du gène de la CLDN1, et d'autre part l'effet d'un traitement par

l'AcM CLDN1, dans des cellules de la lignée d'hépatocarcinome Huh7. Quelle ce soit l'invalidation du gène CLDN1 (CLDN1 KO) ou le traitement des cellules par l'AcM CLDN1 j'ai observé une diminution des capacités de prolifération et d'invasion des cellules Huh7 (**Fig. 2, article de résultats II**). J'ai également constaté un impact du traitement par l'AcM et CLDN1 KO sur les caractéristiques de la lignée cancéreuse, notamment par la capacité réduite de ces cellules à former des sphéroïdes et la diminution de l'expression des marqueurs de cellules souches dans ces cellules (**Fig. 2e et 2k-l, article de résultats II**). De plus, le ciblage de CLDN1 par l'AcM supprime la transition épithélio-mésenchymateuse (EMT) dans les systèmes de co-culture de cellules Huh7 et de fibroblastes associés au cancer (*Cancer associated fibroblasts, CAFs*) (**Fig. 3b, article de résultats II**). L'effet de l'AcM CLDN1 sur les caractéristiques des cellules cancéreuses, telles que la prolifération et l'EMT, a été ensuite évalué dans des modèles sphéroïdes de CHC dérivés de patients. En fait, le traitement par AcM CLDN1 décroît significativement la viabilité cellulaire dans les sphéroïdes de CHC dérivés de patients, avec une efficacité et un taux de réponse supérieurs à ceux du Sorafénib, le traitement standard du CHC (**Fig. 3c-e, article de résultats II**). Enfin, les effets chimiopréventifs du traitement par l'AcM CLDN1 ont été validés dans des modèles murins de xénogreffes de CHC issus de patients (modèles PDX). Collectivement, ces résultats décrivent des effets anti-tumoraux marqués pour ces thérapies basées sur l'utilisation d'AcM ciblant CLDN1.

Les anticorps monoclonaux CLDN1 exercent des effets anti-fibrotiques et anti-tumorigènes en interférant avec la différenciation et la signalisation cellulaires.

A partir de tissus hépatiques provenant de nos modèles murins atteints de fibrose hépatique et de CHC, j'ai étudié le mécanisme moléculaire impliqué dans le traitement par l'AcM CLDN1. Pour cela j'ai mis en oeuvre des techniques de séquençage d'ARN (RNASeq) à haut débit et d'analyse de variation d'expression de groupes de gènes (*Gene Set Enrichment Analysis, GSEA*). Les souris traitées par l'AcM CLDN1 ont montré une forte inhibition de l'expression des groupes de gènes liés aux voies de signalisation pro-fibrogènes et carcinogènes ; les

effets les plus remarquables étaient observés sur les voies de signalisation TNF α -NF κ B, KRAS et STAT3 (**Fig. 5b, article de résultats II et Fig. 5, article de résultats II**).

Concernant le rôle de médiateur potentiel de ces effets pléiotropiques sur la signalisation cellulaire nous avons constaté que l'AcM CLDN1 interfère avec l'activation de Src (**Fig. 5e, article de résultats I et Fig. 5c, article de résultats II**). De plus, l'évaluation par GSEA du lignage cellulaire et de la différenciation cellulaire a montré un rôle fonctionnel de CLDN1 dans la plasticité des cellules hépatiques. Ainsi, le traitement par l'AcM CLDN1 réprime les groupes de gènes associés à la dédifférenciation des hépatocytes dans des modèles murins de fibrose hépatique et de CHC (**Fig. 6e, article de résultats I et Fig. 5a, article de résultats II**). De plus, le traitement par l'AcM CLDN1 inverse nettement les signatures génétiques spécifiques des myofibroblastes associés à la cicatrisation et l'activation pro-inflammatoire des macrophages, à la fois *in vivo* et *in vitro* (**Fig. 6, article de résultats II**). L'ensemble de ces données indique que l'AcM CLDN1 réduit la fibrogénèse et la carcinogénèse hépatiques en interférant avec la signalisation des cellules hôtes et la plasticité des cellules hépatiques.

Discussion

Grâce à ces travaux de thèse, nous avons obtenu un faisceau d'évidence indiquant que CLDN1 non-jonctionnelle est une nouvelle cible d'intérêt majeur pour les traitements de la fibrose hépatique avancée et du CHC. En effet, les résultats obtenus dans différents systèmes d'étude faisant appel à des modèles dérivés de patients, des modèles murins complexes et des cultures cellulaires, démontrent que les AcM ciblant la CLDN1 non-jonctionnelle ont des effets anti-fibrotiques et anti-tumoraux conséquents. Alors qu'une association de CLDN1 avec des maladies fibrotiques n'a jamais été rapportée, le rôle de CLDN1 en tant que moteur de la tumeur est corroboré par des travaux ultérieurs pour d'autres types de cancer (Bhat *et al.*, 2020). Le mécanisme d'action moléculaire des AcM CLDN1 dans la médiation des effets anti-fibrotiques et anti-tumorigènes est différent des stratégies de traitement actuelles. En effet, l'AcM CLDN1 inhibe de multiples voies de signalisation pro-fibrogènes et pro-carcinogènes et

interfère avec la plasticité des cellules hépatiques. Ces données sont conformes aux données précédentes publiées sur le rôle fonctionnel de CLDN1 dans la signalisation et la différenciation cellulaires (Yoon *et al.*, 2010; Suh *et al.*, 2013). A l'inverse, les composés actuellement en développement clinique pour la fibrose hépatique ciblent principalement le métabolisme hépatique et donc les stades précoces de la NASH (Younossi *et al.*, 2019). Les thérapies actuelles pour le CHC ciblent les tyrosines kinases ou le microenvironnement immunitaire, mais elles sont souvent limitées par la résistance (intrinsèque ou acquise) des cellules tumorales aux médicaments. Les effets conséquents de l'AcM CLDN1 sur le caractère souche des cellules tumorales et l'EMT, étroitement liés à la résistance thérapeutique, (Zhu *et al.*, 2017), sont en faveur de possibilités de thérapies combinées efficaces. Enfin, l'une des principales caractéristiques des AcM CLDN1 est la possibilité d'une approche thérapeutique holistique novatrice, qui cible à la fois la tumeur et son environnement fibrotique non-tumoral. Sur la base des solides données précliniques présentées dans ce travail de thèse, de futures études cliniques sont en projet afin de définir le positionnement clinique de l'AcM CLDN1 chez les patients atteints de fibrose hépatique et de CHC.

6 References

- Adams, T. S., et al.** (2020). "Single-cell RNA-seq reveals ectopic and aberrant lung-resident cell populations in idiopathic pulmonary fibrosis." *Sci Adv* 6(28): eaba1983.
- Aizarani, N., et al.** (2019). "A human liver cell atlas reveals heterogeneity and epithelial progenitors." *Nature* 572(7768): 199-204.
- Akinyemiju, T., et al.** (2017). "The Burden of Primary Liver Cancer and Underlying Etiologies From 1990 to 2015 at the Global, Regional, and National Level: Results From the Global Burden of Disease Study 2015." *JAMA Oncol* 3(12): 1683-1691.
- Antoni, D., et al.** (2015). "Three-dimensional cell culture: a breakthrough in vivo." *Int J Mol Sci* 16(3): 5517-5527.
- Aoudjehane, L., et al.** (2015). "Infection of Human Liver Myofibroblasts by Hepatitis C Virus: A Direct Mechanism of Liver Fibrosis in Hepatitis C." *PLoS One* 10(7): e0134141.
- Armingol, E., et al.** (2021). "Deciphering cell-cell interactions and communication from gene expression." *Nat Rev Genet* 22(2): 71-88.
- Arroyo, V., et al.** (2016). "Acute-on-chronic liver failure in cirrhosis." *Nat Rev Dis Primers* 2: 16041.
- Asselah, T., et al.** (2020). "Future treatments for hepatitis delta virus infection." *Liver Int* 40 Suppl 1: 54-60.
- Attia, S. L., et al.** (2021). "Evolving Role for Pharmacotherapy in NAFLD/NASH." *Clin Transl Sci* 14(1): 11-19.
- Babkair, H., et al.** (2016). "Aberrant expression of the tight junction molecules claudin-1 and zonula occludens-1 mediates cell growth and invasion in oral squamous cell carcinoma." *Hum Pathol* 57: 51-60.
- Baglieri, J., et al.** (2019). "The Role of Fibrosis and Liver-Associated Fibroblasts in the Pathogenesis of Hepatocellular Carcinoma." *Int J Mol Sci* 20(7).
- Bataller, R., et al.** (2005). "Liver fibrosis." *J Clin Invest* 115(2): 209-218.

- Bhat, A. A., et al.** (2016). "Claudin-1 promotes TNF-alpha-induced epithelial-mesenchymal transition and migration in colorectal adenocarcinoma cells." *Exp Cell Res* 349(1): 119-127.
- Bhat, A. A., et al.** (2020). "Claudin-1, A Double-Edged Sword in Cancer." *Int J Mol Sci* 21(2).
- Blanchard, A. A., et al.** (2009). "Claudins 1, 3, and 4 protein expression in ER negative breast cancer correlates with markers of the basal phenotype." *Virchows Arch* 454(6): 647-656.
- Borka, K.** (2009). "[Claudin expression in different pancreatic cancers and its significance in differential diagnostics]." *Magy Onkol* 53(3): 273-278.
- Boyault, S., et al.** (2007). "Transcriptome classification of HCC is related to gene alterations and to new therapeutic targets." *Hepatology* 45(1): 42-52.
- Bria, A., et al.** (2017). "Hepatic progenitor cell activation in liver repair." *Liver Res* 1(2): 81-87.
- Broutier, L., et al.** (2017). "Human primary liver cancer-derived organoid cultures for disease modeling and drug screening." *Nat Med* 23(12): 1424-1435.
- Brown, Z. J., et al.** (2018). "Mouse models of hepatocellular carcinoma: an overview and highlights for immunotherapy research." *Nat Rev Gastroenterol Hepatol* 15(9): 536-554.
- Brunt, E. M.** (2000). "Grading and staging the histopathological lesions of chronic hepatitis: the Knodell histology activity index and beyond." *Hepatology* 31(1): 241-246.
- Bukh, J.** (2016). "The history of hepatitis C virus (HCV): Basic research reveals unique features in phylogeny, evolution and the viral life cycle with new perspectives for epidemic control." *J Hepatol* 65(1 Suppl): S2-S21.
- Campana, L., et al.** (2017). "Regression of Liver Fibrosis." *Semin Liver Dis* 37(1): 1-10.
- Chao, Y. C., et al.** (2009). "Claudin-1 is a metastasis suppressor and correlates with clinical outcome in lung adenocarcinoma." *Am J Respir Crit Care Med* 179(2): 123-133.
- Chen, H. N., et al.** (2020). "EpCAM Signaling Promotes Tumor Progression and Protein Stability of PD-L1 through the EGFR Pathway." *Cancer Res* 80(22): 5035-5050.
- Cherradi, S., et al.** (2017). "Antibody targeting of claudin-1 as a potential colorectal cancer therapy." *J Exp Clin Cancer Res* 36(1): 89.
- Choo, Q. L., et al.** (1989). "Isolation of a cDNA clone derived from a blood-borne non-A, non-B viral hepatitis genome." *Science* 244(4902): 359-362.

Collins, M. M., et al. (2013). "Claudin family members exhibit unique temporal and spatial expression boundaries in the chick embryo." *Tissue Barriers* 1(3): e24517.

Colpitts, C. C., et al. (2018). "Humanisation of a claudin-1-specific monoclonal antibody for clinical prevention and cure of HCV infection without escape." *Gut* 67(4): 736-745.

Cooke, G. S., et al. (2019). "Accelerating the elimination of viral hepatitis: a Lancet Gastroenterology & Hepatology Commission." *Lancet Gastroenterol Hepatol* 4(2): 135-184.

Cossart, Y. E., et al. (1970). "Virus-like particles in serum of patients with Australia-antigen-associated hepatitis." *Lancet* 1(7651): 848.

Craig, A. J., et al. (2020). "Tumour evolution in hepatocellular carcinoma." *Nat Rev Gastroenterol Hepatol* 17(3): 139-152.

Crouchet, E., et al. (Accepted 06/21). "A human liver cell-based system modeling a clinical prognostic liver signature combined with single-cell RNA-Seq for discovery of liver disease therapeutics." *Nat Commun*.

D'Ambrosio, R., et al. (2012). "A morphometric and immunohistochemical study to assess the benefit of a sustained virological response in hepatitis C virus patients with cirrhosis." *Hepatology* 56(2): 532-543.

Dahiya, N., et al. (2011). "Claudin-7 is frequently overexpressed in ovarian cancer and promotes invasion." *PLoS One* 6(7): e22119.

De Benedetto, A., et al. (2011). "Tight junction defects in patients with atopic dermatitis." *J Allergy Clin Immunol* 127(3): 773-786 e771-777.

Deng, L., et al. (2021). "The role of tumor-associated macrophages in primary hepatocellular carcinoma and its related targeting therapy." *Int J Med Sci* 18(10): 2109-2116.

DePasquale, E. A. K., et al. (2019). "DoubletDecon: Deconvoluting Doublets from Single-Cell RNA-Sequencing Data." *Cell Rep* 29(6): 1718-1727 e1718.

Dhawan, P., et al. (2005). "Claudin-1 regulates cellular transformation and metastatic behavior in colon cancer." *J Clin Invest* 115(7): 1765-1776.

Dianat, N., et al. (2014). "Generation of functional cholangiocyte-like cells from human pluripotent stem cells and HepaRG cells." *Hepatology* 60(2): 700-714.

- Diehl, A. M., et al.** (2017). "Cause, Pathogenesis, and Treatment of Nonalcoholic Steatohepatitis." *N Engl J Med* 377(21): 2063-2072.
- Dos Reis, P. P., et al.** (2008). "Claudin 1 overexpression increases invasion and is associated with aggressive histological features in oral squamous cell carcinoma." *Cancer* 113(11): 3169-3180.
- Du, G., et al.** (2020). "Targeting Src family kinase member Fyn by Saracatinib attenuated liver fibrosis in vitro and in vivo." *Cell Death Dis* 11(2): 118.
- Eckert, J. J., et al.** (2008). "Tight junction biogenesis during early development." *Biochim Biophys Acta* 1778(3): 717-728.
- Eftang, L. L., et al.** (2013). "Up-regulation of CLDN1 in gastric cancer is correlated with reduced survival." *BMC Cancer* 13: 586.
- Estes, C., et al.** (2018). "Modeling the epidemic of nonalcoholic fatty liver disease demonstrates an exponential increase in burden of disease." *Hepatology* 67(1): 123-133.
- Evans, M. J., et al.** (2007). "Claudin-1 is a hepatitis C virus co-receptor required for a late step in entry." *Nature* 446(7137): 801-805.
- Fallatah, H.** (2014). "Noninvasive Biomarkers of Liver Fibrosis: An Overview." *Adv Hepatol* 2014.
- Fallowfield, J. A., et al.** (2007). "Scar-associated macrophages are a major source of hepatic matrix metalloproteinase-13 and facilitate the resolution of murine hepatic fibrosis." *J Immunol* 178(8): 5288-5295.
- Fattovich, G., et al.** (2008). "Natural history of chronic hepatitis B: special emphasis on disease progression and prognostic factors." *J Hepatol* 48(2): 335-352.
- Feinstone, S. M., et al.** (1975). "Transfusion-associated hepatitis not due to viral hepatitis type A or B." *N Engl J Med* 292(15): 767-770.
- Finn, R. S., et al.** (2020). "Atezolizumab plus Bevacizumab in Unresectable Hepatocellular Carcinoma." *N Engl J Med* 382(20): 1894-1905.
- Fleming, K. M., et al.** (2010). "The rate of decompensation and clinical progression of disease in people with cirrhosis: a cohort study." *Aliment Pharmacol Ther* 32(11-12): 1343-1350.

- Fofana, I., et al.** (2010). "Monoclonal anti-claudin 1 antibodies prevent hepatitis C virus infection of primary human hepatocytes." *Gastroenterology* 139(3): 953-964, 964 e951-954.
- Forbes, S. J., et al.** (2016). "Liver regeneration - mechanisms and models to clinical application." *Nat Rev Gastroenterol Hepatol* 13(8): 473-485.
- Foster, D. J., et al.** (2018). "Advanced siRNA Designs Further Improve In Vivo Performance of GalNAc-siRNA Conjugates." *Mol Ther* 26(3): 708-717.
- French, A. D., et al.** (2009). "PKC and PKA phosphorylation affect the subcellular localization of claudin-1 in melanoma cells." *Int J Med Sci* 6(2): 93-101.
- Furuse, M., et al.** (2002). "Claudin-based tight junctions are crucial for the mammalian epidermal barrier: a lesson from claudin-1-deficient mice." *J Cell Biol* 156(6): 1099-1111.
- Gawrieh, S., et al.** (2021). "Saroglitazar, a PPAR-alpha/gamma Agonist, for Treatment of NAFLD: A Randomized Controlled Double-Blind Phase 2 Trial." *Hepatology*.
- Giannelli, G., et al.** (2016). "Role of epithelial to mesenchymal transition in hepatocellular carcinoma." *J Hepatol* 65(4): 798-808.
- Goossens, N., et al.** (2015). "Molecular classification of hepatocellular carcinoma: potential therapeutic implications." *Hepat Oncol* 2(4): 371-379.
- Guidotti, L. G., et al.** (2006). "Immunobiology and pathogenesis of viral hepatitis." *Annu Rev Pathol* 1: 23-61.
- Guirguis, E., et al.** (2021). "Emerging therapies for the treatment of nonalcoholic steatohepatitis: A systematic review." *Pharmacotherapy* 41(3): 315-328.
- Hagen, S. J.** (2017). "Non-canonical functions of claudin proteins: Beyond the regulation of cell-cell adhesions." *Tissue Barriers* 5(2): e1327839.
- Haghverdi, L., et al.** (2016). "Diffusion pseudotime robustly reconstructs lineage branching." *Nat Methods* 13(10): 845-848.
- Hagstrom, H., et al.** (2017). "Fibrosis stage but not NASH predicts mortality and time to development of severe liver disease in biopsy-proven NAFLD." *J Hepatol* 67(6): 1265-1273.

Harrison, S. A., et al. (2019). "Resmetirom (MGL-3196) for the treatment of non-alcoholic steatohepatitis: a multicentre, randomised, double-blind, placebo-controlled, phase 2 trial." *Lancet* 394(10213): 2012-2024.

Harrison, S. A., et al. (2021). "A structurally optimized FXR agonist, MET409, reduced liver fat content over 12 weeks in patients with non-alcoholic steatohepatitis." *J Hepatol* 75(1): 25-33.

Harrison, S. A., et al. (2021). "Efficacy and Safety of Aldafermin, an Engineered FGF19 Analog, in a Randomized, Double-Blind, Placebo-Controlled Trial of Patients With Nonalcoholic Steatohepatitis." *Gastroenterology* 160(1): 219-231 e211.

Harrison, S. A., et al. (2021). "Efruxifermin in non-alcoholic steatohepatitis: a randomized, double-blind, placebo-controlled, phase 2a trial." *Nat Med* 27(7): 1262-1271.

Hasegawa, K., et al. (2013). "Renal tubular Sirt1 attenuates diabetic albuminuria by epigenetically suppressing Claudin-1 overexpression in podocytes." *Nat Med* 19(11): 1496-1504.

Hashimshony, T., et al. (2016). "CEL-Seq2: sensitive highly-multiplexed single-cell RNA-Seq." *Genome Biol* 17: 77.

Henderson, N. C., et al. (2020). "Fibrosis: from mechanisms to medicines." *Nature* 587(7835): 555-566.

Hill, C., et al. (2019). "Epithelial-mesenchymal transition contributes to pulmonary fibrosis via aberrant epithelial/fibroblastic cross-talk." *J Lung Health Dis* 3(2): 31-35.

Holczbauer, A., et al. (2014). "Increased expression of claudin-1 and claudin-7 in liver cirrhosis and hepatocellular carcinoma." *Pathol Oncol Res* 20(3): 493-502.

Hoshida, Y., et al. (2009). "Integrative transcriptome analysis reveals common molecular subclasses of human hepatocellular carcinoma." *Cancer Res* 69(18): 7385-7392.

Hoshida, Y., et al. (2008). "Gene expression in fixed tissues and outcome in hepatocellular carcinoma." *N Engl J Med* 359(19): 1995-2004.

Hsu, P. C., et al. (2020). "The Crosstalk between Src and Hippo/YAP Signaling Pathways in Non-Small Cell Lung Cancer (NSCLC)." *Cancers (Basel)* 12(6).

Huang, J., et al. (2015). "Claudin-1 enhances tumor proliferation and metastasis by regulating cell anoikis in gastric cancer." *Oncotarget* 6(3): 1652-1665.

Hughes, S. A., et al. (2011). "Hepatitis delta virus." *Lancet* 378(9785): 73-85.

Imamura, H. M., Y. et al. (2003). "Risk factors contributing to early and late phase intrahepatic recurrence of hepatocellular carcinoma after hepatectomy." *J Hepatol* 38(2): 200-207.

Izurieta Pacheco, A. C., et al. (2020). "NISCH syndrome: An extremely rare cause of neonatal cholestasis." *J Hepatol* 73(5): 1257-1258.

Jing, Y., et al. (2018). "Tumor necrosis factor-alpha promotes hepatocellular carcinogenesis through the activation of hepatic progenitor cells." *Cancer Lett* 434: 22-32.

Kanwal, F., et al. (2017). "Risk of Hepatocellular Cancer in HCV Patients Treated With Direct-Acting Antiviral Agents." *Gastroenterology* 153(4): 996-1005 e1001.

Kegel, V., et al. (2016). "Protocol for Isolation of Primary Human Hepatocytes and Corresponding Major Populations of Non-parenchymal Liver Cells." *J Vis Exp*(109): e53069.

Kelley, R. K., et al. (2020). "Cabozantinib in combination with atezolizumab versus sorafenib in treatment-naive advanced hepatocellular carcinoma: COSMIC-312 Phase III study design." *Future Oncol* 16(21): 1525-1536.

Kim, D., et al. (2018). "Changing Trends in Etiology-Based Annual Mortality From Chronic Liver Disease, From 2007 Through 2016." *Gastroenterology* 155(4): 1154-1163 e1153.

Kim, D., et al. (2019). "Changing Trends in Etiology-Based and Ethnicity-Based Annual Mortality Rates of Cirrhosis and Hepatocellular Carcinoma in the United States." *Hepatology* 69(3): 1064-1074.

Kim, J., et al. (2010). "Epithelial-mesenchymal transition gene signature to predict clinical outcome of hepatocellular carcinoma." *Cancer Sci* 101(6): 1521-1528.

Kim, J. H., et al. (2011). "Decreased lactate dehydrogenase B expression enhances claudin 1-mediated hepatoma cell invasiveness via mitochondrial defects." *Exp Cell Res* 317(8): 1108-1118.

Kinugasa, T., et al. (2010). "Increased claudin-1 protein expression contributes to tumorigenesis in ulcerative colitis-associated colorectal cancer." *Anticancer Res* 30(8): 3181-3186.

Kizawa, H., et al. (2017). "Scaffold-free 3D bio-printed human liver tissue stably maintains metabolic functions useful for drug discovery." *Biochem Biophys Rep* 10: 186-191.

Kleinberg, L., et al. (2008). "Claudin upregulation in ovarian carcinoma effusions is associated with poor survival." *Hum Pathol* 39(5): 747-757.

Koh, C., et al. (2019). "HBV/HDV Coinfection: A Challenge for Therapeutics." *Clin Liver Dis* 23(3): 557-572.

Kondo, J., et al. (2008). "Claudin-1 expression is induced by tumor necrosis factor-alpha in human pancreatic cancer cells." *Int J Mol Med* 22(5): 645-649.

Kudo, M., et al. (2018). "Lenvatinib versus sorafenib in first-line treatment of patients with unresectable hepatocellular carcinoma: a randomised phase 3 non-inferiority trial." *Lancet* 391(10126): 1163-1173.

Kulik, L., et al. (2019). "Epidemiology and Management of Hepatocellular Carcinoma." *Gastroenterology* 156(2): 477-491 e471.

Kumar, R., et al. (2017). "Non-alcoholic Fatty Liver Disease in Lean Subjects: Characteristics and Implications." *J Clin Transl Hepatol* 5(3): 216-223.

Kuo, K. T., et al. (2016). "Nm23H1 mediates tumor invasion in esophageal squamous cell carcinoma by regulation of CLDN1 through the AKT signaling." *Oncogenesis* 5(7): e239.

La Manno, G., et al. (2018). "RNA velocity of single cells." *Nature* 560(7719): 494-498.

Lahnemann, D., et al. (2020). "Eleven grand challenges in single-cell data science." *Genome Biol* 21(1): 31.

Lanini, S., et al. (2016). "Hepatitis C: global epidemiology and strategies for control." *Clin Microbiol Infect* 22(10): 833-838.

Lassailly, G., et al. (2020). "Bariatric Surgery Provides Long-term Resolution of Nonalcoholic Steatohepatitis and Regression of Fibrosis." *Gastroenterology* 159(4): 1290-1301 e1295.

Lee, J. H., et al. (2015). "Mitochondrial Respiratory Dysfunction Induces Claudin-1 Expression via Reactive Oxygen Species-mediated Heat Shock Factor 1 Activation, Leading to Hepatoma Cell Invasiveness." *J Biol Chem* 290(35): 21421-21431.

Lefkowitz, J. H. (2005). "Morphology of alcoholic liver disease." *Clin Liver Dis* 9(1): 37-53.

Leotlela, P. D., et al. (2007). "Claudin-1 overexpression in melanoma is regulated by PKC and contributes to melanoma cell motility." *Oncogene* 26(26): 3846-3856.

Li, E., et al. (2019). "Mouse Models for Immunotherapy in Hepatocellular Carcinoma." *Cancers (Basel)* 11(11).

Li, T. Y., et al. (2019). "Immune suppression in chronic hepatitis B infection associated liver disease: A review." *World J Gastroenterol* 25(27): 3527-3537.

Li, W., et al. (2017). "Application of t-SNE to human genetic data." *J Bioinform Comput Biol* 15(4): 1750017.

Lieber, C. S. (2004). "Alcoholic fatty liver: its pathogenesis and mechanism of progression to inflammation and fibrosis." *Alcohol* 34(1): 9-19.

Lindeboom, R. G. H., et al. (2021). "Towards a Human Cell Atlas: Taking Notes from the Past." *Trends Genet* 37(7): 625-630.

Liu, Y., et al. (2012). "Anti-apoptotic effect of claudin-1 on TNF-alpha-induced apoptosis in human breast cancer MCF-7 cells." *Tumour Biol* 33(6): 2307-2315.

Llovet, J. M., et al. (2021). "Hepatocellular carcinoma." *Nat Rev Dis Primers* 7(1): 6.

Llovet, J. M., et al. (2018). "Molecular therapies and precision medicine for hepatocellular carcinoma." *Nat Rev Clin Oncol* 15(10): 599-616.

Llovet, J. M., et al. (2008). "Sorafenib in advanced hepatocellular carcinoma." *N Engl J Med* 359(4): 378-390.

Llovet, J. M., et al. (2016). "Hepatocellular carcinoma." *Nat Rev Dis Primers* 2: 16018.

Lok, A. S., et al. (2016). "Antiviral therapy for chronic hepatitis B viral infection in adults: A systematic review and meta-analysis." *Hepatology* 63(1): 284-306.

Loomba, R., et al. (2018). "GS-0976 Reduces Hepatic Steatosis and Fibrosis Markers in Patients With Nonalcoholic Fatty Liver Disease." *Gastroenterology* 155(5): 1463-1473 e1466.

- Lucifora, J., et al.** (2020). "Fast Differentiation of HepaRG Cells Allowing Hepatitis B and Delta Virus Infections." *Cells* 9(10).
- Luxemburger, H., et al.** (2018). "HCV-Specific T Cell Responses During and After Chronic HCV Infection." *Viruses* 10(11):645.
- Lv, J., et al.** (2017). "CLDN-1 promoted the epithelial to migration and mesenchymal transition (EMT) in human bronchial epithelial cells via Notch pathway." *Mol Cell Biochem* 432(1-2): 91-98.
- Macosko, E. Z., et al.** (2015). "Highly Parallel Genome-wide Expression Profiling of Individual Cells Using Nanoliter Droplets." *Cell* 161(5): 1202-1214.
- Maily, L., et al.** (2015). "Clearance of persistent hepatitis C virus infection in humanized mice using a claudin-1-targeting monoclonal antibody." *Nat Biotechnol* 33(5): 549-554.
- Marcellin, P., et al.** (2013). "Regression of cirrhosis during treatment with tenofovir disoproxil fumarate for chronic hepatitis B: a 5-year open-label follow-up study." *Lancet* 381(9865): 468-475.
- Marquardt, J. U., et al.** (2015). "Functional and genetic deconstruction of the cellular origin in liver cancer." *Nat Rev Cancer* 15(11): 653-667.
- Marrero, J. A., et al.** (2018). "Diagnosis, Staging, and Management of Hepatocellular Carcinoma: 2018 Practice Guidance by the American Association for the Study of Liver Diseases." *Hepatology* 68(2): 723-750.
- Marshall, A. D., et al.** (2018). "Restrictions for reimbursement of interferon-free direct-acting antiviral drugs for HCV infection in Europe." *Lancet Gastroenterol Hepatol* 3(2): 125-133.
- Masterson, J. C., et al.** (2019). "Epithelial HIF-1alpha/claudin-1 axis regulates barrier dysfunction in eosinophilic esophagitis." *J Clin Invest* 129(8): 3224-3235.
- Mee, C. J., et al.** (2009). "Polarization restricts hepatitis C virus entry into HepG2 hepatoma cells." *J Virol* 83(12): 6211-6221.
- Mima, K., et al.** (2013). "Epithelial-mesenchymal transition expression profiles as a prognostic factor for disease-free survival in hepatocellular carcinoma: Clinical significance of transforming growth factor-beta signaling." *Oncol Lett* 5(1): 149-154.

Miwa, N., et al. (2001). "Involvement of claudin-1 in the beta-catenin/Tcf signaling pathway and its frequent upregulation in human colorectal cancers." *Oncol Res* 12(11-12): 469-476.

Moon, A. M., et al. (2020). "Contemporary Epidemiology of Chronic Liver Disease and Cirrhosis." *Clin Gastroenterol Hepatol* 18(12): 2650-2666.

Moreau, R., et al. (2013). "Acute-on-chronic liver failure is a distinct syndrome that develops in patients with acute decompensation of cirrhosis." *Gastroenterology* 144(7): 1426-1437, 1437 e1421-1429.

Nakamuta, M., et al. (2011). "Expression profiles of genes associated with viral entry in HCV-infected human liver." *J Med Virol* 83(5): 921-927.

Nault, J. C., et al. (2014). "Telomerase reverse transcriptase promoter mutation is an early somatic genetic alteration in the transformation of premalignant nodules in hepatocellular carcinoma on cirrhosis." *Hepatology* 60(6): 1983-1992.

Neesse, A., et al. (2012). "Claudin-4 as therapeutic target in cancer." *Arch Biochem Biophys* 524(1): 64-70.

Nemeth, J., et al. (2010). "High expression of claudin-1 protein in papillary thyroid tumor and its regional lymph node metastasis." *Pathol Oncol Res* 16(1): 19-27.

Newsome, P. N., et al. (2021). "A Placebo-Controlled Trial of Subcutaneous Semaglutide in Nonalcoholic Steatohepatitis." *N Engl J Med* 384(12): 1113-1124.

Nieto, M. A., et al. (2016). "Emt: 2016." *Cell* 166(1): 21-45.

Nishikawa, T., et al. (2015). "Resetting the transcription factor network reverses terminal chronic hepatic failure." *J Clin Invest* 125(4): 1533-1544.

Nusrat, S., et al. (2014). "Cirrhosis and its complications: evidence based treatment." *World J Gastroenterol* 20(18): 5442-5460.

Oku, N., et al. (2006). "Tight junction protein claudin-1 enhances the invasive activity of oral squamous cell carcinoma cells by promoting cleavage of laminin-5 gamma2 chain via matrix metalloproteinase (MMP)-2 and membrane-type MMP-1." *Cancer Res* 66(10): 5251-5257.

Page, K., et al. (2021). "Randomized Trial of a Vaccine Regimen to Prevent Chronic HCV Infection." *N Engl J Med* 384(6): 541-549.

- Papastergiou, V., et al.** (2012). "Non-invasive assessment of liver fibrosis." *Ann Gastroenterol* 25(3): 218-231.
- Parola, M., et al.** (2019). "Liver fibrosis: Pathophysiology, pathogenetic targets and clinical issues." *Mol Aspects Med* 65: 37-55.
- Parsons, S. J., et al.** (2004). "Src family kinases, key regulators of signal transduction." *Oncogene* 23(48): 7906-7909.
- Paschoud, S., et al.** (2007). "Claudin-1 and claudin-5 expression patterns differentiate lung squamous cell carcinomas from adenocarcinomas." *Mod Pathol* 20(9): 947-954.
- Petrova, V., et al.** (2018). "The hypoxic tumour microenvironment." *Oncogenesis* 7(1): 10.
- Picelli, S., et al.** (2013). "Smart-seq2 for sensitive full-length transcriptome profiling in single cells." *Nat Methods* 10(11): 1096-1098.
- Pinzani, M., et al.** (2005). "Fibrosis in chronic liver diseases: diagnosis and management." *J Hepatol* 42 Suppl(1): S22-36.
- Pope, J. L., et al.** (2014). "Claudin-1 regulates intestinal epithelial homeostasis through the modulation of Notch-signalling." *Gut* 63(4): 622-634.
- Prior, N., et al.** (2019). "Liver organoids: from basic research to therapeutic applications." *Gut* 68(12): 2228-2237.
- Ramachandran, P., et al.** (2019). "Resolving the fibrotic niche of human liver cirrhosis at single-cell level." *Nature* 575(7783): 512-518.
- Reynolds, G. M., et al.** (2008). "Hepatitis C virus receptor expression in normal and diseased liver tissue." *Hepatology* 47(2): 418-427.
- Roayaie, S., et al.** (2013). "Resection of hepatocellular cancer ≤ 2 cm: results from two Western centers." *Hepatology* 57(4): 1426-1435.
- Roehlen, N., et al.** (2020). "Liver Fibrosis: Mechanistic Concepts and Therapeutic Perspectives." *Cells* 9(4).
- Roehlen, N., et al.** (2020). "Tight Junction Proteins and the Biology of Hepatobiliary Disease." *Int J Mol Sci* 21(3).

Romero-Gomez, M., et al. (2017). "Treatment of NAFLD with diet, physical activity and exercise." *J Hepatol* 67(4): 829-846.

Ruiz de Galarreta, M., et al. (2019). "beta-Catenin Activation Promotes Immune Escape and Resistance to Anti-PD-1 Therapy in Hepatocellular Carcinoma." *Cancer Discov* 9(8): 1124-1141.

Sahin, U., et al. (2021). "FAST: a randomised phase II study of zolbetuximab (IMAB362) plus EOX versus EOX alone for first-line treatment of advanced CLDN18.2-positive gastric and gastro-oesophageal adenocarcinoma." *Ann Oncol* 32(5): 609-619.

Sanyal, A., et al. (2019). "Pegbelfermin (BMS-986036), a PEGylated fibroblast growth factor 21 analogue, in patients with non-alcoholic steatohepatitis: a randomised, double-blind, placebo-controlled, phase 2a trial." *Lancet* 392(10165): 2705-2717.

Saviano, A., et al. (2020). "Single-cell genomics and spatial transcriptomics: Discovery of novel cell states and cellular interactions in liver physiology and disease biology." *J Hepatol* 73(5): 1219-1230.

Schulze, K., et al. (2015). "Exome sequencing of hepatocellular carcinomas identifies new mutational signatures and potential therapeutic targets." *Nat Genet* 47(5): 505-511.

Schuppan, D., et al. (2018). "Liver fibrosis: Direct antifibrotic agents and targeted therapies." *Matrix Biol* 68-69: 435-451.

Seitz, H. K., et al. (2018). "Alcoholic liver disease." *Nat Rev Dis Primers* 4(1): 16.

Seo, K. W., et al. (2010). "Correlation between Claudins Expression and Prognostic Factors in Prostate Cancer." *Korean J Urol* 51(4): 239-244.

Shalek, A. K., et al. (2017). "Single-cell analyses to tailor treatments." *Sci Transl Med* 9(408).

Shen, B., et al. (2021). "Efficacy and safety of drugs for nonalcoholic steatohepatitis." *J Dig Dis* 22(2): 72-82.

Shin, S., et al. (2016). "Genetic lineage tracing analysis of the cell of origin of hepatotoxin-induced liver tumors in mice." *Hepatology* 64(4): 1163-1177.

Shiozaki, A., et al. (2012). "Claudin 1 mediates TNFalpha-induced gene expression and cell migration in human lung carcinoma cells." *PLoS One* 7(5): e38049.

- Sia, D., et al.** (2017). "Liver Cancer Cell of Origin, Molecular Class, and Effects on Patient Prognosis." *Gastroenterology* 152(4): 745-761.
- Singh, A. B., et al.** (2012). "Claudin-1 expression confers resistance to anoikis in colon cancer cells in a Src-dependent manner." *Carcinogenesis* 33(12): 2538-2547.
- Singh, A. B., et al.** (2011). "Claudin-1 up-regulates the repressor ZEB-1 to inhibit E-cadherin expression in colon cancer cells." *Gastroenterology* 141(6): 2140-2153.
- Singh, P., et al.** (2017). "Anti-claudin 18.2 antibody as new targeted therapy for advanced gastric cancer." *J Hematol Oncol* 10(1): 105.
- Song, Y., et al.** (2019). "Restoring E-cadherin Expression by Natural Compounds for Anticancer Therapies in Genital and Urinary Cancers." *Mol Ther Oncolytics* 14: 130-138.
- Stickel, F., et al.** (2017). "Pathophysiology and Management of Alcoholic Liver Disease: Update 2016." *Gut Liver* 11(2): 173-188.
- Subramanian, A., et al.** (2005). "Gene set enrichment analysis: a knowledge-based approach for interpreting genome-wide expression profiles." *Proc Natl Acad Sci U S A* 102(43): 15545-15550.
- Suh, Y., et al.** (2013). "Claudin-1 induces epithelial-mesenchymal transition through activation of the c-Abl-ERK signaling pathway in human liver cells." *Oncogene* 32(41): 4873-4882.
- Sung, H., et al.** (2021). "Global Cancer Statistics 2020: GLOBOCAN Estimates of Incidence and Mortality Worldwide for 36 Cancers in 185 Countries." *CA CANCER J CLIN* 71: 209–249.
- Sureau, C., et al.** (2016). "The hepatitis delta virus: Replication and pathogenesis." *J Hepatol* 64(1 Suppl): S102-S116.
- Suzuki, T.** (2013). "Regulation of intestinal epithelial permeability by tight junctions." *Cell Mol Life Sci* 70(4): 631-659.
- Sven, M. F., et al.** (2020). "A randomised, double-blind, placebo-controlled, multi-centre, dose-range, proof-of-concept, 24-week treatment study of lanifibranor in adult subjects with non-alcoholic steatohepatitis: Design of the NATIVE study." *Contemp Clin Trials* 98: 106170.
- Tahmasebi Birgani, M., et al.** (2017). "Tumor Microenvironment, a Paradigm in Hepatocellular Carcinoma Progression and Therapy." *Int J Mol Sci* 18(2).

Tang, L. S. Y., et al. (2018). "Chronic Hepatitis B Infection: A Review." *JAMA* 319(17): 1802-1813.

Taylor, M. H., et al. (2021). "The LEAP program: lenvatinib plus pembrolizumab for the treatment of advanced solid tumors." *Future Oncol* 17(6): 637-648.

Thrift, A. P., et al. (2017). "Global epidemiology and burden of HCV infection and HCV-related disease." *Nat Rev Gastroenterol Hepatol* 14(2): 122-132.

Timpe, J. M., et al. (2008). "Hepatitis C virus cell-cell transmission in hepatoma cells in the presence of neutralizing antibodies." *Hepatology* 47(1): 17-24.

Trinchet, J. C., et al. (2015). "Complications and competing risks of death in compensated viral cirrhosis (ANRS CO12 CirVir prospective cohort)." *Hepatology* 62(3): 737-750.

Troeger, J. S., et al. (2012). "Deactivation of hepatic stellate cells during liver fibrosis resolution in mice." *Gastroenterology* 143(4): 1073-1083 e1022.

Tsukahara, M., et al. (2005). "Distinct expression patterns of claudin-1 and claudin-4 in intraductal papillary-mucinous tumors of the pancreas." *Pathol Int* 55(2): 63-69.

Tsukita, S., et al. (2000). "The structure and function of claudins, cell adhesion molecules at tight junctions." *Ann N Y Acad Sci* 915: 129-135.

Uhlén M., et al. (Science). "Tissue-based map of the human proteome." *Science* 347(6220): 1260419.

Van den Bossche, J., et al. (2012). "Claudin-1, claudin-2 and claudin-11 genes differentially associate with distinct types of anti-inflammatory macrophages in vitro and with parasite- and tumour-elicited macrophages in vivo." *Scand J Immunol* 75(6): 588-598.

van den Brink, S. C., et al. (2017). "Single-cell sequencing reveals dissociation-induced gene expression in tissue subpopulations." *Nat Methods* 14(10): 935-936.

van der Pol, C. B., et al. (2019). "Accuracy of the Liver Imaging Reporting and Data System in Computed Tomography and Magnetic Resonance Image Analysis of Hepatocellular Carcinoma or Overall Malignancy-A Systematic Review." *Gastroenterology* 156(4): 976-986.

Vare, P., et al. (2008). "Low claudin expression is associated with high Gleason grade in prostate adenocarcinoma." *Oncol Rep* 19(1): 25-31.

Vilar-Gomez, E., et al. (2015). "Weight Loss Through Lifestyle Modification Significantly Reduces Features of Nonalcoholic Steatohepatitis." *Gastroenterology* 149(2): 367-378 e365; quiz e314-365.

Wang, X. (2011). "Identification of common tumor signatures based on gene set enrichment analysis." *In Silico Biol* 11(1-2): 1-10.

Weiskirchen, R., et al. (2019). "Organ and tissue fibrosis: Molecular signals, cellular mechanisms and translational implications." *Mol Aspects Med* 65: 2-15.

WHO (2018). Global status report on alcohol and health 2018.

Wiessing, L., et al. (2014). "Hepatitis C virus infection epidemiology among people who inject drugs in Europe: a systematic review of data for scaling up treatment and prevention." *PLoS One* 9(7): e103345.

Wu, C. J., et al. (2013). "Epithelial cell adhesion molecule (EpCAM) regulates claudin dynamics and tight junctions." *J Biol Chem* 288(17): 12253-12268.

Wu, F., et al. (2019). "Prognostic power of a lipid metabolism gene panel for diffuse gliomas." *J Cell Mol Med* 23(11): 7741-7748.

Xu, J., et al. (2009). "TGF-beta-induced epithelial to mesenchymal transition." *Cell Res* 19(2): 156-172.

Yamada, S., et al. (2014). "Epithelial to mesenchymal transition is associated with shorter disease-free survival in hepatocellular carcinoma." *Ann Surg Oncol* 21(12): 3882-3890.

Yamashita, T., et al. (2009). "EpCAM-positive hepatocellular carcinoma cells are tumor-initiating cells with stem/progenitor cell features." *Gastroenterology* 136(3): 1012-1024.

Yamashita, T., et al. (2013). "Cancer stem cells in the development of liver cancer." *J Clin Invest* 123(5): 1911-1918.

Yang, J., et al. (2020). "EpCAM associates with integrin and regulates cell adhesion in cancer cells." *Biochem Biophys Res Commun* 522(4): 903-909.

Yang, M. H., et al. (2009). "Comprehensive analysis of the independent effect of twist and snail in promoting metastasis of hepatocellular carcinoma." *Hepatology* 50(5): 1464-1474.

- Yanguas, S. C., et al.** (2016). "Experimental models of liver fibrosis." *Arch Toxicol* 90(5): 1025-1048.
- Yau, T., et al.** (2020). "Efficacy and Safety of Nivolumab Plus Ipilimumab in Patients With Advanced Hepatocellular Carcinoma Previously Treated With Sorafenib: The CheckMate 040 Randomized Clinical Trial." *JAMA Oncol* 6(11): e204564.
- Yoon, C. H., et al.** (2010). "Claudin-1 acts through c-Abl-protein kinase Cdelta (PKCdelta) signaling and has a causal role in the acquisition of invasive capacity in human liver cells." *J Biol Chem* 285(1): 226-233.
- Younossi, Z., et al.** (2019). "Global Perspectives on Nonalcoholic Fatty Liver Disease and Nonalcoholic Steatohepatitis." *Hepatology* 69(6): 2672-2682.
- Younossi, Z. M.** (2019). "Non-alcoholic fatty liver disease - A global public health perspective." *J Hepatol* 70(3): 531-544.
- Younossi, Z. M., et al.** (2019). "Obeticholic acid for the treatment of non-alcoholic steatohepatitis: interim analysis from a multicentre, randomised, placebo-controlled phase 3 trial." *Lancet* 394(10215): 2184-2196.
- Yuan, Q., et al.** (2019). "Myofibroblast in Kidney Fibrosis: Origin, Activation, and Regulation." *Adv Exp Med Biol* 1165: 253-283.
- Yuen, M. F., et al.** (2018). "Hepatitis B virus infection." *Nat Rev Dis Primers* 4: 18035.
- Zadori, G., et al.** (2011). "Examination of claudin-1 expression in patients undergoing liver transplantation owing to hepatitis C virus cirrhosis." *Transplant Proc* 43(4): 1267-1271.
- Zappasodi, R., et al.** (2018). "Emerging Concepts for Immune Checkpoint Blockade-Based Combination Therapies." *Cancer Cell* 33(4): 581-598.
- Zeisel, M. B., et al.** (2018). "Tight junction proteins in gastrointestinal and liver disease." *Gut*.
- Zhai, X., et al.** (2014). "Abnormal expression of EMT-related proteins, S100A4, vimentin and E-cadherin, is correlated with clinicopathological features and prognosis in HCC." *Med Oncol* 31(6): 970.

- Zhang, G. J., et al.** (2013). "Upregulation of microRNA-155 promotes the migration and invasion of colorectal cancer cells through the regulation of claudin-1 expression." *Int J Mol Med* 31(6): 1375-1380.
- Zheng, Y., et al.** (2020). "Single-Cell Transcriptomics Reveal Immune Mechanisms of the Onset and Progression of IgA Nephropathy." *Cell Rep* 33(12): 108525.
- Zhou, B., et al.** (2015). "Claudin 1 in Breast Cancer: New Insights." *J Clin Med* 4(12): 1960-1976.
- Zhou, S., et al.** (2015). "Quantification of glypican 3, beta-catenin and claudin-1 protein expression in hepatoblastoma and paediatric hepatocellular carcinoma by colour deconvolution." *Histopathology* 67(6): 905-913.
- Zhu, Y. J., et al.** (2017). "New knowledge of the mechanisms of sorafenib resistance in liver cancer." *Acta Pharmacol Sin* 38(5): 614-622.
- Ziegenhain, C., et al.** (2017). "Comparative Analysis of Single-Cell RNA Sequencing Methods." *Mol Cell* 65(4): 631-643 e634.
- Zihni, C., et al.** (2016). "Tight junctions: from simple barriers to multifunctional molecular gates." *Nat Rev Mol Cell Biol* 17(9): 564-580.
- Zuo, D., et al.** (2020). "Claudin-1 Is a Valuable Prognostic Biomarker in Colorectal Cancer: A Meta-Analysis." *Gastroenterol Res Pract* 2020: 4258035.
- Zwanziger, D., et al.** (2015). "The impact of CLAUDIN-1 on follicular thyroid carcinoma aggressiveness." *Endocr Relat Cancer* 22(5): 819-830.

Introductory article I – Liver fibrosis: Mechanistic concepts and therapeutic perspectives

Review article:

Roehlen N.*, Crouchet E.*, Baumert T.F.: Liver Fibrosis: Mechanistic Concepts and Therapeutic Perspectives. *Cells*. 2020 Apr 3;9(4):875. doi: 10.3390/cells9040875.

*shared first-authorship

Liver Fibrosis: Mechanistic Concepts and Therapeutic Perspectives

Natascha Roehlen ^{1,2,†}, Emilie Crouchet ^{1,2,†} and Thomas F. Baumert ^{1,2,3,*}

¹ Université de Strasbourg, 67000 Strasbourg, France; natascha.roehlen@etu.unistra.fr (N.R.); ecrouchet@unistra.fr (E.C.)

² Institut de Recherche sur les Maladies Virales et Hépatiques U1110, 67000 Strasbourg, France

³ Pôle Hepato-digestif, Institut Hospitalo-Universitaire, Hôpitaux Universitaires de Strasbourg, 67000 Strasbourg, France

* Correspondence: thomas.baumert@unistra.fr; Tel.: +33-366853703

† These authors contributed equally to this work.



Received: 24 February 2020; Accepted: 1 April 2020; Published: 3 April 2020

Abstract: Liver fibrosis due to viral or metabolic chronic liver diseases is a major challenge of global health. Correlating with liver disease progression, fibrosis is a key factor for liver disease outcome and risk of hepatocellular carcinoma (HCC). Despite different mechanism of primary liver injury and disease-specific cell responses, the progression of fibrotic liver disease follows shared patterns across the main liver disease etiologies. Scientific discoveries within the last decade have transformed the understanding of the mechanisms of liver fibrosis. Removal or elimination of the causative agent such as control or cure of viral infection has shown that liver fibrosis is reversible. However, reversal often occurs too slowly or too infrequent to avoid life-threatening complications particularly in advanced fibrosis. Thus, there is a huge unmet medical need for anti-fibrotic therapies to prevent liver disease progression and HCC development. However, while many anti-fibrotic candidate agents have shown robust effects in experimental animal models, their anti-fibrotic effects in clinical trials have been limited or absent. Thus, no approved therapy exists for liver fibrosis. In this review we summarize cellular drivers and molecular mechanisms of fibrogenesis in chronic liver diseases and discuss their impact for the development of urgently needed anti-fibrotic therapies.

Keywords: Hepatic stellate cell; liver myofibroblast; Kupffer cell; liver cirrhosis; anti-fibrotics; TGF- β ; PDGF

1. Introduction

Chronic liver diseases are a major global health burden and account for approximately 2 million deaths per year worldwide [1]. Underlying etiologies in chronic liver disease comprise viral (Hepatitis B; HBV and hepatitis C; HCV) related chronic liver disease, alcoholic steatohepatitis (ASH), and non-alcoholic steatohepatitis (NASH), as well as autoimmune and genetic diseases. Organ fibrosis characterizes disease progression in chronic inflammatory diseases and contributes to 45% of all-cause mortality world-wide [2]. Similarly, in the liver, development of fibrosis mainly determines quality of life, as well as prognosis [3]. Thus, the level of fibrosis correlates with liver function and represents the major risk factor for development of hepatocellular carcinoma (HCC) [4]. Moreover, chronic portal hypertension due to liver fibrosis is the major cause of clinical complications, including hydropic decompensation, and bleeding events, as well as hepatic encephalopathy [3]. Consequently, liver cirrhosis is currently the 11th most common cause of death in the world [1] and the fourth most frequent cause of death in adults in central Europe [5,6].

Liver fibrosis is characterized by progressive accumulation of extracellular matrix (ECM), which destroys the physiological architecture of the liver [7]. Pathogenetically, toxic, metabolic, or viral diseases lead to

damaged hepatocytes and infiltration of immune cells that activate trans-differentiation of Hepatic stellate cells (HSCs) into collagen-producing myofibroblasts [8,9]. Physiologically involved in tissue repair, upon short-term injury this process is balanced by counteracting anti-fibrotic mechanisms resulting in inactivation or apoptosis of myofibroblasts and scar resolution. In contrast, in chronic liver diseases an imbalance of pro-fibrogenic and anti-fibrogenic mechanisms causes persistent activation of proliferating, contractile, and migrating myofibroblasts that lead to excessive production of ECM [8,9]. The liver's fate to either pass into an anti-fibrotic scar-dissolving stage or to proceed into an uninhibited fibrosis-promoting stage is hereby mainly regulated by non-parenchymal cells (NPCs), including Kupffer cells and other immune cells [10–12]. Thus, hepatocyte apoptosis and release of damage-associated patterns (DAMPs) by hepatocytes not only activate HSCs directly but also induce recruitment and activation of lymphocytes and macrophages that contribute to promotion of HSC trans-differentiation and myofibroblast activation by producing pro-inflammatory and pro-fibrogenic cytokines [13,14]. Distinct macrophage subpopulations on the other hand participate in fibrosis resolution due to expression of matrix-metalloproteinases (MMPs) [15,16]. On the molecular basis, a complex network of cytokine-induced signaling pathways orchestrate pro-fibrogenic cell interactions. In fact, Transforming Growth Factor Beta (TGF- β), Platelet Derived Growth Factor (PDGF), and the inflammasome (NLRP3)-Caspase1 pathway, as well as WNT/ β -catenin signaling have been suggested to be key signaling pathways associated with HSC activation and fibrosis progression [17–19]. The general, etiology-independent cell interactions involved in fibrosis development are depicted in Figure 1.

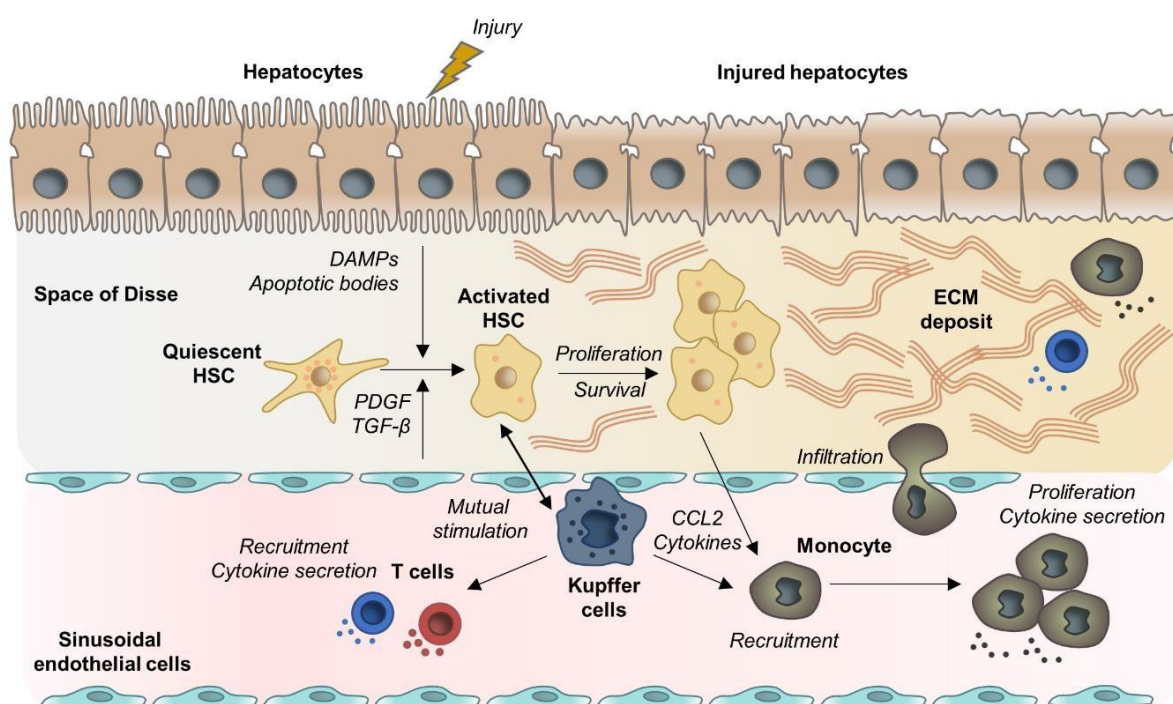


Figure 1. Examples for mechanistic concepts for liver fibrosis. Chronic hepatocyte injury causes release of damage-associated patterns (DAMPs) and apoptotic bodies that activate Hepatic stellate cells (HSCs) and recruit immune cells. Complex multidirectional interactions between activated HSCs and Kupffer cells, as well as innate immune cells promote trans-differentiation into proliferative and extracellularmatrix (ECM) producing myofibroblasts. Abbreviations: PDGF: Platelet Derived Growth Factor; TGF- β : Transforming Growth Factor Beta; CCL2: chemokine (C-C motif) ligand 2.

One approach to prevent liver-related mortality is to prevent progression of fibrogenesis. Within the past years, several in-vitro and in-vivo models have been developed in order to address the unmet medical need of developing efficient and safe anti-fibrotic drugs [20–23]. However, despite increasing knowledge regarding the

molecular mechanisms of liver fibrogenesis, an approved drug to treat liver fibrosis is still pending [24]. In this review we summarize recent advances in the understanding of cellular and molecular drivers of liver fibrogenesis in key etiologies of chronic liver disease. Moreover, anti-fibrotic strategies and agents in clinical development are discussed.

2. Mechanistic Concepts of Liver Fibrosis

2.1 Hepatocyte Cell Death and Apoptosis

Hepatocyte death is an important initial event in all liver disease etiologies. Dead hepatocytes release intracellular compounds termed DAMPs that send out danger signals to surrounding cells including HSCs and Kupffer cells and therefore play an important role in fibrosis development and inflammation. This family of molecules comprise nucleic acids, intracellular proteins, Adenosine Triphosphate (ATP), or mitochondrial or nucleic compounds such as High-Mobility Group Box-1 (HMGB1) [25]. DAMPs can be passively released by necrotic hepatocytes due to the disruption of plasma membrane [25,26]. HMGB1 is one of the most studied DAMPs in the context of liver disease. It is a DNA-binding non-histone nuclear protein ubiquitously expressed in eukaryotic cells. HMGB1 is highly released by necrotic hepatocytes as a danger pattern [26]. In addition, it can be secreted by stressed cells and contribute to immune responses and inflammation by interacting with the Toll Like Receptors (TLR) 4 and 9 [27–30]. Moreover, Li et al. recently provided evidence that HMGB1 directly activates HSCs by regulating HSCs autophagy in a model of HBV-related liver fibrosis progression [31]. Finally, it was recently demonstrated that HMGB1 plays an essential role in the recruitment of pro-inflammatory neutrophils to sites of necrotic injury in the liver [32].

In contrast, apoptosis generates low levels of DAMPs because the cell components are largely retained in apoptotic bodies [25,26]. However, a pro-fibrogenic response can be elicited by hepatocyte apoptosis through activation of the Fas death receptor [33,34]. Moreover, hepatocyte apoptosis induces the release of apoptotic bodies which can be phagocytosed by HSCs and Kupffer and induce a pro-fibrogenic response [35,36]. In addition, DNA from apoptotic hepatocytes triggers TLR9 activation on HSCs and collagen production [37].

Lipid overload in hepatocytes is one of the main drivers of hepatotoxicity, which accelerates the development of progressive inflammation, oxidative stress and fibrosis [38]. In the liver, lipids are mainly stored as triglycerides, an inert and non-cytotoxic form of lipid. Lipotoxicity is rather due to accumulation of toxic intermediates of triglyceride synthesis such as saturated Free Fatty Acids (FFAs) and their derivatives, accumulation of free cholesterol or complex lipids as lysophosphatidylcholine and ceramides [39–41]. Accumulation of these lipids affect cellular function through different mechanisms including oxidative and endoplasmic reticulum stress, mitochondrial dysfunction, and induction of apoptosis [38]. Accumulation of FFAs is one of the strongest apoptosis inducers in hepatocytes. This process is mainly mediated by the Tumor Necrosis Factor-Related Apoptosis-Inducing Ligand Receptor 2 (TRAIL-R2), also known as death receptor 5. TRAIL-R2 especially contributes to cell death caused by palmitic acid, which induces downstream activation of caspase 8 and executionary caspases 3 and 7 [42,43]. Moreover, FFA-induced lipo-apoptosis in hepatocytes stimulates the release of ATP, which stimulates migration of monocytes [44]. In addition to hepatocytes, NPCs are also impacted by the toxic lipid accumulation. FFAs accumulation in HSCs and Kupffer cells especially triggers TLR4 pathway activation, leading to c-Jun N-terminal Kinase (JNK) and NF- κ B pathway activation, as well as secretion of pro-inflammatory and chemoattractant cytokines [38,45].

Dysregulation of hepatic cholesterol metabolism is also a key event leading to hepatocyte death. Free cholesterol causes hepatocyte apoptotic and necrotic death by activating JNK1 [46]. It has recently been shown that high concentration of free cholesterol in hepatocytes of NASH patients leads to cholesterol crystallization [47,48]. Dead hepatocytes containing cholesterol crystals induce the recruitment and aggregation of Kupffer cells in “crown-like structures”, which process dead cells and transform into activated foam cells [48]. Activation of Kupffer cells during this process contributes to HSCs activation through the release of pro-inflammatory cytokines. The group of Hibi et al. also demonstrated that accumulation of free cholesterol in HSCs directly exacerbate liver fibrosis [49,50].

2.2 HSC Activation and Myofibroblast Progenitor Cells

HSCs are the main myofibroblast progenitor cells and therefore key effectors of the fibrogenic response [51]. In normal liver, HSCs are quiescent, non-proliferative perisinusoidal cells, characterized by their star-like morphology and their high number of cytoplasmic lipid droplets [52]. Upon liver injury, HSCs become activated, and transdifferentiate from a quiescent phenotype into a proliferative and contractile myofibroblast phenotype [53]. During this process, activated HSCs progressively lose their star shaped morphology and their lipid droplets, while abundantly producing ECM components (including types I, III, and IV collagens, fibronectin, laminin, and proteoglycans) and pro-inflammatory mediators. In addition, activated cells express high levels of alpha Smooth Muscle Actin (α -SMA) and Tissue Inhibitor of Metalloproteinase 1 (TIMP1) which contribute to the changes from a adipocytic phenotype to a pro-fibrogenic and inflammatory phenotype [54,55].

Physiologically involved in tissue repair, following short-term injury myofibroblasts are rapidly cleared by apoptosis or inactivation [56]. However, under chronic injury, the persistent HSCs activation leads to disruption of the balance between ECM deposition and dissolution and triggers progressive liver fibrosis [51]. Moreover, in advanced fibrosis, the high number of activated HSCs and contractility of the myofibroblasts promote the constriction of hepatic sinusoids, therefore affecting the blood flow and the nutrient exchange and participating in liver dysfunction [9].

Activation of HSCs consists of two major phases (i) the initiation, or pre-inflammatory stage, referring to the early changes in gene expression shortly after injury and (ii) the perpetuation, which corresponds to maintenance of an activated phenotype and fibrosis development [57]. The initiation stage is triggered by paracrine stimulation of HSCs through the products of injured hepatocytes, signals from the resident Kupffer cells and endothelial cells, as well as Reactive Oxygen Species (ROS) and lipid peroxides exposure [58]. Perpetuation results from the continuing effects of these stimuli. These signals induce enhanced proliferation, contractility, pro-inflammatory and chemoattractant mediator synthesis, and fibrogenesis/matrix degradation [57,58].

The production of chemotactic and inflammatory substances induces the activation and the recruitment of other cellular effectors, including Kupffer cells, infiltrating immune cells, endothelial cells, and platelets, which reinforce the pro-fibrogenic environment and the maintenance of HSCs activation [53,59]. TGF- β and PDGF are the two major cytokines contributing to HSCs activation and proliferation. These two major pathways as well as further contributing mediators driving liver fibrosis (i.e., ROS) will be further discussed in this section [57,60]. All these signals lead to ECM accumulation in the extracellular space. Importantly, the matrix-degrading enzymes such as MMPs produced by HSCs and other pro-inflammatory effectors contribute to the replacement of normal ECM by an altered matrix. Indeed, the ECM remodeling involves changes in matrix stiffness, flexibility, and density related to the dysregulation of the components production [61] (Figure 2). Moreover, the ECM is not inert and can also store cytokines and growth factors secreted by the cellular effectors hereby further contributing to inflammation, fibrogenesis, hepatocyte proliferation, and carcinogenesis [53,61].

While activated HSCs are the predominant precursors of myofibroblasts in fibrotic liver (>90% of collagen-producing cells), increasing evidence shows that myofibroblasts can also derive from portal fibroblasts [62,63], bone marrow [64,65], and some studies have suggested Epithelial-To-Mesenchymal Cell Transition (EMT) from hepatocytes or cholangiocytes [66]. However, the contribution of these cells in the development of liver fibrosis is still unclear and differ upon the different liver disease etiologies and stages. For example, the portal fibroblasts are mainly activated by cholestatic injuries and may initiate the periportal fibrosis [67,68]. Indeed, Iwaisako et al. reported that portal fibroblasts contribute to more than 70% of myofibroblasts upon biliary injury [68]. Regarding bone-marrow-derived myofibroblasts two potential sources have been described: fibrocytes and Mesenchymal Stem Cells (MSCs). The fibrocytes can differentiate into myofibroblasts and are recruited in the injured tissue over time, suggesting a role in advanced disease [62]. MSCs are multipotent progenitor that can differentiate into hepatic myofibroblasts [62,64] via mesothelial to mesenchymal transition upon chronic liver

injury [69]. Nonetheless, their exact contribution to liver disease development is still controversial. On one hand, studies indicate their ability to differentiate into pro-fibrogenic myofibroblasts [70], on the other hand several studies demonstrated that injection of MSCs improves liver fibrosis/cirrhosis in mice and could be used as a novel therapeutic approach [71,72]. More studies are therefore needed to clarify the role of these cells. Finally, cholangiocytes and hepatocytes can develop a myofibroblast phenotype via EMT [66,73]. EMT is a reversible process by which epithelial cells lose their polarity and can differentiate into mesenchymal cells. TGF- β , the most potent pro-fibrogenic cytokine upregulated during liver fibrosis is known to be a strong inducer of EMT. However, some controversies remain. Indeed, lineage-tracing experiments have demonstrated that myofibroblasts found in experimental liver fibrosis do not originate from epithelial cells [74,75].

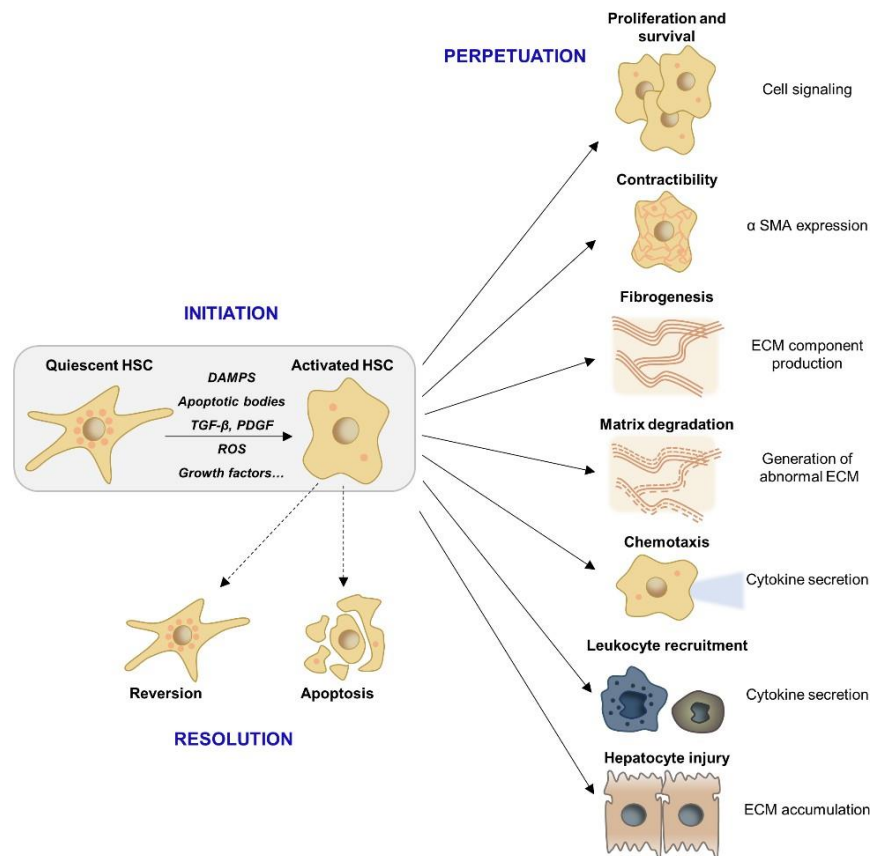


Figure 2. HSC activation and downstream pro-fibrogenic responses. Following the initial event of HSC activation, non-parenchymal cell directed pro- or anti-fibrogenic responses determine whether activated HSCs either transit into spontaneous resolution via reversion and apoptosis or pass into a perpetuated state that results in maintenance of a pro-inflammatory and pro-fibrogenic microenvironment as well as liver degrading ECM accumulation. Abbreviations: α -SMA: α -smooth muscle actin; DAMPS: Damage-associated molecular pattern; ECM: Extracellular matrix; HSC: hepatic stellate cells; PDGF: Platelet-derived growth factor; ROS: Reactive oxygen species; TGF- β : Transforming growth factor β .

2.3 Liver Macrophages

Macrophages represent the largest NPC population in the liver and play a central role in liver inflammation and fibrosis. Hepatic macrophages comprise the liver resident Kupffer cells and monocyte-derived macrophages, originating from the bone-marrow [13]. Activation of Kupffer cells and recruitment of monocyte-derived macrophages are triggered by the release of DAMPs, ROS production, anti-viral response but also by metabolic signaling induced by fat accumulation [76–79].

Macrophages can be classified into a wide spectrum of different phenotypes ranging from the classically activated pro-inflammatory macrophages (M1) to alternatively activated immunoregulatory macrophages (M2). These subclasses are induced by different regulators and exhibit distinct markers and functional activities. M1 are characterized by the expression of pro-inflammatory cytokines (Tumor Necrosis Factor alpha (TNF α), the interleukins (IL) IL6 and IL1 β), whereas M2 express anti-inflammatory mediators (IL4, IL1) [80]. Hepatic macrophages exhibit a remarkable plasticity and can switch to different phenotypes in response to various stimuli of their microenvironment, sometimes expressing both markers of M1 and M2 differentiation. While being difficult to distinctly attribute this dichotomous classification to pro- or anti-fibrogenic actions [13,15], numerous studies indicate distinct subpopulations of macrophages to coexist in the liver and to contribute to different phases of fibrosis. Thus, Duffield et al. demonstrated that macrophage depletion in the early phase of injury decreases the inflammatory response and reduces scarring and the number of myofibroblasts. In contrast, macrophage depletion during recovery leads to a failure of ECM degradation and a less efficient repair [81].

In the early phase of the injury, the dominant macrophage populations are pro-inflammatory. The resident Kupffer cells rapidly secrete IL-1 β , TNF α , chemokine (C-C motif) ligand 2 (CCL2), and CCL5 resulting in activation of HSCs and recruitment of other immune cells including monocyte-derived macrophages [15]. Monocytes infiltration into the liver is primarily controlled by C-C Motif Chemokine Receptor 2 (CCR2) and its ligand CCL2 and is a major contributor of fibrosis development [82,83]. Recruitment of pro-inflammatory cells is the principal driver of hepatic inflammation. Mutual stimulation of inflammatory cells and HSCs results in amplification and perpetuation of the pro-fibrogenic liver state (for a review, see [84]). Activated HSCs modulate immune cell recruitment via secretion of pro-inflammatory and chemoattractant molecules and by secreting ECM which constitutes a network for leukocytes migration and retention [85]. Activated macrophages secrete cytokines to stimulate HSCs, which in turn produce the macrophage colony-stimulating factor, IL6, and other cytokines to perpetuate the pro-fibrotic macrophage activity [85–87]. Moreover, Kupffer cell activation increases the activity of NF- κ B in HSCs, which further promotes pro-inflammatory cytokine secretion [87]. Different studies also described a direct interaction of HSCs with immune cells through expression of adhesion molecules (ICAM-1, VCAM-1), resulting in mutual stimulation and amplification of the pro-fibrogenic response [88,89]. More recently, Lodyga et al. showed that cadherin-11 (CDH11) mediates adhesion of macrophages to myofibroblasts and establishes a pro-fibrotic niche of active TGF- β [90]. Another recent example of mutual stimulation between HSCs and Kupffer cells was reported by Cai et al. They demonstrated that CXCL6 plays an important role in liver fibrosis through stimulating the release of TGF- β by Kupffer cells via an EGFR-dependent pathway [91].

During progression of injury, macrophages exhibit intermediate phenotypes and switch to a mostly anti-inflammatory profile. These macrophages respond to IL10, IL4, and IL13 and secrete anti-inflammatory mediators such as IL-10 and TGF- β [92]. At this stage, some resident macrophages can have a wound healing phenotype characterized by the production of MMPs (i.e., MMP9, MMP12, MMP1), which are involved in matrix degradation and resolution of fibrosis [11,16]. During late-stage injury, the dominant macrophage population is anti-inflammatory due to the abundance of the TGF- β in the fibrotic environment [93]. These macrophages progressively switch to an immunosuppressive phenotype, allowing immune evasion and tumor promotion. Indeed, they produce immunosuppressive mediators such as IL10 and express cell surface receptors like programmed cell death 1 ligand 1 (PD-L1) and the receptor sialic-acid-binding Ig-like lectin 10 that play major roles in suppressing the immune system [94–96]. Therefore, TGF- β provides a link between liver fibrosis and immune responses.

The controlled inflammation and macrophage activation at the different stage of liver injury is an essential feature to control fibrosis development. However, due to the remarkable plasticity of macrophages, translation of this concept into clinical application is challenging. The precise contribution of each macrophage population needs to be fully dissected in the future.

2.4 Lymphocytes

While the role of myofibroblasts and macrophages in fibrogenesis is well described, the role of adaptive immune cells is less defined. Nevertheless, the importance of lymphocytes in fibrogenesis is evidenced by *in vivo* studies showing that inhibition of lymphocyte recruitment in the liver induces a decrease in the fibrogenic responses [97–100].

As described above, chronic liver injury results in the production of pro-inflammatory mediators and the infiltration of leukocytes, including lymphocytes, in the sub-endothelial space. The recruitment of lymphocytes from the circulation is further triggered by interactions with endothelial cells, a process regulated by several chemokines. Importantly, lymphocytes can interact with ECM components and endothelial cells through cell surface integrins, which contribute to cell activation and differentiation as well as fibrogenic responses [101,102]. After migration through the endothelium by a complex mechanism, lymphocytes are recruited at the injury site by chemoattractant molecules [88]. It has been shown that CXCR3 activation by its ligands, including CXCL9, CXCL10, and CXCL11 produced by HSCs and endothelial cells, promotes lymphocytes trans-endothelial migration [103]. Myofibroblasts also secrete cytokines promoting lymphocyte migration, including IL-6, hepatocyte growth factor and TGF- β [97].

CD4⁺ T cell responses have been shown to be critical for fibrosis development. Polarization of CD4⁺ T cells in distinct T-helper (TH) lineages is critical for defining cell properties and cytokine production. The TH2-polarized T cells are directly involved in fibrosis development by stimulating pro-fibrogenic gene expression in myofibroblasts (pro-collagen I and III, MMP2, MMP9, and TIMPs) and the synthesis of immunoregulatory mediators in macrophages (IL10, TGF- β) [14]. These processes are mainly driven by IL4 and IL13 [14,104]. IL17-producing CD4⁺ T cells and regulatory T cells (Tregs) have also been identified as effectors of liver fibrogenesis. It was observed that IL-17 expression is upregulated in fibrotic liver tissue and promotes pro-inflammatory cytokine expression, neutrophil influx, liver injury, and fibrosis [105,106]. Similarly, an increase of the Treg population was observed in patients with advanced fibrosis, which may promote fibrosis through secretion of IL8 [107,108]. The role of B-lymphocytes and CD8⁺ T cells in liver fibrosis is less well understood. It is possible that these cells could promote fibrosis by secreting pro-fibrotic cytokines or by amplifying tissue injury [88,97,109].

2.5 Gut Dysbiosis

Numerous studies suggest a key role of gut dysbiosis in the progression of liver fibrosis. The term liver-gut axis describes the close bidirectional interaction between the gut and its microbiota with the liver. Thus, 75% of the portal vein blood derives from the gut and transports intestinal products to the liver. The liver in turn secretes bile and antibodies into the gut [110]. The interface between the liver and the gut microbiota is shaped by the mucosal barrier, consisting of the gut epithelial barrier and the gut vascular barrier. The integrity of this intestinal mucus barrier and the physiological composition of the intestinal microbiome are critical for maintaining homeostasis of the liver-gut axis [111]. Metabolic toxins, especially alcohol abuse or high fat/low fiber diet in NAFLD have been described to disrupt intestinal homeostasis by increasing intestinal permeability and altering microbiota [112,113]. Consequentially, the relative overgrowth of potentially pathogenic bacteria not only drives hepatic inflammatory immune responses and HSC activation due to portal delivery of pathogen-associated molecular patterns (PAMPs, as lipopolysaccharides, peptidoglycans, and flagellin), the altered microbiome also results in intestinal deconjugation of bile acids and therefore production of so-called secondary bile acids that suppress Farnesoid-X Receptor (FXR) signaling [111]. FXR is a nuclear receptor activated by bile acids that regulates bile acid, lipid, and glucose metabolism [114,115]. Intestinal FXR signaling physiologically exerts protective effects on intestinal epithelial barrier properties [116] and accelerates gut vascular barrier repair [113]. Intestinal accumulation of secondary FXR-suppressing bile acids in chronic liver disease therefore promotes disruption of the intestinal barrier.

Independent of the underlying etiology and presence of the causal toxin, liver fibrosis itself is typically accompanied by gut dysbiosis [117,118]. These etiology-independent alterations in the gut microbiome [117,119] are due to reduced small bowel motility e.g., in the context of ascites [119–121] and compromised intestinal immunity [122]. Moreover, highlighting the reciprocal interaction of bile acids and the gut microbiome, reduced excretion of primary bile acids in liver fibrosis with compromised liver function directly affects composition of the gut microbiome [119,121]. Typical features of gut dysbiosis in liver cirrhosis are reduced diversity and relative overgrowth of potentially pathogenic bacteria as *Enterococcaceae* and *Enterobacteriaceae* or bacteria of buccal origin [118]. Together with the typical severely compromised gut barrier, gut dysbiosis promotes cirrhosis inflammatory state due to hepatic accumulation of PAMPs and toxic bacteria products [123] and correlates with liver disease progression [124,125]. Nevertheless, abundance of pathogenic taxa associates with risk of decompensation in patients with liver cirrhosis and enteral bacterial translocation is involved in outcome-determining complications as spontaneous bacterial peritonitis and hepatoencephalopathy [124,126].

2.6 Molecular Signaling Pathways Involved in Liver Fibrogenesis

2.6.1 PDGF Signaling

PDGF is a growth factor promoting HSCs division and proliferation. Four different PDGF subunits, termed PDGF-A, -B, -C, and -D, were identified and can produce five different polymers (PDGF-AA, -BB, -AB, -CC, and -DD), via a disulfide bond linkage, which have different functions [127]. PDGF-AA mainly controls cell proliferation and chemotaxis, while PDGFR-AB and -BB promote collagen synthesis [17]. Moreover, several studies demonstrated that the subunit PDGF-B is the most potent factor associated with early HSCs activation. Indeed, PDGF-B expression is transiently increased during the early stage of activation. In contrast, PDGF-C and -D levels are increased during the trans-differentiation and persist upon the perpetuation, suggesting a role of these subunits in the late phase of fibrogenesis [128–130].

Under healthy conditions, PDGF is produced by platelets. During liver injury, Kupffer cells mediate intrahepatic recruitment of platelets [59]. Moreover, PDGF can also be expressed by Kupffer cells, endothelial cells, and activated HSCs. Finally, PDGF receptor (PDGFR) is expressed at the membrane of HSCs and can therefore stimulate HSCs activation through autocrine mechanisms [131,132].

The binding of PDGFs on their corresponding receptors induces receptor dimerization and phosphorylation which in turn phosphorylate tyrosine residues on different intracellular substrates. Stimulation of PDGFR triggers activation of several signaling pathways including the Ras/Raf system, the phospholipase C γ (PLC γ), the phosphatidylinositol 3-kinase (PI3K)/Akt pathway, and the JAK/signal transducer and activator of transcription (STAT) pathway [17]. These downstream elements then regulate the expression levels of pro-fibrotic target genes such as type I collagen (COL1A1), metalloproteinase inhibitors (TIMPs), and MMPs but also the apoptosis regulator Bcl 2, resulting in cell proliferation and survival [17].

2.6.2 TGF- β Signaling

In cooperation with PDGF, the TGF- β signaling is considered as one of the most important pathways driving HSC activation and fibrogenesis [133]. The TGF- β family comprises 33 members. While TGF- β 2 plays an important role in biliary fibrogenesis, TGF- β 1 is the most widely investigated isoform in liver fibrogenesis [134]. TGF- β is synthesized as a latent precursor by a variety of cells including endothelial cells, macrophages, and hepatocytes. Moreover, platelets were recently identified as an important source of TGF- β in the liver [135]. The inactive TGF- β molecules bind to the latency associated protein (LAP) and accumulate in the ECM and must be cleaved by specific proteases to become active. Endothelial cells participate in the conversion of TGF- β from the latent to the active form. Moreover, interactions with transmembrane integrins are considered as the principal activating mechanism for latent TGF- β [136]. The active form binds to and activates the TGF- β type II receptor (T β RII), which recruits the TGF- β type I receptor (T β RI). The downstream canonical signaling of TGF- β 1 converges on SMAD proteins.

The SMAD protein family can be classified into three groups based on their functions. The receptor-regulated SMADs (R-SMADs) include SMAD1, SMAD2, SMAD3, SMAD5, and SMAD8. The inhibitory SMADs include SMAD6 and SMAD7. SMAD4 is the only member of the third category, named common SMAD. R-SMADs are activated by phosphorylation at their C-terminus, i.e., pSMAD2 and pSMAD3, and form a complex with SMAD4, which translocates into the nucleus to regulate gene expression. SMAD3 is crucial for inducing HSCs activation and pro-fibrogenic gene transcription such as α -SMA or COL1A1 [116]. Of note, activation of the SMAD3-dependent TGF- β signaling in hepatocytes was also demonstrated to contribute to fibrosis development, especially in NASH, by inducing hepatocyte death and lipid accumulation [137]. In contrast to SMAD3, SMAD2 has no DNA binding capacity and is described as an anti-fibrotic molecule. The underlying mechanism could involve the ability of SMAD2 to induce TRAIL-mediated HSC apoptosis [138]. Moreover, SMAD6 and SMAD7, which negatively regulate TGF- β signaling, are considered as anti-fibrotic factors [139,140]. As a proof of concept, the group of Mertens showed that overexpression of SMAD7 in transgenic mice interferes with liver fibrosis progression and liver damage [141].

The canonical pathway in which SMAD3 is phosphorylated at its C-terminus (pSMAD3C) is described as the main fibrogenic pathway [60,142]. However, a non-canonical and pro-fibrogenic pathway was recently described, in which PDGF activates JNK that phosphorylates SMAD3 in its linker domain (pSMAD3L). pSMAD3L is able to rapidly translocate into the nucleus to stimulate HSC proliferation and induces a pro-fibrogenic response [143,144]. This non-canonical pathway is therefore crucial for the induction of ECM production and is now considered as an attractive therapeutic target [143]. Other studies have also identified TGF- β non-canonical pathways such as mitogen-activated protein kinase (MAPK), mammalian target of rapamycin (mTOR), PI3K/Akt, JAK1/STAT3, and Rho GTPase pathways. Both the canonical and the non-canonical pathways contribute to HSCs activation but also to macrophages activation and polarization [136]. TGF- β production is also associated with the activation of the connective tissue growth factor (CTGF) in HSCs and hepatocytes, a mitogenic factor playing an important role in liver fibrosis development [60]. Finally, it was shown that ROS can act as inducers or effectors of the TGF- β signaling and therefore generate a vicious cycle for fibrosis [145]. Moreover, high levels of TGF- β induce a massive hepatocyte cell death, contributing to chronic liver damage [88].

2.6.3 Oxidative Stress

Oxidative stress (OS) is a key process driving liver damage and initiation of liver fibrosis. It corresponds to an altered balance between cellular pro-oxidant and antioxidant factors, which results in ROS and reactive nitrogen species (RNS) production. ROS constitute a family of pro-fibrotic mediators including superoxides, hydrogen peroxide (H_2O_2), and hydroxyl radicals [146]. They are generated during normal cellular metabolism and in particular during oxidative phosphorylation and lipid peroxidation in hepatocytes, HSCs, and macrophages. At low levels, ROS can serve as secondary messengers to activate different cellular responses [147]. However, at high levels, they provoke disruption of cellular lipids, proteins and DNA and lead to hepatocyte necrosis and apoptosis. Moreover, ROS stimulate pro-inflammatory and pro-fibrogenic factor production by activated HSCs, Kupffer cells, and other pro-inflammatory cells [77,148]. ROS production is exacerbated by ethanol, FFA accumulation, iron deposit, and chronic viral infection [146,149,150].

The NADPH oxidases (NOXs) are a major source of ROS in the liver and mediate fibrogenic responses induced by angiotensin II, PDGF, and TGF- β in HSCs and macrophages [151,152]. Zhan et al. notably showed that phagocytosis of apoptotic bodies by HSCs following hepatocyte death results in NOX activation and collagen production [35]. Other studies demonstrated that the TGF- β -SMAD3 pathway increases NOX1 and NOX4 expression in HSCs, which correlates with the degree of fibrosis [153–155]. ROS signaling also regulates

the expression and the activity of the transcription factor NF- κ B. NF- κ B has a key role in the regulation of cell death, inflammation, and wound healing and is therefore an important modulator of liver fibrosis progression [156]. Indeed, several studies have shown that inhibition of NF- κ B activity protects from hepatic fibrosis in-vivo [157]. Moreover, in contrast to quiescent HSCs where NF- κ B activity is suppressed, myofibroblasts display a high NF- κ B activity, suggesting that NF- κ B activity is linked with HSC proliferation [156]. In line with this observation, it was demonstrated that Kupffer cell activation increases the activity of NF- κ B in HSCs, which in turn promotes pro-inflammatory cytokine secretion [87,156].

Over the last few years, epigenetic regulation of fibrosis progression has emerged as another process which orchestrates several aspects of the fibrogenic response in the liver (for a review, see [158]). Important epigenetic changes are induced by ROS in the HSCs, including chromatin remodeling by histone modification, DNA methylation and gene silencing by microRNAs (miRs) [158]. In-vitro and in-vivo approaches have demonstrated that HSCs show a global demethylation of fibrogenic genes during transdifferentiation into myofibroblasts, which is associated with liver fibrosis development [159–161].

2.6.4 The Inflammasome (NLRP3)-Caspase1 Pathway

Hepatic inflammation is a pan-etiology driver of hepatic damage and liver fibrosis. Inflammasomes are intracellular multiprotein complexes expressed in hepatocytes and NPCs including HSCs and Kupffer cells [162]. From the various inflammasomes, the NOD-like receptor (NLR) NLRP3 inflammasome is the best characterized. It has been shown to play a crucial role in the progression of NAFLD to NASH [163,164]. NLRP3 inflammasome consists of an intracellular multiprotein complex that activates caspase 1 by cleavage, which further cleaves pro-IL1 β and pro-IL18 into mature forms. IL1 β and IL18 are important mediators of the innate inflammatory response which initiate and perpetuate an abnormal wound-healing response and facilitate the progression of hepatic fibrosis.

Even if NLRP3 inflammasome activation in different cell types has not been completely elucidated, several evidences demonstrated that accumulation of toxic lipids and DAMPs- and PAMPS-mediated TLR signaling activates NLRP3 inflammasome [45,163,165]. It was notably demonstrated that TLR2 and palmitic acid cooperatively activate NLRP3 inflammasome in Kupffer cells and promote HSCs activation through pro-inflammatory cytokine secretion [166]. Moreover, it was speculated that phagocytosis of cholesterol crystals from hepatocytes can activate NLRP3 inflammasome in macrophages and may contribute to inflammation and fibrosis in NASH [47]. Finally, it was shown that activation of NLRP3 in hepatocytes results in pyroptosis, a form of programmed cell death involving caspase 1, liver inflammation, and fibrosis [167]. Therefore, blockade of NLRP3 pathway emerges as a novel therapeutic target to reduce liver inflammation and fibrosis in NASH [168].

2.6.5 Wnt/ β -Catenin Signaling

Physiologically, the Wnt/ β -catenin pathway is necessary for organ development. However, Wnt/ β -catenin signaling has also been associated with the development of fibrosis in different organs, including the liver [19]. β -catenin is a protein which acts as both adhesion molecule and transcription factor. Its expression is regulated by the Wnt protein. When the pathway is inactive, β -catenin level in the cytoplasm is regulated by a destruction complex which includes the glycogen synthase kinase 3 β and casein kinase 1 α . In contrast, when the pathway is active, Wnt binds the receptor Frizzled and the low-density lipoprotein-receptor-related protein 5/6 to form a complex, which inhibits β -catenin degradation. β -catenin in turn translocates in the nucleus to activate target genes transcription. However, β -catenin must recruit coactivators to be fully active, such as p300 or the cyclic AMP response element-binding protein-binding protein (CBP) [19]. During liver injury, the Wnt signaling is upregulated in the HSCs compared to quiescent cells and contribute to the pro-fibrogenic response by promoting α -SMA expression and collagen deposition [169].

3. Disease-Related Pro-fibrogenic Mechanisms in Chronic Liver Diseases

3.1 Chronic Hepatitis C

Chronic hepatitis C affects around 70 million people worldwide and still represents a leading cause of HCC and liver transplantation [170]. In most cases, infection by the hepatitis C virus (HCV) does not resolve spontaneously. Thus, approximately 80% of infected patients become chronic carriers and 20–30% develop liver cirrhosis within 25–30 years [171]. Chronic hepatitis C can now efficiently be cured by direct acting antivirals (for review see [172]). Chronic HCV infection induces hepatocyte cell death, that leads to release of DAMPs that can directly activate HSCs [31,35,77]. However, chronic inflammation due to antiviral immune response is still regarded as the most important driver of myofibroblast activation and ECM production in HCV infected patients [173]. Thus, immune response to HCV infection results in enhanced secretion of multiple growth factors, inflammatory cytokines, and chemokines by Kupffer cells and lymphocytes [174,175]. Moreover, HCV replicating hepatocytes have been shown to secrete pro-fibrogenic cytokines [176].

HCV viral proteins have also been shown to directly modulate signaling and metabolic pathways implicated in fibrogenesis. Thus, several studies indicate activation of HSCs into myofibroblasts by the HCV core protein, as well as non-structural HCV proteins. In fact, HCV core protein activates HSC proliferation in an Ras/ERK and PI3K/AKT dependent manner. The non-structural NS3 and NS5 proteins on the other hand induce inflammatory signaling pathways, including NF- κ B [177]. Moreover, hepatocyte expression of HCV core protein is associated with decreased intracellular and mitochondrial glutathione levels, an important antioxidant [178,179]. Further promoting oxidative stress, the HCV protein NS3 can directly activate NOX2 in Kupffer cells and T cells [149,180]. The HCV envelope protein E2 on the other hand has been shown to bind to CD81 on HSC and activates MMP2, which have been hypothesized to promote inflammatory infiltration and enhanced parenchymal damage due to degradation of normal hepatic ECM [181]. Finally, human myofibroblasts have been reported to express HCV host factors and to be permissive to HCV. Increased proliferation and collagen production in these cells indicates further potential direct pro-fibrogenic effects of HCV on these fibrosis-driving cell population [182].

While cure of HCV infection has been shown to reduce liver disease complications and HCC risk, a significant risk to develop HCC persists in advanced fibrosis [183,184]. Several studies have shown that chronic HCV infection results in persistent epigenetic and transcriptional changes associated with the stage of fibrosis and HCC risk [185,186], suggesting that viral cure only partially eliminates the virus-induced pro-fibrogenic and carcinogenic drivers particularly in advanced fibrosis [187].

3.2 Chronic Hepatitis B

Despite the presence of an efficient vaccine, chronic HBV infection still affects currently approximately 260 million people, mostly in Africa and Asia [188]. While horizontal transmission of adults often results in self-limiting acute infection, vertical transmission mostly leads to chronic infection [189,190]. Currently available therapeutic therapies for chronically infected patients include interferon-based therapies and several nucleos(t)ide analogues. While nucleos(t)ide analogues rarely result in viral cure, suppression of viral replication slows down disease progression, that can eventually end in liver cirrhosis and HCC [191]. As in chronic hepatitis C, chronic hepatitis B triggers HSCs activation via DAMPs release and the host antiviral immune response leading to chronic inflammation [31,35,76,77,192]. However, in contrast to HCV, the direct involvement of HBV infection in HSC activation remains less defined. A recent study showed that the HBV encoded x protein (HBx) induces overexpression of the special AT-rich binding protein 1 (SATB1) in hepatocytes, which in turn promotes the activation and proliferation of HSCs through the secretion of CTGF and PDGF [193]. Moreover, Liu et al. observed that HBV can transiently infect and replicate in cultured HSCs in-vitro and that production of HBV S protein (HBs) affects their proliferation and expression of collagen type I [194]. Moreover, a direct activation of Tregs by HBx was observed in HBV-infected patients [105,106]. While pharmacological control of HBV infection markedly reduces liver disease progression and HCC risk, the absence of effective curative therapies still poses a challenge for the long-term management of patients [195].

3.3 Alcoholic Liver Disease

Alcoholic liver disease is a major cause of liver fibrosis world-wide. Chronic alcohol intake activates pro-fibrogenic mechanisms: the metabolism of alcohol in hepatocytes to acetaldehyde causes release of ROS, that can activate HSCs in a paracrine way [196]. Moreover, the ethanol metabolite acetaldehyde itself is fibrogenic and induces secretion of TGF- β [197]. Furthermore, both collagen type 1 genes have acetaldehyde-responsive elements that allow acetaldehyde-induced collagen expression in HSCs within hours [197,198]. Several studies further indicate alcohol-induced apoptosis of hepatocytes as a mechanism of liver fibrosis. Thus, hepatocyte apoptosis increases upon alcoholic liver injury [199], which not only induces production of chemokines and pro-inflammatory cytokines that activate HSCs [200] but also induces phagocytosis of the apoptotic bodies by Kupffer cells, that become pro-fibrogenic and release HSC activating cytokines as TNF α and TGF- β [36,201–203]. Finally, chronic alcoholic intake has been correlated with suppression of innate immunity [204–206]. Innate cytokines [207], natural killer (NK) cells [208], and macrophages [209] have been reported to inhibit liver fibrosis by clearance or inactivation of HSCs and therefore may underlie decompensation of the physiological balance of pro- and anti-fibrogenic mechanisms in chronic ASH.

3.4 Non-Alcoholic Liver Disease

NAFLD represents the fastest growing etiology of chronic liver disease and currently affects 15–30% of the global adult population [210] with expected further exponential increase within the next years [211]. NASH describes currently the inflammatory form of NAFLD characterized by disease progression and increased HCC risk. For many years, diagnosis of NASH required the exclusion of other potential triggers of chronic liver disease as alcohol abuse or viral infection. However, due to the variety of etiologies and pathologies there is overlap. Recently, another term “metabolic associated fatty liver disease (MAFLD)” has been suggested as a more appropriate and defining nomenclature for the heterogeneous population of patients with this disease. By avoiding the description “non-alcoholic”, this new terminology is supposed to address the high prevalence of co-existing toxic (e.g., alcohol) or viral contributors that do not exclude the affiliation to a metabolic liver disease [212]. Instead, thorough patient stratification according to present risk factors and chronic liver disease contributors should be performed to allow preventive and therapeutic recommendations that address the underlying disease in its whole complexity [212].

HSCs activation by oxidative stress and inflammation plays a leading role in NASH disease progression and fibrosis development [213]. Accelerated by insulin resistance accumulating metabolites of saturated fatty acids cause lipotoxicity that damages hepatocytes and results in oxidative stress [214, 215]. Hepatocyte released DAMPs activate Kupffer cells via TLR and hereby create a pro-inflammatory microenvironment that promotes a HSC activating fibrogenic adaptive immune response [216]. Moreover, it has been shown that the high levels of oxidative stress in NASH hamper the physiologic regenerative proliferation of mature hepatocytes [217] and triggers recruitment of hepatic progenitor cells. These cells form the so called ductular reaction at the interface of hepatocytes and the biliary tree and are able to differentiate into both hepatocytes and cholangiocytes [218]. Of note, pro-fibrogenic cytokines, including TGF- β have been shown to be released by the ductular reaction [219]. Moreover, it has been shown that cholangiocytes can transform into collagen-producing myofibroblasts by EMT [220]. Further highlighting the potential role of HPC expansion/ductular reaction in NASH associated fibrosis progression, portal fibrosis that represents a key feature in progressive NASH livers correlates with the extent of ductular reactions and the degree of fibrosis [221]. However, demonstrating ECM accumulation and myofibroblast activation prior to PLC expansion in a murine mouse model of NASH, Van Hul et al. elegantly indicated LPC expansion to be only part of the complex pathogenesis of fibrosis in NASH, that is further depending on the inflammatory microenvironment [222]. While there is a large pipeline of compounds for treatment of NASH, there are currently no approved therapies [223].

4. Resolution of Liver Fibrosis

Progression into liver fibrosis and cirrhosis account for high morbidity and mortality in patients with chronic liver diseases, causing substantial economic burden. Patients with compensated liver cirrhosis have a 2–7% risk for hepatic decompensation and 1–7% risk of HCC development per year [224]. In NASH patients, fibrosis is the only histological feature that independently correlates with clinical outcomes [225–227]. Emphasizing the urgent need for efficient anti-fibrotic drugs, liver cirrhosis is currently the 11th most frequent cause of death worldwide [1].

Removal of the main inducer of chronic inflammation have been shown to be able to induce regression of advanced liver fibrosis (up to Metavir stages 3 and 4) due to chronic HBV and HCV infection [228–230]. However, approximately 15% of patient with chronic viral liver infection do not show any reversal in liver fibrosis despite sustained viral response [228,229]. In metabolic liver disease, lifestyle changes and bariatric surgery can induce regression of histological fibrosis [231], however, licensed therapeutic compounds for NASH are absent. Finally, spontaneous resolution after removal or treatment of the trigger of chronic inflammation occurs slowly and may not prevent life-threatening complications. Thus, besides causal therapies of underlying pathologies of chronic liver disease, anti-fibrotic strategies are needed to inhibit trigger-dissociated progression of liver fibrosis and to accelerate fibrosis resolution.

4.1 Molecular Mechanisms of Fibrosis Regression

Fibrosis regression is associated with inactivation or apoptosis of HSCs and myofibroblasts [56,232]. Thus, whereas increased cell death in hepatocytes contributes to fibrogenesis, cell death in HSCs is an important mechanism for the resolution of liver fibrosis. Indeed, TRAIL-mediated HSCs apoptosis is associated with an improvement of liver fibrosis [233–235]. Dissolution of the fibrotic scar is mainly mediated by macrophages that secrete the matrix-degrading enzymes collagenase and MMPs [10,16]. Macrophages associated with the resolution of hepatic fibrosis have been termed scar-associated macrophages (SAMs) and exhibit a phenotype outside the M1/M2 classification [16]. Thus, while pro-fibrotic macrophages have been characterized by a high expression of Ly-6C or Gr1 [16], CD11b^{neg} macrophages with low expression of Ly-6C are associated with MMPs production and fibrosis resolution [236,237]. Using single-cell RNA-Seq of patient-derived liver tissue, Ramachandran et al. elegantly demonstrated that distinct macrophage subpopulations inhabit the fibrotic niche [238]. Moreover, they identified a novel scar-associated TREM2⁺ CD9⁺ subpopulation of macrophages with a hybrid phenotype, which expands in liver fibrosis and is pro-fibrogenic. In addition to macrophages, NK cells exhibit an anti-fibrotic activity by mediating HSCs apoptosis through the production of interferon gamma (IFN γ) [239–243]. Moreover, activation of NK cells and their cytolytic activity are important to control premalignant cell growth in fibrotic environment [244].

4.2 Candidate Targets and Pathways for Therapeutic Intervention

Generally, anti-fibrotic therapies can be divided into agents that mediate its anti-fibrotic effects by i) hepatocyte protection, ii) inhibition of HSC activation and fibrotic scar evolution, or iii) immune modulation (for recent reviews see [24] and [245]). Moreover, several phytodrugs have been characterized to potentially exert multidimensional protective effects on liver fibrosis progression [246,247].

However, despite numerous preclinical and clinical trials, to date, no Food and Drug Administration (FDA)-approved anti-fibrotic drugs exist and the only available curative treatment option for patient with advanced liver cirrhosis is liver transplantation [248]. Examples of anti-fibrotics, that are currently in clinical trial are reviewed in the following and further summarized in Tables 1–3.

4.2.1 Hepatic Protection via Inhibition of Apoptosis

Hepatocyte cell death by apoptosis is a major trigger of inflammation and HSC activation in the evolution of liver fibrogenesis in all etiologies [249,250]. Accordingly, inhibition of hepatocyte apoptosis decreased HSC activation in animal models of liver fibrosis [251,252]. Following a promising pre-clinical study in a carbon tetrachloride (CCl₄)-based liver fibrosis rat model [253], just recently two randomized placebo-controlled trials investigated the pan-caspase inhibitor Emricasan in NASH patients with F1-F3 fibrosis [254] or cirrhosis with severe portal hypertension [255]. Garcia-Tsao et al. reported small reductive effects on hepatic venous pressure gradient (HVPG) in cirrhotic NASH patients [255]. No effects were seen in patients with acutely decompensated cirrhosis [256]. In contrast, 72 week administration of Emricasan in patients with NASH-associated F1-F3 fibrosis did not improve liver inflammation or fibrosis but rather tended to worsen hepatocyte-ballooning, potentially due to activation of other mechanisms of cell death and necrosis [254]. Results from a recently completed clinical trial of Emricasan in the setting of post-transplant HCV-induced fibrosis after SVR are awaited 2020 (NCT02138253).

Another approach to reduce liver injury associated hepatocyte cell death is to inhibit stress signals. Apoptosis signal-regulating kinase (ASK1) belongs to the MAPK pathways and is involved in hepatocellular apoptosis, inflammation and fibrosis [257–259]. The selective ASK1 inhibitor Selonsertib improved fibrosis in a murine NASH model [257]. In a multicenter phase II clinical trial, 24 week treatment of patients with NASH F2-3 improved histological degree of fibrosis [260]. However, considering frequently reported improvement of fibrosis due to enforced patient's compliance and therapeutic monitoring, the absent inclusion of a placebo-control group in this study substantiates the need for further confirmatory studies. Phase 3 clinical trials in patients with NASH associated F3 (NCT03053050) and F4 fibrosis (NCT03053063) have just been completed and results are awaited to be published in 2020.

4.2.2 Hepatic Protection via Reduction of Oxidative Stress

Oxidative Stress is one of the major drivers in liver fibrosis progression, especially in NASH [261]. Consequently, several strategies to reduce oxidative stress have been developed and investigated in terms of anti-fibrotic potency [262–265]. NOXs are membrane-bound enzyme complexes that catalyze the reduction of NADH, hereby producing superoxide radicals. NOX 1, 2, and 4 exert key roles in the activation of HSCs during liver fibrogenesis [155,266] and NOX4 is involved in hepatocyte apoptosis [155]. GKT137831, a dual NOX1/4 inhibitor suppressed ROS production in HSCs in-vitro and in-vivo and significantly attenuated liver fibrogenesis in CCl₄ and bile duct ligation based mouse models of liver fibrosis [267]. According to a first interim analysis of a phase 2 clinical trial in patients with primary biliary cholangitis, GKT137831 showed significant effects on serological cholestasis parameters. Publication of effects on additional endpoints, including fibrosis after a treatment duration of 24 weeks are expected to be published soon (NCT03226067).

4.2.3 Hepatic Protection via Restoration of Gut Microbiome

Considering the pathophysiological implication of gut dysbiosis in chronic liver disease progression and fibrogenesis, numerous studies investigated the potential of probiotics, prebiotics, and fecal microbiota transplantation for anti-fibrotic therapy [268]. Probiotics are living micro-organisms and prebiotics are indigestible food ingredients that are supposed to improve or restore the gut microflora. Confirming the pathological relevance of gut dysbiosis in chronic liver diseases, prebiotics and probiotics have shown protective effects on steatosis and liver inflammation in animal models of chronic liver injury [269–272]. In line with the pre-clinical data, VSL#3, the most studied probiotic formulation, showed potential anti-inflammatory and insulin-sensitizing effects according to a meta-analysis in NASH/NAFLD patients [273]. Recently, Bajaj et al. reported association of a diet rich in cereals, fermented milk, vegetables, and coffee/tea, with microbial diversity and lower risk of hospitalization in cirrhotic patients [125]. However, evidence for systematical clinical application of pro- and prebiotics is still lacking due to limitations of clinical studies in sample size, placebo-control and precise information regarding patients' diet and lifestyle [268].

Fecal microbiota transplantation (FMT) describes the transfer of a fecal suspension from a healthy donor into the intestine of a patient. Interestingly, FMT reduced liver injury in a mouse model of alcohol-induced chronic liver disease [269]. Moreover, FMT was superior to probiotics in prevention of hepatic encephalopathy

due to protective effects on intestinal mucosal barrier function [274]. Few small clinical trials further indicated potential protective effects of FMT on chronic liver disease progression. Thus, Philips et al. reported single FMT in patients with severe ASH to reduce hepatic inflammation and improve survival during one year of follow-up [275]. Moreover, a randomized clinical trial with 20 patients with cirrhosis and recurrent hepatic encephalopathy revealed improved cognition and reduced hospitalizations following FMT compared to standard care [276]. However, lethal *Escherichia coli* bacteremia have been reported in patients that have undergone FMT [277]. Thus, further studies are needed to evaluate the potential and especially safety profile of FMT in chronic liver disease patients that are at high risk of bacteremia due to bacterial translocation.

4.2.4 Hepatic Protection via Lipid-Lowering Agents

Statins are widely used lipid-lowering agents that decrease serum cholesterol levels by inhibition of the activity of 3-hydroxy-3-methylglutaryl co-enzyme A reductase [278]. Considering its lipid lowering properties, several studies addressed the consequential hypothesis of statins to decrease experimental liver steatosis with controversial results [279–281]. However, recent evidence for independent pleiotropic effects of statins on chronic liver diseases have led to increasing interest among hepatologists (for a recent review see [282]). Thus, several studies on animal models of liver fibrosis reported statins to decrease oxidative stress, hepatic inflammation, and fibrogenesis [283–285]. Moreover, retrospective analyses of patients with chronic liver diseases and hypercholesterolemia indicated statin-use revealed association with reduced risk of disease progression, as well as complications, including HCC development [286]. Moreover, several retrospective cohort studies and randomized controlled trials reported reduced HVG and decreased risk of decompensation, HCC development and death in statin-treated patients with liver cirrhosis of different etiologies [287–289]. Finally, statins are described to exert beneficial effects on cardiovascular mortality and morbidity, that is especially of interest in patients with NASH [290].

Despite consistent data indicating potential anti-fibrotic effects, validity of these studies is limited due to retrospective design and lack of hard clinical endpoints, e.g., histological assessment of fibrosis. Moreover, considering drug-induced hepatotoxicity as a rare, though well-described side effect of statin as well as increased risk of rhabdomyolysis in patients with chronic liver disease due to impaired CYP3A4 metabolism in the liver, the safety profile of statins in patients with chronic liver disease and liver cirrhosis needs to be evaluated in detail. Thus, just recently Pose et al. reported rhabdomyolysis requiring treatment discontinuation in 19% (3/18) of patients with decompensated liver cirrhosis and treatment with 40mg simvastatin per day compared to 14% in 20mg simvastatin or placebo treated patients, respectively [291]. Another study reported severe rhabdomyolysis in 3% of patients with liver cirrhosis and statin use [289]. Taken together, growing experimental and clinical evidence suggest statins to exert beneficial pleiotropic effects on chronic liver disease progression and fibrosis. However, large prospective placebo-controlled trials with strong clinical endpoints as well as extended safety evaluation are awaited before recommendation of statins in patients with liver fibrosis (NCT03780673; NCT02968810; NCT04072601).

4.2.5 Inhibition of HSC Activation

Numerous studies indicate Wnt/ β -catenin signaling to be implicated in HSC activation and to contribute to liver fibrosis [169,292,293]. ICG-001 is a small molecule inhibitor that specifically disrupts the interaction between CBP and β -catenin. Initially developed for colon cancer therapy, ICG-001 [294] has been tested in several fibrosis studies and has been shown to inhibit TGF- β mediated upregulation of α -SMA and collagen 1 in mouse fibroblasts and human HSCs. Moreover, ICG-001 administration in a murine CCl₄ induced mouse model of fibrosis attenuated HSC activation and ECM accumulation. Mechanistically, ICG-001 was found to affect macrophage infiltration and thereby reduce hepatic inflammation by affecting Wnt-dependent secretion of CCL12 by HSCs [295]. Apart from the liver, ICG-001 has also been reported to suppress pulmonary [296] and renal interstitial fibrosis [297].

As another member of CBP/ β -catenin inhibitors, PRI-724 have been shown to inhibit HSC activation and collagen production in HCV transgenic mice [298]. Moreover, an independent study reported anti-fibrotic effects of PRI-724 in CCl₄ induced murine liver fibrosis. In addition to confirmation of suppressed HSC activation, this study further indicated improved fibrosis resolution due to an increased F4/80+ CD11b+ and Ly6C low

CD11b+ macrophage population [11,299]. In a NASH mouse model, PRI-724 was shown to decrease hepatocyte apoptosis as well as fibrosis degree. Similar observations in CBP KO mice highlighted the CBP/ β -catenin specific anti-fibrotic mode of action of PRI-724 [300]. A single-center, open label phase I clinical trial of PRI-724 in patients with HCV-associated liver cirrhosis showed dose dependent histological improvement (> 2 points decrease in histologic activity index score) in 3/12 patients, but deterioration by 2 points in 2/12 patients. A phase I/IIa clinical trial of PRI-724 in patients with hepatitis B or C related liver cirrhosis is expected to be completed in July 2020 and will further clarify the yet uncertain potential of PRI-724 in fibrosis treatment (NCT03620474).

FXR ligands have first been developed in the context of cholestatic liver diseases, as primary biliary cirrhosis. Thus, primary bile acids bind to FXR, that heterodimerizes with the retinoid X receptor, resulting in activation of its function as a transcription factor. FXR activation in hepatocytes and enterocytes hereby downregulates bile acid production, export as well as enteral and hepatic uptake. Moreover, it protects the intestinal mucosal barrier contributing to maintenance of the physiological gut microbiome and ultimately homeostasis of the liver-gut axis. FXR agonists such as obeticholic acid (OCA), may support reconstitution of gut microbiome composition, reduce bacterial translocation and inflammation [301,302]. Moreover, interfering the physiological feedback control system of bile acid production, synthetic FXR agonists as OCA have been developed and shown anti-cholestatic potency, leading to its approval for second-line treatment in PBC [303,304]. Recent clinical studies further indicate improvement of histological features, including fibrosis in patients with PBC after long-terms OCA treatment [305]. Moreover, FXR has been described to mediate inhibitory effects on HSCs activation [306]. Investigation of OCA in animal models of fibrosis further emphasized anti-fibrotic activity of FXR activation [306–308]. In 2015, the FLINT study, a phase 2b clinical trial reported histological improvement of fibrosis in NASH patients after short-term treatment with OCA for 72 weeks [309]. Just recently the first 18 month interim results of a multicenter, randomized placebo-controlled phase 3 clinical trial of long-term OCA treatment in NASH patients with fibrosis F1-F3 (NCT02548351) have been published and reports dose-dependent improvement of fibrosis in 23% of OCA 25 mg treated compared to 12% placebo treated participants. Moreover, OCA-treated patients showed less hepatocellular inflammation and ballooning. Reports regarding impact on non-invasive markers of fibrosis, long-term safety as well as clinical outcomes of this ongoing clinical trial (NCT02548351) are awaited in the future [310].

4.2.6 Reduction of Fibrotic Scar evolution and Contractility

In liver cirrhosis up to 50% of the livers' dry weight consists of collagens [311]. Collagen 1 (Col1) represents the most abundant collagen in fibrotic livers [312]. Jimenez et al. reported specific inhibition of Col1A1 siRNA containing lipoplexes in mouse models of liver fibrosis. Parenteral treatment hereby led to a 90% decrease in collagen production and 50% decrease of total collagen accumulation [313]. Another study on transgenic mice with inducible Col1 knockdown further reported additional anti-inflammatory effects [314]. Hsp47 is a Col1 chaperone and knockdown by siRNA can be used to block collagen synthesis. In order to target mainly fibrosis-effector cells, Sato et al. used Hsp47 siRNA containing vitamin A-coupled liposomes, which are predominantly uptaken by HSCs and achieved significant anti-fibrotic effects in 3 in-vivo models of liver fibrosis [315]. A clinical trial, investigating BMS 986263, an HSP47 siRNA delivering Lipid Nanoparticle, did not reveal any toxicity in healthy humans [316]. A phase 1b/2 open label dose escalation study of BMS 986,263 has recently been completed (NCT02227459). More studies on collagen inhibitors are expected to start in the next years.

Lysyl oxidases (LOXs), that are secreted by HSCs or MFs deamidate lysine or hydroxylysine residues in collagen or elastin and hereby crosslink collagen with each further [317,318]. These enzymes are therefore contributing to the stiffness of the ECM and impair degradation of deposited collagen fibrils by MMPs [319,320]. ECM stiffness in turn further promotes proliferation and activity of myofibroblasts via integrins [319,321]. LOX enzymes further exert functions on gene regulation [322], receptor function, and growth factor activity [323]. In fact, LOX enzymes impact on Collagen 3 expression [322]. Moreover, LOX members have been shown to oxidize PDGFR β , thereby increasing the affinity to its ligand [324]. Development of liver fibrosis in a CCl₄ based mouse model was shown to be accompanied by a 30-fold increase in LOX activity. Inhibition of all LOX members by β -aminopropionitrile decreased number and activity of MFs leading to a lower degree of liver fibrosis in this CCl₄ induced liver fibrosis mouse model [325–327]. However, despite promising results in a mouse model of

liver fibrosis [328], clinical trials investigating the LOXL2 blocking antibody Simtuzumab in patients with NASH, human immunodeficiency virus (HIV), or HCV-associated liverfibrosis as well as primary sclerosing cholangitis gave only disappointing results with no effect on liver fibrosis [329–331]. A later study showing rapid downregulation of LOXL2 after liver injury in contrast to stable upregulation of LOX and LOXL1, suggests a rather minor role of LOXL2 in liver fibrosis [317]. Future studies should address this observation by specific targeting of LOX or LOXL1.

4.2.7 Immune Modulation

Considering macrophages as the first pro-inflammatory response to liver injury [15,332,333], modulation of their first innate immune response represents a potential target for anti-fibrotic treatment approaches. Reduction of pro-inflammatory macrophage recruitment, using a dual CCR2/CCR5 inhibitor (Cenicriviroc) revealed anti-fibrotic effects in animal models of liver fibrosis [334–336]. Anti-fibrotic efficacy was also reported in a phase II clinical trial (CENTAUR; NCT02217475 [337]) of Cenicriviroc in NASH patients. In fact, especially patients with high disease activity and fibrosis stage benefit from oral Cenicriviroc treatment for 2 years. Surprisingly this was not accompanied by an anti-inflammatory activity [338]. Cenicriviroc was well tolerated, regardless of hepatic insufficiency. Headache and gastrointestinal disorders of mild severity were most frequent adverse events [338,339]. A phase 3 study on patients with advanced fibrosis and cirrhosis will further unravel the potency of CCR2/CCR5 inhibition for fibrosis therapy (AURORA; NCT 03028740).

Galectins are carbohydrate-binding proteins that get secreted by different cell types upon liver injury [340]. Extracellularly, these proteins bind to components of the ECM or to cell surface receptors [341,342]. Several studies indicate increased levels of galectin in inflammatory, fibrotic, or malignant liver tissue [343–345]. Due to its anti-apoptotic, cell differentiating and chemotactic properties, especially Gal-3, that is mainly secreted by activated macrophages, is involved in the pathophysiology of liver fibrosis [346–348]. Belapectin, an inhibitor or galectin-3 has shown potent anti-fibrotic efficacy in mouse and rat models of liver fibrosis [349,350] and was well tolerated in a phase 1 clinical trial [351]. However, just recently published results of a phase 2b placebo-controlled clinical study of belapectin in patients with NASH and liver fibrosis showed no effect on fibrosis following treatment for 52 weeks [352]. Still, considering significant protective effects on hepatocyte ballooning as well as significant lower HPVG and varices development in a subgroup of patients with NASH cirrhosis, a phase 3 clinical study in patients with NASH cirrhosis without varices at baseline timepoint is currently being initiated. The medication was well tolerated by NASH patients. Most frequently reported mild-moderate adverse events included infections, gastrointestinal, and musculoskeletal, as well as connective tissue disorders [352].

4.2.8 Phytodrugs with Multi-Dimensional Effects on Liver Fibrosis

Several studies investigated herbal formulations and phytodrugs in treatment of liver fibrosis. Among many other phytochemicals, resveratrol, silymarin, and curcumin are the most extensively studied phytodrugs with potential anti-fibrotic activity [246,247].

Resveratrol is a natural antioxidant that can be found in a wide variety of plants. Frequently reported beneficial effects of resveratrol on health have been attributed to its mimicry of calorie restriction via activation of AMP-activated kinase (AMPK), nuclear factor (erythroid-derived)-like 2 (Nrf2), and nicotinamide adenine dinucleotide NAD⁺-dependent deacetylase (SIRT1) [353–355]. Treatment with resveratrol improves NASH and chronic liver disease in mouse models [264,353,356]. In NAFLD patients, a randomized, double-blinded clinical trial of oral resveratrol supplementation compared to placebo for 12 weeks revealed significant protective effects on markers of liver inflammation (serum level of alanine aminotransferase, NF- κ B activity) and hepatic steatosis grade, but not on fibrosis [357].

Silymarin is an extract of the milk thistle (*Silybum marianum*), consisting of a mixture of different flavonoids and is applied as a supportive, hepatoprotective medication in patients with liver cirrhosis, chronic inflammatory, and toxic liver diseases since ages [358]. The consideration as a hepatoprotective agent is due to experimental data indicating potential prevention of hepatic injury by toxins and deceleration of fibrosis progression by the main

ingredient, silibinin [359,360]. Moreover, long clinical experience exists for silymarin in prevention of alpha-amanitin-induced hepatotoxicity [361]. Thus, silibinin is regarded as a specific antidote of amanitin [362]. In terms of therapeutic application, small clinical studies reported anti-viral, anti-oxidative, anti-inflammatory, and insulin-sensitizing effects of silymarin in different etiologies of chronic liver disease, including ALD, NASH, and viral hepatitis [363–366]. Thus, silymarin administration for four weeks reduced oxidative stress, fibrosis score, and activation of HSCs as well as Kupffer cells in a CCl₄ based rat model of liver fibrosis [367,368]. However, in clinical practice low water solubility and limited oral bioavailability due to poor enteral absorption (23–47%) and high first-pass metabolism in the liver hamper use of silymarin [359,369]. Recently, new formulations of silymarin, including complexes with phosphatidylcholine and glyco-conjugates, have bypassed these limitations in oral application [370]. First studies using orally bioavailable silybin-vitamin E-phospholipids complexes for 12 months showed potential effects on hepatocyte ballooning, steatosis and liver fibrosis in 180 patients with NAFLD or NASH and 36 patients with HCV [371]. However, large double-blind, placebo-controlled studies of silymarin in treatment of chronic liver diseases are still missing, but needed to define its clinical value in not only supportive but also therapeutic applications [358].

Curcumin, the active compound of *Curcuma longa* have been investigated in several medical diseases and reported to exert tumor preventive, antiviral and anti-inflammatory effects in chronic liver disease [372,373]. Thus, curcumin administration inhibited hepatic inflammation, steatosis, fibrosis development, and progression in NASH in-vivo models [374,375]. Few clinical studies exist regarding the therapeutic potential of curcumin in chronic liver diseases. As observed for silymarin, curcumin is characterized by low oral bioavailability [376]. However, two independent randomized, placebo-controlled clinical trials reported decrease of biochemical and ultrasonographic markers of liver inflammation and steatosis by short-term curcumin administration (500–1000 mg/d) in 87 and 80 patients with NAFLD, respectively. Considering the low bioavailability of curcumin, these clinical effects are thought to be mediated by its metabolites [377,378]. Nevertheless, absent histological evaluation of changes following curcumin treatment strongly limits impact of the studies especially in terms of their anti-fibrotic capacity [379,380]. Moreover, a recent placebo-controlled clinical trial investigating lifestyle modification plus curcumin supplementation vs. placebo in 50 patients with NASH did not find significant advantages of curcumin in amelioration of biochemical and sonographic liver inflammation, steatosis, and fibrosis compared to lifestyle intervention alone [381]. Well-designed randomized placebo-controlled trials including histological examination are needed to define curcumin's significance in clinical practice.

4.3 From Mouse to Men: Challenges in the Clinical Development of Anti-Fibrotic Compounds

The largely disappointing results of clinical phase 2 and 3 trials contrasts a long pipeline of promising anti-fibrotic candidate agents in preclinical models. This indicates the yet insufficient investigation or representation of disease biology by cell culture and animal models of fibrosis. Thus, conventional cell culture models of fibrosis do not recapitulate the multicellular and multidirectional evolution of fibrosis in humans. In fact, some agents have strong inhibitory effects on HSCs and myofibroblasts but mediate pro-fibrogenic mechanisms in other liver cells. Moreover, animal models of liver fibrosis have been shown to only partially reflect the human disease and reliable fibrotic readouts have long been undefined. In the past years, more and more guidelines for pre-clinical investigation and validation of potential anti-fibrotic agents have been proposed [24]. Thus, investigation of anti-fibrotic drugs in 2–3 validated and complementary fibrosis models are recommended. Widely accepted experimental approaches are CCl₄ or Thioacetamide (TAA)-induced fibrosis, nutritional models mimicking NASH or biliary models [24,382,383]. Moreover, novel 3D in-vitro models that incorporate multiple parenchymal and non-parenchymal cell types as well as the fibrosis-driving fibrotic ECM itself are more and more established [20,384,385]. Consideration of the complex disease pathophysiology, implementation of complementary cell culture, and animal models of liver fibrosis as well as use of validated endpoints will hopefully revolutionize future anti-fibrotic opportunities.

5. Conclusions

Despite different mechanisms of primary liver injury, the progression of fibrotic liver disease follows shared patterns across the main liver disease etiologies. For all the etiologies, the development of hepatic fibrosis is

initiated in response to hepatocytes or cholangiocytes damage, while progression of the fibrotic disease is mainly driven by dysregulated inflammatory processes. Thus, chronic viral infection triggers robust immune responses leading to chronic inflammation and hepatocyte death. The progression of ALD and NASH is marked by the accumulation of fat in the liver leading to hepatocyte apoptosis and oxidative stress. Repetitive peaks of inflammation, followed by anti-inflammatory, reparative immune responses activate collagen-producing myofibroblasts that account for excessive accumulation of ECM, the cellular correlate of tissue fibrosis. Removal or elimination of the initial trigger such as viral cure may slow down or reverse liver fibrosis, but mostly occurs often too slowly or too infrequent to avoid life-threatening complications in particular in late-stage disease. While many anti-fibrotic candidate agents have shown robust effects in experimental animal models, their anti-fibrotic effects in clinical trials are less clear. The fact that selected anti-fibrotic agents have shown evidence for potential effect on fibrosis progression in clinical trials, suggests that it is possible to target liver fibrosis by pharmacological intervention. However, additional clinical studies are needed to confirm the long-term impact and robustness of these findings. Given the still limited clinical efficacy and adverse effects of the current compounds in clinical development, there is a high unmet medical need for more efficient and safe anti-fibrotic drugs to significantly improve the patients' outcome. The recent development of innovative patient-derived models for liver fibrosis may advance the development of compounds with anti-fibrotic properties in the future.

Table 1. Examples for compounds in clinical development aiming to reduce fibrosis by inhibition of hepatocyte apoptosis and reduction of oxidative stress.

Anti-fibrotic Mechanism	Agent	Rationale	Molecular Mode of Action in Preclinical Studies	Key Findings in Clinical Trials
Inhibition of hepatocyte apoptosis	Pan-caspase inhibitor Emricasan	Hepatocyte apoptosis is a major trigger of inflammation and HSC activation [249,250].	Decreased HSCs activation and improvement of liver function in ratCCl ₄ model [253]. No effects in patients with acutely decompensated cirrhosis [256].	Phase 2: Improvement of liver inflammation or fibrosis and tendency towards worsening of hepatocyte ballooning in NASH patients with F1-F3 fibrosis [254]. Small reductive effect on HVPg in cirrhotic NASH patients [255]. NCT02138253: clinical trial of Emricasan in the setting of post-transplant HCV-induced fibrosis after SVR: awaited 2020.
	ASK1 inhibitor, selonsertib	Mediation of hepatocyte apoptosis via activation of JNK and p38 MAP kinases [257].	Improvement of steatosis and fibrosis in NASH mouse model [257].	Phase 2: Improvement of histological degree of fibrosis in patients with NASH F2-3 [260]. Decrease of liver stiffness by MRE and improvements of non-invasive markers of fibrosis and inflammation [386]. Phase 3: STELLAR-3 and 4: Selonsertib in NASH patients and bridging fibrosis or cirrhosis: ongoing (NCT03053050; NCT03053063)
Reduction of oxidative stress	Natural antioxidant with several targets, Resveratrol	Anti-inflammatory and antioxidant activity	Resveratrol reduces inflammation, fibrosis [264] as well as steatosis [387] in a mice models of NASH.	Phase 2: significant protective effects of resveratrol on markers of liver inflammation and hepatic steatosis grade within 12 weeks of treatment, no effect on fibrosis [357].
	Dual NOX1/4 inhibitor, GKT137831	Activation of HSCs (NOX1) and induction of apoptosis in hepatocytes (NOX4) by production of superoxide radicals [155,266].	Anti-fibrotic effect in CCl ₄ and bile duct ligation based mouse models of liver fibrosis via suppression of ROS production in HSCs in-vitro and in-vivo [267].	Phase 2: significant effects on serological cholestasis parameters after 6 weeks of treatment in PBC. Ongoing study (NCT03226067).

Table 2. Examples for compounds in clinical development aiming to reduce fibrosis by inhibition of HSC activation and reduction of fibrotic scar evolution.

Anti-fibrotic Mechanism	Agent	Rationale	Molecular Mode of Action in Preclinical Studies	Key Findings in Clinical Trials
Inhibition of HSC activation	FXR agonist, Obeticholic acid	Transcriptional regulation of fibrogenic genes in HSCs [306]. Improvement of intestinal mucosal barrier and homeostasis of gut-liver axis [301,302].	Downregulation of collagen 1 synthesis in HSCs, potent anti-fibrotic effect in animal models of liver fibrosis [306].	Phase 2: Improvement of fibrosis after 72 weeks treatment with OCA [309] Phase 3 (CENTAUR): dose-dependent improvement of fibrosis in 23% of OCA 25 mg treated compared to 12% placebo treated participants. Reduction of hepatocellular inflammation and ballooning [310].
	CBP/ β -catenin small molecule inhibitor PRI-724	Implication of Wnt/ β -catenin signaling in HSC activation and liver fibrosis [169,292,293].	Inhibition of HSC activation in HCV transgenic mice as well as CCl ₄ based murine liver fibrosis [298]. Beneficial effects on fibrosis resolution by activating anti-fibrotic macrophage subpopulations [299]. Decrease of hepatocyte apoptosis as well as fibrosis degree in NASH mouse model [300].	Phase 1: dose dependent histological improvement (>2 point decrease in histologic activity index score) in 3/12 patients, but deterioration by 2 points in 2/12 patients with HCV associated cirrhosis [388]. Phase 2: PRI-724 in patients with hepatitis B or C related liver cirrhosis: expected to be completed in July 2020 (NCT03620474).
Reduction of fibrotic scar evolution and contractility	Hsp47 siRNA delivering lipid nanoparticle, BMS 986263	Function of Hsp47 as a collagen1 chaperone [315].	Significant anti-fibrotic effects in 3 and in-vivo models of liver fibrosis [315].	Phase 1b/2: open label dose escalation study of BMS 986,263 in patients with moderate to severe fibrosis: completed, not yet published (NCT02227459).
	LOXL2 specific monoclonal antibody, AB0023 (Simtuzumab)	Contributing of LOXL2 to ECM stiffness and hampered degradation of deposited collagen fibrils [317–320] Implication in Collagen 3 expression [322] and PDGFR sensitivity [324].	Potent anti-fibrotic activity in bleomycin based mouse model of liver fibrosis via inhibition of collagen-crosslinking and its downstream activating effect on TGF- β 1 signaling that contributes to myofibroblast simulation [328].	Phase 2: No effect on fibrosis in NASH, PSC, or patients with HIV and/or HCV-infected patients with liver fibrosis [329–331].

Table 3. Examples for compounds in clinical development aiming to reduce fibrosis by immune modulation

Antifibrotic mechanism	Agent	Rationale	Molecular Mechanism of Action in Preclinical Studies	Key Findings in Clinical Trials
Immune modulation	CCR2/CCR5 inhibitor, <u>Cenicriviroc</u>	Involvement of CCR2/CCR5 mediated monocyte and macrophage recruitment during early pro-fibrogenic response [15,332,333].	Dose-dependent decrease in monocyte/macrophage recruitment [334–336]. Significant decrease in lobular inflammation, hepatocellular ballooning as well as collagen 1 and α -SMA protein expression in NASH mouse model [334].	Phase 2: Improvement of fibrosis stage (>1 stage) without worsening of steatohepatitis especially in patients with high disease activity (NAS > 5, prominent hepatocyte ballooning, F2-F3 fibrosis) [338]. No effect on lobular inflammation, but decrease in serological markers of systemic inflammation (hsCRP IL6, fibrinogen) [338]. Phase 3: AURORA, NASH patients with advanced fibrosis and cirrhosis (NCT03028740): ongoing
	Inhibitor of galectin-3, Belapectin	Function of galectin-3 as a chemoattractant for macrophages and monocytes, hereby accelerating further pro-inflammatory and pro-fibrogenic immune responses [347,348]. Activator of MMP2 and MMP9 [342].	Dose-dependent reduction of NAS, fibrosis and portal pressure in rat and murine models of NASH potentially due to an impact on macrophage polarization and reduced activation of HSCs [349,350].	Phase 2: No effect on fibrosis within 52 weeks of treatment in NASH patients. Significant protective effects on hepatocyte ballooning as well as significant lower HPVG and varices development in a subgroup of patients with NASH cirrhosis [352].

Author Contributions: Wrote—N.R. and E.C. conceptualized and edited—T.F.B. All authors have read and agreed to the published version of the manuscript.

Funding: TFB acknowledges funding by the European Union (ERC-AdG-2014-HEPCIR #671231, EU H2020-HEPCAR #667273 and ERC PoC-HEPCAN #862551), ARC, Paris and Institut Hospitalo-Universitaire, Strasbourg (TheraHCC and TheraHCC2.0 IHUARC IHU201301187 and IHU201901299), the foundation of the University of Strasbourg (HEPKIN), the Agence National de Recherches sur le Sida et les Hépatites Virales (ANRS 2017/1633) and the US National Institute of Health (R01CA233794 and NCI 1R21CA209940-01A1). This work has been published under the framework of LABEX ANR-10-LABX-0028-HEPSYS and PLAN CANCER 2014-2019 HCCMICTAR and benefits from the state managed funding by the French National Research Agency as part of the Investments for the Future Program, National Institute for Cancer (INCa) and Inserm. N. R. is supported by a fellowship of the German Research Foundation (DFG) (RO 5983/1-1 to NR).

Conflicts of Interest: The authors declare no conflict of interest. Inserm, the University of Strasbourg and IHU Strasbourg have filed patent applications with T.F.B. as a co-inventor on compounds for prevention and treatment of HCV infection, liver disease and HCC which have been licensed to Alentis Therapeutics, Basel.

References

- Asrani, S.K.; Devarbhavi, H.; Eaton, J.; Kamath, P.S. Burden of liver diseases in the world. *J. Hepatol.* **2019**, *70*, 151–171. [CrossRef]
- Wynn, T.A. Fibrotic disease and the T(H)1/T(H)2 paradigm. *Nat. Rev. Immunol.* **2004**, *4*, 583–594. [CrossRef]
- D’Amico, G.; Morabito, A.; D’Amico, M.; Pasta, L.; Malizia, G.; Rebora, P.; Valsecchi, M.G. New concepts on the clinical course and stratification of compensated and decompensated cirrhosis. *Hepatol. Int.* **2018**, *12*, 34–43. [CrossRef]
- Llovet, J.M.; Zucman-Rossi, J.; Pikarsky, E.; Sangro, B.; Schwartz, M.; Sherman, M.; Gores, G. Hepatocellular carcinoma. *Nat. Rev. Dis. Primers* **2016**, *2*, 16018. [CrossRef]
- D’Amico, G.; Morabito, A.; D’Amico, M.; Pasta, L.; Malizia, G.; Rebora, P.; Valsecchi, M.G. Clinical states of cirrhosis and competing risks. *J. Hepatol.* **2018**, *68*, 563–576. [CrossRef]
- Marcellin, P.; Kutala, B.K. Liver diseases: A major, neglected global public health problem requiring urgent actions and large-scale screening. *Liver Int. Off. J. Int. Assoc. Study Liver* **2018**, *38*, 2–6. [CrossRef]
- Iredale, J.P. Models of liver fibrosis: Exploring the dynamic nature of inflammation and repair in a solid organ. *J. Clin. Invest.* **2007**, *117*, 539–548. [CrossRef]
- Elpek, G.O. Cellular and molecular mechanisms in the pathogenesis of liver fibrosis: An update. *World J. Gastroenterol.* **2014**, *20*, 7260–7276. [CrossRef]
- Zhou, W.C.; Zhang, Q.B.; Qiao, L. Pathogenesis of liver cirrhosis. *World J. Gastroenterol.* **2014**, *20*, 7312–7324. [CrossRef]
- Campana, L.; Iredale, J.P. Regression of Liver Fibrosis. *Semin. Liver Dis.* **2017**, *37*, 1–10. [CrossRef]
- Ramachandran, P.; Pellicoro, A.; Vernon, M.A.; Boulter, L.; Aucott, R.L.; Ali, A.; Hartland, S.N.; Snowden, V.K.; Cappon, A.; Gordon-Walker, T.T.; et al. Differential Ly-6C expression identifies the recruited macrophage phenotype, which orchestrates the regression of murine liver fibrosis. *Proc. Natl. Acad. Sci. USA* **2012**, *109*, E3186–E3195. [CrossRef]
- Natarajan, V.; Harris, E.N.; Kidambi, S. SECs (Sinusoidal Endothelial Cells), Liver Microenvironment, and Fibrosis. *Biomed. Res. Int* **2017**, *2017*, 4097205. [CrossRef]
- Krenkel, O.; Tacke, F. Liver macrophages in tissue homeostasis and disease. *Nat. Rev. Immunol.* **2017**, *17*, 306–321. [CrossRef]
- Barron, L.; Wynn, T.A. Fibrosis is regulated by Th2 and Th17 responses and by dynamic interactions between fibroblasts and macrophages. *Am. J. Physiol. Gastrointest. Liver Physiol.* **2011**, *300*, G723–G728. [CrossRef]
- Tacke, F.; Zimmermann, H.W. Macrophage heterogeneity in liver injury and fibrosis. *J. Hepatol.* **2014**, *60*, 1090–1096. [CrossRef]
- Fallowfield, J.A.; Mizuno, M.; Kendall, T.J.; Constandinou, C.M.; Benyon, R.C.; Duffield, J.S.; Iredale, J.P. Scar-associated macrophages are a major source of hepatic matrix metalloproteinase-13 and facilitate the resolution of murine hepatic fibrosis. *J. Immunol.* **2007**, *178*, 5288–5295. [CrossRef]
- Ying, H.Z.; Chen, Q.; Zhang, W.Y.; Zhang, H.H.; Ma, Y.; Zhang, S.Z.; Fang, J.; Yu, C.H. PDGF signaling pathway in hepatic fibrosis pathogenesis and therapeutics (Review). *Mol. Med. Rep.* **2017**, *16*, 7879–7889. [CrossRef]
- Xu, F.; Liu, C.; Zhou, D.; Zhang, L. TGF-beta/SMAD Pathway and Its Regulation in Hepatic Fibrosis. *J. Histochem. Cytochem.* **2016**, *64*, 157–167. [CrossRef]
- Nishikawa, K.; Osawa, Y.; Kimura, K. Wnt/beta-Catenin Signaling as a Potential Target for the Treatment of Liver Cirrhosis Using Antifibrotic Drugs. *Int. J. Mol. Sci.* **2018**, *19*, 3103. [CrossRef]
- van Grunsven, L.A. 3D in vitro models of liver fibrosis. *Drug Deliv. Rev.* **2017**, *121*, 133–146. [CrossRef]
- Van de Bovenkamp, M.; Groothuis, G.M.; Meijer, D.K.; Olinga, P. Liver fibrosis in vitro: Cell culture models and precision-cut liver slices. *Toxicol. Vitro* **2007**, *21*, 545–557. [CrossRef]
- Kim, Y.O.; Popov, Y.; Schuppan, D. Optimized Mouse Models for Liver Fibrosis. *Methods Mol. Biol* **2017**, *1559*, 279–296. [CrossRef]

23. Yanguas, S.C.; Cogliati, B.; Willebrords, J.; Maes, M.; Colle, I.; van den Bossche, B.; de Oliveira, C.; Andraus, W.; Alves, V.A.F.; Leclercq, I.; et al. Experimental models of liver fibrosis. *Arch. Toxicol.* **2016**, *90*, 1025–1048. [CrossRef]
24. Schuppan, D.; Ashfaq-Khan, M.; Yang, A.T.; Kim, Y.O. Liver fibrosis: Direct antifibrotic agents and targeted therapies. *Matrix Biol.* **2018**, *68–69*, 435–451. [CrossRef]
25. Mihm, S. Danger-Associated Molecular Patterns (DAMPs): Molecular Triggers for Sterile Inflammation in the Liver. *Int. J. Mol. Sci.* **2018**, *19*, 3104. [CrossRef]
26. Scaffidi, P.; Misteli, T.; Bianchi, M.E. Release of chromatin protein HMGB1 by necrotic cells triggers inflammation. *Nature* **2002**, *418*, 191–195. [CrossRef]
27. Gardella, S.; Andrei, C.; Ferrera, D.; Lotti, L.V.; Torrisi, M.R.; Bianchi, M.E.; Rubartelli, A. The nuclear protein HMGB1 is secreted by monocytes via a non-classical, vesicle-mediated secretory pathway. *EMBO Rep.* **2002**, *3*, 995–1001. [CrossRef]
28. Tian, J.; Avalos, A.M.; Mao, S.-Y.; Chen, B.; Senthil, K.; Wu, H.; Parroche, P.; Drabic, S.; Golenbock, D.; Sirois, C.; et al. Toll-like receptor 9-dependent activation by DNA-containing immune complexes is mediated by HMGB1 and RAGE. *Nat. Immunol.* **2007**, *8*, 487–496. [CrossRef]
29. Tsung, A.; Sahai, R.; Tanaka, H.; Nakao, A.; Fink, M.P.; Lotze, M.T.; Yang, H.; Li, J.; Tracey, K.J.; Geller, D.A.; et al. The nuclear factor HMGB1 mediates hepatic injury after murine liver ischemia-reperfusion. *J. Exp. Med.* **2005**, *201*, 1135–1143. [CrossRef]
30. Li, J.; Wang, F.-P.; She, W.-M.; Yang, C.-Q.; Li, L.; Tu, C.-T.; Wang, J.-Y.; Jiang, W. Enhanced high-mobility group box 1 (HMGB1) modulates regulatory T cells (Treg)/T helper 17 (Th17) balance via toll-like receptor (TLR)-4-interleukin (IL)-6 pathway in patients with chronic hepatitis B. *J. Viral Hepat.* **2014**, *21*, 129–140. [CrossRef]
31. Li, J.; Zeng, C.; Zheng, B.; Liu, C.; Tang, M.; Jiang, Y.; Chang, Y.; Song, W.; Wang, Y.; Yang, C. HMGB1-induced autophagy facilitates hepatic stellate cells activation: A new pathway in liver fibrosis. *Clin. Sci.* **2018**, *132*, 1645–1667. [CrossRef]
32. Huebener, P.; Pradere, J.-P.; Hernandez, C.; Gwak, G.-Y.; Caviglia, J.M.; Mu, X.; Loike, J.D.; Jenkins, R.E.; Antoine, D.J.; Schwabe, R.F. The HMGB1/RAGE axis triggers neutrophil-mediated injury amplification following necrosis. *J. Clin. Invest.* **2015**, *125*, 539–550. [CrossRef]
33. Canbay, A.; Higuchi, H.; Bronk, S.F.; Taniai, M.; Sebo, T.J.; Gores, G.J. Fas enhances fibrogenesis in the bile duct ligated mouse: A link between apoptosis and fibrosis. *Gastroenterology* **2002**, *123*, 1323–1330. [CrossRef]
34. Feldstein, A.E.; Canbay, A.; Angulo, P.; Taniai, M.; Burgart, L.J.; Lindor, K.D.; Gores, G.J. Hepatocyte apoptosis and fas expression are prominent features of human nonalcoholic steatohepatitis. *Gastroenterology* **2003**, *125*, 437–443. [CrossRef]
35. Zhan, S.-S.; Jiang, J.X.; Wu, J.; Halsted, C.; Friedman, S.L.; Zern, M.A.; Torok, N.J. Phagocytosis of apoptotic bodies by hepatic stellate cells induces NADPH oxidase and is associated with liver fibrosis in vivo. *Hepatology* **2006**, *43*, 435–443. [CrossRef]
36. Canbay, A.; Feldstein, A.E.; Higuchi, H.; Werneburg, N.; Grambihler, A.; Bronk, S.F.; Gores, G.J. Kupffer cell engulfment of apoptotic bodies stimulates death ligand and cytokine expression. *Hepatology* **2003**, *38*, 1188–1198. [CrossRef]
37. Watanabe, A.; Hashmi, A.; Gomes, D.A.; Town, T.; Badou, A.; Flavell, R.A.; Mehal, W.Z. Apoptotic hepatocyte DNA inhibits hepatic stellate cell chemotaxis via toll-like receptor 9. *Hepatology* **2007**, *46*, 1509–1518. [CrossRef]
38. Musso, G.; Cassader, M.; Paschetta, E.; Gambino, R. Bioactive Lipid Species and Metabolic Pathways in Progression and Resolution of Nonalcoholic Steatohepatitis. *Gastroenterology* **2018**, *155*, 282–302 e288. [CrossRef]
39. Chiappini, F.; Coilly, A.; Kadar, H.; Gual, P.; Tran, A.; Desterke, C.; Samuel, D.; Duclos-Vallée, J.C.; Touboul, D.; Bertrand-Michel, J.; et al. Metabolism dysregulation induces a specific lipid signature of nonalcoholic steatohepatitis in patients. *Sci. Rep.* **2017**, *7*, 46658. [CrossRef]
40. Chaurasia, B.; Summers, S.A. Ceramides - Lipotoxic Inducers of Metabolic Disorders. *Trends Endocrinol. Metab.* **2015**, *26*, 538–550. [CrossRef]
41. Neuschwander-Tetri, B.A. Hepatic lipotoxicity and the pathogenesis of nonalcoholic steatohepatitis: The central role of nontriglyceride fatty acid metabolites. *Hepatology* **2010**, *52*, 774–788. [CrossRef] [PubMed]
42. Cazanave, S.C.; Mott, J.L.; Bronk, S.F.; Werneburg, N.W.; Fingas, C.D.; Meng, X.W.; Finnberg, N.; El-Deiry, W.S.; Kaufmann, S.H.; Gores, G.J. Death receptor 5 signaling promotes hepatocyte lipoapoptosis. *J. Biol. Chem.* **2011**, *286*, 39336–39348. [CrossRef]
43. Cazanave, S.C.; Wang, X.; Zhou, H.; Rahmani, M.; Grant, S.; Durrant, D.E.; Klaassen, C.D.; Yamamoto, M.; Sanyal, A.J. Degradation of Keap1 activates BH3-only proteins Bim and PUMA during hepatocyte lipoapoptosis. *Cell Death Differ.* **2014**, *21*, 1303–1312. [CrossRef]
44. Xiao, F.; Waldrop, S.L.; Bronk, S.F.; Gores, G.J.; Davis, L.S.; Kilic, G. Lipoapoptosis induced by saturated free fatty acids stimulates monocyte migration: A novel role for Pannexin1 in liver cells. *Purinergic Signal.* **2015**, *11*, 347–359. [CrossRef]
45. Shi, H.; Kokoeva, M.V.; Inouye, K.; Tzameli, I.; Yin, H.; Flier, J.S. TLR4 links innate immunity and fatty acid-induced insulin resistance. *J. Clin. Invest.* **2006**, *116*, 3015–3025. [CrossRef]

46. Gan, L.T.; Van Rooyen, D.M.; Koina, M.E.; McCuskey, R.S.; Teoh, N.C.; Farrell, G.C. Hepatocyte free cholesterol lipotoxicity results from JNK1-mediated mitochondrial injury and is HMGB1 and TLR4-dependent. *J. Hepatol.* **2014**, *61*, 1376–1384. [CrossRef]
47. Ioannou, G.N. The Role of Cholesterol in the Pathogenesis of NASH. *Trends Endocrinol Metab.* **2016**, *27*, 84–95. [CrossRef]
48. Ioannou, G.N.; Haigh, W.G.; Thorning, D.; Savard, C. Hepatic cholesterol crystals and crown-like structures distinguish NASH from simple steatosis. *J. Lipid Res.* **2013**, *54*, 1326–1334. [CrossRef]
49. Teratani, T.; Tomita, K.; Suzuki, T.; Oshikawa, T.; Yokoyama, H.; Shimamura, K.; Tominaga, S.; Hiroi, S.; Irie, R.; Okada, Y.; et al. A high-cholesterol diet exacerbates liver fibrosis in mice via accumulation of free cholesterol in hepatic stellate cells. *Gastroenterology* **2012**, *142*, 152–164 e110. [CrossRef] Tomita, K.; Teratani, T.; Suzuki, T.; Shimizu, M.; Sato, H.; Narimatsu, K.; Okada, Y.; Kurihara, C.; Irie, R.; Yokoyama, H.; et al. Free cholesterol accumulation in hepatic stellate cells: Mechanism of liver fibrosis aggravation in nonalcoholic steatohepatitis in mice. *Hepatology* **2014**, *59*, 154–169. [CrossRef]
50. Mederacke, I.; Hsu, C.C.; Troeger, J.S.; Huebener, P.; Mu, X.; Dapito, D.H.; Pradere, J.P.; Schwabe, R.F. Fate tracing reveals hepatic stellate cells as dominant contributors to liver fibrosis independent of its aetiology. *Nat. Commun.* **2013**, *4*, 2823. [CrossRef] [PubMed]
51. Testerink, N.; Ajat, M.; Houweling, M.; Brouwers, J.F.; Pully, V.V.; van Manen, H.-J.; Otto, C.; Helms, J.B.; Vaandrager, A.B. Replacement of Retinyl Esters by Polyunsaturated Triacylglycerol Species in Lipid Droplets of Hepatic Stellate Cells during Activation. *PLoS ONE* **2012**, *7*. [CrossRef] [PubMed]
52. Affo, S.; Yu, L.X.; Schwabe, R.F. The Role of Cancer-Associated Fibroblasts and Fibrosis in Liver Cancer. *Annu. Rev. Pathol. Mech. Dis.* **2017**, *12*, 153–186. [CrossRef] [PubMed]
53. Friedman, S.L. Mechanisms of Hepatic Fibrogenesis. *Gastroenterology* **2008**, *134*, 1655–1669. [CrossRef]
54. Hazra, S.; Xiong, S.; Wang, J.; Rippe, R.A.; Krishna, V.; Chatterjee, K.; Tsukamoto, H. Peroxisome Proliferator-activated Receptor γ Induces a Phenotypic Switch from Activated to Quiescent Hepatic Stellate Cells. *J. Biol. Chem.* **2004**, *279*, 11392–11401. [CrossRef]
55. Kisseleva, T.; Cong, M.; Paik, Y.; Scholten, D.; Jiang, C.; Benner, C.; Iwaisako, K.; Moore-Morris, T.; Scott, B.; Tsukamoto, H.; et al. Myofibroblasts revert to an inactive phenotype during regression of liver fibrosis. *Proc. Natl. Acad. Sci. USA* **2012**, *109*, 9448–9453. [CrossRef]
56. Tsuchida, T.; Friedman, S.L. Mechanisms of hepatic stellate cell activation. *Nat. Rev. Gastroenterol. Hepatol.* **2017**, *14*, 397–411. [CrossRef]
57. Friedman, S.L. Hepatic Stellate Cells: Protean, Multifunctional, and Enigmatic Cells of the Liver. *Physiol. Rev.* **2008**, *88*, 125–172. [CrossRef]
58. Malehmir, M.; Pfister, D.; Gallage, S.; Szydlowska, M.; Inverso, D.; Kotsiliti, E.; Leone, V.; Peiseler, M.; Surewaard, B.G.J.; Rath, D.; et al. Platelet GPIIb/IIIa is a mediator and potential interventional target for NASH and subsequent liver cancer. *Nat. Med.* **2019**, *25*, 641–655. [CrossRef]
59. Fabregat, I.; Moreno-Càceres, J.; Sánchez, A.; Dooley, S.; Dewidar, B.; Giannelli, G.; Dijke, P.t. TGF- β signalling and liver disease. *FEBS J.* **2016**, *283*, 2219–2232. [CrossRef]
60. Baiocchi, A.; Montaldo, C.; Conigliaro, A.; Grimaldi, A.; Correani, V.; Mura, F.; Ciccocanti, F.; Rotiroli, N.; Brenna, A.; Montalbano, M.; et al. Extracellular Matrix Molecular Remodeling in Human Liver Fibrosis Evolution. *PLoS ONE* **2016**, *11*. [CrossRef] [PubMed]
61. Kisseleva, T.; Uchinami, H.; Feirt, N.; Quintana-Bustamante, O.; Segovia, J.C.; Schwabe, R.F.; Brenner, D.A. Bone marrow-derived fibrocytes participate in pathogenesis of liver fibrosis. *J. Hepatol.* **2006**, *45*, 429–438. [CrossRef] [PubMed]
62. Wells, R.G.; Kruglov, E.; Dranoff, J.A. Autocrine release of TGF- β by portal fibroblasts regulates cell growth. *FEBS Lett.* **2004**, *559*, 107–110. [CrossRef]
63. Forbes, S.J.; Russo, F.P.; Rey, V.; Burra, P.; Rugge, M.; Wright, N.A.; Alison, M.R. A significant proportion of myofibroblasts are of bone marrow origin in human liver fibrosis. *Gastroenterology* **2004**, *126*, 955–963. [CrossRef] [PubMed]
64. Quante, M.; Tu, S.P.; Tomita, H.; Gonda, T.; Wang, S.S.W.; Takashi, S.; Baik, G.H.; Shibata, W.; DiPrete, B.; Betz, K.S.; et al. Bone Marrow-Derived Myofibroblasts Contribute to the Mesenchymal Stem Cell Niche and Promote Tumor Growth. *Cancer Cell* **2011**, *19*, 257–272. [CrossRef] [PubMed]
65. Zeisberg, M.; Yang, C.; Martino, M.; Duncan, M.B.; Rieder, F.; Tanjore, H.; Kalluri, R. Fibroblasts Derive from Hepatocytes in Liver Fibrosis via Epithelial to Mesenchymal Transition. *J. Biol. Chem.* **2007**, *282*, 23337–23347. [CrossRef]
66. Beaussier, M.; Wendum, D.; Schiffer, E.; Dumont, S.; Rey, C.; Lienhart, A.; Housset, C. Prominent contribution of portal mesenchymal cells to liver fibrosis in ischemic and obstructive cholestatic injuries. *Lab. Invest.* **2007**, *87*, 292–303. [CrossRef]

67. Iwaisako, K.; Jiang, C.; Zhang, M.; Cong, M.; Moore-Morris, T.J.; Park, T.J.; Liu, X.; Xu, J.; Wang, P.; Paik, Y.H.; et al. Origin of myofibroblasts in the fibrotic liver in mice. *Proc. Natl. Acad. Sci. USA* **2014**, *111*, E3297–3305. [CrossRef]
68. Li, Y.; Wang, J.; Asahina, K. Mesothelial cells give rise to hepatic stellate cells and myofibroblasts via mesothelial–mesenchymal transition in liver injury. *Proc. Natl. Acad. Sci. USA* **2013**, *110*, 2324–2329. [CrossRef]
69. Baertschiger, R.M.; Serre-Beinier, V.; Morel, P.; Bosco, D.; Peyrou, M.; Clément, S.; Sgroi, A.; Kaelin, A.; Buhler, L.H.; Gonelle-Gispert, C. Fibrogenic Potential of Human Multipotent Mesenchymal Stromal Cells in Injured Liver. *PLoS ONE* **2009**, *4*, e6657. [CrossRef]
70. Watanabe, Y.; Tsuchiya, A.; Seino, S.; Kawata, Y.; Kojima, Y.; Ikarashi, S.; Starkey Lewis, P.J.; Lu, W.Y.; Kikuta, J.; Kawai, H.; et al. Mesenchymal Stem Cells and Induced Bone Marrow-Derived Macrophages Synergistically Improve Liver Fibrosis in Mice. *Stem Cells Transl. Med.* **2018**, *8*, 271–284. [CrossRef]
71. An, S.Y.; Jang, Y.J.; Lim, H.-J.; Han, J.; Lee, J.; Lee, G.; Park, J.Y.; Park, S.-Y.; Kim, J.H.; Do, B.-R.; et al. Milk Fat Globule-EGF Factor 8, Secreted by Mesenchymal Stem Cells, Protects Against Liver Fibrosis in Mice. *Gastroenterology* **2017**, *152*, 1174–1186. [CrossRef]
72. ZHAO, Y.-L.; ZHU, R.-T.; SUN, Y.-L. Epithelial-mesenchymal transition in liver fibrosis. *Biomed. Rep.* **2016**, *4*, 269–274. [CrossRef] [PubMed]
73. Taura, K.; Miura, K.; Iwaisako, K.; Österreicher, C.H.; Kodama, Y.; Penz-Österreicher, M.; Brenner, D.A. Hepatocytes Do Not Undergo Epithelial-Mesenchymal Transition in Liver Fibrosis in Mice. *Hepatology (Baltimore, Md.)* **2010**, *51*, 1027–1036. [CrossRef] [PubMed]
74. Chu, A.S.; Diaz, R.; Hui, J.-J.; Yanger, K.; Zong, Y.; Alpini, G.; Stanger, B.Z.; Wells, R.G. Lineage tracing demonstrates no evidence of cholangiocyte epithelial-to-mesenchymal transition in murine models of hepatic fibrosis. *Hepatology (Baltimore, Md.)* **2011**, *53*, 1685–1695. [CrossRef] [PubMed]
75. Nishitsuji, H.; Funami, K.; Shimizu, Y.; Ujino, S.; Sugiyama, K.; Seya, T.; Takaku, H.; Shimotohno, K. Hepatitis C Virus Infection Induces Inflammatory Cytokines and Chemokines Mediated by the Cross Talk between Hepatocytes and Stellate Cells. *J. Virol.* **2013**, *87*, 8169–8178. [CrossRef] [PubMed]
76. Luedde, T.; Kaplowitz, N.; Schwabe, R.F. Cell Death and Cell Death Responses in Liver Disease: Mechanisms and Clinical Relevance. *Gastroenterology* **2014**, *147*, 765–783.e764. [CrossRef] [PubMed]
77. Leroux, A.; Ferrere, G.; Godie, V.; Cailleux, F.; Renoud, M.-L.; Gaudin, F.; Naveau, S.; Prévot, S.; Makhzami, S.; Perlemuter, G.; et al. Toxic lipids stored by Kupffer cells correlates with their pro-inflammatory phenotype at an early stage of steatohepatitis. *J. Hepatology* **2012**, *57*, 141–149. [CrossRef]
78. Bieghs, V.; Hendriks, T.; Gorp, P.J.V.; Verheyen, F.; Guichot, Y.D.; Walenbergh, S.M.A.; Jeurissen, M.L.J.; Gijbels, M.; Rensen, S.S.; Bast, A.; et al. The Cholesterol Derivative 27-Hydroxycholesterol Reduces Steatohepatitis in Mice. *Gastroenterology* **2013**, *144*, 167–178.e161. [CrossRef]
79. Mosser, D.M.; Edwards, J.P. Exploring the full spectrum of macrophage activation. *Nat. Rev. Immunol.* **2008**, *8*, 958–969. [CrossRef]
80. Duffield, J.S.; Forbes, S.J.; Constandinou, C.M.; Clay, S.; Partolina, M.; Vuthoori, S.; Wu, S.; Lang, R.; Iredale, J.P. Selective depletion of macrophages reveals distinct, opposing roles during liver injury and repair. *J. Clin. Invest.* **2005**, *115*, 56–65. [CrossRef]
81. Karlmark, K.R.; Weiskirchen, R.; Zimmermann, H.W.; Gassler, N.; Ginhoux, F.; Weber, C.; Merad, M.; Luedde, T.; Trautwein, C.; Tacke, F. Hepatic recruitment of the inflammatory Gr1+ monocyte subset upon liver injury promotes hepatic fibrosis. *Hepatology* **2009**, *50*, 261–274. [CrossRef] [PubMed]
82. Seki, E.; Minicis, S.d.; Inokuchi, S.; Taura, K.; Miyai, K.; Rooijen, N.v.; Schwabe, R.F.; Brenner, D.A. CCR2 promotes hepatic fibrosis in mice. *Hepatology* **2009**, *50*, 185–197. [CrossRef] [PubMed]
83. Marra, F.; Tacke, F. Roles for Chemokines in Liver Disease. *Gastroenterology* **2014**, *147*, 577–594.e571. [CrossRef]
84. Sahin, H.; Trautwein, C.; Wasmuth, H.E. Functional role of chemokines in liver disease models. *Nat. Rev. Gastroenterol. Hepatol.* **2010**, *7*, 682–690. [CrossRef] [PubMed]
85. Lee, U.E.; Friedman, S.L. Mechanisms of Hepatic Fibrogenesis. *Best Pr. Res. Clin. Gastroenterol.* **2011**, *25*, 195–206. [CrossRef] [PubMed]
86. Liu, C.; Tao, Q.; Sun, M.; Wu, J.Z.; Yang, W.; Jian, P.; Peng, J.; Hu, Y.; Liu, C.; Liu, P. Kupffer cells are associated with apoptosis, inflammation and fibrotic effects in hepatic fibrosis in rats. *Lab. Invest.* **2010**, *90*, 1805–1816. [CrossRef] [PubMed]
87. Holt, A.P.; Salmon, M.; Buckley, C.D.; Adams, D.H. Immune interactions in hepatic fibrosis. or “Leucocyte-stromal interactions in hepatic fibrosis”. *Clin. Liver Dis.* **2008**, *12*, 861. [CrossRef]
88. Muhanna, N.; Horani, A.; Doron, S.; Safadi, R. Lymphocyte–hepatic stellate cell proximity suggests a direct interaction. *Clin. Exp. Immunol.* **2007**, *148*, 338–347. [CrossRef]
89. Lodyga, M.; Cambridge, E.; Karvonen, H.M.; Pakshir, P.; Wu, B.; Boo, S.; Kiebalo, M.; Kaarteenaho, R.; Glogauer, M.; Kapoor, M.; et al. Cadherin-11–mediated adhesion of macrophages to myofibroblasts establishes a profibrotic niche of active TGF- β . *Sci. Signal.* **2019**, *12*. [CrossRef] [PubMed]

90. Cai, X.; Li, Z.; Zhang, Q.; Qu, Y.; Xu, M.; Wan, X.; Lu, L. CXCL6-EGFR-induced Kupffer cells secrete TGF- β 1 promoting hepatic stellate cell activation via the SMAD2/BRD4/C-MYC/EZH2 pathway in liver fibrosis. *J. Cell. Mol. Med.* **2018**, *22*, 5050–5061. [CrossRef]
91. Ramachandran, P.; Iredale, J.P.; Fallowfield, J.A. Resolution of liver fibrosis: Basic mechanisms and clinical relevance. *Semin. Liver Dis.* **2015**, *35*, 119–131. [CrossRef]
92. Flavell, R.A.; Sanjabi, S.; Wrzesinski, S.H.; Licona-Limon, P. The polarization of immune cells in the tumour environment by TGF β . *Nat. Rev. Immunol.* **2010**, *10*, 554–567. [CrossRef]
93. Barenwaldt, A.; Laubli, H. The sialoglycan-Siglec glyco-immune checkpoint - a target for improving innate and adaptive anti-cancer immunity. *Expert Opin. Ther. Targets* **2019**, *23*, 839–853. [CrossRef]
94. Shouval, D.S.; Biswas, A.; Goettel, J.A.; McCann, K.; Conaway, E.; Redhu, N.S.; Mascanfroni, I.D.; Adham, Z.A.; Lavoie, S.; Ibourk, M.; et al. Interleukin-10 Receptor Signaling in Innate Immune Cells Regulates Mucosal Immune Tolerance and Anti-Inflammatory Macrophage Function. *Immunity* **2014**, *40*, 706–719. [CrossRef] [PubMed]
95. Calderaro, J.; Rousseau, B.; Amaddeo, G.; Mercey, M.; Charpy, C.; Costentin, C.; Luciani, A.; Zafrani, E.-S.; Laurent, A.; Azoulay, D.; et al. Programmed death ligand 1 expression in hepatocellular carcinoma: Relationship With clinical and pathological features. *Hepatology* **2016**, *64*, 2038–2046. [CrossRef] [PubMed]
96. Holt, A.P.; Stamatakis, Z.; Adams, D.H. Attenuated liver fibrosis in the absence of B cells. *Hepatology* **2006**, *43*, 868–871. [CrossRef]
97. Safadi, R.; Ohta, M.; Alvarez, C.E.; Fiel, M.I.; Bansal, M.; Mehal, W.Z.; Friedman, S.L. Immune stimulation of hepatic fibrogenesis by CD8 cells and attenuation by transgenic interleukin-10 from hepatocytes. *Gastroenterology* **2004**, *127*, 870–882. [CrossRef]
98. Novobrantseva, T.I.; Majeau, G.R.; Amatucci, A.; Kogan, S.; Brenner, I.; Casola, S.; Shlomchik, M.J.; Kotliansky, V.; Hochman, P.S.; Ibraghimov, A. Attenuated liver fibrosis in the absence of B cells. *J. Clin. Invest.* **2005**, *115*, 3072–3082. [CrossRef] [PubMed]
99. Wang, Y.; Zhang, C. The Roles of Liver-Resident Lymphocytes in Liver Diseases. *Front. Immunol.* **2019**, *10*. [CrossRef] [PubMed]
100. Lee, W.-Y.; Kubes, P. Leukocyte adhesion in the liver: Distinct adhesion paradigm from other organs. *J. Hepatol.* **2008**, *48*, 504–512. [CrossRef] [PubMed]
101. Patsenker, E.; Stickel, F. Role of integrins in fibrosing liver diseases. *Am. J. Physiol. Gastrointest. Liver Physiol.* **2011**, *301*, G425–434. [CrossRef] [PubMed]
102. Curbishley, S.M.; Eksteen, B.; Gladue, R.P.; Lalor, P.; Adams, D.H. CXCR3 Activation Promotes Lymphocyte Transendothelial Migration across Human Hepatic Endothelium under Fluid Flow. *Am. J. Pathol.* **2005**, *167*, 887–899. [CrossRef]
103. Weng, H.-L.; Liu, Y.; Chen, J.-L.; Huang, T.; Xu, L.-J.; Godoy, P.; Hu, J.-H.; Zhou, C.; Stickel, F.; Marx, A.; et al. The etiology of liver damage imparts cytokines transforming growth factor β 1 or interleukin-13 as driving forces in fibrogenesis. *Hepatology* **2009**, *50*, 230–243. [CrossRef]
104. Tan, Z.; Qian, X.; Jiang, R.; Liu, Q.; Wang, Y.; Chen, C.; Wang, X.; Ryffel, B.; Sun, B. IL-17A Plays a Critical Role in the Pathogenesis of Liver Fibrosis through Hepatic Stellate Cell Activation. *J. Immunol.* **2013**, *191*, 1835–1844. [CrossRef]
105. Li, X.; Su, Y.; Hua, X.; Xie, C.; Liu, J.; Huang, Y.; Zhou, L.; Zhang, M.; Li, X.; Gao, Z. Levels of hepatic Th17 cells and regulatory T cells upregulated by hepatic stellate cells in advanced HBV-related liver fibrosis. *J. Transl. Med.* **2017**, *15*, s12967–s13017. [CrossRef]
106. Tu, J.-F.; Ding, Y.-H.; Ying, X.-H.; Wu, F.-Z.; Zhou, X.-M.; Zhang, D.-K.; Zou, H.; Ji, J.-S. Regulatory T cells, especially ICOS + FOXP3 + regulatory T cells, are increased in the hepatocellular carcinoma microenvironment and predict reduced survival. *Sci. Rep.* **2016**, *6*, 1–8. [CrossRef]
107. Fu, J.; Xu, D.; Liu, Z.; Shi, M.; Zhao, P.; Fu, B.; Zhang, Z.; Yang, H.; Zhang, H.; Zhou, C.; et al. Increased Regulatory T Cells Correlate With CD8 T-Cell Impairment and Poor Survival in Hepatocellular Carcinoma Patients. *Gastroenterology* **2007**, *132*, 2328–2339. [CrossRef]
108. Faggioli, F.; Palagano, E.; Tommaso, L.D.; Donadon, M.; Marrella, V.; Recordati, C.; Mantero, S.; Villa, A.; Vezzoni, P.; Cassani, B. B lymphocytes limit senescence-driven fibrosis resolution and favor hepatocarcinogenesis in mouse liver injury. *Hepatology* **2018**, *67*, 1970–1985. [CrossRef]
109. Henao-Mejia, J.; Elinav, E.; Thaïs, C.A.; Licona-Limon, P.; Flavell, R.A. Role of the intestinal microbiome in liver disease. *J. Autoimmun.* **2013**, *46*, 66–73. [CrossRef]

110. Albillos, A.; de Gottardi, A.; Rescigno, M. The gut-liver axis in liver disease: Pathophysiological basis for therapy. *J. Hepatol.* **2020**, *72*, 558–577. [CrossRef] [PubMed]
111. Bull-Otterson, L.; Feng, W.; Kirpich, I.; Wang, Y.; Qin, X.; Liu, Y.; Gobejishvili, L.; Joshi-Barve, S.; Ayvaz, T.; Petrosino, J.; et al. Metagenomic analyses of alcohol induced pathogenic alterations in the intestinal microbiome and the effect of *Lactobacillus rhamnosus* GG treatment. *PLoS ONE* **2013**, *8*, e53028. [CrossRef] [PubMed]
112. Mouries, J.; Brescia, P.; Silvestri, A.; Spadoni, I.; Sorribas, M.; Wiest, R.; Mileti, E.; Galbiati, M.; Invernizzi, P.; Adorini, L.; et al. Microbiota-driven gut vascular barrier disruption is a prerequisite for non-alcoholic steatohepatitis development. *J. Hepatol.* **2019**, *71*, 1216–1228. [CrossRef]
113. Sinal, C.J.; Tohkin, M.; Miyata, M.; Ward, J.M.; Lambert, G.; Gonzalez, F.J. Targeted disruption of the nuclear receptor FXR/BAR impairs bile acid and lipid homeostasis. *Cell* **2000**, *102*, 731–744. [CrossRef]
114. Claudel, T.; Staels, B.; Kuipers, F. The Farnesoid X receptor: A molecular link between bile acid and lipid and glucose metabolism. *Arter. Thromb. Vasc. Biol.* **2005**, *25*, 2020–2030. [CrossRef] [PubMed]
115. Gadaleta, R.M.; van Erpecum, K.J.; Oldenburg, B.; Willemsen, E.C.; Renooij, W.; Murzilli, S.; Klomp, L.W.; Siersema, P.D.; Schipper, M.E.; Danese, S.; et al. Farnesoid X receptor activation inhibits inflammation and preserves the intestinal barrier in inflammatory bowel disease. *Gut* **2011**, *60*, 463–472. [CrossRef] [PubMed]
116. Chen, Y.; Yang, F.; Lu, H.; Wang, B.; Chen, Y.; Lei, D.; Wang, Y.; Zhu, B.; Li, L. Characterization of fecal microbial communities in patients with liver cirrhosis. *Hepatology* **2011**, *54*, 562–572. [CrossRef]
117. Qin, N.; Yang, F.; Li, A.; Prifti, E.; Chen, Y.; Shao, L.; Guo, J.; Le Chatelier, E.; Yao, J.; Wu, L.; et al. Alterations of the human gut microbiome in liver cirrhosis. *Nature* **2014**, *513*, 59–64. [CrossRef]
118. Kakiyama, G.; Pandak, W.M.; Gillevet, P.M.; Hylemon, P.B.; Heuman, D.M.; Daita, K.; Takei, H.; Muto, A.; Nittono, H.; Ridlon, J.M.; et al. Modulation of the fecal bile acid profile by gut microbiota in cirrhosis. *J. Hepatol.* **2013**, *58*, 949–955. [CrossRef]
119. Gunnarsdottir, S.A.; Sadik, R.; Shev, S.; Simren, M.; Sjøvall, H.; Stotzer, P.O.; Abrahamsson, H.; Olsson, R.; Björnsson, E.S. Small intestinal motility disturbances and bacterial overgrowth in patients with liver cirrhosis and portal hypertension. *Am. J. Gastroenterol.* **2003**, *98*, 1362–1370. [CrossRef]
120. Kakiyama, G.; Hylemon, P.B.; Zhou, H.; Pandak, W.M.; Heuman, D.M.; Kang, D.J.; Takei, H.; Nittono, H.; Ridlon, J.M.; Fuchs, M.; et al. Colonic inflammation and secondary bile acids in alcoholic cirrhosis. *Am. J. Physiol. Liver Physiol.* **2014**, *306*, G929–937. [CrossRef] [PubMed]
121. Teltschik, Z.; Wiest, R.; Beisner, J.; Nuding, S.; Hofmann, C.; Schoelmerich, J.; Bevins, C.L.; Stange, E.F.; Wehkamp, J. Intestinal bacterial translocation in rats with cirrhosis is related to compromised Paneth cell antimicrobial host defense. *Hepatology* **2012**, *55*, 1154–1163. [CrossRef] [PubMed]
122. Albillos, A.; Lario, M.; Alvarez-Mon, M. Cirrhosis-associated immune dysfunction: Distinctive features and clinical relevance. *J. Hepatol.* **2014**, *61*, 1385–1396. [CrossRef] [PubMed]
123. Bajaj, J.S.; Heuman, D.M.; Hylemon, P.B.; Sanyal, A.J.; White, M.B.; Monteith, P.; Noble, N.A.; Unser, A.B.; Daita, K.; Fisher, A.R.; et al. Altered profile of human gut microbiome is associated with cirrhosis and its complications. *J. Hepatol.* **2014**, *60*, 940–947. [CrossRef]
124. Bajaj, J.S.; Idilman, R.; Mabudian, L.; Hood, M.; Fagan, A.; Turan, D.; White, M.B.; Karakaya, F.; Wang, J.; Atalay, R.; et al. Diet affects gut microbiota and modulates hospitalization risk differentially in an international cirrhosis cohort. *Hepatology* **2018**, *68*, 234–247. [CrossRef]
125. Bajaj, J.S.; Hylemon, P.B.; Ridlon, J.M.; Heuman, D.M.; Daita, K.; White, M.B.; Monteith, P.; Noble, N.A.; Sikaroodi, M.; Gillevet, P.M. Colonic mucosal microbiome differs from stool microbiome in cirrhosis and hepatic encephalopathy and is linked to cognition and inflammation. *Am. J. Physiol. Liver Physiol.* **2012**, *303*, G675–685. [CrossRef]
126. Borkham-Kamphorst, E.; Weiskirchen, R. The PDGF system and its antagonists in liver fibrosis. *Cytokine Growth Factor Rev.* **2016**, *28*, 53–61. [CrossRef]
127. Breitkopf, K.; Roeyen, C.V.; Sawitz, I.; Wickert, L.; Floege, J.; Gressner, A.M. Expression patterns of PDGF-A, -B, -C and -D and the PDGF-receptors α and β in activated rat hepatic stellate cells (HSC). *Cytokine* **2005**, *31*, 349–357. [CrossRef]
128. Czochra, P.; Klopčič, B.; Meyer, E.; Herkel, J.; Garcia-Lazaro, J.F.; Thieringer, F.; Schirmacher, P.; Biesterfeld, S.; Galle, P.R.; Lohse, A.W.; et al. Liver fibrosis induced by hepatic overexpression of PDGF-B in transgenic mice. *J. Hepatol.* **2006**, *45*, 419–428. [CrossRef]
129. Campbell, J.S.; Hughes, S.D.; Gilbertson, D.G.; Palmer, T.E.; Holdren, M.S.; Haran, A.C.; Odell, M.M.; Bauer, R.L.; Ren, H.-P.; Haugen, H.S.; et al. Platelet-derived growth factor C induces liver fibrosis, steatosis, and hepatocellular carcinoma. *Proc. Natl. Acad. Sci. USA* **2005**, *102*, 3389–3394. [CrossRef]
130. Hayes, B.J.; Riehle, K.J.; Shimizu-Albergine, M.; Bauer, R.L.; Hudkins, K.L.; Johansson, F.; Yeh, M.M.; Jr, W.M.M.; Yeung, R.S.; Campbell, J.S. Activation of Platelet-Derived Growth Factor Receptor Alpha Contributes to Liver Fibrosis. *PLoS ONE* **2014**, *9*, e92925. [CrossRef] [PubMed]
131. Kocabayoglu, P.; Lade, A.; Lee, Y.A.; Dragomir, A.-C.; Sun, X.; Fiel, M.I.; Thung, S.; Aloman, C.; Soriano, P.; Hoshida, Y.;

- et al. β -PDGF receptor expressed by hepatic stellate cells regulates fibrosis in murine liver injury, but not carcinogenesis. *J. Hepatol.* **2015**, *63*, 141–147. [CrossRef] [PubMed]
132. Dewidar, B.; Meyer, C.; Dooley, S.; Meindl-Beinker, A.N. TGF- β in Hepatic Stellate Cell Activation and Liver Fibrogenesis-Updated 2019. *Cells* **2019**, *8*, 1419. [CrossRef] [PubMed]
133. Dropmann, A.; Dediulia, T.; Breikopf-Heinlein, K.; Korhonen, H.; Janicot, M.; Weber, S.N.; Thomas, M.; Piiper, A.; Bertran, E.; Fabregat, I.; et al. TGF- β 1 and TGF- β 2 abundance in liver diseases of mice and men. *Oncotarget* **2016**, *7*, 19499–19518. [CrossRef]
134. Ghafoory, S.; Varshney, R.; Robison, T.; Kouzbari, K.; Woolington, S.; Murphy, B.; Xia, L.; Ahamed, J. Platelet TGF- β 1 deficiency decreases liver fibrosis in a mouse model of liver injury. *Blood Adv.* **2018**, *2*, 470–480. [CrossRef] [PubMed]
135. Derynck, R.; Budi, E.H. Specificity, versatility, and control of TGF- β family signaling. *Sci. Signal.* **2019**, *12*. [CrossRef]
136. Yang, L.; Roh, Y.S.; Song, J.; Zhang, B.; Liu, C.; Loomba, R.; Seki, E. Transforming growth factor beta signaling in hepatocytes participates in steatohepatitis through regulation of cell death and lipid metabolism in mice. *Hepatology* **2014**, *59*, 483–495. [CrossRef]
137. Xu, F.; Zhou, D.; Meng, X.; Wang, X.; Liu, C.; Huang, C.; Li, J.; Zhang, L. Smad2 increases the apoptosis of activated human hepatic stellate cells induced by TRAIL. *Int. Immunopharmacol.* **2016**, *32*, 76–86. [CrossRef]
138. Inagaki, Y.; Okazaki, I. Emerging insights into Transforming growth factor β Smad signal in hepatic fibrogenesis. *Gut* **2007**, *56*, 284–292. [CrossRef]
139. Park, S.-H. Fine Tuning and Cross-talking of TGF- β Signal by Inhibitory Smads. *BMB Rep.* **2005**, *38*, 9–16. [CrossRef]
140. Dooley, S.; Hamzavi, J.; Ciucan, L.; Godoy, P.; Ilkavets, I.; Ehner, S.; Ueberham, E.; Gebhardt, R.; Kanzler, S.; Geier, A.; et al. Hepatocyte-specific Smad7 expression attenuates TGF-beta-mediated fibrogenesis and protects against liver damage. *Gastroenterology* **2008**, *135*, 642–659. [CrossRef] [PubMed]
141. Liu, X.; Wang, W.; Hu, H.; Tang, N.; Zhang, C.; Liang, W.; Wang, M. Smad3 specific inhibitor, naringenin, decreases the expression of extracellular matrix induced by TGF-beta1 in cultured rat hepatic stellate cells. *Pharm Res.* **2006**, *23*, 82–89. [CrossRef] [PubMed]
142. Hernandez-Aquino, E.; Zarco, N.; Casas-Grajales, S.; Ramos-Tovar, E.; Flores-Beltran, R.E.; Arauz, J.; Shibayama, M.; Favari, L.; Tsutsumi, V.; Segovia, J.; et al. Naringenin prevents experimental liver fibrosis by blocking TGFbeta-Smad3 and JNK-Smad3 pathways. *World J. Gastroenterol.* **2017**, *23*, 4354–4368. [CrossRef] [PubMed]
143. Yoshida, K.; Murata, M.; Yamaguchi, T.; Matsuzaki, K.; Okazaki, K. Reversible Human TGF-beta Signal Shifting between Tumor Suppression and Fibro-Carcinogenesis: Implications of Smad Phospho-Isoforms for Hepatic Epithelial-Mesenchymal Transitions. *J. Clin. Med.* **2016**, *5*, 7. [CrossRef] [PubMed]
144. Liu, R.-M.; Desai, L.P. Reciprocal regulation of TGF- β and reactive oxygen species: A perverse cycle for fibrosis. *Redox Biol.* **2015**, *6*, 565–577. [CrossRef] [PubMed]
145. Sánchez-Valle, V.; Chávez-Tapia, N.C.; Uribe, M.; Méndez-Sánchez, N. Role of oxidative stress and molecular changes in liver fibrosis: A review. *Curr. Med. Chem.* **2012**, *19*, 4850–4860. [CrossRef]
146. Reth, M. Hydrogen peroxide as second messenger in lymphocyte activation. *Nat. Immunol.* **2002**, *3*, 1129–1134. [CrossRef]
147. Zhang, Q.; Raoof, M.; Chen, Y.; Sumi, Y.; Sursal, T.; Junger, W.; Brohi, K.; Itagaki, K.; Hauser, C.J. Circulating mitochondrial DAMPs cause inflammatory responses to injury. *Nature* **2010**, *464*, 104–107. [CrossRef]
148. Choi, J.; James Ou, J.-H. Mechanisms of Liver Injury. III. Oxidative stress in the pathogenesis of hepatitis C virus. *Am. J. Physiol. Liver Physiol.* **2006**, *290*, G847–G851. [CrossRef]
149. Ivanov, A.V.; Valuev-Elliston, V.T.; Tyurina, D.A.; Ivanova, O.N.; Kochetkov, S.N.; Bartosch, B.; Isagulants, M.G. Oxidative stress, a trigger of hepatitis C and B virus-induced liver carcinogenesis. *Oncotarget* **2016**, *8*, 3895–3932. [CrossRef]
150. Liang, S.; Kisseleva, T.; Brenner, D.A. The Role of NADPH Oxidases (NOXs) in Liver Fibrosis and the Activation of Myofibroblasts. *Front. Physiol.* **2016**, *7*. [CrossRef] [PubMed]
151. Bataller, R.; Sancho-bru, P.; Ginès, P.; Lora, J.M.; Al-garawi, A.; Solé, M.; Colmenero, J.; Nicolás, J.M.; Jiménez, W.; Weich, N.; et al. Activated human hepatic stellate cells express the renin-angiotensin system and synthesize angiotensin II. *Gastroenterology* **2003**, *125*, 117–125. [CrossRef]
152. Sancho, P.; Mainez, J.; Crosas-Molist, E.; Roncero, C.; Fernández-Rodríguez, C.M.; Pinedo, F.; Huber, H.; Eferl, R.; Mikulits, W.; Fabregat, I. NADPH Oxidase NOX4 Mediates Stellate Cell Activation and Hepatocyte Cell Death during Liver Fibrosis Development. *PLoS ONE* **2012**, *7*, e45285. [CrossRef] [PubMed]
153. Bettaieb, A.; Jiang, J.X.; Sasaki, Y.; Chao, T.-I.; Kiss, Z.; Chen, X.; Tian, J.; Katsuyama, M.; Yabe-Nishimura, C.; Xi, Y.; et al. Hepatocyte NADPH Oxidase 4 Regulates Stress Signaling, Fibrosis, and Insulin Sensitivity During Development of Steatohepatitis in Mice. *Gastroenterology* **2015**, *149*, 468–480. [CrossRef] [PubMed]
154. Jiang, J.X.; Chen, X.; Serizawa, N.; Szyndralewicz, C.; Page, P.; Schroder, K.; Brandes, R.P.; Devaraj, S.; Torok, N.J. Liver fibrosis and hepatocyte apoptosis are attenuated by GKT137831, a novel NOX4/NOX1 inhibitor in vivo. *Free Radic. Biol. Med.* **2012**, *53*, 289–296. [CrossRef]
155. Luedde, T.; Schwabe, R.F. NF- κ B in the liver—linking injury, fibrosis and hepatocellular carcinoma. *Nat. Rev.*

- Gastroenterol. Hepatol.* **2011**, *8*, 108–118. [CrossRef]
156. Muriel, P. NF- κ B in liver diseases: A target for drug therapy. *J. Appl. Toxicol.* **2009**, *29*, 91–100. [CrossRef]
157. Moran-Salvador, E.; Mann, J. Epigenetics and Liver Fibrosis. *Cell. Mol. Gastroenterol. Hepatol.* **2017**, *4*, 125–134. [CrossRef]
158. Götze, S.; Schumacher, E.C.; Kordes, C.; Häussinger, D. Epigenetic Changes during Hepatic Stellate Cell Activation. *PLoS ONE* **2015**, *10*, e0128745. [CrossRef]
159. El Taghdouini, A.; Sørensen, A.L.; Reiner, A.H.; Coll, M.; Verhulst, S.; Mannaerts, I.; Øie, C.I.; Smedsrød, B.; Najimi, M.; Sokal, E.; et al. Genome-wide analysis of DNA methylation and gene expression patterns in purified, uncultured human liver cells and activated hepatic stellate cells. *Oncotarget* **2015**, *6*, 26729–26745. [CrossRef]
160. Komatsu, Y.; Waku, T.; Iwasaki, N.; Ono, W.; Yamaguchi, C.; Yanagisawa, J. Global analysis of DNA methylation in early-stage liver fibrosis. *BMC Med. Genom.* **2012**, *5*, 5. [CrossRef] [PubMed]
161. Del Campo, J.A.; Gallego, P.; Grande, L. Role of inflammatory response in liver diseases: Therapeutic strategies. *World J. Hepatol.* **2018**, *10*, 1–7. [CrossRef] [PubMed]
162. Csak, T.; Ganz, M.; Pespisa, J.; Kodys, K.; Dolganiuc, A.; Szabo, G. Fatty acid and endotoxin activate inflammasomes in mouse hepatocytes that release danger signals to stimulate immune cells. *Hepatology* **2011**, *54*, 133–144. [CrossRef] [PubMed]
163. Wree, A.; McGeough, M.D.; Pena, C.A.; Schlattjan, M.; Li, H.; Inzaugarat, M.E.; Messer, K.; Canbay, A.; Hoffman, H.M.; Feldstein, A.E. NLRP3 inflammasome activation is required for fibrosis development in NAFLD. *J. Mol. Med. (Berl)* **2014**, *92*, 1069–1082. [CrossRef] [PubMed]
164. Wen, H.; Gris, D.; Lei, Y.; Jha, S.; Zhang, L.; Huang, M.T.; Brickey, W.J.; Ting, J.P. Fatty acid-induced NLRP3-ASC inflammasome activation interferes with insulin signaling. *Nat. Immunol.* **2011**, *12*, 408–415. [CrossRef] [PubMed]
165. Miura, K.; Yang, L.; van Rooijen, N.; Brenner, D.A.; Ohnishi, H.; Seki, E. Toll-like receptor 2 and palmitic acid cooperatively contribute to the development of nonalcoholic steatohepatitis through inflammasome activation in mice. *Hepatology* **2013**, *57*, 577–589. [CrossRef] [PubMed]
166. Wree, A.; Eguchi, A.; McGeough, M.D.; Pena, C.A.; Johnson, C.D.; Canbay, A.; Hoffman, H.M.; Feldstein, A.E. NLRP3 inflammasome activation results in hepatocyte pyroptosis, liver inflammation, and fibrosis in mice. *Hepatology* **2014**, *59*, 898–910. [CrossRef] [PubMed]
167. Mridha, A.R.; Wree, A.; Robertson, A.A.B.; Yeh, M.M.; Johnson, C.D.; Van Rooyen, D.M.; Haczejni, F.; Teoh, N.C.; Savard, C.; Ioannou, G.N.; et al. NLRP3 inflammasome blockade reduces liver inflammation and fibrosis in experimental NASH in mice. *J. Hepatol.* **2017**, *66*, 1037–1046. [CrossRef] [PubMed]
168. Berg, T.; DeLanghe, S.; Al Alam, D.; Utley, S.; Estrada, J.; Wang, K.S. beta-catenin regulates mesenchymal progenitor cell differentiation during hepatogenesis. *J. Surg. Res.* **2010**, *164*, 276–285. [CrossRef] [PubMed]
169. Lavanchy, D. The global burden of hepatitis C. *L Liver Int.* **2009**, *29* (Suppl. 1), 74–81. [CrossRef]
170. Lingala, S.; Ghany, M.G. Natural History of Hepatitis, C. *Gastroenterol. Clin. North. Am.* **2015**, *44*, 717–734. [CrossRef] [PubMed]
171. Baumert, T.F.; Berg, T.; Lim, J.K.; Nelson, D.R. Status of Direct-Acting Antiviral Therapy for Hepatitis C Virus Infection and Remaining Challenges. *Gastroenterology* **2019**, *156*, 431–445. [CrossRef] [PubMed]
172. Jacobson Brown, P.M.; Neuman, M.G. Immunopathogenesis of hepatitis C viral infection: Th1/Th2 responses and the role of cytokines. *Clin. Biochem.* **2001**, *34*, 167–171. [CrossRef]
173. Boltjes, A.; Movita, D.; Boonstra, A.; Woltman, A.M. The role of Kupffer cells in hepatitis B and hepatitis C virus infections. *J. Hepatol.* **2014**, *61*, 660–671. [CrossRef]
174. Baskic, D.; Vukovic, V.; Popovic, S.; Jovanovic, D.; Mitrovic, S.; Djurdjevic, P.; Avramovic, D.; Arsovic, A.; Bankovic, D.; Cukic, J.; et al. Chronic Hepatitis C: Conspectus of immunological events in the course of fibrosis evolution. *PLoS ONE* **2019**, *14*, e0219508. [CrossRef]
175. Schulze-Krebs, A.; Preimel, D.; Popov, Y.; Bartenschlager, R.; Lohmann, V.; Pinzani, M.; Schuppan, D. Hepatitis C virus-replicating hepatocytes induce fibrogenic activation of hepatic stellate cells. *Gastroenterology* **2005**, *129*, 246–258. [CrossRef]
176. Bataller, R.; Paik, Y.H.; Lindquist, J.N.; Lemasters, J.J.; Brenner, D.A. Hepatitis C virus core and nonstructural proteins induce fibrogenic effects in hepatic stellate cells. *Gastroenterology* **2004**, *126*, 529–540. [CrossRef]
177. Korenaga, M.; Wang, T.; Li, Y.; Showalter, L.A.; Chan, T.; Sun, J.; Weinman, S.A. Hepatitis C Virus Core Protein Inhibits Mitochondrial Electron Transport and Increases Reactive Oxygen Species (ROS) Production. *J. Biol. Chem.* **2005**, *280*, 37481–37488. [CrossRef]
178. Okuda, M.; Li, K.; Beard, M.R.; Showalter, L.A.; Scholle, F.; Lemon, S.M.; Weinman, S.A. Mitochondrial injury, oxidative stress, and antioxidant gene expression are induced by hepatitis C virus core protein. *Gastroenterology* **2002**, *122*, 366–375. [CrossRef]
179. Thorén, F.; Romero, A.; Lindh, M.; Dahlgren, C.; Hellstrand, K. A hepatitis C virus-encoded, nonstructural protein (NS3) triggers dysfunction and apoptosis in lymphocytes: Role of NADPH oxidase-derived oxygen radicals. *J. Leukoc. Biol.* **2004**, *76*, 1180–1186. [CrossRef]

180. Mazzocca, A.; Sciammetta, S.C.; Carloni, V.; Cosmi, L.; Annunziato, F.; Harada, T.; Abrignani, S.; Pinzani, M. Binding of hepatitis C virus envelope protein E2 to CD81 up-regulates matrix metalloproteinase-2 in human hepatic stellate cells. *J. Biol. Chem.* **2005**, *280*, 11329–11339. [CrossRef] [PubMed]
181. Aoudjehane, L.; Bisch, G.; Scatton, O.; Granier, C.; Gaston, J.; Housset, C.; Roingeard, P.; Cosset, F.L.; Perdigo, F.; Balladur, P.; et al. Infection of Human Liver Myofibroblasts by Hepatitis C Virus: A Direct Mechanism of Liver Fibrosis in Hepatitis C. *PLoS ONE* **2015**, *10*, e0134141. [CrossRef] [PubMed]
182. Kanwal, F.; Kramer, J.; Asch, S.M.; Chayanupatkul, M.; Cao, Y.; El-Serag, H.B. Risk of Hepatocellular Cancer in HCV Patients Treated With Direct-Acting Antiviral Agents. *Gastroenterology* **2017**, *153*, 996–1005 e1001. [CrossRef] [PubMed]
183. Kanwal, F.; Kramer, J.R.; Asch, S.M.; Cao, Y.; Li, L.; El-Serag, H.B. Long-Term Risk of Hepatocellular Carcinoma in HCV Patients Treated With Direct Acting Antiviral Agents. *Hepatology* **2020**, *71*, 44–55. [CrossRef] [PubMed]
184. Hamdane, N.; Juhling, F.; Crouchet, E.; El Saghire, H.; Thumann, C.; Oudot, M.A.; Bandiera, S.; Saviano, A.; Ponsolles, C.; Roca Suarez, A.A.; et al. HCV-Induced Epigenetic Changes Associated With Liver Cancer Risk Persist After Sustained Virologic Response. *Gastroenterology* **2019**, *156*, 2313–2329.e2317. [CrossRef] [PubMed]
185. Perez, S.; Kaspi, A.; Domovitz, T.; Davidovich, A.; Lavi-Itzkovitz, A.; Meirson, T.; Alison Holmes, J.; Dai, C.Y.; Huang, C.F.; Chung, R.T.; et al. Hepatitis C virus leaves an epigenetic signature post cure of infection by direct-acting antivirals. *PLoS Genet.* **2019**, *15*, e1008181. [CrossRef]
186. Lohmann, V.; Bartenschlager, R. Indelibly Stamped by Hepatitis C Virus Infection: Persistent Epigenetic Signatures Increasing Liver Cancer Risk. *Gastroenterology* **2019**, *156*, 2130–2133. [CrossRef]
187. Childs, L.; Roesel, S.; Tohme, R.A. Status and progress of hepatitis B control through vaccination in the South-East Asia Region, 1992–2015. *Vaccine* **2018**, *36*, 6–14. [CrossRef]
188. Milich, D.; Liang, T.J. Exploring the biological basis of hepatitis B e antigen in hepatitis B virus infection. *Hepatology* **2003**, *38*, 1075–1086. [CrossRef]
189. Shin, E.C.; Sung, P.S.; Park, S.H. Immune responses and immunopathology in acute and chronic viral hepatitis. *Nat. Rev. Immunol.* **2016**, *16*, 509–523. [CrossRef]
190. Tang, C.M.; Yau, T.O.; Yu, J. Management of chronic hepatitis B infection: Current treatment guidelines, challenges, and new developments. *World J. Gastroenterol.* **2014**, *20*, 6262–6278. [CrossRef] [PubMed]
191. Levrero, M.; Zucman-Rossi, J. Mechanisms of HBV-induced hepatocellular carcinoma. *J. Hepatol.* **2016**, *64*, S84–S101. [CrossRef] [PubMed]
192. Gong, J.; Tu, W.; Han, J.; He, J.; Liu, J.; Han, P.; Wang, Y.; Li, M.; Liu, M.; Liao, J.; et al. Hepatic SATB1 induces paracrine activation of hepatic stellate cells and is upregulated by HBx. *Sci. Rep.* **2016**, *6*, 1–13. [CrossRef] [PubMed]
193. Liu, X. Hepatitis B virus infects hepatic stellate cells and affects their proliferation and expression of collagen type I. *Chin. Med J.* **2009**, *122*, 1455–1461. [PubMed]
194. Martinez, M.G.; Villeret, F.; Testoni, B.; Zoulim, F. Can we cure hepatitis B virus with novel direct-acting antivirals? *Liver Int.* **2020**, *40* (Suppl. 1), 27–34. [CrossRef] [PubMed]
195. Nieto, N.; Friedman, S.L.; Cederbaum, A.I. Cytochrome P450 2E1-derived reactive oxygen species mediate paracrine stimulation of collagen I protein synthesis by hepatic stellate cells. *J. Biol. Chem.* **2002**, *277*, 9853–9864. [CrossRef]
196. Svegliati-Baroni, G.; Inagaki, Y.; Rincon-Sanchez, A.R.; Else, C.; Saccomanno, S.; Benedetti, A.; Ramirez, F.; Rojkind, M. Early response of alpha2(I) collagen to acetaldehyde in human hepatic stellate cells is TGF-beta independent. *Hepatology* **2005**, *42*, 343–352. [CrossRef]
197. Greenwel, P.; Dominguez-Rosales, J.A.; Mavi, G.; Rivas-Estilla, A.M.; Rojkind, M. Hydrogen peroxide: A link between acetaldehyde-elicited alpha1(I) collagen gene up-regulation and oxidative stress in mouse hepatic stellate cells. *Hepatology* **2000**, *31*, 109–116. [CrossRef]
198. Natori, S.; Rust, C.; Stadheim, L.M.; Srinivasan, A.; Burgart, L.J.; Gores, G.J. Hepatocyte apoptosis is a pathologic feature of human alcoholic hepatitis. *J. Hepatol.* **2001**, *34*, 248–253. [CrossRef]
199. Faouzi, S.; Burckhardt, B.E.; Hanson, J.C.; Campe, C.B.; Schrum, L.W.; Rippe, R.A.; Maher, J.J. Anti-Fas induces hepatic chemokines and promotes inflammation by an NF-kappa B-independent, caspase-3-dependent pathway. *J. Biol. Chem.* **2001**, *276*, 49077–49082. [CrossRef]
200. Wheeler, M.D.; Kono, H.; Yin, M.; Nakagami, M.; Uesugi, T.; Arteel, G.E.; Gabele, E.; Rusyn, I.; Yamashina, S.; Froh, M.; et al. The role of Kupffer cell oxidant production in early ethanol-induced liver disease. *Free Radic. Biol. Med.* **2001**, *31*, 1544–1549. [CrossRef]
201. Pastorino, J.G.; Shulga, N.; Hoek, J.B. TNF-alpha-induced cell death in ethanol-exposed cells depends on p38 MAPK signaling but is independent of Bid and caspase-8. *Am. J. Physiol. Liver Physiol.* **2003**, *285*, G503–516. [CrossRef]
202. Matsuoka, M.; Tsukamoto, H. Stimulation of hepatic lipocyte collagen production by Kupffer cell-derived transforming growth factor beta: Implication for a pathogenetic role in alcoholic liver fibrogenesis. *Hepatology* **1990**, *11*, 599–605. [CrossRef] [PubMed]
203. Cook, R.T. Alcohol abuse, alcoholism, and damage to the immune system—A review. *Alcohol. Clin. Exp. Res.* **1998**, *22*, 1927–1942.

204. Guo, T.L.; Zhang, L.X.; Chen, J.P.; Nguyen, V.A.; White, K.L., Jr.; Gao, B. Differential STAT5 activation and phenotypic marker expression by immune cells following low levels of ethanol consumption in mice. *Immunopharmacol. Immunotoxicol.* **2002**, *24*, 121–138. [CrossRef]
205. Collier, S.D.; Pruett, S.B. Mechanisms of suppression of poly I:C-induced activation of NK cells by ethanol. *Alcoholism* **2000**, *21*, 87–95. [CrossRef]
206. Inagaki, Y.; Nemoto, T.; Kushida, M.; Sheng, Y.; Higashi, K.; Ikeda, K.; Kawada, N.; Shirasaki, F.; Takehara, K.; Sugiyama, K.; et al. Interferon alfa down-regulates collagen gene transcription and suppresses experimental hepatic fibrosis in mice. *Hepatology* **2003**, *38*, 890–899. [CrossRef]
207. Radaeva, S.; Sun, R.; Jaruga, B.; Nguyen, V.T.; Tian, Z.; Gao, B. Natural killer cells ameliorate liver fibrosis by killing activated stellate cells in NKG2D-dependent and tumor necrosis factor-related apoptosis-inducing ligand-dependent manners. *Gastroenterology* **2006**, *130*, 435–452. [CrossRef]
208. Friedman, S.L. Mac the knife? Macrophages- the double-edged sword of hepatic fibrosis. *J. Clin. Investig.* **2005**, *115*, 29–32. [CrossRef]
209. Younossi, Z.M.; Koenig, A.B.; Abdelatif, D.; Fazel, Y.; Henry, L.; Wymer, M. Global epidemiology of nonalcoholic fatty liver disease-Meta-analytic assessment of prevalence, incidence, and outcomes. *Hepatology* **2016**, *64*, 73–84. [CrossRef]
210. Estes, C.; Razavi, H.; Loomba, R.; Younossi, Z.; Sanyal, A.J. Modeling the epidemic of nonalcoholic fatty liver disease demonstrates an exponential increase in burden of disease. *Hepatology* **2018**, *67*, 123–133. [CrossRef]
211. Eslam, M.; Sanyal, A.J.; George, J.; an international consensus panel. MAFLD: A consensus-driven proposed nomenclature for metabolic associated fatty liver disease. *Gastroenterology* **2020**. [CrossRef] [PubMed]
212. Tilg, H.; Moschen, A.R. Evolution of inflammation in nonalcoholic fatty liver disease: The multiple parallel hits hypothesis. *Hepatology* **2010**, *52*, 1836–1846. [CrossRef] [PubMed]
213. Peverill, W.; Powell, L.W.; Skoien, R. Evolving concepts in the pathogenesis of NASH: Beyond steatosis and inflammation. *Int. J. Mol. Sci.* **2014**, *15*, 8591–8638. [CrossRef] [PubMed]
214. De Minicis, S.; Agostinelli, L.; Rychlicki, C.; Sorice, G.P.; Saccomanno, S.; Candelaresi, C.; Giaccari, A.; Trozzi, L.; Pierantonelli, I.; Mingarelli, E.; et al. HCC development is associated to peripheral insulin resistance in a mouse model of NASH. *PLoS ONE* **2014**, *9*, e97136. [CrossRef]
215. Wong, V.W.; Chitturi, S.; Wong, G.L.; Yu, J.; Chan, H.L.; Farrell, G.C. Pathogenesis and novel treatment options for non-alcoholic steatohepatitis. *Lancet Gastroenterol. Hepatol.* **2016**, *1*, 56–67. [CrossRef]
216. Sell, S. Heterogeneity and plasticity of hepatocyte lineage cells. *Hepatology* **2001**, *33*, 738–750. [CrossRef]
217. Roskams, T.A.; Theise, N.D.; Balabaud, C.; Bhagat, G.; Bhathal, P.S.; Bioulac-Sage, P.; Brunt, E.M.; Crawford, J.M.; Crosby, H.A.; Desmet, V.; et al. Nomenclature of the finer branches of the biliary tree: Canals, ductules, and ductular reactions in human livers. *Hepatology* **2004**, *39*, 1739–1745. [CrossRef]
218. Svegliati-Baroni, G.; De Minicis, S.; Marziani, M. Hepatic fibrogenesis in response to chronic liver injury: Novel insights on the role of cell-to-cell interaction and transition. *Liver Int.* **2008**, *28*, 1052–1064. [CrossRef]
219. Xia, J.L.; Dai, C.; Michalopoulos, G.K.; Liu, Y. Hepatocyte growth factor attenuates liver fibrosis induced by bile duct ligation. *Am. J. Pathol.* **2006**, *168*, 1500–1512. [CrossRef]
220. Richardson, M.M.; Jonsson, J.R.; Powell, E.E.; Brunt, E.M.; Neuschwander-Tetri, B.A.; Bhathal, P.S.; Dixon, J.B.; Weltman, M.D.; Tilg, H.; Moschen, A.R.; et al. Progressive fibrosis in nonalcoholic steatohepatitis: Association with altered regeneration and a ductular reaction. *Gastroenterology* **2007**, *133*, 80–90. [CrossRef] [PubMed]
221. Van Hul, N.K.; Abarca-Quinones, J.; Sempoux, C.; Horsmans, Y.; Leclercq, I.A. Relation between liver progenitor cell expansion and extracellular matrix deposition in a CDE-induced murine model of chronic liver injury. *Hepatology* **2009**, *49*, 1625–1635. [CrossRef] [PubMed]
222. Ocker, M. Challenges and opportunities in drug development for nonalcoholic steatohepatitis. *Eur. J. Pharmacol.* **2020**, *870*, 172913. [CrossRef] [PubMed]
223. Schuppan, D.; Afdhal, N.H. Liver cirrhosis. *Lancet* **2008**, *371*, 838–851. [CrossRef]
224. Angulo, P.; Kleiner, D.E.; Dam-Larsen, S.; Adams, L.A.; Bjornsson, E.S.; Charatcharoenwitthaya, P.; Mills, P.R.; Keach, J.C.; Lafferty, H.D.; Stahler, A.; et al. Liver Fibrosis, but No Other Histologic Features, Is Associated With Long-term Outcomes of Patients With Nonalcoholic Fatty Liver Disease. *Gastroenterology* **2015**, *149*, 389–397.e310. [CrossRef]
225. Ekstedt, M.; Hagstrom, H.; Nasr, P.; Fredrikson, M.; Stal, P.; Kechagias, S.; Hultcrantz, R. Fibrosis stage is the strongest predictor for disease-specific mortality in NAFLD after up to 33 years of follow-up. *Hepatology* **2015**, *61*, 1547–1554. [CrossRef]
226. Younossi, Z.M.; Stepanova, M.; Rafiq, N.; Makhlof, H.; Younoszai, Z.; Agrawal, R.; Goodman, Z. Pathologic criteria for nonalcoholic steatohepatitis: Interprotocol agreement and ability to predict liver-related mortality. *Hepatology* **2011**, *53*, 1874–1882. [CrossRef]
227. Marcellin, P.; Gane, E.; Buti, M.; Afdhal, N.; Sievert, W.; Jacobson, I.M.; Washington, M.K.; Germanidis, G.; Flaherty, J.F.; Aguilar Schall, R.; et al. Regression of cirrhosis during treatment with tenofovir disoproxil fumarate for chronic hepatitis B: A 5-year open-label follow-up study. *Lancet* **2013**, *381*, 468–475. [CrossRef]

228. D'Ambrosio, R.; Aghemo, A.; Rumi, M.G.; Ronchi, G.; Donato, M.F.; Paradis, V.; Colombo, M.; Bedossa, P. A morphometric and immunohistochemical study to assess the benefit of a sustained virological response in hepatitis C virus patients with cirrhosis. *Hepatology* **2012**, *56*, 532–543. [CrossRef]
229. Levrero, M.; Subic, M.; Villeret, F.; Zoulim, F. Perspectives and limitations for nucleo(t)side analogs in future HBV therapies. *Curr. Opin. Virol.* **2018**, *30*, 80–89. [CrossRef]
230. Vilar-Gomez, E.; Martinez-Perez, Y.; Calzadilla-Bertot, L.; Torres-Gonzalez, A.; Gra-Oramas, B.; Gonzalez-Fabian, L.; Friedman, S.L.; Diago, M.; Romero-Gomez, M. Weight Loss Through Lifestyle Modification Significantly Reduces Features of Nonalcoholic Steatohepatitis. *Gastroenterology* **2015**, *149*, 367–378. [CrossRef] [PubMed]
231. Troeger, J.S.; Mederacke, I.; Gwak, G.Y.; Dapito, D.H.; Mu, X.; Hsu, C.C.; Pradere, J.P.; Friedman, R.A.; Schwabe, R.F. Deactivation of hepatic stellate cells during liver fibrosis resolution in mice. *Gastroenterology* **2012**, *143*, 1073–1083 e1022. [CrossRef] [PubMed]
232. Singh, H.D.; Otano, I.; Rombouts, K.; Singh, K.P.; Peppas, D.; Gill, U.S.; Böttcher, K.; Kennedy, P.T.F.; Oben, J.; Pinzani, M.; et al. TRAIL regulatory receptors constrain human hepatic stellate cell apoptosis. *Sci. Rep.* **2017**, *7*, 1–11. [CrossRef] [PubMed]
233. Arabpour, M.; Cool, R.H.; Faber, K.N.; Quax, W.J.; Haisma, H.J. Receptor-specific TRAIL as a means to achieve targeted elimination of activated hepatic stellate cells. *J. Drug Target.* **2017**, *25*, 360–369. [CrossRef]
234. Park, S.-J.; Sohn, H.-Y.; Yoon, J.; Park, S.I. Down-regulation of FoxO-dependent c-FLIP expression mediates TRAIL-induced apoptosis in activated hepatic stellate cells. *Cell. Signal.* **2009**, *21*, 1495–1503. [CrossRef]
235. Fukushima, J.; Kamada, Y.; Matsumoto, H.; Yoshida, Y.; Ezaki, H.; Takemura, T.; Saji, Y.; Igura, T.; Tsutsui, S.; Kihara, S.; et al. Adiponectin prevents progression of steatohepatitis in mice by regulating oxidative stress and Kupffer cell phenotype polarization. *Hepatol. Res.* **2009**, *39*, 724–738. [CrossRef]
236. Franchi, L.; Warner, N.; Viani, K.; Nuñez, G. Function of Nod-like Receptors in Microbial Recognition and Host Defense. *Immunol. Rev.* **2009**, *227*, 106–128. [CrossRef]
237. Ramachandran, P.; Dobie, R.; Wilson-Kanamori, J.R.; Dora, E.F.; Henderson, B.E.P.; Luu, N.T.; Portman, J.R.; Matchett, K.P.; Brice, M.; Marwick, J.A.; et al. Resolving the fibrotic niche of human liver cirrhosis at single-cell level. *Nature* **2019**, *575*, 512–518. [CrossRef]
238. Glässner, A.; Eisenhardt, M.; Kokordelis, P.; Krämer, B.; Wolter, F.; Nischalke, H.D.; Boesecke, C.; Sauerbruch, T.; Rockstroh, J.K.; Spengler, U.; et al. Impaired CD4+ T cell stimulation of NK cell anti-fibrotic activity may contribute to accelerated liver fibrosis progression in HIV/HCV patients. *J. Hepatol.* **2013**, *59*, 427–433. [CrossRef]
239. Muhanna, N.; Tair, L.A.; Doron, S.; Amer, J.; Azzeh, M.; Mahamid, M.; Friedman, S.; Safadi, R. Amelioration of hepatic fibrosis by NK cell activation. *Gut* **2011**, *60*, 90–98. [CrossRef]
240. Melhem, A.; Muhanna, N.; Bishara, A.; Alvarez, C.E.; Ilan, Y.; Bishara, T.; Horani, A.; Nassar, M.; Friedman, S.L.; Safadi, R. Anti-fibrotic activity of NK cells in experimental liver injury through killing of activated HSC. *J. Hepatol.* **2006**, *45*, 60–71. [CrossRef] [PubMed]
241. JEONG, W.I.; PARK, O.; GAO, B. Abrogation of the Antifibrotic Effects of Natural Killer Cells/Interferon-γ Contributes to Alcohol Acceleration of Liver Fibrosis. *Gastroenterology* **2008**, *134*, 248–258. [CrossRef] [PubMed]
242. Gur, C.; Doron, S.; Kfir-Erenfeld, S.; Horwitz, E.; Abu-tair, L.; Safadi, R.; Mandelboim, O. NKp46-mediated killing of human and mouse hepatic stellate cells attenuates liver fibrosis. *Gut* **2012**, *61*, 885–893. [CrossRef] [PubMed]
243. Tian, Z.; Chen, Y.; Gao, B. Natural Killer Cells in Liver Disease. *Hepatol. (Baltimore, Md.)* **2013**, *57*, 1654–1662. [CrossRef] [PubMed]
244. Bansal, M.B.; Chamroonkul, N. Antifibrotics in liver disease: Are we getting closer to clinical use? *Hepatol. Int.* **2019**, *13*, 25–39. [CrossRef] [PubMed]
245. Latief, U.; Ahmad, R. Herbal remedies for liver fibrosis: A review on the mode of action of fifty herbs. *J. Tradit. Complement. Med.* **2018**, *8*, 352–360. [CrossRef]
246. Duval, F.; Moreno-Cuevas, J.E.; Gonzalez-Garza, M.T.; Maldonado-Bernal, C.; Cruz-Vega, D.E. Liver fibrosis and mechanisms of the protective action of medicinal plants targeting inflammation and the immune response. *Int. J. Inflam.* **2015**, *2015*, 943497. [CrossRef]
247. Neong, S.F.; Adebayo, D.; Wong, F. An update on the pathogenesis and clinical management of cirrhosis with refractory ascites. *Expert. Rev. Gastroenterol. Hepatol.* **2019**, *13*, 293–305. [CrossRef]
248. Wree, A.; Mehal, W.Z.; Feldstein, A.E. Targeting Cell Death and Sterile Inflammation Loop for the Treatment of Nonalcoholic Steatohepatitis. *Semin. Liver Dis.* **2016**, *36*, 27–36. [CrossRef]
249. Schwabe, R.F.; Luedde, T. Apoptosis and necroptosis in the liver: A matter of life and death. *Nat. Rev. Gastroenterol. Hepatol.* **2018**, *15*, 738–752. [CrossRef]
250. Thapaliya, S.; Wree, A.; Povero, D.; Inzaugarat, M.E.; Berk, M.; Dixon, L.; Papouchado, B.G.; Feldstein, A.E. Caspase 3 inactivation protects against hepatic cell death and ameliorates fibrogenesis in a diet-induced NASH model. *Dig. Dis. Sci.* **2014**, *59*, 1197–1206. [CrossRef] [PubMed]
251. Witek, R.P.; Stone, W.C.; Karaca, F.G.; Syn, W.K.; Pereira, T.A.; Agboola, K.M.; Omenetti, A.; Jung, Y.; Teaberry, V.; Choi, S.S.; et al. Pan-caspase inhibitor VX-166 reduces fibrosis in an animal model of nonalcoholic steatohepatitis.

- Hepatology* **2009**, *50*, 1421–1430. [CrossRef] [PubMed]
252. Gracia-Sancho, J.; Manicardi, N.; Ortega-Ribera, M.; Maeso-Diaz, R.; Guixé-Muntet, S.; Fernandez-Iglesias, A.; Hide, D.; Garcia-Caldero, H.; Boyer-Diaz, Z.; Contreras, P.C.; et al. Emricasan Ameliorates Portal Hypertension and Liver Fibrosis in Cirrhotic Rats Through a Hepatocyte-Mediated Paracrine Mechanism. *Hepatol. Commun.* **2019**, *3*, 987–1000. [CrossRef] [PubMed]
253. Harrison, S.A.; Goodman, Z.; Jabbar, A.; Vemulapalli, R.; Younes, Z.H.; Freilich, B.; Sheikh, M.Y.; Schattenberg, J.M.; Kayali, Z.; Zivony, A.; et al. A randomized, placebo-controlled trial of emricasan in patients with NASH and F1-F3 fibrosis. *J. Hepatol.* **2019**. [CrossRef]
254. Garcia-Tsao, G.; Bosch, J.; Kayali, Z.; Harrison, S.A.; Abdelmalek, M.F.; Lawitz, E.; Satapathy, S.K.; Ghabril, M.; Shiffman, M.L.; Younes, Z.H.; et al. Randomized Placebo-Controlled Trial of Emricasan in Non-alcoholic Steatohepatitis (NASH) Cirrhosis with Severe Portal Hypertension. *J. Hepatol.* **2019**. [CrossRef]
255. Mehta, G.; Rousell, S.; Burgess, G.; Morris, M.; Wright, G.; McPherson, S.; Frenette, C.; Cave, M.; Hagerty, D.T.; Spada, A.; et al. A Placebo-Controlled, Multicenter, Double-Blind, Phase 2 Randomized Trial of the Pan-Caspase Inhibitor Emricasan in Patients with Acutely Decompensated Cirrhosis. *J. Clin. Exp. Hepatol.* **2018**, *8*, 224–234. [CrossRef]
256. Budas, G.; Karnik, S.; Jonnson, T.; Watkins, S.; Breckenridge, D. Reduction of liver steatosis and fibrosis with an ASK1 inhibitor in a murine model of NASH is accomplished by improvements in cholesterol, bile acid and lipid metabolism. *J. Hepatol.* **2016**, *64*, S170. [CrossRef]
257. Yamamoto, E.; Dong, Y.F.; Kataoka, K.; Yamashita, T.; Tokutomi, Y.; Matsuba, S.; Ichijo, H.; Ogawa, H.; Kim-Mitsuyama, S. Olmesartan prevents cardiovascular injury and hepatic steatosis in obesity and diabetes, accompanied by apoptosis signal regulating kinase-1 inhibition. *Hypertension* **2008**, *52*, 573–580. [CrossRef]
258. Wang, P.X.; Ji, Y.X.; Zhang, X.J.; Zhao, L.P.; Yan, Z.Z.; Zhang, P.; Shen, L.J.; Yang, X.; Fang, J.; Tian, S.; et al. Targeting CASP8 and FADD-like apoptosis regulator ameliorates nonalcoholic steatohepatitis in mice and nonhuman primates. *Nat. Med.* **2017**, *23*, 439–449. [CrossRef]
259. Loomba, R.; Lawitz, E.; Mantry, P.S.; Jayakumar, S.; Caldwell, S.H.; Arnold, H.; Diehl, A.M.; Djedjos, C.S.; Han, L.; Myers, R.P.; et al. The ASK1 inhibitor selonsertib in patients with nonalcoholic steatohepatitis: A randomized, phase 2 trial. *Hepatology* **2018**, *67*, 549–559. [CrossRef]
260. Schuppan, D.; Surabattula, R.; Wang, X.Y. Determinants of fibrosis progression and regression in NASH. *J. Hepatol.* **2018**, *68*, 238–250. [CrossRef] [PubMed]
261. Wu, L.; Zhang, Q.; Mo, W.; Feng, J.; Li, S.; Li, J.; Liu, T.; Xu, S.; Wang, W.; Lu, X.; et al. Quercetin prevents hepatic fibrosis by inhibiting hepatic stellate cell activation and reducing autophagy via the TGF- β 1/Smads and PI3K/Akt pathways. *Sci. Rep.* **2017**, *7*, 9289. [CrossRef] [PubMed]
262. Cai, Z.; Lou, Q.; Wang, F.; Li, E.; Sun, J.; Fang, H.; Xi, J.; Ju, L. N-acetylcysteine protects against liver injury induced by carbon tetrachloride via activation of the Nrf2/HO-1 pathway. *Int. J. Clin. Exp. Pathol.* **2015**, *8*, 8655–8662. [PubMed]
263. Kessoku, T.; Imajo, K.; Honda, Y.; Kato, T.; Ogawa, Y.; Tomeno, W.; Kato, S.; Mawatari, H.; Fujita, K.; Yoneda, M.; et al. Resveratrol ameliorates fibrosis and inflammation in a mouse model of nonalcoholic steatohepatitis. *Sci. Rep.* **2016**, *6*, 22251. [CrossRef]
264. Sanyal, A.J.; Chalasani, N.; Kowdley, K.V.; McCullough, A.; Diehl, A.M.; Bass, N.M.; Neuschwander-Tetri, B.A.; Lavine, J.E.; Tonascia, J.; Unalp, A.; et al. Pioglitazone, vitamin E, or placebo for nonalcoholic steatohepatitis. *N. Engl. J. Med.* **2010**, *362*, 1675–1685. [CrossRef]
265. Paik, Y.H.; Iwaisako, K.; Seki, E.; Inokuchi, S.; Schnabl, B.; Osterreicher, C.H.; Kisseleva, T.; Brenner, D.A. The nicotinamide adenine dinucleotide phosphate oxidase (NOX) homologues NOX1 and NOX2/gp91(phox) mediate hepatic fibrosis in mice. *Hepatology* **2011**, *53*, 1730–1741. [CrossRef]
266. Aoyama, T.; Paik, Y.H.; Watanabe, S.; Laleu, B.; Gaggini, F.; Fioraso-Cartier, L.; Molango, S.; Heitz, F.; Merlot, C.; Szyndralewicz, C.; et al. Nicotinamide adenine dinucleotide phosphate oxidase in experimental liver fibrosis: GKT137831 as a novel potential therapeutic agent. *Hepatology* **2012**, *56*, 2316–2327. [CrossRef]
267. Milosevic, I.; Vujovic, A.; Barac, A.; Djelic, M.; Korac, M.; Radovanovic Spurnic, A.; Gmizic, I.; Stevanovic, O.; Djordjevic, V.; Lekic, N.; et al. Gut-Liver Axis, Gut Microbiota, and Its Modulation in the Management of Liver Diseases: A Review of the Literature. *Int. J. Mol. Sci.* **2019**, *20*, 395. [CrossRef]
268. Ferrere, G.; Wrzosek, L.; Cailleux, F.; Turpin, W.; Puchois, V.; Spatz, M.; Ciocan, D.; Rainteau, D.; Humbert, L.; Hugot, C.; et al. Fecal microbiota manipulation prevents dysbiosis and alcohol-induced liver injury in mice. *J. Hepatol.* **2017**, *66*, 806–815. [CrossRef]
269. Li, Z.; Yang, S.; Lin, H.; Huang, J.; Watkins, P.A.; Moser, A.B.; Desimone, C.; Song, X.Y.; Diehl, A.M. Probiotics and antibodies to TNF inhibit inflammatory activity and improve nonalcoholic fatty liver disease. *Hepatology* **2003**, *37*, 343–350. [CrossRef]
270. Chen, L.; Pan, D.D.; Zhou, J.; Jiang, Y.Z. Protective effect of selenium-enriched Lactobacillus on CCl4-induced liver injury in mice and its possible mechanisms. *World J. Gastroenterol.* **2005**, *11*, 5795–5800. [CrossRef]
271. Velayudham, A.; Dolganiuc, A.; Ellis, M.; Petrascu, J.; Kodys, K.; Mandrekar, P.; Szabo, G. VSL#3 probiotic treatment attenuates fibrosis without changes in steatohepatitis in a diet-induced nonalcoholic steatohepatitis model in mice.

- Hepatology* **2009**, *49*, 989–997. [CrossRef] [PubMed]
272. Ma, Y.Y.; Li, L.; Yu, C.H.; Shen, Z.; Chen, L.H.; Li, Y.M. Effects of probiotics on nonalcoholic fatty liver disease: A meta-analysis. *World J. Gastroenterol.* **2013**, *19*, 6911–6918. [CrossRef] [PubMed]
273. Wang, W.W.; Zhang, Y.; Huang, X.B.; You, N.; Zheng, L.; Li, J. Fecal microbiota transplantation prevents hepatic encephalopathy in rats with carbon tetrachloride-induced acute hepatic dysfunction. *World J. Gastroenterol.* **2017**, *23*, 6983–6994. [CrossRef] [PubMed]
274. Philips, C.A.; Pande, A.; Shasthry, S.M.; Jamwal, K.D.; Khillan, V.; Chandel, S.S.; Kumar, G.; Sharma, M.K.; Maiwall, R.; Jindal, A.; et al. Healthy Donor Fecal Microbiota Transplantation in Steroid-Ineligible Severe Alcoholic Hepatitis: A Pilot Study. *Clin. Gastroenterol. Hepatol.* **2017**, *15*, 600–602. [CrossRef]
275. Bajaj, J.S.; Kassam, Z.; Fagan, A.; Gavis, E.A.; Liu, E.; Cox, I.J.; Kheradman, R.; Heuman, D.; Wang, J.; Gurry, T.; et al. Fecal microbiota transplant from a rational stool donor improves hepatic encephalopathy: A randomized clinical trial. *Hepatology* **2017**, *66*, 1727–1738. [CrossRef]
276. DeFilipp, Z.; Bloom, P.P.; Torres Soto, M.; Mansour, M.K.; Sater, M.R.A.; Huntley, M.H.; Turbett, S.; Chung, R.T.; Chen, Y.B.; Hohmann, E.L.; et al. coli Bacteremia Transmitted by Fecal Microbiota Transplant. *N. Engl. J. Med.* **2019**, *381*, 2043–2050. [CrossRef]
277. Chou, R.; Dana, T.; Blazina, I.; Daeges, M.; Jeanne, T.L. Statins for Prevention of Cardiovascular Disease in Adults: Evidence Report and Systematic Review for the US Preventive Services Task Force. *JAMA* **2016**, *316*, 2008–2024. [CrossRef]
278. Schierwagen, R.; Maybuchen, L.; Zimmer, S.; Hittatiya, K.; Back, C.; Klein, S.; Uschner, F.E.; Reul, W.; Boor, P.; Nickenig, G.; et al. Seven weeks of Western diet in apolipoprotein-E-deficient mice induce metabolic syndrome and non-alcoholic steatohepatitis with liver fibrosis. *Sci. Rep.* **2015**, *5*, 12931. [CrossRef]
279. Gracia-Sancho, J.; Garcia-Caldero, H.; Hide, D.; Marrone, G.; Guixé-Muntet, S.; Peralta, C.; Garcia-Pagan, J.C.; Abruñales, J.G.; Bosch, J. Simvastatin maintains function and viability of steatotic rat livers procured for transplantation. *J. Hepatol.* **2013**, *58*, 1140–1146. [CrossRef]
280. Schierwagen, R.; Maybuchen, L.; Hittatiya, K.; Klein, S.; Uschner, F.E.; Braga, T.T.; Franklin, B.S.; Nickenig, G.; Strassburg, C.P.; Plat, J.; et al. Statins improve NASH via inhibition of RhoA and Ras. *Am. J. Physiol. Liver Physiol.* **2016**, *311*, G724–G733. [CrossRef] [PubMed]
281. Pose, E.; Trebicka, J.; Mookerjee, R.P.; Angeli, P.; Gines, P. Statins: Old drugs as new therapy for liver diseases? *J. Hepatol.* **2019**, *70*, 194–202. [CrossRef] [PubMed]
282. Chong, L.W.; Hsu, Y.C.; Lee, T.F.; Lin, Y.; Chiu, Y.T.; Yang, K.C.; Wu, J.C.; Huang, Y.T. Fluvastatin attenuates hepatic steatosis-induced fibrogenesis in rats through inhibiting paracrine effect of hepatocyte on hepatic stellate cells. *BMC Gastroenterol.* **2015**, *15*, 22. [CrossRef] [PubMed]
283. Arab, J.P.; Shah, V.H. Statins and portal hypertension: A tale of two models. *Hepatology* **2016**, *63*, 2044–2047. [CrossRef]
284. Moreno, M.; Ramalho, L.N.; Sancho-Bru, P.; Ruiz-Ortega, M.; Ramalho, F.; Abruñales, J.G.; Colmenero, J.; Dominguez, M.; Egido, J.; Arroyo, V.; et al. Atorvastatin attenuates angiotensin II-induced inflammatory actions in the liver. *Am. J. Physiol. Liver Physiol.* **2009**, *296*, G147–156. [CrossRef] [PubMed]
285. Kamal, S.; Khan, M.A.; Seth, A.; Cholankeril, G.; Gupta, D.; Singh, U.; Kamal, F.; Howden, C.W.; Stave, C.; Nair, S.; et al. Beneficial Effects of Statins on the Rates of Hepatic Fibrosis, Hepatic Decompensation, and Mortality in Chronic Liver Disease: A Systematic Review and Meta-Analysis. *Am. J. Gastroenterol.* **2017**, *112*, 1495–1505. [CrossRef]
286. Pollo-Flores, P.; Soldan, M.; Santos, U.C.; Kunz, D.G.; Mattos, D.E.; da Silva, A.C.; Marchiori, R.C.; Rezende, G.F. Three months of simvastatin therapy vs. placebo for severe portal hypertension in cirrhosis: A randomized controlled trial. *Dig. Liver Dis.* **2015**, *47*, 957–963. [CrossRef]
287. Chang, F.M.; Wang, Y.P.; Lang, H.C.; Tsai, C.F.; Hou, M.C.; Lee, F.Y.; Lu, C.L. Statins decrease the risk of decompensation in hepatitis B virus- and hepatitis C virus-related cirrhosis: A population-based study. *Hepatology* **2017**, *66*, 896–907. [CrossRef]
288. Abruñales, J.G.; Albillos, A.; Banares, R.; Turnes, J.; Gonzalez, R.; Garcia-Pagan, J.C.; Bosch, J. Simvastatin lowers portal pressure in patients with cirrhosis and portal hypertension: A randomized controlled trial. *Gastroenterology* **2009**, *136*, 1651–1658. [CrossRef]
289. Naci, H.; Brugts, J.J.; Fleurence, R.; Tsoi, B.; Toor, H.; Ades, A.E. Comparative benefits of statins in the primary and secondary prevention of major coronary events and all-cause mortality: A network meta-analysis of placebo-controlled and active-comparator trials. *Eur. J. Prev Cardiol.* **2013**, *20*, 641–657. [CrossRef]
290. Pose, E.; Napoleone, L.; Amin, A.; Campion, D.; Jimenez, C.; Piano, S.; Roux, O.; Uschner, F.E.; de Wit, K.; Zaccherini, G.; et al. Safety of two different doses of simvastatin plus rifaximin in decompensated cirrhosis (LIVERHOPE-SAFETY): A randomised, double-blind, placebo-controlled, phase 2 trial. *Lancet Gastroenterol. Hepatol.* **2020**, *5*, 31–41. [CrossRef]
291. Cheng, J.H.; She, H.; Han, Y.P.; Wang, J.; Xiong, S.; Asahina, K.; Tsukamoto, H. Wnt antagonism inhibits hepatic stellate cell activation and liver fibrosis. *Am. J. Physiol. Liver Physiol.* **2008**, *294*, G39–49. [CrossRef] [PubMed]

292. Kordes, C.; Sawitzka, I.; Haussinger, D. Canonical Wnt signaling maintains the quiescent stage of hepatic stellate cells. *Biochem. Biophys. Res. Commun.* **2008**, *367*, 116–123. [CrossRef] [PubMed]
293. Emami, K.H.; Nguyen, C.; Ma, H.; Kim, D.H.; Jeong, K.W.; Eguchi, M.; Moon, R.T.; Teo, J.L.; Kim, H.Y.; Moon, S.H.; et al. A small molecule inhibitor of beta-catenin/CREB-binding protein transcription [corrected]. *Proc. Natl. Acad. Sci. USA* **2004**, *101*, 12682–12687. [CrossRef] [PubMed]
294. Akcora, B.O.; Storm, G.; Bansal, R. Inhibition of canonical WNT signaling pathway by beta-catenin/CBP inhibitor ICG-001 ameliorates liver fibrosis in vivo through suppression of stromal CXCL12. *Biochim. Biophys. Acta Mol. Basis Dis.* **2018**, *1864*, 804–818. [CrossRef] [PubMed]
295. Henderson, W.R., Jr.; Chi, E.Y.; Ye, X.; Nguyen, C.; Tien, Y.T.; Zhou, B.; Borok, Z.; Knight, D.A.; Kahn, M. Inhibition of Wnt/beta-catenin/CREB binding protein (CBP) signaling reverses pulmonary fibrosis. *Proc. Natl. Acad. Sci. USA* **2010**, *107*, 14309–14314. [CrossRef]
296. Hao, S.; He, W.; Li, Y.; Ding, H.; Hou, Y.; Nie, J.; Hou, F.F.; Kahn, M.; Liu, Y. Targeted inhibition of beta-catenin/CBP signaling ameliorates renal interstitial fibrosis. *J. Am. Soc. Nephrol.* **2011**, *22*, 1642–1653. [CrossRef]
297. Tokunaga, Y.; Osawa, Y.; Ohtsuki, T.; Hayashi, Y.; Yamaji, K.; Yamane, D.; Hara, M.; Munekata, K.; Tsukiyama-Kohara, K.; Hishima, T.; et al. Selective inhibitor of Wnt/beta-catenin/CBP signaling ameliorates hepatitis C virus-induced liver fibrosis in mouse model. *Sci. Rep.* **2017**, *7*, 325. [CrossRef]
298. Osawa, Y.; Oboki, K.; Imamura, J.; Kojika, E.; Hayashi, Y.; Hishima, T.; Saibara, T.; Shibasaki, F.; Kohara, M.; Kimura, K. Inhibition of Cyclic Adenosine Monophosphate (cAMP)-response Element-binding Protein (CREB)-binding Protein (CBP)/beta-Catenin Reduces Liver Fibrosis in Mice. *EBioMedicine* **2015**, *2*, 1751–1758. [CrossRef]
299. Osawa, Y.; Kojika, E.; Hayashi, Y.; Kimura, M.; Nishikawa, K.; Yoshio, S.; Doi, H.; Kanto, T.; Kimura, K. Tumor necrosis factor-alpha-mediated hepatocyte apoptosis stimulates fibrosis in the steatotic liver in mice. *Hepatol. Commun.* **2018**, *2*, 407–420. [CrossRef]
300. Ubeda, M.; Lario, M.; Munoz, L.; Borrero, M.J.; Rodriguez-Serrano, M.; Sanchez-Diaz, A.M.; Del Campo, R.; Lledo, L.; Pastor, O.; Garcia-Bermejo, L.; et al. Obeticholic acid reduces bacterial translocation and inhibits intestinal inflammation in cirrhotic rats. *J. Hepatol.* **2016**, *64*, 1049–1057. [CrossRef]
301. Schwabl, P.; Hambruch, E.; Seeland, B.A.; Hayden, H.; Wagner, M.; Garnys, L.; Strobel, B.; Schubert, T.L.; Riedl, F.; Mitteregger, D.; et al. The FXR agonist PX20606 ameliorates portal hypertension by targeting vascular remodelling and sinusoidal dysfunction. *J. Hepatol.* **2017**, *66*, 724–733. [CrossRef] [PubMed]
302. Gulamhusein, A.F.; Hirschfield, G.M. Primary biliary cholangitis: Pathogenesis and therapeutic opportunities. *Nat. Rev. Gastroenterol. Hepatol.* **2019**. [CrossRef]
303. Nevens, F.; Andreone, P.; Mazzella, G.; Strasser, S.I.; Bowlus, C.; Invernizzi, P.; Drenth, J.P.; Pockros, P.J.; Regula, J.; Beuers, U.; et al. A Placebo-Controlled Trial of Obeticholic Acid in Primary Biliary Cholangitis. *N. Engl. J. Med.* **2016**, *375*, 631–643. [CrossRef]
304. Bowlus, C.L.; Pockros, P.J.; Kremer, A.E.; Pares, A.; Forman, L.M.; Drenth, J.P.H.; Ryder, S.D.; Terracciano, L.; Jin, Y.; Liberman, A.; et al. Long-Term Obeticholic Acid Therapy Improves Histological Endpoints in Patients With Primary Biliary Cholangitis. *Clin. Gastroenterol. Hepatol.* **2019**. [CrossRef] [PubMed]
305. Fiorucci, S.; Antonelli, E.; Rizzo, G.; Renga, B.; Mencarelli, A.; Riccardi, L.; Orlandi, S.; Pellicciari, R.; Morelli, A. The nuclear receptor SHP mediates inhibition of hepatic stellate cells by FXR and protects against liver fibrosis. *Gastroenterology* **2004**, *127*, 1497–1512. [CrossRef] [PubMed]
306. Modica, S.; Gadaleta, R.M.; Moschetta, A. Deciphering the nuclear bile acid receptor FXR paradigm. *Nucl. Recept. Signal.* **2010**, *8*, e005. [CrossRef]
307. Wang, Y.D.; Chen, W.D.; Wang, M.; Yu, D.; Forman, B.M.; Huang, W. Farnesoid X receptor antagonizes nuclear factor kappaB in hepatic inflammatory response. *Hepatology* **2008**, *48*, 1632–1643. [CrossRef]
308. Neuschwander-Tetri, B.A.; Loomba, R.; Sanyal, A.J.; Lavine, J.E.; Van Natta, M.L.; Abdelmalek, M.F.; Chalasani, N.; Dasarthy, S.; Diehl, A.M.; Hameed, B.; et al. Farnesoid X nuclear receptor ligand obeticholic acid for non-cirrhotic, non-alcoholic steatohepatitis (FLINT): A multicentre, randomised, placebo-controlled trial. *Lancet* **2015**, *385*, 956–965. [CrossRef]
309. Younossi, Z.M.; Ratziu, V.; Loomba, R.; Rinella, M.; Anstee, Q.M.; Goodman, Z.; Bedossa, P.; Geier, A.; Beckebaum, S.; Newsome, P.N.; et al. Obeticholic acid for the treatment of non-alcoholic steatohepatitis: Interim analysis from a multicentre, randomised, placebo-controlled phase 3 trial. *Lancet* **2019**, *394*, 2184–2196. [CrossRef]
310. Schuppan, D. Structure of the extracellular matrix in normal and fibrotic liver: Collagens and glycoproteins. *Semin. Liver Dis.* **1990**, *10*, 1–10. [CrossRef]
311. Karsdal, M.A.; Nielsen, S.H.; Leeming, D.J.; Langholm, L.L.; Nielsen, M.J.; Manon-Jensen, T.; Siebuhr, A.; Gudmann, N.S.; Ronnow, S.; Sand, J.M.; et al. The good and the bad collagens of fibrosis-Their role in signaling and organ function. *Adv. Drug Deliv. Rev.* **2017**, *121*, 43–56. [CrossRef] [PubMed]
312. Jimenez Calvente, C.; Sehgal, A.; Popov, Y.; Kim, Y.O.; Zevallos, V.; Sahin, U.; Diken, M.; Schuppan, D. Specific hepatic delivery of procollagen alpha1(I) small interfering RNA in lipid-like nanoparticles resolves liver fibrosis. *Hepatology* **2015**, *62*, 1285–1297. [CrossRef] [PubMed]

313. Molokanova, O.; Schonig, K.; Weng, S.Y.; Wang, X.; Bros, M.; Diken, M.; Ohngemach, S.; Karsdal, M.; Strand, D.; Nikolaev, A.; et al. Inducible knockdown of procollagen I protects mice from liver fibrosis and leads to dysregulated matrix genes and attenuated inflammation. *Matrix Biol.* **2018**, *66*, 34–49. [CrossRef] [PubMed]
314. Sato, Y.; Murase, K.; Kato, J.; Kobune, M.; Sato, T.; Kawano, Y.; Takimoto, R.; Takada, K.; Miyanishi, K.; Matsunaga, T.; et al. Resolution of liver cirrhosis using vitamin A-coupled liposomes to deliver siRNA against a collagen-specific chaperone. *Nat. Biotechnol.* **2008**, *26*, 431–442. [CrossRef] [PubMed]
315. Soule, B.; Tiruchera, G.; Kavita, U.; Kundu, S.R.C. Safety, tolerability, and pharmacokinetics of BMS-986263/ND-L02-s0201, a novel targeted lipid nanoparticle delivering HSP47siRNA, in healthy participants: A randomised, placebo-controlled, double-blind, phase 1 study. *J. Hepatol.* **2018**, *68*, S112. [CrossRef]
316. Perepelyuk, M.; Terajima, M.; Wang, A.Y.; Georges, P.C.; Janmey, P.A.; Yamauchi, M.; Wells, R.G. Hepatic stellate cells and portal fibroblasts are the major cellular sources of collagens and lysyl oxidases in normal liver and early after injury. *Am. J. Physiol. Liver Physiol.* **2013**, *304*, G605–G614. [CrossRef] [PubMed]
317. Smith-Mungo, L.I.; Kagan, H.M. Lysyl oxidase: Properties, regulation and multiple functions in biology. *Matrix Biol.* **1998**, *16*, 387–398. [CrossRef]
318. Elbjerrami, W.M.; Yonter, E.O.; Starcher, B.C.; West, J.L. Enhancing mechanical properties of tissue-engineered constructs via lysyl oxidase crosslinking activity. *J. Biomed. Mater. Res. A* **2003**, *66*, 513–521. [CrossRef]
319. van der Slot-Verhoeven, A.J.; van Dura, E.A.; Attema, J.; Blauw, B.; Degroot, J.; Huizinga, T.W.; Zuurmond, A.M.; Bank, R.A. The type of collagen cross-link determines the reversibility of experimental skin fibrosis. *Biochim Biophys Acta* **2005**, *1740*, 60–67. [CrossRef]
320. Huang, D.; Chang, T.R.; Aggarwal, A.; Lee, R.C.; Ehrlich, H.P. Mechanisms and dynamics of mechanical strengthening in ligament-equivalent fibroblast-populated collagen matrices. *Ann. Biomed. Eng.* **1993**, *21*, 289–305. [CrossRef]
321. Giampuzzi, M.; Botti, G.; Di Duca, M.; Arata, L.; Ghiggeri, G.; Gusmano, R.; Ravazzolo, R.; Di Donato, A. Lysyl oxidase activates the transcription activity of human collagen III promoter. Possible involvement of Ku antigen. *J. Boil. Chem.* **2000**, *275*, 36341–36349. [CrossRef]
322. Atsawasuwan, P.; Mochida, Y.; Katafuchi, M.; Kaku, M.; Fong, K.S.; Csiszar, K.; Yamauchi, M. Lysyl oxidase binds transforming growth factor-beta and regulates its signaling via amine oxidase activity. *J. Boil. Chem.* **2008**, *283*, 34229–34240. [CrossRef] [PubMed]
323. Lucero, H.A.; Ravid, K.; Grimsby, J.L.; Rich, C.B.; DiCamillo, S.J.; Maki, J.M.; Myllyharju, J.; Kagan, H.M. Lysyl oxidase oxidizes cell membrane proteins and enhances the chemotactic response of vascular smooth muscle cells. *J. Boil. Chem.* **2008**, *283*, 24103–24117. [CrossRef] [PubMed]
324. Fiume, L.; Favilli, G. Inhibition of experimental cirrhosis by carbon tetrachloride following treatment with aminoacetonitrile. *Nature* **1961**, *189*, 71–72. [CrossRef] [PubMed]
325. Liu, S.B.; Ikenaga, N.; Peng, Z.W.; Sverdlov, D.Y.; Greenstein, A.; Smith, V.; Schuppan, D.; Popov, Y. Lysyl oxidase activity contributes to collagen stabilization during liver fibrosis progression and limits spontaneous fibrosis reversal in mice. *FASEB J.* **2016**, *30*, 1599–1609. [CrossRef] [PubMed]
326. Ikenaga, N.; Peng, Z.W.; Vaid, K.A.; Liu, S.B.; Yoshida, S.; Sverdlov, D.Y.; Mikels-Vigdal, A.; Smith, V.; Schuppan, D.; Popov, Y.V. Selective targeting of lysyl oxidase-like 2 (LOXL2) suppresses hepatic fibrosis progression and accelerates its reversal. *Gut* **2017**, *66*, 1697–1708. [CrossRef]
327. Barry-Hamilton, V.; Spangler, R.; Marshall, D.; McCauley, S.; Rodriguez, H.M.; Oyasu, M.; Mikels, A.; Vaysberg, M.; Ghermazien, H.; Wai, C.; et al. Allosteric inhibition of lysyl oxidase-like-2 impedes the development of a pathologic microenvironment. *Nat. Med.* **2010**, *16*, 1009–1017. [CrossRef]
328. Harrison, S.A.; Abdelmalek, M.F.; Caldwell, S.; Shiffman, M.L.; Diehl, A.M.; Ghalib, R.; Lawitz, E.J.; Rockey, D.C.; Schall, R.A.; Jia, C.; et al. Simtuzumab Is Ineffective for Patients With Bridging Fibrosis or Compensated Cirrhosis Caused by Nonalcoholic Steatohepatitis. *Gastroenterology* **2018**, *155*, 1140–1153. [CrossRef]
329. Muir, A.J.; Levy, C.; Janssen, H.L.A.; Montano-Loza, A.J.; Shiffman, M.L.; Caldwell, S.; Luketic, V.; Ding, D.; Jia, C.; McColgan, B.J.; et al. Simtuzumab for Primary Sclerosing Cholangitis: Phase 2 Study Results With Insights on the Natural History of the Disease. *Hepatology* **2019**, *69*, 684–698. [CrossRef]
330. Meissner, E.G.; McLaughlin, M.; Matthews, L.; Gharib, A.M.; Wood, B.J.; Levy, E.; Sinkus, R.; Virtaneva, K.; Sturdevant, D.; Martens, C.; et al. Simtuzumab treatment of advanced liver fibrosis in HIV and HCV-infected adults: Results of a 6-month open-label safety trial. *Liver Int.* **2016**, *36*, 1783–1792. [CrossRef]
331. Pradere, J.P.; Kluwe, J.; De Minicis, S.; Jiao, J.J.; Gwak, G.Y.; Dapito, D.H.; Jang, M.K.; Guenther, N.D.; Mederacke, I.; Friedman, R.; et al. Hepatic macrophages but not dendritic cells contribute to liver fibrosis by promoting the survival of activated hepatic stellate cells in mice. *Hepatology* **2013**, *58*, 1461–1473. [CrossRef] [PubMed]
332. Baek, C.; Wehr, A.; Karlmark, K.R.; Heymann, F.; Vucur, M.; Gassler, N.; Huss, S.; Klussmann, S.; Eulberg, D.; Luedde, T.; et al. Pharmacological inhibition of the chemokine CCL2 (MCP-1) diminishes liver macrophage infiltration and steatohepatitis in chronic hepatic injury. *Gut* **2012**, *61*, 416–426. [CrossRef] [PubMed]
333. Lefebvre, E.; Moyle, G.; Reshef, R.; Richman, L.P.; Thompson, M.; Hong, F.; Chou, H.L.; Hashiguchi, T.; Plato, C.; Poulin, D.; et al. Antifibrotic Effects of the Dual CCR2/CCR5 Antagonist Cenicriviroc in Animal Models of Liver and Kidney

- Fibrosis. *PLoS ONE* **2016**, *11*, e0158156. [CrossRef] [PubMed]
334. Mossanen, J.C.; Krenkel, O.; Ergen, C.; Govaere, O.; Liepelt, A.; Puengel, T.; Heymann, F.; Kalthoff, S.; Lefebvre, E.; Eulberg, D.; et al. Chemokine (C-C motif) receptor 2-positive monocytes aggravate the early phase of acetaminophen-induced acute liver injury. *Hepatology* **2016**, *64*, 1667–1682. [CrossRef]
335. Puengel, T.; Krenkel, O.; Mossanen, J.; Longerich, E.; Trautwein, C. The dual CCR/CCR5 antagonist Cenicriviroc ameliorates steatohepatitis and fibrosis in vivo by inhibiting the infiltration of inflammatory monocytes into injured liver. *J. Hepatol.* **2016**, s159–s182.
336. Friedman, S.; Sanyal, A.; Goodman, Z.; Lefebvre, E.; Gottwald, M.; Fischer, L.; Ratzu, V. Efficacy and safety study of cenicriviroc for the treatment of non-alcoholic steatohepatitis in adult subjects with liver fibrosis: CENTAUR Phase 2b study design. *Contemp Clin. Trials* **2016**, *47*, 356–365. [CrossRef]
337. Friedman, S.L.; Ratzu, V.; Harrison, S.A.; Abdelmalek, M.F.; Aithal, G.P.; Caballeria, J.; Francque, S.; Farrell, G.; Kowdley, K.V.; Craxi, A.; et al. A randomized, placebo-controlled trial of cenicriviroc for treatment of nonalcoholic steatohepatitis with fibrosis. *Hepatology* **2018**, *67*, 1754–1767. [CrossRef]
338. Lefebvre, E.; Gottwald, M.; Lasseter, K.; Chang, W.; Willett, M.; Smith, P.F.; Somasunderam, A.; Utay, N.S. Pharmacokinetics, Safety, and CCR2/CCR5 Antagonist Activity of Cenicriviroc in Participants With Mild or Moderate Hepatic Impairment. *Clin. Transl. Sci.* **2016**, *9*, 139–148. [CrossRef]
339. Barondes, S.H.; Castronovo, V.; Cooper, D.N.; Cummings, R.D.; Drickamer, K.; Feizi, T.; Gitt, M.A.; Hirabayashi, J.; Hughes, C.; Kasai, K.; et al. Galectins: A family of animal beta-galactoside-binding lectins. *Cell* **1994**, *76*, 597–598. [CrossRef]
340. Davidson, P.J.; Li, S.Y.; Lohse, A.G.; Vandergaast, R.; Verde, E.; Pearson, A.; Patterson, R.J.; Wang, J.L.; Arnoys, E.J. Transport of galectin-3 between the nucleus and cytoplasm. I. Conditions and signals for nuclear import. *Glycobiology* **2006**, *16*, 602–611. [CrossRef]
341. Ochieng, J.; Fridman, R.; Nangia-Makker, P.; Kleiner, D.E.; Liotta, L.A.; Stetler-Stevenson, W.G.; Raz, A. Galectin-3 is a novel substrate for human matrix metalloproteinases-2 and -9. *Biochemistry* **1994**, *33*, 14109–14114. [CrossRef] [PubMed]
342. Fujita, K.; Niki, T.; Nomura, T.; Oura, K.; Tadokoro, T.; Sakamoto, T.; Tani, J.; Yoneyama, H.; Morishita, A.; Kuroda, N.; et al. Correlation between serum galectin-9 levels and liver fibrosis. *J. Gastroenterol. Hepatol.* **2018**, *33*, 492–499. [CrossRef] [PubMed]
343. Matter, M.S.; Marquardt, J.U.; Andersen, J.B.; Quintavalle, C.; Korokhov, N.; Stauffer, J.K.; Kaji, K.; Decaens, T.; Quagliata, L.; Elloumi, F.; et al. Oncogenic driver genes and the inflammatory microenvironment dictate liver tumor phenotype. *Hepatology* **2016**, *63*, 1888–1899. [CrossRef] [PubMed]
344. Bacigalupo, M.L.; Manzi, M.; Rabinovich, G.A.; Troncoso, M.F. Hierarchical and selective roles of galectins in hepatocarcinogenesis, liver fibrosis and inflammation of hepatocellular carcinoma. *World, J. Gastroenterol.* **2013**, *19*, 8831–8849. [CrossRef] [PubMed]
345. Yang, R.Y.; Hsu, D.K.; Liu, F.T. Expression of galectin-3 modulates T-cell growth and apoptosis. *Proc. Natl. Acad. Sci. USA* **1996**, *93*, 6737–6742. [CrossRef] [PubMed]
346. Jeng, K.C.; Frigeri, L.G.; Liu, F.T. An endogenous lectin, galectin-3 (epsilon BP/Mac-2), potentiates IL-1 production by human monocytes. *Immunol. Lett.* **1994**, *42*, 113–116. [CrossRef]
347. Sano, H.; Hsu, D.K.; Yu, L.; Apgar, J.R.; Kuwabara, I.; Yamanaka, T.; Hirashima, M.; Liu, F.T. Human galectin-3 is a novel chemoattractant for monocytes and macrophages. *J. Immunol.* **2000**, *165*, 2156–2164. [CrossRef]
348. Traber, P.G.; Zomer, E. Therapy of experimental NASH and fibrosis with galectin inhibitors. *PLoS ONE* **2013**, *8*, e83481. [CrossRef]
349. Traber, P.G.; Chou, H.; Zomer, E.; Hong, F.; Klyosov, A.; Fiel, M.I.; Friedman, S.L. Regression of fibrosis and reversal of cirrhosis in rats by galectin inhibitors in thioacetamide-induced liver disease. *PLoS ONE* **2013**, *8*, e75361. [CrossRef]
350. Harrison, S.A.; Marri, S.R.; Chalasani, N.; Kohli, R.; Aronstein, W.; Thompson, G.A.; Irish, W.; Miles, M.V.; Xanthakos, S.A.; Lawitz, E.; et al. Randomised clinical study: GR-MD-02, a galectin-3 inhibitor, vs. placebo in patients having non-alcoholic steatohepatitis with advanced fibrosis. *Aliment. Pharmacol.* **2016**, *44*, 1183–1198. [CrossRef]
351. Chalasani, N.; Abdelmalek, M.F.; Garcia-Tsao, G.; Vuppalanchi, R.; Alkhouli, N.; Rinella, M.; Noureddin, M.; Pyko, M.; Shiffman, M.; Sanyal, A.; et al. Effects of Belapectin, an Inhibitor of Galectin-3, in Patients with Nonalcoholic Steatohepatitis With Cirrhosis And Portal Hypertension. *Gastroenterology* **2019**. [CrossRef] [PubMed]
352. Baur, J.A.; Pearson, K.J.; Price, N.L.; Jamieson, H.A.; Lerin, C.; Kalra, A.; Prabhu, V.V.; Allard, J.S.; Lopez-Lluch, G.; Lewis, K.; et al. Resveratrol improves health and survival of mice on a high-calorie diet. *Nature* **2006**, *444*, 337–342. [CrossRef] [PubMed]
353. Lagouge, M.; Argmann, C.; Gerhart-Hines, Z.; Meziane, H.; Lerin, C.; Daussin, F.; Messadeq, N.; Milne, J.; Lambert, P.; Elliott, P.; et al. Resveratrol improves mitochondrial function and protects against metabolic disease by activating SIRT1 and PGC-1alpha. *Cell* **2006**, *127*, 1109–1122. [CrossRef] [PubMed]
354. Price, N.L.; Gomes, A.P.; Ling, A.J.; Duarte, F.V.; Martin-Montalvo, A.; North, B.J.; Agarwal, B.; Ye, L.; Ramadori, G.; Teodoro, J.S.; et al. SIRT1 is required for AMPK activation and the beneficial effects of resveratrol on mitochondrial

- function. *Cell Metab.* **2012**, *15*, 675–690. [CrossRef] [PubMed]
355. Muriel, P.; Rivera-Espinoza, Y. Beneficial drugs for liver diseases. *J. Appl. Toxicol.* **2008**, *28*, 93–103. [CrossRef] [PubMed]
356. Faghihzadeh, F.; Adibi, P.; Rafiei, R.; Hekmatdoost, A. Resveratrol supplementation improves inflammatory biomarkers in patients with nonalcoholic fatty liver disease. *Nutr. Res.* **2014**, *34*, 837–843. [CrossRef]
357. Ferenci, P. Silymarin in the treatment of liver diseases: What is the clinical evidence? *Clin. Liver Dis. (Hoboken)* **2016**, *7*, 8–10. [CrossRef]
358. Dehmlow, C.; Erhard, J.; de Groot, H. Inhibition of Kupffer cell functions as an explanation for the hepatoprotective properties of silibinin. *Hepatology* **1996**, *23*, 749–754. [CrossRef]
359. Boigk, G.; Stroedter, L.; Herbst, H.; Waldschmidt, J.; Riecken, E.O.; Schuppan, D. Silymarin retards collagen accumulation in early and advanced biliary fibrosis secondary to complete bile duct obliteration in rats. *Hepatology* **1997**, *26*, 643–649. [CrossRef]
360. Enjalbert, F.; Rapior, S.; Nouguié-Soule, J.; Guillon, S.; Amouroux, N.; Cabot, C. Treatment of amatoxin poisoning: 20-year retrospective analysis. *J. Toxicol. Clin. Toxicol.* **2002**, *40*, 715–757. [CrossRef]
361. Sonnenbichler, J.; Zetl, I. Biochemical effects of the flavonolignan silibinin on RNA, protein and DNA synthesis in rat livers. *Prog Clin. Biol Res.* **1986**, *213*, 319–331. [PubMed]
362. Loguercio, C.; Federico, A.; Trappoliere, M.; Tuccillo, C.; de Sio, I.; Di Leva, A.; Niosi, M.; D’Auria, M.V.; Capasso, R.; Del Vecchio Blanco, C.; et al. The effect of a silybin-vitamin E-phospholipid complex on nonalcoholic fatty liver disease: A pilot study. *Dig. Dis. Sci.* **2007**, *52*, 2387–2395. [CrossRef] [PubMed]
363. Ferenci, P.; Scherzer, T.M.; Kerschner, H.; Rutter, K.; Beinhardt, S.; Hofer, H.; Schoniger-Hekele, M.; Holzmann, H.; Steindl-Munda, P. Silibinin is a potent antiviral agent in patients with chronic hepatitis C not responding to pegylated interferon/ribavirin therapy. *Gastroenterology* **2008**, *135*, 1561–1567. [CrossRef] [PubMed]
364. Lucena, M.I.; Andrade, R.J.; de la Cruz, J.P.; Rodriguez-Mendizabal, M.; Blanco, E.; Sanchez de la Cuesta, F. Effects of silymarin MZ-80 on oxidative stress in patients with alcoholic cirrhosis. Results of a randomized, double-blind, placebo-controlled clinical study. *Int J. Clin. Pharmacol. Ther.* **2002**, *40*, 2–8. [CrossRef] [PubMed]
365. Velussi, M.; Cernigoi, A.M.; De Monte, A.; Dapas, F.; Caffau, C.; Zilli, M. Long-term (12 months) treatment with an anti-oxidant drug (silymarin) is effective on hyperinsulinemia, exogenous insulin need and malondialdehyde levels in cirrhotic diabetic patients. *J. Hepatol.* **1997**, *26*, 871–879. [CrossRef]
366. Clichici, S.; Olteanu, D.; Nagy, A.L.; Oros, A.; Filip, A.; Mircea, P.A. Silymarin inhibits the progression of fibrosis in the early stages of liver injury in CCl₄-treated rats. *J. Med. Food* **2015**, *18*, 290–298. [CrossRef]
367. Tsai, J.H.; Liu, J.Y.; Wu, T.T.; Ho, P.C.; Huang, C.Y.; Shyu, J.C.; Hsieh, Y.S.; Tsai, C.C.; Liu, Y.C. Effects of silymarin on the resolution of liver fibrosis induced by carbon tetrachloride in rats. *J. Viral. Hepat.* **2008**, *15*, 508–514. [CrossRef]
368. Wu, J.W.; Lin, L.C.; Hung, S.C.; Chi, C.W.; Tsai, T.H. Analysis of silibinin in rat plasma and bile for hepatobiliary excretion and oral bioavailability application. *J. Pharm. Biomed. Anal.* **2007**, *45*, 635–641. [CrossRef]
369. Zarrelli, A.; Romanucci, V.; Tuccillo, C.; Federico, A.; Loguercio, C.; Gravante, R.; Di Fabio, G. New silibinin glyco-conjugates: Synthesis and evaluation of antioxidant properties. *Bioorg. Med. Chem. Lett.* **2014**, *24*, 5147–5149. [CrossRef]
370. Loguercio, C.; Andreone, P.; Brisc, C.; Brisc, M.C.; Bugianesi, E.; Chiaramonte, M.; Cursaro, C.; Danila, M.; de Sio, I.; Floreani, A.; et al. Silybin combined with phosphatidylcholine and vitamin E in patients with nonalcoholic fatty liver disease: A randomized controlled trial. *Free Radic. Biol. Med.* **2012**, *52*, 1658–1665. [CrossRef]
371. Tu, C.T.; Han, B.; Liu, H.C.; Zhang, S.C. Curcumin protects mice against concanavalin A-induced hepatitis by inhibiting intrahepatic intercellular adhesion molecule-1 (ICAM-1) and CXCL10 expression. *Mol. Cell Biochem* **2011**, *358*, 53–60. [CrossRef] [PubMed]
372. Rivera-Espinoza, Y.; Muriel, P. Pharmacological actions of curcumin in liver diseases or damage. *Liver Int.* **2009**, *29*, 1457–1466. [CrossRef] [PubMed]
373. Vizzutti, F.; Provenzano, A.; Galastri, S.; Milani, S.; Delogu, W.; Novo, E.; Caligiuri, A.; Zamara, E.; Arena, U.; Laffi, G.; et al. Curcumin limits the fibrogenic evolution of experimental steatohepatitis. *Lab. Invest.* **2010**, *90*, 104–115. [CrossRef] [PubMed]
374. Li, B.; Wang, L.; Lu, Q.; Da, W. Liver injury attenuation by curcumin in a rat NASH model: An Nrf2 activation-mediated effect? *Ir. J. Med. Sci.* **2016**, *185*, 93–100. [CrossRef]
375. Ireson, C.; Orr, S.; Jones, D.J.; Verschoyle, R.; Lim, C.K.; Luo, J.L.; Howells, L.; Plummer, S.; Jukes, R.; Williams, M.; et al. Characterization of metabolites of the chemopreventive agent curcumin in human and rat hepatocytes and in the rat in vivo, and evaluation of their ability to inhibit phorbol ester-induced prostaglandin E₂ production. *Cancer Res.* **2001**, *61*, 1058–1064.
376. Huang, Y.; Cao, S.; Zhang, Q.; Zhang, H.; Fan, Y.; Qiu, F.; Kang, N. Biological and pharmacological effects of hexahydrocurcumin, a metabolite of curcumin. *Arch. Biochem. Biophys.* **2018**, *646*, 31–37. [CrossRef]
377. Wang, J.; Yu, X.; Zhang, L.; Wang, L.; Peng, Z.; Chen, Y. The pharmacokinetics and tissue distribution of curcumin and its metabolites in mice. *Biomed. Chromatogr.* **2018**, e4267. [CrossRef]

378. Panahi, Y.; Kianpour, P.; Mohtashami, R.; Jafari, R.; Simental-Mendia, L.E.; Sahebkar, A. Efficacy and Safety of Phytosomal Curcumin in Non-Alcoholic Fatty Liver Disease: A Randomized Controlled Trial. *Drug Res.(Stuttg)* **2017**, *67*, 244–251. [CrossRef]
379. Rahmani, S.; Asgari, S.; Askari, G.; Keshvari, M.; Hatamipour, M.; Feizi, A.; Sahebkar, A. Treatment of Non-alcoholic Fatty Liver Disease with Curcumin: A Randomized Placebo-controlled Trial. *Phytother Res.* **2016**, *30*, 1540–1548. [CrossRef]
380. Saadati, S.; Sadeghi, A.; Mansour, A.; Yari, Z.; Poustchi, H.; Hedayati, M.; Hatami, B.; Hekmatdoost, A. Curcumin and inflammation in non-alcoholic fatty liver disease: A randomized, placebo controlled clinical trial. *BMC Gastroenterol.* **2019**, *19*, 133. [CrossRef]
381. Torok, N.J.; Dranoff, J.A.; Schuppan, D.; Friedman, S.L. Strategies and endpoints of antifibrotic drug trials: Summary and recommendations from the AASLD Emerging Trends Conference, Chicago, June 2014. *Hepatology* **2015**, *62*, 627–634. [CrossRef] [PubMed]
382. Popov, Y.; Schuppan, D. Targeting liver fibrosis: Strategies for development and validation of antifibrotic therapies. *Hepatology* **2009**, *50*, 1294–1306. [CrossRef] [PubMed]
383. Reimer, K.C.; Wree, A.; Roderburg, C.; Tacke, F. New drugs for NAFLD: Lessons from basic models to the clinic. *Hepatol. Int.* **2019**. [CrossRef] [PubMed]
384. Igal, G.; Evelyn, A.; Jennifer, C.X.; Natalia, K.; Alexandra, N.; Eddie, G.; John, D. Fibrotic Human Lung Extracellular Matrix as a Disease-Specific Substrate for Models of pulmonary Fibrosis. *J. Respir Med. Lung Dis.* **2019**, *4*, 1043.
385. Loomba, R.L.E.; Ghalib, R.; Elkhatab, M.; Caldwell, S.; Abdelmalek, M. Longitudinal changes in liver stiffness by magnetic resonance elastography (MRE), liver fibrosis, and serum markers of fibrosis in a multi-center clinical trial in nonalcoholic steatohepatitis (NASH). *J. Hepatol.* **2017**, *66*, S671. [CrossRef]
386. Nishikawa, K.; Iwaya, K.; Kinoshita, M.; Fujiwara, Y.; Akao, M.; Sonoda, M.; Thirupathi, S.; Suzuki, T.; Hiroi, S.; Seki, S.; et al. Resveratrol increases CD68(+) Kupffer cells colocalized with adipose differentiation-related protein and ameliorates high-fat-diet-induced fatty liver in mice. *Mol. Nutr. Food Res.* **2015**, *59*, 1155–1170. [CrossRef]
387. Kimura, K.; Ikoma, A.; Shibakawa, M.; Shimoda, S.; Harada, K.; Saio, M.; Imamura, J.; Osawa, Y.; Kimura, M.; Nishikawa, K.; et al. Safety, Tolerability, and Preliminary Efficacy of the Anti-Fibrotic Small Molecule PRI-724, a CBP/beta-Catenin Inhibitor, in Patients with Hepatitis C Virus-related Cirrhosis: A Single-Center, Open-Label, Dose Escalation Phase 1 Trial. *EBioMedicine* **2017**, *23*, 79–87. [CrossRef]



© 2020 by the authors. Licensee MDPI, Basel, Switzerland. This article is an open access article distributed under the terms and conditions of the Creative Commons Attribution (CC BY) license (<http://creativecommons.org/licenses/by/4.0/>).

Introductory article II - The role of the liver microenvironment in liver carcinogenesis

Book chapter:

Saviano A*, **Roehlen N***, Virzì A, Roca Suarez AA, Hoshida Y, Lupberger J, Baumert TF. Stromal and Immune Drivers of Hepatocarcinogenesis. In: Hoshida Y, editor. Hepatocellular Carcinoma: Translational Precision Medicine Approaches [Internet]. Cham (CH): Humana Press; 2019. Chapter 15.

* shared first authorship.

Stromal and Immune Drivers of Hepatocarcinogenesis



Antonio Saviano, Natascha Roehlen, Alessia Virzi,

Armando Andres Roca Suarez, Yujin Hoshida, Joachim Lupberger, and Thomas F. Baumert

* Antonio Saviano and Natascha Roehlen are co-first authors of this chapter

A. Saviano · T. F. Baumert (*)

Inserm U1110, Institut de Recherche sur les Maladies Virales et Hépatiques, Université de Strasbourg, Strasbourg, France

Pôle Hépato-digestif, Institut Hospitalo-Universitaire, Hôpitaux Universitaires,
Strasbourg, France

e-mail: thomas.baumert@unistra.fr

N. Roehlen · A. Virzi · A. A. R. Suarez · J. Lupberger

Inserm U1110, Institut de Recherche sur les Maladies Virales et Hépatiques, Université de Strasbourg, Strasbourg, France

Y. Hoshida

Liver Tumor Translational Research Program, Simmons Comprehensive Cancer Center, Division of Digestive and Liver
Diseases, Department of Internal Medicine,
University of Texas Southwestern Medical Center, Dallas, TX, USA

© Springer Nature Switzerland AG 2019

Y. Hoshida (ed.), *Hepatocellular Carcinoma*, Molecular and Translational Medicine, https://doi.org/10.1007/978-3-030-21540-8_15

Introduction

The liver is a multifunctional organ that plays a key role in metabolism and detoxification as well as in regulation of immune response and tolerance. The liver is physiologically exposed to many pathogens and toxic substances derived from the gut and has the largest population of resident macrophages (i.e., Kupffer cells, KCs) in the body and a high prevalence of natural killer cells (NK), natural killer T cells (NKT), and T cells. In normal conditions, the liver removes a large amount of microbes and pathogen-associated and damage-associated molecular patterns (PAMPs and DAMPs) and maintains an immunosuppressive environment [1].

Following chronic hepatocyte damage, immune and stromal cells modify a liver environment, which triggers chronic inflammation and ultimately promotes hepatocellular carcinoma (HCC) [2]. Indeed, independently from the etiology, chronic liver disease is characterized by a deregulation in the liver immune network that stimulates cellular stress and death favoring liver fibrosis, hepatocyte proliferation, and epithelial-to-mesenchymal transition (EMT) [2]. A combination of EMT, genetic mutations, and epigenetic alterations that accumulate during cell proliferation is the most important driver of hepatocarcinogenesis [3].

Once HCC has developed, liver microenvironment greatly affects tumor progression and response to therapy [4]. This is the reason why gene expression signatures in liver tissues adjacent to the HCC—and not in the tumor itself—highly correlate with long-term survival of patients with liver fibrosis [5]. Similarly, HCC infiltration by non-parenchymal cells (e.g., regulatory T cells, T_{reg}) has been associated with tumor progression [5–8]. New therapies targeting liver microenvironment are recently developed or under clinical investigation for both chronic liver disease (e.g., nonalcoholic steatohepatitis, NASH) and HCC.

Hence, liver microenvironment plays an essential role in both hepatocarcinogenesis and tumor progression and it is an important therapeutic target for HCC prevention and treatment.

From Chronic Inflammation to Hepatocellular Carcinoma

HCC almost universally evolves on the background of chronic liver inflammation and liver fibrosis [9]. Chronic hepatocyte cell injury induces activation of the immune system that initiates and supports chronic inflammation by generation of proinflammatory cytokines and chemokines and activation of hepatic stellate cells (HSCs), finally resulting in liver fibrosis, cirrhosis, and cancer [10] (Fig. 15.1).

During chronic infections (e.g., hepatitis B virus, HBV, or hepatitis C virus, HCV) as well as metabolic (e.g., NASH) or toxic diseases (e.g., alcoholic steatohepatitis, ASH), immune cells—first of all KCs—are activated by the release of PAMPs and DAMPs produced by hepatocyte apoptosis and death. Activated KCs present viral antigens to T cells and/or secrete cytokines and chemokines that recruit circulating monocytes, lymphocytes, and neutrophils [11]. Proinflammatory signals are mainly mediated by the accumulation of tumor necrosis factor alpha (TNF- α); interleukins (IL) such as IL-6, IL-1 β , IL-2, IL-7, IL-15, IL-17; C-C motif chemokine ligand 2 (CCL2); and interferon gamma (IFN- γ).

Following activation by antigen-presenting cells, T cells and especially T-helper17 (Th17) cells and the mucosal-associated invariant T (MAIT) cells are major promoters of liver inflammation primarily by secretion of IL-17 [12, 13]. IL-17 secreted by T cells as well as transforming growth factor beta 1 (TGF- β 1) and platelet-derived growth factor subunit B (PDGF-B) secreted by KCs and monocyte-derived macrophages are able to activate and differentiate HSC into collagen-producing myofibroblasts [12, 13]. Finally, also DAMPs can directly activate HSC and participate in fibrosis [7, 14]. HSC-derived myofibroblasts account for abnormal production of collagen in the liver and are main components of the hepatic precancerous microenvironment [15].

The inflammatory microenvironment causes hepatocellular stress, accompanied by epigenetic modifications, mitochondrial alterations, DNA damage, and chromosomal alterations that determine cell transformations [7]. Inflammation has been shown to upregulate nuclear factor kappa B (NF- κ B) and signal transducer and activator of transcription 3 (STAT3) thereby affecting cell proliferation, survival, angiogenesis, and chemotaxis [16–18]. STAT3 is further induced by several other cytokines and growth factors that are known to be upregulated under conditions of chronic liver inflammation [19]. Regarding chronic HBV and HCV infection, upregulation of the cytokines lymphotoxin beta and TNF- α in CD4⁺ and CD8⁺ T cells has been shown to promote hepatocarcinogenesis [20, 21].

Collectively, persistence of infection by hepatotropic viruses or toxic condition may cause a chronic inflammatory state, accompanied by continual cell death and promotion of compensatory tissue repair mechanisms, finally resulting in liver cirrhosis and cell transformation. Since chronic inflammation induces impaired immune surveillance due to exhausted T cells, chronic inflammatory liver status not only provokes cell transformation but also attenuates physiological antitumor defense mechanisms by the immune system. Thus, tumor cell attack by cytolytic T cells is weakened in chronic inflammatory liver tissue and HCC microenvironment [22–24].

Moreover, upregulation of immunosuppressive T_{reg} cells has been related to chronic inflammation associated with attenuated immune surveillance contributing to risk of HCC development [25, 26]. The inducible type 1 T regulatory (Tr1) cells possess many immunosuppressive functions by secretion of the cytokines IL-10 and TGF- β , as well as by expression of the checkpoint inhibitors cytotoxic T-lymphocyte-associated protein 4 (CTLA-4) and programmed death 1 (PD1) on the cell surface [27–29]. T_{reg} or KC-secreted IL-10 was reported to reduce immune surveillance by suppressing macrophage activation, T-cell proliferation, and IFN- γ production, hereby inhibiting antitumor response mediated by the immune system [30–32]. Moreover, TGF- β is known to inhibit IL-2-dependent T-cell proliferation as well as production of proinflammatory cytokines and performance of cytolytic functions by effector cells [33–35]. Suggesting its involvement in chronic inflammatory liver disease and contribution to hepatocarcinogenesis, levels of the immunoregulatory cytokine IL-10 and TGF- β have been reported to be elevated in patients with chronic liver disease and related to disease progression and patients' survival [30, 36, 37].

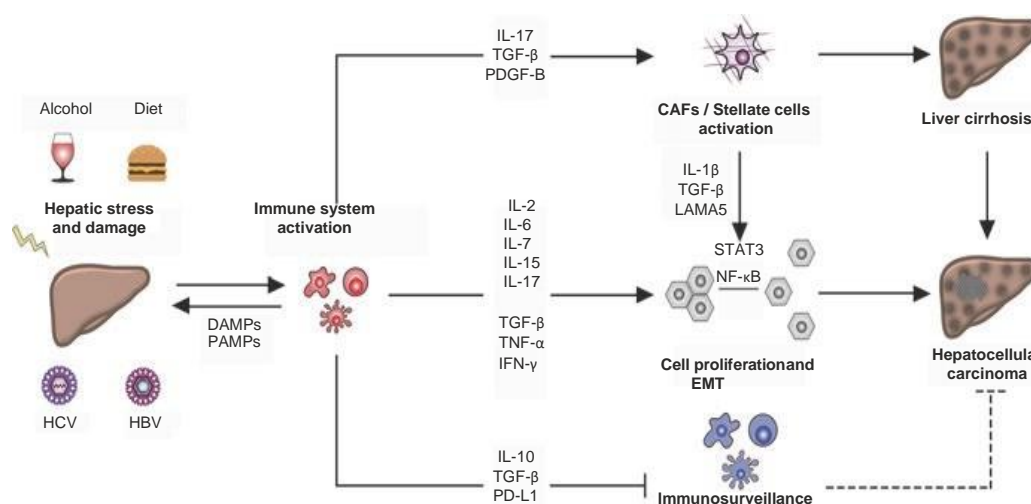


Fig. 15.1 Chronic inflammation is a pan-etiological driver of hepatocarcinogenesis. Hepatocarcinogenesis can be induced by multiple etiological and environmental conditions. Chronic HBV and HCV infections, as well as chronic alcohol abuse and metabolic syndrome trigger the activation of the innate immune system via release of Damage-Associated Molecular Patterns (DAMPs) and Pathogen Associated Molecular Patterns (PAMPs). The persistent dysregulation of the immunological network of the liver, promoted by the secretion of pro-inflammatory cytokines/chemokines (e.g. IL-2, IL-6, IL-7, IL-15, IL-17, TGF-β, TNF-α, IFN-γ), leads to cells death, compensatory hepatocellular proliferation, activation of cancer-associated fibroblasts (CAFs) and hepatic stellate cells (HSCs) as well as epithelial-to-mesenchymal transition (EMT). Moreover, sustained necro-inflammatory status attenuates immune-surveillance and anti-tumor immune response, by secretion of anti-inflammatory molecules (e.g. IL-10, TGF-β, PD-L1). In addition, the activation of HSCs contributes significantly to cell proliferation (by the release of IL-1β, TGF-β and LAMA5) and cirrhosis. In conclusion, cellular proliferation and EMT, further sustained by STAT3/NF-κB pathway activation, cirrhosis and impaired immunosurveillance activity collectively contribute to HCC development.

Immune Cells in HCC Microenvironment

Leukocytes are one of the main drivers in chronic inflammation. They are highly enriched in both the precancerous state of liver cirrhosis and in malignant tissue of HCC. Indeed, liver carcinoma is characterized by an immunogenic micro-environment, consisting of high amounts of lymphocytes, including NK cells, NKT cells, B cells, and T cells [38]. T-cell exhaustion due to chronic inflammation hereby shapes an immunogenic microenvironment that is characterized by an enhanced immunotolerance. Thus, the endogenous antitumor function of cytotoxic lymphocytes can be restored by antigen-presenting cells, which are typically reduced in the HCC microenvironment [39]. Indeed, decreased activity of NK cells, one of the most important antigen-presenting cells, correlates with an increased incidence of HCC in patients with liver cirrhosis [40]. Moreover, infiltration and density of T cells in human HCCs correlate with better patient prognosis, whereas tumor-infiltrating B cells reduce tumor viability [41].

Macrophages perpetuate chronic inflammation following liver injury and promote fibrogenesis via HSC activation. This therefore represents a significant component of HCC microenvironment. Of note, tumor-associated macrophages (TAMs) are considered to promote tumor development and favor angiogenesis and tumor cell migration [42, 43]. Moreover, TAMs may stimulate tumor growth by suppression of the adaptive immune system. They express high levels of cell death-ligand 1 (PD-L1), thereby suppressing the antitumor cytotoxic T-cell responses [44]. TAMs provide cytokines and growth factors that enhance tumor cell proliferation and NF-κB-mediated protection from cancer cell apoptosis and angiogenesis [45]. Accordingly, TAM infiltration correlates with HCC progression and poor survival [46, 47].

Dendritic cells (DCs) are a heterogeneous cell population and one of the most powerful antigen-presenting cells which regulate the primary immune response and the immune homeostasis in the liver [48]. By forming a bridge between the innate and the adaptive immune system [49], DCs are regarded as key players in immune regulation [50, 51]. An impaired DC function has frequently been suggested as an important factor contributing to an immunosuppressive microenvironment in chronic liver disease, which is favoring tumor development. Accordingly, several studies report lower DC numbers in both the peripheral blood and liver

tissue of patients with HCC [52, 53]. A reduced IL-12 secretion by DCs is hereby attributed to an attenuated stimulation of T cells [54]. Moreover, DC inhibition and its effect on downstream effector cells have further been identified as immune escape mechanisms of HCC [55, 56].

Stromal Cells Participate in HCC Development and Progression

Liver cirrhosis is one of the main risk factors for hepatocarcinogenesis and therefore regarded as a precancerous liver state [57]. Thus, the lifetime risk of HCC development in patients with advanced liver cirrhosis is approximately 30%, and 80–90% of HCCs evolve in cirrhotic liver tissue [58, 59]. Considering HSCs as the most important progenitor cells of myofibroblasts that account for enhanced production of the extracellular matrix in liver fibrosis and liver cirrhosis, HSC-derived myofibroblasts are the main components of the hepatic precancerous microenvironment as well as the HCC tumor environment. Indeed, differentiation of HSCs from pericyte-like cells to collagen-producing myofibroblasts provides 85–95% of the myofibroblasts in liver fibrosis and liver cirrhosis, independent of the underlying trigger [15]. Hence, together with bone marrow (BM)-derived fibroblasts and portal fibroblasts (PF), HSC-derived myofibroblasts compose the stromal population of cancer-associated myofibroblasts (CAFs) that contribute actively to HCC development and progression [60]. Of note, CAFs show a markedly altered phenotype compared to normal fibroblasts [61, 62]. Normal fibroblasts may suppress tumor growth by contact inhibition [62], whereas CAFs promote an immune-tolerant tumor environment by interaction with monocytes and lymphocytes [63]. Indeed, CAFs inhibit lymphocyte tumor infiltration, increase the activity of immunosuppressive regulatory T cells, and induce apoptosis in monocytes [64, 65]. Furthermore, CAFs were reported to impair antitumor functions of T cells via activation of neutrophils [66]. CAFs may further promote hepatocarcinogenesis by downregulation of tumor-suppressive microRNAs [67, 68]. CAF activity has also been associated with tumor angiogenesis. CAFs have been shown to secrete vascular endothelial growth factor (VEGF) and angiopoietin 1 or 2 [69–71]. The cross talk between CAFs and cancer cells is crucial for HCC biology. The secretion of laminin5 (LAMA5) [72] and IL-1 β [73] by CAFs has been shown to promote HCC migration, and on the other hand, highly metastatic HCC cells were found to be able to convert normal fibroblasts to CAFs, which in turn promote cancer progression by secretion of proinflammatory cytokines [74]. Several studies further suggest an association of CAFs and CSCs that are thought to promote tumor development and to mediate therapeutic resistance. CAFs have been reported to recruit CSCs and to drive their self-renewal [75, 76]. Moreover, CAFs have been observed to increase expression of keratin 19 by paracrine interactions [77], a marker for hepatic stem cells that has been observed to be correlated with poor prognosis [78]. In summary, CAFs are key drivers in hepatic carcinogenesis by increasing angiogenesis, inflammation, and proliferation and attenuating immune surveillance [60] (Fig. 15.2). CAFs correlate with HCC tumor stage and progression, tumor recurrence after surgery, as well as overall prognosis [79–81].

Lymphatic vessels function as a tissue drainage and immunological control system. They are highly enriched in the liver, carrying approximately 25–50% of the thoracic duct's lymph flow [82]. For a long time, lymphatic vessels were considered to affect carcinogenesis only by providing the structural pathway for metastatic spread of tumor cells. However, recent observations indicate a functional role of the lymphatic endothelium also in the hepatocytes' immunogenic microenvironment, which is affecting the development of chronic liver disease and hepatocarcinogenesis [83]. Thus, lymphatic endothelial cells (LECs) guide immune cell migration by lining the inner surface of lymphatic capillaries and regulate the expression of adhesion molecules and cytokines [84, 85]. Moreover, by secretion of immunosuppressive cytokines (i.e., TGF- β) and the overexpression of co-inhibitory checkpoint proteins (i.e., PD-L1), LECs suppress a maturation and proliferation of circulating immune cells [84–86]. LECs further mediate CD4⁺ and CD8⁺ T-cell tolerance by expression of self-antigens in the presence of inhibitory ligands [87].

Lymphangiogenesis is increased in liver fibrosis and cirrhosis and positively correlate with portal venous pressure and disease severity [88–90]. The enhanced interstitial flow and increased number of LECs is accompanied by increased cytokine production and immune cell recruitment to the inflammatory environment present in almost all chronic liver diseases [91]. The primarily immunosuppressive functions of LECs hereby contribute to an immunotolerant microenvironment favoring HCC development [83, 92]. Moreover, expression of chemokines by LECs may facilitate lymphogenic metastatic tumor spread [84].

Vascular endothelial growth factor C (VEGF-C) is an important stimulator of LEC growth and lymphangiogenesis. VEGF-C is enhanced in liver cirrhosis and HCC, and its expression in HCCs correlates with metastasis and poor patients' outcome [93, 94].

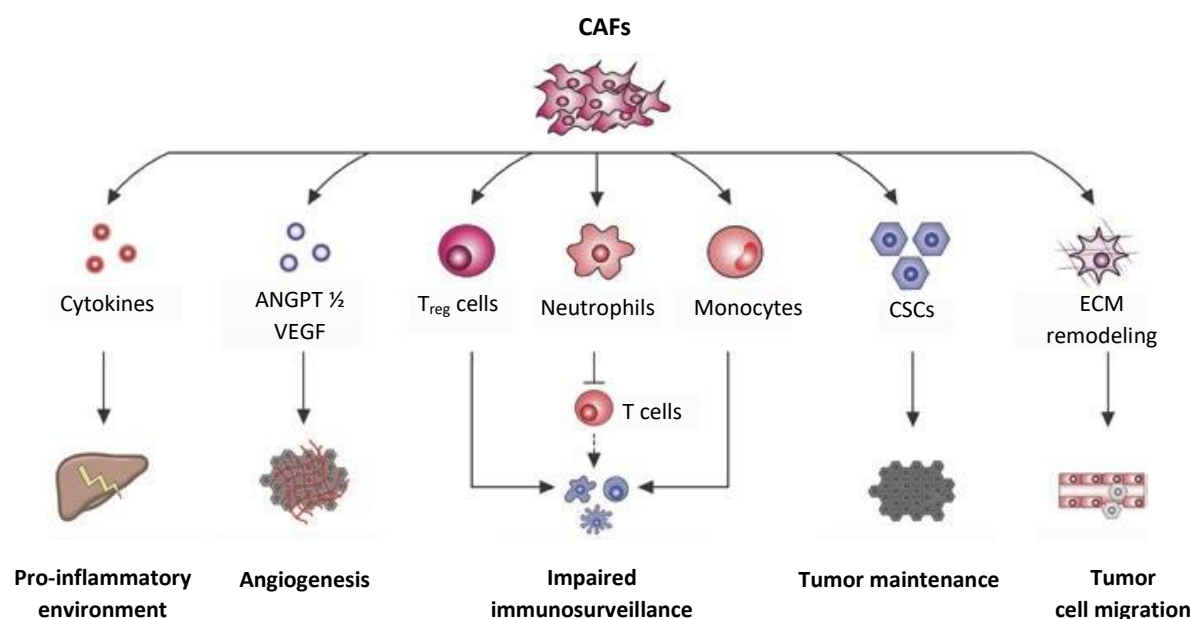


Fig. 15.2 Cancer-associated fibroblasts (CAFs) characterize the stromal tumor microenvironment and promote hepatocarcinogenesis, tumor progression and treatment resistance. Tumor microenvironment in HCC is predominantly characterized by cancer-associated fibroblasts (CAFs) that contribute actively to tumor development, progression and metastatic spread. Interacting with the immune cells and secreting angiogenic factors, these cells reduce immune surveillance and drive tumor angiogenesis. Moreover, CAFs promote cancer cell proliferation by paracrine interactions as well as production of prooncogenic cytokines (e.g. TGF- β). CAFs are also reported to recruit cancer stem cells, hereby affecting tumor maintenance, heterogeneity and treatment resistance. Finally, CAFs are responsible for the alteration of liver extracellular matrix by production and secretion of Laminin 5 and Integrin β 1 that further promote HCC cell invasion and migration.

Epithelial-to-Mesenchymal Transition in HCC

Epithelial-to-mesenchymal transition (EMT) describes a reversible process, by which epithelial cell types gradually develop mesenchymal characteristics leading to higher motility and invasive properties that are essential in embryogenic development and wound healing but also implicated in hepatic fibrogenesis and carcinogenesis [95, 96]. Thus, while epithelial cells are characterized by polarity and stable morphology, mesenchymal cells lack polarity, show a loose arrangement, and exhibit the capacity of migration [97]. EMT can be divided in three different biological subtypes [98]. While type 1 EMT determines embryonal development and organogenesis, types 2 and 3 EMT affect liver disease progression and can be activated by several proinflammatory cytokines and growth factors present in the inflammatory state of the liver [99].

Type 2 EMT occurs in response to cell injury as a mechanism of tissue repair and may cause fibrosis due to generation of collagen-producing fibroblasts. TGF- β , a cytokine increased under condition of chronic inflammation, has been shown to be one of the strongest activators of type 2 EMT that can affect hepatocytes, cholangiocytes, and hepatic stellate cells (HSC) [100]. Quiescent HSCs, the most frequent progenitor cells of collagen-producing fibroblasts [15], are actually regarded as transitional cells that have undergone partial EMT from epithelial cells and may complete transition upon inflammatory signals [101]. Hence, EMT is regarded as one of the most important promoters of liver fibrogenesis in response to chronic inflammation [101].

Type 3 EMT may occur due to genetic and epigenetic changes during malignant transformation of epithelial cells and is implicated in HCC growth and progression [3]. Cells generated by type 3 EMT differ significantly

from types 1 and 2 EMT cells and develop properties of invasion and migration as well as escape from apoptosis. Weakened or loss of E-cadherin expression, characteristic for development of the mesenchymal unpolarized phenotype, could be revealed in 58% of human HCC patients and correlated with the presence of metastases and patients' survival [102]. Besides proinflammatory cytokines and growth factors, several studies further indicate induction of type 3 EMT by core proteins of HCV itself [103]. Given not only the correlation of EMT with tumor stage but also response to therapy [104], therapeutic targeting of molecular key players in EMT is highly clinically relevant.

Clinical Perspectives

Considering the implication of stromal and immunogenic cell compounds in HCC development and progression, medical treatments targeting these factors represent promising tools for future medical treatment of advanced HCC. Presently, sorafenib, an oral multikinase inhibitor targeting vascular endothelial growth factor receptor (VEGFR-2/VEGFR-3) and platelet-derived growth factor receptor (PDGFR), produced by the stromal HCC microenvironment already represents the standard of care treatment for patients with advanced HCC [105]. Lenvatinib, another tyrosine kinase inhibitor with multiple targets, has recently been revealed to be noninferior compared to sorafenib according to the REFLECT trial and has lately been approved by the FDA as first-line treatment for unresectable HCC [106]. Moreover, recently therapeutic strategies targeting the immunogenic tumor microenvironment have been demonstrated to be effective as systemic therapy for several cancer types. Consequently, drugs targeting exhausted lymphocytes expressing PD1 and infiltrating the tumor are able to activate T-cell-driven immune response against cancer cells and were approved for melanoma and non-small cell lung cancer treatment [107, 108]. Preliminary results from open-label trials of these drugs in HCC treatment are encouraging. Indeed, nivolumab and pembrolizumab, anti-PD1 monoclonal antibodies, have been demonstrated to be more effective than placebo in patients with advanced unresectable HCC previously treated with sorafenib [109, 110]. For that reason, these compounds were recently approved by FDA as a second-line treatment for advanced HCC. Moreover, currently several randomized controlled trials investigate the effects of other drugs targeting the HCC immunogenic and stromal microenvironment. Thus, aiming to activate tumor-targeting cytotoxic T lymphocytes, a growing number of studies recently worked on ex vivo tumor-antigen-loaded dendritic cells as an approach of cancer immunotherapy by DC vaccination [111–113]. Several other studies are focused on immunotherapy targeting TAMs, aiming to decrease TAM population present in the HCC by elimination, blocking recruitment, or functional reprogramming of TAM polarization [43]. The results of current ongoing clinical studies are expected in the next few years and may revolutionize future HCC medical treatment.

References

1. Jenne CN, Kubes P. Immune surveillance by the liver. *Nat Immunol.* 2013;14:996. <https://doi.org/10.1038/ni.2691>. <https://www.nature.com/articles/ni.2691#supplementary-information>.
2. Marrone G, Shah VH, Gracia-Sancho J. Sinusoidal communication in liver fibrosis and regeneration. *J Hepatol.* 2016;65(3):608–17. <https://doi.org/10.1016/j.jhep.2016.04.018>.
3. van Zijl F, Zulehner G, Petz M, Schneller D, Kornauth C, Hau M, et al. Epithelial-mesenchymal transition in hepatocellular carcinoma. *Future Oncol.* 2009;5(8):1169–79. <https://doi.org/10.2217/fon.09.91>.
4. Nishida N, Kudo M. Oncogenic signal and tumor microenvironment in hepatocellular carcinoma. *Oncology.* 2017;93(Suppl 1):160–4. <https://doi.org/10.1159/000481246>.
5. Hoshida Y, Villanueva A, Kobayashi M, Peix J, Chiang DY, Camargo A, et al. Gene expression in fixed tissues and outcome in hepatocellular carcinoma. *N Engl J Med.* 2008;359(19):1995–2004. <https://doi.org/10.1056/NEJMoa0804525>.
6. Caja L, Dituri F, Mancarella S, Caballero-Diaz D, Moustakas A, Giannelli G, et al. TGF-beta and the tissue microenvironment: relevance in fibrosis and cancer. *Int J Mol Sci.* 2018;19(5). <https://doi.org/10.3390/ijms19051294>.
7. Ringelhan M, Pfister D, O'Connor T, Pikarsky E, Heikenwalder M. The immunology of hepatocellular carcinoma. *Nat Immunol.* 2018;19(3):222–32. <https://doi.org/10.1038/s41590-018-0044-z>.
8. Robinson MW, Harmon C, O'Farrelly C. Liver immunology and its role in inflammation and homeostasis. *Cell Mol Immunol.* 2016;13(3):267–76. <https://doi.org/10.1038/cmi.2016.3>.
9. Llovet JM, Zucman-Rossi J, Pikarsky E, Sangro B, Schwartz M, Sherman M, et al. Hepatocellular carcinoma. *Nat Rev Dis*

- Primers. 2016;2:16018. <https://doi.org/10.1038/nrdp.2016.18>.
10. Pellicoro A, Ramachandran P, Iredale JP, Fallowfield JA. Liver fibrosis and repair: immunoregulation of wound healing in a solid organ. *Nat Rev Immunol*. 2014;14(3):181–94. <https://doi.org/10.1038/nri3623>.
11. Mossanen JC, Krenkel O, Ergen C, Govaere O, Liepelt A, Puengel T, et al. Chemokine (C-C motif) receptor 2-positive monocytes aggravate the early phase of acetaminophen-induced acute liver injury. *Hepatology*. 2016;64(5):1667–82. <https://doi.org/10.1002/hep.28682>.
12. Lemmers A, Moreno C, Gustot T, Marechal R, Degre D, Demetter P, et al. The interleukin-17 pathway is involved in human alcoholic liver disease. *Hepatology*. 2009;49(2):646–57. <https://doi.org/10.1002/hep.22680>.
13. Meng F, Wang K, Aoyama T, Grivennikov SI, Paik Y, Scholten D, et al. Interleukin-17 signaling in inflammatory, Kupffer cells, and hepatic stellate cells exacerbates liver fibrosis in mice. *Gastroenterology*. 2012;143(3):765–76 e3. <https://doi.org/10.1053/j.gastro.2012.05.049>.
14. Tu T, Calabro SR, Lee A, Maczurek AE, Budzinska MA, Warner FJ, et al. Hepatocytes in liver injury: victim, bystander, or accomplice in progressive fibrosis? *J Gastroenterol Hepatol*. 2015;30(12):1696–704. <https://doi.org/10.1111/jgh.13065>.
15. Mederacke I, Hsu CC, Troeger JS, Huebener P, Mu X, Dapito DH, et al. Fate tracing reveals hepatic stellate cells as dominant contributors to liver fibrosis independent of its aetiology. *Nat Commun*. 2013;4:2823. <https://doi.org/10.1038/ncomms3823>.
16. Maeda S, Kamata H, Luo JL, Leffert H, Karin M. IKK β couples hepatocyte death to cytokine-driven compensatory proliferation that promotes chemical hepatocarcinogenesis. *Cell*. 2005;121(7):977–90. <https://doi.org/10.1016/j.cell.2005.04.014>.
17. Akira S, Nishio Y, Inoue M, Wang XJ, Wei S, Matsusaka T, et al. Molecular cloning of APRF, a novel IFN-stimulated gene factor 3 p91-related transcription factor involved in the gp130-mediated signaling pathway. *Cell*. 1994;77(1):63–71.
18. Mackey-Lawrence NM, Petri WA Jr. Leptin and mucosal immunity. *Mucosal Immunol*. 2012;5(5):472–9. <https://doi.org/10.1038/mi.2012.40>.
19. McCartney EM, Helbig KJ, Narayana SK, Eyre NS, Aloia AL, Beard MR. Signal transducer and activator of transcription 3 is a proviral host factor for hepatitis C virus. *Hepatology*. 2013;58(5):1558–68. <https://doi.org/10.1002/hep.26496>.
20. Haybaeck J, Zeller N, Wolf MJ, Weber A, Wagner U, Kurrer MO, et al. A lymphotoxin-driven pathway to hepatocellular carcinoma. *Cancer Cell*. 2009;16(4):295–308. <https://doi.org/10.1016/j.ccr.2009.08.021>.
21. Wolf MJ, Adili A, Piotrowitz K, Abdullah Z, Boege Y, Stemmer K, et al. Metabolic activation of intrahepatic CD8⁺ T cells and NKT cells causes nonalcoholic steatohepatitis and liver cancer via cross-talk with hepatocytes. *Cancer Cell*. 2014;26(4):549–64. <https://doi.org/10.1016/j.ccr.2014.09.003>.
22. Kang TW, Yevsa T, Woller N, Hoenicke L, Wuestefeld T, Dauch D, et al. Senescence surveillance of pre-malignant hepatocytes limits liver cancer development. *Nature*. 2011;479(7374):547–51. <https://doi.org/10.1038/nature10599>.
23. Ma C, Kesarwala AH, Eggert T, Medina-Echeverez J, Kleiner DE, Jin P, et al. NAFLD causes selective CD4⁺ T lymphocyte loss and promotes hepatocarcinogenesis. *Nature*. 2016;531(7593):253–7. <https://doi.org/10.1038/nature16969>.
24. van der Windt DJ, Sud V, Zhang H, Varley PR, Goswami J, Yazdani HO, et al. Neutrophil extracellular traps promote inflammation and development of hepatocellular carcinoma in nonalcoholic steatohepatitis. *Hepatology*. 2018;68(4):1347–60. <https://doi.org/10.1002/hep.29914>.
25. Jiang R, Tang J, Chen Y, Deng L, Ji J, Xie Y, et al. The long noncoding RNA lnc-EGFR stimulates T-regulatory cells differentiation thus promoting hepatocellular carcinoma immune evasion. *Nat Commun*. 2017;8:15129. <https://doi.org/10.1038/ncomms15129>.
26. Li K, Liu H, Guo T. Th17/Treg imbalance is an indicator of liver cirrhosis process and a risk factor for HCC occurrence in HBV patients. *Clin Res Hepatol Gastroenterol*. 2017;41(4):399–407. <https://doi.org/10.1016/j.clinre.2016.12.004>.
27. Read S, Malmstrom V, Powrie F. Cytotoxic T lymphocyte-associated antigen 4 plays an essential role in the function of CD25⁺CD4⁺ regulatory cells that control intestinal inflammation. *J Exp Med*. 2000;192(2):295–302.
28. Nishimura H, Nose M, Hiai H, Minato N, Honjo T. Development of lupus-like autoimmune diseases by disruption of the PD-1 gene encoding an ITIM motif-carrying immunoreceptor. *Immunity*. 1999;11(2):141–51.
29. Carter L, Fouser LA, Jussif J, Fitz L, Deng B, Wood CR, et al. PD-1:PD-L inhibitory pathway affects both CD4⁺ and CD8⁺ T cells and is overcome by IL-2. *Eur J Immunol*. 2002;32(3):634–43. [https://doi.org/10.1002/1521-4141\(200203\)32:3<634::AID-IMMU634>3.0.CO;2-9](https://doi.org/10.1002/1521-4141(200203)32:3<634::AID-IMMU634>3.0.CO;2-9).
30. Knolle P, Schlaak J, Uhrig A, Kempf P, Meyer zum Buschenfelde KH, Gerken G. Human Kupffer cells secrete IL-10 in response to lipopolysaccharide (LPS) challenge. *J Hepatol*. 1995;22(2):226–9.
31. Hattori E, Okumoto K, Adachi T, Takeda T, Ito J, Sugahara K, et al. Possible contribution of circulating interleukin-10 (IL-10) to anti-tumor immunity and prognosis in patients with unresectable hepatocellular carcinoma. *Hepatol Res*. 2003;27(4):309–14.
32. Moore KW, de Waal Malefyt R, Coffman RL, O’Garra A. Interleukin-10 and the interleukin-10 receptor. *Annu Rev Immunol*. 2001;19:683–765. <https://doi.org/10.1146/annurev.immunol.19.1.683>.
33. Kehrl JH, Wakefield LM, Roberts AB, Jakowlew S, Alvarez-Mon M, Derynck R, et al. Production of transforming growth factor β by human T lymphocytes and its potential role in the regulation of T cell growth. *J Exp Med*. 1986;163(5):1037–50.
34. Espevik T, Waage A, Faxvaag A, Shalaby MR. Regulation of interleukin-2 and interleukin-6 production from T-cells: involvement of interleukin-1 β and transforming growth factor- β . *Cell Immunol*. 1990;126(1):47–56.
35. Smyth MJ, Strobl SL, Young HA, Ortaldo JR, Ochoa AC. Regulation of lymphokine-activated killer activity and pore-forming protein gene expression in human peripheral blood CD8⁺ T lymphocytes. Inhibition by transforming growth factor- β . *J Immunol*. 1991;146(10):3289–97.
36. Othman MS, Aref AM, Mohamed AA, Ibrahim WA. Serum levels of Interleukin-6 and Interleukin-10 as biomarkers for hepatocellular carcinoma in Egyptian patients. *ISRN Hepatol*. 2013;2013:412317. <https://doi.org/10.1155/2013/412317>.
37. El-Emshaty HM, Nasif WA, Mohamed IE. Serum cytokine of IL-10 and IL-12 in chronic liver disease: the immune and

- inflammatory response. *Dis Markers*. 2015;2015:707254. <https://doi.org/10.1155/2015/707254>.
38. Thomson AW, Knolle PA. Antigen-presenting cell function in the tolerogenic liver environment. *Nat Rev Immunol*. 2010;10(11):753–66. <https://doi.org/10.1038/nri2858>.
39. Chen DS, Mellman I. Oncology meets immunology: the cancer-immunity cycle. *Immunity*. 2013;39(1):1–10. <https://doi.org/10.1016/j.immuni.2013.07.012>.
40. Nakajima T, Mizushima N, Kanai K. Relationship between natural killer activity and development of hepatocellular carcinoma in patients with cirrhosis of the liver. *Jpn J Clin Oncol*. 1987;17(4):327–32.
41. Garnelo M, Tan A, Her Z, Yeong J, Lim CJ, Chen J, et al. Interaction between tumour-infiltrating B cells and T cells controls the progression of hepatocellular carcinoma. *Gut*. 2017;66(2):342–51. <https://doi.org/10.1136/gutjnl-2015-310814>.
42. Condeelis J, Pollard JW. Macrophages: obligate partners for tumor cell migration, invasion, and metastasis. *Cell*. 2006;124(2):263–6. <https://doi.org/10.1016/j.cell.2006.01.007>.
43. Degroote H, Van Dierendonck A, Geerts A, Van Vlierberghe H, Devisscher L. Preclinical and clinical therapeutic strategies affecting tumor-associated macrophages in hepatocellular carcinoma. *J Immunol Res*. 2018;2018:7819520. <https://doi.org/10.1155/2018/7819520>.
44. Wu K, Kryczek I, Chen L, Zou W, Welling TH. Kupffer cell suppression of CD8+ T cells in human hepatocellular carcinoma is mediated by B7-H1/programmed death-1 interactions. *Cancer Res*. 2009;69(20):8067–75. <https://doi.org/10.1158/0008-5472.CAN-09-0901>.
45. Tacke F. Targeting hepatic macrophages to treat liver diseases. *J Hepatol*. 2017;66(6):1300–12. <https://doi.org/10.1016/j.jhep.2017.02.026>.
46. Yeung OW, Lo CM, Ling CC, Qi X, Geng W, Li CX, et al. Alternatively activated (M2) macrophages promote tumour growth and invasiveness in hepatocellular carcinoma. *J Hepatol*. 2015;62(3):607–16. <https://doi.org/10.1016/j.jhep.2014.10.029>.
47. Ding T, Xu J, Wang F, Shi M, Zhang Y, Li SP, et al. High tumor-infiltrating macrophage density predicts poor prognosis in patients with primary hepatocellular carcinoma after resection. *Hum Pathol*. 2009;40(3):381–9. <https://doi.org/10.1016/j.humpath.2008.08.011>.
48. Banchereau J, Steinman RM. Dendritic cells and the control of immunity. *Nature*. 1998;392(6673):245–52. <https://doi.org/10.1038/32588>.
49. Steinman RM, Hemmi H. Dendritic cells: translating innate to adaptive immunity. *Curr Top Microbiol Immunol*. 2006;311:17–58.
50. Almand B, Resser JR, Lindman B, Nadaf S, Clark JI, Kwon ED, et al. Clinical significance of defective dendritic cell differentiation in cancer. *Clin Cancer Res*. 2000;6(5):1755–66.
51. Steinman RM. Lasker Basic Medical Research Award. Dendritic cells: versatile controllers of the immune system. *Nat Med*. 2007;13(10):1155–9. <https://doi.org/10.1038/nm1643>.
52. Kakumu S, Ito S, Ishikawa T, Mita Y, Tagaya T, Fukuzawa Y, et al. Decreased function of peripheral blood dendritic cells in patients with hepatocellular carcinoma with hepatitis B and C virus infection. *J Gastroenterol Hepatol*. 2000;15(4):431–6.
53. Chen S, Akbar SM, Tanimoto K, Ninomiya T, Iuchi H, Michitaka K, et al. Absence of CD83-positive mature and activated dendritic cells at cancer nodules from patients with hepatocellular carcinoma: relevance to hepatocarcinogenesis. *Cancer Lett*. 2000;148(1):49–57.
54. Ormandy LA, Farber A, Cantz T, Petrykowska S, Wedemeyer H, Horning M, et al. Direct ex vivo analysis of dendritic cells in patients with hepatocellular carcinoma. *World J Gastroenterol*. 2006;12(20):3275–82.
55. Gabrilovich DI, Chen HL, Girgis KR, Cunningham HT, Meny GM, Nadaf S, et al. Production of vascular endothelial growth factor by human tumors inhibits the functional maturation of dendritic cells. *Nat Med*. 1996;2(10):1096–103.
56. Beckebaum S, Zhang X, Chen X, Yu Z, Frilling A, Dworacki G, et al. Increased levels of interleukin-10 in serum from patients with hepatocellular carcinoma correlate with profound numerical deficiencies and immature phenotype of circulating dendritic cell subsets. *Clin Cancer Res*. 2004;10(21):7260–9. <https://doi.org/10.1158/1078-0432.CCR-04-0872>.
57. Maier KP. Cirrhosis of the liver as a precancerous condition. *Praxis (Bern 1994)*. 1998;87(44):1462–5.
58. Singal AG, El-Serag HB. Hepatocellular carcinoma from epidemiology to prevention: translating knowledge into practice. *Clin Gastroenterol Hepatol*. 2015;13(12):2140–51. <https://doi.org/10.1016/j.cgh.2015.08.014>.
59. El-Serag HB. Hepatocellular carcinoma. *N Engl J Med*. 2011;365(12):1118–27. <https://doi.org/10.1056/NEJMra1001683>.
60. Affo S, Yu LX, Schwabe RF. The role of cancer-associated fibroblasts and fibrosis in liver cancer. *Annu Rev Pathol*. 2017;12:153–86. <https://doi.org/10.1146/annurev-pathol-052016-100322>.
61. Hanahan D, Weinberg RA. Hallmarks of cancer: the next generation. *Cell*. 2011;144(5):646–74. <https://doi.org/10.1016/j.cell.2011.02.013>.
62. Bissell MJ, Hines WC. Why don't we get more cancer? A proposed role of the microenvironment in restraining cancer progression. *Nat Med*. 2011;17(3):320–9. <https://doi.org/10.1038/nm.2328>.
63. Ji J, Eggert T, Budhu A, Forgues M, Takai A, Dang H, et al. Hepatic stellate cell and monocyte interaction contributes to poor prognosis in hepatocellular carcinoma. *Hepatology*. 2015;62(2):481–95. <https://doi.org/10.1002/hep.27822>.
64. Zhao W, Su W, Kuang P, Zhang L, Liu J, Yin Z, et al. The role of hepatic stellate cells in the regulation of T-cell function and the promotion of hepatocellular carcinoma. *Int J Oncol*. 2012;41(2):457–64. <https://doi.org/10.3892/ijo.2012.1497>.
65. Zhao W, Zhang L, Yin Z, Su W, Ren G, Zhou C, et al. Activated hepatic stellate cells promote hepatocellular carcinoma development in immunocompetent mice. *Int J Cancer*. 2011;129(11):2651–61. <https://doi.org/10.1002/ijc.25920>.
66. Cheng Y, Li H, Deng Y, Tai Y, Zeng K, Zhang Y, et al. Cancer-associated fibroblasts induce PDL1+ neutrophils through the IL6-STAT3 pathway that fosters immune suppression in hepatocellular carcinoma. *Cell Death Dis*. 2018;9(4):422. <https://doi.org/10.1038/s41419-018-0458-4>.
67. Zhang Z, Li X, Sun W, Yue S, Yang J, Li J, et al. Loss of exosomal miR-320a from cancer-associated fibroblasts contributes to HCC proliferation and metastasis. *Cancer Lett*. 2017;397:33–42. <https://doi.org/10.1016/j.canlet.2017.03.004>.
68. Wang F, Li L, Piontek K, Sakaguchi M, Selaru FM. Exosome miR-335 as a novel therapeutic strategy in hepatocellular

- carcinoma. *Hepatology*. 2018;67(3):940–54. <https://doi.org/10.1002/hep.29586>.
69. Torimura T, Ueno T, Kin M, Harada R, Taniguchi E, Nakamura T, et al. Overexpression of angiopoietin-1 and angiopoietin-2 in hepatocellular carcinoma. *J Hepatol*. 2004;40(5):799–807. <https://doi.org/10.1016/j.jhep.2004.01.027>.
70. Taura K, De Minicis S, Seki E, Hatano E, Iwaisako K, Osterreicher CH, et al. Hepatic stellate cells secrete angiopoietin 1 that induces angiogenesis in liver fibrosis. *Gastroenterology*. 2008;135(5):1729–38. <https://doi.org/10.1053/j.gastro.2008.07.065>.
71. Lin N, Chen Z, Lu Y, Li Y, Hu K, Xu R. Role of activated hepatic stellate cells in proliferation and metastasis of hepatocellular carcinoma. *Hepatol Res*. 2015;45(3):326–36. <https://doi.org/10.1111/hepr.12356>.
72. Santamato A, Fransvea E, Dituri F, Caligiuri A, Quaranta M, Niimi T, et al. Hepatic stellate cells stimulate HCC cell migration via laminin-5 production. *Clin Sci (Lond)*. 2011;121(4):159–68. <https://doi.org/10.1042/CS20110002>.
73. Okabe H, Beppu T, Ueda M, Hayashi H, Ishiko T, Masuda T, et al. Identification of CXCL5/ENA-78 as a factor involved in the interaction between cholangiocarcinoma cells and cancer-associated fibroblasts. *Int J Cancer*. 2012;131(10):2234–41. <https://doi.org/10.1002/ijc.27496>.
74. Fang T, Lv H, Lv G, Li T, Wang C, Han Q, et al. Tumor-derived exosomal miR-1247-3p induces cancer-associated fibroblast activation to foster lung metastasis of liver cancer. *Nat Commun*. 2018;9(1):191. <https://doi.org/10.1038/s41467-017-02583-0>.
75. Jiang J, Ye F, Yang X, Zong C, Gao L, Yang Y, et al. Peri-tumor associated fibroblasts promote intrahepatic metastasis of hepatocellular carcinoma by recruiting cancer stem cells. *Cancer Lett*. 2017;404:19–28. <https://doi.org/10.1016/j.canlet.2017.07.006>.
76. Liu C, Liu L, Chen X, Cheng J, Zhang H, Zhang C, et al. LSD1 stimulates cancer-associated fibroblasts to drive Notch3-dependent self-renewal of liver cancer stem-like cells. *Cancer Res*. 2018;78(4):938–49. <https://doi.org/10.1158/0008-5472.CAN-17-1236>.
77. Rhee H, Kim HY, Choi JH, Woo HG, Yoo JE, Nahm JH, et al. Keratin 19 expression in hepatocellular carcinoma is regulated by fibroblast-derived HGF via a MET-ERK1/2-AP1 and SP1 axis. *Cancer Res*. 2018;78(7):1619–31. <https://doi.org/10.1158/0008-5472.CAN-17-0988>.
78. Kim H, Choi GH, Na DC, Ahn EY, Kim GI, Lee JE, et al. Human hepatocellular carcinomas with “Stemness”-related marker expression: keratin 19 expression and a poor prognosis. *Hepatology*. 2011;54(5):1707–17. <https://doi.org/10.1002/hep.24559>.
79. Coulouarn C, Corlu A, Glaise D, Guenon I, Thorgerisson SS, Clement B. Hepatocyte-stellate cell cross-talk in the liver engenders a permissive inflammatory microenvironment that drives progression in hepatocellular carcinoma. *Cancer Res*. 2012;72(10):2533–42. <https://doi.org/10.1158/0008-5472.CAN-11-3317>.
80. Ju MJ, Qiu SJ, Fan J, Xiao YS, Gao Q, Zhou J, et al. Peritumoral activated hepatic stellate cells predict poor clinical outcome in hepatocellular carcinoma after curative resection. *Am J Clin Pathol*. 2009;131(4):498–510. <https://doi.org/10.1309/AJCP86PPBNGOHNLL>.
81. Zhang DY, Goossens N, Guo J, Tsai MC, Chou HI, Altunkaynak C, et al. A hepatic stellate cell gene expression signature associated with outcomes in hepatitis C cirrhosis and hepatocellular carcinoma after curative resection. *Gut*. 2016;65(10):1754–64. <https://doi.org/10.1136/gutjnl-2015-309655>.
82. Pupulin LF, Vilgrain V, Ronot M, Becker CD, Breguet R, Terraz S. Hepatic lymphatics: anatomy and related diseases. *Abdom Imaging*. 2015;40(6):1997–2011. <https://doi.org/10.1007/s00261-015-0350-y>.
83. Lund AW, Wagner M, Fankhauser M, Steinskog ES, Broggi MA, Spranger S, et al. Lymphatic vessels regulate immune microenvironments in human and murine melanoma. *J Clin Invest*. 2016;126(9):3389–402. <https://doi.org/10.1172/JCI79434>.
84. Swartz MA. Immunomodulatory roles of lymphatic vessels in cancer progression. *Cancer Immunol Res*. 2014;2(8):701–7. <https://doi.org/10.1158/2326-6066.CIR-14-0115>.
85. Lukacs-Kornek V, Malhotra D, Fletcher AL, Acton SE, Elpek KG, Tayalia P, et al. Regulated release of nitric oxide by nonhematopoietic stroma controls expansion of the activated T cell pool in lymph nodes. *Nat Immunol*. 2011;12(11):1096–104. <https://doi.org/10.1038/ni.2112>.
86. Fletcher AL, Lukacs-Kornek V, Reynoso ED, Pinner SE, Bellemare-Pelletier A, Curry MS, et al. Lymph node fibroblastic reticular cells directly present peripheral tissue antigen under steady-state and inflammatory conditions. *J Exp Med*. 2010;207(4):689–97. <https://doi.org/10.1084/jem.20092642>.
87. Rouhani SJ, Eccles JD, Riccardi P, Peske JD, Tewalt EF, Cohen JN, et al. Roles of lymphatic endothelial cells expressing peripheral tissue antigens in CD4 T-cell tolerance induction. *Nat Commun*. 2015;6:6771. <https://doi.org/10.1038/ncomms7771>.
88. Vollmar B, Wolf B, Siegmund S, Katsen AD, Menger MD. Lymph vessel expansion and function in the development of hepatic fibrosis and cirrhosis. *Am J Pathol*. 1997;151(1):169–75.
89. Yamauchi Y, Michitaka K, Onji M. Morphometric analysis of lymphatic and blood vessels in human chronic viral liver diseases. *Am J Pathol*. 1998;153(4):1131–7. [https://doi.org/10.1016/S0002-9440\(10\)65657-X](https://doi.org/10.1016/S0002-9440(10)65657-X).
90. Yokomori H, Oda M, Kaneko F, Kawachi S, Tanabe M, Yoshimura K, et al. Lymphatic marker podoplanin/D2-40 in human advanced cirrhotic liver—re-evaluations of microlymphatic abnormalities. *BMC Gastroenterol*. 2010;10:131. <https://doi.org/10.1186/1471-230X-10-131>.
91. Limatola E, Filosa S. Exogenous vitellogenesis and micropinocytosis in the lizard, *Podarcis sicula*, treated with follicle-stimulating hormone. *Gen Comp Endocrinol*. 1989;75(2):165–76.
92. Shields JD, Kourtis IC, Tomei AA, Roberts JM, Swartz MA. Induction of lymphoid-like stroma and immune escape by tumors that express the chemokine CCL21. *Science*. 2010;328(5979):749–52. <https://doi.org/10.1126/science.1185837>.
93. Xiang Z, Zeng Z, Tang Z, Fan J, Sun H, Wu W, et al. Increased expression of vascular endothelial growth factor-C and nuclear CXCR4 in hepatocellular carcinoma is correlated with lymph node metastasis and poor outcome. *Cancer J*. 2009;15(6):519–

25. <https://doi.org/10.1097/PPO.0b013e3181c6aa6b>.
94. Yamaguchi R, Yano H, Nakashima O, Akiba J, Nishida N, Kurogi M, et al. Expression of vascular endothelial growth factor-C in human hepatocellular carcinoma. *J Gastroenterol Hepatol*. 2006;21(1 Pt 1):152–60. <https://doi.org/10.1111/j.1440-1746.2005.04217.x>.
95. Nieto MA, Huang RY, Jackson RA, Thiery JP. Emt: 2016. *Cell*. 2016;166(1):21–45. <https://doi.org/10.1016/j.cell.2016.06.028>.
96. Dongre A, Weinberg RA. New insights into the mechanisms of epithelial-mesenchymal transition and implications for cancer. *Nat Rev Mol Cell Biol*. 2018; <https://doi.org/10.1038/s41580-018-0080-4>.
97. Polyak K, Weinberg RA. Transitions between epithelial and mesenchymal states: acquisition of malignant and stem cell traits. *Nat Rev Cancer*. 2009;9(4):265–73. <https://doi.org/10.1038/nrc2620>.
98. Acloque H, Adams MS, Fishwick K, Bronner-Fraser M, Nieto MA. Epithelial-mesenchymal transitions: the importance of changing cell state in development and disease. *J Clin Invest*. 2009;119(6):1438–49. <https://doi.org/10.1172/JCI38019>.
99. Yan L, Xu F, Dai CL. Relationship between epithelial-to-mesenchymal transition and the inflammatory microenvironment of hepatocellular carcinoma. *J Exp Clin Cancer Res*. 2018;37(1):203. <https://doi.org/10.1186/s13046-018-0887-z>.
100. Zavadil J, Bottinger EP. TGF-beta and epithelial-to-mesenchymal transitions. *Oncogene*. 2005;24(37):5764–74. <https://doi.org/10.1038/sj.onc.1208927>.
101. Choi SS, Diehl AM. Epithelial-to-mesenchymal transitions in the liver. *Hepatology*. 2009;50(6):2007–13. <https://doi.org/10.1002/hep.23196>.
102. Zhai B, Yan HX, Liu SQ, Chen L, Wu MC, Wang HY. Reduced expression of E-cadherin/ catenin complex in hepatocellular carcinomas. *World J Gastroenterol*. 2008;14(37):5665–73.
103. Battaglia S, Benzoubir N, Nobilet S, Charneau P, Samuel D, Zignego AL, et al. Liver cancer-derived hepatitis C virus core proteins shift TGF-beta responses from tumor suppression to epithelial-mesenchymal transition. *PLoS One*. 2009;4(2):e4355. <https://doi.org/10.1371/journal.pone.0004355>.
104. Fuchs BC, Fujii T, Dorfman JD, Goodwin JM, Zhu AX, Lanuti M, et al. Epithelial-to- mesenchymal transition and integrin-linked kinase mediate sensitivity to epidermal growth factor receptor inhibition in human hepatoma cells. *Cancer Res*. 2008;68(7):2391–9. <https://doi.org/10.1158/0008-5472.CAN-07-2460>.
105. Llovet JM, Ricci S, Mazzaferro V, Hilgard P, Gane E, Blanc JF, et al. Sorafenib in advanced hepatocellular carcinoma. *N Engl J Med*. 2008;359(4):378–90. <https://doi.org/10.1056/NEJMoa0708857>.
106. Kudo M, Finn RS, Qin S, Han KH, Ikeda K, Piscaglia F, et al. Lenvatinib versus sorafenib in first-line treatment of patients with unresectable hepatocellular carcinoma: a randomised phase 3 non-inferiority trial. *Lancet*. 2018;391(10126):1163–73. [https://doi.org/10.1016/S0140-6736\(18\)30207-1](https://doi.org/10.1016/S0140-6736(18)30207-1).
107. Sui H, Ma N, Wang Y, Li H, Liu X, Su Y, et al. Anti-PD-1/PD-L1 therapy for non-small- cell lung cancer: toward personalized medicine and combination strategies. *J Immunol Res*. 2018;2018:6984948. <https://doi.org/10.1155/2018/6984948>.
108. Herzberg B, Fisher DE. Metastatic melanoma and immunotherapy. *Clin Immunol*. 2016;172:105–10.
109. Killock D. Immunotherapy: Nivolumab keeps HCC in check and opens avenues for check- mate. *Nat Rev Clin Oncol*. 2017;14(7):392.
110. Zhu AX, Finn RS, Edeline J, Cattani S, Ogasawara S, Palmer D, et al. Pembrolizumab in patients with advanced hepatocellular carcinoma previously treated with sorafenib (KEYNOTE-224): a non-randomised, open-label phase 2 trial. *Lancet Oncol*. 2018;19(7):940–52. [https://doi.org/10.1016/S1470-2045\(18\)30351-6](https://doi.org/10.1016/S1470-2045(18)30351-6).
111. Shang N, Figini M, Shangguan J, Wang B, Sun C, Pan L, et al. Dendritic cells based immunotherapy. *Am J Cancer Res*. 2017;7(10):2091–102.
112. Palmer DH, Midgley RS, Mirza N, Torr EE, Ahmed F, Steele JC, et al. A phase II study of adoptive immunotherapy using dendritic cells pulsed with tumor lysate in patients with hepatocellular carcinoma. *Hepatology*. 2009;49(1):124–32. <https://doi.org/10.1002/hep.22626>.
113. El Ansary M, Mogawer S, Elhamid SA, Alwakil S, Aboelkasem F, Sabaawy HE, et al. Immunotherapy by autologous dendritic cell vaccine in patients with advanced HCC. *J Cancer Res Clin Oncol*. 2013;139(1):39–48. <https://doi.org/10.1007/s00432-012-1298-8>.

Introductory article III – Tight Junction Proteins and the Biology of Hepatobiliary Disease

Review article:

Roehlen N, Roca Suarez AA, El Saghire H, Saviano A, Schuster C, Lupberger J, Baumert TF. Tight Junction Proteins and the Biology of Hepatobiliary Disease. *Int J Mol Sci.* 2020 Jan 28;21(3):825. doi: 10.3390/ijms21030825.



Tight Junction Proteins and the Biology of Hepatobiliary Disease

Natascha Roehlen^{1,2}, Armando Andres Roca Suarez^{1,2}, Houssein El Saghire^{1,2}, Antonio Saviano^{1,2,3}, Catherine Schuster^{1,2}, Joachim Lupberger^{1,2} and Thomas F. Baumert^{1,2,3*}

¹ Institut de Recherche sur les Maladies Virales et Hépatiques, Inserm UMR1110, F-67000 Strasbourg, France; natascha.roehlen@etu.unistra.fr (N.R.); andres.roca-suarez@etu.unistra.fr (A.A.R.S.); elsaghire@unistra.fr (H.E.S.); saviano@unistra.fr (A.S.); catherine.schuster@unistra.fr (C.S.); joachim.lupberger@unistra.fr (J.L.)

² Université de Strasbourg, F-67000 Strasbourg, France

³ Pôle Hepato-digestif, Institut Hospitalo-universitaire, Hôpitaux Universitaires de Strasbourg, F-67000 Strasbourg, France

* Correspondence: thomas.baumert@unistra.fr; Tel.: +33-3688-53703



check for
updates

Received: 4 November 2019; Accepted: 21 January 2020; Published: 28 January 2020

Abstract: Tight junctions (TJ) are intercellular adhesion complexes on epithelial cells and composed of integral membrane proteins as well as cytosolic adaptor proteins. Tight junction proteins have been recognized to play a key role in health and disease. In the liver, TJ proteins have several functions: they contribute as gatekeepers for paracellular diffusion between adherent hepatocytes or cholangiocytes to shape the blood-biliary barrier (BBIB) and maintain tissue homeostasis. At non-junctional localizations, TJ proteins are involved in key regulatory cell functions such as differentiation, proliferation, and migration by recruiting signaling proteins in response to extracellular stimuli. Moreover, TJ proteins are hepatocyte entry factors for the hepatitis C virus (HCV)—a major cause of liver disease and cancer worldwide. Perturbation of TJ protein expression has been reported in chronic HCV infection, cholestatic liver diseases as well as hepatobiliary carcinoma. Here we review the physiological function of TJ proteins in the liver and their implications in hepatobiliary diseases.

Keywords: Claudin; occludin; blood-biliary barrier; chronic liver disease; hepatocellular carcinoma; cholangiocellular carcinoma; NISCH syndrome

1. Introduction

Tight junctions (TJ) are protein complexes on epithelial cells in all organs of the body and establish paracellular diffusion barriers between different compartments. The distinct cell polarity and selective paracellular diffusion hereby provides the molecular basis of tissue homeostasis [1]. Structurally, TJs consist of transmembrane proteins that function as the diffusion barriers and cytosolic proteins that interface the junctional complexes with the cytoskeleton [1]. While initially TJs were believed to serve as simple paracellular gates, in the past years, accumulating data have identified additional functions of TJs proteins. By maintaining cellular differentiation, intercellular communication as well as assembly of signaling proteins, TJ proteins have been shown to orchestrate inside-out and outside-in signaling, hereby affecting cell proliferation, migration, apoptosis, and inflammation [2–4]. On the other hand, several growth factors, cytokines, and signaling cascades induce and regulate localization and expression of TJ proteins, hereby affecting epithelial differentiation and barrier integrity [5,6].

In the healthy liver, TJ proteins are expressed on hepatocytes, cholangiocytes, and nonparenchymal cells such as endothelial cells [5,7,8]. While TJ proteins on hepatocytes build the blood-biliary barrier

(BBIB) and are hijacked during hepatitis C virus (HCV) infection, TJ proteins on cholangiocytes line the intrahepatic bile ducts [7,9,10]. Besides their localization at the apical membrane, TJ proteins have also been described to be localized at the basolateral membrane and in the cytoplasm of hepatocytes. In these non-junctional localizations, TJ proteins regulate cell-matrix interactions, intracellular signaling and proliferation, migration, and invasion [11]. Perturbation of TJ structure, protein expression, and localization have frequently been described in chronic liver and biliary diseases, indicating their fundamental role in liver biology [12]. This review provides an overview of TJ proteins being expressed in the liver, their function in maintaining TJ structure and cell signaling outside of TJs, as well as their implication in hepatobiliary diseases.

2. Biology of Tight Junction Proteins

1.1. Structure and Composition of Tight Junctions

Tight junctions are shaped by intercellular protein-protein complexes connecting plasma membranes of neighboring cells. Thus, TJs often appear as “kissing points” by electron microscopy. Two models of TJ structure exist: the protein model and the protein-lipid hybrid model. The protein model postulates construction of the junctional diffusion barrier by transmembrane proteins on both sides, interacting in a homotypic or heterotypic way (shown in Figure 1a), whereas the hybrid model proposes membrane hemifusions built by inverted lipid micelles and stabilized by transmembrane proteins [1]. Yet no consensus on the ultrastructural appearance has been reached. However, in both cases, TJs build a regulatory semipermeable gate that enables selective paracellular diffusion depending on the size and charge of the corresponding molecule [1]. Moreover, TJs form an intramembrane barrier (also referred to as “fence function”), that restricts exchange between the cells’ apical and basolateral surfaces [13]. However, whether the fence function of TJs is critical or not for the establishment of a polarized phenotype has been a matter of debate, taking into account that it has been observed how epithelial cells are able to polarize in the absence of cell-cell junctions [14,15].

The transmembrane domains of TJs on epithelial cells are mainly built by tetraspanin-associated proteins of the claudin (CLDN) family and the junctional proteins occludin (OCLN) and MarvelD3, which contain a MAL and related proteins for vesicle trafficking and membrane link (MARVEL) domain. Moreover, junctional adhesion molecules (JAMs) have been reported as integral membrane proteins in TJs [16,17]. Tricellular TJ proteins characterize cell adhesion between three neighboring cells and include tricellulin [18], lipolysis-stimulated lipoprotein receptor (LSR) [19], as well as immunoglobulin-like domain containing receptor (ILDR1 and ILDR2) [20]. Representatives of the cytosolic junctional plaque on the other hand are adapter proteins as Zonula occludens 1-3 (ZO1-3), membrane-associated guanylate kinase inverted (MAGI) proteins, and cingulin [1] (Figure 1a).

OCLN was the first identified transmembrane protein in TJs and belongs to the large protein family of Marvel-domain-containing proteins [21]. In contrast to the multiple and differentially expressed members of CLDN family, only one OCLN transcript has been described, which however occurs in differently spliced variants. With a size of 65 kDa, OCLN contains four transmembrane domains, one small intracellular loop, two extracellular loops, and intracellular localized C and N terminals (Figure 1a) [22].

The family of CLDN proteins comprises 27 members in mammals [23]. According to their physiological role in paracellular permeability, CLDNs can further be subgrouped into sealing CLDNs (CLDN1, 3, 5, 11, 14, and 19), cation-selective (CLDN2, 10b and 15) and anion-selective paracellular channel forming CLDNs (CLDN10a and 17), as well as water-permeable CLDNs (CLDN2 and 15). For the remaining CLDNs, their roles on epithelial barriers are not yet fully understood [24]. These 20–27 kDa proteins consist of four transmembrane domains, two extracellular loops, and a cytoplasmatic carboxyl tail (Figure 1a). As integral proteins of TJs, CLDNs are reported to regulate ion and water permeability of the paracellular barrier [1,25,26].

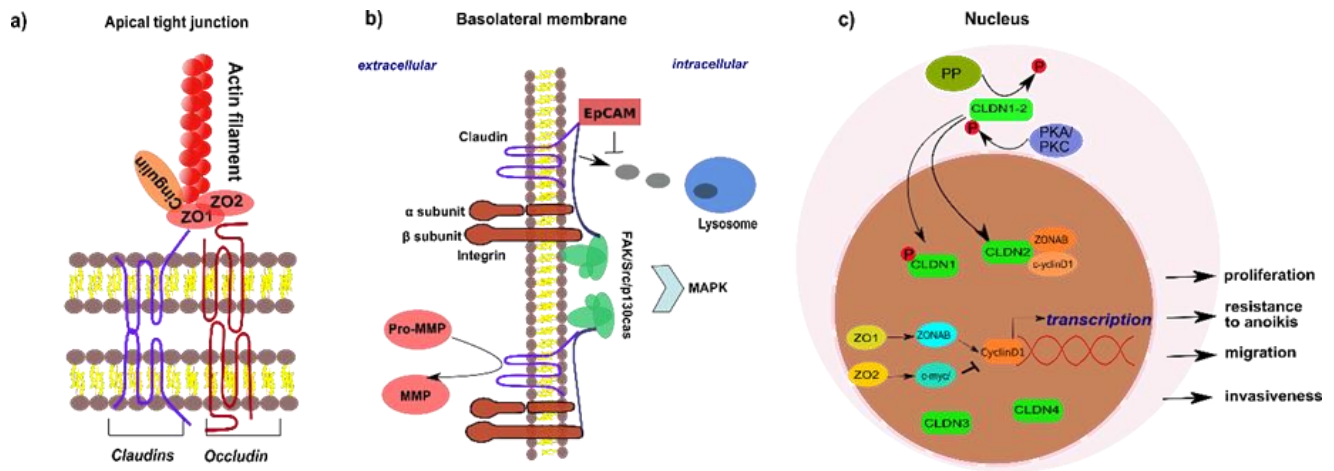


Figure 1. Functions of tight junction proteins at different subcellular localizations. Tight junction proteins are expressed at three different locations within epithelial cells with different functions including the apical membrane (a), the basolateral membrane (b), and in the nucleus (c). (a) At the apical membrane, tight junctions (TJs) are typically built by integral membrane proteins of the CLDN or Marvel-domain containing protein family (e.g., occludin—OCLN) that connect via C-terminus bound adapter proteins to intracellular actin filaments. (b) In the normal intestinal mucosa and in various cancer cell types, basolateral localized CLDNs have been found to regulate activation of pro-MMPs into MMPs and to interact with integrins at focal adhesion complexes, hereby affecting main intracellular signaling cascades such as the MAPK pathway. Investigations on colon cancer cell lines indicate EpCAM to specifically stabilize expression of CLDN1 and 7 at the basolateral membrane and to prevent their lysosomal degradation. (c) Nuclear localization has been reported for ZO1 and ZO2 as well as CLDN1–4 in various cancer cell types and is regulated by posttranslational modification. Within the nucleus, CLDN2 retains cyclinD1 and ZONAB hereby enhancing cell proliferation. Specific interaction of ZO1 with the transcription factor ZONAB regulates G1/S-phase progression by increasing cyclin D1, while ZO2 inhibits transcription of cyclin D1 by binding to c-myc. CLDN (Claudin); c-myc(MYC proto-oncogene); EpCAM (epithelial cell adhesion molecule); FAK (focal adhesion kinase); MAPK (Mitogen-activated protein kinase); MMP (Matrix-metalloproteinase); PKA (protein kinase A); PKC (protein kinase C); PP (protein phosphatase); Src (steroid receptor coactivator); ZO1 (Zonula occludens 1); ZO2 (Zonula occludens 2); ZONAB (ZO1-associated nucleic acid binding protein).

With four transmembrane domains, cytoplasmatic C- and N-terminals, and two extracellular loops, tricellulin shows strong structural similarity to CLDNs and OCLN [18,27]. While OCLN and CLDN represent the main transmembrane proteins of apical cell adhesions between two cells (bicellular tight junction, bTJ), tricellulin is mainly enriched at tricellular contact regions (tricellular tight junction, tTJ), although also been identified in bTJs [18]. LSR, ILDR1 and 2, which are commonly described as the angulin family, have been reported to recruit tricellulin to tTJ [20].

JAMs belong to the immunoglobulin superfamily (IgSF). Originally discovered on leucocytes as key players of leucocyte-endothelial cell interaction and trans-endothelial migration, JAM-A-C as well as the related IgSF members CAR, endothelial cell-selective adhesion molecule (ESAM), and JAM-4 were later described to be enriched in epithelial and endothelial TJs. Consisting of two IgSF domains, two Ig-like domains, one single transmembrane domain, and a PDZ-domain binding cytoplasmatic tail, these proteins contribute to barrier formation and TJ associated signaling [16,17].

Besides transmembrane proteins, TJs consist of junctional plaque components that connect the junctional membrane with the cytoskeleton. ZO proteins are the most important adapter proteins, that connect CLDN, OCLN, and tricellulin with the cytoskeleton, hereby enabling clustering of protein complexes to the intracellular domains of TJs (Figure 1a). Apart from TJs, ZO proteins have also been described in cadherin-based adherens junctions and gap junctions [28]. Three ZO proteins (ZO1–3) with high structural similarity have been discovered. ZO1, the best described member of the family of ZO proteins represents a 220 kDa scaffolding protein, that includes three types of functional domains, a Src homology 3 domain (SH3), three PDZ domains, a proline rich and a guanylate kinase domain [29,30].

ZO proteins directly interact with the intracellular actin filaments and the first PDZ domain has been shown to associate with the C-terminus of CLDN and OCLN proteins, hereby regulating TJ assembly (Figure 1a) [31,32]. Other representatives of the junctional plaque are cingulin and 7H6 [33,34]. For a detailed review regarding the general structure and composition of TJs see [35,36].

The TJ complex is known to be highly dynamic with continuous remodeling by clathrin-mediated endocytic recycling [37–40]. Recycled or newly produced TJ proteins are sorted in the Golgi-network and transported by specific trafficking proteins to the desired localizations [41,42]. On the other hand, several growth factors, cytokines, and signaling cascades induce and regulate localization and expression of TJ proteins, hereby affecting epithelial differentiation and barrier integrity [5,6].

Knockout (KO) studies in cultured epithelial cells indicate an increase of paracellular permeability by loss of single CLDN proteins [43,44]. In contrast, KO of OCLN does not alter baseline barrier function, but attenuates cytokine-induced increase in trans-epithelial resistance [45]. Knockdown of tricellulin using siRNA decreases trans-epithelial electrical resistance and increases the paracellular permeability in cultured epithelial cells [18]. JAM-A in vitro and in vivo KO studies revealed increased epithelial permeability potentially due to perturbed regulation of CLDN expression and induction of apoptosis [46,47]. Loss of ZO1 retards but not completely hampers TJ formation, probably due to compensatory upregulation of ZO2. Thus, assembly of CLDN and OCLN proteins to TJs takes longer in the absence of ZO1 but does not block eventual establishment of the polarized epithelial structure with functional TJs within hours in cell culture [15]. However, KO of ZO1 and knockdown of ZO2 by RNA interference results in diffuse distribution of integral TJ proteins in epithelial cells with severe perturbation of the paracellular barrier [48]. While to our knowledge KO of 7H6 in epithelial cells has not yet been analyzed, its localization would suggest a paracellular barrier function [49,50]. In mice in vivo KO or knockdown of TJ proteins results in a wide variety of phenotypes, ranging from a normal phenotype without any disease to lethality [51–55]. Furthermore, there are differences in the phenotype of TJ protein loss of function in mice and humans: e.g., while CLDN1 KO in a mouse model has shown to be lethal [52], congenital CLDN1 KO loss-of function mutations in human patients can manifest in a highly variable phenotype ranging from normal health without disease to neonatal sclerosing cholangitis and ichthyosis of variable severity (NISCH syndrome), potentially due to compensatory upregulation of other CLDN members [56]. This indicates differential functions of the TJ orthologs in mice and humans and suggests that a complete loss of TJ proteins can be functionally compensated as shown for CLDN1 in humans.

1.2. Non-Junctional Localization of Tight Junction Proteins

Several TJ proteins have been described to be also localized outside of TJs at the basolateral membrane, in the cytoplasm, and in the nucleus. Non-junctional TJ proteins exert key regulatory functions on cell proliferation, cell adhesion, as well as migration and invasion [11]. As an example, CLDN1, 2, and 7 regulate cell-matrix interaction by forming complexes with integrin proteins at focal adhesions on the basolateral membrane of human lung, melanoma, colon, as well as breast cancer cells (Figure 1b) [57–61]. These interactions have not only been shown to affect epithelial adhesion to the matrix and cell proliferation [59], but also to be associated with cancer progression and metastasis [61]. The epithelial cell adhesion molecule (EpCAM) specifically stabilizes this non-junctional CLDN expression and regulates its lysosomal degradation (Figure 1b) [62]. In line with the potential pro-oncogenic function of CLDN proteins at the basolateral membrane, interaction of EpCAM with CLDN7 was reported to promote tumor progression and cell dissemination [63].

Several studies link basolateral CLDN expression with expression and activity of matrix metalloproteinases (MMPs) [64–66]. At the basolateral membrane of epithelial cells, secreted MMPs are able to degrade extracellular matrix proteins [67]. Interestingly, CLDN proteins have been shown to recruit and activate pro-MMP, hereby promoting migration and invasion of the corresponding cancer cells (Figure 1b) [68].

Nuclear localization has been reported for ZO1/ZO2 [69,70] and CLDN1-4 [71–74] in several types of cancer cells. The conditions or inducers under which these TJ proteins localize in the nucleus are poorly understood. However, in the case of CLDN1, phosphorylation by protein kinase A and C (PKA and PKC) has been shown to promote nuclear import [75]. Nuclear import of CLDN2 on the other hand is induced by dephosphorylation [72]. Functional investigations in colon cancer cells indicate nuclear localization of CLDN proteins to be associated with resistance to anoikis as well as migration and invasiveness [71], while nuclear localization of ZO1/ZO2 affects cell cycle progression and cell proliferation by transcriptional regulation of cyclin D1 in tumorous and non-tumorous epithelial cells [76,77] (Figure 1c).

3. Tight Junction Proteins and Their Role in Signaling

In colon and liver cancer cells, TJ proteins functionally crosstalk with key cellular signaling pathways, including PI3K/AKT, Wnt/ β -catenin, and EGFR/ERK signaling [78–80]. Proteomic analysis of OCLN and CLDNs revealed numerous binding partners, that are known to be involved in cell signaling and trafficking, such as kinases, phosphatases, signaling adaptors, and receptor proteins [81,82]. A strong body of evidence indicates functional crosstalk of CLDN proteins with the EGFR signaling pathway. Dhawan et al. reported CLDN2 overexpression to promote cell proliferation in an EGFR-dependent manner in colon tumor cells [79]. De Souza et al. found EGF to increase CLDN3 expression via ERK and PI3K signaling, hereby accelerating colorectal tumor cell migration in vitro [83]. Finally, EGFR signaling has been shown to mediate the formation of a CD81-CLDN1 complex, hereby enabling entry of HCV into hepatocytes [82,84] (Figure 2).

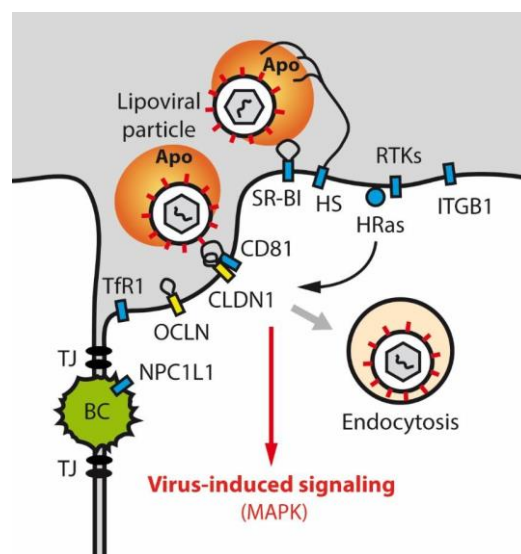


Figure 2. Hepatitis C virus (HCV) entry process and signaling. HCV lipoviral particle entry into hepatocytes requires a complex orchestration of entry factors that involves non-junctional TJ proteins CLDN1 and OCLN and virus-induced host signaling. Apo (Apolipoproteins), BC (Bile canaliculi), CD81 (Cluster of Differentiation 81), CLDN1 (Claudin-1), HRas (H-Ras Proto-Oncogene, GTPase), HS (Heparan sulfate), ITGB1 (Integrin Subunit Beta 1), MAPK (Mitogen-activated protein kinase), NPC1L1 (Niemann-Pick C1-like protein 1), OCLN (Occludin), RTK (Receptor tyrosine kinases), SR-BI (Scavenger Receptor Class B Member 1), TfR1 (Transferrin Receptor 1), TJ (Tight junction).

Several studies further associate CLDN proteins with proapoptotic signaling. Singh et al. indicated CLDN1 as a driver of resistance to anoikis in colon cancer cells, a form of self-programmed death in epithelial cells following detachment from the surrounding extracellular matrix. Mechanistically, CLDN1 was found to directly interact with steroid receptor coactivator (Src), a non-receptor tyrosine kinase that binds to extracellular matrix proteins and plays a pivotal role in cellular signal transduction, promoting survival, proliferation, and angiogenesis in its activated form. The authors postulated the presence of a multiprotein complex consisting of CLDN1, ZO1, and Src2 that regulates activation of Src downstream oncogenic signaling [85]. Another cellular self-defense mechanism, Fas-mediated apoptosis, has been shown to alter OCLN and ZO1 expression in lung epithelia [86].

Furthermore, several studies indicate TJ proteins to function as intracellular signaling platforms, involved in regulation of cell differentiation and growth. Indeed, Spadaro et al. reported conformational changes of ZO1 to induce recruitment of the transcription factor DbpA to TJs in epithelial (Eph4) cells, hereby affecting cell proliferation [87]. In lung cells, interaction between CLDN18 and the signaling molecule Yes-associated protein (YAP) has been shown to affect colony formation and progenitor cell proliferation [88].

Posttranslational modification of TJ transmembrane proteins by growth factor signaling pathways fine-tune the TJ barrier function. Mitogen-activated protein kinase (MAPK) [89] and PKA [90] have been shown to phosphorylate CLDN1 at TJs of cerebral and lung endothelial cells, hereby affecting TJ permeability. Phosphorylation of CLDN5, induced by cyclic-AMP potentiates the blood–brain barrier [90], while PKA mediated phosphorylation of CLDN16 affects Mg²⁺ transport in kidney cells [91]. Vascular endothelial growth factor (VEGF) signaling perturbs hepatocellular TJ integrity by targeting OCLN via the PKC pathway [92]. Moreover, several studies indicate that cytokines, which are upregulated during inflammation, affect TJ protein expression. For example, Ni and coworkers demonstrated that TNF- α -induced phosphorylation of OCLN in human cerebral endothelial cells via MAPK, modulates TJ permeability [93]. Moreover, OCLN phosphorylation regulates its interaction with ZO1 in kidney cancer cells [94]. Exposure of intestinal epithelial cells with TNF- α hampers TJ permeability via NF- κ B-dependent downregulation of ZO1 expression and altered junctional localization [95]. Loss of epithelial cell-to-cell junctions including TJs, represents a typical and early event in the evolution of epithelial-mesenchymal transition (EMT). EMT describes a process by which epithelial cells lose epithelial characteristics and acquire mesenchymal properties including the ability of migration and invasion [96,97].

4. Tight Junction Proteins in the Liver and the Blood-Biliary Barrier

Epithelial cells in the liver, namely hepatocytes and cholangiocytes, form the parenchymal structure of the organ and are characterized by a distinct cell polarity. TJs between neighboring hepatocytes separate the hepatocyte cell membrane into basal (sinusoidal), basolateral, and apical (bile canalicular) domains. By sealing the paracellular space, TJs and other adhesion complexes build the physiological BBIB, that segregates blood-containing basal hepatic sinusoids from apical bile canaliculi [9]. The BBIB hereby enables simultaneous execution of two major functions of the liver: the production and secretion of bile and the continuous metabolic exchange with the portal and systemic circulation allowing detoxification and excretion of proteins and coagulation factors. In particular, the apical bile canalicular domain of hepatocytes is characterized by numerous bile transporters and microvilli, that are required for bile secretion and absorption, while the basolateral sinusoidal domain is specialized in metabolic exchange with the blood [98]. CLDNs 1-3 and OCLN are expressed in TJs of hepatocytes and cholangiocytes [53,99,100]. While transmembrane TJ proteins on hepatocytes build the BBIB and shape bile canaliculi, TJs on cholangiocytes line the intrahepatic bile ducts [7]. The gallbladder on the other hand, shows physiologically strong expression of CLDNs 2, 3, 7, and OCLN. The hepatic sinusoidal endothelium strongly expresses CLDN5 [8].

In the normal liver and in contrast to other TJ proteins, tricellulin expression in hepatocytes and biliary epithelial cells strongly varies between individuals but is accentuated at tricellular contacts in colocalization with CLDN1 and CLDN4 [101]. In contrast to their weak expression on hepatocytes, the junctional adaptor proteins 7H6 and ZO1 are enriched in bile canaliculi [33,102].

KO studies in mice suggest a crucial role of CLDN2 and 3 for the BBIB. Thus, KO of the channel-forming CLDN2 lead to cholesterol gallstone disease due to a decrease in paracellular water transport [53]. CLDN3 KO in mice on the other hand, increases the paracellular phosphate ion transport of hepatic tight junctions, resulting in calcium phosphate core formation. Cholesterol overdose causes the cholesterol gallstone disease in these mice [99].

5. Tight Junction Proteins in Chronic Hepatobiliary Diseases

Chronic liver diseases constitute a global health problem, associated with high mortality due to its complications of liver cirrhosis and cancer [103]. Major causes comprise chronic hepatitis B virus (HBV) and HCV infection, alcoholic and metabolic liver disease such as non-alcoholic steatohepatitis.

Decompensated liver cirrhosis is the fourth most common cause of death in adults in central Europe [104,105]. Downregulated expression or impaired function of TJ proteins have frequently been associated with chronic liver diseases [12]. Loss of the BBIB, which is maintained by junctional adhesion complexes including TJs represents a common feature in mice models of chronic liver injury [106,107]. Takaki et al. observed loss of TJ protein expression, including CLDN3 and ZO1 following hepatectomy and reappearance several days after surgery. This suggests a functional role of TJ proteins in liver regeneration [108]. Moreover, alterations related to the expression of TJ proteins have been implicated in chronic HCV infection, biliary diseases, and liver cancer.

1.3. Tight Junction Proteins and HCV Infection

Chronic HCV infection represents a serious global health problem affecting more than 71 million people worldwide and potentially leads to liver fibrosis, cirrhosis, and hepatocellular carcinoma (HCC) [109–111]. Cell entry is a critical step in the HCV life cycle and involves a complex multi-step process consisting of viral attachment to the hepatocyte cell membrane and internalization [10,112]. HCV requires a complex orchestration of host dependency factors including among others CLDN1, OCLN, CD81, and SR-B1. Mechanistically, EGFR signaling promotes CLDN1-CD81 coreceptor association, which is a prerequisite for the internalization of the virus (Figure 2).

OCLN on the other hand, is believed to act downstream of the other cell entry factors CD81, CLDN1, and SRB1 during the HCV entry process [113,114]. OCLN interacts with HCV surface glycoprotein E2 via its extracellular loop 2 (ECL2) [115]. Of note, transgenic expression of human OCLN enables HCV infection of non-permissive species like mice [116–118]. However, the exact mechanism and localization of OCLN-HCV interaction is not fully understood. Considering its role for HCV cell entry, alterations in CLDN1 and OCLN expression levels and their functional consequences have been a focus of interest in the HCV field within the last years. Hepatic expression of CLDN1 and OCLN was found to be increased in liver biopsies of patients with chronic HCV infection [119]. In accordance, HCV liver graft infection is associated with OCLN and CLDN1 upregulation [120].

Anti-CLDN1 antibodies prevent and eliminate chronic HCV infection in cell-based and animal models without any detectable adverse effects and especially without disrupting TJ integrity or function [121–124]. The safety profile was further confirmed in human liver-chimeric mice and is most likely related to the molecular mechanism of action of CLDN1 monoclonal antibodies (mAbs) targeting the non-junctional expressed CLDN1 on hepatocytes without binding to CLDN1 localized in TJs [123–125]. Xiao et al. reported synergistic effects of anti-CLDN1 mAb with direct-acting antivirals as antiviral approaches for difficult-to-treat patients [126,127]. Confirming the functional role of OCLN in HCV entry, previous mechanistic monoclonal antibodies targeting ECL2 of OCLN were efficient in the prevention of infection both in cell culture and human liver chimeric mice without detectable side effects [114,128,129].

1.4. Tight Junction Proteins in Hepatocellular Carcinoma

Primary liver cancer is the sixth most frequent and second most deadly type of cancer in the world, with HCC being the most common histological subtype (75%–85%) [130]. Several members of the CLDN family have been reported to be perturbed during hepatocarcinogenesis. CLDN1, 4, 5, 7, and 10 are overexpressed in HCC [80,131–135]. Low levels of CLDN5 and high levels of CLDN7 were found to be independent prognostic factors [131]. Similarly, CLDN10 overexpression in HCC correlated with poor patients' outcome and tumor recurrence [133,136]. In contrast, CLDN14 downregulation in HCCs correlates with advanced tumor stage and poor overall survival [137] and CLDN3 expression is decreased in HCC [138]. Bouchagier and coworkers reported an overexpression of OCLN in HCC tumors compared to non-neoplastic liver tissues, which positively correlated with a favorable prognosis [131]. Orban et al. on the other hand, found decreased OCLN mRNA and protein levels in HCC [102]. These opposing findings may be due to different histological grading of the analyzed HCC samples and a potential dedifferentiation characterized by decreased OCLN levels. Decreased cell migration and proliferation following treatment of HCC cells with different compounds was accompanied by upregulation of OCLN expression, indicating mesenchymal-epithelial transition (MET) [139–141] and thus supporting the findings from Bouchagier et al. Expression of tricellulin is very heterogeneous in HCC tissues, but seems to be positively correlated with poor prognosis [101]. Downregulation of ZO1 on the other hand,

associates with poor prognosis in HCC patients undergoing hepatectomy [142]. Collectively, these studies suggest a pathogenic role of TJ proteins in hepatocarcinogenesis.

Studies on TJ protein expression in chronic liver diseases together with clinical correlations are summarized in Table 1.

Table 1. Perturbation of TJ proteins in chronic liver diseases.

Liver Disease	Tight Junction Protein	Perturbation	Potential Clinical Impact	References
HCV infection	CLDN1	<ul style="list-style-type: none"> • Overexpression in chronically HCV- infected liver tissue • Upregulation upon HCV liver graft infection 	<ul style="list-style-type: none"> • SNPs in <i>CLDN1</i> promoter confer susceptibility to HCV infection • Crucial HCV entry factor, antiviral target 	[143,144] [119,121,124], [120,122,123]
	OCLN	<ul style="list-style-type: none"> • Overexpression in chronically HCV- infected liver tissue • Upregulation upon HCV liver graft infection 	<ul style="list-style-type: none"> • Crucial HCV entry factor, antiviral target 	[114,119,120,128,129,145]
HCC	CLDN1	<ul style="list-style-type: none"> • Upregulated in the large majority of HCCs 	<ul style="list-style-type: none"> • Correlation of expression with patients' survival • Therapeutic target 	[80,131,132,134,135]
	CLDN3, CLDN14	<ul style="list-style-type: none"> • Downregulated/low expression in HCC 	<ul style="list-style-type: none"> • Unknown 	[137, 138]
	CLDN4, 5, 7 and 10	<ul style="list-style-type: none"> • Upregulated in HCC 	<ul style="list-style-type: none"> • Unknown 	[131] [133,136]
	OCLN	<ul style="list-style-type: none"> • Both downregulated and upregulated described in HCC 	<ul style="list-style-type: none"> • Positive correlation of expression with good prognosis 	[102] [131]
	Tricellulin	<ul style="list-style-type: none"> • Heterogeneous 	<ul style="list-style-type: none"> • Positive correlation with poor prognosis 	[101]
	ZO1	-	<ul style="list-style-type: none"> • Low expression correlates with HCC recurrence after hepatic resection 	[142]

6. Tight Junction Proteins in Biliary Diseases

Considering that TJ proteins on bile canaliculi are major contributors to the BBIB, TJ integrity has frequently been investigated in biliary diseases. Indeed, disruption of bile duct epithelial barrier plays a crucial role in the pathogenesis of chronic biliary diseases [7]. Studies in animal models of cholestatic disease hereby revealed secondary expressional and morphologic alterations of the tight junctional network upon cholestatic liver injury [146]. Perturbation of TJ proteins could further be found in human biliary liver diseases as primary sclerosing cholangitis (PSC) [147] and cholangiocellular carcinoma (CCA) [148]. Moreover, primary perturbation of TJ proteins caused by homozygous mutations have been identified to account for cholestatic syndromes, including progressive familial intrahepatic cholestasis (PFIC) type 4 [149,150] and the neonatal ichthyosis-sclerosing cholangitis (NISCH) syndrome [151].

1.5. Tight Junction Proteins in Primary Biliary Cirrhosis and Secondary Sclerosing Cholangitis

Primary biliary cirrhosis (PBC) and PSC represent etiologies of chronic liver disease that are characterized by cholestasis and an increased risk of developing liver cirrhosis and cancer. Mediated by immunological mechanisms of bile duct destruction, patients typically present with elevated serum levels of bile acids [152,153]. Ultrastructural studies of damaged bile ducts in PBC show electron-dense deposits in enlarged intercellular spaces, infiltrated by immune cells indicating perturbed barrier integrity [154]. TJ proteins are responsible for the main barrier formations maintaining the BBIB and preventing bile regurgitation from the biliary tract. In this context, downregulation of the TJ proteins 7H6 and ZO1 in bile ducts in PBC and in hepatocytes in PSC has been suggested to account for the increased paracellular permeability observed in chronic cholestatic liver diseases. Consequently, toxic bile acids can enter the periductal area and promote the infiltration of immune cells, eventually leading to inflammatory driven progression of bile injury. Interestingly, the expression of these TJ proteins is preserved in PBC patients treated with ursodeoxycholic acid [147].

1.6. Primary Perturbation of Tight Junction Proteins in Biliary Diseases: NISCH Syndrome and PFIC Type 4

NISCH syndrome represents an extremely rare autosomal-recessive ichthyosis syndrome caused by mutations in the *CLDN1* gene leading to its abolished expression in liver and skin (KO phenotype). First being described in 2002, only 12 cases have been reported [151,155–161]. The clinical manifestation is variable ranging from absent or regressive cholestasis to progressive liver disease with liver failure. The hepatic feature of this syndrome is characterized by neonatal sclerosing cholangitis with elevated serum bile acids and hepatomegaly. Additional non-hepatic manifestations can include dental anomalies, mild psychomotor delay, ichthyosis, and scalp hypotrichosis as well as scarring alopecia [56,151]. The human phenotype hereby strongly deviates from the one observed in *CLDN1*-KO mice that present severely wrinkled appearance of the skin and death within 24 h after birth [52], indicating differential function of CLDNs in mice and humans. Thus, increased paracellular permeability and secondary bile injury due to *CLDN1* absence in patients with NISCH syndrome [44] may be compensated by overexpression of other TJ protein members in the liver, explaining the variable phenotype [56]. Alternatively, mutations in other genes may be responsible for part of the observed phenotype. In conclusion, these findings demonstrate that *CLDN1* is not essential for life in humans and its absence has a variable clinical phenotype.

Loss of ZO2 on the other hand, is observed in PFIC type 4 [149,150]. Mechanistically, a mutation in the *ZO2* gene has been described to hamper proper localization of *CLDN1* in TJs of cholangiocytes in the liver despite normal protein levels, hereby increasing paracellular permeability to bile acids [149]. Clinical signs of cholestasis appear within the first year of life in patients homozygous for this mutation and are typically contrasted by normal levels of γ -glutamyl transferase activity (GGT). Progressing into secondary biliary cirrhosis, affected patients present with severe liver disease at a young age, often requiring liver transplantation [149]. A missense mutation in the first PDZ domain of ZO2, that binds to *CLDN1* in TJs has further been described in patients with familial hypercholestanemia, characterized by pruritus and fat malabsorption but without progressive liver disease [162].

1.7. Tight Junction Proteins in Cholangiocellular Carcinoma

Cholangiocellular carcinoma (CCA) represents the second most common primary liver cancer type. With an overall incidence rate of 2/100 000 it belongs to the rather rare cancer subtypes, though within the last few years, a dramatic increase in prevalence and mortality have been documented [163–165]. In contrast to the strong linkage of liver fibrosis/cirrhosis with HCC, most CCAs occur sporadically. However, known risk factors are PSC and HBV/HCV associated liver cirrhosis [166–169].

Several studies have reported evidence for potential functional implication of TJ proteins in CCA. CLDN3, 7, 8, and 10 expression were found to be decreased in intrahepatic CCAs compared to normal tissues. Significantly lower expression of CLDN1, 8, and 10 was also found in extrahepatic CCA, while CLDN1, 2, 3, 7, 8, and 10 are decreased in CCA of the gallbladder [148]. The most significant alteration of CLDN expression between CCA and adjacent liver tissue was found for CLDN10, as it was markedly decreased in all forms of bile duct cancers [148]. Moreover, in contrast to its restricted membrane localization in normal bile epithelia, intrahepatic CCA showed cytoplasmatic localization of CLDN10. Based on the negative staining in HCC and normal mature hepatocytes, CLDN4 and CLDN7 have been suggested as immunohistochemical markers of cholangiocellular differentiation in primary liver cancer [170,171]. In view of its preserved or even elevated expression in intra- and extrahepatic CCA, especially CLDN4 represents an attractive histological marker of CCA [148]. Interestingly, downregulation of CLDN4 by siRNA led to decreased migration and invasion of CCA cell lines [172]. CLDN18, that has been intensively studied in relation to gastric cancer is expressed in 40% of intrahepatic CCAs and is associated with lymph node metastasis and poor prognosis [173].

In intrahepatic CCA, tricellulin is decreased compared to adjacent tumor tissue, while patients with preserved tricellulin expression had significantly better clinical outcome and lower histological grading [101]. Downregulation of ZO1 and OCLN are associated with progression in biliary tract cancers [174].

All reported perturbations of TJ protein expressions in chronic hepatobiliary diseases are summarized in Table 2.

Table 2. Perturbation of TJ proteins in chronic biliary diseases.

Biliary Disease	TJ Protein	Perturbation	Potential Clinical implication	References
Primary biliary cirrhosis (PBC)	ZO1	<ul style="list-style-type: none"> Downregulation in bile ducts of patients with PBC 	<ul style="list-style-type: none"> Increased paracellular permeability Preservation of ZO-1 expression in patients treated with ursodeoxycholic acid 	[147]
Primary sclerosing cholangitis (PSC)	ZO1	<ul style="list-style-type: none"> Downregulation on hepatocytes of patients with PSC 	<ul style="list-style-type: none"> Increased paracellular permeability 	[147]
Progressive familial intrahepatic cholestasis (PFIC) type 4	CLDN1	<ul style="list-style-type: none"> Loss of expression 	<ul style="list-style-type: none"> Failed localization of CLDN1 to TJs on cholangiocytes despite normal CLDN1 protein levels Increased paracellular permeability Progressive chronic liver disease 	[149,150]
Familial hypercholelasmia	ZO2	<ul style="list-style-type: none"> Missense mutation in the first PDZ domain of ZO2 	<ul style="list-style-type: none"> Perturbed localization of CLDN1 in TJ Pruritus, fat malabsorption, elevated serum bileacid concentrations 	[162]
NISCH syndrome	CLDN1	<ul style="list-style-type: none"> Loss of CLDN1 expression due to homozygous CLDN1 mutation (functional KO) 	<ul style="list-style-type: none"> Variable clinical outcome from mild to absent disease to neonatal sclerosing cholangitis and ichthyosis (with functional impact of additional mutations unknown) Increased paracellular permeability 	[56,151]
CCA	CLDN1–3, 7, 8, and 10	<ul style="list-style-type: none"> Perturbed expression in intrahepatic, extrahepatic CCA, and/or CCA of the gallbladder 	<ul style="list-style-type: none"> CLDN7: suggested as histological marker to distinguish CCA from HCC 	[148,170]
	CLDN4	<ul style="list-style-type: none"> Perturbed expression in CCA 	<ul style="list-style-type: none"> Suggested as histological marker to distinguish CCA from HCC 	[148,170–172]
	CLDN18	<ul style="list-style-type: none"> Expressed in 40% of intrahepatic CCA 	<ul style="list-style-type: none"> Expression is associated with lymph node metastasis and poor prognosis 	[173]
	Tricellulin	<ul style="list-style-type: none"> Downregulated in CCA 	<ul style="list-style-type: none"> Positive correlation of expression with clinical outcome 	[101]
	OCLN	<ul style="list-style-type: none"> Downregulated in CCA 	<ul style="list-style-type: none"> Correlation of downregulated expression with tumor progression 	[148]
	ZO1	<ul style="list-style-type: none"> Downregulated in CCA 	<ul style="list-style-type: none"> Correlation of downregulated expression with tumor progression 	[148]

7. Summary

Tight junction proteins on hepatocytes and cholangiocytes play an important functional role as paracellular gatekeepers and represent the molecular basis of the BBIB, enabling exertion of two major function of the liver: production and secretion of bile as well as metabolic exchange and detoxification. Moreover, non-junctional TJ proteins at the basolateral membrane and in the nucleus exert key functions in cellular signaling, apoptosis, and migration. The TJ proteins CLDN1 and OCLN on the basolateral membrane of hepatocytes serve as entry factors for HCV—a major cause of liver disease and cancer worldwide. Highlighting its function as regulators of paracellular permeability enabling maintenance of the BBIB, secondary perturbation of TJ proteins has been described in biliary diseases, including PSC and PBC. In humans, the complete loss of distinct TJ proteins is not lethal, and the associated clinical phenotypes are highly variable as described for NISCH-syndrome or PFIC type 3. Finally, up- or downregulation of TJ protein expression in hepatobiliary cancer suggests a functional implication of TJ proteins in key cell regulatory signaling cascades potentially associated with carcinogenesis.

Author Contributions: N.R. and T.F.B. conceptualized the N.R. performed the literature review and wrote the manuscript. J.L., C.S. and T.F.B. revised the manuscript, J.L., A.S., H.E.S. and A.A.R.S. prepared original figures. All authors have read and agreed to the published version of the manuscript.

Funding: The authors acknowledge support by ARC, Paris and Institut Hospital-Universitaire, Strasbourg (TheraHCC, TheraHCC2.0 IHUARC IHU201301187 and IHUARC2019 IHU201901299 to T.F.B.), the European Union (ERC-AdG-2014-671231-HEPCIR, EU H2020-667273-HEPCAR and ERC-PoC-2016-PRELICAN, ERC-PoC-2018-HEPCAN to T.F.B.), Agence nationale de recherche sur le sida et les hépatites virales (ANRS, ECTZ35076) and the Foundation of the University of Strasbourg. This work was done under the framework of the LABEX ANR-10-LABX-0028_HEPSYS and Inserm Plan Cancer (Plan Cancer 2014-2019, Action 13.1, appel à projets 2018) and benefits from funding from the state managed by the French National Research Agency as part of the Investments for the future. N. R. is supported by a fellowship of the German Research Foundation (DFG) (RO 5983/1-1 to NR).

Conflicts of Interest: Inserm, the University of Strasbourg, the Strasbourg University Hospitals and the IHU have filed patent applications and patents on Claudin-1 specific monoclonal antibodies for prevention and treatment of HCV infection and hepatocellular carcinoma which have been licensed to Alentis Therapeutics, Basel, Switzerland.

Abbreviations

Akt	AKT serine/threonine kinase
Apo	Apolipoprotein
BBIB	Blood-biliary barrier
bTJ	Bicellular tight junction
CCA	Cholangiocellular carcinoma
CD81	Cluster of differentiation 81
CLDN	Claudin
c-myc	MYC proto-oncogene
ECL2	Extracellular loop 2
EGFR	Epidermal growth factor receptor
EMT	Epithelial-mesenchymal transition
EpCAM	Epithelial cell adhesion molecule
ESAM	Endothelial cell-selective adhesion molecule
FAK	Focal adhesion kinase
GGT	γ-glutamyl transferase
HBV	Hepatitis B virus
HCC	Hepatocellular carcinoma
HCV	Hepatitis C virus
HRas	HRas proto-oncogene, GTPase
HS	Heparan sulfate
IgSF	Immunoglobulin superfamily
ILDR	Immunoglobulin-like domain containing receptor
ITGB1	Integrin subunit beta 1
JAM	Junctional adhesion molecules
KO	Knockout
LSR	Lipolysis-stimulated lipoprotein receptor
mAbs	Monoclonal antibodies
MAGI	Membrane-associated guanylate kinase inverted

MAPK	Mitogen-activated protein kinase
MARVEL	MAL and related proteins for vesicle trafficking and membrane link
MET	Mesenchymal-epithelial transition
MMP	Matrix metalloproteinase
NISCH	Neonatal ichthyosis-sclerosing cholangitis
NPC1L1	Niemann-Pick C1-like protein 1
OCLN	Occludin
PBC	Primary biliary cirrhosis
PFIC	Progressive familial intrahepatic cholestasis
PKA	Protein kinase A
PKC	Protein kinase C
PP	Protein phosphatase
PSC	Primary sclerosing cholangitis
RTK	Receptor tyrosine kinase
SH3	Src homology 3 domain
SNPs	Single nucleotide polymorphisms
SR-BI	Scavenger receptor class B member 1
Src	Steroid receptor coactivator
TfR1	Transferrin receptor 1
TJ	Tight junction
tTJ	Tricellular tight junction
TNF- α	Tumor necrosis factor alpha
VEGF	Vascular endothelial growth factor
YAP	Yes-associated protein
ZO	Zonula occludens
ZONAB	ZO1-associated nucleic acid binding protein

References

1. Zihni, C.; Mills, C.; Matter, K.; Balda, M.S. Tight junctions: From simple barriers to multifunctional molecular gates. *Nat. Rev. Mol. Cell Biol.* **2016**, *17*, 564–580. [CrossRef] [PubMed]
2. Severson, E.A.; Parkos, C.A. Mechanisms of outside-in signaling at the tight junction by junctional adhesion molecule A. *Ann. N. Y. Acad. Sci.* **2009**, *1165*, 10–18. [CrossRef] [PubMed]
3. Singh, A.B.; Uppada, S.B.; Dhawan, P. Claudin proteins, outside-in signaling, and carcinogenesis. *Pflug. Arch.* **2017**, *469*, 69–75. [CrossRef] [PubMed]
4. Farkas, A.E.; Capaldo, C.T.; Nusrat, A. Regulation of epithelial proliferation by tight junction proteins. *Ann. N. Y. Acad. Sci.* **2012**, *1258*, 115–124. [CrossRef]
5. Kojima, T.; Sawada, N. Expression and function of claudins in hepatocytes. *Methods Mol. Biol.* **2011**, *762*, 233–244. [CrossRef]
6. Gonzalez-Mariscal, L.; Tapia, R.; Chamorro, D. Crosstalk of tight junction components with signaling pathways. *Biochim. Biophys. Acta* **2008**, *1778*, 729–756. [CrossRef]
7. Rao, R.K.; Samak, G. Bile duct epithelial tight junctions and barrier function. *Tissue Barriers* **2013**, *1*, e25718. [CrossRef]
8. Sakaguchi, T.; Suzuki, S.; Higashi, H.; Inaba, K.; Nakamura, S.; Baba, S.; Kato, T.; Konno, H. Expression of tight junction protein claudin-5 in tumor vessels and sinusoidal endothelium in patients with hepatocellular carcinoma. *J. Surg. Res.* **2008**, *147*, 123–131. [CrossRef]
9. Kojima, T.; Yamamoto, T.; Murata, M.; Chiba, H.; Kokai, Y.; Sawada, N. Regulation of the blood-biliary barrier: Interaction between gap and tight junctions in hepatocytes. *Med. Electron. Microsc.* **2003**, *36*, 157–164. [CrossRef]
10. Miao, Z.; Xie, Z.; Miao, J.; Ran, J.; Feng, Y.; Xia, X. Regulated Entry of Hepatitis C Virus into Hepatocytes. *Viruses* **2017**, *9*, 100. [CrossRef]
11. Hagen, S.J. Non-canonical functions of claudin proteins: Beyond the regulation of cell-cell adhesions. *Tissue Barriers* **2017**, *5*, e1327839. [CrossRef]
12. Zeisel, M.B.; Dhawan, P.; Baumert, T.F. Tight junction proteins in gastrointestinal and liver disease. *Gut* **2018**. [CrossRef]
13. Markov, A.G.; Aschenbach, J.R.; Amasheh, S. The epithelial barrier and beyond: Claudins as amplifiers of physiological organ functions. *IUBMB Life* **2017**, *69*, 290–296. [CrossRef]
14. Baas, A.F.; Kuipers, J.; van der Wel, N.N.; Batlle, E.; Koerten, H.K.; Peters, P.J.; Clevers, H.C. Complete polarization of single intestinal epithelial cells upon activation of LKB1 by STRAD. *Cell* **2004**, *116*, 457–466. [CrossRef]

15. Umeda, K.; Matsui, T.; Nakayama, M.; Furuse, K.; Sasaki, H.; Furuse, M.; Tsukita, S. Establishment and characterization of cultured epithelial cells lacking expression of ZO-1. *J. Biol. Chem.* **2004**, *279*, 44785–44794. [CrossRef]
16. Ebnet, K.; Suzuki, A.; Ohno, S.; Vestweber, D. Junctional adhesion molecules (JAMs): More molecules with dual functions? *J. Cell Sci.* **2004**, *117*, 19–29. [CrossRef]
17. Ebnet, K. Junctional Adhesion Molecules (JAMs): Cell Adhesion Receptors with Pleiotropic Functions in Cell Physiology and Development. *Physiol. Rev.* **2017**, *97*, 1529–1554. [CrossRef]
18. Ikenouchi, J.; Furuse, M.; Furuse, K.; Sasaki, H.; Tsukita, S.; Tsukita, S. Tricellulin constitutes a novel barrier at tricellular contacts of epithelial cells. *J. Cell Biol.* **2005**, *171*, 939–945. [CrossRef]
19. Masuda, S.; Oda, Y.; Sasaki, H.; Ikenouchi, J.; Higashi, T.; Akashi, M.; Nishi, E.; Furuse, M. LSR defines cell corners for tricellular tight junction formation in epithelial cells. *J. Cell Sci.* **2011**, *124*, 548–555. [CrossRef]
20. Higashi, T.; Tokuda, S.; Kitajiri, S.; Masuda, S.; Nakamura, H.; Oda, Y.; Furuse, M. Analysis of the ‘angulin’ proteins LSR, ILDR1 and ILDR2—tricellulin recruitment, epithelial barrier function and implication in deafness pathogenesis. *J. Cell Sci.* **2013**, *126*, 966–977. [CrossRef]
21. Furuse, M.; Hirase, T.; Itoh, M.; Nagafuchi, A.; Yonemura, S.; Tsukita, S.; Tsukita, S. Occludin: A novel integral membrane protein localizing at tight junctions. *J. Cell Biol.* **1993**, *123*, 1777–1788. [CrossRef] [PubMed]
22. Cummins, P.M. Occludin: One protein, many forms. *Mol. Cell. Biol.* **2012**, *32*, 242–250. [CrossRef] [PubMed]
23. Mineta, K.; Yamamoto, Y.; Yamazaki, Y.; Tanaka, H.; Tada, Y.; Saito, K.; Tamura, A.; Igarashi, M.; Endo, T.; Takeuchi, K.; et al. Predicted expansion of the claudin multigene family. *FEBS Lett.* **2011**, *585*, 606–612. [CrossRef] [PubMed]
24. Gunzel, D.; Fromm, M. Claudins and other tight junction proteins. *Compr. Physiol.* **2012**, *2*, 1819–1852. [CrossRef]
25. Tamura, A.; Tsukita, S. Paracellular barrier and channel functions of TJ claudins in organizing biological systems: Advances in the field of barrierology revealed in knockout mice. *Semin. Cell Dev. Biol.* **2014**, *36*, 177–185. [CrossRef]
26. Tanaka, H.; Tamura, A.; Suzuki, K.; Tsukita, S. Site-specific distribution of claudin-based paracellular channels with roles in biological fluid flow and metabolism. *Ann. N. Y. Acad. Sci.* **2017**, *1405*, 44–52. [CrossRef]
27. Chiba, H.; Osanai, M.; Murata, M.; Kojima, T.; Sawada, N. Transmembrane proteins of tight junctions. *Biochim. Biophys. Acta* **2008**, *1778*, 588–600. [CrossRef]
28. Bauer, H.; Zweimüller-Mayer, J.; Steinbacher, P.; Lametschwandtner, A.; Bauer, H.C. The dual role of zonula occludens (ZO) proteins. *J. Biomed. Biotechnol.* **2010**, *2010*, 402593. [CrossRef]
29. Tsukita, S.; Furuse, M.; Itoh, M. Molecular architecture of tight junctions: Occludin and ZO-1. *Soc. Gen. Physiol. Ser.* **1997**, *52*, 69–76.
30. Willott, E.; Balda, M.S.; Fanning, A.S.; Jameson, B.; Van Itallie, C.; Anderson, J.M. The tight junction protein ZO-1 is homologous to the Drosophila discs-large tumor suppressor protein of septate junctions. *Proc. Natl. Acad. Sci. USA* **1993**, *90*, 7834–7838. [CrossRef]
31. Guillemot, L.; Paschoud, S.; Pulimeno, P.; Foglia, A.; Citi, S. The cytoplasmic plaque of tight junctions: A scaffolding and signalling center. *Biochim. Biophys. Acta* **2008**, *1778*, 601–613. [CrossRef] [PubMed]
32. Li, Y.; Fanning, A.S.; Anderson, J.M.; Lavie, A. Structure of the conserved cytoplasmic C-terminal domain of occludin: Identification of the ZO-1 binding surface. *J. Mol. Biol.* **2005**, *352*, 151–164. [CrossRef] [PubMed]
33. Zhong, Y.; Saitoh, T.; Minase, T.; Sawada, N.; Enomoto, K.; Mori, M. Monoclonal antibody 7H6 reacts with a novel tight junction-associated protein distinct from ZO-1, cingulin and ZO-2. *J. Cell Biol.* **1993**, *120*, 477–483. [CrossRef] [PubMed]
34. Citi, S.; Sabanay, H.; Jakes, R.; Geiger, B.; Kendrick-Jones, J. Cingulin, a new peripheral component of tight junctions. *Nature* **1988**, *333*, 272–276. [CrossRef] [PubMed]
35. Tsukita, S.; Furuse, M.; Itoh, M. Multifunctional strands in tight junctions. *Nat. Rev. Mol. Cell Biol.* **2001**, *2*, 285–293. [CrossRef]
36. Tsukita, S.; Tanaka, H.; Tamura, A. The Claudins: From Tight Junctions to Biological Systems. *Trends Biochem. Sci.* **2019**, *44*, 141–152. [CrossRef] [PubMed]
37. Shen, L.; Weber, C.R.; Turner, J.R. The tight junction protein complex undergoes rapid and continuous molecular remodeling at steady state. *J. Cell Biol.* **2008**, *181*, 683–695. [CrossRef]
38. Chalmers, A.D.; Whitley, P. Continuous endocytic recycling of tight junction proteins: How and why? *Essays Biochem.* **2012**, *53*, 41–54. [CrossRef]
39. Ivanov, A.I.; Nusrat, A.; Parkos, C.A. Endocytosis of the apical junctional complex: Mechanisms and possible roles in regulation of epithelial barriers. *Bioessays* **2005**, *27*, 356–365. [CrossRef]
40. Ivanov, A.I.; Nusrat, A.; Parkos, C.A. Endocytosis of epithelial apical junctional proteins by a clathrin-mediated pathway into a unique storage compartment. *Mol. Biol. Cell* **2004**, *15*, 176–188. [CrossRef]
41. Lu, R.; Stewart, L.; Wilson, J.M. Scaffolding protein GOPC regulates tight junction structure. *Cell Tissue Res.* **2015**, *360*, 321–332. [CrossRef] [PubMed]
42. Lu, R.; Johnson, D.L.; Stewart, L.; Waite, K.; Elliott, D.; Wilson, J.M. Rab14 regulation of claudin-2 trafficking modulates epithelial permeability and lumen morphogenesis. *Mol. Biol. Cell* **2014**, *25*, 1744–1754. [CrossRef]

43. Gunzel, D.; Yu, A.S. Claudins and the modulation of tight junction permeability. *Physiol. Rev.* **2013**, *93*, 525–569. [CrossRef]
44. Grosse, B.; Cassio, D.; Yousef, N.; Bernardo, C.; Jacquemin, E.; Gonzales, E. Claudin-1 involved in neonatalichthyosis sclerosing cholangitis syndrome regulates hepatic paracellular permeability. *Hepatology* **2012**, *55*, 1249–1259. [CrossRef] [PubMed]
45. Van Itallie, C.M.; Fanning, A.S.; Holmes, J.; Anderson, J.M. Occludin is required for cytokine-induced regulation of tight junction barriers. *J. Cell Sci.* **2010**, *123*, 2844–2852. [CrossRef] [PubMed]
46. Laukoetter, M.G.; Nava, P.; Lee, W.Y.; Severson, E.A.; Capaldo, C.T.; Babbitt, B.A.; Williams, I.R.; Koval, M.; Peatman, E.; Campbell, J.A.; et al. JAM-A regulates permeability and inflammation in the intestine in vivo. *J. Exp. Med.* **2007**, *204*, 3067–3076. [CrossRef]
47. Vetrano, S.; Rescigno, M.; Cera, M.R.; Correale, C.; Rumio, C.; Doni, A.; Fantini, M.; Sturm, A.; Borroni, E.; Repici, A.; et al. Unique role of junctional adhesion molecule-a in maintaining mucosal homeostasis in inflammatory bowel disease. *Gastroenterology* **2008**, *135*, 173–184. [CrossRef] [PubMed]
48. Umeda, K.; Ikenouchi, J.; Katahira-Tayama, S.; Furuse, K.; Sasaki, H.; Nakayama, M.; Matsui, T.; Tsukita, S.; Furuse, M.; Tsukita, S. ZO-1 and ZO-2 independently determine where claudins are polymerized in tight-junction strand formation. *Cell* **2006**, *126*, 741–754. [CrossRef] [PubMed]
49. Satoh, H.; Zhong, Y.; Isomura, H.; Saitoh, M.; Enomoto, K.; Sawada, N.; Mori, M. Localization of 7H6 tightjunction-associated antigen along the cell border of vascular endothelial cells correlates with paracellular barrier function against ions, large molecules, and cancer cells. *Exp. Cell Res.* **1996**, *222*, 269–274. [CrossRef]
50. Zhong, Y.; Enomoto, K.; Isomura, H.; Sawada, N.; Minase, T.; Oyamada, M.; Konishi, Y.; Mori, M. Localization of the 7H6 antigen at tight junctions correlates with the paracellular barrier function of MDCK cells. *Exp. Cell Res.* **1994**, *214*, 614–620. [CrossRef]
51. Kage, H.; Flodby, P.; Gao, D.; Kim, Y.H.; Marconett, C.N.; DeMaio, L.; Kim, K.J.; Crandall, E.D.; Borok, Z. Claudin 4 knockout mice: Normal physiological phenotype with increased susceptibility to lung injury. *Am. J. Physiol. Lung Cell. Mol. Physiol.* **2014**, *307*, L524–L536. [CrossRef] [PubMed]
52. Furuse, M.; Hata, M.; Furuse, K.; Yoshida, Y.; Haratake, A.; Sugitani, Y.; Noda, T.; Kubo, A.; Tsukita, S. Claudin-based tight junctions are crucial for the mammalian epidermal barrier: A lesson from claudin-1-deficient mice. *J. Cell Biol.* **2002**, *156*, 1099–1111. [CrossRef] [PubMed]
53. Matsumoto, K.; Imasato, M.; Yamazaki, Y.; Tanaka, H.; Watanabe, M.; Eguchi, H.; Nagano, H.; Hikita, H.; Tatsumi, T.; Takehara, T.; et al. Claudin 2 deficiency reduces bile flow and increases susceptibility to cholesterol gallstone disease in mice. *Gastroenterology* **2014**, *147*, 1134–1145. [CrossRef] [PubMed]
54. Katsuno, T.; Umeda, K.; Matsui, T.; Hata, M.; Tamura, A.; Itoh, M.; Takeuchi, K.; Fujimori, T.; Nabeshima, Y.; Noda, T.; et al. Deficiency of zonula occludens-1 causes embryonic lethal phenotype associated with defected yolk sac angiogenesis and apoptosis of embryonic cells. *Mol. Biol. Cell* **2008**, *19*, 2465–2475. [CrossRef]
55. Saitou, M.; Furuse, M.; Sasaki, H.; Schulzke, J.D.; Fromm, M.; Takano, H.; Noda, T.; Tsukita, S. Complex phenotype of mice lacking occludin, a component of tight junction strands. *Mol. Biol. Cell* **2000**, *11*, 4131–4142. [CrossRef]
56. Hadj-Rabia, S.; Baala, L.; Vabres, P.; Hamel-Teillac, D.; Jacquemin, E.; Fabre, M.; Lyonnet, S.; De Prost, Y.; Munnich, A.; Hadchouel, M.; et al. Claudin-1 gene mutations in neonatal sclerosing cholangitis associated with ichthyosis: A tight junction disease. *Gastroenterology* **2004**, *127*, 1386–1390. [CrossRef]
57. Izraely, S.; Sagi-Assif, O.; Klein, A.; Meshel, T.; Ben-Menachem, S.; Zaritsky, A.; Ehrlich, M.; Prieto, V.G.; Bar-Eli, M.; Pirker, C.; et al. The metastatic microenvironment: Claudin-1 suppresses the malignant phenotype of melanoma brain metastasis. *Int. J. Cancer* **2015**, *136*, 1296–1307. [CrossRef]
58. Ding, L.; Lu, Z.; Foreman, O.; Tatum, R.; Lu, Q.; Renegar, R.; Cao, J.; Chen, Y.H. Inflammation and disruption of the mucosal architecture in claudin-7-deficient mice. *Gastroenterology* **2012**, *142*, 305–315. [CrossRef]
59. Lu, Z.; Kim, D.H.; Fan, J.; Lu, Q.; Verbanac, K.; Ding, L.; Renegar, R.; Chen, Y.H. A non-tight junction function of claudin-7-Interaction with integrin signaling in suppressing lung cancer cell proliferation and detachment. *Mol. Cancer* **2015**, *14*, 120. [CrossRef]
60. Ding, L.; Wang, L.; Sui, L.; Zhao, H.; Xu, X.; Li, T.; Wang, X.; Li, W.; Zhou, P.; Kong, L. Claudin-7 indirectly regulates the integrin/FAK signaling pathway in human colon cancer tissue. *J. Hum. Genet.* **2016**, *61*, 711–720. [CrossRef]
61. Tabaries, S.; Dong, Z.; Annis, M.G.; Omeroglu, A.; Pepin, F.; Ouellet, V.; Russo, C.; Hassanain, M.; Metrakos, P.; Diaz, Z.; et al. Claudin-2 is selectively enriched in and promotes the formation of breast cancer liver metastases through engagement of integrin complexes. *Oncogene* **2011**, *30*, 1318–1328. [CrossRef] [PubMed]
62. Wu, C.J.; Mannan, P.; Lu, M.; Udey, M.C. Epithelial cell adhesion molecule (EpCAM) regulates claudin dynamics and tight junctions. *J. Biol. Chem.* **2013**, *288*, 12253–12268. [CrossRef] [PubMed]
63. Nubel, T.; Preobraschenski, J.; Tuncay, H.; Weiss, T.; Kuhn, S.; Ladwein, M.; Langbein, L.; Zoller, M. Claudin-7 regulates EpCAM-mediated functions in tumor progression. *Mol. Cancer Res* **2009**, *7*, 285–299. [CrossRef] [PubMed]
64. Agarwal, R.; D’Souza, T.; Morin, P.J. Claudin-3 and claudin-4 expression in ovarian epithelial cells enhances invasion and is associated with increased matrix metalloproteinase-2 activity. *Cancer Res.* **2005**, *65*, 7378–7385. [CrossRef]

65. Leotlela, P.D.; Wade, M.S.; Duray, P.H.; Rhode, M.J.; Brown, H.F.; Rosenthal, D.T.; Dissanayake, S.K.; Earley, R.; Indig, F.E.; Nickoloff, B.J.; et al. Claudin-1 overexpression in melanoma is regulated by PKC and contributes to melanoma cell motility. *Oncogene* **2007**, *26*, 3846–3856. [CrossRef]
66. Yoon, C.H.; Kim, M.J.; Park, M.J.; Park, I.C.; Hwang, S.G.; An, S.; Choi, Y.H.; Yoon, G.; Lee, S.J. Claudin-1 acts through c-Abl-protein kinase Cdelta (PKCdelta) signaling and has a causal role in the acquisition of invasive capacity in human liver cells. *J. Biol. Chem.* **2010**, *285*, 226–233. [CrossRef]
67. Conlon, G.A.; Murray, G.I. Recent advances in understanding the roles of matrix metalloproteinases in tumour invasion and metastasis. *J. Pathol.* **2019**, *247*, 629–640. [CrossRef]
68. Torres-Martinez, A.C.; Gallardo-Vera, J.F.; Lara-Holguin, A.N.; Montano, L.F.; Rendon-Huerta, E.P. Claudin-6 enhances cell invasiveness through claudin-1 in AGS human adenocarcinoma gastric cancer cells. *Exp. Cell Res.* **2017**, *350*, 226–235. [CrossRef]
69. Gottardi, C.J.; Arpin, M.; Fanning, A.S.; Louvard, D. The junction-associated protein, zonula occludens-1, localizes to the nucleus before the maturation and during the remodeling of cell-cell contacts. *Proc. Natl. Acad. Sci. USA* **1996**, *93*, 10779–10784. [CrossRef]
70. Islas, S.; Vega, J.; Ponce, L.; Gonzalez-Mariscal, L. Nuclear localization of the tight junction protein ZO-2 in epithelial cells. *Exp. Cell Res.* **2002**, *274*, 138–148. [CrossRef]
71. Dhawan, P.; Singh, A.B.; Deane, N.G.; No, Y.; Shiou, S.R.; Schmidt, C.; Neff, J.; Washington, M.K.; Beauchamp, R.D. Claudin-1 regulates cellular transformation and metastatic behavior in colon cancer. *J. Clin. Investig.* **2005**, *115*, 1765–1776. [CrossRef] [PubMed]
72. Ikari, A.; Watanabe, R.; Sato, T.; Taga, S.; Shimobaba, S.; Yamaguchi, M.; Yamazaki, Y.; Endo, S.; Matsunaga, T.; Sugatani, J. Nuclear distribution of claudin-2 increases cell proliferation in human lung adenocarcinoma cells. *Biochim. Biophys. Acta* **2014**, *1843*, 2079–2088. [CrossRef] [PubMed]
73. Todd, M.C.; Petty, H.M.; King, J.M.; Piana Marshall, B.N.; Sheller, R.A.; Cuevas, M.E. Overexpression and delocalization of claudin-3 protein in MCF-7 and MDA-MB-415 breast cancer cell lines. *Oncol. Lett.* **2015**, *10*, 156–162. [CrossRef] [PubMed]
74. Cuevas, M.E.; Gaska, J.M.; Gist, A.C.; King, J.M.; Sheller, R.A.; Todd, M.C. Estrogen-dependent expression and subcellular localization of the tight junction protein claudin-4 in HEC-1A endometrial cancer cells. *Int. J. Oncol.* **2015**, *47*, 650–656. [CrossRef] [PubMed]
75. French, A.D.; Fiori, J.L.; Camilli, T.C.; Leotlela, P.D.; O’Connell, M.P.; Frank, B.P.; Subaran, S.; Indig, F.E.; Taub, D.D.; Weeraratna, A.T. PKC and PKA phosphorylation affect the subcellular localization of claudin-1 in melanoma cells. *Int. J. Med. Sci.* **2009**, *6*, 93–101. [CrossRef] [PubMed]
76. Sourisseau, T.; Georgiadis, A.; Tsapara, A.; Ali, R.R.; Pestell, R.; Matter, K.; Balda, M.S. Regulation of PCNA and cyclin D1 expression and epithelial morphogenesis by the ZO-1-regulated transcription factor ZONAB/DbpA. *Mol. Cell. Biol.* **2006**, *26*, 2387–2398. [CrossRef]
77. Huerta, M.; Munoz, R.; Tapia, R.; Soto-Reyes, E.; Ramirez, L.; Recillas-Targa, F.; Gonzalez-Mariscal, L.; Lopez-Bayghen, E. Cyclin D1 is transcriptionally down-regulated by ZO-2 via an E box and the transcription factor c-Myc. *Mol. Biol. Cell* **2007**, *18*, 4826–4836. [CrossRef]
78. Singh, A.B.; Sharma, A.; Smith, J.J.; Krishnan, M.; Chen, X.; Eschrich, S.; Washington, M.K.; Yeatman, T.J.; Beauchamp, R.D.; Dhawan, P. Claudin-1 up-regulates the repressor ZEB-1 to inhibit E-cadherin expression in colon cancer cells. *Gastroenterology* **2011**, *141*, 2140–2153. [CrossRef]
79. Dhawan, P.; Ahmad, R.; Chaturvedi, R.; Smith, J.J.; Midha, R.; Mittal, M.K.; Krishnan, M.; Chen, X.; Eschrich, S.; Yeatman, T.J.; et al. Claudin-2 expression increases tumorigenicity of colon cancer cells: Role of epidermal growth factor receptor activation. *Oncogene* **2011**, *30*, 3234–3247. [CrossRef]
80. Suh, Y.; Yoon, C.H.; Kim, R.K.; Lim, E.J.; Oh, Y.S.; Hwang, S.G.; An, S.; Yoon, G.; Gye, M.C.; Yi, J.M.; et al. Claudin-1 induces epithelial-mesenchymal transition through activation of the c-Abl-ERK signaling pathway in human liver cells. *Oncogene* **2013**, *32*, 4873–4882. [CrossRef]
81. Fredriksson, K.; Van Itallie, C.M.; Aponte, A.; Gucsek, M.; Tietgens, A.J.; Anderson, J.M. Proteomic analysis of proteins surrounding occludin and claudin-4 reveals their proximity to signaling and trafficking networks. *PLoS ONE* **2015**, *10*, e0117074. [CrossRef] [PubMed]
82. Zona, L.; Lupberger, J.; Sidahmed-Adrar, N.; Thumann, C.; Harris, H.J.; Barnes, A.; Florentin, J.; Tawar, R.G.; Xiao, F.; Turek, M.; et al. HRas signal transduction promotes hepatitis C virus cell entry by triggering assembly of the host tetraspanin receptor complex. *Cell Host Microbe* **2013**, *13*, 302–313. [CrossRef] [PubMed]
83. De Souza, W.F.; Fortunato-Miranda, N.; Robbs, B.K.; de Araujo, W.M.; de-Freitas-Junior, J.C.; Bastos, L.G.; Viola, J.P.; Morgado-Diaz, J.A. Claudin-3 overexpression increases the malignant potential of colorectal cancer cells: Roles of ERK1/2 and PI3K-Akt as modulators of EGFR signaling. *PLoS ONE* **2013**, *8*, e74994. [CrossRef]
84. Lupberger, J.; Zeisel, M.B.; Xiao, F.; Thumann, C.; Fofana, I.; Zona, L.; Davis, C.; Mee, C.J.; Turek, M.; Gorke, S.; et al. EGFR and EphA2 are host factors for hepatitis C virus entry and possible targets for antiviral therapy. *Nat. Med.* **2011**, *17*, 589–595. [CrossRef] [PubMed]

85. Singh, A.B.; Sharma, A.; Dhawan, P. Claudin-1 expression confers resistance to anoikis in colon cancer cells in a Src-dependent manner. *Carcinogenesis* **2012**, *33*, 2538–2547. [CrossRef] [PubMed]
86. Herrero, R.; Prados, L.; Ferruelo, A.; Puig, F.; Pandolfi, R.; Guillaumat-Prats, R.; Moreno, L.; Matute-Bello, G.; Artigas, A.; Esteban, A.; et al. Fas activation alters tight junction proteins in acute lung injury. *Thorax* **2019**, *74*, 69–82. [CrossRef] [PubMed]
87. Spadaro, D.; Le, S.; Laroche, T.; Mean, I.; Jond, L.; Yan, J.; Citi, S. Tension-Dependent Stretching Activates ZO-1 to Control the Junctional Localization of Its Interactors. *Curr. Biol.* **2017**, *27*, 3783–3795. [CrossRef]
88. Zhou, B.; Flodby, P.; Luo, J.; Castillo, D.R.; Liu, Y.; Yu, F.X.; McConnell, A.; Varghese, B.; Li, G.; Chimgé, N.O.; et al. Claudin-18-mediated YAP activity regulates lung stem and progenitor cell homeostasis and tumorigenesis. *J. Clin. Invest.* **2018**, *128*, 970–984. [CrossRef]
89. Fujibe, M.; Chiba, H.; Kojima, T.; Soma, T.; Wada, T.; Yamashita, T.; Sawada, N. Thr203 of claudin-1, a putative phosphorylation site for MAP kinase, is required to promote the barrier function of tight junctions. *Exp. Cell Res.* **2004**, *295*, 36–47. [CrossRef]
90. Ishizaki, T.; Chiba, H.; Kojima, T.; Fujibe, M.; Soma, T.; Miyajima, H.; Nagasawa, K.; Wada, I.; Sawada, N. Cyclic AMP induces phosphorylation of claudin-5 immunoprecipitates and expression of claudin-5 gene in blood-brain-barrier endothelial cells via protein kinase A-dependent and -independent pathways. *Exp. Cell Res.* **2003**, *290*, 275–288. [CrossRef]
91. Ikari, A.; Ito, M.; Okude, C.; Sawada, H.; Harada, H.; Degawa, M.; Sakai, H.; Takahashi, T.; Sugatani, J.; Miwa, M. Claudin-16 is directly phosphorylated by protein kinase A independently of a vasodilator-stimulated phosphoprotein-mediated pathway. *J. Cell. Physiol.* **2008**, *214*, 221–229. [CrossRef]
92. Schmitt, M.; Horbach, A.; Kubitz, R.; Frilling, A.; Haussinger, D. Disruption of hepatocellular tight junctions by vascular endothelial growth factor (VEGF): A novel mechanism for tumor invasion. *J. Hepatol.* **2004**, *41*, 274–283. [CrossRef] [PubMed]
93. Ni, Y.; Teng, T.; Li, R.; Simonyi, A.; Sun, G.Y.; Lee, J.C. TNF α alters occludin and cerebral endothelial permeability: Role of p38MAPK. *PLoS ONE* **2017**, *12*, e0170346. [CrossRef] [PubMed]
94. Elias, B.C.; Suzuki, T.; Seth, A.; Giorgianni, F.; Kale, G.; Shen, L.; Turner, J.R.; Naren, A.; Desiderio, D.M.; Rao, R. Phosphorylation of Tyr-398 and Tyr-402 in occludin prevents its interaction with ZO-1 and destabilizes its assembly at the tight junctions. *J. Biol. Chem.* **2009**, *284*, 1559–1569. [CrossRef] [PubMed]
95. Ma, T.Y.; Iwamoto, G.K.; Hoa, N.T.; Akotia, V.; Pedram, A.; Boivin, M.A.; Said, H.M. TNF- α -induced increase in intestinal epithelial tight junction permeability requires NF- κ B activation. *Am. J. Physiol. Gastrointest. Liver Physiol.* **2004**, *286*, G367–G376. [CrossRef]
96. Kalluri, R. EMT: When epithelial cells decide to become mesenchymal-like cells. *J. Clin. Invest.* **2009**, *119*, 1417–1419. [CrossRef]
97. Lamouille, S.; Xu, J.; Derynck, R. Molecular mechanisms of epithelial-mesenchymal transition. *Nat. Rev. Mol. Cell Biol.* **2014**, *15*, 178–196. [CrossRef]
98. Gissen, P.; Arias, I.M. Structural and functional hepatocyte polarity and liver disease. *J. Hepatol.* **2015**, *63*, 1023–1037. [CrossRef]
99. Tanaka, H.; Imasato, M.; Yamazaki, Y.; Matsumoto, K.; Kunimoto, K.; Delpierre, J.; Meyer, K.; Zerial, M.; Kitamura, N.; Watanabe, M.; et al. Claudin-3 regulates bile canalicular paracellular barrier and cholesterol gallstone core formation in mice. *J. Hepatol.* **2018**, *69*, 1308–1316. [CrossRef]
100. Rahner, C.; Mitic, L.L.; Anderson, J.M. Heterogeneity in expression and subcellular localization of claudins 2, 3, 4, and 5 in the rat liver, pancreas, and gut. *Gastroenterology* **2001**, *120*, 411–422. [CrossRef]
101. Somoracz, A.; Korompay, A.; Torzsok, P.; Patonai, A.; Erdelyi-Belle, B.; Lotz, G.; Schaff, Z.; Kiss, A. Tricellulin expression and its prognostic significance in primary liver carcinomas. *Pathol. Oncol. Res.* **2014**, *20*, 755–764. [CrossRef] [PubMed]
102. Orban, E.; Szabo, E.; Lotz, G.; Kupcsulik, P.; Paska, C.; Schaff, Z.; Kiss, A. Different expression of occludin and ZO-1 in primary and metastatic liver tumors. *Pathol. Oncol. Res.* **2008**, *14*, 299–306. [CrossRef] [PubMed]
103. Byass, P. The global burden of liver disease: A challenge for methods and for public health. *BMC Med.* **2014**, *12*, 159. [CrossRef] [PubMed]
104. D’Amico, G.; Morabito, A.; D’Amico, M.; Pasta, L.; Malizia, G.; Rebora, P.; Valsecchi, M.G. Clinical states of cirrhosis and competing risks. *J. Hepatol.* **2018**, *68*, 563–576. [CrossRef]
105. Marcellin, P.; Kutala, B.K. Liver diseases: A major, neglected global public health problem requiring urgent actions and large-scale screening. *Liver Int.* **2018**, *38*, 2–6. [CrossRef]
106. Pradhan-Sundd, T.; Zhou, L.; Vats, R.; Jiang, A.; Molina, L.; Singh, S.; Poddar, M.; Russell, J.; Stolz, D.B.; Oertel, M.; et al. Dual catenin loss in murine liver causes tight junctional deregulation and progressive intrahepatic cholestasis. *Hepatology* **2018**, *67*, 2320–2337. [CrossRef]
107. Pradhan-Sundd, T.; Vats, R.; Russell, J.O.; Singh, S.; Michael, A.A.; Molina, L.; Kakar, S.; Cornuet, P.; Poddar, M.; Watkins, S.C.; et al. Dysregulated Bile Transporters and Impaired Tight Junctions During Chronic Liver Injury in Mice. *Gastroenterology* **2018**, *155*, 1218–1232-e24. [CrossRef]

108. Takaki, Y.; Hirai, S.; Manabe, N.; Izumi, Y.; Hirose, T.; Nakaya, M.; Suzuki, A.; Mizuno, K.; Akimoto, K.; Tsukita, S.; et al. Dynamic changes in protein components of the tight junction during liver regeneration. *Cell Tissue Res.* **2001**, *305*, 399–409. [CrossRef]
109. Liang, T.J.; Rehermann, B.; Seeff, L.B.; Hoofnagle, J.H. Pathogenesis, natural history, treatment, and prevention of hepatitis C. *Ann. Intern. Med.* **2000**, *132*, 296–305. [CrossRef]
110. Thrift, A.P.; El-Serag, H.B.; Kanwal, F. Global epidemiology and burden of HCV infection and HCV-related disease. *Nat. Rev. Gastroenterol. Hepatol.* **2017**, *14*, 122–132. [CrossRef]
111. WHO. *Global Hepatitis Report*; WHO: Geneva, Switzerland, 2017.
112. Douam, F.; Lavillette, D.; Cosset, F.L. The mechanism of HCV entry into host cells. *Prog. Mol. Biol. Transl. Sci.* **2015**, *129*, 63–107. [CrossRef] [PubMed]
113. Sourisseau, M.; Michta, M.L.; Zony, C.; Israelow, B.; Hopcraft, S.E.; Narbus, C.M.; Parra Martin, A.; Evans, M.J. Temporal analysis of hepatitis C virus cell entry with occludin directed blocking antibodies. *PLoS Pathog.* **2013**, *9*, e1003244. [CrossRef] [PubMed]
114. Shimizu, Y.; Shirasago, Y.; Kondoh, M.; Suzuki, T.; Wakita, T.; Hanada, K.; Yagi, K.; Fukasawa, M. Monoclonal Antibodies against Occludin Completely Prevented Hepatitis C Virus Infection in a Mouse Model. *J. Virol.* **2018**, *92*, e02258–17. [CrossRef] [PubMed]
115. Liu, S.; Kuo, W.; Yang, W.; Liu, W.; Gibson, G.A.; Dorko, K.; Watkins, S.C.; Strom, S.C.; Wang, T. The second extracellular loop dictates Occludin-mediated HCV entry. *Virology* **2010**, *407*, 160–170. [CrossRef] [PubMed]
116. Dorner, M.; Horwitz, J.A.; Robbins, J.B.; Barry, W.T.; Feng, Q.; Mu, K.; Jones, C.T.; Schoggins, J.W.; Catanese, M.T.; Burton, D.R.; et al. A genetically humanized mouse model for hepatitis C virus infection. *Nature* **2011**, *474*, 208–211. [CrossRef] [PubMed]
117. Dorner, M.; Horwitz, J.A.; Donovan, B.M.; Labitt, R.N.; Budell, W.C.; Friling, T.; Vogt, A.; Catanese, M.T.; Satoh, T.; Kawai, T.; et al. Completion of the entire hepatitis C virus life cycle in genetically humanized mice. *Nature* **2013**, *501*, 237–241. [CrossRef] [PubMed]
118. Ding, Q.; von Schaewen, M.; Hrebikova, G.; Heller, B.; Sandmann, L.; Plaas, M.; Ploss, A. Mice Expressing Minimally Humanized CD81 and Occludin Genes Support Hepatitis C Virus Uptake In Vivo. *J. Virol.* **2017**, *91*, e01799–16. [CrossRef]
119. Nakamuta, M.; Fujino, T.; Yada, R.; Aoyagi, Y.; Yasutake, K.; Kohjima, M.; Fukuizumi, K.; Yoshimoto, T.; Harada, N.; Yada, M.; et al. Expression profiles of genes associated with viral entry in HCV-infected human liver. *J. Med. Virol.* **2011**, *83*, 921–927. [CrossRef]
120. Mensa, L.; Crespo, G.; Gastinger, M.J.; Kabat, J.; Perez-del-Pulgar, S.; Miquel, R.; Emerson, S.U.; Purcell, R.H.; Forns, X. Hepatitis C virus receptors claudin-1 and occludin after liver transplantation and influence on early viral kinetics. *Hepatology* **2011**, *53*, 1436–1445. [CrossRef]
121. Krieger, S.E.; Zeisel, M.B.; Davis, C.; Thumann, C.; Harris, H.J.; Schnober, E.K.; Mee, C.; Soulier, E.; Royer, C.; Lambotin, M.; et al. Inhibition of hepatitis C virus infection by anti-claudin-1 antibodies is mediated by neutralization of E2-CD81-claudin-1 associations. *Hepatology* **2010**, *51*, 1144–1157. [CrossRef]
122. Fofana, I.; Krieger, S.E.; Grunert, F.; Glauben, S.; Xiao, F.; Fafi-Kremer, S.; Soulier, E.; Royer, C.; Thumann, C.; Mee, C.J.; et al. Monoclonal anti-claudin 1 antibodies prevent hepatitis C virus infection of primary human hepatocytes. *Gastroenterology* **2010**, *139*, 953–964. [CrossRef] [PubMed]
123. Colpitts, C.C.; Tawar, R.G.; Mailly, L.; Thumann, C.; Heydmann, L.; Durand, S.C.; Xiao, F.; Robinet, E.; Pessaux, P.; Zeisel, M.B.; et al. Humanisation of a claudin-1-specific monoclonal antibody for clinical prevention and cure of HCV infection without escape. *Gut* **2018**, *67*, 736–745. [CrossRef] [PubMed]
124. Mailly, L.; Xiao, F.; Lupberger, J.; Wilson, G.K.; Aubert, P.; Duong, F.H.T.; Calabrese, D.; Leboeuf, C.; Fofana, I.; Thumann, C.; et al. Clearance of persistent hepatitis C virus infection in humanized mice using a claudin-1-targeting monoclonal antibody. *Nat. Biotechnol.* **2015**, *33*, 549–554. [CrossRef] [PubMed]
125. Fofana, I.; Fafi-Kremer, S.; Carolla, P.; Fauvelle, C.; Zahid, M.N.; Turek, M.; Heydmann, L.; Cury, K.; Hayer, J.; Combet, C.; et al. Mutations that alter use of hepatitis C virus cell entry factors mediate escape from neutralizing antibodies. *Gastroenterology* **2012**, *143*, 223–233. [CrossRef]
126. Xiao, F.; Fofana, I.; Thumann, C.; Mailly, L.; Alles, R.; Robinet, E.; Meyer, N.; Schaeffer, M.; Habersetzer, F.; Doffoel, M.; et al. Synergy of entry inhibitors with direct-acting antivirals uncovers novel combinations for prevention and treatment of hepatitis C. *Gut* **2014**. [CrossRef]
127. Xiao, F.; Fofana, I.; Heydmann, L.; Barth, H.; Soulier, E.; Habersetzer, F.; Doffoel, M.; Bukh, J.; Patel, A.H.; Zeisel, M.B.; et al. Hepatitis C virus cell-cell transmission and resistance to direct-acting antiviral agents. *PLoS Pathog.* **2014**, *10*, e1004128. [CrossRef]
128. Okai, K.; Ichikawa-Tomikawa, N.; Saito, A.C.; Watabe, T.; Sugimoto, K.; Fujita, D.; Ono, C.; Fukuhara, T.; Matsuura, Y.; Ohira, H.; et al. A novel occludin-targeting monoclonal antibody prevents hepatitis C virus infection in vitro. *Oncotarget* **2018**, *9*, 16588–16598. [CrossRef]
129. Michta, M.L.; Hopcraft, S.E.; Narbus, C.M.; Kratovac, Z.; Israelow, B.; Sourisseau, M.; Evans, M.J. Species-specific

- regions of occludin required by hepatitis C virus for cell entry. *J. Virol.* **2010**, *84*, 11696–11708. [CrossRef]
130. Bray, F.; Ferlay, J.; Soerjomataram, I.; Siegel, R.L.; Torre, L.A.; Jemal, A. Global cancer statistics 2018, GLOBOCAN estimates of incidence and mortality worldwide for 36 cancers in 185 countries. *CA Cancer J. Clin.* **2018**, *68*, 394–424. [CrossRef]
131. Bouchagier, K.A.; Assimakopoulos, S.F.; Karavias, D.D.; Maroulis, I.; Tzelepi, V.; Kalofonos, H.; Kardamakis, D.; Scopa, C.D.; Tsamandas, A.C. Expression of claudins-1, -4, -5, -7 and occludin in hepatocellular carcinoma and their relation with classic clinicopathological features and patients' survival. *In Vivo* **2014**, *28*, 315–326.
132. Holczbauer, A.; Gyongyosi, B.; Lotz, G.; Torzsok, P.; Kaposi-Novak, P.; Szijarto, A.; Tatrai, P.; Kupcsulik, P.; Schaff, Z.; Kiss, A. Increased expression of claudin-1 and claudin-7 in liver cirrhosis and hepatocellular carcinoma. *Pathol. Oncol. Res.* **2014**, *20*, 493–502. [CrossRef]
133. Huang, G.W.; Ding, X.; Chen, S.L.; Zeng, L. Expression of claudin 10 protein in hepatocellular carcinoma: Impact on survival. *J. Cancer Res. Clin. Oncol.* **2011**, *137*, 1213–1218. [CrossRef] [PubMed]
134. Zhou, S.; Parham, D.M.; Yung, E.; Pattengale, P.; Wang, L. Quantification of glypican 3, beta-catenin and claudin-1 protein expression in hepatoblastoma and paediatric hepatocellular carcinoma by colour deconvolution. *Histopathology* **2015**, *67*, 905–913. [CrossRef] [PubMed]
135. Kim, J.H.; Kim, E.L.; Lee, Y.K.; Park, C.B.; Kim, B.W.; Wang, H.J.; Yoon, C.H.; Lee, S.J.; Yoon, G. Decreased lactate dehydrogenase B expression enhances claudin 1-mediated hepatoma cell invasiveness via mitochondrial defects. *Exp. Cell Res.* **2011**, *317*, 1108–1118. [CrossRef] [PubMed]
136. Cheung, S.T.; Leung, K.L.; Ip, Y.C.; Chen, X.; Fong, D.Y.; Ng, I.O.; Fan, S.T.; So, S. Claudin-10 expression level is associated with recurrence of primary hepatocellular carcinoma. *Clin. Cancer Res.* **2005**, *11*, 551–556. [PubMed]
137. Li, C.P.; Cai, M.Y.; Jiang, L.J.; Mai, S.J.; Chen, J.W.; Wang, F.W.; Liao, Y.J.; Chen, W.H.; Jin, X.H.; Pei, X.Q.; et al. CLDN14 is epigenetically silenced by EZH2-mediated H3K27ME3 and is a novel prognostic biomarker in hepatocellular carcinoma. *Carcinogenesis* **2016**, *37*, 557–566. [CrossRef]
138. Jiang, L.; Yang, Y.D.; Fu, L.; Xu, W.; Liu, D.; Liang, Q.; Zhang, X.; Xu, L.; Guan, X.Y.; Wu, B.; et al. CLDN3 inhibits cancer aggressiveness via Wnt-EMT signaling and is a potential prognostic biomarker for hepatocellular carcinoma. *Oncotarget* **2014**, *5*, 7663–7676. [CrossRef]
139. Gerardo-Ramirez, M.; Lazzarini-Lechuga, R.; Hernandez-Rizo, S.; Jimenez-Salazar, J.E.; Simoni-Nieves, A.; Garcia-Ruiz, C.; Fernandez-Checa, J.C.; Marquardt, J.U.; Coulouarn, C.; Gutierrez-Ruiz, M.C.; et al. GDF11 exhibits tumor suppressive properties in hepatocellular carcinoma cells by restricting clonal expansion and invasion. *Biochim. Biophys. Acta Mol. Basis Dis.* **2019**, *1865*, 1540–1554. [CrossRef]
140. Hou, X.; Yang, L.; Jiang, X.; Liu, Z.; Li, X.; Xie, S.; Li, G.; Liu, J. Role of microRNA-141-3p in the progression and metastasis of hepatocellular carcinoma cell. *Int. J. Biol. Macromol.* **2019**, *128*, 331–339. [CrossRef]
141. Wang, S.C.; Lin, X.L.; Li, J.; Zhang, T.T.; Wang, H.Y.; Shi, J.W.; Yang, S.; Zhao, W.T.; Xie, R.Y.; Wei, F.; et al. MicroRNA-122 triggers mesenchymal-epithelial transition and suppresses hepatocellular carcinoma cell motility and invasion by targeting RhoA. *PLoS ONE* **2014**, *9*, e101330. [CrossRef]
142. Nagai, T.; Arao, T.; Nishio, K.; Matsumoto, K.; Hagiwara, S.; Sakurai, T.; Minami, Y.; Ida, H.; Ueshima, K.; Nishida, N.; et al. Impact of Tight Junction Protein ZO-1 and TWIST Expression on Postoperative Survival of Patients with Hepatocellular Carcinoma. *Dig. Dis.* **2016**, *34*, 702–707. [CrossRef]
143. Bekker, V.; Chanock, S.J.; Yeager, M.; Hutchinson, A.A.; von Hahn, T.; Chen, S.; Xiao, N.; Dotrang, M.; Brown, M.; Busch, M.P.; et al. Genetic variation in CLDN1 and susceptibility to hepatitis C virus infection. *J. Viral. Hepat.* **2010**, *17*, 192–200. [CrossRef]
144. Zadori, G.; Gelley, F.; Torzsok, P.; Sarvary, E.; Doros, A.; Deak, A.P.; Nagy, P.; Schaff, Z.; Kiss, A.; Nemes, B. Examination of claudin-1 expression in patients undergoing liver transplantation owing to hepatitis C virus cirrhosis. *Transplant. Proc.* **2011**, *43*, 1267–1271. [CrossRef] [PubMed]
145. Liu, S.; Yang, W.; Shen, L.; Turner, J.R.; Coyne, C.B.; Wang, T. Tight junction proteins claudin-1 and occludin control hepatitis C virus entry and are downregulated during infection to prevent superinfection. *J. Virol.* **2009**, *83*, 2011–2014. [CrossRef]
146. De Vos, R.; Desmet, V.J. Morphologic changes of the junctional complex of the hepatocytes in rat liver after bile duct ligation. *Br. J. Exp. Pathol.* **1978**, *59*, 220–227.
147. Sakisaka, S.; Kawaguchi, T.; Taniguchi, E.; Hanada, S.; Sasatomi, K.; Koga, H.; Harada, M.; Kimura, R.; Sata, M.; Sawada, N.; et al. Alterations in tight junctions differ between primary biliary cirrhosis and primary sclerosing cholangitis. *Hepatology* **2001**, *33*, 1460–1468. [CrossRef]
148. Nemeth, Z.; Szasz, A.M.; Tatrai, P.; Nemeth, J.; Gyorffy, H.; Somoracz, A.; Szijarto, A.; Kupcsulik, P.; Kiss, A.; Schaff, Z. Claudin-1, -2, -3, -4, -7, -8, and -10 protein expression in biliary tract cancers. *J. Histochem. Cytochem.* **2009**, *57*, 113–121. [CrossRef]
149. Sambrotta, M.; Strautnieks, S.; Papouli, E.; Rushton, P.; Clark, B.E.; Parry, D.A.; Logan, C.V.; Newbury, L.J.; Kamath, B.M.; Ling, S.; et al. Mutations in TJP2 cause progressive cholestatic liver disease. *Nat. Genet.* **2014**, *46*, 326–328. [CrossRef]

150. Vitale, G.; Gitto, S.; Vukotic, R.; Raimondi, F.; Andreone, P. Familial intrahepatic cholestasis: New and wide perspectives. *Dig. Liver Dis.* **2019**, *51*, 922–933. [CrossRef]
151. Baala, L.; Hadj-Rabia, S.; Hamel-Teillac, D.; Hadchouel, M.; Prost, C.; Leal, S.M.; Jacquemin, E.; Sefiani, A.; De Prost, Y.; Courtois, G.; et al. Homozygosity mapping of a locus for a novel syndromic ichthyosis to chromosome 3q27–q28. *J. Invest. Dermatol.* **2002**, *119*, 70–76. [CrossRef]
152. Lindor, K.D.; Gershwin, M.E.; Poupon, R.; Kaplan, M.; Bergasa, N.V.; Heathcote, E.J. American Association for Study of Liver, D. Primary biliary cirrhosis. *Hepatology* **2009**, *50*, 291–308. [CrossRef] [PubMed]
153. Karlsen, T.H.; Folseraas, T.; Thorburn, D.; Vesterhus, M. Primary sclerosing cholangitis—A comprehensive review. *J. Hepatol.* **2017**, *67*, 1298–1323. [CrossRef] [PubMed]
154. Nakanuma, Y.; Tsuneyama, K.; Gershwin, M.E.; Yasoshima, M. Pathology and immunopathology of primary biliary cirrhosis with emphasis on bile duct lesions: Recent progress. *Semin. Liver Dis.* **1995**, *15*, 313–328. [CrossRef] [PubMed]
155. Feldmeyer, L.; Huber, M.; Fellmann, F.; Beckmann, J.S.; Frenk, E.; Hohl, D. Confirmation of the origin of NISCH syndrome. *Hum. Mutat.* **2006**, *27*, 408–410. [CrossRef] [PubMed]
156. Nagtzaam, I.F.; van Geel, M.; Driessen, A.; Steijlen, P.M.; van Steensel, M.A. Bile duct paucity is part of the neonatal ichthyosis-sclerosing cholangitis phenotype. *Br. J. Dermatol.* **2010**, *163*, 205–207. [CrossRef] [PubMed]
157. Shah, I.; Bhatnagar, S. NISCH syndrome with hypothyroxinemia. *Ann. Hepatol.* **2010**, *9*, 299–301. [CrossRef]
158. Kirchmeier, P.; Sayar, E.; Hotz, A.; Hausser, I.; Islek, A.; Yilmaz, A.; Artan, R.; Fischer, J. Novel mutation in the CLDN1 gene in a Turkish family with neonatal ichthyosis sclerosing cholangitis (NISCH) syndrome. *Br. J. Dermatol.* **2014**, *170*, 976–978. [CrossRef]
159. Youssefian, L.; Vahidnezhad, H.; Saeidian, A.H.; Sotoudeh, S.; Zeinali, S.; Uitto, J. Gene-Targeted Next-Generation Sequencing Identifies a Novel CLDN1 Mutation in a Consanguineous Family With NISCH Syndrome. *Am. J. Gastroenterol.* **2017**, *112*, 396–398. [CrossRef]
160. Nagtzaam, I.F.; Peeters, V.P.M.; Vreeburg, M.; Wagner, A.; Steijlen, P.M.; van Geel, M.; van Steensel, M.A.M. Novel CLDN1 mutation in ichthyosis-hypotrichosis-sclerosing cholangitis syndrome without signs of liver disease. *Br. J. Dermatol.* **2018**, *178*, e202–e203. [CrossRef]
161. Szepeowski, S.; Lacoste, C.; Mallet, S.; Roquelaure, B.; Badens, C.; Fabre, A. NISCH syndrome, a rare cause of neonatal cholestasis: A case report. *Arch. Pediatr.* **2017**, *24*, 1228–1234. [CrossRef]
162. Carlton, V.E.; Harris, B.Z.; Puffenberger, E.G.; Batta, A.K.; Knisely, A.S.; Robinson, D.L.; Strauss, K.A.; Shneider, B.L.; Lim, W.A.; Salen, G.; et al. Complex inheritance of familial hypercholanemia with associated mutations in TJP2 and BAAT. *Nat. Genet.* **2003**, *34*, 91–96. [CrossRef] [PubMed]
163. Patel, T. Increasing incidence and mortality of primary intrahepatic cholangiocarcinoma in the United States. *Hepatology* **2001**, *33*, 1353–1357. [CrossRef] [PubMed]
164. Saha, S.K.; Zhu, A.X.; Fuchs, C.S.; Brooks, G.A. Forty-Year Trends in Cholangiocarcinoma Incidence in the U.S: Intrahepatic Disease on the Rise. *Oncologist* **2016**, *21*, 594–599. [CrossRef] [PubMed]
165. Von Hahn, T.; Ciesek, S.; Wegener, G.; Plentz, R.R.; Weismüller, T.J.; Wedemeyer, H.; Manns, M.P.; Greten, T.F.; Malek, N.P. Epidemiological trends in incidence and mortality of hepatobiliary cancers in Germany. *Scand. J. Gastroenterol.* **2011**, *46*, 1092–1098. [CrossRef]
166. Ehlken, H.; Schramm, C. Primary sclerosing cholangitis and cholangiocarcinoma: Pathogenesis and modes of diagnostics. *Dig. Dis.* **2013**, *31*, 118–125. [CrossRef]
167. Shaib, Y.H.; El-Serag, H.B.; Davila, J.A.; Morgan, R.; McGlynn, K.A. Risk factors of intrahepatic cholangiocarcinoma in the United States: A case-control study. *Gastroenterology* **2005**, *128*, 620–626. [CrossRef]
168. Ralphs, S.; Khan, S.A. The role of the hepatitis viruses in cholangiocarcinoma. *J. Viral. Hepat.* **2013**, *20*, 297–305. [CrossRef]
169. Tyson, G.L.; El-Serag, H.B. Risk factors for cholangiocarcinoma. *Hepatology* **2011**, *54*, 173–184. [CrossRef]
170. Jakab, C.; Kiss, A.; Schaff, Z.; Szabo, Z.; Rusvai, M.; Galfi, P.; Szabara, A.; Sterczar, A.; Kulka, J. Claudin-7 protein differentiates canine cholangiocarcinoma from hepatocellular carcinoma. *Histol. Histopathol.* **2010**, *25*, 857–864. [CrossRef]
171. Lodi, C.; Szabo, E.; Holczbauer, A.; Batmunkh, E.; Szijarto, A.; Kupcsulik, P.; Kovalszky, I.; Paku, S.; Illyes, G.; Kiss, A.; et al. Claudin-4 differentiates biliary tract cancers from hepatocellular carcinomas. *Mod. Pathol.* **2006**, *19*, 460–469. [CrossRef]
172. Bunthot, S.; Obchoei, S.; Kraiklang, R.; Pirojkul, C.; Wongkham, S.; Wongkham, C. Overexpression of claudin-4 in cholangiocarcinoma tissues and its possible role in tumor metastasis. *Asian Pac. J. Cancer Prev.* **2012**, *13*, 71–76. [PubMed]
173. Shinozaki, A.; Shibahara, J.; Noda, N.; Tanaka, M.; Aoki, T.; Kokudo, N.; Fukayama, M. Claudin-18 in biliary neoplasms. Its significance in the classification of intrahepatic cholangiocarcinoma. *Virchows Arch.* **2011**, *459*, 73–80. [CrossRef] [PubMed]

174. Nemeth, Z.; Szasz, A.M.; Somoracz, A.; Tatnai, P.; Nemeth, J.; Gyorffy, H.; Szijarto, A.; Kupcsulik, P.; Kiss, A.; Schaff, Z. Zonula occludens-1, occludin, and E-cadherin protein expression in biliary tract cancers. *Pathol. Oncol. Res.* **2009**, *15*, 533–539. [CrossRef] [PubMed]



© 2020 by the authors. Licensee MDPI, Basel, Switzerland. This article is an open access article distributed under the terms and conditions of the Creative Commons Attribution (CC BY) license (<http://creativecommons.org/licenses/by/4.0/>).

8 Curriculum vitae

Personal data

Name: Natascha Röhlen
Date of birth: 05.06.1990 in Karlsruhe
Nationality: German
Address: Rue du Général Leclerc 44,
67202 Wolfisheim, France
Phone: (+49) 157/33743410
E-Mail: natascha.roehlen@etu.unistra.fr

Education and Employment Record

Employment

Since 10/2018: Postdoctoral fellow at Inserm Unit UMR_S1110, Institute of Viral and Liver Disease, Strasbourg, France.

02/2016-09/2018: Medical Doctor at Department of Internal Medicine II, Gastroenterology, Endocrinology and Infectious Diseases, University Hospital Freiburg, Freiburg, Germany.

Academic Education and University Degrees

Since 10/2018: PhD thesis at University Strasbourg, Ecole doctorale des Sciences de la vie et de la Santé (ED414):
“The functional role of Claudin-1 as a mediator and therapeutic target in liver fibrogenesis and hepatocarcinogenesis”

03/2013-01/2018: Dissertation at the Department of Internal Medicine I, Endocrinology, Goethe University Frankfurt:
“Die Bedeutung des Vitamin D-Sirtuin1-Forkheadbox-Protein O3a-Signalweges in der Pathogenese autoimmuner und maligner Schilddrüsenerkrankungen”

01/2018: Doctorate of Medicine, Grade: magna cum laude

10/2009-11/2015: Study of Medicine at Goethe University Frankfurt
11/2015: Graduation in Human Medicine, Grade: 1.16

School Education

09/2000-07/2009: Goethe Gymnasium Gaggenau (Secondary School),
Germany
07/2009: Abitur, Grade: 1.8

09/1996-07/2000: Grundschule Bischweier (Primary school), Germany

Scholarships

Since 10/2019: Individual Research grant by the German Research
Foundation (DFG)

10/2013-10/2014: Receipt of the scholarship „Deutschlandstipendium“
(National scholarship programme)

09/2013-10/2013: Receipt of the DAAD scholarship
(Foreign exchange scholarship for an elective abroad)

Language skills:

German: Mother language

English: Advanced (C1)

French: Intermediate (B1)

Scientific output:

Original articles:

- **Roehlen N***, Saviano A*, El Saghire H*, Crouchet E, Duong FHT, Juehling F, Cherradi S, Oudot MA, Gonzalez Motos V, Durand SC, Pessaux P, Felli E, Thumann C, Koutsopoulos O, Fuchs B, Hoshida Y, Elson G, Meyer M, Iacone R, Schweighoffer T, Heikenwälder M, Mailly L, Schuster C, Lupberger J, Zeisel MB, Baumert TF. Claudin-1 is a mediator and therapeutic target for organ fibrosis. In Revision in *Sci Transl Med*. *shared first-authorship.
- **Roehlen N**, Muller M, Cherradi S, Jühling F, Duong FHT, Almeida N, Del Zompo F, Fernandez M, Riedl T, El Saghire H, Saviano A, Durand S, Ponsolles C, Oudot M, Felli E, Pessaux P, Davidson I, Crouchet E, Bandiera S, Thumann C, Nicolay B, Bardeesy N, Laquerriere P, Heikenwälder M, Iacone R, Meyer M, Elson G, Schweighoffer T, Schuster C, Mailly L, Lupberger J, Baumert TF. A humanized Claudin-1 specific monoclonal antibody for treatment of hepatocellular carcinoma. In preparation for submission to *Cancer Discovery*.
- Crouchet E, Bandiera S, Fujiwara N, Li S, El Saghire H, Sun X, Hirschfield H, Juehling F, **Roehlen N**, Zhu S, Heydmann L, Saviano A, Qian T, González Motos V, Venkatesh A, Ponsolles C, Verrier ER, Lupberger J, Sojoodi M, Oudot MA, Duong FHT, Masia R, Wei L, Thumann C, Durand SC, Nakagawa S, Ono A, Song WM, Higashi T, Sanchez R, Kim RS, Bian CB, Kiani K, Croonenborghs T, Subramanian A, Chung RT, Heide D, Hetzer J, Straub BK, Schuppan D, Ankavay M, Cocquerel L, Schaeffer E, Goossens N, Koh AP, Mahajan M, Nair VD, Gunasekaran G, Schwartz ME, Bardeesy N, Shalek AK, Rozenblatt-Rosen A, Regev A, Heikenwalder M, Felli E, Pessaux P, Tanabe KK, Schuster C, Pochet N, Zeisel MB, Fuchs BC, Hoshida Y, Baumert TF. A human liver cell-based system modeling a clinical prognostic liver signature combined with single-cell RNA-Seq for discovery of liver disease therapeutics. Accepted in *Nat Commun* (08/2021).
- **Roehlen N**, Laubner K, Bettinger D, Schwacha H, Hilger H, Koenig C, Grueninger D, Krebs A, Seufert J. Duodenal-Jejunal Bypass Liner Improves Cardiovascular Risk Biomarkers and Predicted 4-Year Risk of Major CV Events in Patients with Type 2 Diabetes and Metabolic Syndrome. *Obes Surg*. 2020 Apr;30(4):1200-1210.
- **Roehlen N**, Doering C, Hansmann ML, Gruenwald F, Vorlaender C, Bechstein WO, Holzer K, Badenhop K, Penna-Martinez M. Vitamin D, FOXO3a, and Sirtuin1 in Hashimoto's Thyroiditis and Differentiated Thyroid Cancer. *Front Endocrinol (Lausanne)*. 2018 Sep 11;9:527.

Reviews, book chapters and Editorials:

- **Roehlen N**, Baumert RF. Uncovering the Mechanism of Action of Aspirin in HCC Chemoprevention. *EBioMedicine*. 2019 Aug 6. (Editorial)
- Saviano A*, **Roehlen N***, Virzì A, Roca Suarez A.A., Hoshida Y, Lupberger J, Baumert TF (2019). Stromal and immune drivers of hepatocarcinogenesis. Hoshida J (Ed.), Hepatocellular Carcinoma: Translational Precision Medicine Approach_Series:

Molecular and Translational Medicine. Springer p317-331. *shared first-authorship. (Book chapter)

- **Roehlen N**, Roca Suarez AA, El Saghire H, Saviano A, Schuster C, Lupberger J, Baumert TF. Tight Junction Proteins and the Biology of Hepatobiliary Disease. *Int J Mol Sci*. 2020 Jan 28;21(3):825. (Review).
- **Roehlen N**, Crouchet E, Baumert TF. Liver Fibrosis: Mechanistic Concepts and Therapeutic Perspectives. *Cells*. 2020 Apr 3;9(4):875. (Review)
- **Roehlen N**, Knoop RF, Laubner K, Seufert J, Schwacha H, Thimme R, Fischer A. Ischemic Duodenal Ulceration after Transarterial Chemoembolization for Hepatocellular Carcinoma: A Case Report. *Case Rep Gastroenterol*. 2018 Jun 28;12(2):352-359. (Case report)
- **Roehlen N**, Takacs S, Ebeling O, Seufert J, Laubner K. Ectopic papillary thyroid carcinoma within a thyroglossal duct cyst: A case report. *Medicine (Baltimore)*. 2017 Dec;96(48):e8921. (Case report)
- **Roehlen N**, Hilger H, Stock F, Gläser B, Guhl J, Schmitt-Graeff A, Seufert J, Laubner K. 17q12 Deletion Syndrome as a Rare Cause for Diabetes Mellitus Type MODY5. *J Clin Endocrinol Metab*. 2018 Oct 1. (Review)

Oral presentations:

- **Roehlen N**, Cherradi S, Muller M, Almeida N, Duong FHT, Crouchet E, El Saghire H, Durand S, Ponsolles C, Oudot M, Saviano A, Felli E, Pessaux P, Cristofori C, Lupberger J, Elson G, Meyer M, Iacone R, Schweighoffer T, Laquerriere P, Schuster C, Mailly L, Baumert TFB. A humanized Claudin-1-specific monoclonal antibody for treatment of hepatocellular carcinoma. Oral presentation at the International Liver Congress (EASL), 2021.
- El Saghire H*, Saviano A*, **Roehlen N***, Crouchet E, Duong FHT, Juehling F, Cherradi S, Oudot MA, Gonzalez Motos V, Durand SC, Pessaux P, Felli E, Thumann C, Koutsopoulos O, Fuchs B, Hoshida Y, Elson G, Meyer M, Iacone R, Schweighoffer T, Heikenwälder M, Mailly L, Schuster C, Lupberger J, Zeisel MB, Baumert TF. Claudin-1 is a target for treatment of advanced liver fibrosis and cancer prevention. *shared first-authorship. Oral presentation at the International Liver Congress (EASL), 2021.
- **Roehlen N**. Claudin-1 as a therapeutic target for HCC- molecular mechanisms and role of the microenvironment. Oral presentation at the Annual TheraHCC Workshop, March 2021.
- **Roehlen N**. Claudin-1 and cancer biology - what can we learn from other cancers. Oral presentation at the ERC HEPCAN Symposium, May 2020.
- **Roehlen N**. Role of CAFs in HCC. Oral presentation at the ERC HEPCAN Symposium, May 2020

The functional role of Claudin-1 as a mediator and therapeutic target in liver fibrogenesis and hepatocarcinogenesis

Résumé

La fibrose hépatique et le carcinome hépatocellulaire (CHC) constituent des problèmes majeurs de santé publique. A ce jour, l'augmentation constante de l'incidence des maladies hépatiques avancées, l'absence de thérapies anti-fibrotiques approuvées et l'efficacité limitée des options thérapeutiques actuelles pour les patients atteints de CHC avancé démontrent l'urgence à adresser ce besoin médical non résolu. La claudine-1 (CLDN1) est une protéine membranaire qui intervient dans l'adhésion des cellules au niveau des jonctions serrées et dans la signalisation cellulaire. En utilisant des anticorps monoclonaux (mAb) ciblant la forme non-jonctionnelle de CLDN1, nous avons étudié le potentiel de CLDN1 à être une cible thérapeutique pour lutter contre la fibrose hépatique et le CHC. En effet, des mAb CLDN1, issus du laboratoire, ont montré des effets antifibrotiques, chimiopréventifs et anti-tumorigènes très significatifs dans plusieurs modèles de fibrose hépatique avancée et de CHC dérivés de tissus de patients, à la fois *in vitro*, *ex vivo* et *in vivo*. Des études mécanistiques ont révélé que l'AcM CLDN1 est impliqué dans la différenciation cellulaire ainsi que dans la régulation de certaines voies de signalisation cellulaire. Ces données révèlent que CLDN1 non-jonctionnelle est une nouvelle cible pour le traitement de la fibrose hépatique et pour la chimioprévention et la thérapie du CHC. Mots-clés : CHC, CLDN1, fibrose hépatique.

Résumé en anglais

Liver fibrosis and hepatocellular carcinoma (HCC) are major public health burden. However, approved antifibrotic therapies are absent and current treatment options for patients with advanced HCC show only limited efficacy. Thus, an urgent medical need exists for the development of new therapies to treat advanced liver disease and HCC. Claudin-1 (CLDN1) is a cell membrane protein mediating cell adhesion and signaling. Using monoclonal antibodies (mAbs) targeting non-junctional CLDN1, we aimed to investigate the role of CLDN1 as a therapeutic target for liver fibrosis and HCC. In fact, CLDN1 mAbs showed marked and significant antifibrotic, chemopreventive and anti-tumorigenic effects in several patient-derived cell-based, *ex vivo* and *in vivo* models of advanced liver fibrosis and HCC. Mechanistic studies suggested CLDN1 mAb to interfere with cell differentiation as well as cell signaling. These data indicate non-junctional CLDN1 as a novel target for treatment of advanced liver fibrosis, HCC chemoprevention and HCC therapy. Keywords : HCC, CLDN1, liver fibrosis